The Dissertation Committee for Ali Goudarzi Certifies that this is the approved version of the following dissertation:

Modeling Conformance Control and Chemical EOR Processes Using Different Reservoir Simulators

Committee:

Keith P. Johnston, Co-Supervisor

Kamy Sepehrnoori, Co-Supervisor

Mojdeh Delshad, Co-Supervisor

Mukul M. Sharma

Roger T. Bonnecaze

Modeling Conformance Control and Chemical EOR Processes Using Different Reservoir Simulators

by

Ali Goudarzi, B.E.; M.S.; M.S.E.

Dissertation

Presented to the Faculty of the Graduate School of

The University of Texas at Austin

in Partial Fulfillment

of the Requirements

for the Degree of

Doctor of Philosophy

The University of Texas at Austin

August 2015

Dedication

To my parents and my brothers for their unconditional support

Acknowledgements

This dissertation would never be possible without the support and help from many people. It is really a great honor for me to express my deepest gratitude to some of those many. I would like to express my sincere gratitude to my co-supervisors Dr. Keith P. Johnston, Dr. Kamy Sepehrnoori, and Dr. Mojdeh Delshad for their continuous guidance, support, and encouragement. I am privileged to have had an opportunity to work with them. I have learned a lot from their profound insight, vast knowledge, and keen observations. I personally believe that their invaluable support, encouragement, and endless patience were the principal keys to my success.

I would also like to express my sincere gratitude to my committee members, Dr. Mukul Sharma, and Dr. Roger T. Bonnecaze. I really appreciate the time, valuable comments, and feedback of my committee.

I would also thank Dr. Chowdhury K. Mamun for grammatical and extensive technical review and for helpful comments on my dissertation.

I would like to acknowledge the faculty and staff of the Petroleum and Geosystems Engineering Department and also Chemical Engineering Department at The University of Texas at Austin: Dr. Isaac C. Sanchez, Dr. Hal Alper, Dr. Roger Terzian, John Cassibry, Joanna Castillo, Cheryl Kruzie, Frankie Hart, Mary Pettengill, Kate W. Baird, Carrie Brown, Kevin J. Haynes, and Kelly McQueary for their technical and administrative support.

I am indebted to many of my friends and colleagues who through their sincere suggestions and fruitful discussions shaped this dissertation in so many ways. Without their support, this important research would have not been possible. In particular, I would like to thank Dr. Abdoljalil Varavei for description of UTCHEM and UTGEL and having

extensive technical discussion; Dr. Baojun Bai for great support on providing conformance control laboratory data and having related technical discussion; Jing Wang for extensive discussion about gel kinetics; Hamid Lashgari for related technical discussion; Aboulghasem Kazemi Nia for technical discussion; Pongpak Taksaudom for running and reporting the bugs of code; Mahmood Shakiba for helping on discrete fracture model of the code; Peila Chen for providing static imbibition tests laboratory data; Jun Lu for providing coreflood experiments laboratory data; Farag Muhammed for related technical discussion; Abdulmohsin Imqam and Ayman Almohsin for providing laboratory data on preformed particle gels; Hao Zhang for providing laboratory data on microgels.

I would like to thank my friends Mohsen Rezaveisi, Mojtaba Ghasemi Doroh, Javad Behseresht, Saeedeh Mohebbinia, Amir Frooqnia, Rohollah Abdollah-Pour, Mahdy Shirdel, Hamed Darabi, Ali Moinfar, Mohsen Taghavifar, Reza Ganjedanesh, Mehdi Haghshenas, Gholamreza Garmeh, Seyed Reza Yousefi, Amirreza Rahmani, Ali Farhadinia, Mohammad Lotfollahi, Mohammadreza Beigi, Alireza Mollaei, Mahdi Habibi, Hossein Roodi, Mahdi Haddad, Masoud Behzadi Nasab, Wei Yu, Sergio Jose Cavalcante Filho, Saeid Enayat-Pour, Ehsan Saadat-Pour, Rouzbeh Ghanbarnezhad, Amin Ettehadtavakkol, Ali Abouie, Ahmad Sakhaee-Pour, Reza Tavakoli, Shayan Tavassoli, Zoya Heidari, Vahid Shabro, Maryam Mirabolghasemi, Alireza Sanaei, Behzad Eftekhari, Mohammad Mirzaei, Mohammad Hosein Kalaei, Mohammad O. Eshkalak, Emad Al-Shalabi, Elif Ozdingis, and Pooneh Hosseininoosheri as well as many other friends I have not mentioned names for all their support and making my life so pleasant during these years.

The work presented in this dissertation was funded from RPSEA subcontract#11123-32 for water management in a small producer program. Additional

support came from the Reservoir Simulation Joint Industry Project (RSJIP) at the Center for Petroleum and Geosystems Engineering at The University of Texas at Austin.

Finally, I would like to extend my appreciation to my parents for their love, patience, understanding, and encouragement towards my achievements.

Modeling Conformance Control and Chemical EOR Processes Using Different Reservoir Simulators

Ali Goudarzi, Ph.D.

The University of Texas at Austin, 2015

Supervisors: Keith P. Johnston

Kamy Sepehrnoori

Mojdeh Delshad

Successful field waterflood is a crucial prerequisite for improving the performance before EOR methods, such as ASP, SP, and P flooding, are applied in the field. Excess water production is a major problem in mature waterflooded oil fields that leads to early well abandonment and unrecoverable hydrocarbon. Gel treatments at the injection and production wells to preferentially plug the thief zones are cost-effective methods to improve sweep efficiency in reservoirs and reduce excess water production during hydrocarbon recovery. There are extensive experimental studies performed by some researchers in the past to investigate the performance of gels in conformance control and decreasing water production in mature waterflooded reservoirs, but no substantial modeling work has been done to simulate these experiments and predict the results for large field cases.

We developed a novel, 3-dimensional chemical compositional and robust general reservoir simulator (UTGEL) to model gel treatment processes. The simulator has the capability to model different types of microgels, such as preformed particle gels (PPG),

thermally active polymers (TAP), pH-sensitive microgels, and colloidal dispersion gels (CDG). The simulator has been validated for gel flooding using laboratory and field scale data. The simulator helps to design and optimize the flowing gel injection for conformance control processes in larger field cases.

The gel rheology, adsorption, resistance factor and residual resistance factor with salinity effect, gel viscosity, gel kinetics, and swelling ratio were implemented in UTGEL. Several simulation case studies in fractured and heterogeneous reservoirs were performed to illustrate the effect of gel on production behavior and water control. Laboratory results of homogeneous and heterogeneous sandpacks, and Berea sandstone corefloods were used to validate the PPG transport models. Simulations of different heterogeneous field cases were performed and the results showed that PPG can improve the oil recovery by 5-10% OOIP compared to waterflood.

For recovery from fractured reservoirs by waterflooding, injected water will flow easily through fractures and most part of reservoir oil will remain in matrix blocks unrecovered. Recovery from these reservoirs depends on matrix permeability, wettability, fracture intensity, temperature, pressure, and fluid properties. Chemical processes such as polymer flooding (P), surfactant/polymer (SP) flooding and alkali/surfactant/polymer (ASP) flooding are being used to enhance reservoir energy and increase the recovery. Chemical flooding has much broader range of applicability than in the past. These include high temperature reservoirs, formations with extreme salinity and hardness, naturally fractured carbonates, and sandstone reservoirs with heavy and viscous crude oils.

The recovery from fractured carbonate reservoirs is frequently considered to be dominated by spontaneous imbibition. Therefore, any chemical process which can enhance the rate of imbibition has to be studied carefully. Wettability alteration using

chemicals such as surfactant and alkali has been studied by many researchers in the past years and is recognized as one of the most effective recovery methods in fractured carbonate reservoirs. Injected surfactant will alter the wettability of matrix blocks from oil-wet to water-wet and also reduce the interfacial tension to ultra-low values and consequently more oil will be recovered by spontaneous co-current or counter-current imbibition depending on the dominant recovery mechanism.

Accurate and reliable up-scaling of chemical enhanced oil recovery processes (CEOR) are among the most important issues in reservoir simulation. The important challenges in up-scaling CEOR processes are predictability of developed dimensionless numbers and also considering all the required mechanisms including wettability alteration and interfacial tension reduction. Thus, developing new dimensionless numbers with improved predictability at larger scales is of utmost importance in CEOR processes. There are some scaling groups developed in the past for either imbibition or coreflood experiments but none of them were predictive because all the physics related to chemical EOR processes (interfacial tension reduction and wettability alteration) were not included.

Furthermore, most of commercial reservoir simulators do not have the capability to model imbibition tests due to lack of some physics, such as surfactant molecular diffusion. The modeling of imbibition cell tests can aid to understand the mechanisms behind wettability alteration and consequently aid in up-scaling the process. Also, modeling coreflood experiments for fractured vuggy carbonates is challenging. Different approaches of random permeability distribution and explicit fractures were used to model the experiments which demonstrate the validity and ranges of applicability of upscaled procedures, and also indicate the importance of viscous and capillary forces in larger

scales. The simulation models were then used to predict the recovery response times for larger cores.

Table of Contents

List of Tables

List of Figures

Chapter 1: Introduction

The demand for energy and new oil reservoirs around the world has increased rapidly while oil recovery from depleted reservoirs has become more difficult. Oil production from fractured carbonate reservoirs by water flooding is often inefficient due to the commonly oil-wet nature of matrix rocks and lack of sufficient spontaneous capillary imbibition driving force to push oil out from the matrix to the fracture network. Chemical processes such as surfactant/alkali-induced wettability alteration and interfacial tension (IFT) reduction have shown great potential to reduce the residual oil saturation in matrix blocks, leading to significant incremental oil recovery (IOR). However, the IOR response time is the most crucial decision factor in field projects.

This chapter firstly describes the problem and also discusses the main objectives and the overall scope of this dissertation. Moreover, a brief description of the structure of different chapters of this dissertation will be given.

1.1 DESCRIPTION OF THE PROBLEM

Excess water production is a major problem that leads to early well abandonment and unrecoverable hydrocarbon in mature oil fields. Gel treatments at the injection wells to preferentially plug the thief zones are cost-effective methods to improve sweep efficiency in reservoirs and reduce excess water production during hydrocarbon recovery (Seright, 1995, 1999, 2000, 2004; Bai *et al.*, 1999, 2004, 2007, 2008, 2010; Sydansk and Moore, 1992; Cheung *et al.*, 2007; Wu *et al.*, 2008; Shi *et al.*, 2011; Zhang and Bai,

2010; Garmeh *et al.*, 2011). A recent gel process uses the preformed particle gels (PPGs) to overcome distinct drawbacks inherent in in-situ gelation systems, i.e. lack of control on gelation time, uncertain gelling due to shear degradation, chromatographic fractionation or change of gel compositions, and dilution by formation water.

Unfortunately, publications on mechanistically modeling conformance control processes for mature waterflooding are limited. Therefore, reservoir simulator with special features is needed to represent coupled chemical and physical mechanisms present in conformance control processes. The simulator needs to be first validated against well controlled lab-scale experiments to have reliable predictions of the full field implementations.

Optimization of any EOR and IOR processes requires a predictive model. A predictive model is also needed to fully understand the underlying mechanisms driving the recovery processes. To the best of author's knowledge, there is no comprehensive conformance control reservoir simulation model in the industry for controlling excess water production in mature waterflooded reservoirs.

Most of the fractured reservoirs (around 80%) are mixed-wet to oil-wet carbonates (Treiber et al., 1972; Roehl and Choquette, 1985; Borchardt and Yen, 1989) and therefore water flooding cannot be effective for these fractured reservoirs. Matrix permeability, wettability, fracture intensity, geological heterogeneity, and fluid properties are the main factors controlling the recovery factor in these reservoirs (Adibhatla and Mohanty, 2005). Interest in chemical enhanced oil recovery (CEOR) processes has intensified in recent years because of rising oil prices as well as the advancement in chemical formulations and injection techniques. Polymer (P), surfactant/polymer (SP), and alkaline/surfactant/polymer (ASP) are techniques for improving sweep and

displacement efficiencies with the aim of improving oil production in both secondary and tertiary floods (Lake, 1989; Green and Willhite, 1998; Delshad *et al*., 2006, 2009; Seethepalli *et al*., 2004; Abidhatla and Mohanty, 2006). More oil reservoirs are reaching maturity where secondary polymer floods and tertiary surfactant methods have become increasingly important. This significance has added to the industry's interest in using reservoir simulator as a tool for reservoir evaluation and management to minimize costs and to increase the process efficiency.

Understanding the mechanisms of oil production from tight matrix blocks in fractured carbonate heterogeneous rocks requires performing different kinds of experiment (mainly imbibition cell tests and corefloods). For scaleup purposes, there is need to model these experiments using CEOR simulator and try developing dimensionless groups to investigate the oil recovery prediction for large scale field cases. There are different scaling groups developed in the past for either imbibition or coreflood experiments but none of them are predictive because all the physics related to chemical EOR processes (interfacial tension reduction and wettability alteration) were not included (Mattax and Kyte, 1962; Parsons and Chaney, 1966; Hagoort, 1980; Al-Lawati, 1996; Ma et al., 1997; Li and Horne, 2002). Designing cost-effective, successful chemical processes for heterogeneous fractured carbonate reservoirs requires scale-up studies and comprehensive understanding of involved mechanisms for oil recovery during a chemical flood.

1.2 RESEARCH OBJECTIVES

In the first part of this dissertation, we developed a numerical reservoir simulator for conformance control processes using different types of bulk gels and microgels. Different types of laboratory experiments were used to validate various physical models for resistance factor, residual resistance factor, swelling ratio, and gel in-situ rheology implemented in the simulator in addition to gel transport models. Empirical correlations for resistance factor and residual resistance factor of different microgels for wide range of brine salinity and hardness are developed and implemented in the simulator. We then applied our integrated simulator (i.e., UTGEL) to model conformance control processes in both highly heterogeneous and fractured reservoirs. Different sensitivity simulations were performed to optimize the main design variables for a conformance control process and evaluate reservoir parameters which influence the performance of microgels in blocking high permeability channels and diverting injected water into low permeability areas.

In the second part of this dissertation, we developed dimensionless scaling groups to aid in upscaling of laboratory results to field-scale applications using controlled and systematic laboratory measurements for several core sizes. The modified dimensionless group includes the IFT reduction effect which can be the main advantage compared to previous developed dimensionless times. Imbibition and coreflood tests on different core sizes are used to validate the scaling group; oil recovery could be predicted for the large cores at reservoir temperature using the new scaling group and recovery result from smaller cores. This new finding can be significant as it demonstrates the extent of IFT reduction and wettability alteration in fractured reservoirs.

1.3 BRIEF DESCRIPTION OF THE CHAPTERS

Chapter 2 focuses on a literature review of different approaches for wettability alteration in fractured carbonate reservoirs. A discussion will be provided on both experimental and simulation work conducted in the past. Then this chapter will discuss different types of bulk gels and microgels comprehensively. The advantages and disadvantages of different microgels will be reviewed in more detail compared to bulk gels; also the main mechanisms of each microgel in its performance and water control will be discussed.

Chapter 3 discusses with details all mathematical formulations of multi component, multiphase flow for gel component in porous media. The chapter includes the formulation (i.e., the mass conservation equation) implemented in UTGEL to transport the gel species. Then three different types of bulk gels (KGOPT = 1 or 2 or 3) will be explained including the detailed reaction mechanisms and permeability reduction factors. Subsequently, colloidal dispersion gels or CDG (KGOPT=5) will be covered, including detailed equations for CDG viscosity and transport though porous media.

Chapter 4 presents with detail all the mathematical equations and models for propagation of preformed particle gels (PPG) in a reservoir. This includes correlations for viscosity, swelling ratio, gel rheology, resistance factor, residual resistance factor, adsorption and kinetics regarding the flow of PPG in porous media. Then different types of PPG injection experiments on both sandpack and sandstone cores are discussed. The experiments include both homogenous and heterogeneous porous media which includes different permeability layered systems with crossflow and without crossflow. Then simulation results of these experiments using an inhouse simulator (UTGEL) will be presented, which will aid in designing large field-scale conformance control processes.

Different simulations on synthetic cases will be covered to investigate the effect of key controlling factors, such as slug size, PPG concentration, permeability contrast, etc. on the performance of PPG for excess water production control. After that, several heterogeneous field cases were chosen to compare the effect of PPG and other types of gels, such as bulk gels on increasing oil recovery and reducing water cut.

Chapter 5 presents with detail all the mathematical equations and models for activation and propagation of thermally active polymers (TAP) in a reservoir. This includes correlations for TAP viscosity, rheology, resistance factor, residual resistance factor, adsorption and retention during the flow of TAP in porous media. Different simulations on synthetic cases will be covered to investigate the effect of key controlling factor, such as slug size, TAP concentration, permeability contrast, etc. on the performance of TAP for blocking high permeability thief zones.

Chapter 6 discusses different types of chemical EOR experiments, including coreflood and imbibition tests using new surfactant formulations, and how these experiments can be modeled using an inhouse chemical flooding simulator (UTCHEM). The commonly used dimensionless groups are presented and their advantages and disadvantages are explained. After that, the experimental results for different core sizes are used to introduce a new dimensionless group, including the IFT reduction effect.

Chapter 7 presents the benchmark study of different reservoir simulators for modeling chemical EOR processes. Different chemical simulators (UTCHEM, CMG-STARS, and ECLIPSE) were used to model coreflood experiments and field-scale simulations. The chemical tables in CMG-STARS and ECLIPSE were carefully matched with correlations in UTCHEM to get a close agreement between different simulators for modeling chemical EOR processes.

Chapter 8 presents the summary of the dissertation and the concluding remarks. We further propose some recommendations that can be considered for further enhancements in UTGEL simulator.

Chapter 2: Background and Literature Review

Conventional recovery from oil reservoirs based on natural depletion by energy of fluid is referred to primary production. After pressure depletion due to production, it is required to enhance reservoir pressure and this can be performed either by injecting water or gas. This stage of production by pressure maintenance is called secondary recovery. However, it was recognized that water flooding cannot mobilize droplets of original oil trapped in smaller pores due to capillary forces, especially in fractured carbonate reservoirs. Injected water will flow through fractures easily and residual oil will remain unswept in the matrix. There can be further oil recovery after secondary flood by changing the wettability of the rock or decreasing IFT between water and oil by injected chemicals, such as surfactant or alkali, referred to as chemical EOR processes (Lake, 1989; Green and Willhite, 1998).

Excess water production is a major problem that leads to early well abandonment and unrecoverable hydrocarbon in mature oil fields. Excess water production through fractures and high permeability thief zones is a growing concern for sweep efficiency and oil production. Water management in mature waterflooded reservoirs is a top priority to push more oil out and control water production. Gel treatments at the injection wells to preferentially plug the thief zones are cost-effective methods to improve sweep efficiency in reservoirs and reduce excess water production during hydrocarbon recovery.

This chapter is divided into two parts. The first part will be an introduction to conformance control processes using different polymer/gel chemistries (bulk gels and microgels). The second part will be an overview of the chemical EOR processes in

fractured carbonate reservoir, focusing on wettability alteration and upscaling methodologies.

2.1 CONFORMANCE CONTROL PROCESSES

Excess water production due to heterogeneity or existence of fractures and high permeability channels causes water conning, which is a major issue for field operators. Among different methods, polymer or gel injection can reduce water cut. Several researchers have shown that polymer or gel have capability to reduce water relative permeability without considerable change in oil relative permeability (Schneider and Owens, 1982; Zaitoun and Kohler, 1988; Zaitoun *et al.*, 1991; Liang *et al.*, 1995). Several physical processes are proposed for the action of polymer on relative permeability modification which can be categorized as: a) Shrinking of the polymer in the presence of oil, b) Partitioning of fluid, c) Water effect and adsorption, and d) Wettability effect. Several experimental studies (both steady and unsteady-state conditions) were completed to measure the effect of polymer on relative permeability and capillary pressure (Barreau *et al.*, 1997). The permeability modification by polyacrylamide in two-phase flow can be explained in terms of the adsorbed polymer layer on pore walls but wettability effect of polymer can mainly be attributed to IFT reduction and residual oil saturation reduction (Zaitoun *et al.*, 1998). However, there are some concerns and issues with polymer flooding which can be summarized as following:

- Classical polymer flooding for mobility control requires high pressure drop for injecting at specific rate due to its high viscosity.
- A large volume of polymer is required because some polymer mass will be lost due to adsorption and retention in the reservoir.

- Due to shear-thinning behavior, a viscous bulk will be generated around the wellbore because its shear rate will decrease rapidly as it enters the formation.

The field trial of relative permeability modification in the Marmul field (Oman) using a polymer/crosslinker combination gave a substantial decrease in water-cut with a considerable increase in oil production (Faber *et al.*, 1998). The simulation results of the Marmul field showed that the reservoir characterization and layering was one of the key success factors. The volume and concentrations of polymer/crosslinker required was based upon the reservoir heterogeneity and production results. Liang *et al.* (2000) studied the mechanisms for this permeability reduction and found out it is based on a combined "wall-effect" from an adsorbed polymer layer on the pore walls and "gel-droplet" at the center of a pore throat. If the gelant is prepared by the wetting phase, wall-effect model can explain the permeability reduction and if the gelant is prepared by the non-wetting phase, gel-droplet model should be used for explaining the phenomena. Ogunberu and Asghari (2004) investigated the effect of anionic polymers for reducing water production which can result from polymer flow-induced adsorption on porous media surface.

The mechanism for disproportionate permeability reduction (DPR) was investigated extensively by Stavland and Nilsson (2001). It was agreed that DPR can be suitable for water shut-off, where it reduces water permeability more than oil. The following most popular methods were proposed for DPR:

- Polymer adsorption at the pore surface and wettability change towards more water-wet
- Selective dehydration and swelling of polymer and crosslinker
- Segregated flow of oil and water
- Balancing between elastic confining forces and opposing capillary forces

Also there are some ideas that combination of the above mechanisms can also be another mechanism for DPR. The experimental results using Berea sandstone cores showed that lower range of pressure gradient will cause larger DPR due to relatively large residual oil saturation in the new pore space (Ganguly *et al.,* 2003). Also, the experimental results showed that permeability variation with pressure gradient is due to gel elasticity and deformation with pressure changes. Willhite *et al.* (2001) illustrated that DPR occurs when both water and oil flow through new pore structures generated by gel dehydration in the treated porous rock. Chauveteau *et al.* (2004) reported some laboratory experiments on a new type of microgel which is a very valuable DPR product. This new type of microgel was essentially a combination of polymer chains and two crosslinkers; neutral acrylamide (AM) and sulfonate (AMPS) which can be at different composition and concentration based on reservoir conditions. The remarkable point about this new type of microgel is that oil permeability does not decrease at all and they have very high thermal and mechanical stability. The degree of DPR depends on the characteristics of gel, pore size, and the flow rate. The new type of conformance-polymers as organically crosslinked polymer (OCP) was tested for high-temperature fields up to 350 ^{0}F in southern Mexico and the results proved that OCP is successful for permeability reduction in both sandstone and carbonate formations (Mercado *et al.,* 2009). The OCP system has very good thermal stability with high resistance to acid, CO_2, and H_2S. Sydansk and Seright (2007) provided some guidelines about under what conditions disproportionate permeability reduction (DPR) and water shutoff (WSO) can be applied successfully (Figure 2-1). The ideal DPR/WSO treatment is referred to one which does not reduce oil relative permeability and also which does not cause any reduction in the post treatment oil-production rate.

Unfortunately, there is still no ideal DPR/WSO treatment and all conformance control applications provide some degree of permeability reduction to oil. It should be noted that although the main focus of DPR/WSO treatment is for oil production wells but they can also be applied to gas production wells. The guidelines for ideal DPR/WSO treatment especially with regard to reservoir heterogeneity, geology, and production conditions are given in Table 2-1. The following shows the main key factors for successful DPR (Sydansk and Seright, 2007):

- High permeability producing intervals
- Long gel onset times
- Thick hydrocarbon producing areas
- Low oil viscosity
- Higher density contrast between oil and treatment fluid

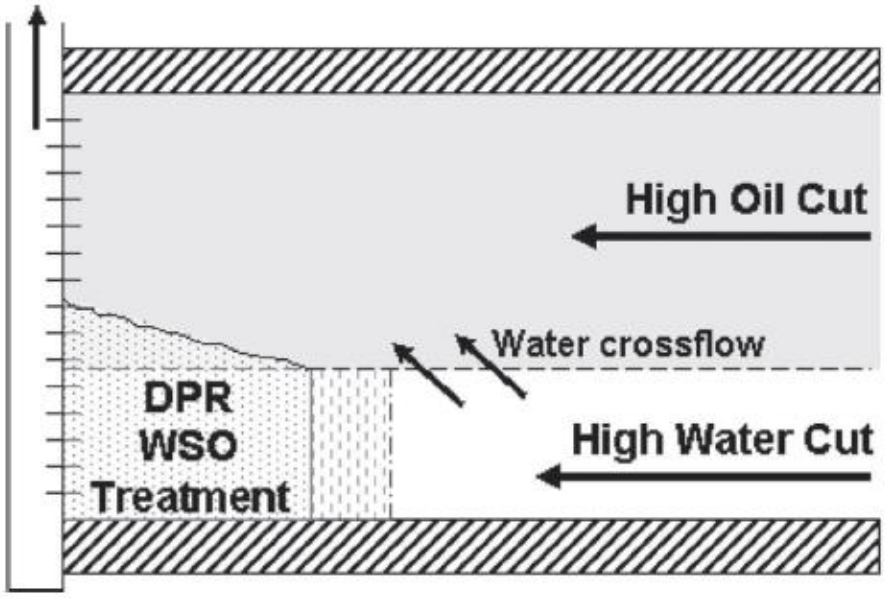

Figure 2-1: A representation of DPR/WSO treatment (Sydansk and Seright, 2007).

Table 2-1: Guidelines for the conditions of ideal DPR/WSO treatments (Sydansk and Seright, 2007).

GUIDELINES – WHEN & WHERE IDEAL RPM/DPR WSO TREATMENTS ARE APPLICABLE	Applicable
• Matrix-reservoir-rock radial-flow vertical wells	
➢ Fully drawn down wells	
▪ Long-term WSO	
⅄ Single homogeneous oil-producing zone	**No**
⅄ Multiple zones	
♦ Cross flow exists	**No**
♦ No crossflow exists	
▫ Oil zone(s) producing at 100% oil cut	**Yes**
▫ Oil zone(s) producing at a finite-water cut	**No**
▪ Short-term WSO	
⅄ Single homogeneous oil-producing zone	**Possibly**
⅄ Multiple zones	**Possibly**
➢ Wells not fully drawn down	
▪ Long-term WSO	
⅄ Single oil-producing zone	**No**
⅄ Multiple zones	
♦ Oil zone(s) producing at 100% oil cut	**Yes**
♦ Oil zone(s) producing at a finite water cut	**Depends***
▪ Short-term WSO	
⅄ Single homogeneous oil-producing zone	**Possibly**
⅄ Multiple zones	**Possibly**
• Matrix-reservoir-rock radial-flow horizontal wells (long-term WSO)	
➢ Water coning	**No**
• Fractured wells	
➢ Vertical wells	
▪ Hydraulic fracture extending into a fracture	**Yes**
▪ Single natural-fracture problem	**Yes**
▪ Limited natural-fracture-network problem	**Yes**
▪ Extensive natural-fracture-network problem	**Challenging**
➢ Horizontal wells	
▪ Fracture(s) connected to an aquifer	**Yes**

* depends on drawdown pressure

Gatooni *et al.* (2001) measured rheology of gels formed by crosslinking polyacrylamide polymers with chromium (III) and correlated with permeability of the gel to water over a wide range of polymer concentrations. The experimental results showed that permeability of gel to water increases with flow velocity and decreases with polymer concentration. The behavior can be modeled with a power-law expression and the results imply that the velocity-dependent behavior of the gel's permeability to water is due to its elasticity. Seright (2009) investigated pore-filling gels like chromium (III)-acetate-hydrolyzed polyacrylamide [Cr(III)-acetate-HPAM] to overcome the problem of reducing permeability to oil during treatment. Cr(III)-acetate-HPAM gels can dehydrate and increase oil permeability. In some tests gels had water residual resistance factor greater than 2,000 and final oil residual resistance factor less than 2. If the gel provides considerable water residual resistance factor, water entry into the fracture can be greatly limited with minimum reduction in oil recovery as shown in Figure 2-2.

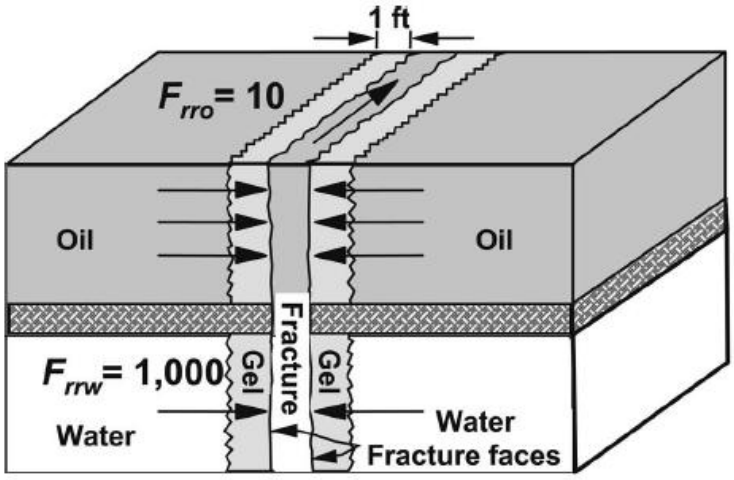

Figure 2-2: A representation of gel restricting water entry into a fracture (Seright, 2009).

2.1.1 Water Production Control Using Gels

Excess water production is becoming a major problem in mature oil fields as the oil reservoir is subjected to long water flooding process. Gel treatments, if applied correctly, can reduce excess water production and improve conformance by filling water channels and fractures. Each year many billions of barrels of water are produced world-wide and this produced water can stem from natural water-drive or waterflood through the mechanisms of coning, casing leaks or channeling (Seright, 1997). The produced water compromises the oil recovery and is expensive to be disposed. It was estimated that the cost-savings for the oil industry can be up to around 100 million USD per year for each 1% reduction in produced water (Seright, 1997). Water production control or water shut-off can be accomplished by several methods. The traditional method is to squeeze cement in the near-wellbore formation which hardens once in place (Sparlin and Hagen, 1984). However, there are some concerns and problems with cement squeezing. The first problem is that the slurry is very viscous and therefore a very low injection rate is required to be applied in order to stay under the critical fracturing pressure (Zitha, 2000). The second problem is that due to the brittle nature of cements the blocking capacity may be temporary. Furthermore, since the cement slurry is a dispersion of solids there is a high risk of permeability damage in the oil-producing zones.

The water production control methods often involve the injection of gel-forming chemicals (also referred to as gelants) in the near-wellbore formation. Ideally, the formed gel changes the permeability of the reservoir rock selectively such that the oil flow is not hindered, whereas the water flow is reduced or blocked completely as shown in Figure 2-3.

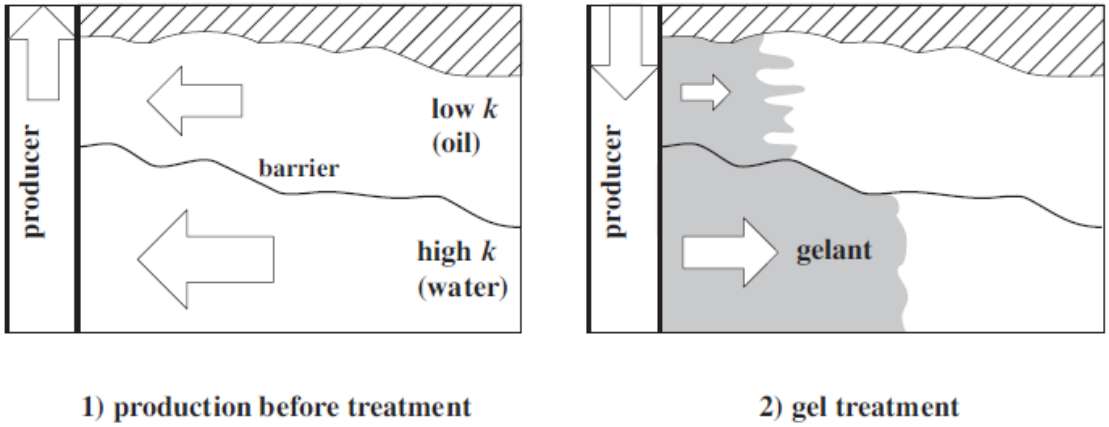

Figure 2-3: A representation of gel treatment in the reservoir after water breakthrough (Castelijns, 2007).

There are economic and environmental incentives to develop methods that reduce water production without significantly affecting oil production. Many gel floods have been tested and applied in the field and the results are often unpublished, classified, or reported but lack details. Nevertheless, 30–40% of the treatments proved to be successful over many years (Zitha, 2000). Depending on reservoir conditions and economics, each field project requires a specific choice of gelant and treatment procedure. By placing gelant in matrix containing residual oil, dehydration of the gel reconnects some of the trapped oil and consequently the oil permeability increases. Before gelation, it is a liquid composed of several compositions, polymer (HPAM), crosslinker (Cr^{3+}, Cr^{6+}, or Al^{3+}) and some additives. The liquid is called gelant. At some conditions, such as higher critical temperature, pH change, the gelant can crosslink to form gel as shown in Figure 2-4. Gel strength can be controlled by its gelant compositions; it can be weak like flowing gel, or very rigid, like rubber. Additives are used to control gelation time, gel strength, and thermal stability.

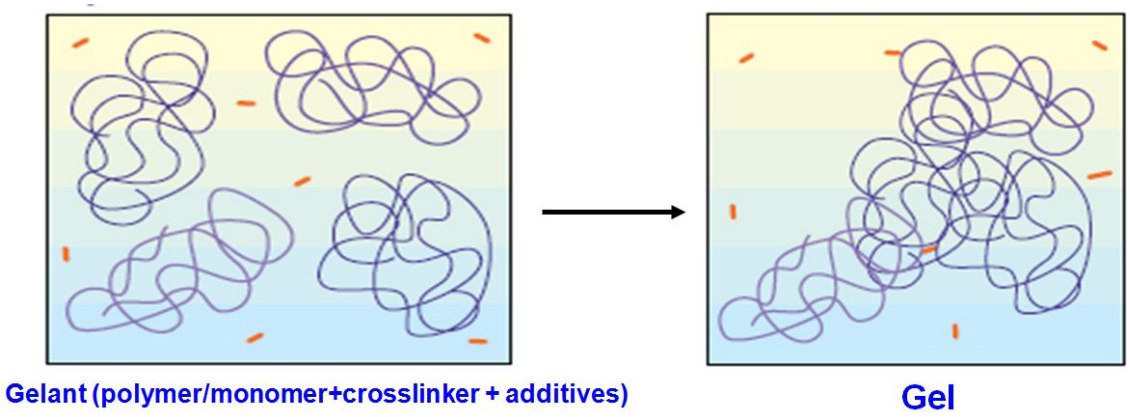

Figure 2-4: A representation of gel composition and its formation.

In the following sections, we will overview the bulk gels for near wellbore treatment and water production control. Then different kinds of microgels for in-depth conformance will be discussed.

2.1.2 Bulk Gels

It is well known that treatment with gelled polymer can reduce the water permeability at residual oil saturation by one to three orders of magnitude compared to oil permeability at the residual water saturation. This process is called disproportionate permeability reduction (DPR) and is of great interest because application of gel treatments in mature waterflooded reservoirs has potential to reduce water production (Willhite *et al.*, 2002). The mechanisms are not yet well understood. Willhite *et al.* (2012) performed experiments in unconsolidated sandpacks and in Berea sandstone cores to describe how permeability to oil and water is developed in pore space that is filled with chromium acetate/partially hydrolyzed polyacrylamide (HPAM) gel and proposed a mechanism for DPR.

Wang *et al.* (2003) performed experiments on single and parallel sandpacks to investigate the mechanism of weak gels for conformance control. They noted that when the polymer and crosslinker are injected into heterogeneous porous media, they selectively penetrate into high permeability zones which lead to in-situ formation of the weak gel. In subsequent waterflooding or polymer flooding, the weak gel system can be gradually pushed into a deeper formation with increased injection pressure and the weak gel is ruptured or squeezed into fine gel particles during this process. When these mobile gel particles migrate to pore throats, some of them are squeezed through the throats, while others are trapped at the throats to form blockages. These blockages can plug some large channels and divert the subsequently injected water into those untouched low permeability zones. Thus, weak gel improves the overall injection profile and improves the areal and vertical sweep efficiencies.

During evaluation of gels for conformance improvement in treating channeling through fractures, rheology measurements can be prepared much faster and with much lower cost than measurements made during extrusion of gels through fractured cores. Wang and Seright (2006) investigated the rheology data as the good substitute for the extrusion experiments thought the fractures. Results showed that the measured pressure gradients during gel extrusion experiments for a given aperture (fracture width) were much higher than anticipated based on rheology measurements. The actual gel flow path through wormholes is significantly narrower than the fracture width and this can be a possible reason for this relatively high pressure gradient.

Seright (1999) emphasized the mechanism of gel extrusion through fractures in designing gel composition, gel volume, and optimum gel placement. He showed that during extrusion of gel through fractures, gel moved as a plug and that negligible viscous dissipation occurred during the gel plug movement. Coreflooding experiments by Seright (1995) demonstrated that gel cannot flow through porous media after gelation and highlighted that preformed gel can reduce water flow through fracture without inducing substantial formation damage. The effect of salts on gelation time was examined for two gelling systems (Al-Muntasheri *et al.*, 2009). The pH of the gelling solutions at these conditions was 10. The results clearly show that both systems exhibited a delay in the gelation time because polymer network shrinkage results in less crosslinking sites which leads to longer gelation times. The initial pH was found to change the gelation time for polyacrylamide homopolymers (PAM) gel systems in which polyethyleneimine (PEI) was used as organic crosslinker. It was found that lower initial pH delayed the gelation of the PAM/PEI systems (Al-Muntasheri *et al.*, 2007).

For a gel with yield stress τ_y , under steady rate conditions, Bird *et al.* (1983) used a simple force balance to calculate the minimum pressure gradient, , $\frac{dp}{dl}$ required to extrude gel through two parallel plates separated by a distance of w:

$$\frac{dp}{dl} = \frac{2\tau_y}{w}. \tag{2.1}$$

For fluid flow through tubes (Bird *et al.*, 1976):

$$\tau = \frac{p_O - p_L}{2L} R, \tag{2.2}$$

Where L is the length of the tube and R is the radius, p_O and p_L are the inlet and outlet pressures, respectively. For Newtonian materials,

$$\tau = -\eta \frac{d\gamma}{dt}, \tag{2.3}$$

where τ is the shear stress, η is the Newtonian viscosity, γ is shear strain, and t is time.

The pressure gradient required for gel extrusion is inversely proportional to the square of the fracture width (Seright; 1999, 2001, 2003). For Cr(III)-acetate-HPAM gel, the required pressure gradient ($\frac{dp}{dl}$, in psi/ft) could be estimated as following (if fracture width, w_f, is expressed in inches):

$$\frac{dp}{dl} = \frac{0.02}{(w_f)^2}. \tag{2.4}$$

Improvement of mobility ratio can be one of the goals in polymer and gel treatment. The concept of mobility ratio explains the behavior of stable and unstable displacement as shown in

Figure 2-5. Mobility, k/μ, is defined as effective permeability to a given phase divided by the viscosity of that phase. Mobility ratio, M, is defined as the mobility of the displacing phase divided by the mobility of the displaced phase. The displacement is stable when M<1 and unstable when M>1.

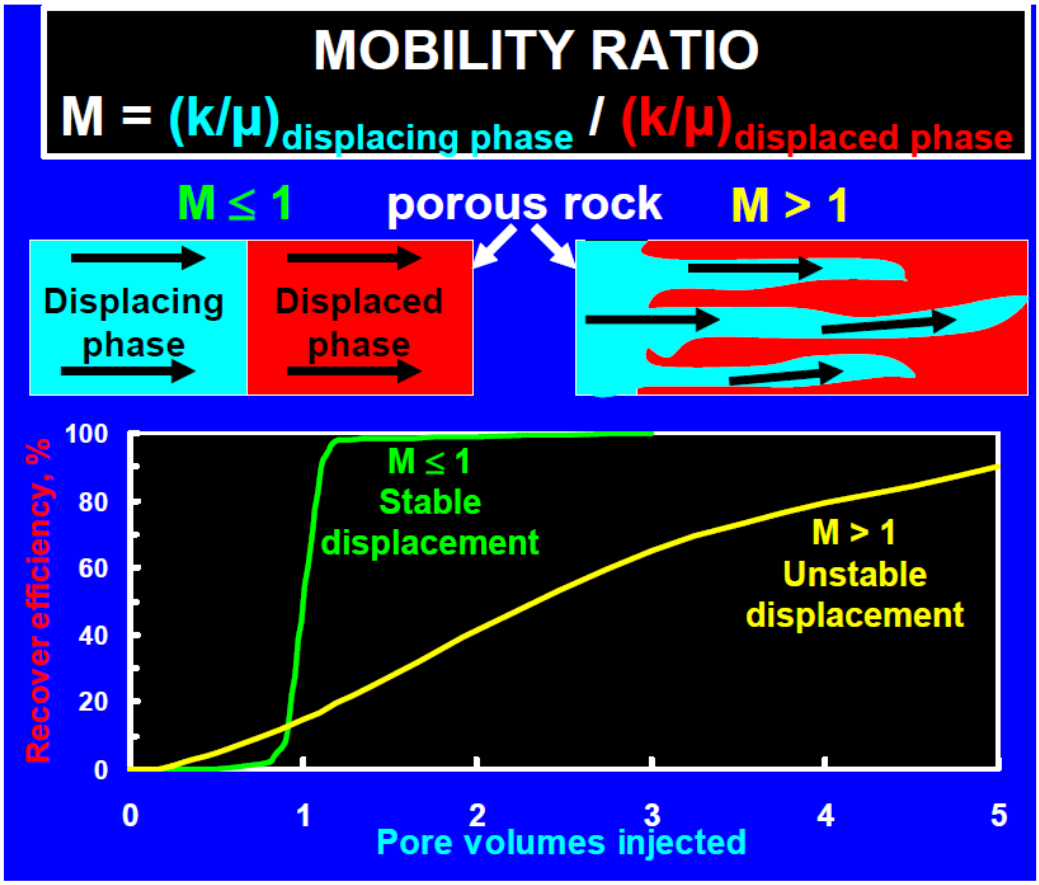

Figure 2-5: A representation of mobility ratio effect on recovery efficiency (Seright, 2006).

It should be noted that the main objective in gel treatment is to reduce flow through fractures or high-permeability zones while diverting injected water into low permeability hydrocarbon-bearing strata and therefore gel penetration into low permeability zones should be minimized. On the other hand, polymer can be used as mobility control agent and therefore penetration into low permeability zones should be maximized (Figure 2-6).

Crossflow can occur to some extent in most of the reservoirs and there is a need to characterize the effect of crossflow on gel performance. The performance of gel placement is strongly affected by the level of communication between reservoir layers, which is characterized by the vertical equilibrium (VE) conditions. Sorbie and Seright (1992) showed that in viscous-stable injection of gelant in systems close to vertical equilibrium, considerable volumes of injected material can crossflow into the low-permeability layers, and subsequent gel formation can seriously reduce the performance of the continuing waterflood as shown in Figure 2-7. For reservoirs with crossflow, the efficiency of the gel injection critically depends on whether the displacement is "understable" or "overstable". An under-stable displacement happens when $FR < \frac{k_{high\ permeability}}{k_{low\ permeability}}$, where FR is the gel resistance factor and over-stable displacement is defined by $FR > \frac{k_{high\ permeability}}{k_{low\ permeability}}$. For viscous over-stable gelant slugs in systems with free crossflow, both the original placement of the gelant and the subsequent propagation away from the well are very unsatisfactory due to the extensive level of viscous crossflow.

In practice, some degree of viscosity of the gelant can be "tolerated"; however, this must still give a viscous under-stable displacement in the initial stages to reduce crossflow to acceptable levels. Sorbie and Seright (1992) suggested that an approximate practical guideline for gelant placement in reservoirs with crossflow is to maintain $FR * \frac{k_{lowpermeability}}{k_{high\ permeability}} \leq 0.3$. Figure 2-8 illustrates the main steps for the gel injection. A gelant with a water-like viscosity is first injected (Figure 2-16a). Secondly, water is injected to displace the gelant away from the wellbore (Figure 2-16b). In the third step (Figure 2-16c), the well is shut in to allow gelation to occur. Finally, if the gel treatment is applied in a waterflood injection well, water injection is resumed. A pathway will be available for water to crossflow from the high permeability zone into the low permeability zone leading to improvement in sweep efficiency (Figure 2-16d).

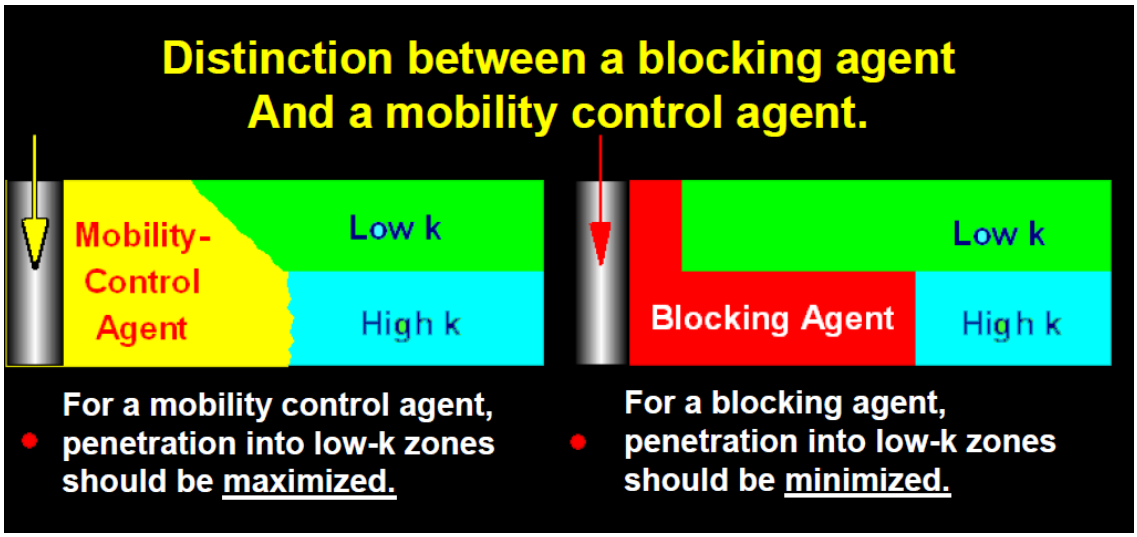

Figure 2-6: A representation of difference between gel blocking agent and mobility control agent (Sorbie and Seright, 1992).

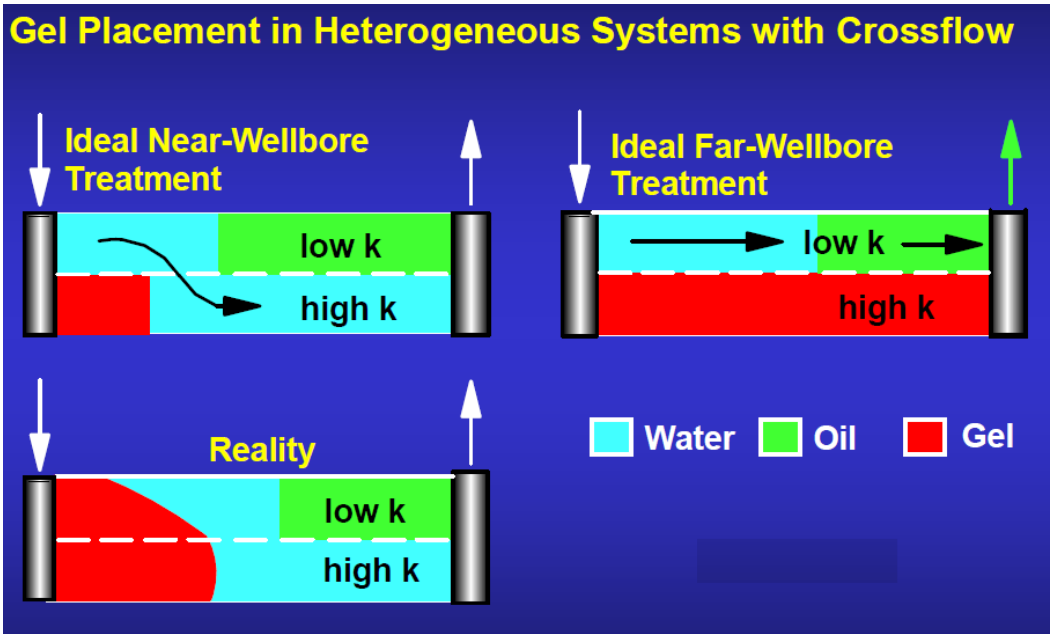

Figure 2-7: Crossflow effect on gel placement for near wellbore treatment (Sorbie and Seright, 1992).

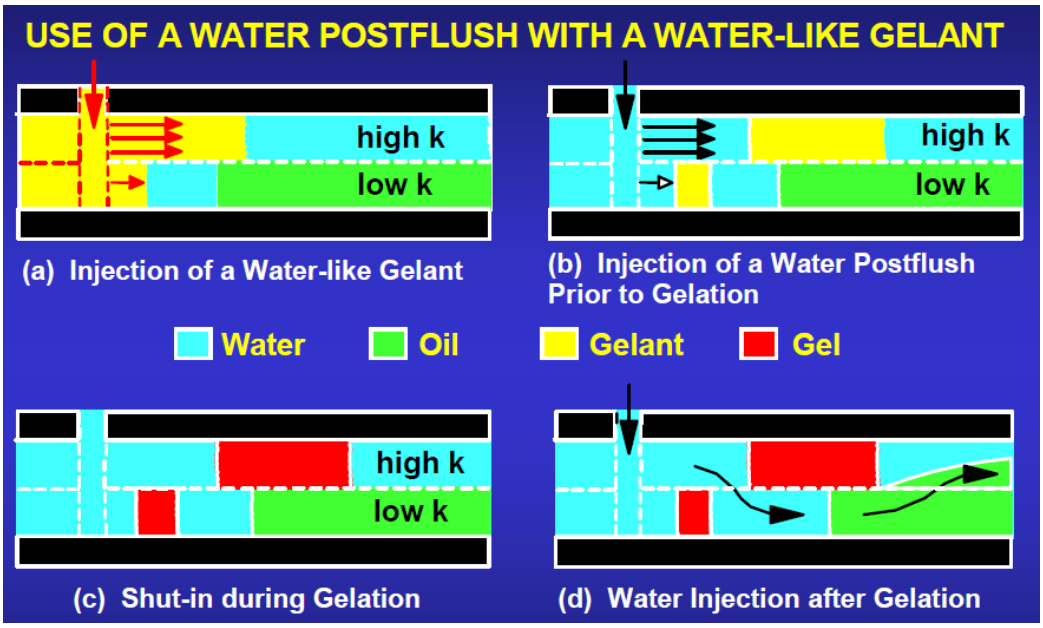

Figure 2-8: Representation of the gelation steps and water postflush with a gelant (Sorbie and Seright, 1992).

From different case studies for gel profile modification, it is revealed that it can be most appropriate for high permeability contrasts, high thickness layers, and relatively low oil viscosity. However, it should be noted that ultimate recovery by profile modifications using gels may be considerably less than from a traditional polymer flood.

Daqing filed in China is a great example for large scale gel injection. Laboratory research began in the 1960s, investigating the potential of enhanced oil recovery (EOR) processes in the Daqing oil field. Use of polymer flooding was identified as the key method to improve areal and vertical sweep efficiency, as well as providing mobility control. At Daqing, the endpoint relative permeabilities were k_{rw}~0.5 and k_{ro}~0.8, oil viscosity was 9 mPa-s, and water viscosity was 0.6 mPa-s. Thus, during waterflooding, the endpoint mobility ratio was 9.4. Due to this unfavorable mobility ratio, viscous fingers can form that lead to severe channeling, especially when zones with different permeability exist. By injecting a viscous polymer solution, the mobility ratio was decreased to favorable conditions (Seright, 2006). In Daqing field, naturally fractures may exist. If fractures are responsible for significant channeling between wells, gel treatments could be a viable solution. If fractures are not responsible for channeling, other sweep improvement options may be more appropriate. CDG gels (HPAM crosslinked with aluminum citrate) were field tested at Daqing (Chang *et al.*, 2004) and claims were made for the success of these treatments. Careful analysis of the Daqing field data and additional unpublished data associated with the project indicates no significant difference between CDG flood and the normal polymer flood. Injectivity behavior was not significantly different for the two cases and also water/oil ratios and production trends cannot be distinguished for the two processes.

2.1.3 Microgels

This section describes four different types of microgels:

- Colloidal dispersion gels (CDG)
- pH-sensitive gels
- Preformed particle gels (PPG)
- Thermally active polymers (TAP)

The comprehensive study of governing flow equations and simulations for PPG and TAP as the main focus of conformance control for this research will be discussed in Chapters 4 and 5.

2.1.3.1 Colloidal Dispersion Gels (CDG)

Application of gelled polymer treatments can significantly improve the amount of oil recoverable by displacement in waterflooding and other enhanced recovery mechanisms in heterogeneous reservoirs containing zones of high permeability. The use of a partially hydrolyzed polyacrylamide/aluminum citrate (CDG) has been claimed to produce long-term, in-depth permeability modification in certain reservoirs resulting in significant incremental oil recoveries and has been the subject of an extensive laboratory study (March and Smith, 1994; Fielding *et al.*, 1994).

The polyacrylamide/aluminum citrate CDG system, developed by Tiorco Inc., consists of low concentrations of HiVis 350, a partially hydrolyzed polyacrylamide with an average molecular weight of 27 million, and Tiorco 677, a chelated aluminum citrate solution. Typical concentrations used in this system are 300 ppm polymer and 15 ppm Al^{3+} as crosslinker. This system is reported to be slow forming, thus allowing for in-depth permeability treatment of oil reservoirs. It is hypothesized that polymer colloids, or gel

aggregates, are formed, which are then filtered from solution by the porous media, thereby reducing the permeability. These claims are based on interpretation of field performance in which large volumes of colloidal dispersed gel have been injected (Ranganathan *et al.*, 1998). Abdulbaki (2012) performed numerous simulations on optimization of CDG for maximized hydrocarbon recovery efficiency.

CDGs are composed of polymer and crosslinker, combined in low concentrations so that a bulk gel cannot form (Mack and Smith 1994; Fielding et al. 1994; Coste et al. 2000; Sheng 2011). The key characteristic of CDGs distinguishing them from polymer bulk gels is that they are not continuous intermolecular gel networks; this is a direct result of the low concentration of reactants required to formulate CDGs. Instead, CDGs are micro-scale separate gels/colloids that came about from primarily intramolecular forces (Mack and Smith, 1994; Diaz *et al.*, 2008). Abdulbaki *et al.* (2014) provided a comprehensive literature survey of different microgels, especially CDG, and concluded that despite uncertainty around the mechanism by which microgels divert flow, numerous lab and field applications demonstrate its ability to improve sweep efficiency.

Figure 2-9 shows the difference between CDG and bulk gels. Mack and Smith (1994) recommended the use of a pure, partially hydrolyzed polyacrylamide for CDG preparation which is the most commonly used polymer reported in the literature.

Ranganathan *et al.* (1998) performed laboratory investigation of a polyacrylamide/aluminum citrate CDG system in unconsolidated sandpacks and the study includes flow of the polymer and in-situ gelation behavior of the gelant in porous media as well. They concluded that gel solution flows through porous media in a manner similar to polymer and gel retention happens at the inlet of sandpack.

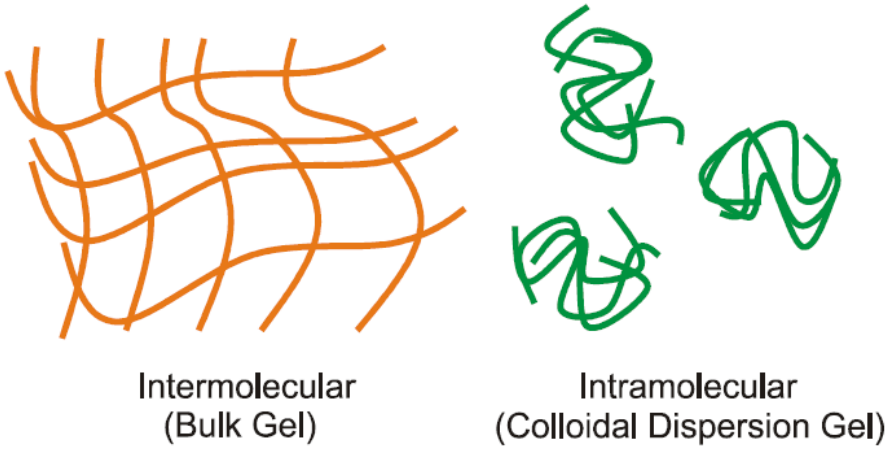

Figure 2-9: Distinction between Bulk Gel and CDG (Diaz *et al.*, 2008).

CDG flow resistance/gelation is triggered by a specific "transition pressure". When subjected to high pressure differentials above the transition pressure, CDGs are in the form of gelant and flow as easily as an uncrosslinked polymer. Below the transition pressure, gelation occurs and pore throats are filled/plugged leading to resistance during flow and permeability reductions (Mack and Smith, 1994; Sheng, 2011). The pressure difference around the wellbores is typically above the transition pressure and therefore CDGs are easily injected even when preformed at the surface (CDGs are generally injected as a gelant which form strengthened gels in-situ).

The rate of intramolecular crosslinking is expressed as a function of polymer concentration, polymer/crosslinker ratio, water salinity, temperature, and shear (Mack and Smith, 1994). Another crucial point to be addressed is that the gelation time is controllable, and can be on the order of hours to weeks. For field applications, it must be ensured that the time is long enough such that gelation does not occur near the wellbore and it is in high permeability zone deep in the reservoir (Sheng, 2011).

In field applications, CDG water control process can offer distinct advantages. First and foremost, the low reactant concentration requirement enables large quantities of CDGs to be generated economically. It also enables a relatively slow rate of crosslinking, giving the flooding solution more time to enter the depths of the reservoir formation before crosslinking happens. The shear-thinning behavior of CDGs further guarantees that the CDGs only alter matrix permeability deep inside the reservoir. Finally, this new technology is a potential method to the problems brought about by high permeability-variance and channeling, offering a viable means of conformance control (Mack and Smith, 1994). However, there are some limitations for CDG conformance process which can be summarized as following:

- Target reservoirs are mature waterflooded (Mack and Smith 1994). However, some CDG field implementations have been successful even with non-mature waterflooded fields (Chang *et al.,* 2004, 2006; Diaz *et al.,* 2008).
- Injection is not within the appropriate production zones (Mack and Smith, 1994).
- Wells with poor wellbore completions in which skin or very low permeability exists.
- High salinity reservoirs: Coste *et al.* (2000) specified an upper salinity limit of 5000 ppm. Mack and Smith (1994) specified an upper limit of 30,000 ppm total dissolved solids (TDS).
- High temperature reservoirs: Coste *et al.* (2000) specified an upper limit of 90˚C. Mack and Smith (1994) and Fielding *et al.* (1994) illustrated successful CDG applications at temperatures as high as 94.4˚C.

The field results from a North Sea reservoir that had been waterflooded to residual oil saturation showed increased recovery from increased microscopic diversion caused by blocking of pores with CDG injection. The linear coreflood results for this reservoir showed that almost 40% of the remaining oil saturation after waterflooding was produced by CDG injection (Spildo *et al.*, 2009).

Lu and Song (2000) provided a study of the performances and characteristics of the CDG gels that were made up of aluminum citrate, produced water and polymer and is used for sweep efficiency improvement in Daqing oil field. Smith *et al.* (2000) carried out experiments to determine the optimal CDG formulation for a Daqing field pilot and performed laboratory experiments to determine the effect of CDGs on RF, RRF and oil recovery.

Mack and Smith (1994) reported the successful use of CDGs in 22 of 29 field projects applied in the Rocky Mountain Region in the U.S.A. Fielding *et al.* (1994) reported an incremental oil recovery of 5% the OOIP and a decrease in water-oil-ratio (WOR) resulting from the use of CDGs in the North Rainbow Ranch Unit in Wyoming, U.S.A. There are other examples of successful implementations of CDG technology including their use in the Comodoro Rivadavia Formation in southern Argentina, in the Loma Alta Sur field in Argentina, as well as in the Adon Road Field in Wyoming, U.S.A. (Muruaga *et al.*, 2008; Diaz *et al.*, 2008; Smith *et al.*, 1996). Figure 2-10 effectively shows the improved sweep profile created by CDG use in the Loma Alta Sur field in Argentina (Diaz *et al.*, 2008).

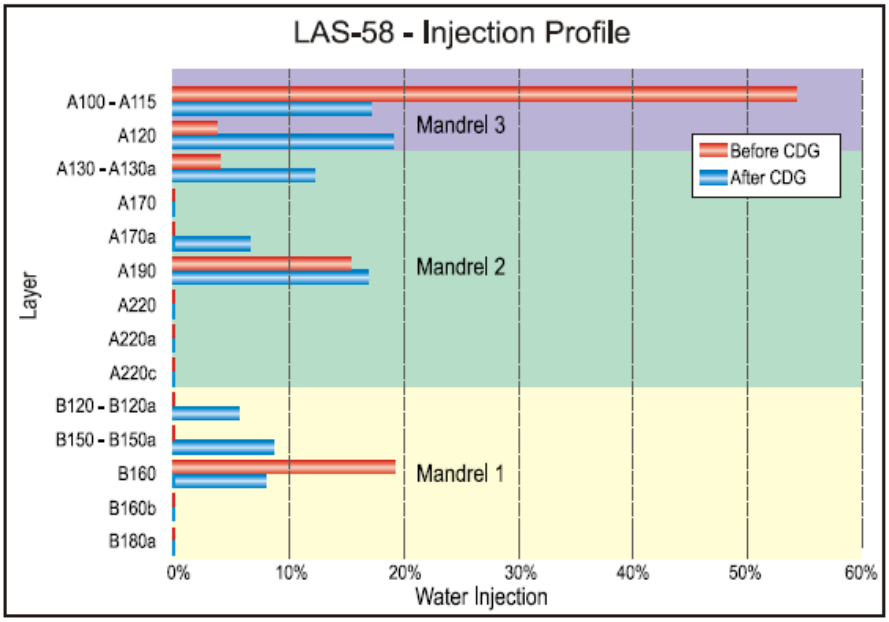

Figure 2-10: Improved sweep profile after CDG used in Loma Alta Sur field (Diaz *et al.*, 2008).

2.1.3.2 pH-sensitive Gels

It is tough to control the transport and reaction of the chemicals in a heterogeneous reservoir and the success of the field applications of in-situ gellation has been challenging (Seright and Liang 1994). Preformed microgels at the surface do not have the above reaction control problem but are difficult to place deep in the reservoir, because they make large pressure drops near the injection well and also tend to show mechanical trapping and filtration. During the last 15 years, use of preformed soft microgels has been investigated by researchers as an effective method for in-depth permeability control and/or relative permeability modification for excess water production control (Chauveteau *et al.*, 2001, 2003, 2004; Feng *et al.*, 2003). Because of their controlled, small size, their softness, and flexibility, the new microgels could be transported in reservoir rock without mechanical trapping if the permeability is

sufficiently high. Adhesion of microgel globules on pore wall provides the desired permeability and relative permeability modification.

Polyelectrolytes are water-soluble polymers that form molecular networks by association in solution. The properties of such polymers are very sensitive to the pH and ionic content of the solution (Huh *et al.*, 2005). Polyelectrolytes can swell up to around 1,000 times of their own volume by retaining a huge volume of water, or they may reversibly de-swell to their original volume. Their solution viscosity can accordingly be changed by several orders of magnitude in a controlled manner by adjusting the solution pH. This remarkable property of pH-sensitive polymers can be exploited for a number of improved oil recovery (IOR) applications, as proposed by Al-Anazi and Sharma (2002a).

Huh *et al.* (2005) developed a comprehensive rheology model by combining the ionic hydrogel swelling theory of Brannon-Peppas and Peppas (1988) with the Mark-Houwink equation that relates the polymer intrinsic viscosity with polymer molecular size; the Martin equation that relates the characteristic Newtonian viscosity with polymer concentration and intrinsic viscosity; and the Carreau equation that relates polymer viscosity with shear rate. Therefore the polymer viscosity can be calculated as a function of pH, salinity, polymer concentration, and shear rate.

Al-Anazi and Sharma (2002a) investigated the possibility of using a high-viscosity polyacrylic acid solution as a carrier fluid to transport sands for gravel packing, which can be easily removed afterwards from the gravel pack zone by lowering its viscosity with acid injection. Extensive measurements of poly(acrylic acid) solution viscosity as a function of pH, salinity, polymer concentration, and shear rate were performed. For pH sensitive gels, it was proposed to utilize pH change as the trigger, which has a number of advantages. For example, for the problem of improving

injectivity, polyacrylic acid solution exhibits a low viscosity at low pH, but at pH values higher than a critical value, the viscosity increases drastically and remains at a plateau value with further increases in pH (Al-Anazi and Sharma, 2002b). By injecting a polyelectrolyte at low-pH, a low viscosity and good injectivity can be achieved. Once deeper in the reservoir, the pH of water can increase due to reaction of injected acid with the carbonate and other minerals in the reservoir rock (and to a certain extent, due to mixing between injected water and the bypassed resident water). For the critical concern of chemical loss, the preliminary study (Al-Anazi and Sharma, 2002b) indicated that adsorption of polyacryl acid is small compared to the conventional polymers used for IOR. Also, due to its large manufacturing scale, unit cost for polyacrylic acid is small, again compared to other IOR polymers. As with other anionic polymers, sensitivity to divalent ions remains an issue. The use of pre-flushes and buffers can minimize the impact of divalent ions on the polymer.

For modeling the apparent viscosity of microgel suspensions, two approaches are proposed. The first is to treat the microgel globules as colloidal particles and to employ suspension rheology models and the second approach is to treat the microgel globules as highly entangled polymer "molecules" and to employ a polymer-solution rheology model (Bird *et al*., 1977; Bohdanecky and Kovar, 1982). Huh *et al.* (2005) emphasized that the second approach of treating the swollen gel micro-globules as if they were individual polymer molecules with a very large molecular weight is physically more reasonable. Budtova *et al*. (1994) suggested that such an approximation is reasonably acceptable because the swollen gel network is highly flexible at the high volume fraction of brine as solvent. Because highly swollen large gel globules would be much more deformable than un-swollen gel globules when subjected to shear, the second approach is also more

reasonable in representing their shear dependence. Huh *et al.* (2005) concluded that the apparent viscosity of hydrogel suspensions can be reasonably modeled by substituting the gel globule's hydrodynamic radius for the polymer molecule's hydrodynamic radius in the polymer-solution viscosity model. The modified pH-sensitive gel model in UTGEL calculates the equilibrium swelling ratio in terms of pH and ionic strength of solution (Onbergenov, 2012).

Choi *et al.* (2006) performed experimental study on ion transportation in Berea sandstone and polymer transport in sandpacks and concluded that the equilibrium simulations (without kinetics) are a useful way of setting bounds for the subsequent geochemical reactions and transport, and help better understand the effects of varying mineralogy on the pH history for acid-mineral reaction in the rock. The results showed that crosslinked polyacrylic acid microgels in brine undergo retention mainly due to attraction between microgels during propagation in a pure silica sandpack. The high crosslink density polymers form harder microgels due to its more rigid network, resulting in less retention during flow than the low crosslink density polymers. Evaluation of permeability reduction fronts from sandpack experiments suggests that polymer retention is more from adsorption on the silica surface than from straining by deep-bed filtration. Rheological measurements by Choi *et al.* (2010) showed that shear viscosities of HPAM solution has a noticeable, but reversible, dependence on pH. The observed peak pHs indicates that spontaneous geochemical reactions can return the polymer solution to its original high viscosity. Also, the experimental results showed that two factors affect the viscosity of HPAM mainly at low pH: polymer concentration and molecular weight. The salinity change does not have considerable impact on HPAM viscosity at low pH. It should be noted that polymer adsorption increases as pH decreases.

2.1.3.3 Preformed Particle Gels (PPG)

Particle gels can be divided into in-situ gels and preformed particle gels (PPG). Traditionally in-situ gels were used for controlling water production where a mixture of polymer and crosslinker which is called a gelant, is injected into the formation to form gel at reservoir conditions for blocking the channels (Sydansk and Moore, 1992; Jain et al., 2005). Disadvantages of this method are the effect of adsorption and formation water on the crosslinking reaction and possible damages on the low permeability un-swept oil zone (Bai, 2010). The new technology for gel treatment is to form the gel at surface conditions and inject the preformed gel into the reservoir. This new process, referred to as preformed particle gel, can overcome problems, such as lack of control on gelation time and uncertainties due to the effect of adsorption and shear degradation which usually occur in traditional in-situ gel systems. PPGs are dried superabsorbent crosslinked polymer powders that can swell up to 200 times their original size (Bai *et al.*, 2007a, 2007b; Muhammed, 2011). These particles are prepared by combining monomers, controlled monomers, stable cross-linkers, initiators, and other agents in aqueous solution. This new technology can be used for either conformance control or water shutoff or even both in some cases. This technology has been successfully applied for more than 5000 wells (Bai *et al.*, 2013).

Bai *et al.* (1999) used gel to divert injected water into un-swept oil zones of the formation and decrease the flow capacity of channels or fractures. Seright (2000) showed that preformed gels have better efficiency through fractures compared to in-situ gels and impose less damage in low permeability oil zones. Feng *et al.* (2003) showed that microgels are good candidates for water shutoff and profile control without any problem

of plugging. Rousseau *et al.* (2005) used sandpack experiments to study the flow and transport of microgels.

Another type of particles gels called nanoparticles have drawn a great deal of attention from the oil industry for their EOR potential (Hendraningrat *et al.*, 2013), namely, their ability to modify certain factors in reservoir formations. Kong and Ohadi (2010) emphasized that nano-agents may significantly increase oil recovery by modifying surface tension. Hendraningrat *et al.* (2013) studied the disjoining pressure as a displacement mechanism due to the existence of nanoparticles in various permeability core plugs. The results show that hydrophilic nanoparticles have capability to decrease the contact angle of the aqueous phase and increase water-wetness. Ogolo *et al.* (2012) investigated the effect of some nanoparticles (oxides of aluminum, zinc, magnesium, iron, zirconium, nickel, tin and silicon) on oil recovery. The coreflood tests on transport behavior of nanogel through sandpack showed that both the resistance factor and the residual resistance factor decrease with an increase in the size of the swollen particles, because the larger particles were weaker than the small particles, indicating that the gel strength is more important than the particle size for nanogel particle injectivity and permeability reduction (Almohsin *et al.*, 2014).

PPG strength is an essential parameter for designing gel treatment in conformance control processes. There are several measurements for gel strength (Sydansk, 1990). One such measurement is the elastic strength which can be defined as the resistance to physical deformation that a gel will exhibit while extruding through a restriction in its flow path, such as the restriction in a fracture flow path. Another measurement is the yield strength. This gel strength is measured by placing a gel sample in a large container having a small orifice and then increasing the pressure in the container until the gel flows

through the orifice. The yield strength of a gel is often much larger than its elastic strength (Sydansk, 1990).

There are several developed methods to measure bulk gel strength. Gardner (1983) used rheometers to study the rheology of relatively weak gels and polymers. Meister (1985) designed a simple gel strength tester with a 30-mesh screen to quantitatively compare strong bulk gels. Smith (1989) developed a similar screen model to quantify the gel strength of weak bulk gels using screen packs of 100-mesh size. Sydansk (1990) proposed bottle-test gel strength codes that can semi-quantitatively evaluate the gel strength for rigid, rubbery gels. Riccardo (1994) proposed measuring the gel strength based on the maximum diameter of a steel ball that could settle through the gel. Another proposed method for quantifying the gel strength of PPGs involves using a dynamic oscillatory rheometer to measure the elastic or storage modulus (G') and the viscous or loss modulus (G"), which represents the PPGs elastic energy and viscous energy, respectively (Muhammed *et al.*, 2014). The main advantage of this technique is that it quickly and practically allows for a quantitative evaluation of the particle gel strength both in a laboratory and on site during PPG treatment. Two parameters of PPGs characterization, the threshold pressure and apparent viscosity, can be quantitatively determined using this method. Muhammed *et al.* (2014) introduced two empirical correlations based on measured data: one model correlates the threshold pressure with the gel strength and the other correlates the apparent viscosity with the shear rate and both models have reasonably good correlation factors.

Wang and Seright (2006) examined whether or not using rheology measurements to evaluate gel properties in fractures is an acceptable substitute for extrusion experiments as a way to reduce costs. McCool *et al.* (2009) investigated the effect of

shear on flow properties during the placement of gelants in fractures. Imqam *et al.* (2014) studied the effect of the conduit's opening size and salt concentration on the injectivity index, resistance factor, gel dehydration, particle opening ratio, and plugging efficiency. They concluded that both the gel threshold pressure and the stable injection pressure increased as the particle opening ratio increased. Both pressures, however, did not increase significantly after a specific ratio. Additionally, the gel strength impacted the gel injection pressure more than the particle opening ratio did (Imqam, 2015a, 2015b).

Feng *et al.* (2003) prepared two microgel samples by crosslinking an acrylamide-based polymer solution with a non-toxic zirconium crosslinker under controlled shear flow. The evaluation of their performance showed that they have long term stability and excellent propagation in porous media. Tongwa and Bai (2014) synthesized a nanocomposite preformed particle gel has using Calcium Montmorillonite as nanomaterial, and evaluated for mobility control and fracture plugging applications in mature reservoirs. It was observed that gel strength increased with increasing nanomaterial concentration. They also observed that long-term thermal stability of hydrogels was directly proportional to nanomaterial concentration. The higher the nanomaterial concentration, the longer the thermal stability of the hydrogels.

Elsharafi and Bai (2012) designed a filtration apparatus to determine the possible penetration of PPG into low-permeable sandstone rocks. They concluded that the damage of particle gel on unswept, low-permeable zones/areas can be effectively reduced by controlling both the particle size and the concentration of brine that was used to prepare swollen PPG. The PPG damage was affected by the particle sizes, brine concentrations, and core permeability; more damage occurred with a small particle size (100−120 mesh), low salinity (0.05 wt % NaCl), and high- permeability (290-320 mD). Zhang *et al.* (2010)

designed a screen model test to evaluate the rheological behavior of the swollen PPG. They concluded that a swollen PPG is a shear-thinning material with properties that can be expressed using a power-law equation from which an apparent consistency constant and an apparent flow index can be obtained. The experimental results showed that for a given flow rate and brine concentration, PPG injection pressure decreases as the mesh size decreases or the fracture width increases.

The study of PPG enhanced surfactant-polymer system in Shengli Oilfield showed significant improvement in oil recovery compared to polymer or SP flooding (Cui *et al.*, 2011). It is because of the enhanced sweep efficiency by mixed PPG-polymer with higher viscosity and also the improved displacement efficiency by surfactant. Muhammed (2014) studied the chemical compatibility between PPGs and surfactants. The interaction between surfactant and PPGs depends on surfactant concentration. The higher the surfactant concentration, the more influence on PPGs properties. The elevated temperature partially affected the swelling ratio of the PPGs but it reduced the PPGs strength (G'). The combined injection of PPGs and surfactant resulted in a higher injection pressure gradient in the reservoir because of the high flow resistance created from the particles. This increased pressure produced an additional force to drive surfactant into the matrix or low-permeability areas and therefore resulted in practical forced imbibition (Muhammed, 2014). It was found that two different designs of PPGs-surfactant together and PPGs followed by surfactant both improves oil recovery significantly and reduces excess water production.

2.1.3.4 Thermally Active Polymers (TAP)

Thermally active polymers (TAP) are deep diverting gels developed by an industry research consortium (known as BrightWater®) among BP, Chevron, Texaco and Nalco (Frampton *et al.*, 2004). The TAP microgels improve waterflooding sweep efficiency by its time-delayed, high-volume swelling ability where the aim is to plug the high permeability thief zones and divert injected water into low permeability areas. Pritchett *et al.* (2003) stated that "an essential feature was seen as having only one injected component, so that no chromatographic separation could occur". Thermally active sub-micron gel particles (0.1 to 1 micron in size un-swelled often referred to as "kernels") are injected into the reservoir with cold injection water compared to the reservoir temperature. The microgel kernels in the coldwater move primarily to thief zones due to their higher permeabilities, while slowly adsorbing heat from the surrounding warmer reservoir rock. At a specific pre-determined critical temperature (a key design parameter), the kernels "pop" like popcorn in the way that they swell irreversibly. This results in their viscosification and the plugging of the thief zones, and thus increases residual resistance factor. Therefore, it leads to the diversion of subsequent injected water to other relatively unswept portions of the reservoir and increasing sweep efficiency, as well as reducing excess water production as shown in Figure 2-11 (Frampton *et al.*, 2004; Garmeh *et al.*, 2012; Pritchett *et al.*, 2003; Yanez *et al.*, 2007).

The TAP microgels activation is controlled by two types of crosslinking agents, labile and non-labile (stable) crosslinkers. Chang *et al.* (2002) and Kurian and Chang (2011) emphasized that the microparticle content should ideally contain between 20,000 to 60,000 ppm labile crosslinker (preferably polyethyleneglycol diacrylate) and between 0 to 100 ppm non-labile (stable) crosslinker (preferably methylene bisacrylamide). Their

patents also describe the use of an inverse emulsion process for the TAP microgel synthesis, which ensures that the sub-micron size microgels are prepared, through the use of a dispersing surfactant additive (Frampton *et al.*, 2004; Yanez *et al.*, 2007).

TAP's small particle size and low viscosity make it easy to inject and possible to achieve great depths within a reservoir before expanding. As soon as the cool injected aqueous phase, including TAP suspensions, heats up to a certain pre-specified temperature in the reservoir, the labile crosslinkers begin breaking down and imposing microgel swelling through the absorption of water; hence, time and heat are two key design parameters for activation of TAP (Figure 2-12). The swelling leads to the plugging of high permeability thief zone and diversion of trailing injected fluid. The expanded particle size (and rate of de-crosslinking/swelling) should be designed for each specific target porous media and can be controlled through the proper selection of polymer as well as the types and degree of labile and non-labile crosslinkers. The use of TAP requires the knowledge of high permeability thief zone pore size, formation temperature, and microparticle propagation rate. Garmeh *et al.* (2012) presented a workflow for TAP treatment design and also discussed different simulation approaches using CMG-STARS to evaluate the effects of treatment concentration, slug size, permeability contrast, k_v/k_h, mobility ratio, and gel activation location. Izgec and Shook (2012) carried out a similar simulation study and concluded that gel placement location and permeability contrast (between the thief zone and surrounding layers) are the most important factors determining the success of a TAP treatment. Izgec and Shook (2012) also presented an approach to determine the slug size of a TAP treatment and concluded that injection of TAP at lower concentration but longer injection time (big slug) can provide better diversion compared to higher concentration and shorter injection (small slug).

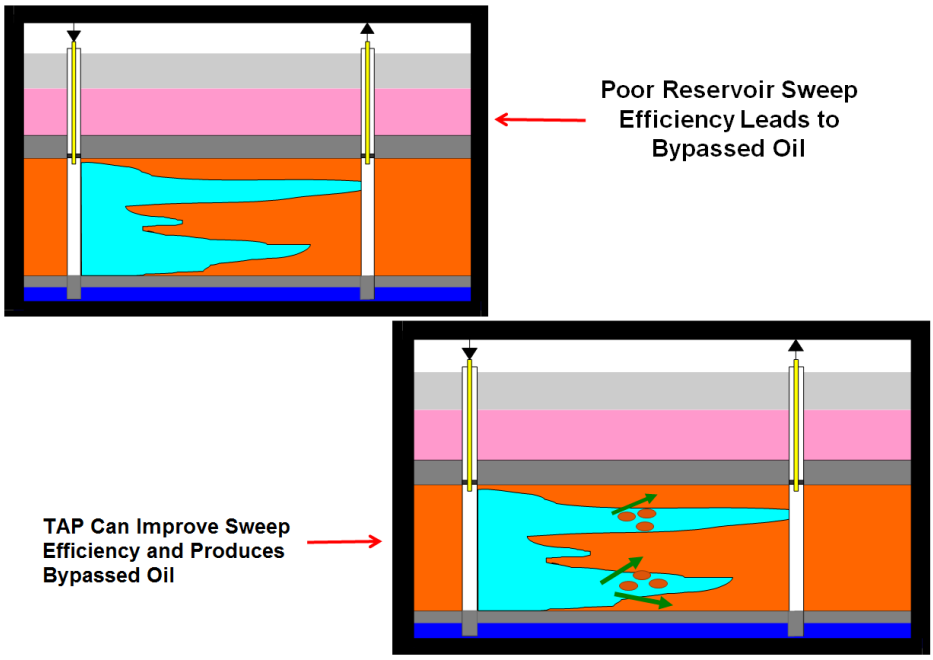

Figure 2-11: A schematic representation of sweep efficiency improvement using TAP.

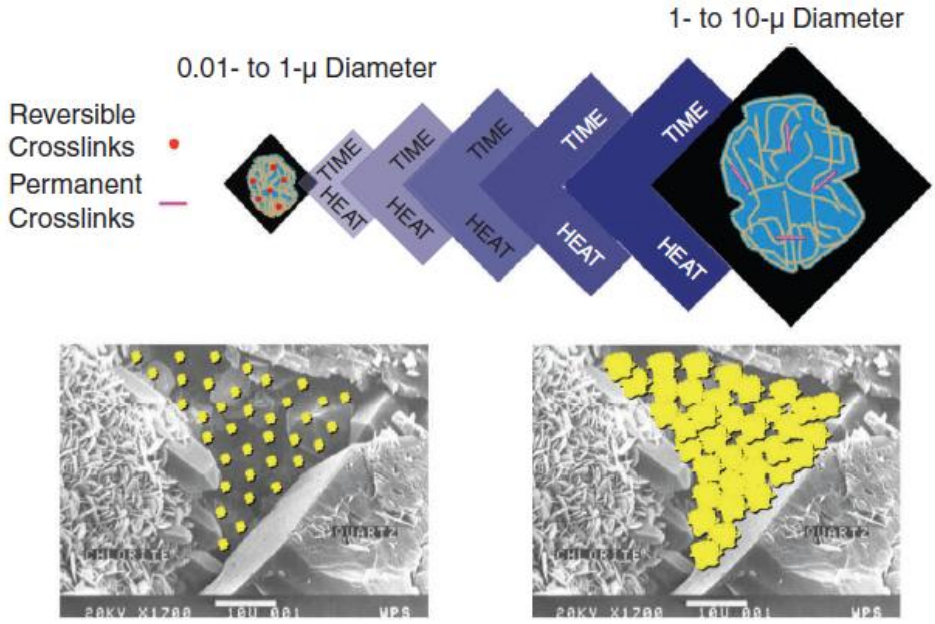

Figure 2-12: TAP microgels is activated by heat and time and the particles expand up to 10 times their original size (Garmeh *et al.*, 2012).

Manrique *et al.* (2012) proposed a list of screening criteria for TAP design and implementation which can be divided into two major steps: basic or decision making criteria and extended criteria.

Basic Screening Criteria:

- Early water breakthrough and high water cut.
- High permeability contrast between reservoir layers.
- Reservoir temperature between 20 ^{0}C (68 ^{0}F) and 120 ^{0}C (248 ^{0}F)
- TAP works only in sandstone reservoirs because carbonate reservoirs have low pH which prevents TAP activation.
- Injection water should have pH greater than six because lower pH shrinks the TAP particle size and reduces its viscosifying power.
- Injection water salinity should be below 150,000 ppm.

Extended Screening Criteria:

- Higher amount of movable oil in the pattern which leads to higher incremental oil recovery.
- Better TAP treatment results are seen in patterns that have lower number of fracture jobs.
- Reservoirs with higher temperature gradient between injection and reservoir temperature show better results.
- Reservoirs with high heterogeneity (Dykstra-Parson coefficient greater than 0.8 is recommended).
- Net pay thickness (Greater than 10 m thickness and high permeability contrast).
- Well configuration and completions. Well design and completions with better flexibility for monitoring TAP performance are always preferred.

First commercial field implementations were in Milne Point field and Prudhoe Bay field, both in Alaska (Ohms *et al.*, 2009; Husband *et al.*, 2010). In the Milne Point field, Ohms *et al.* (2009) reported promising results for a TAP trial in an isolated pattern containing three wells (1 injector and 2 producers). Around 60,000 bbls of incremental oil were recovered over 4 years, at a cost of below $5/incremental bbls of oil, illustrating TAP's commercial potential. In the Prudhoe Bay field, Husband *et al.* (2010) also reported highly encouraging results that demonstrated TAP's commercial potential. The use of TAP in a moderate-sized pilot pattern led to reduced water cuts and the production of around 500,000 incremental barrels of oil, at a competitive cost. Figure 2-13 demonstrates positive effect of TAP on vertical sweep efficiency, as can be seen from the simulation evaluation of the vertical distribution of oil and water saturations, in particular at the producer. Figure 2-14 which clearly shows the effect of sweep improvement by TAP on oil production rate above the normal decline. It should be noted that in both TAP field implementations discussed above, there were reasons to believe in the existence of significant bypassed oil; this is an important prerequisite to utilizing such a technology economically.

Mustoni *et al.* (2012) reported over 60,000 incremental bbls of oil over six TAP pilot treatments, and significant reduction in combined WOR in the field in Argentina. Yanez *et al.* (2007) provided a list of screening criteria for TAP floods. There were some other successful projects of TAP treatment in Russia, Tunisia, Brazil, and Gulf of Suez (Thrasher *et al.*, 2013; Ghaddab *et al.*, 2010; Galli *et al.*, 2012; Roussennac and Toschi, 2010; Towns *et al.*, 2013).

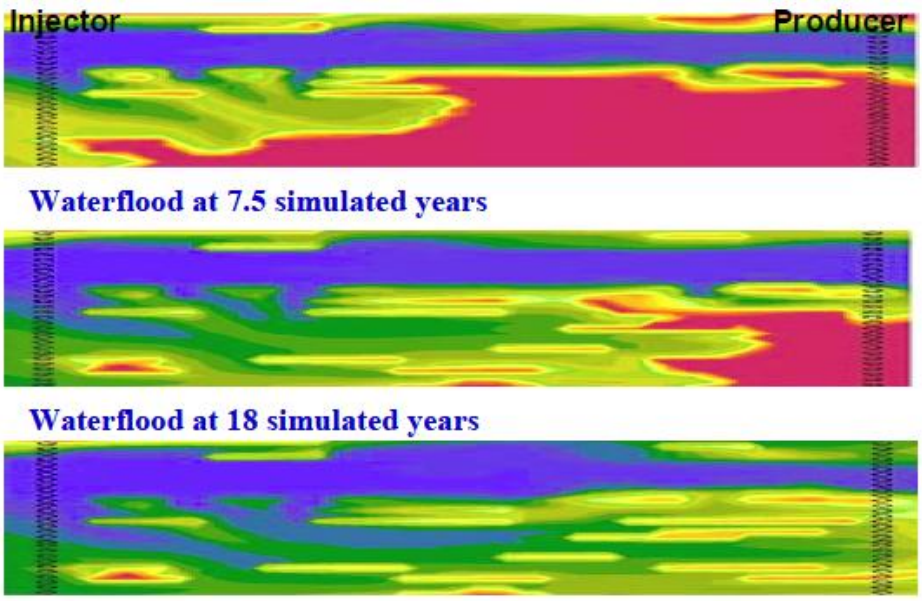

Figure 2-13: Vertical sweep improvement due to TAP treatment (Husband *et al.*, 2010).

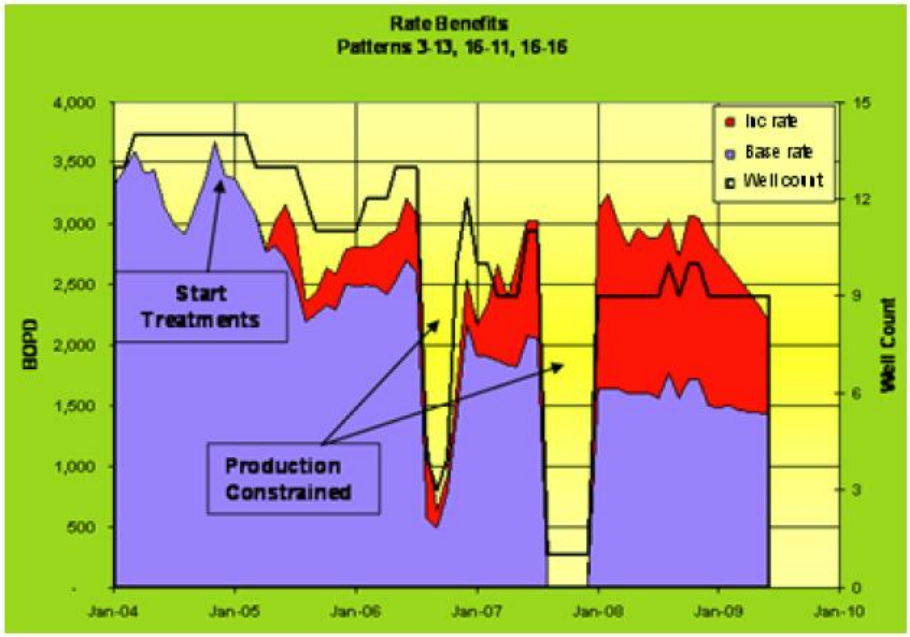

Figure 2-14: The effect of sweep improvement by TAP on oil production rate. Red line represents incremental oil compared to the base case in blue (Husband et al., 2010).

2.2 CHEMICAL EOR PROCESSES

2.2.1 Contact Angle and Wettability

When a liquid is subject to contact with a solid surface, the liquid can either expand over the whole surface or form small drops on the surface. In the first case, the liquid will wet the solid completely, while in the later case, a contact angle $\theta > 0$ will develop between the surface and the drop (Torsaeter and Abtahi, 2003).

When two immiscible fluids contact a solid surface, one of them tends to spread or adhere over the surface more than the other. For a water-oil-solid system at equilibrium, the following equation (known as Young's equation) can be expressed:

$$\sigma_{so} - \sigma_{sw} = \sigma_{wo} \cos\theta, \tag{2.5}$$

where σ_{so} is the interfacial tension between the oil and solid surface, σ_{sw} is the interfacial tension between the water and solid surface, σ_{wo} interfacial tension between the oil and water and θ is the contact angle measured through the water phase as shown in Figure 2-15.

Adhesion tension which is a function of the interfacial tension determines which fluid wets the solid surface. In the case of water-oil-solid, the adhesion tension, A_T, is defined as the following:

$$A_T = \sigma_{so} - \sigma_{sw} = \sigma_{wo} \cos\theta. \tag{2.6}$$

A positive A_T indicates that water preferentially wets the solid surface (water-wet). Zero value of A_T indicates that both phases have an equal attraction for the surface (neutral system). A negative A_T indicates that the oil wets the solid surface (oil-wet). The

magnitude of the adhesion tension determines the ability of the wetting fluid to adhere to the solid and spread over the surface of the solid.

The wettability of a reservoir rock-fluid system is defined as the ability of one fluid in the presence of another to spread on the rock surface. Wettability plays an important role in the production of oil and gas as it not only determines initial fluid distributions, but also is a main factor in the flow processes through reservoir rock. The intensity for the wetting of a solid by liquids is usually measured by the contact angle that a liquid-liquid interface makes with a solid and it can either be oil-wet, mixed-wet, or water-wet as shown in Figure 2-16.

The wettability of a reservoir rock system will depend on reservoir rock material and pore geometry, geological mechanisms (accumulation and migration), composition and amount of oil and brine, physical conditions; pressure and temperature as well as mechanisms occurring during production, *i.e*., change in saturations, pressure, and composition (Torsaeter and Abtahi, 2003). Note that it is difficult to make a general model of wettability including all these factors. Although a lot of work has been done on wettability, it is not fully understood how the wettability of a porous rock surface is composed.

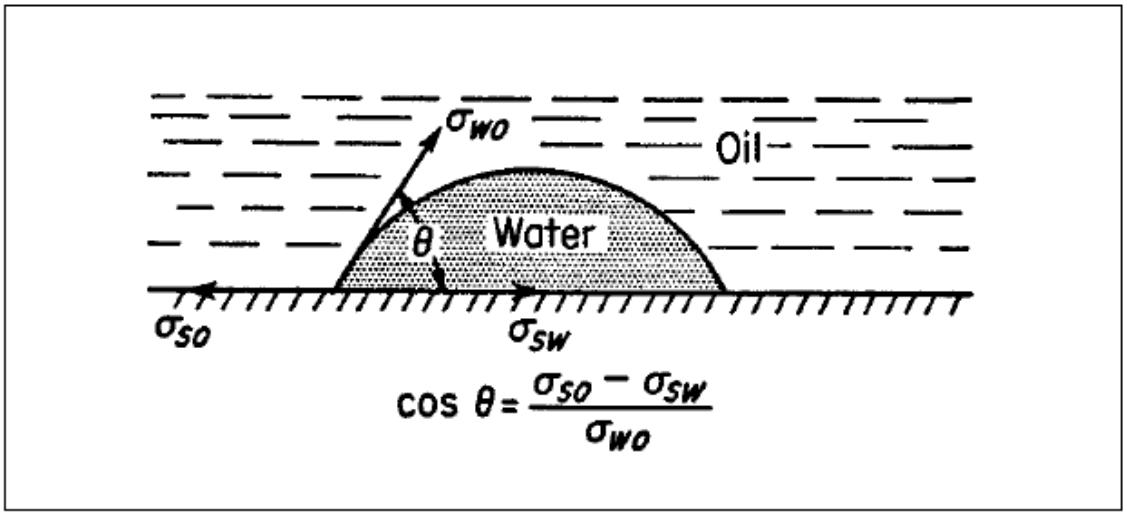

Figure 2-15: Interfacial tensions for a water-oil-solid system at equilibrium (Torsaeter and Abtahi, 2003).

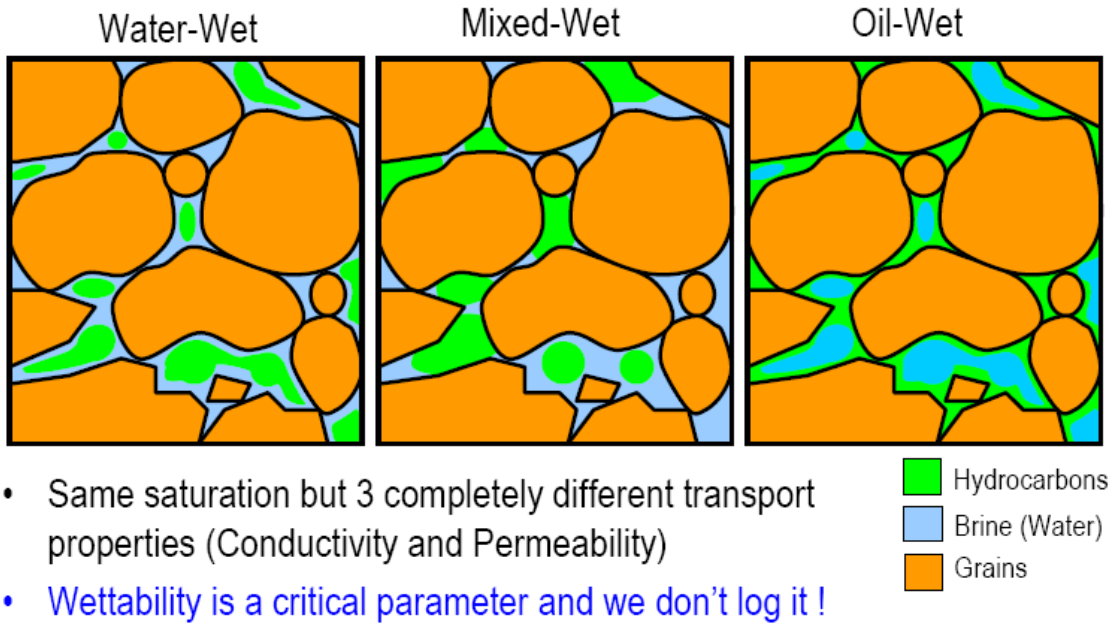

Figure 2-16: Schematic representation of wettability in carbonate reservoirs (Torsaeter and Abtahi, 2003).

2.2.2 Wettability Measurement

Three methods have been proposed for measuring wettability of reservoir rocks:

- Amott-Harvey
- Centrifuge
- Contact angle

2.2.2.1 Amott-Harvey Method

In principle, a core sample is chosen and saturated with oil. The oil-saturated sample is then placed in imbibition cell surrounded by water. As shown in Figure 2-17, the water is allowed to imbibe into the core displacing oil out of the core until equilibrium is reached. The volume of water imbibed is measured. The core sample is then removed and the remaining oil in the sample is forced down to residual saturation by displacement with water. This may be performed either in a centrifuge or displaced with a pump in a sealed core holder. The volume of oil displaced may be measured directly or determined by weight measurements.

The core (saturated with water at residual oil saturation) is placed in an imbibition cell and surrounded by oil. The oil is allowed to imbibe into the core displacing water out of the sample. The volume of water displaced is measured (equal to volume of oil imbibed). The core is removed from the cell after equilibrium is reached and the remaining water in the core is forced out by displacement in a centrifuge. The volume of water displaced is measured. By recording all volumes produced, it is possible to calculate wettability-index WI :

$$WI = \frac{V_{O1}}{V_{O1} + V_{O2}} - \frac{V_{W1}}{V_{W1} + V_{W2}} = r_W - r_o, \tag{2.7}$$

where V_{O1} is the volume of oil produced during water imbibition; V_{O2} is volume of oil produced during water flooding; V_{W1} is volume of water produced during oil imbibition; V_{W2} is volume of water produced during oil flooding; r_W is displacement-with-water-ratio and r_o is displacement-with-oil-ratio.

The wettability index has a value between -1.0 and 1.0 where: WI = 1.0 refers to completely water wet and WI = 0.0 is neutral and finally WI = -1.0 is completely oil wet.

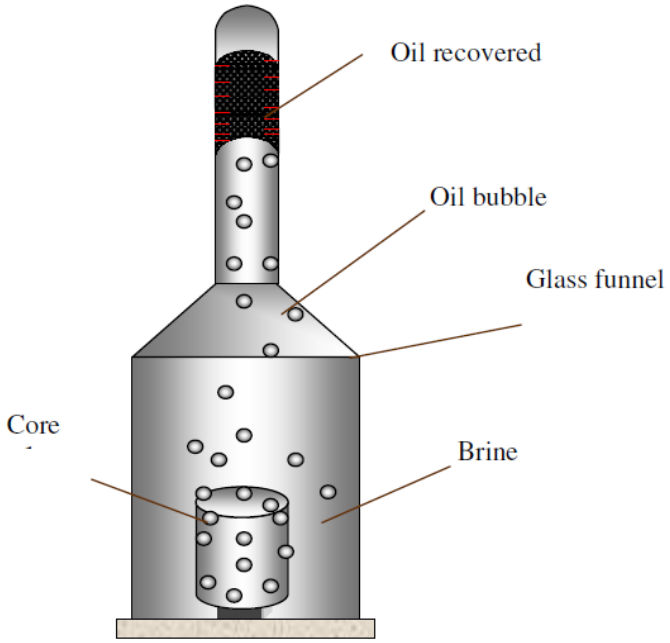

Figure 2-17: Amott cell test method for measuring wettability (Putra *et al.*, 1999).

2.2.2.2 Centrifuge Method

The centrifuge method is based on a correlation between the degree of wetting and the areas under the capillary pressure curves. The method employs two areas under the oil-water capillary pressure curves obtained from the centrifuge method often referred to as USBM (United States Bureau of Mines). The area ratio is selected to define the

wettability scale; $WI_{USBM} = log(A_1/A_2)$. The relative wetting tendencies of the liquids in a porous medium and the distribution of pore sizes determine the shape of the capillary-pressure curves (Torsaeter and Abtahi, 2003). In general, water-wet systems should have a larger area in the drainage curves than the area under the imbibition curves. Therefore, the logarithm of the area ratio for the water-wet system is greater than zero. Conversely, the area ratio is less than unity for oil-wet systems and the logarithm of the ratio is negative. A graphical description of capillary pressure method for calculating wettability is shown in Figure 2-18.

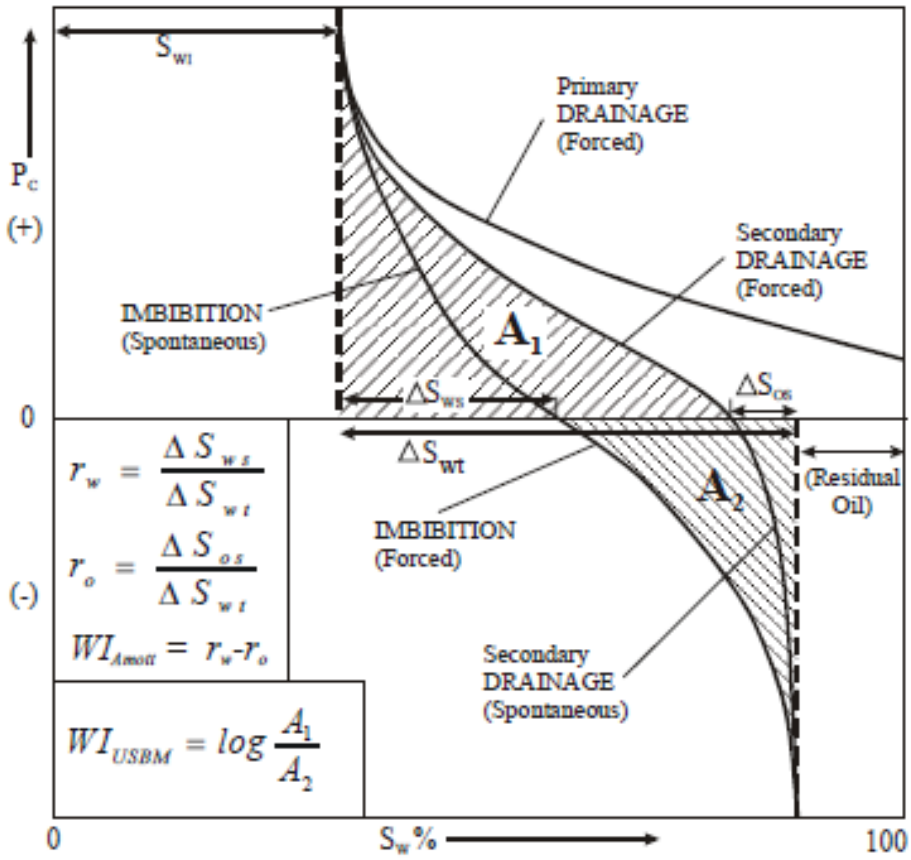

Figure 2-18: Wettability measurement by USMB and Amott method (Torsaeter and Abtahi, 2003).

2.2.2.3 Contact Angle Method

The measurement of contact angles is based on Young's equation. When placing a drop of liquid on a solid surface, a finite angle of contact in most cases will be observed. However, complete spreading may also occur and then Young's equation ceases to hold. The measurement of the contact angle is simple in concept, but in practice it is a very complex topic and the interpretation of results is not straightforward. The contact angle between oil, water and a solid surface will depend on crude oil composition, surface electric properties, solid surface itself, roughness, and heterogeneity of the solid surface.

In practice, it is even more complex for a porous material, because of different pore shapes and complex mineralogy. The solid surface must be carefully polished and measurements on mineral surfaces are often performed on the natural plane of cleavage. A drop of liquid is placed on the solid surface and an enlarged picture of drop is obtained by photographing. The dimensions of the drop image are then measured and used to determine the contact angle. The contact angle measurements can also be performed at reservoir conditions which are one of the main advantages in crude oil-brine-rock system. It has been shown that temperature can change the wettability significantly.

2.2.3 Wettability and Interfacial Tension Effect on Petrophysical Properties

In the following section, the effect of wettability and interfacial tension on some of reservoir petrophysical properties such as residual oil saturation, relative permeability, capillary pressure, and capillary desaturation curves will be presented.

2.2.3.1 Wettability-IFT Effect on Residual Oil Saturation

Wettability may be the single most important factor affecting residual oil saturation in reservoirs (Graue *et al.*, 1999). Wettability plays the main role for distribution of fluids in the pore structure of the rock and also fractures; therefore, its effect on fluid movement through reservoir and recovery is inevitable. Residual oil saturation, S_{or}, is defined as the oil saturation where no further oil production was observed by forced imbibition (Schembre *et al.*, 2006).

A significant mobilization of the residual oil saturation is only possible by interfacial tension (IFT) reduction or surfactant-induced wettability alteration. The IFT reduction will affect capillary desaturation curves by increasing capillary number and this increment will reduce the required capillary forces for mobilizing the trapped residual oil in smaller pores. A static imbibition by surfactant solution imbibition process recovers residual oil by reducing the surface forces between oil and the imbibing fluid (Al-Lawati and Saleh, 1996).

The goal of using a dilute surfactant solution is to reduce the IFT of the water/oil system to low values in order to release the residual oil (Al-Lawati and Saleh, 1996). Gupta *et al.* (2009) conducted a series of displacement experiments and showed that low IFT fluid displacement leads to a reduction in residual oil saturation and low IFT causes the residual oil bubbles to become smaller. Patil *et al.* (2008) examined the impact of

wettability alteration on residual oil saturation reduction in the core and the observed results indicated that the decrease in residual oil saturation corresponds to an increase in water-wetness. However, in some other core flood experiments in which many pore volumes were injected, the observed trapped/residual saturation did not follow a monotonic trend as a function of wettability and was actually lowest for intermediate-wet to oil-wet rocks as Figure 2-19 illustrates (Anderson, 2006). Therefore, wettability alteration can be considered as the main mechanism for lowering residual oil saturation; but this area is still open for further research.

The salinity of formation water has a considerable effect on residual oil saturation. Experimental results show that a low salinity water flood results in the considerable reduction of residual oil. Jadhunandan and Morrow (1995) performed a comprehensive experimental study on the effect of wettability over recovery and showed that maximum oil recovery can be achieved at intermediate-wet conditions. The experimental results showed that an increase in temperature caused a slight reduction in residual oil saturation (Schembre *et al.*, 2006).

Some studies showed a decrease in residual oil saturation by water injection with an increase in temperature systematically for both consolidated and unconsolidated sand (Edmondson, 1965; Poston *et al*., 1970; Maini and Batycky, 1985). However, the effect of temperature on residual oil saturation is negligible and can be neglected in coreflood experiments. The effect of capillary number on residual oil saturation shows that an increase of four to five orders of magnitude in capillary number is required in any EOR process in order to reduce the residual oil saturation significantly.

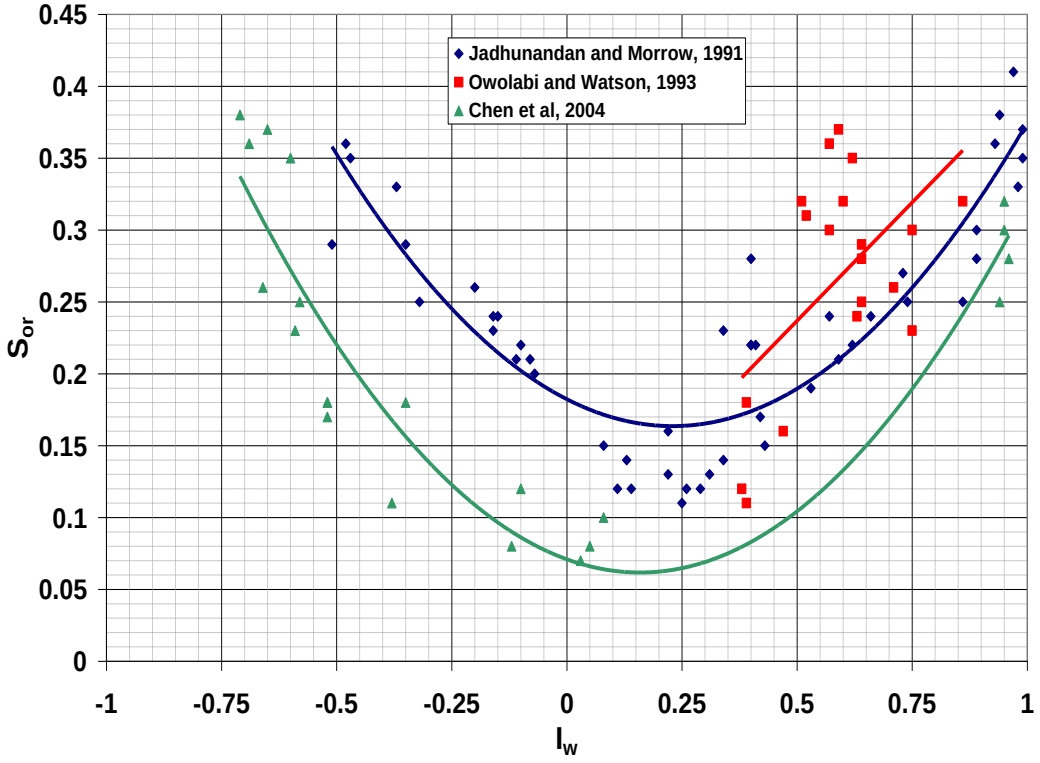

Figure 2-19: Effect of wettability on residual oil saturation (Anderson, 2006).

2.2.3.2 Wettability-IFT Effects on Relative Permeability

Wettability for a phase impacts the amount trapped in smaller pores and cannot move by natural mechanisms. Therefore, it is inversely proportional to relative permeability which shows the ease of phase movement. Then, it can be concluded that under wettability alteration from oil-wet to water-wet, relative permeability with respect to water will decrease but for the oil, it will increase. Studying the effect of wettability on the non-wetting phase is more complex due to saturation history and hysteresis (Anderson, 1986). The study of relative permeability during wettability alteration should be conducted very carefully for the static imbibition cell with counter-current flow and

dynamic coreflood experiments with co-current flow. For both drainage and imbibition processes, a large increase in relative permeabilities occurred below IFT of 5.5 dyne/cm indicating a critical point when fluid begins to move easily. Based on conventional description of immiscible flow, relative permeabilities are unique functions of saturation in 2-phase flow regime. However, this theory may not hold for spontaneous imbibition where viscous and capillary forces may play an important role in fluid flow and final recovery factor (Fischer and Morrow, 2005). Craig (1971) showed certain conditions for distinguishing water-wet compared to oil-wet systems based on relative permeability curves as presented in Table 2-2.

The second most important rule of Craig (1971) is that the intersection of relative permeability curves for water-wet systems occurs at saturations greater than 50% and for the oil-wet systems, it will be less than 50% and probably around 35%. Relative permeability curves for water-wet systems are dependent on initial water saturation to some extent. Reduction in initial water saturation causes a shift in the location and shape of the curves. However, initial water saturation has little effect on relative permeability curves for oil-wet systems. Morrow *et al.* (1986) proved that relative permeability data at residual oil saturation are not well defined for oil-wet systems.

Table 2-2: Rules of thumb for determining wettability (Craig, 1971).

TABLE 1—CRAIG'S[6] RULES OF THUMBS FOR DETERMINING WETTABILITY

	Water-Wet	Oil-Wet
Interstitial water saturation	Usually greater than 20 to 25% PV.	Generally less than 15% PV. Frequently less than 10%.
Saturation at which oil and water relative permeabilities are equal.	Greater than 50% water saturation.	Less than 50% water saturation.
Relative permeability to water at the maximum water saturation (i.e., floodout); based on the effective oil permeability at reservoir interstitial water saturation.	Generally less than 30%.	Greater than 50% and approaching 100%.

2.2.3.3 Wettability-IFT Effects on Capillary Pressure and Trapping Number

Capillary pressure arises from discontinuity between water and oil pressure at their interface in the presence of porous rock. Capillary pressure is defined as the difference between non-wetting and wetting phase pressures.

$$P_c = P_{non-wetting} - P_{wetting}\,. \tag{2.8}$$

At reservoir conditions, the fluids are oil/water, oil/gas or water/gas. Based on the Young-Laplace equation, the capillary pressure is proportional directly to the interfacial tension and inversely to the pore curvature as shown in the following equation:

$$P_2 - P_1 = \sigma\left(\frac{1}{r_1} + \frac{1}{r_2}\right), \tag{2.9}$$

where r_1 and r_2 are the principal radii of curvature for the pores assuming cylinder shape. For simplification, the mean radius of curvature r_m is introduced as following:

$$\frac{1}{r_m} = \frac{1}{2}\left(\frac{1}{r_1} + \frac{1}{r_2}\right). \tag{2.10}$$

Substituting Eq. (2.10) into (2.9) and including the effect of wettability by contact angle leads to the following equation for capillary pressure:

$$P_c = \frac{2\sigma Cos(\theta)}{R}, \tag{2.11}$$

where P_c stands for the capillary pressure, σ is the IFT between two phases, θ is the contact angle, and R is the pore radius of curvature. There are two primary capillary pressure curves: drainage and imbibition. The drainage mechanism is referred to displacing of wetting-phase by non-wetting phase and imbibition is the displacement of non-wetting phase by wetting-phase. In general capillary pressure/saturation relationship is a function of pore structure, wettability, and saturation history. It seems these two curves should be identical as they are the reverse of each other, but in reality there is hysteresis as the saturation is varied during capillary process. It is necessary that these two processes be considered to construct the capillary pressure/saturation relationship for a specific rock.

The combined effects of capillary, viscous, and buoyancy forces are described by a dimensionless parameter, trapping number, which is the sum of capillary number and bond number (Delshad *et al.*, 2006). By diffusing surfactant into the rock, IFT will be reduced and this will result in an increase in trapping number. There will be considerable

reduction in residual oil saturation and increase in incremental in oil recovery when trapping number significantly increases. Capillary Desaturation Curves (CDC) illustrates the reduction of residual oil during wettability alteration as a function of trapping number (Lake, 1989). Lake (1989) pointed out two important observations about the effect of wettability on CDC curves. First, the plateau value for non-wetting phase is higher than the wetting-phase and the second point is that the wetting-phase has higher critical trapping number. Critical trapping number is the capillary number at which residual oil saturation begins to decrease and there will be no effect on mobilization of trapped oil until this point. The results indicate that the residual oil saturation increases for more non-wetting conditions as illustrated in Figure 2-20.

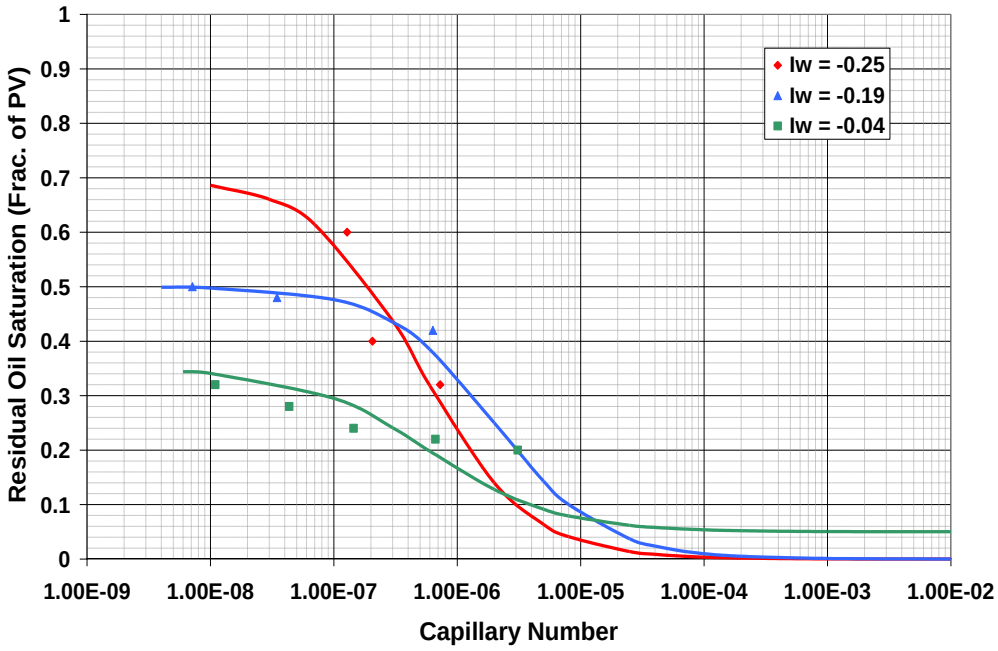

Figure 2-20: Wettability effect on capillary desaturation curves for three carbonate rocks (Kamath *et al.*, 2001). Figure regenerated by Anderson (2006).

2.2.4 An Overview of Fractured Carbonate Reservoirs

Large fractions of fractured reservoirs in the world are oil-wet and injected water will preferentially flow through high permeability fractures. For example, North Ghaba in Oman is a fractured reservoir with only 20 percent of total oil in place produced after 20 years of water injection. Experimental results on core plugs of this reservoir showed that by increasing temperature, the wettability will change from oil-wet to water-wet. The change in wettability was explained by removal of adsorbed asphaltene from rock surface at high temperatures.

The main characteristic of fractured reservoirs is that they are composed of two systems of matrix and fracture. Actually, matrix forms the original structure of porous media that is separated into different parts by internal fractures as shown in Figure 2-21. Many of the fractured reservoirs have a high rate of production initially, because of oil storage inside fractures. After a short time, however, this rate will drop to a constant value. This plateau production will be controlled by matrix-fracture interactions and different mechanisms will cause flow of oil from the matrix to fractures, and then towards production wells. Therefore, successful simulation of fractured reservoirs needs an understanding of matrix-fracture interactions and introducing of a mathematical model.

For reservoir simulation, Darcy's law and mass balance equations for each phase (oil, gas, and water) are used. The resulting system of equations will be solved using different numerical methods. If we use the information of current time step for calculating properties in the next time step, the method will be called explicit, whereas if the information at each time step is used for reservoir evaluation at the same time step, the method will be implicit. There is one other popular method known as IMPES

(Implicit Pressure Explicit Saturation). In this method, saturation at each time step will be calculated using explicit method but the pressure will be evaluated using implicit method. This method may result in high numerical instability when there is a high rate of flow in reservoir leading to smaller time steps. For this reason, a new more advanced method known as AIM (Adaptive Implicit) is introduced for regions close to wells, an implicit method; at distances far from wells, an explicit method is suggested for reducing run time. The AIM method will be very useful for fractured reservoirs when there is large variance in pressure through the reservoir.

After dividing the reservoir into separate matrix blocks, energy and continuity equations with some phenomenological laws (Darcy Law, Capillary Pressure Law, etc) have to be used for matrix-fracture and matrix-matrix interactions. Therefore, understanding mechanisms of fluid flow through matrix-fracture media is essential for model development of different oil recovery processes from naturally fractured reservoirs. Dynamic imbibition is one of the important mechanisms in fractured reservoirs as shown in Figure 2-22. As illustrated in Figure 2-23, the mechanisms of fluid flow in fractured reservoirs is a combination of viscous force, gravity force, and capillary force that should be accounted for in any model for describing these reservoirs. Lashgari et al. (2014c) developed an approach to estimate the performance of hydraulic fractured well and the relative contribution of the matrix and the fracture to the total flow rate in the presence of different skins which causes resistances around fracture, matrix, and wellbore.

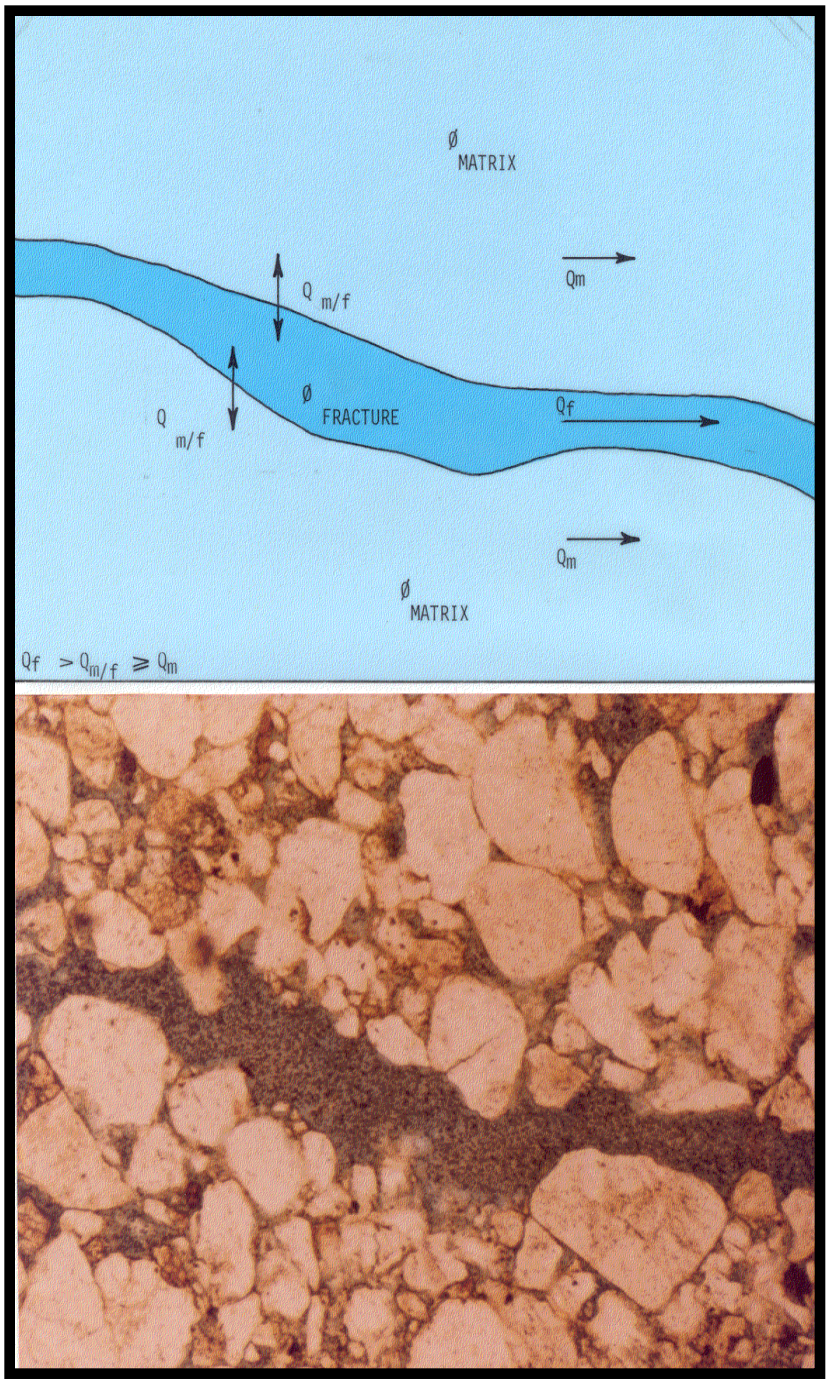

Figure 2-21: Carbonate reservoir with open fractures and no interface region (Nelson, 2001).

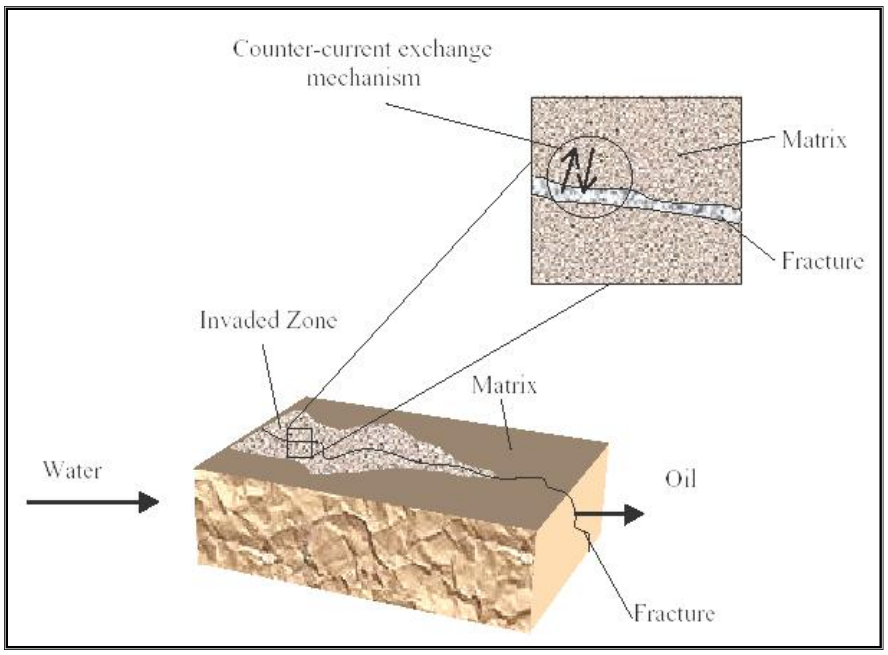

Figure 2-22: Dynamic imbibition process in fractured reservoirs (Putra *et al.*, 1999).

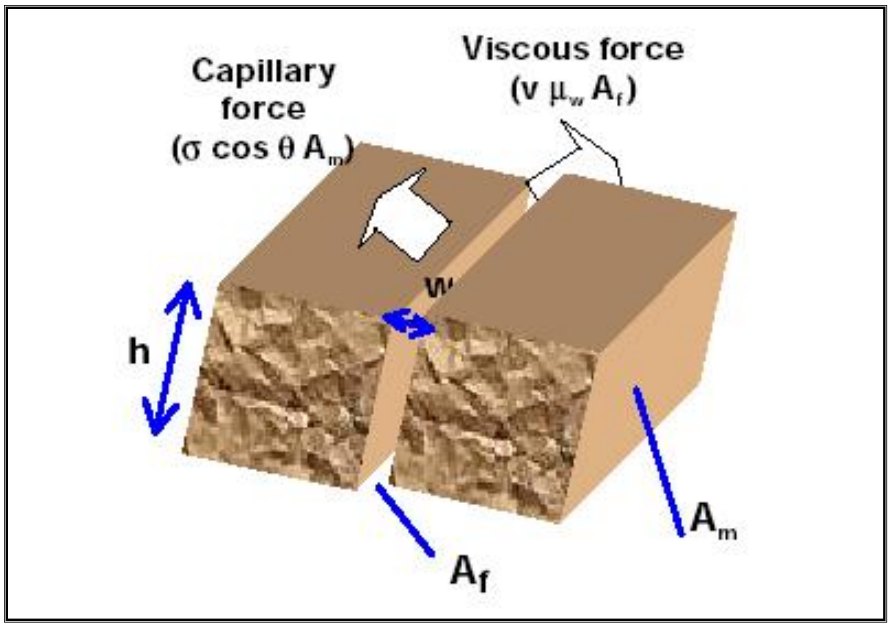

Figure 2-23: Viscous and capillary forces in a fracture-matrix system (Putra *et al.*, 1999).

2.2.5 Wettability Alteration in Fractured Carbonate Reservoirs

In carbonate reservoirs, fractures will act as transport path for injected fluid and, therefore, injected water will flow primarily through fractures. The reason for this is negative or low values of capillary pressure in oil-wet carbonate matrix which limits water imbibition from fracture to matrix to displace oil. It has been shown by Hirasaki (1991) that the thickness of water or oil film on the rock is the main contributor of wettability state. If the film thickness is high, the system will probably maintain its wettability but for the thin films, by using some chemical or thermal methods, water film can break leading to wettability alteration.

Buckley *et al.* (1998) observed that interactions between solid surface and polar oil components in one side and ion coupling on the other side can be the main reasons for the oil-wet nature of minerals on the rock surface. It was demonstrated by laboratory experiments that some surface active components (surfactant) have ability to change wettability of rock from oil-wet to water-wet and mobilize more oil from matrix blocks (Austad and Milter, 1997). Later on, the Amott-Harvey index of the core before and after spontaneous imbibitions by using surfactants was used to evaluate the degree of wettability alteration (Standnes and Austad, 2000).

Standnes and Austad (2000) investigated the effect of surfactant type on oil recovery from oil-wet chalk reservoir using both cationic and anionic surfactants. He found out that in general, cationic surfactants have better potential to recover more oil from oil-wet rocks in comparison with anionic surfactant. He concluded that the main mechanism for wettability alteration of carbonate rocks by cationic surfactants is the removal of Naphthenic acids (NA) compounds from the rock surface. The loss of cationic surfactant during wettability alteration can be low due to weak adsorption of Ca^{2+} groups

on calcite surfaces. The effect of surfactant concentration on oil recovery is also interesting because by increasing concentration, final oil recovery will decrease due to solubilization of more oil in micelles at higher surfactant concentrations.

There is an optimal concentration for different salinities at which the wettability alteration will be highest for anionic surfactants. Gupta and Mohanty (2008) showed that increasing the reservoir salinity will lower the surfactant concentration needed for wettability alteration but the magnitude of wettability alteration will decrease. Tweheyo *et al.* (1999) considered wettability alteration in the presence of divalent cations and realized that SO_4^{2-}, Ca^{2+} and Mg^{2+} ions can change the wettability of rock at 100 ^{0}C and higher temperatures without the need for surfactant.

Adibhatla and Mohanty (2006) and Gupta and Mohanty (2007) have demonstrated that dilute anionic and non-ionic surfactants can recover around 60% of OOIP from oil-wet fractured carbonate cores by imbibition laboratory tests. The recovery from fractured reservoirs is a combination of gravity and capillary forces and in many situations gravity is dominated especially for anionic surfactants due to low capillary pressure of oil-wet rocks. At early times of imbibition, diffusion is the main mechanism for penetration of surfactant into matrix blocks. Standnes and Austad (2000) showed that spontaneous imbibitions will occur faster for the cores with initial water saturation rather than the ones with 100 % oil saturation. The imbibition rate should be optimized because the economic feasibility will be questionable if the rate is slow and if the process is too fast; then injected water will flow through fractures without much impact on matrix wettability. Two important factors which control wettability alteration are critical micelle concentration (CMC) and surfactant hydrophobicity. Hydrophobic surfactants have more

desire to contact the adsorbed carboxylic acids at the water-oil interface and also dissolution of ions in the organic phase will be enhanced (Standnes and Austad, 2000).

In general, mineralogy of the rock surface, oil composition, pore roughness, surfactant type, water saturation, water composition and temperature are all critical parameters affecting wettability alteration (Graue *et al.*, 1998; Morrow *et al*., 1986; Buckley and Morrow, 1990). Experimental results showed that wettability alteration is reproducible for carbonate chalk rocks and degree of imbibition rate decreases by increasing aging time (Graue and Bogne, 1999). Afterwards, Graue *et al.* (2002) showed that most uniform wettability alteration will occur during the aging process where core is saturated with crude oil and the direction of flood get reversed several times. In recent years chemical processes and wettability alteration are considered as valuable EOR methods for mature depleted light oil conventional reservoirs, non-thermal recovery of viscous oils, and also for fractured carbonate reservoirs (Delshad *et al*., 2006; Farhadinia *et al.*, 2011; Chen and Mohanty, 2012; Darabi *et al.*, 2012; Kalaei *et al.*, 2012; Mirzaei *et al.*, 2013; Mohebbinia *et al.*, 2014).

2.2.6 An Overview of Chemical Enhanced Oil Recovery Processes

2.2.6.1 Polymer (P) Flooding

Polymer flooding is considered the basic chemical process used for improving mobility ratio in the reservoir leading to better sweep of remained oil. Mobility ratio of water with respect to oil can be defined as

$$M = \frac{\lambda_w}{\lambda_o} = \frac{(\frac{k_w}{\mu_w})}{(\frac{k_o}{\mu_o})} = \frac{k_w}{k_o} \times \frac{\mu_o}{\mu_w}, \tag{2.12}$$

where k, λ, and μ stand for effective permeability, mobility, and viscosity and the subscripts o and w refer to oil and water phases. Higher mobility ratio indicates that either the viscosity of water is low or its permeability is high which in both cases causes the fingering of water through oil and low sweep of original oil. The main purpose of polymer is to increase viscosity of the water or, in some cases, decrease water effective permeability. There were considerable number of field projects in polymer flooding during the 1960s and 1970s. There are some issues about polymer flooding such as the stability of polymer at high temperatures, good transport in porous media, shear stability, and solubility in water with high salinity and hardness.

There are essentially two types of polymers commonly used in EOR projects: hydrolyzed polyacrylamide (HPAM) and Xanthan gum. The main advantages of HPAM are low cost and resistance to biodegradation; however, on the other hand, almost all HPAM show sensitivity to hardness and salinity. Xanthan gum is relatively expensive and more susceptible to bacterial attack, but they do not show much sensitivity to salinity and hardness (Lake, 1989).

2.2.6.2 Surfactant-Polymer (SP) Flooding

After water-flooding, oil droplets can be trapped due to capillary forces and further water injection will be inefficient for mobilizing trapped oil. This trapping can be shown as a competition between viscous forces which mobilize the oil and capillary forces which cause trapping of oil (Lake, 1989). Surfactant injection into reservoirs for interfacial tension reduction between water and oil in not a new topic and was first done by Uren and Fahmy (1927). IFT can be reduced from *30* dynes/cm in a typical waterflood to around 10^{-2} dynes/cm, which causes a significant reduction in residual oil saturation (Green and Willhite, 1998). Surfactant injection is usually followed by polymer flooding in order to improve sweep efficiency and control mobility.

Capillary number, which is the ratio of viscous forces to capillary forces, controls the amount of residual oil saturation in reservoir. IFT reduction will increase the capillary number and, consequently, more residual oil will be mobilized. Another useful approach is to generate surfactant in-situ instead of injecting expensive surfactants. This can be achieved by using alkaline to convert naphthenic acids in active acidic oils into soap and surfactant. We should always inject enough surfactant for sweeping a large portion of reservoir and actively reduce IFT where surfactant propagates close to optimal conditions (Gilliland and Conley, 1976). Having optimal conditions in a reservoir is crucial for an efficient surfactant-polymer flood and the salinity gradient technique is one of the most effective methods for achieving these conditions (Nelson and Pope, 1978; Hirasaki, 1982). Based on previous discussions, it is suggested to select a concentrated surfactant slug, which will minimize the effect of dispersive mixing in the reservoir (Lake, 1989). Mollaei *et al.* (2011) used an analytical chemical flood predictive model (CFPM) to predict the SP flood performance and the results helped to specify the best candidates for

SP flooding based on reservoir rock and fluid properties. Gravity-stable surfactant flood is applicable for thick reservoirs with high temperature and also when the use of polymer becomes increasingly challenging (Tavassoli *et al.*, 2014). The main point which needs to be considered to minimize the surfactant loss is the use of phase gradient during flood. It is necessary to use Type II(-) at the rear of microemulsion phase to avoid surfactant loss because of phase trapping (Austad and Milter, 1997). Standnes and Austad (2002) showed that by lowering the salinity, Type III will shift into II(-) at the rear of microemulsion phase and, consequently, surfactant trapping will be reduced.

Alkaline flooding was proposed by Nelson and Pope (1978) and includes injection of high-pH chemical plus surfactant into reservoir. The main goal of alkali injection is to reduce the adsorption of surfactant on rock surfaces and also generate in-situ soap when contacted with naphthenic acids in the crude oil (Johnson, 1976). Another important benefit from alkali injection especially in fractured carbonate reservoirs is in altering the wettability of matrix blocks from oil-wet to water-wet. Some tests have been conducted on calcite plates for wettability alteration; it was found that sodium carbonate is very effective for wettability alteration since sodium carbonate has low adsorption compared to other alkali, reduces the extent of ion exchange and does not affect permeability considerably (Hirasaki and Zhang, 2004).

Surfactant flooding will not benefit much from capillary pressure if IFT is reduced to ultra low values and gravity is dominated for oil recovery. It was shown that for fractured oil-wet rock sample with negative capillary pressure, wettability alteration using alkaline plus IFT reduction by surfactant improved recovery and pressure gradient became favorable for displacing oil by viscous forces (Delshad *et al.*, 2006). It was known that having soap/surfactant gradient will lead to a gradient in optimum salinity

which is very beneficial for moving phase behavior from Type III to Type II(-), where there is minimum surfactant oil retention. The effect of soap/surfactant gradient on optimum salinity was studied widely by Liu *et al.* (2008) for 1-D cases. In addition, generated soap causes the formation of a middle layer and an ultra-low IFT is achieved over an extended range of salinity (Hirasaki *et al.*, 2008).

Chapter 3: Description of UTGEL Reservoir Simulator for Conformance Control

3.1 UTGEL RESERVOIR SIMULATOR

UTGEL is a finite difference three-dimensional multiphase multi-component chemical compositional reservoir simulator which can be used for modeling conformance control processes. The simulator can model both bulk gels and microgels. A comprehensive module is available for polymer and gel rheological and transport properties, such as shear thinning viscosity, adsorption, resistance factor, and inaccessible pore volume. UTGEL can be used to model various types of laboratory experiments including open fracture, conduit, sandpack (homogeneous or heterogeneous permeability), and sandstone coreflood which provide an understanding of conformance control mechanism and its impact on improving oil recovery. The main goal of this chapter is to introduce different capabilities existing in UTGEL for modeling conformance control processes. The formulation in UTGEL is IMPEC similar to UTCHEM and it can model different types of wells (vertical, horizontal, and deviated wells). UTGEL can model both in-situ bulk gels which are formed inside the reservoir and also microgels which are usually prepared at the surface and then injected into the reservoir. The simulator can model three-phase relative permeabilities (water/gas/organic phases or water/organic/microemulsion phases), polymer with non-Newtonian rheology, dispersion, diffusion, adsorption, chemical reactions, non equilibrium mass transfer between phases and other related phenomena.

Some of the useful features of UTGEL which are mainly for conformance control purposes are listed below (UTGEL technical manual, 2014).

UTGEL Conformance Control Applications:

- Water production control
- Polymer flooding
- Polymer-gel conformance control
- Bulk Gel Flooding (BG)
- Microgel Flooding
  - ✓ Preformed Particle Gels (PPG)
  - ✓ Thermally Active Polymers (TAP)
  - ✓ Colloidal Dispersion Gels (CDG)
  - ✓ pH-sensitive Microgels

A brief description of existing phases and components in UTGEL is first described. The mathematical formulation including mass balance equation, pressure equation, and energy balance equation is derived for four phases including, water phase ($\ell = 1$), Oil phase ($\ell = 2$), microemulsion phase ($\ell = 3$), and gas phase ($\ell = 4$).

The following components can exist in the phases:

$\kappa = 1$: Water (volume fraction)

$\kappa = 2$: Oil (volume fraction)

$\kappa = 3$: Surfactant (volume fraction)

$\kappa = 4$: Polymer (weight percent)

$\kappa = 5$: Total anions concentration, assumed all be chloride anions (meq/ml)

$\kappa = 6$: Total divalent cations concentration, assumed all be calcium (meq/ml water)

To activate the gel model, two conditions of $IREACT = 1$ and $NG > 0$ are selected. Different values of the flag "KGOPT" refer to different gel models (Table 3-1). The gel components are numbered from NG1 through NG8. The gel properties modeled in UTGEL include:

- Effect of gel on aqueous-phase viscosity
- Gel retention and adsorption on matrix rock
- Aqueous phase permeability reduction

Table 3-1: Gel model components and units in simulator.

Gel species	KGOPT=1	KGOPT=2	KGOPT=3	KGOPT=4	KGOPT=5	KGOPT=6
NG1	$Na_2Cr_2O_7$ (ppm)	…..	…..	…..	…..	…..
NG2	CSN_2H_4 (ppm)	Malonate ion (ppm)	…..	…..	…..	…..
NG3	Cr^{3+} (ppm)	Cr^{3+} (ppm)	OH^- (ppm)	…..	…..	…..
NG4	Gel (ppm)	Gel (ppm)	Gel (ppm)	…..	…..	…..
NG5	Hydrogen (meq/ml)	Hydrogen (meq/ml)	…..	…..	…..	…..
NG6	…..	…..	…..	PPG (ppm)	…..	…..
NG7	…..	…..	…..	…..	CDG (ppm)	…..
NG8	…..	…..	…..	…..	…..	TAP (ppm)

3.2 MATHEMATICAL FORMULATION

3.2.1 Mass Balance Equation

The gel particle is treated as a "solute" in the aqueous phase. The mass balance equations are solved for water, oil, total anions, total divalent cations, and gel species. The aqueous phase pressure is obtained by an overall mass balance of water and oil. The assumptions for developing flow equations are as following:

- The rock and fluids are slightly compressible.
- Fluid flow with Dacry law will apply for multiphase flow.
- The liquid is ideal mixture.
- Fickian dispersion with full tensor dispersion coefficient is used.
- The boundary conditions of no flow and no dispersive flux across the impermeable boundaries will be used for flow equations.
- Local equilibrium exists between surfactant/oil/water except for specified chemical reactions.

The mass conservation equation for each component in terms of overall volume per unit pore volume is defined as

$$\frac{\partial}{\partial t}\left(\phi \tilde{C}_\kappa \rho_\kappa\right) + \vec{\nabla}\bullet\left[\sum_{\ell=1}^{2} \rho_\kappa \left(C_{\kappa\ell}\vec{u}_\ell - \vec{\tilde{D}}_{\kappa\ell}\right)\right] = R_\kappa, \tag{3.1}$$

where $\tilde{C}_\kappa$ is overall volumetric concentration of component κ, ρ_κ is density of pure component κ, $C_{\kappa\ell}$ is concentration of component κ in phase ℓ, $\vec{u}_\ell$ is volumetric flux of phase ℓ, $\vec{\tilde{D}}_{\kappa\ell}$ is dispersive flux of component κ in phase ℓ, and R_κ is the source term for component κ which is a combination of all rate terms for that component.

The overall volume of component κ per unit pore volume will be computed as follows:

$$\tilde{C}_\kappa = \left(1 - \sum_{k=1}^{n_{cv}} \hat{C}_\kappa\right) \sum_{\ell=1}^{n_p} S_\ell C_{\kappa\ell} + \hat{C}_\kappa, \qquad \text{for } \kappa = 1,\ldots, \mathrm{n_c} \tag{3.2}$$

where

$\tilde{C}_\kappa$ = overall volumetric concentration of component κ, (L^3/L^3)

n_{cv} = total number of volume-occupying components

$\hat{C}_\kappa$ = adsorbed concentration of species κ, (L^3/L^3)

n_p = number of phases

S_ℓ = saturation of phase ℓ, (L^3/L^3)

The volumetric concentration of component κ in phase ℓ can be easily defined as

$$C_{\kappa\ell} = \frac{w_{\kappa\ell}\rho_\ell}{\rho_\kappa}, \tag{3.3}$$

where $w_{\kappa\ell}$ is the mass fraction of component κ in phase ℓ, ρ_ℓ is density of phase ℓ, and ρ_κ is the density of component κ. For example in two-phase flow of water/oil (no surfactant), the concentration equations are

$$C_1 = C_{11}S_1, \tag{3.4}$$

$$C_2 = C_{21}S_1 + S_2, \tag{3.5}$$

where 1 refers to water phase and 2 refers to oil phase ($C_{12} = 0$, $C_{22} = 1$). The phase saturations can be computed as

$$S_2 = \frac{C_2 - C_{21}}{1 - C_{21}}, \tag{3.6}$$

$$S_1 = 1.0 - S_2 . \tag{3.7}$$

The overall mass fraction of component κ can be easily calculated as

$$w_\kappa = \phi \rho_\ell \tilde{C}_\kappa . \tag{3.8}$$

The mixing is ideal with constant compressibility C_κ^0. The density of a component κ at phase pressure P compared to reference pressure P_{R0} is calculated as following:

$$\rho_\kappa = 1 + C_\kappa^0 (P - P_{R0}). \tag{3.9}$$

The dispersive flux has Fickian form as following:

$$\vec{\tilde{D}}_{\kappa\ell} = \phi S_\ell \overline{\overline{K}}_{\kappa\ell} \cdot \overline{\nabla} C_{\kappa\ell}, \tag{3.10}$$

where the dispersion tensor for a component κ in phase ℓ can be expanded as

$$\overline{\overline{K}}_{\kappa\ell} = \begin{bmatrix} K_{xx,\kappa\ell} & K_{xy,\kappa\ell} & K_{xz,\kappa\ell} \\ K_{yx,\kappa\ell} & K_{yy,\kappa\ell} & K_{yz,\kappa\ell} \\ K_{zx,\kappa\ell} & K_{zy,\kappa\ell} & K_{zz,\kappa\ell} \end{bmatrix}. \tag{3.11}$$

The elements of $\overline{\overline{K}}_{\kappa\ell}$ for multiphase, multicomponent flow in permeable media with molecular diffusion in Cartesian coordinates and the main diagonal are given by the following expressions:

$$K_{xx,\kappa\ell} = \frac{D_{\kappa\ell}}{\tau} + \frac{\alpha_{L\ell}}{\phi S_\ell}\frac{u_{x\ell}^2}{|u_\ell|} + \frac{\alpha_{T\ell}}{\phi S_\ell}\left(\frac{u_{y\ell}^2}{|u_\ell|} + \frac{u_{z\ell}^2}{|u_\ell|}\right), \tag{3.12}$$

$$K_{yy,\kappa\ell} = \frac{D_{\kappa\ell}}{\tau} + \frac{\alpha_{L\ell}}{\phi S_\ell}\frac{u_{y\ell}^2}{|u_\ell|} + \frac{\alpha_{T\ell}}{\phi S_\ell}\left(\frac{u_{x\ell}^2}{|u_\ell|} + \frac{u_{z\ell}^2}{|u_\ell|}\right), \tag{3.13}$$

$$K_{zz,\kappa\ell} = \frac{D_{\kappa\ell}}{\tau} + \frac{\alpha_{L\ell}}{\phi S_\ell}\frac{u_{z\ell}^2}{|u_\ell|} + \frac{\alpha_{T\ell}}{\phi S_\ell}\left(\frac{u_{x\ell}^2}{|u_\ell|} + \frac{u_{y\ell}^2}{|u_\ell|}\right), \tag{3.14}$$

where $D_{\kappa\ell}$ is molecular diffusivity of component κ in phase ℓ and τ is the tortuosity of reservoir formation. $\alpha_{L\ell}$ is longitudinal dispersion coefficient of phase ℓ and $\alpha_{T\ell}$ is transverse dispersion coefficient of phase ℓ. Upper and lower diagonals are given by

$$K_{xy,\kappa\ell} = K_{yx,\kappa\ell} = \frac{\alpha_{L\ell} - \alpha_{T\ell}}{\phi S_\ell}\frac{u_{x\ell}u_{y\ell}}{|u_\ell|}, \tag{3.15}$$

$$K_{xz,\kappa\ell} = K_{zx,\kappa\ell} = \frac{\alpha_{L\ell} - \alpha_{T\ell}}{\phi S_\ell}\frac{u_{x\ell}u_{z\ell}}{|u_\ell|}, \tag{3.16}$$

$$K_{yz,\kappa\ell} = K_{zy,\kappa\ell} = \frac{\alpha_{L\ell} - \alpha_{T\ell}}{\phi S_\ell}\frac{u_{y\ell}u_{z\ell}}{|u_\ell|}. \tag{3.17}$$

The magnitude of the vector flux for each phase, $\vec{u}_\ell$, will be computed as follows:

$$|\vec{u}_\ell| = \sqrt{\left(u_{x\ell}\right)^2 + \left(u_{y\ell}\right)^2 + \left(u_{z\ell}\right)^2}. \tag{3.18}$$

The phase flux calculated from Darcy's law is

$$\vec{u}_\ell = -\frac{k_{r\ell}\vec{\vec{K}}}{\mu_\ell}\left(\vec{\nabla}P_\ell - \gamma_\ell\vec{\nabla}h\right), \tag{3.19}$$

where

$\vec{\vec{K}}$ = permeability tensor, (L^2)

$k_{r\ell}$ = relative permeability of phase ℓ, (L^2/L^2)

μ_ℓ = viscosity of phase ℓ, (m/Lt)

γ_ℓ = specific weight of phase ℓ, (m/L^2t^2)

h = vertical depth, (L)

The source term, R_κ, is a combination of all rate terms for component κ as follows:

$$R_\kappa = \phi \sum_{\ell=1}^{n_p} S_\ell r_{\kappa\ell} + (1-\phi) r_{\kappa s} + Q_\kappa, \tag{3.20}$$

where

Q_κ = injection or production rate for component κ per bulk volume

$r_{\kappa\ell}$ = reaction rate for component κ in phase ℓ

$r_{\kappa s}$ = reaction rate for component κ with solid phase

3.2.2 Pressure Equation

The pressure equation will be formed by summing up the mass balances over all volume-occupying components, and substituting Darcy's law in each of phase flux terms, using the definition of capillary pressure. By knowing that $\sum_{\kappa=1}^{n_{cv}} C_{\kappa\ell} = 1$ (sum of concentrations of all the components in each phase equals to l), the pressure equation in terms of the reference phase pressure (phase 1) will be:

$$\phi C_t \frac{\partial P_1}{\partial t} + \vec{\nabla} \bullet \vec{\vec{K}} \bullet \lambda_{rTc} \vec{\nabla} P_1 = -\vec{\nabla} \bullet \sum_{\ell=1}^{n_p} \vec{\vec{K}} \bullet \lambda_{r\ell c} \vec{\nabla} D + \vec{\nabla} \bullet \sum_{\ell=1}^{n_p} \vec{\vec{K}} \bullet \lambda_{r\ell c} \vec{\nabla} P_{c\ell 1} + \sum_{\kappa=1}^{n_{cv}} Q_\kappa, \tag{3.21}$$

where

C_t = total system compressibility, (Lt^2/m)

$\vec{\vec{K}}$ = permeability tensor, (L^2)

P_1 = pressure of phase 1, (Lt^2/m)

Q_κ = source/sink flow for component κ per bulk volume. (L^3/L^3t)

$P_{c\ell 1}$ = capillary pressure between the given phase ℓ and phase 1, (Lt^2/m)

D = depth, (L)

$\lambda_{r\ell c}$ = relative mobility, (m/Lt)

λ_{rTc} = total relative mobility, (m/Lt)

The relative mobilities ($\lambda_{r\ell c}$ and λ_{rTc}) and total compressibility (C_t) are calculated using

$$\lambda_{r\ell c} = \frac{k_{r\ell}}{\mu_\ell} \sum_{\kappa=1}^{n_{cv}} \rho_\kappa C_{\kappa\ell}, \tag{3.22}$$

$$\lambda_{rTc} = \sum_{\ell=1}^{n_p} \lambda_{r\ell c}, \tag{3.23}$$

$$C_t = C_r + \sum_{\kappa=1}^{n_{cv}} C_\kappa^o \tilde{C}_\kappa, \tag{3.24}$$

where

C_r = rock compressibility

C_κ^o = component compressibility

The porosity is calculated as

$$\phi = \phi_R \left[1 + C_r (P_1 - P_R)\right], \tag{3.25}$$

where ϕ_R is the porosity at a specific pressure P_R, P_1 is the water phase pressure, and C_r is the rock compressibility at P_R.

3.2.3 Energy Balance Equation

The energy balance equation is derived by assuming that energy is a function of temperature only and energy flux in the reservoir occurs by advection and heat conduction only as shown below:

$$\frac{\partial}{\partial t}\left[(1-\phi)\rho_s C_{vs} + \phi \sum_{\ell=1}^{n_p} \rho_\ell S_\ell C_{v\ell}\right] T + \vec{\nabla} \cdot \left(\sum_{\ell=1}^{n_p} \rho_\ell C_{p\ell} u_\ell T - \lambda_{eff,T} \vec{\nabla} T\right) = q_H - E_L, \tag{3.26}$$

where

T = reservoir temperature

C_{vs} = rock heat capacity at constant volume, (Q/T)

$C_{v\ell}$ = phase ℓ heat capacity at constant volume, (Q/T)

$C_{p\ell}$ = phase ℓ heat capacity at constant pressure, (Q/T)

$\lambda_{eff,T}$ = effective thermal conductivity, (QL/Tt)

q_H = enthalpy source term per bulk volume, (Q/L^3)

E_L = heat loss to overburden and underburden formations or rock computed using the Vinsome and Westerveld (1980) heat loss method.

where $\lambda_{eff,T}$ is effective thermal conductivity which can be defined as follows:

$$\lambda_{eff} = (1-\phi)\lambda_r + \phi\sum_{\ell=1}^{n_p} s_\ell \lambda_\ell, \tag{3.27}$$

where λ_r is thermal conductivity of the rock, ϕ is porosity, and λ_ℓ is thermal conductivity of phase ℓ.

3.2.4 Well Model

The injection and production wells are assumed as source and sink terms in the flow equations. Wells can be completed vertically in several layers of the aquifer or horizontally with any length and both pressure and rate constraints are available for well conditions. The well models used are based on Peaceman (1983) and Babu and Odeh (1988) formulations. Abouie (2015) developed a wellbore simulator which could model homogeneous and heterogeneous, non-isobaric aqueous phase reactions assuming local equilibrium or kinetic conditions.

The boundary condition assumed in UTCHEM is no convective, no dispersive, and no thermal flux through all boundaries. Conductive thermal fluxes through the upper and lower boundaries of the aquifer may be modeled using the Vinsome and Westerveld (1980) method. If temperature variation is modeled, the boundary temperature is set to the initial temperature.

The main options for well model in UTGEL are as following:

- Any arbitrary number of producers in any gridblock can be specified.
- Skin factor (S) and completion interval can be specified and given as input.
- Both injection wells and producers can be shut in or opened at anytime during the

simulation. The well type can also be changed during the simulation (e.g., an injector changes to a producer).

- Each injection well can inject multiple slugs with different component concentrations.
- Wells can be completed in any direction parallel to the axes or deviated with the completion trajectory specified.

3.2.4.1 Vertical Wells with Cartesian or Corner Point Grid Options

Two basic well conditions of constant flow rate or constant flowing bottomhole pressure are implemented. Application of Darcy's law to a wellblock (i,j,k) results in

$$Q = \sum_{\ell=1}^{n_p} Q_\ell = \sum_{\ell=1}^{n_p} PI_\ell \left(P_{wf} - P_\ell \right), \tag{3.28}$$

where PI_ℓ is the productivity index and $P_\ell = P_1 + P_{c\ell 1}$ in which $P_{c\ell 1}$ is the capillary pressure between water and ℓ phases. For two-dimensional areal (x-y) and three-dimensional simulation, the PI_ℓ is given by

$$PI_\ell = \frac{2\pi\sqrt{k_x k_y}\,\Delta z}{(0.15802)\left(\ln \frac{r_o}{r_w} + S \right)} \lambda_{r\ell}, \tag{3.29}$$

and for one-dimensional simulation by

$$PI_\ell = \frac{k_x \Delta y \Delta z}{0.15802 \frac{\Delta x}{2}} \lambda_{r\ell}, \tag{3.30}$$

where the constant in the above equations is the unit conversion factors where the permeability is in Darcy and gridblock size in ft and $\lambda_{r\ell} = \dfrac{k_{r\ell}}{\mu_\ell}$ is in (cp)$^{-1}$ to result PI_ℓ in (psi)$^{-1}$.

The equivalent radius, r_o, is calculated using Peaceman's model (Peaceman, 1983)

$$r_o = 0.28 \frac{\left(\left(\dfrac{k_x}{k_y} \right)^{1/2} \Delta y^2 + \left(\dfrac{k_y}{k_x} \right)^{1/2} \Delta x^2 \right)^{1/2}}{\left(\dfrac{k_x}{k_y} \right)^{1/4} + \left(\dfrac{k_y}{k_x} \right)^{1/4}}. \tag{3.31}$$

The bottomhole flowing pressure in layer *k*, $(P_{wf})_k$ is given by

$$(P_{wf})_k = (P_{wf})_{k-1} + \bar{\gamma}_k, \qquad k = 2, ..., n_{bz} \tag{3.32}$$

where n_{bz} is the number of layers perforated and

$$\bar{\gamma}_k = \gamma_k \frac{\Delta z_k}{2} + \gamma_{k-1} \frac{\Delta z_{k-1}}{2}, \tag{3.33}$$

where γ_k is calculated from:

$$\gamma_k = \frac{\sum_{\ell=1}^{n_p} \gamma_\ell PI_\ell}{\sum_{\ell=1}^{n_p} PI_\ell}. \tag{3.34}$$

For the producer wellblock, specific weights of the produced fluids, γ_ℓ, are used in the calculations while for the injection wells, the specific weights of the injected fluids are calculated using

$$\gamma_\ell = \sum_{k=1}^{n_c} \left((C_{inj})_{k,\ell} \right) \gamma_k . \tag{3.35}$$

3.2.4.2 Well Constraint for Injection Wells

3.2.4.2.1 Rate Constraint

Once the phase injection rates, $Q_{inj,\ell}$, are specified, the positive injection rates can be assigned to the individual layer *k* that is perforated according to

$$Q_\ell = Q_{inj,\ell} \frac{\sum_{\ell=1}^{n_p} PI_\ell}{\sum_{k=1}^{n_{bz}} \sum_{\ell=1}^{n_p} PI_\ell} . \tag{3.36}$$

The total injection rate for the ijk block is given by

$$Q = \sum_{\ell=l}^{n_p} Q_\ell . \tag{3.37}$$

The above term is then added to the constant vector of the pressure equation at the ijk block. In Eq. (3.36), it is assumed that the potential gradient between the wellbore and the gridblock pressure is the same for all the layers in the reservoir model. Nolen and Berry (1972) have shown that including the potential differences in Eq. (3.36) may result

in stability problems. Eq. (3.36) may give erroneous results in the case of large vertical heterogeneity and especially in the presence of non-communicating layers. However, in the case of a very low permeability zone or small crossflow, the above formulation does not result in a significant error.

3.2.4.2.2 Pressure Constraint

When bottomhole injection pressure for the first perforated layer, $(P_{wf})_{ij,k=1}$, is specified, then Eq. (3.28) will be used. The term $\sum_{\ell=1}^{n_p} \mathrm{PI}_\ell \left(\mathrm{P_{wf}} - \mathrm{P_{c1\,\ell}}\right)$ in Eq. (3.28) is added to the constant vector of the pressure equation for block ijk and term $\sum_{\ell=1}^{n_p} \mathrm{PI}_\ell$ to the $(P_1)^{n+1}$ term (diagonal element in the pressure matrix).

After the pressure equation is solved, Eq. (3.28) is used to obtain the total injection rate at the end of the time step, Q. The injected phase cuts for each layer are the same as the total injected cuts.

$$Q_\ell = Q \frac{Q_{inj,\ell}}{\sum_{\ell=1}^{n_p} Q_{inj,\ell}}. \tag{3.38}$$

The phase injection rates, $\mathrm{Q_{inj,\ell}}$, specified as input values, are treated as phase cuts.

3.2.4.3 Well Constraint for Production Wells

3.2.4.3.1 Rate Constraint

When the total production rate, input as a negative value (Qprod) is specified, the withdrawal rate for each layer k is calculated using

$$Q = Q_{prod} \frac{\sum_{\ell=1}^{n_p} PI_\ell}{\sum_{k=1}^{n_{bz}} \sum_{\ell=1}^{n_p} PI_\ell}, \tag{3.39}$$

and the produced phase cuts are then calculated using

$$Q_\ell = Q \frac{\lambda_{r\ell}}{\sum_{\ell=1}^{n_p} \lambda_{r\ell}}. \tag{3.40}$$

3.2.4.3.2 Pressure Constraint

When bottomhole pressure for a producer is specified, Eq. (3.28) is used to calculate the total production rate (Q) in the same manner as was described above for the injection well on pressure constraint. The produced phase cuts are then obtained from

$$Q_\ell = Q \frac{PI_\ell}{\sum_{\ell=1}^{n_p} PI_\ell}. \tag{3.41}$$

3.3 GEL OPTIONS

This section firstly describes the bulk gels and also discusses about two types of microgels; colloidal dispersion gels and pH-sensitive gels. The preformed particle gels (PPG) and thermally active polymers (TAP) will be discussed extensively in Chapters 4 and 5.

3.3.1 Bulk Gels

Bulk gels can be generated to squeeze the fractures or very high permeability streaks to control excess water production. The gelling system composed of a polymer and crosslinker which is injected to form gel in-situ and thus block the high permeability streaks. Different gel properties such as viscosity, adsorption, and permeability reduction are discussed here. A brief description of three different types of bulk gels of Polymer/Chromium Chloride, Polymer/Chromium Malonate, and Silicate gels is described.

3.3.1.1 Bulk Gel Viscosity

The viscosity of an aqueous solution containing bulk gel can be modeled using the Flory-Huggins equation with additional terms for bulk gel (Thurston *et al.*, 1987).

$$\mu_1 = \mu_w\left[1+\left(A_{p1}C_{4,1}+A_{p2}C_{4,1}{}^2+A_{p3}C_{4,1}{}^3\right)C_{SEP}^{S_P}+A_{g1}C_{15,1}+A_{g2}C_{15,1}{}^2\right], \tag{3.42}$$

where $C_{4,1}$, $C_{15,1}$ are polymer and bulk gel concentration in aqueous phase, μ_w is the water viscosity, C_{SEP} is effective salinity ($\left(\mathrm{C_{SEP}}=\frac{\mathrm{C_5}+\beta_\mathrm{p}\mathrm{C_6}}{\mathrm{C_1}}\right)$), S_p is a parameter for the effect of salinity, and A_{p1}, A_{p2}, A_{p3}, A_{g1} , A_{g2} are input parameters.

3.3.1.2 Bulk Gel Adsorption

We use Langmuir isotherm for gel adsorption which is a function of gel concentration and salinity as given below:

$$\hat{C}_{15} = \frac{a_{15}\left(C_{15,1}\right)}{1+b_{15}C_{15,1}}, \tag{3.43}$$

$$\mathrm{a}_{15} = \left(\mathrm{a}_{15,1} + \mathrm{a}_{15,2}\mathrm{C}_{\mathrm{SEP}}\right), \tag{3.44}$$

where $C_{15,1}$ is the bulk gel concentration in the aqueous phase 1 and $a_{15,1}$, $a_{15,2}$, and b_{15} are model parameters.

3.3.1.3 Bulk Gel Permeability Reduction

The effect of gel on aqueous-phase permeability reduction is taken into account through a residual resistance factor also commonly used for polymer flooding.

$$R_{RF} = 1+\frac{\left(R_{RFMax}-1\right)A_{gk}C_{15,1}}{1 + B_{gk}C_{15,1}}, \tag{3.45}$$

where the maximum residual resistance factor is calculated by

$$R_{RF\max} = \left[1-\frac{c_{rg}\left(A_{p1}C_{SEP}^{S_p}\right)^{1/3}}{\left(\frac{\sqrt{k_x k_y}}{\phi}\right)^{1/2}}\right]^{-4}, \tag{3.46}$$

where $C_{15,1}$ is the gel concentration in the aqueous phase 1, R_{RFMax} is the maximum permeability reduction, A_{gk}, and B_{gk} are input parameters. The parameter c_{rg} is an input parameter depending on the gel type. The permeability reduction for silicate gel

(KGOPT=3) is independent of the silicate viscosity and the maximum residual resistance factor (R_{RFMax}) is equal to 10.

3.3.1.4 Polymer/Chromium Chloride Bulk Gel *(KGOPT = 1)*

There are two sets of reactions for polymer/chromium chloride. The first is in-situ gelation of polymer with sodium dichromate and reducing agent thiourea, and the second is the gelation of Cr(III) with polymer to form gel.

The kinetics for the reaction between polymer and chromium has been generalized to allow for any exponent (Hunt, 1987). The gel is formed by fast reaction between trivalent chromium Cr(III) and polymer. There is an option for the slow delayed reaction between Cr (VI) and thiourea. The sodium dichromate ($Na_2Cr_2O_7$) and thiourea $[CS(NH_2)]_2$ are treated like conservative tracers and do not occupy any volume. The Cr(III) for the gelation can be generated in-situ by redox reaction between Cr(VI) and thiourea.

$$Cr_2O_7^{2-} + 6CS(NH_2)_2 + 8H^+ \xrightarrow{k_1} 2Cr^{3+} + 3\left[CS(NH_2)_2\right]_2 + 7H_2O. \qquad (3.47)$$

The gel reaction is highly dependent on pH (Lockhart and Albonico, 1994; Seright and Martin, 1991). The pH effect on gel kinetic equation is considered as hydrogen ion concentration to simulate gel reactions more mechanistically.

3.3.1.5 Polymer/Chromium Malonate Bulk Gel *(KGOPT = 2)*

The components of polymer/chromium chloride gel are as follows:

- Polymer: Hydrolyzed polyacrylamide (HPAM) and HE-100 (acrylamido-3-propane sulfonic acid co-polymer) were used. HE-100/chromium malonate is reported to have a longer gelation time than HPAM/chromium malonate (Lockhart and Albonico, 1994).
- Crosslinker (Chromium malonate): Gelation time with chromium malonate is the longest with better stability at high temperature compared to other various complexes of chromium (Lockhart and Albonico, 1994).
- Delaying Ligand (Malonate ion-uncomplexed): The uncomplexed malonate ion as a delaying ligand is an optional component that gives longer gelation time.

3.3.1.5.1 Polymer and Crosslinker Only

The kinetics for this gel is the same as the kinetics of chromium chloride gel except with different exponents:

$$Polymer + n\,Cr(III) \longrightarrow Gel, \tag{3.48}$$

$$\frac{d[Cr(III)]}{dt} = -k\,\frac{[Cr(III)]^{X14}[Polymer]^{X4}}{[H^+]^{X16}}, \tag{3.49}$$

$$\frac{d[Gel]}{dt} = -\frac{1}{n}\,\frac{d[Cr(III)]}{dt}, \tag{3.50}$$

where the possible values for exponents are X4=2.6, X14=0.6, and X16=1.0.

3.3.1.5.2 Polymer, Crosslinker, and Malonate ion

When the malonate ion is used as a delaying ligand, the gelation kinetics is different, with zero-order reaction for chromium:

$$\frac{d[Cr(III)]}{dt} = -k \frac{[Polymer]^{X4}}{[Malonate]^{X13}[H^+]^{X16}}, \tag{3.51}$$

$$\frac{d[Gel]}{dt} = -\frac{1}{n} \frac{d[Cr(III)]}{dt}, \tag{3.52}$$

where the possible values for exponents are $X_4 = 2.6$, $X_{13} = 0.3$, and $X_{16} = 1.0$.

3.3.1.6 Silicate Bulk Gel *(KGOPT=3)*

Polymer and chromium are replaced with silicate (SiO_2) and hydroxyl ion (OH^-), respectively. The gelation was limited to occur only for pH > 7 (Bennett *et al.*, 1988; Iler, 1979) to eliminate complex behavior of gel reaction rate at pH < 7. The aqueous phase permeability reduction was not dependent on silicate viscosity.

Silicate gel is formed by polymerization when appropriate conditions are established. However, the exact mechanism of gelation is not clear yet. The general process of gelation is as follows (Jurinak *et al*., 1989):

- The monomer and dimer silicate species are condensed to form higher-order oligomers.
- Intramolecular condensation of silanol groups within polymers leads to ring closure and eventual particle formation.
- The individual particles are aggregated to form chains and microgel.

The rate of gelation (Kristensen *et al.*, 1993) is a function of

- silicate concentration
- pH
- ionic strength
- temperature

The basic equations that govern polymerization of silicate (Iler, 1979) are as follows:

$$SiO_2 + 2H_2O \longrightarrow Si(OH)_4, \tag{3.53}$$

$$SiOH^- + SiOH^- \longrightarrow Si_2O^{2-} + H_2O, \tag{3.54}$$

$$SiO_2 + mOH^- \longrightarrow SilicateGel, \tag{3.55}$$

where m is the stoichiometric ratio.

The gelation kinetics equation is derived using Eq. (3.55) as following:

$$\frac{d[SiO_2]}{dt} = -k\left[SiO_2\right]^{X4}\left[OH^-\right]^{X14}, \tag{3.56}$$

where $X4$ is gelation kinetics exponent for silicate and $X14$ is gelation kinetics exponent for hydroxyl ion.

$$\frac{d[Gel]}{dt} = -\frac{d[SiO_2]}{dt}, \tag{3.57}$$

where the possible values for exponents are X_4 = 3.8, and X_{14} = -2.5 (Kristensen *et al.*, 1993).

3.3.2 Colloidal Dispersion Gels, CDG (*KGOPT=5)*

CDGs or stable, soft, size-controlled microgels are injected to increase the resistance factor of the high permeability zones and divert the flow to the low permeability zones. This diversion will lead to improvement in macroscopic sweep efficiency and also block the large pore throats with high permeability zones and divert the water to the smaller pore throats with lower permeability which reduces the water production as well.

CDG can be divided into two types: gel formed in-situ and preformed gel. CDG formed in-situ is predominantly intermolecular crosslinked gel in which polymer and crosslinker will react to form microgels and viscosity will increase following mixing. This form is called in-situ because it is not stable at surface and it doesn't form microgel until it arrives to the target in deep reservoir. This kind normally should be injected into the well immediately or after a short while (1 or 2 hours). Otherwise, the gel forms in the vicinity of wellbore and thus blocks the rock surface leading a hard injectivity and failure of in-depth treatment. If the polymer molecules inter-crosslink very fast leading to formation of CDG aggregates in the first part of core, the failure of in-depth transportation will happen most probably. Preformed gel is predominantly intramolecular crosslinked CDG whose viscosity will decrease significantly after addition of the crosslinker and then decrease gradually and finally reach a constant value lasting for at least 15 days. Preformed gel is stable at surface at least for 15 days, and the size of gel stays constant while propagating through the porous media. Transport model of CDG through porous media and also viscosity models will be discussed in the following sections.

3.3.2.1 CDG Transport Model

The jamming ratio, proposed by Cozic *et al.* (2009), represents the ratio between the mean pore diameter and the mean diameter of microgels which can be determined as following:

$$J_r = \frac{d_h}{d_m} = \frac{2r_h}{d_m}, \tag{3.58}$$

where d_h is the mean pore diameter, d_m is the microgels mean diameter, and r_h is radius of the pore throat. The adsorbed layer thickness may be smaller than the diameter of microgel due to the shear rate effect when microgels adsorb to the pore throat wall in a monolayer way. On the other side, the adsorbed layer thickness might be greater than the diameter of microgel due to the interaction between the microgels when microgels adsorb to the pore throat wall in a multilayer way.

The dynamic jamming ratio, which is the ratio between the diameter of the pore throat and the adsorbed layer thickness of microgels, will be used extensively for CDG transport in porous media and is proposed to evaluate the permeability reduction for each gridblock. The dynamic jamming ration can be calculated with the following correlation:

$$JR = \frac{d_h}{\varepsilon_h} = \frac{2r_h}{\varepsilon_h}, \tag{3.59}$$

where ε_h is the adsorbed layer thickness of microgels. Dynamic jamming ratio can be used to determine whether the stable microgels such as CDG can go through the pore throat in each grid block or not.

The permeability reduction with respect to water phase can happen near the wellbore due to the adsorption of microgels on the pore wall. The hydrodynamic thickness of adsorbed layers ε_{h} can be estimated by the following capillary model relationship (Chauveteau and Sorbie 1991):

$$\varepsilon_{\mathrm{h}} = r_{\mathrm{h}}\left(1 - R_{\mathrm{k}}^{-1/4}\right). \tag{3.60}$$

The equation which predicts adsorbed layer thickness can be expressed as following:

$$\varepsilon_{\mathrm{h}} = \varepsilon_{\mathrm{h1}}\dot{\gamma}_{\mathrm{eq}}^{\ B}, \tag{3.61}$$

$$\varepsilon_{\mathrm{h1}} = d_2 C_{\mathrm{m}} + e_2 , \tag{3.62}$$

where C_m is the microgel concentration in the aqueous phase 1, $\dot{\gamma}_{\mathrm{eq}}$ is the equivalent shear rate ($\sec^{-1}$), $\varepsilon_{\mathrm{h1}}$ is the adsorbed layer thickness when equivalent shear rate is equal to 1 $\sec^{-1}$, and d_2, and e_2 are parameters which can be obtained by fitting the experimental data for adsorbed layer thickness. Substitution of Eq. (3.62) into Eq. (3.61) yields the following:

$$\varepsilon_{\mathrm{h}} = \left(d_2 C_{\mathrm{m}} + e_2\right)\dot{\gamma}_{\mathrm{eq}}^{\ B}. \tag{3.63}$$

Substituting Eq. (3.63) into the Eq. (3.62) yields the following equation for permeability reduction:

$$R_{\mathrm{k}}=\left(\frac{r_{\mathrm{h}}}{r_{\mathrm{h}}-\left(d_2 C_{\mathrm{m}}+e_2\right)\dot{\gamma}_{\mathrm{eq}}{}^{B}}\right)^4, \tag{3.64}$$

where the pore throat radius r_{h} can be estimated using the following equation:

$$r_h=1.15\sqrt{\frac{8\bar{k}}{\phi}}, \tag{3.65}$$

where $\bar{k}$ is the average permeability, and ϕ is porosity. The in-situ shear rate for phase l is modeled by the modified Blake-Kozeny capillary bundle equation for multiphase flow (Lin, 1981; Sorbie, 1991) as following:

$$\dot{\gamma}_{\mathrm{eq}}=\frac{\dot{\gamma}_{\mathrm{c}}|u|}{\sqrt{\bar{k}k_{\mathrm{rl}}\phi S_{\mathrm{l}}}}, \tag{3.66}$$

where $|u|$ is the magnitude of apparent velocity, k_{rl} is the relative permeability to phase l, $\bar{k}$ is the average permeability, S_{l} is the saturation of the phase l; $\dot{\gamma}_{\mathrm{c}}$ is equal to 3.97C and C is the shear rate coefficient used to account for non-ideal effects such as slip at the pore walls (Wreath *et al.*, 1990; Sorbie, 1991). After calculating the pore throat radius and the adsorbed layer thickness, Eq. (3.59) can be used to calculate dynamic jamming ratio. If the dynamic jamming ratio if greater than 4, then the following equation can be used to calculate permeability reduction to water (Shi *et al.*, 2011a):

$$R_k = \left(\frac{JR}{JR-2} \right)^4 . \tag{3.67}$$

The trend in permeability reduction with JR for the whole range is similar to log-normal distribution by analyzing the change of permeability reduction in the above discussion; therefore log-normal distribution can be used to match the change of permeability reduction with JR. In probability theory, a log-normal distribution is a probability distribution of a random variable with normally distributed logarithm. The probability density function of log-normal distribution can be expressed as following:

$$Y = \frac{1}{X\sqrt{2\pi\sigma^2}} \exp\left(-\frac{\left(\ln X - \mu\right)^2}{2\sigma^2} \right), \qquad X > 0 \tag{3.68}$$

where μ and σ are the mean and standard deviation of the variable's logarithm (by definition, the variable's logarithm is normally distributed). The probability density function of log-normal distribution can be modified to match the theoretical Eq. (3.67) which will give the following equation for permeability reduction:

$$R_k = 1.5 + \left[\frac{c}{(JR-1)\sqrt{2\pi\sigma^2}} \exp\left(-\frac{\left(\ln\left(JR-1\right) - \mu\right)^2}{2\sigma^2} \right) \right]^f . \tag{3.69}$$

3.3.2.2 CDG Viscosity Models

The viscosity of CDG at low concentrations of less than 2000 ppm and low shear rate will be calculated using Huggin's equation (Russel *et al.*, 1989) as shown below:

$$\mu_{CDG}^{0} = \mu_s(1+[\eta]C_{CDG} + K_H[\eta]^2 C_{CDG}{}^2), \qquad C_{CDG} \langle\ 2000\ ppm \qquad (3.70)$$

where K_H is the Huggins constant which is an indication for interaction of particle colloids inside the solution, μ_s is the solvent viscosity, $[\eta]$ is the intrinsic viscosity at zero shear rate which is an indication of the microgel colloids density, C_{CDG} is the gel concentration, and μ_{CDG}^{0} is the viscosity at zero shear rate.

The above equation is valid for low CDG concentrations ($C_{CDG} \langle\ 2000\ ppm$). However, Maclaurin model was proposed for higher concentrations as shown below:

$$\mu_{CDG}^{0} = \mu_s(1+[\eta]C_{CDG} + [\eta]^2 K_H C_{CDG}{}^2 + \frac{[\eta]^3 K_H{}^2}{2} C_{CDG}{}^3 + ...). \qquad C_{CDG} \rangle\ 2000\ ppm \qquad (3.71)$$

It is obvious that Eq. (3.71) for high concentrations will be simplified to Eq. (3.70) for low concentrations by removing the third term.

Carreau's model (Bird *et al.*, 1977) failed to represent the effect of shear rate on microgel viscosity when it was tested for different concentrations. Shi *et al.* (2011b) modified Carreau' model to consider shear effect at any arbitrary concentration as shown below:

$$\frac{\mu_M - \mu_s}{\mu_M^0 - \mu_s} = \left[1+(\lambda \dot{\gamma}_{eq})^2\right]^{(n-1)/2}, \qquad (3.72)$$

$$\lambda = ae^{bC_M}. \qquad (3.73)$$

Chapter 4: Study of Preformed Particle Gels (PPG) for Conformance Control

4.1 INTRODUCTION

Preformed particle gel (PPG) is an improved super absorbent polymer (SAP) for conformance control. Traditional SAPs cannot be used for conformance control due to their low strength, instability at high temperatures, and fast swelling time (Bai *et al.*, 2008). However, new series of SAPs, known as preformed particle gel (PPG), were developed for conformance control (Bai *et al.*, 2004a, 2007a). There are different types of PPGs, such as preformed bulk gels (Seright, 2004), partially preformed gels (Sydansk *et al.*, 2004), millimeter-sized preformed particle gels (Bai *at al.*, 2004a), and pH sensitive crosslinked polymers (Huh *et al.*, 2005). The main differences are in their swelling times and particle sizes. There have been several well tests using a temperature sensitive microgel system, called BrightWater® from TIORCO (Cheung *et al.*, 2007). Swelling gels were also successfully employed to control CO_2 breakthrough in CO_2 enhanced oil recovery projects (Wu and Bai, 2008).

Bai *et al.* (2007b, 2010) performed extensive experimental research to investigate the propagation of PPG through porous media and the influencing parameters, such as particle size, swelling capacity, injectivity, etc. However, no mathematical model has been proposed for propagation of gel and very few simulation studies have been done to model laboratory results.

Transport ability of PPG through pores depends on several parameters, such as pore diameter, structure of particles, particle size, and salinity. In fact, particle size is not

the diameter of each particle, but it is the average size of randomly selected number of particles through a sample. Particles can swell considerably; swelling ratio is a function of salinity. The particles, depending on the salinity, are defined as weak or strong.

Based on the study by Li and Bai (2001), parameters for evaluating gel performance were swelling capacity, elastic modulus, swelling rate, and fracture stress. The swelling capacity, A, can be defined as

$$A = \frac{M_l - M_s}{M_s}, \tag{4.1}$$

where M_l is the volume after swelling, and M_s is the dried gel volume. The change in elastic modulus versus time can be used as an indication of thermal stability and strength. It should be noted that gel strength is a function of both monomer and crosslinker concentrations and by increasing the crosslinker concentration, the strength will increase due to the rapid increase in network density. However, swelling capacity will be lost if the crosslinker concentration is too high and this is an important consideration for designing gel treatments. Thermal stability can be enhanced from 90 ^{0}C to 120 ^{0}C when only 0.2 wt% thermal stabilizing agent is added. Higher temperatures are favorable, as the swelling capacity of gels increases considerably at higher temperatures.

In this chapter, PPG experiments are presented first. Experiments discussed in this chapter are all conducted by Dr. Bai and his research staff at Missouri University of Science and Technology, Rolla. Next, we describe the mechanistic model developed and implemented in an in-house reservoir simulator, UTGEL. The simulation results are validated with different experimental and field data.

4.2 EXPERIMENTAL PROCEDURE

4.2.1 Gels and Materials

A superabsorbent polymer comprised mainly of a potassium salt of cross-linked polyacrylamide copolymer was used as the PPGs in all experiments. When dry, these PPGs are white, sugar-like, granular powder. Table 4-1 lists the typical characteristics of the PPGs used in this study. In aqueous solution, PPGs can absorb a large amount of water because of their hydrophilicity which allows hydrogen bonding with water molecules, although the swelling solution salinity affects ability to adsorb water. Table 4-2 shows that PPG swelling ratio is greatly affected by brine salinity. Figure 4-1 shows a comparison of dry gel particles and fully swollen particles in 1.0 wt. % sodium chloride (NaCl) solution. The laboratory data shows that swelling ratio decrease as brine concentration increases as shown in Figure 4-2.

Table 4-1: Characteristics of PPG used in the experiments.

Properties	Value
Absorption Deionized Water (g/g)	>200
Apparent Bulk Density (g/l)	540
Moisture Content (%)	5
pH Value	5.5-6.0 (+/- 0.5; 1% gel in 0.9% NaCl)

Table 4-2: Effect of brine salinity on swelling ratio.

Brine Salinity, wt. % NaCl	Swelling Ratio, g/g
0.05	194
0.25	98
1	52
10	32

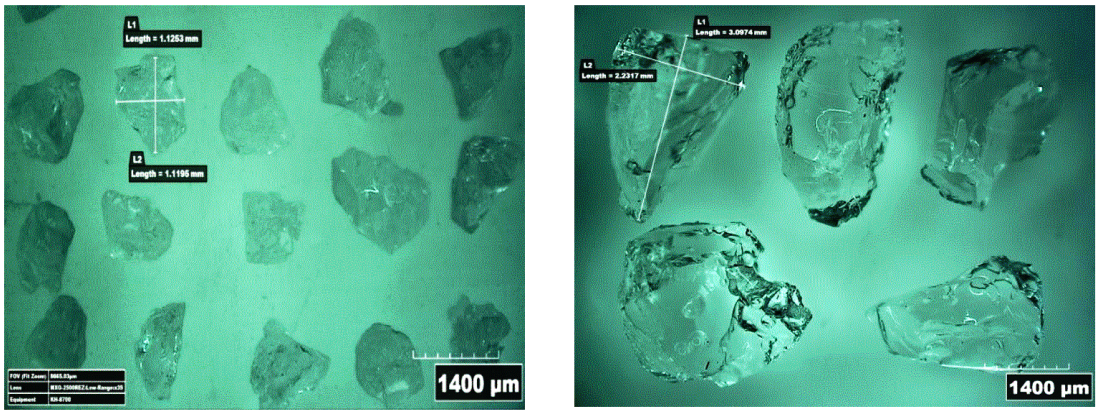

Figure 4-1: Comparison of dry and swollen PPG particles: (a) Dry PPGs with 18/20 mesh size, (b) Fully swollen PPGs in 1.0 wt. % NaCl (Bai, 2013).

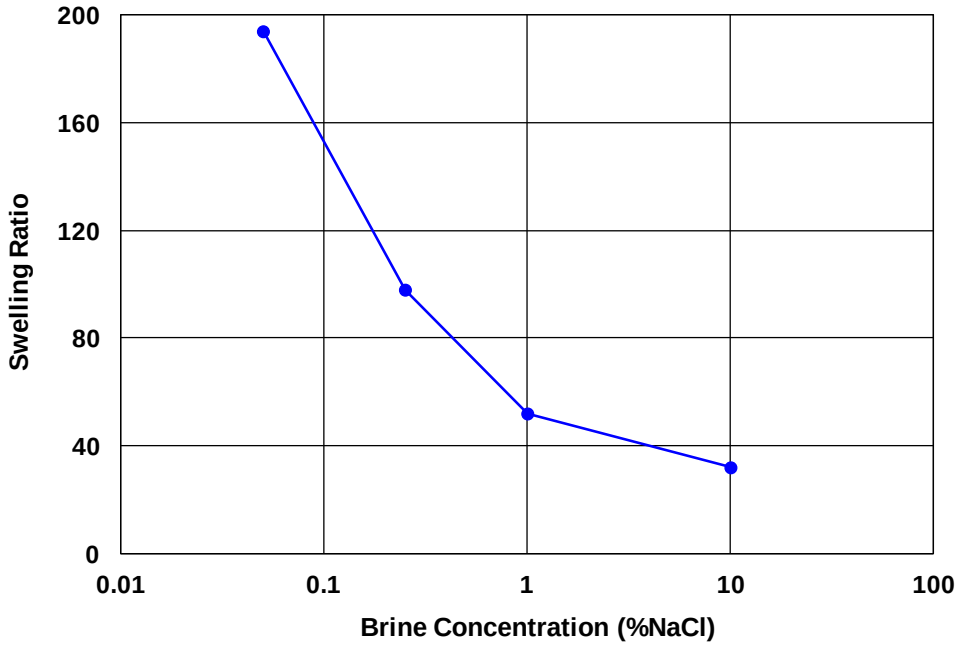

Figure 4-2: The swelling ratio as a function of brine concentration.

The following section represents different experiments designed and conducted for evaluating PPG performance. Experimental data is used to model the flow and transport of PPG in porous media.

4.2.2 Transparent Open Fracture Experiment

A 1-D transparent model constitutes two parallel acrylic plates between which there is a rubber O-ring. Bolts, nuts, and shims are used to fix the two parallel acrylic plates and control the fracture width. On one side of the plate, there is a hole as inlet for the injection of fluids and PPG; on the other side, there is another hole as the outlet to discharge fluids and PPG. In addition, there are three extra holes on a plate as pressure taps, connecting to the pressure transducers. The schematic diagram of the experimental setup is shown in Figure 4-3. The model was used to study the particle strength and size effect on the injectivity and to visually observe particle movement in a single fracture. Brine was injected at different flow rates and then PPG was extruded into the fracture to evaluate the injection pressure. Before PPG injection, the fracture system is saturated with brine to characterize using flow measurements. Completely swollen PPG sample with 40-mesh size was prepared with four different brine salinities (0.05, 0.25, 1, and 10 %wt NaCl) for the experiment.

The test was conducted in three fracture widths (0.5, 1, and 1.5 mm) and at different salinities. After gel placement, water was injected to evaluate plugging efficiency of the gel. The gel moves along the fracture like a piston and gravity effects on PPG shape and movement are neglected. Injection pressure measurements were recorded at different injection flow rates and used for comparison with simulation results. The measured PPG injection pressures for different fracture widths (0.5, 1, 1.5 mm) are shown in Figure 4-4 through Figure 4-6. The pressure gradient remained stable during the experiment and there was no considerable plugging (continuous pressure gradient increase) at the end of gel injection. Also, resistance factor and residual resistance factor data were measured at different salinities and different fracture widths which helped us to

develop a model for resistance factor and residual resistance factor as a function of salinity and injection rate.

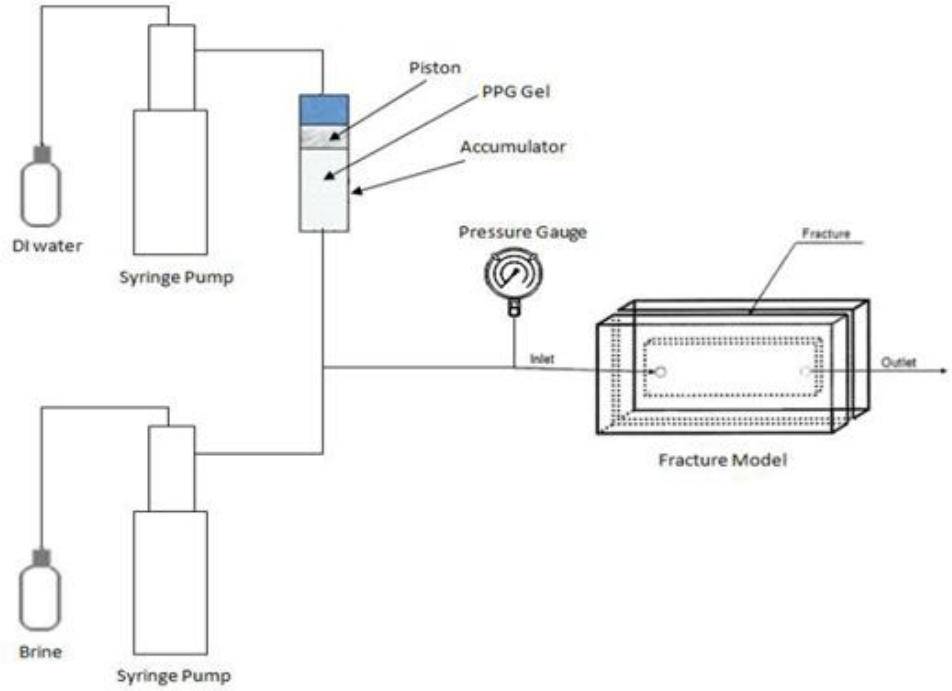

Figure 4-3: Experimental setup for PPG injection into an open fracture (Bai, 2013).

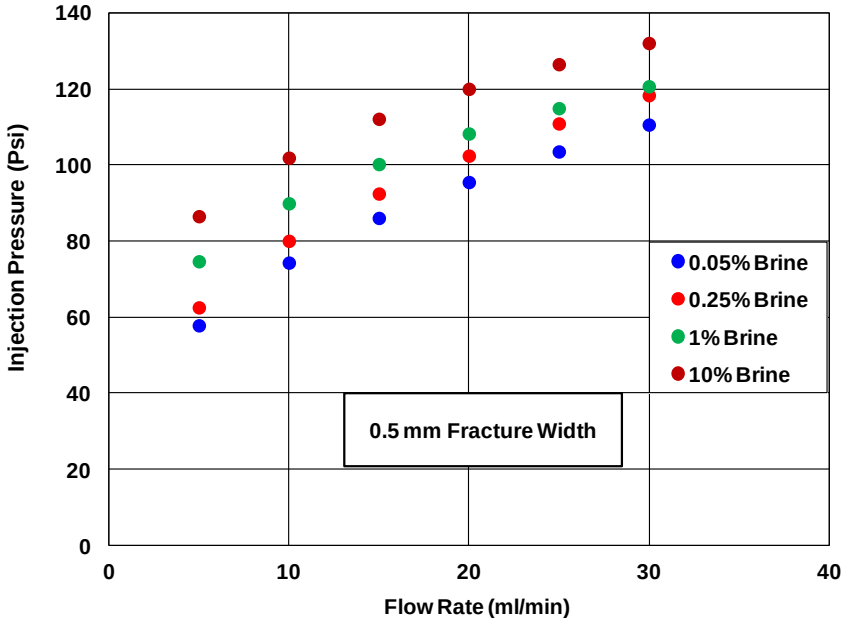

Figure 4-4: PPG injection pressure vs. flow rate for 0.5 mm fracture width: 0.05 wt.% NaCl, (b) 0.25 wt.% NaCl, (c) 1 wt.% NaCl, (d) 10 wt.% NaCl.

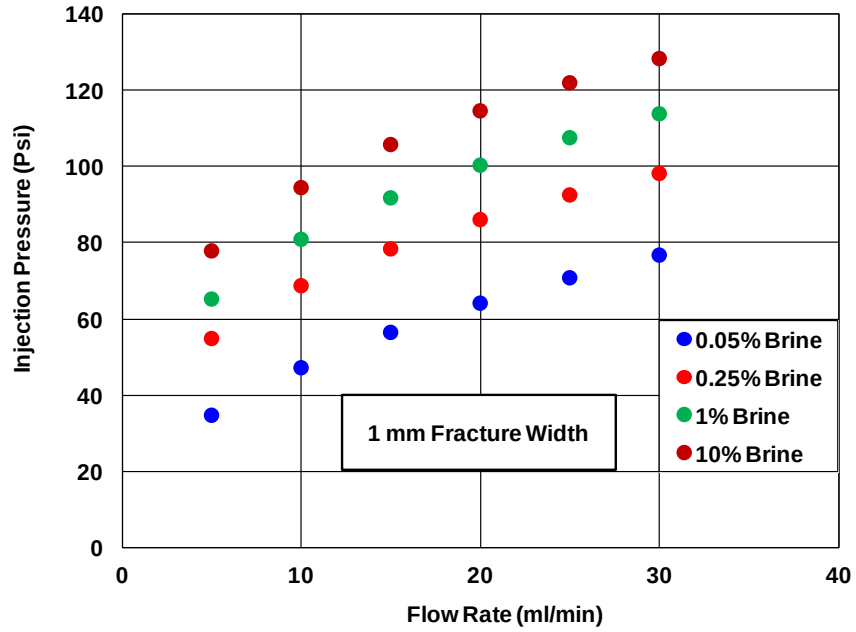

Figure 4-5: PPG injection pressure vs. flow rate for 1 mm fracture width: 0.05 wt.% NaCl, (b) 0.25 wt.% NaCl, (c) 1 wt.% NaCl, (d) 10 wt.% NaCl.

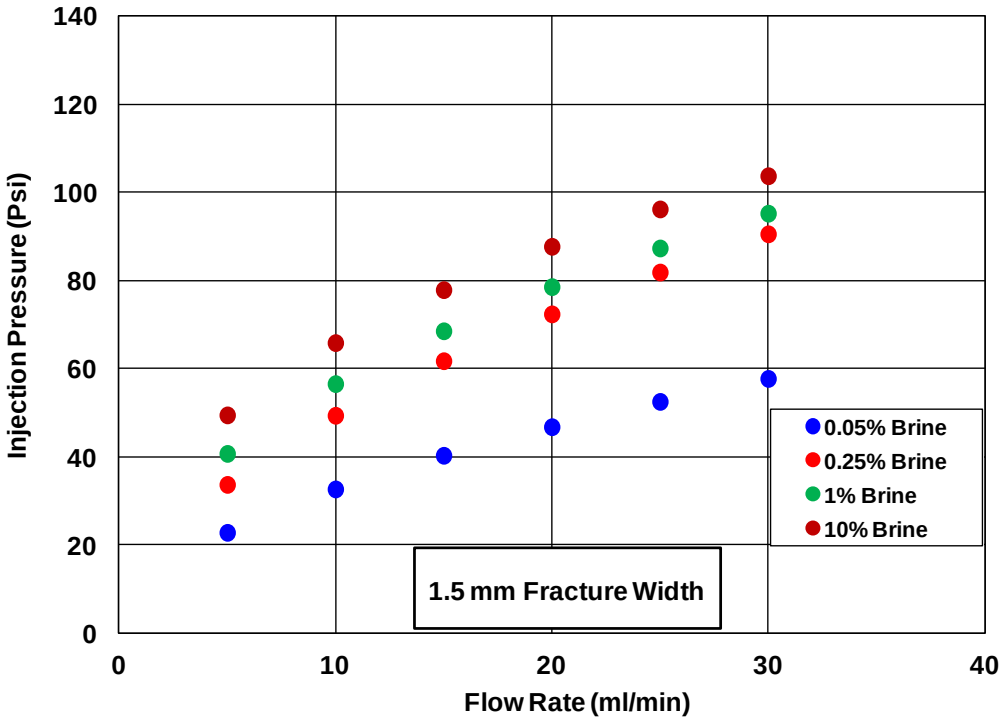

Figure 4-6: PPG injection pressure vs. flow rate for 1.5 mm fracture width: 0.05 wt.% NaCl, (b) 0.25 wt.% NaCl, (c) 1 wt.% NaCl, (d) 10 wt.% NaCl.

4.2.3 Homogeneous Sandpack Experiment

Sandpack with 1 inch diameter and 20 inches length (Figure 4-7) was divided into four sections with equal lengths by three pressure taps. Four pressure transducers were mounted on the inlet and on the pressure taps along the sand pack for monitoring the pressure behavior of the injection process. Stainless steel screens were used on each end of the sand pack and all pressure taps to prevent sand migration. Dry Ottawa sands with particle size of 354 - 420 micron (40/45 mesh) were used with a measured water permeability of 27.29 Darcy. Figure 4-8 shows sand particles and homogeneous sandpack porous media. Sands were gradually packed into the model with a constant packing pressure (200 psi) to ensure all sections of the sandpack having the same porosity.

Consistent permeability value was measured for each section of the sandpack as shown in Figure 4-9 and homogenous porous media model was assumed in the following experimental discussion and simulation work. The pore volume of the sand pack was 49.7 ml with the porosity of the sandpack measured as 0.193. The brine used in the experiment was 1 wt.% KCl and 2000 ppm preformed particle gel was used for the gel injection. The experimental procedure is presented below:

- Sandpack was initially saturated with 1 wt% KCl brine and the pore volume was calculated.
- Brine was injected at different flow rates and the absolute permeability was calculated.
- Oil was injected to displace water until no water came out and the oil in place was calculated based on the volume of water displaced.
- Brine was injected at 2 ml/min rate and the differential pressure with time was recorded in each section of the sandpack to obtain the injectivity curve. The volume of oil produced was also recorded every 2.5 minutes to obtain the oil recovery curve for the water flooding process.
- PPG was injected at 2 ml/min. The injection pressure was monitored in each section and the oil production was recorded.
- Brine was injected again at 2 ml/min rate and the pressure behavior, oil recovery, and water cut were observed.

The sandpack results of oil recovery and water cut are given in Figure 4-10 and Figure 4-11. Waterflood oil recovery was 62% OOIP and PPG and subsequent waterflood increased the recovery by additional 20%. The water cut was reduced from 99% to almost 79% during microgel injection which is a good indication for effectiveness of this microgel in reducing water cut.

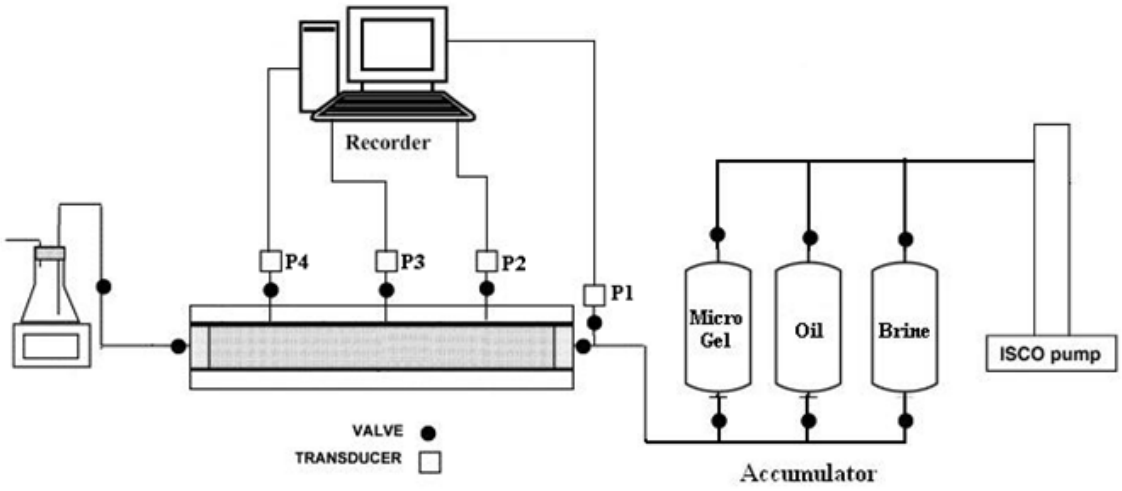

Figure 4-7: Schematic representation of homogeneous sandpack model for PPG injection (Bai, 2013).

Figure 4-8: Dry Ottawa sands used in the sandpack model (homogeneous porous media is achieved for sandpack experiment).

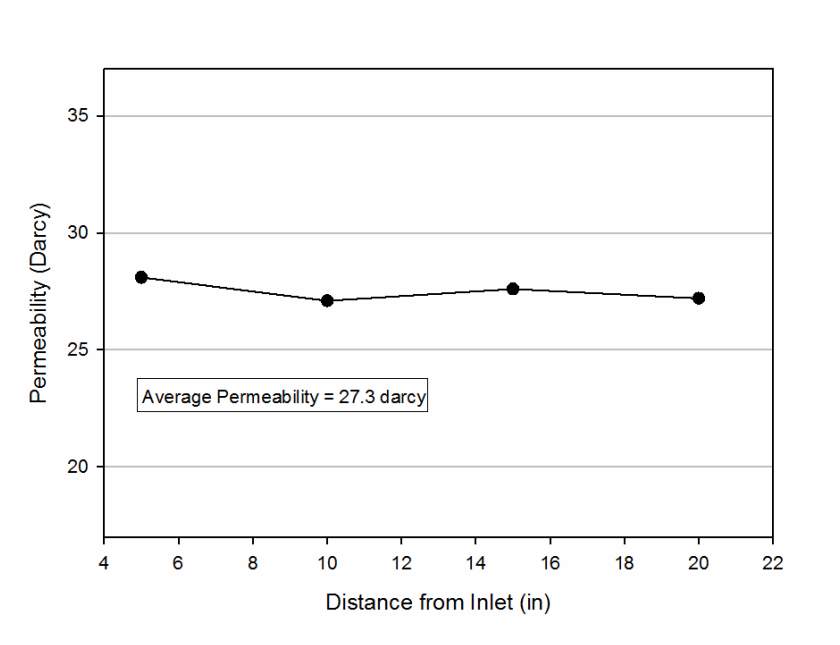

Figure 4-9: Permeability profile along the sandpack model (Bai, 2013).

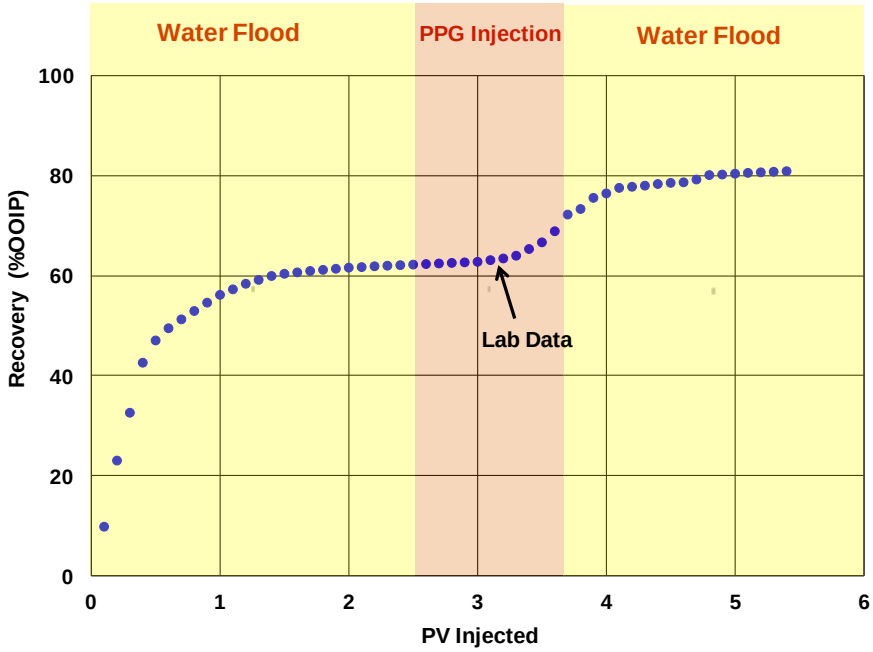

Figure 4-10: Measured oil recovery for homogeneous sandpack experiment (Bai, 2013).

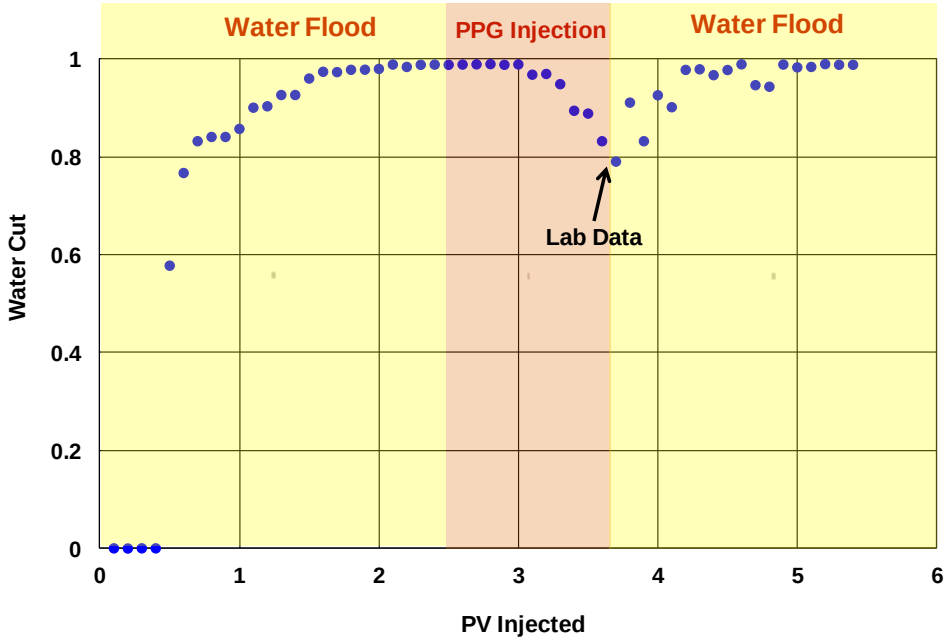

Figure 4-11: Measured water cut for homogeneous sandpack experiment (Bai, 2013).

4.2.4 Heterogeneous Sandpack Experiment (No Crosslow)

The main objective of these experiments is to evaluate PPG performance in heterogeneous porous media and to achieve this two different heterogeneous systems are designed. The first is two parallel sandpacks with different permeabilities and without any crossflow between two packs as shown in Figure 4-12. The flow rates are the same for both sandpacks and the PPG performance in each pack will be evaluated based on the measured oil recovery and water cut.

The experimental procedure is presented below:

- Both Sandpacks were initially saturated with 1 wt% KCl brine and the pore volumes were calculated.
- Brine was injected at different flow rates and the absolute permeability of each sanpack was calculated.
- Oil was injected to displace water until no water was produced and the oil saturation is calculated based on the volume of water displaced.
- Brine was injected at 1 ml/min and the differential pressure with time was recorded to obtain the injectivity curve. The volume of oil produced from each sandpack was also recorded every 2.5 minutes to obtain the oil recovery curve for the water flooding process in both sandpacks.
- PPG (2000 ppm concentration) was injected at 1 ml/min for 0.2 PVs. The injection pressure was monitored in each section and the oil production was recorded.
- Brine was injected again at 1 ml/min and the pressure behavior, the oil recovered, and the water cut were observed.

The sandpack results of oil recovery and water cut are given in Figure 4-13 and Figure 4-14. Waterflood oil recovery was 39% OOIP and PPG and subsequent waterflood increased the recovery by about 17%. The water cut was reduced from 99% to almost 79% during microgel injection which is a good indication for effectiveness of this microgel in reducing water cut.

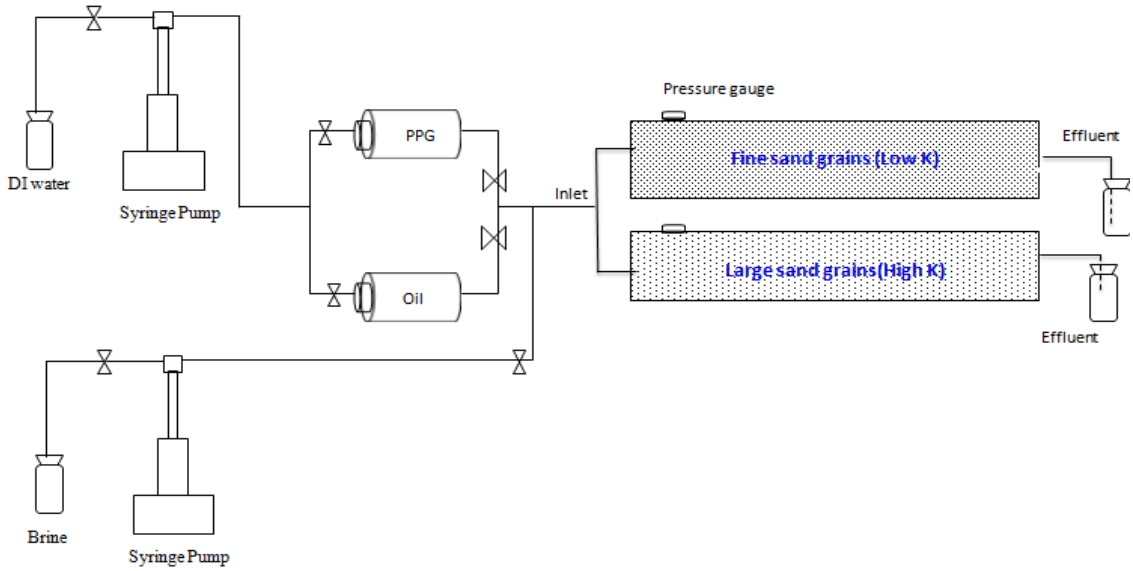

Figure 4-12: Schematic representation of heterogeneous sandpack model with different permeabilities (no crossflow) for PPG injection (Bai, 2014).

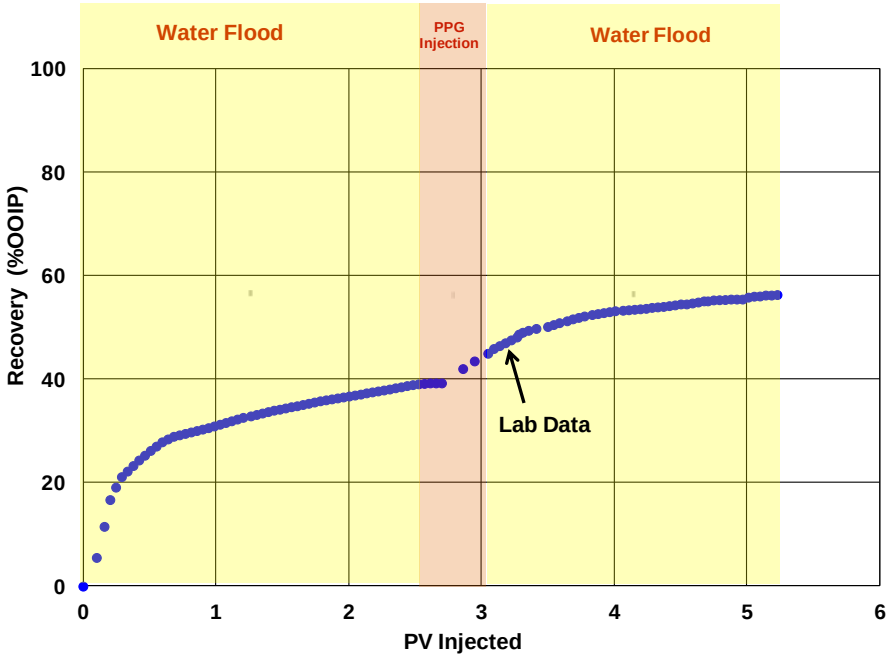

Figure 4-13: Measured oil recovery for heterogeneous sandpack experiment without crossflow (Bai, 2014).

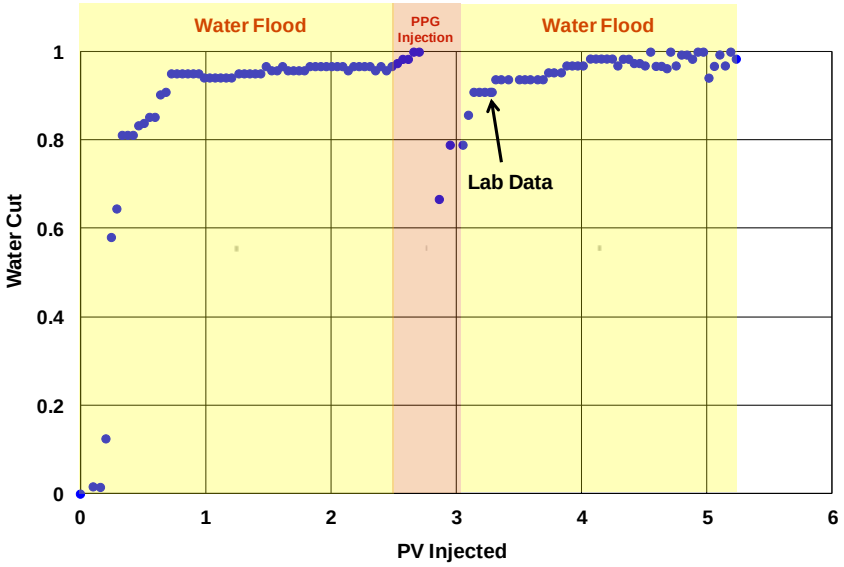

Figure 4-14: Measured water cut for heterogeneous sandpack experiment without crossflow (Bai, 2014).

4.2.5 Heterogeneous Sandpack Experiment (With Crosslow)

The second heterogeneous system is two parallel sandpack with different permeabilities (inner low permeability zone and outer high permeability zone) and with crossflow between two porous media as shown in Figure 4-15. A perforated screen tube with diameter less than 1 inch was placed inside the stainless steel round tube to design high and low permeability zones in contact with each other. Large sand grain was poured first inside the stainless steel around perforated screen tube to create high permeability media. Fine sand grain was then poured inside perforated screen to obtain low permeability zone. The outer high permeability zone was filled with sand of 20-30 mesh size and the inner low permeability zone was filled with sand of 80-100 mesh size. The oil recovery and water cut from the combined sandpack system were measured at the effluent. The size of the sandpacks was 5.08 cm in diameter and 30.48 cm in length.

The coreflood results of oil recovery and water cut for heterogeneous case with no crossflow are given in Figure 4-16 and Figure 4-17. Waterflood oil recovery was 65% OOIP and PPG and subsequent waterflood increased the recovery by about 6%.

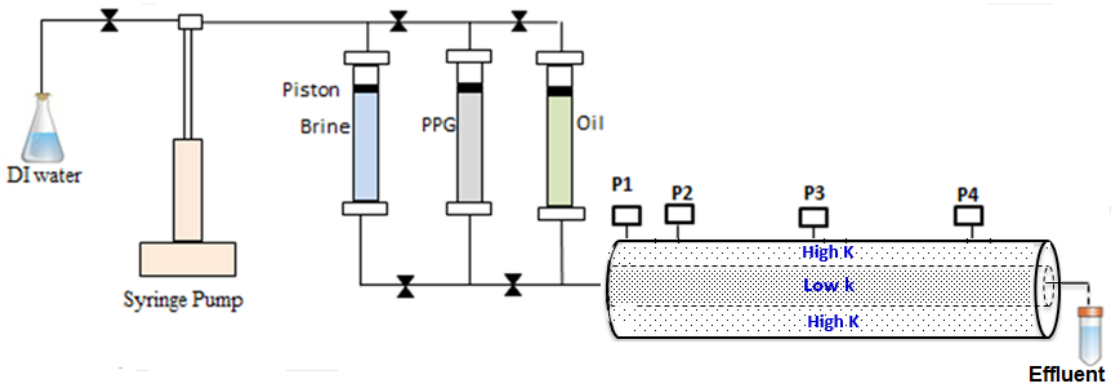

Figure 4-15: Schematic representation of heterogeneous sandpack model with different permeabilities (with crossflow) for PPG injection (Bai, 2014).

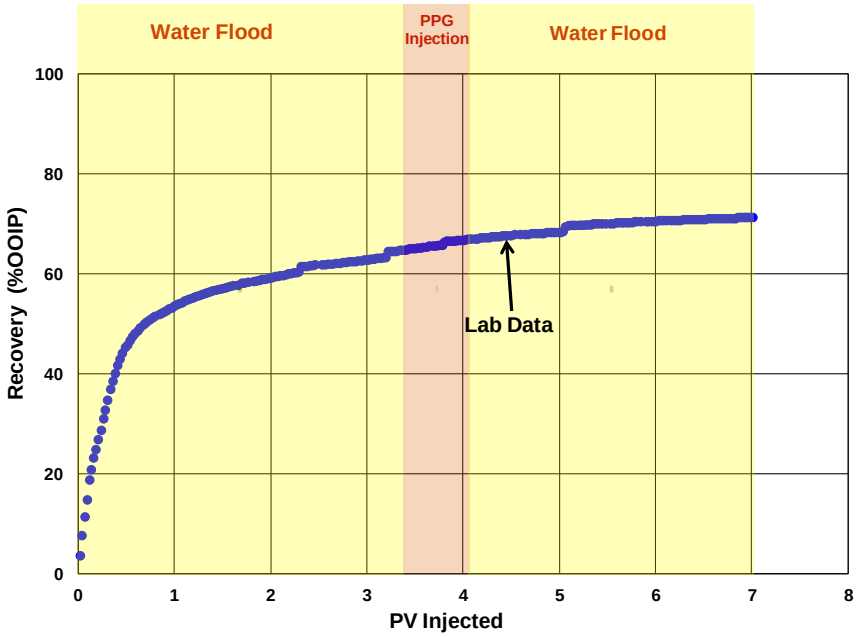

Figure 4-16: Measured oil recovery for heterogeneous sandpack experiment with crossflow (Bai, 2014).

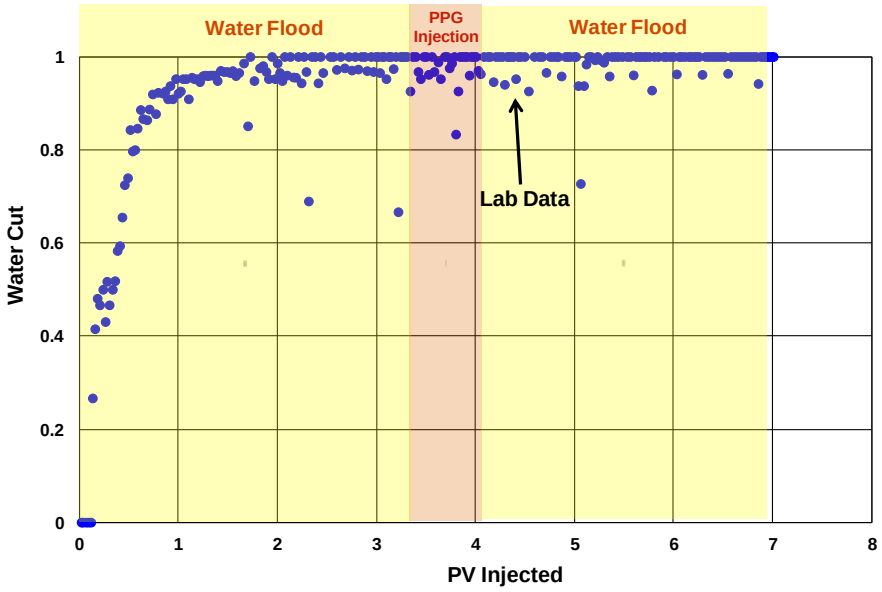

Figure 4-17: Measured water cut for heterogeneous sandpack experiment with crossflow (Bai, 2014).

4.2.6 Nanogel Berea Sandstone Coreflood Experiment

A high permeability Berea sandstone core was used in this study (Figure 4-18). Liquid permeability, pore volume, and porosity of the core were determined by routine core analysis. The core is homogeneous with dimensions of 3.9×3.9×53.1 cm, porosity of 0.23, permeability of 550 mD, and pore volume of 185.1 cm^3.

The microgel used in the work was provided by Poweltec in France. It is crosslinked hydrophilic gel with the particle size of 100-200 nanometers. It was in liquid form with 30 wt% of solid. 1000 ppm microgel composed of 1 wt% KCl brine was prepared using energic stirring (warring blender 11000 rpm for 10 minutes) for coreflooding tests. Figure 4-19 shows the image of particles from ESM (Environmental Scanning Electron Microscope). Figure 4-20 shows the particle size distribution of the microgel prepared by 1 wt% KCl brine at 25 ^{0}C measured by a sysmex FPIA3000 (Malvern) particle size analyzer.

Figure 4-21 shows the experimental set up which consists of one ISCO pump to inject brine, oil, and microgel. A hassler type core holder is designed for the core with the dimension of 3.85×3.85×60 cm. The coreholder has five pressure taps enabling pressure drop measurements at different sections: 12-24 cm, 24-32 cm, 32-36 cm, 36-48 cm, and total length 0-60 cm. The core holder contains rubber sleeve that provides a seal around the core in order to prevent any leakage. The seal is achieved by hydraulic pumping water into the annular space between the rubber sleeve and the core holder outer wall.

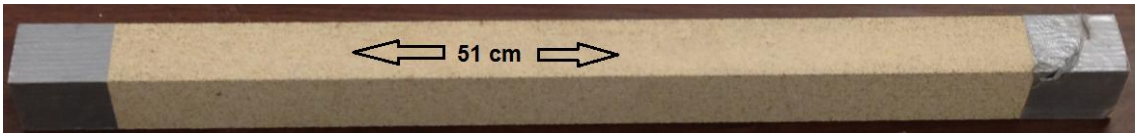

Figure 4-18: The image of the long Berea sandstone core used for gel conformance control study.

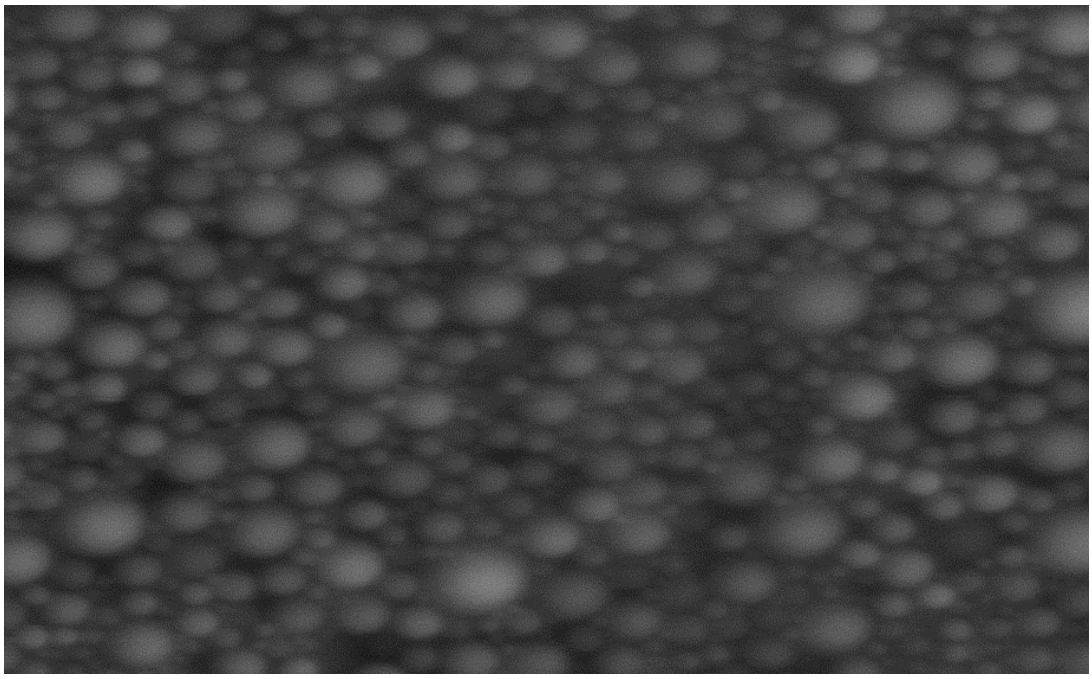

Figure 4-19: The image of the swollen microgel before injection (Bai, 2013).

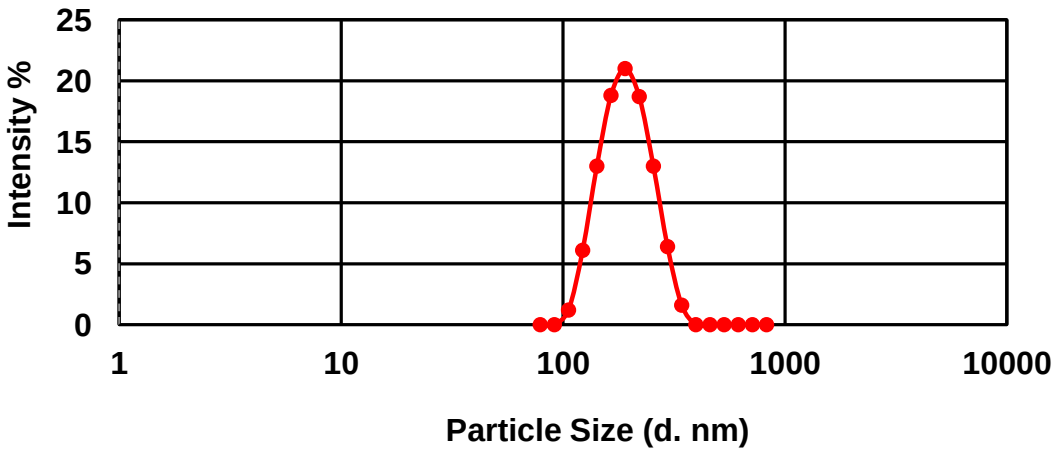

Figure 4-20: Microgel characterization with microparticle distribution analyzer using Sysmex FPIA3000 (Malvern) with a salinity of 10,000 mg/L (Bai, 2013).

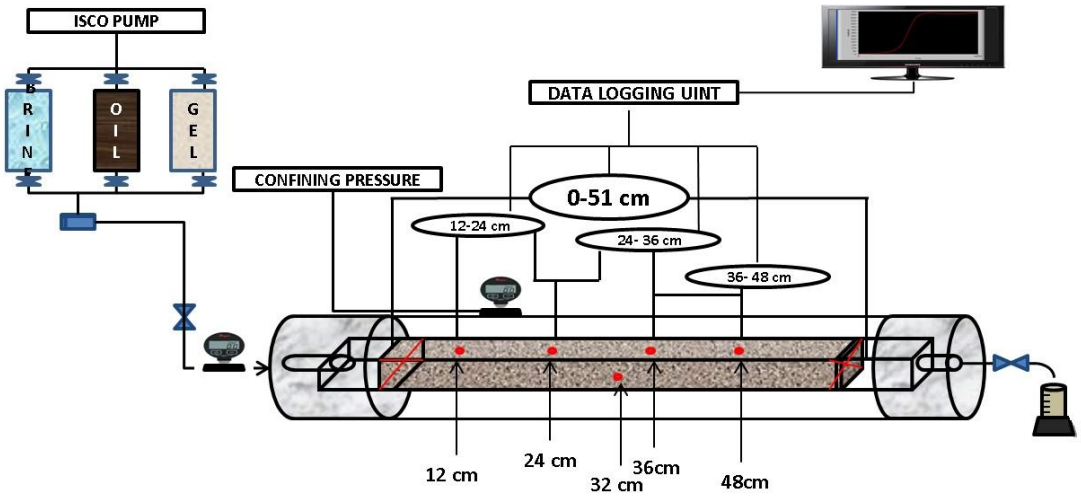

Figure 4-21: Experimental set up used for Berea sandstone coreflood experiment (Bai, 2013).

The experiment is designed to determine microgel propagation, permeability reduction, oil recovery, and water cut. The Berea sandstone core with water permeability of 558.62 mD was used for this experiment at room temperature of 25 ^{0}C. After saturating and preparing the core, it was flooded with 0.97 PV of brine at the flow rate of 1.5 cm^3/min and then flooded with 0.9 PVs of microgel at the rate of 1.5 cm^3/min. Finally, 1.16 PVs of post water was injected again at the same rate of 1.5 cm^3/min. The mineral oil from Fisher Scientific was used for the oil recovery experiment. A brief summary of the experimental procedure is outlined as

- The core was prepared, dry weight was measured and then it was under vacuum for one day.
- The core was saturated with 1 wt% KCl brine and the pore volume was calculated.
- Brine was injected at different flow rates and the absolute permeability was calculated using measured pressure drop.
- Mineral oil was injected at 1.5 cm^3/min to displace water until no water comes out and the oil in place was calculated based on the volume of water displaced.
- Brine was injected at 1.5 cm^3/min rate and the differential pressure with time was recorded. The volume of produced oil was also recorded every few minutes to obtain waterflood oil recovery curve.
- One PV of microgel was injected at the same injection rate of 1.5 cm^3/min. The injection pressure was monitored in each section and the oil production was recorded every few minutes.
- Brine was injected again at 1.5 cm^3/min rate and the pressure behavior, the oil recovered, and water cut were monitored.

The coreflood results of oil recovery and water cut are given in Figure 4-22 and Figure 4-23. Waterflood oil recovery was 40% OOIP and PPG and subsequent waterflood increased the recovery by about 20%. The water cut was reduced from 99% to almost 90% during microgel injection which is a good indication for effectiveness of this microgel in reducing water cut. The experimental results indicated that residual oil saturation was reduced from 0.374 during primary waterflood to 0.289 during microgel injection and finally to 0.223 during post water injection.

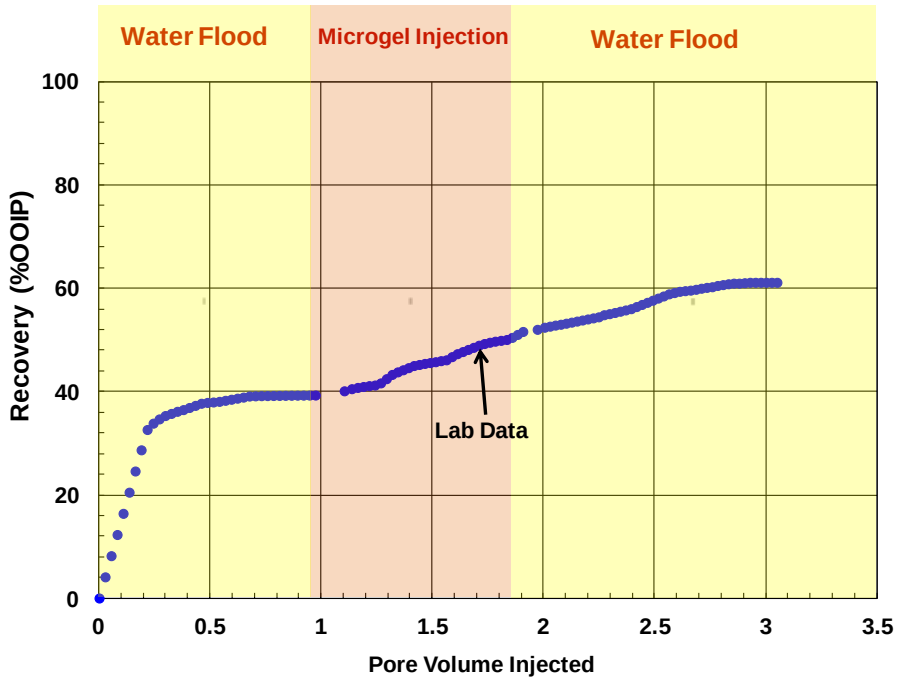

Figure 4-22: Measured oil recovery for Berea sandstone coreflood (Bai, 2013).

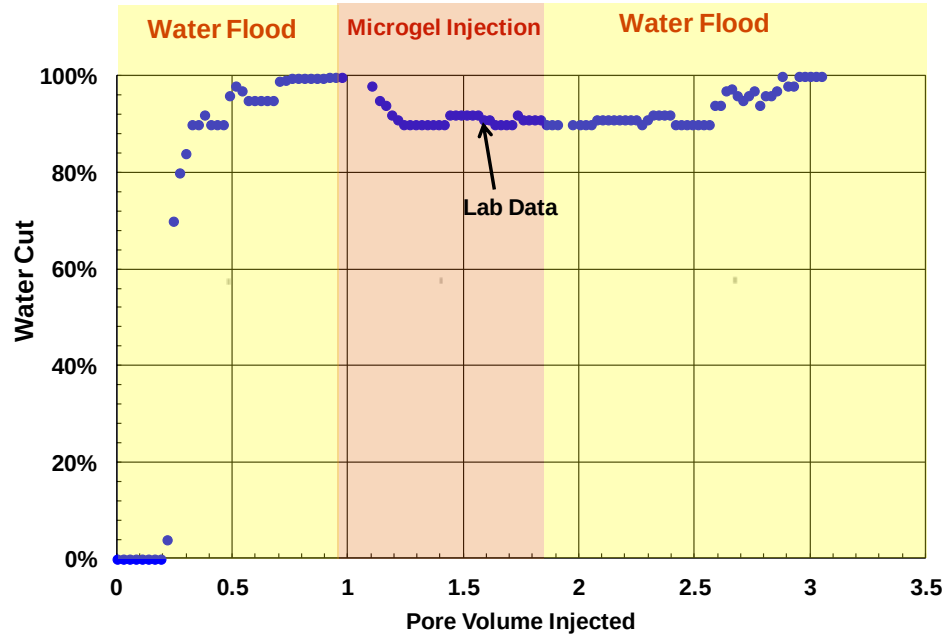

Figure 4-23: Measured water cut for Berea sandstone coreflood (Bai, 2013).

4.3 PPG MODEL DESCRIPTION

4.3.1 PPG Transport Model

There are different conditions for particles to flow and transport through porous media. Viscosity and resistance factor are two important properties for modeling PPG flow in porous media. The resistance factor is a function of salinity and flow rate based on the laboratory results. The swelling ratio and subsequent size of swelled particles are calculated.

The average pore throat radius is calculated using porosity and permeability.

$$r_h = 1.15\sqrt{\frac{8\bar{k}}{\phi}}, \tag{4.2}$$

where the average permeability, $\bar{k}$, is approximated from

$$\bar{k} = \left[\frac{1}{k_x}\left(\frac{u_{x\ell}}{u_\ell}\right)^2 + \frac{1}{k_y}\left(\frac{u_{y\ell}}{u_\ell}\right)^2 + \frac{1}{k_z}\left(\frac{u_{z\ell}}{u_\ell}\right)^2\right]^{-1}, \tag{4.3}$$

where k_x, k_y, k_z are directional permeabilities, $u_{x\ell}, u_{y\ell}, u_{z\ell}$ are components of fluxes in each direction for the aqueous phase and u_ℓ is aqueous phase flux.

In each grid cell, we calculate the pore throat size using Eq. (4.2) and permeability and porosity assigned to that grid cell. PPG will move out of a gridblock depending on the size of particles in comparison to the pore throat diameter assigned to the gridblock. If PPG cannot pass through the gridblock, the resistance factor is calculated and the aqueous viscosity is increased accordingly. The conditions for passing PPG particle through the pore throat for weak and strong PPG particles (Bai *et al.*,

2004b) are as follows:

- For weak PPG particles: If PPG particle diameter is less than $5.7 \times d_p$.
- For strong PPG particles: If PPG particle diameter is less than $1.3 \times d_p$.

Under the above criteria for weak and strong gels, the PPG particles will pass through the pore throat. If above conditions for a specific gridlock hold and PPG can pass through pore throat, gel particles will enter that specific gridblock and resistance to water flow by PPG will happen (Goudarzi *et al.*, 2013, 2014). The PPG will increase the viscosity of aqueous phase and new effective viscosity for water will be calculated as defined below:

$$\mu_{effective} = RF \times \mu_{aqueous\ phase}\ , \qquad During\ \ PPG\ \ Injection \tag{4.4}$$

$$\mu_{effective} = RRF \times \mu_{aqueous\ phase}\ . \qquad During\ \ Post\, Water\ \ Injection \tag{4.5}$$

The resistance factor (RF) is used during PPG injection and residual resistance factor (RRF) is for post water injection and will be explained in more detail later. This increase in water viscosity will lead to reduction of water phase mobility, improvement in mobility ratio, and subsequently delay water production.

4.3.2 Swelling Ratio

Swelling ratio is defined as the ratio of PPG particle volume after and before swelling. Bai (2010) and Imqam *et al.* (2014) reported a relationship for swelling ratio as a function of salinity based on laboratory measurements. They showed that the particles can swell very fast within 60 minutes and the final swelling ratio depends on salt concentration, with higher salt concentration leading to the smaller swelling ratio. It is

presumably due to the static electric repulsive force and charge balance. At low salt concentrations, the electric repulsive force will separate the gel molecules and create more space for water to enter (Bai *et al.*, 2004b).

We developed an empirical correlation for swelling ratio vs. effective salinity to fit their laboratory data.

$$SF = a_p (C_{SEP})^{n_p}, \tag{4.6}$$

where a_p and n_p are model parameters, *SF* is the swelling ratio, and C_{SEP} is the effective salinity $\left(\mathrm{C_{SEP}} = \mathrm{C_5} + \beta_\mathrm{p}\mathrm{C_6}\right)$ in meq/ml which takes into account the combined effect of anions ($\mathrm{C_5}$) and divalent cations ($\mathrm{C_6}$) on swelling ratio. The effect of pH is not considered in this model.

4.3.3 PPG Viscosity

UTGEL models viscosity of aqueous solution containing gel as a function of gel concentration and water viscosity as shown below (Thurston *et al.*, 1987):

$$\mu_1 = \mu_w \left[1 + A_{ppg,1} C_{ppg,1} + A_{ppg,2} C_{ppg,1}^2\right], \tag{4.7}$$

where $C_{ppg,1}$ is the PPG concentration in aqueous phase, μ_w is the water viscosity, and $A_{ppg,1}$ and $A_{ppg,2}$ are model parameters.

4.3.4 PPG In-situ Rheology

The viscosity of gel decreases by increasing shear rate. The relationship between gel viscosity and shear rate is modeled using Meter's equation (Meter and Bird, 1964) as follows:

$$\mu_1 = \mu_w + \frac{\mu_1^0 - \mu_w}{1 + \left(\frac{\dot{\gamma}_{eq}}{\dot{\gamma}_{1/2}} \right)^{P_\alpha - 1}}, \tag{4.8}$$

$$\dot{\gamma}_{eq} = \frac{\dot{\gamma}_c |u_\ell|}{\sqrt{\bar{k} k_{r\ell} \phi S_\ell}}, \tag{4.9}$$

where μ_1^0 is the gel solution viscosity at low shear rate, $\dot{\gamma}_{1/2}$ and P_α are model parameters, $\dot{\gamma}_c$ is the shear rate correction, $|u_\ell|$ is magnitude of flux, and $k_{r\ell}$ is relative permeability of phase ℓ.

The empirical correlations for resistance factor/apparent viscosity are developed based on the measured resistance factor at different salinities, injection rates, and fracture widths. The proposed models use resistance factor as major input parameters with consideration of flow rate and salinity on resistance factor.

4.3.5 PPG Resistance Factor with Salinity Effect

Gel can reduce the water effective permeability where the degree of permeability reduction depends on gel type, salinity, hardness, shear effects, and rock properties. Resistance factor (*RF*) is determined by the ratio of the differential pressure for microgel injection to that of initial water injection as

$$RF = \frac{(k_w/\mu_w)_{BaseWater}}{k_{microgel}/\mu_{microgel}} = \frac{\Delta P_{microgel}}{\Delta P_{BaseWater}}, \quad (4.10)$$

where k_w, $k_{microgel}$ are effective permeabilities during waterflood and microgel injection, and μ_w, $\mu_{microgel}$ are water and microgel viscosities, and ΔP_w, $\Delta P_{microgel}$ are the pressure drop during waterflood and microgel injection.

Measured data for resistance factor as a function of flow rate and salinity for different fracture widths are reported. Table 4-3 gives the empirical correlations developed based on measured resistance factor at different salinities and fracture widths. It is clear that resistance factor decreases as flow rate increases indicating the shear thinning behavior of microgels (Zhang et al., 2010). The viscoelastic behavior of PPG is related to coil structure of polyacrylamide molecules with a flexible nature (Green and Willhite, 1998).

For each fracture width, the coefficient "a_1" varies significantly with salinity but relatively a minor variation in the exponents "b_1". Therefore, an exponential function was used to fit the data as shown in Figure 4-24. We believe that resistance factor is sensitive to the water hardness (i.e. calcium and magnesium concentrations). We have proposed the following correlation but additional laboratory data are required to validate it (Goudarzi *et al.*, 2015).

$$a_1 = a_{11}(C_{SEP})^{a_{12}}. \quad (4.11)$$

The resistance factor is expressed as

$$RF = a_{11}(C_{SEP})^{a_{12}}(\dot{\gamma}_{eq})^{b_1}, \quad (4.12)$$

where a_{11}, a_{12}, and b_1 are model parameters, $\dot{\gamma}_{eq}$ is shear rate, and C_{SEP} is the effective salinity $\left(C_{SEP} = C_5 + \beta_p C_6\right)$ in meq/ml which takes into account the combined effect of anions (C_5) and divalent cations (C_6) on resistance factor. The proposed model considers the effect of shear rate and salinity on resistance factor.

Table 4-3: Resistance factor correlations based on fracture experiments (Zhang and Bai, 2010).

Fracture Width (mm)	Salinity (wt%)	Resistance Factor
0.5	0.05	$RF = 24130\,q^{-0.616}$
	0.25	$RF = 27640\,q^{-0.643}$
	1	$RF = 37976\,q^{-0.731}$
	10	$RF = 46353\,q^{-0.764}$
1	0.05	$RF = 106646\,q^{-0.556}$
	0.25	$RF = 203784\,q^{-0.674}$
	1	$RF = 247784\,q^{-0.689}$
	10	$RF = 311457\,q^{-0.72}$
1.5	0.05	$RF = 207954\,q^{-0.48}$
	0.25	$RF = 291839\,q^{-0.446}$
	1	$RF = 400038\,q^{-0.525}$
	10	$RF = 536435\,q^{-0.585}$

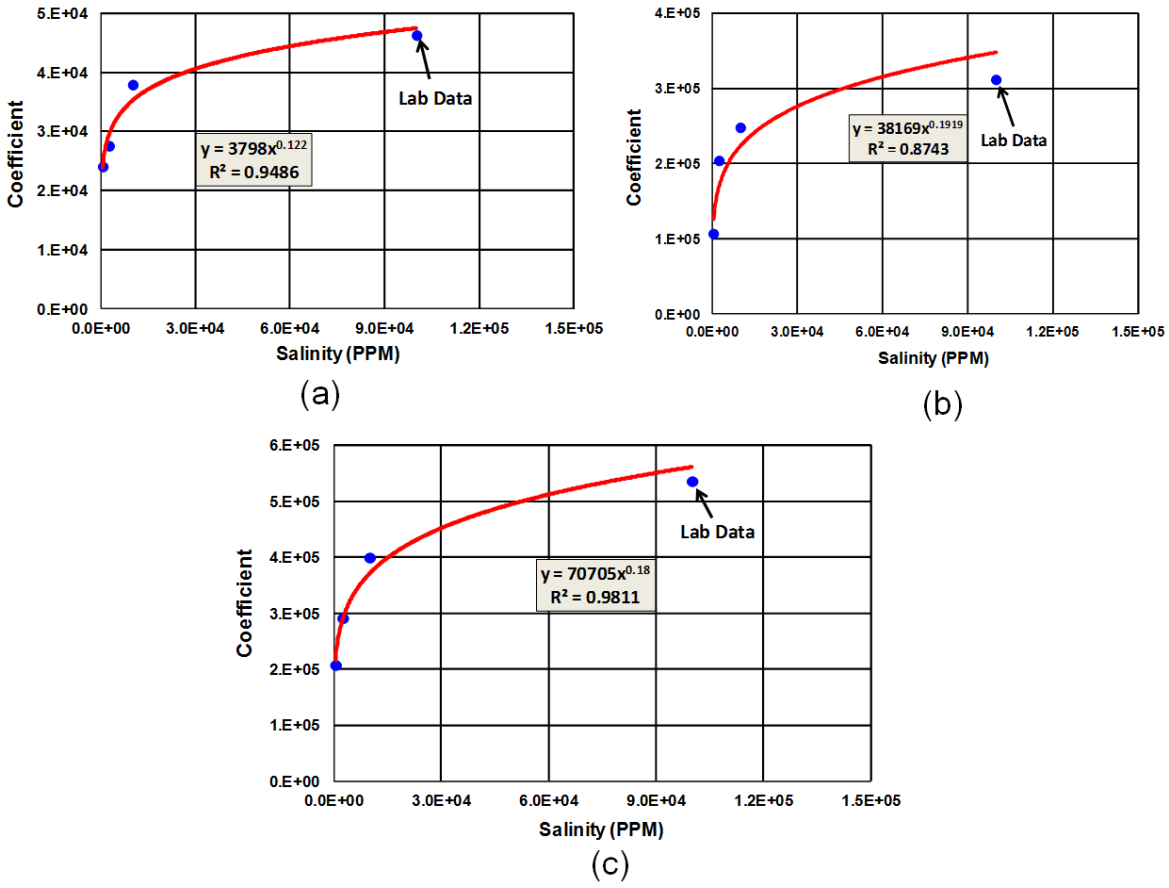

Figure 4-24: Calculated (curve) and measured (points) resistance factor coefficients (a_1) as a function of salinity for different fracture widths: (a) 0.5 mm, (b) 1 mm, (c) 1.5 mm.

4.3.6 Residual Resistance Factor with Salinity Effect

Residual resistance factor, RRF, is defined to ensure that permeability reduction will remain in post water injection. RRF is defined as the ratio of pressure drop during post water injection to the pressure drop during initial waterflood as follows:

$$RRF = \frac{(k_w/\mu_w)_{BaseWater}}{(k_w/\mu_w)_{PostWater}} = \frac{\Delta P_{PostWater}}{\Delta P_{BaseWater}}. \tag{4.13}$$

where $\Delta P_{BaseWater}$, $\Delta P_{PostWater}$ are the pressure drop during initial water and post water injection.

Measured data for residual resistance factor as a function of flow rate and salinity for different fracture widths are reported. Table 4-4 gives the empirical correlations developed using measured residual resistance factor for different salinities and fracture widths. Similar to resistance factor, residual resistance factor decreases as flow rate increases.

The coefficient "a_2" is changing with salinity considerably for each fracture width with minor change in the exponents "b_2". Therefore, an exponential function can be used to fit the data as shown in Figure 4-25. We believe that residual resistance factor is sensitive to the brine hardness (i.e. calcium and magnesium concentrations). We have used the following correlation but need additional laboratory data for validation.

$$a_2 = a_{21}(C_{SEP})^{a_{22}}. \tag{4.14}$$

Accordingly final developed model for resistance factor will be expressed as following:

$$RRF = a_{21}(C_{SEP})^{a_{22}}(\dot{\gamma}_{eq})^{b_2}, \tag{4.15}$$

where a_{21}, a_{22}, and b_2 are model parameters. The proposed model considers combined effects of shear rate and salinity on residual resistance factor.

Table 4-4: Residual resistance factor correlations based on fracture experiments (Zhang and Bai, 2010).

Fracture Width (mm)	Salinity (wt%)	Residual Resistance Factor
0.5	0.05	$RRF = 4439.3q^{-1.057}$
	0.25	$RRF = 5490.4q^{-1.062}$
	1	$RRF = 21766q^{-1.482}$
	10	$RRF = 30776q^{-1.503}$
1	0.05	$RRF = 26980q^{-0.975}$
	0.25	$RRF = 48265q^{-1.155}$
	1	$RRF = 59764q^{-1.199}$
	10	$RRF = 136059q^{-1.418}$
1.5	0.05	$RRF = 76385q^{-1.012}$

4.3.7 PPG Retention Model

A new retention model was developed and implemented into the simulator to consider the PPG retention. UTGEL uses Langmuir isotherm for PPG retention (adsorption) and includes PPG concentration and salinity as shown below:

$$\hat{C}_{PPG} = \frac{a_{14}\left(C_{PPG,1}\right)}{1 + b_{14}C_{PPG,1}}, \tag{4.16}$$

$$\mathrm{a}_{14} = \left(\mathrm{a}_{14,1} + \mathrm{a}_{14,2}\mathrm{C}_{\mathrm{SEP}}\right), \tag{4.17}$$

where $C_{PPG,1}$ is the PPG concentration in the aqueous phase 1 and the parameters $\mathrm{a}_{14,1}$, $\mathrm{a}_{14,2}$, and b_{14} are input parameters.

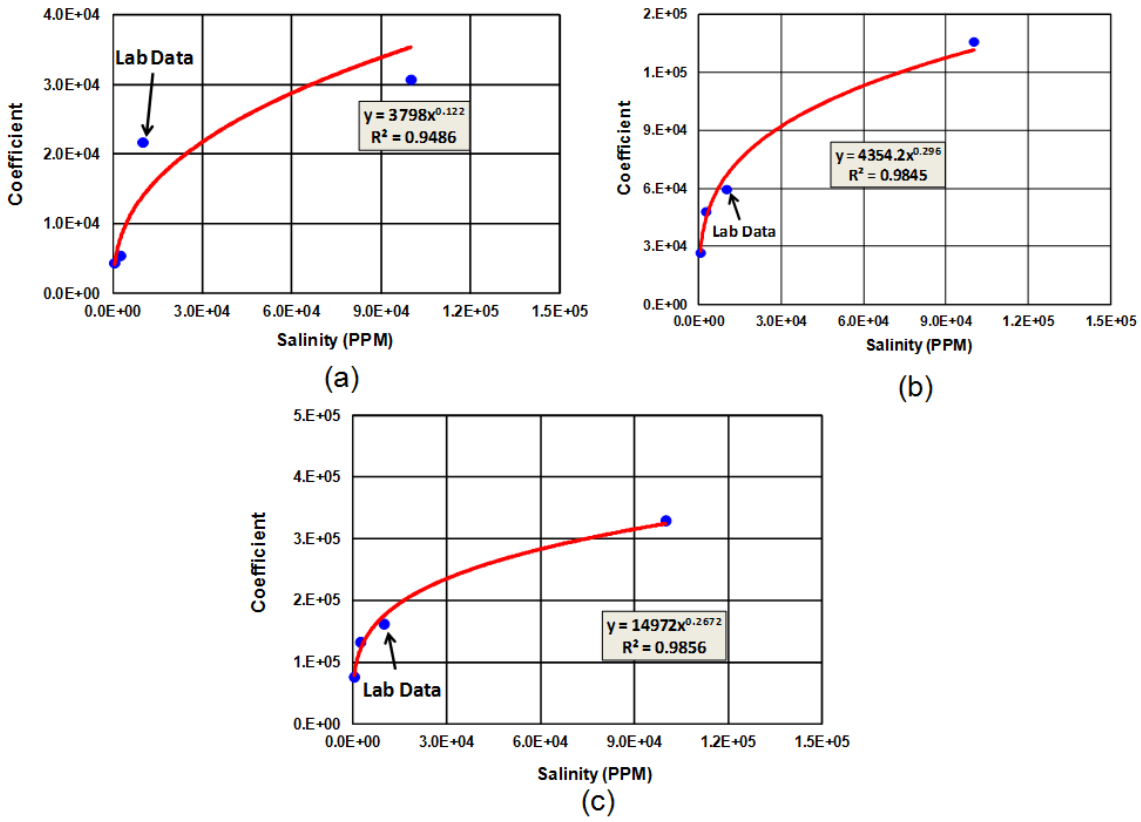

Figure 4-25: Calculated (curve) and measured (points) residual resistance factor coefficients (a_2) as a function of salinity for different fracture widths: (a) 0.5 mm, (b) 1 mm, (c) 1.5 mm.

4.3.8 PPG Transport Kinetics

Wang *et al.* (2012) proposed a novel mathematical model that reflects pore-throat plugging by PPG, particle plugging to reduce the permeability, pressure gradient, throat size, and plugged particle restarting to deform and flow through pore throats. The plugging will happen when PPG particle diameter is larger than the pore throat. However, under the effect of large pressure gradient, the PPG particle will deform and pass through the pore throat. Hence, the net rate of PPG plugging will be the difference between the rate of plugging, r_p, and the rate of restarting of previously plugged particles, r_r (Wang *et al.*, 2013). Therefore the following equation represents a kinetic model for this statement:

$$\frac{\partial \sigma}{\partial t} = r_p - r_r. \tag{4.18}$$

The plugging probability of PPG particles through the pore throat is related to the diameter distribution of PPG and pore throats. The extensive laboratory research showed that PPG diameter has normal distribution after drying, crushing and swelling. The experimental results by Wang (2013) showed that the critical restarting pressure gradient of PPG has exponential relationship with the ratio of particle diameter to pore throat diameter.

$$\nabla p_G = K_A * \exp(K_B * D_{PPG} / 2r_h), \tag{4.19}$$

where K_A, and K_B are model parameters. According to Eq. (4.19), it can be seen that under a pressure gradient less than critical pressure gradient, the plugging will happen and under higher gradient than critical pressure gradient, the particles will pass though the pore throat. Generally, larger particles are trapped first when passing through the pore throat and the concentration of PPG suspension decreases. As PPG particles transport in

the reservoir, the plugging particles will deform and restart if the pressure gradient is higher than critical restarting pressure gradient. The restarting rate is proportional to particle concentration, pressure gradient, and flow rate and the following function can be used to describe the rate of particle restarting r_r of previously plugged particle:

$$r_r = \chi\sigma v_{\mathrm{p}} \frac{\nabla p - \nabla p_{\mathrm{G}}}{\nabla p} \cdot \Theta\left(\nabla p - \nabla p_{\mathrm{G}}\right), \tag{4.20}$$

$$\Theta\left(\nabla p - \nabla p_{\mathrm{G}}\right) = \begin{cases} 0 & \nabla p < \nabla p_{\mathrm{G}} \\ 1 & \nabla p \geq \nabla p_{\mathrm{G}} \end{cases}, \tag{4.21}$$

Where χ is the removal coefficient of plugging particles which is used for characterizing the probability of particles restarting, $\Theta(x)$ is the Heaviside function, v_{p} is the flow velocity, and ∇p is the instantaneous pressure gradient.

The PPG is approximately regarded as a sphere and the expansion is a 3D volume expansion. The swelling of three kinds of PPG is shown in Figure 4-26. It can be seen from the figure that the initial swelling ratio of PPG with water increases drastically with time and tends to reach stable plateau after almost 120 mins. In fact, swelling of PPG and suspension property of particles in solution determines whether the PPG can reach deep into the reservoir to change the flow direction. The experimental results show that PPG swelling can increase to some extent at temperatures above 80 ^{0}C as shown in Figure 4-27.

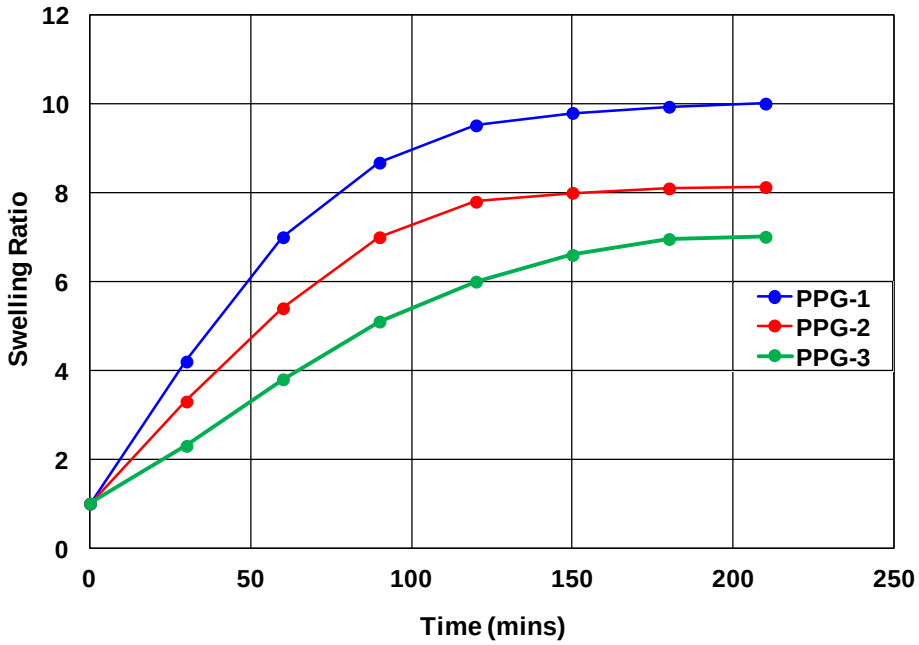

Figure 4-26: PPG swelling as a function of time (Wang *et al.*, 2013).

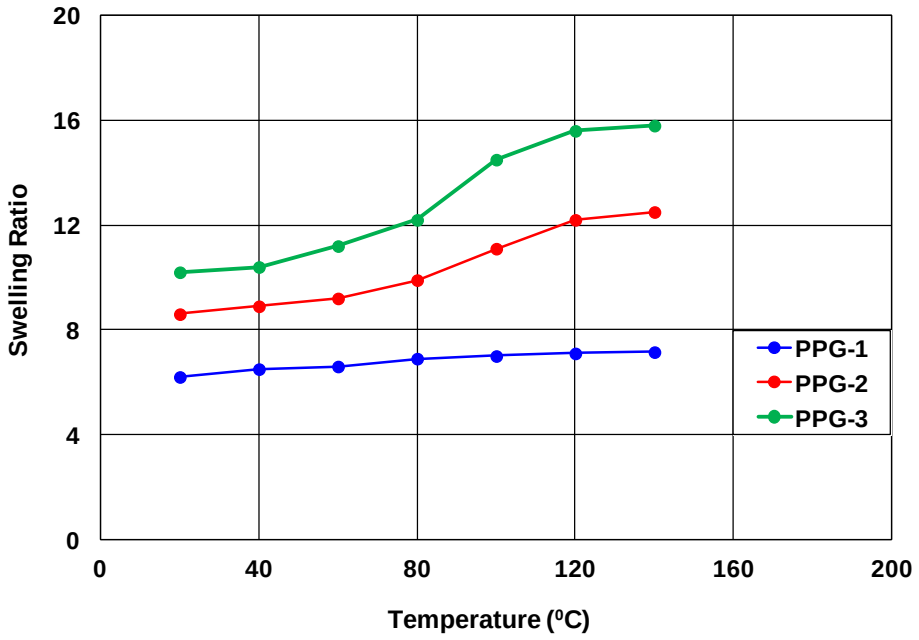

Figure 4-27: PPG swelling dependence on temperature (Wang *et al.*, 2012).

4.3.9 Embedded Discrete Fracture Model (EDFM)

The conformance control processes including PPG treatment are usually performed in mature waterflooded reservoirs which typically contain fractures or very high permeability streaks. Modeling the propagation of PPG through these fractures and conduits was considered as new challenges for this research study. Numerical simulation of fluid-flow in fractured reservoirs is complex due to the large contrast between matrix and fracture permeabilities, the extremely small size of fracture apertures, and the unstructured grid.

Several approaches have been proposed to model fracture networks that can be classified into two major classes of models: Dual continuum (Dual Porosity/Dual Permeability, DPDP) and Discrete Fracture Models (DFM). The Dual continuum models provide an efficient approach to describe highly heterogeneous fractured formations using two domains, one for fracture system and other one for rock matrix. However, they suffer from high degree of simplification in a way that they cannot consider the effect of each fracture explicitly. On the other side, discrete fracture models are limited by unstructured gridding algorithms and simulation times even though they are more accurate. Unstructured gridding imposes more complexity for field-scale simulations (Figure 4-28).

To overcome problems associated with unstructured gridding, a new model has been developed called Embedded Discrete Fracture Model (EDFM). First, Li and Lee (2008) adopted a hierarchical modeling approach to represent fractures with different length scales. Later, Moinfar *et al.* (2013) employed this model to represent fractures with different dip and orientations in GPAS (in-house fully implicit parallel

compositional reservoir simulator). A 3D synthetic illustration of fracture inclination which comprises eight fractures is shown in Figure 4-29.

In this model, fracture planes are discretized by cell boundaries. In fact, for flow in rock matrix, the structured grid is used and unstructured grid is used to model flow in fracture network. The fracture control volumes are considered as non-neighboring connections (NNC). A preprocessing step is developed to locate the fractures and to calculate the transmissibility factors among non-neighboring connections (Cavalcante Filho *et al.*, 2015). Since the fracture control volumes are introduced inside the matrix grid domain, three new connections are defined based on non-neighboring connections. For each of these new connections, a transmissibility factor is calculated as a preprocessing step explained briefly in the following:

a) For matrix-fracture connection (Connection type I)

$$T = \frac{kA}{d}, \tag{4.22}$$

where A is the area of fracture cell inside the grid block, k is the harmonic average of permeability, and d is the normal distance between center of matrix gridblock and fracture cell.

b) For fracture-fracture intersection (Connection type II)

$$\frac{kA}{d} = \frac{T_1 T_2}{T_1 + T_2}, \tag{4.23}$$

$$T_1 = \frac{k_{f_1} \omega_{f_1} L}{d_{f_1}}, \tag{4.24}$$

$$T_2 = \frac{k_{f_2} \omega_{f_2} L}{d_{f_2}}, \tag{4.25}$$

where k is the fracture permeability, ω is the fracture aperture, L is the length of intersection line between two fractures bounded in a gridblock, and the subscripts f_1 and f_2 represent the intersected fracture number 1 and number 2.

c) For fracture-fracture connection of the same fracture plane (Connection type III)

$$T = \frac{kA}{d}, \tag{4.26}$$

where k is the fracture permeability, A is the length of intersection times the aperture, and d is the distance between center of two segments.

The EDFM approach was implemented into UTGEL to provide efficient and robust tool to study the flow of gels in complex fracture system (Shakiba, 2014). The EDFM implementations created a more realistic environment to study the behavior of fractured reservoirs and aid in designing gel injection through fractures and conduits. Taksaudom (2014) investigated the effect of PPG for a complex fracture conduit model which contains many fracture streaks with different dip angles and the results showed that there was approximately 7% improvement in oil recovery with PPG treatment compared to waterflood.

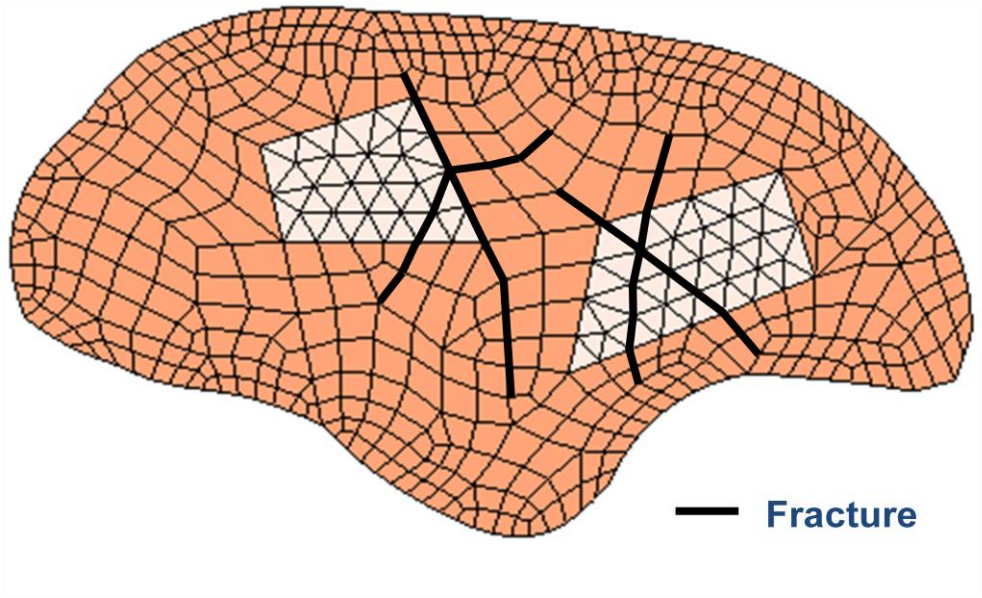

Figure 4-28: Discrete fracture model using unstructured grid.

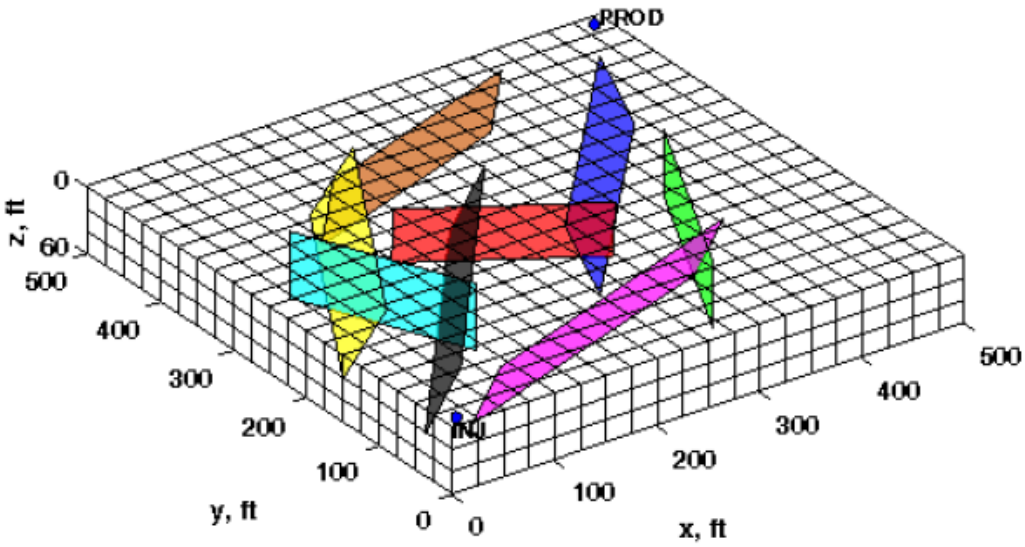

Figure 4-29: A synthetic 3D fractured reservoir with eight inclined macrofractures (Moinfar *et al.*, 2012).

4.4 RESULTS AND DISCUSSION

4.4.1 Simulation of Open Fracture Experiment

A Cartesian 1-D model was set up to simulate the fracture with single phase gel injection (Figure 4-30). Similar to the fracture experiment, six injection rates of 5, 10, 15, 20, 25, and 30 ml/min were selected and the simulation continued until the point where injection pressure became stable at steady state conditions. The PPG injection concentration, swelling ratio, and resistance factor information were selected based on the measured data from the lab. The open fracture media has porosity of one and the permeability was calculated for each fracture width using the equation for laminar flow between two parallel plates. The simulations are done at room temperature with twelve hours simulation time. The injection was at constant rate and production was at constant pressure. Totally, twelve simulations were performed to model the effect of salinity, flow rate, and fracture widths on PPG injection pressure and injectivity.

The injection pressure depends on flow rate, salinity, fracture width, and gel properties. Different simulations were performed to investigate the effect of these properties on injection pressure. Table 4-5 gives the summary of data used for different fracture width simulations. Comparisons of lab data and simulations are shown in Figure 4-31 through Figure 4-33. The comparison of injection pressure shows that there is good agreement between lab data and simulation results. The results demonstrate that PPG injection pressure increases with flow rate and salinity. The injection pressure depends on softness and deformability of swollen PPG particles rather than the particle size and PPG particles are softer and deformable at lower salinity brine which justifies the reason for high PPG injection pressure at higher salinity. The comparison shows that PPG injection

pressure decreases and the fracture width increases. This can be due to more conductivity of fracture at higher widths which lowers the injection pressure.

Table 4-5: Model parameters for the open fracture experiment.

Model	1-Dimensional Cartesian
No. of grids	20×1×1
Δx , Δz	55, 10 cm
Porosity	100 %
Δy (fracture width)	0.5, 1, 1.5 mm
Fracture Permeability	20833, 83333, 187500 Darcy
Water Saturation	100 %
Temperature	25 ^{0}C
Injection Rate (constant rate)	5, 10, 15, 20, 25, 30 ml/min
Outlet Pressure	14.7 psi
Simulation Time	12 hour

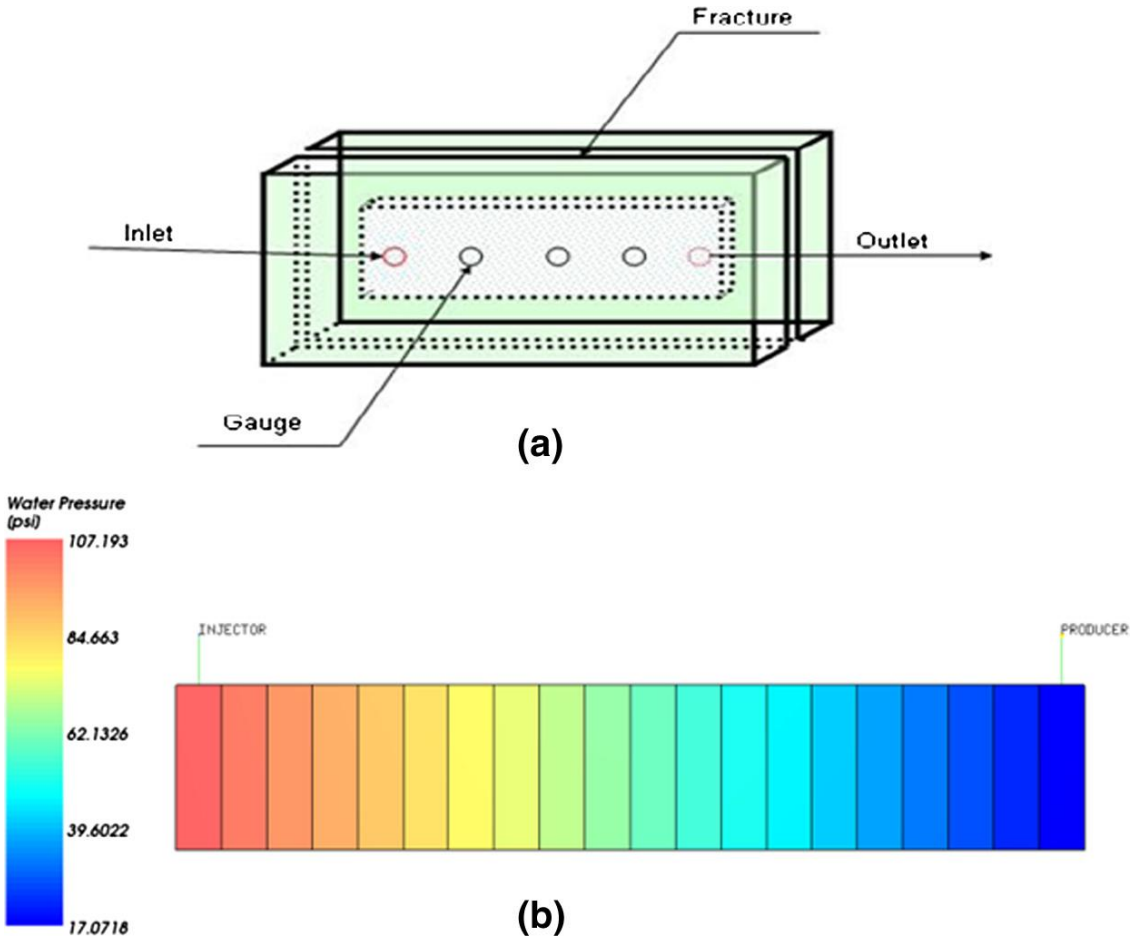

Figure 4-30: Open fracture experiment: (a) experimental setup, (b) simulation model.

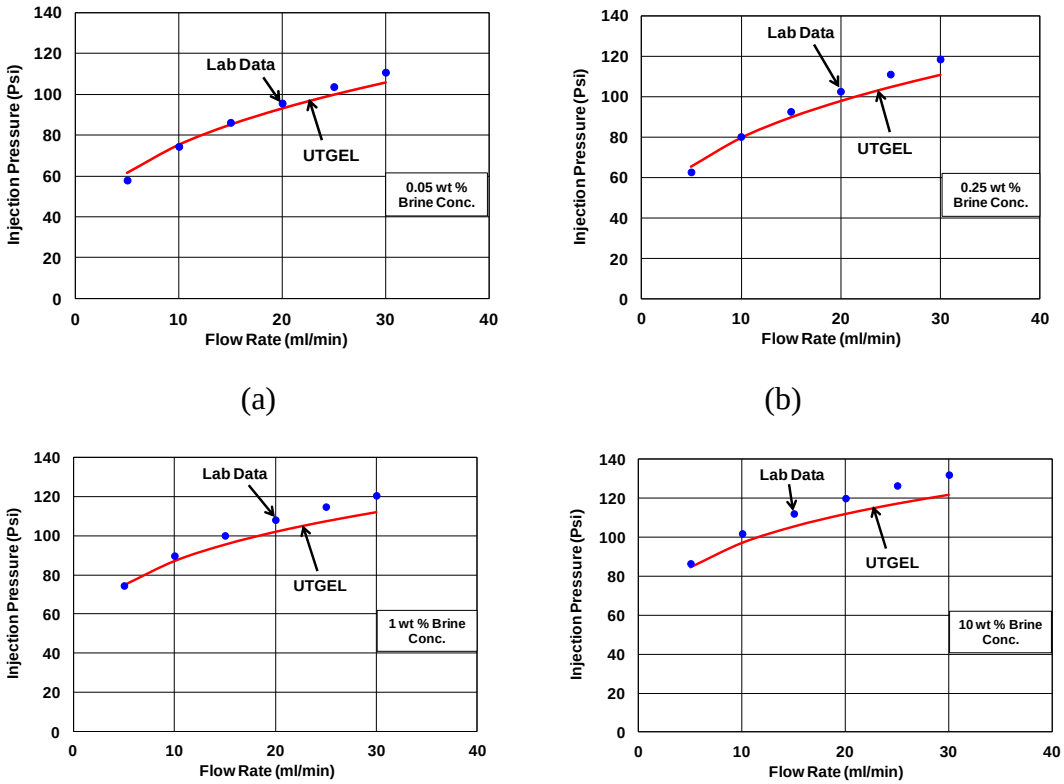

Figure 4-31: Comparison of measured and simulated PPG injection pressures as a function of flow rate for 0.5 mm fracture width:
(a) 0.05 wt.% NaCl, (b) 0.25 wt.% NaCl, (c) 1 wt.% NaCl, (d) 10 wt.% NaCl.

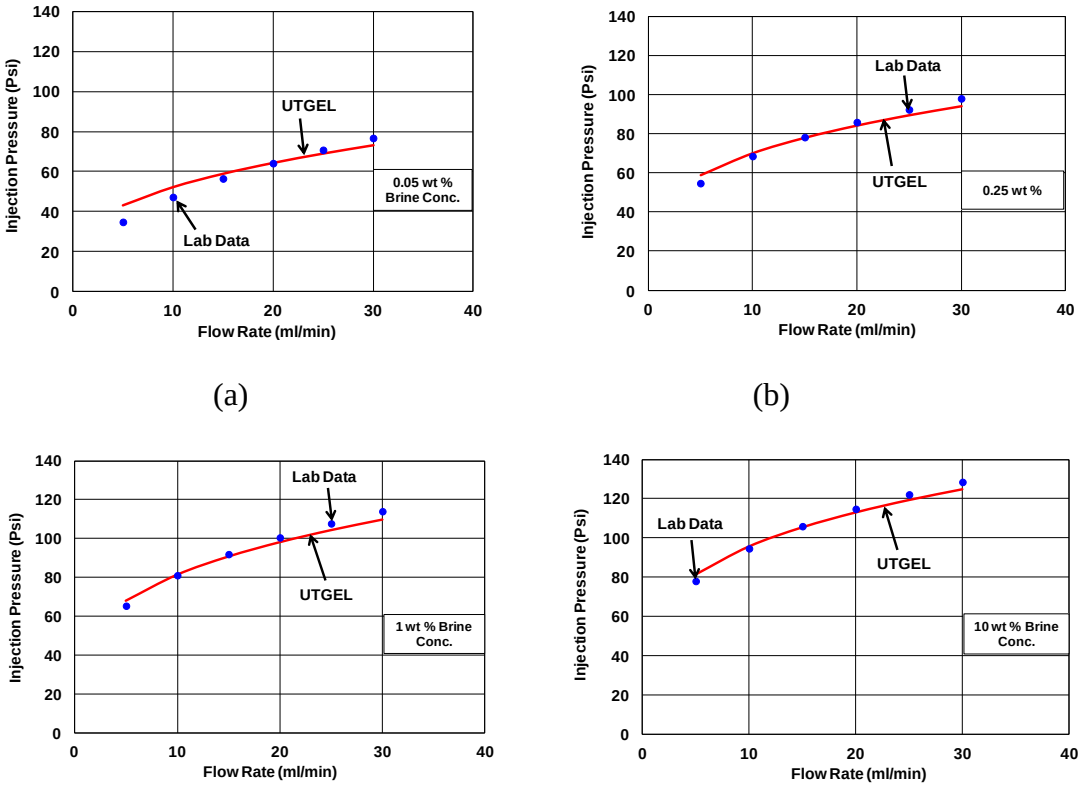

Figure 4-32: Comparison of measured and simulated PPG injection pressures as a function of flow rate for 1 mm fracture width:
(a) 0.05 wt.% NaCl, (b) 0.25 wt.% NaCl, (c) 1 wt.% NaCl, (d) 10 wt.% NaCl.

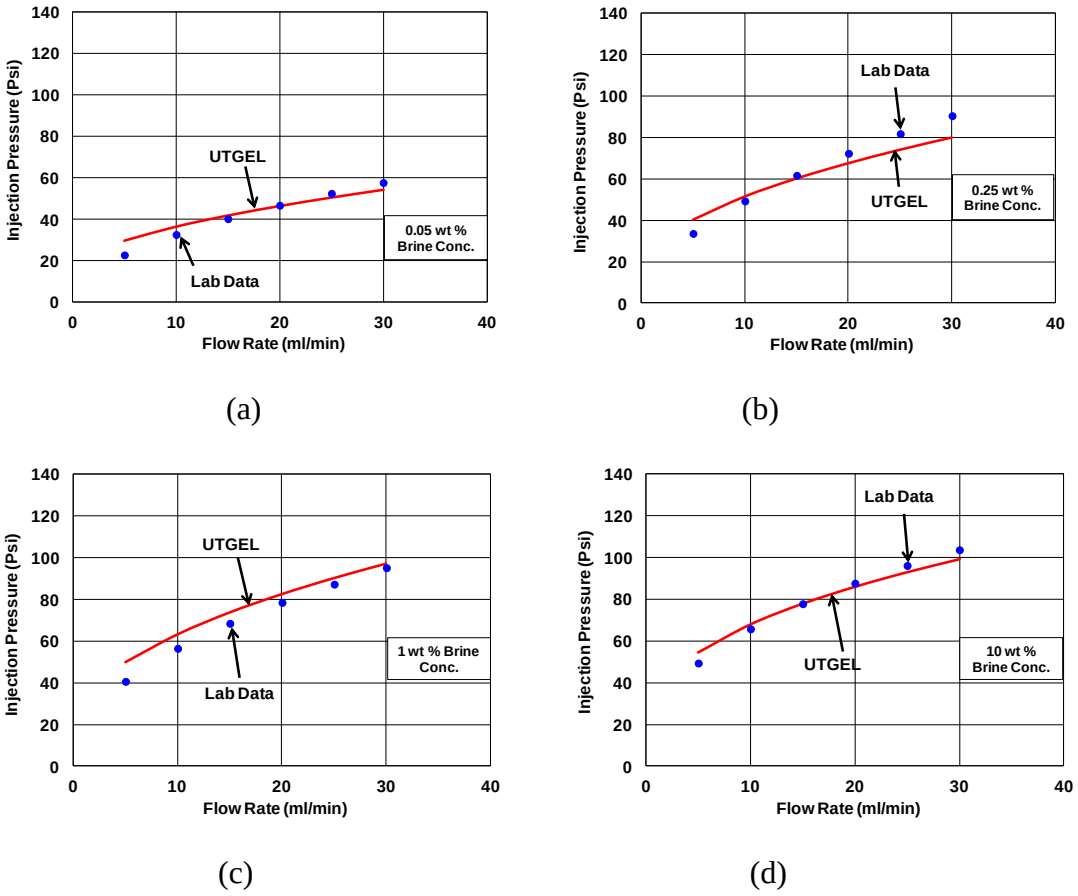

Figure 4-33: Comparison of measured and simulated PPG injection pressures as a function of flow rate for 1.5 mm fracture width:
(a) 0.05 wt.% NaCl, (b) 0.25 wt.% NaCl, (c) 1 wt.% NaCl, (d) 10 wt.% NaCl.

4.4.2 Simulation of Homogeneous Sandpack Experiment

A Cartesian 1-D model was used to simulate the water and PPG injection into the sandpack to history match the measured oil recovery and water cut (Figure 4-34). After packing and saturating the sandpack, it was flooded with 2.5 PVs of brine at a flow rate of 2 ml/min and then flooded with 1.2 PVs of PPG at the rate of 2 ml/min. Finally, 1.7 PVs of post-water was injected at the same rate of 2 ml/min. The mineral oil from Fisher Scientific was used for this experiment. Oil recovery was nearly 81% OOIP. A summary of rock and fluid properties is shown in Table 4-6.

In order to history match the oil recovery and water cut results, parameters were assigned for swelling ratio, resistance factor, and residual resistance factor. The coefficient and exponent parameters for swelling ratio were used based on the lab data to calculate swelling ratio as a function of salinity shown below:

$$SF = 34.26(C_{SEP})^{-0.343}. \tag{4.27}$$

In addition, resistance factor and residual resistance factor parameters were assigned in the INPUT file based on measured data. The following equations for resistance factor (RF) and residual resistance factor (RRF) are used.

$$RF = 203503(C_{SEP})^{-0.52}(\dot{\gamma}_{eq})^{-0.619}, \tag{4.28}$$

$$RRF = 86220(C_{SEP})^{-0.54}(\dot{\gamma}_{eq})^{-1.21}. \tag{4.29}$$

A comparison of measured and simulated oil recovery is shown in Figure 4-35. Water cut is compared in Figure 4-36. The favorable comparison of the simulated and the experimental results indicate that the gel transport model implemented in the simulator can accurately model gel injection behavior.

Table 4-6: Fluid and petrophysical properties for homogeneous sandpack experiment.

Diameter and Length	2.54 cm, 50.8 cm
Porosity, Permeability	0.386, 27290 md
Initial oil Saturation	0.88
Irreducible Water Saturation	0.12
Pore Volume	99.4 cm^3
Temperature	22.5 ^0C
Salinity	1 wt% KCl (0.134 meq/ml)
Mineral Oil Viscosity	37 cp
Residual Oil Saturation	0.265
Duration of Experiment	268 min
Gel flood:	Pore volumes injected:
1 wt% KCl flood	2.5 PV
2000 ppm PPG in 1 wt% KCl	1.2 PV
1 wt % KCl post flush	1.7 PV

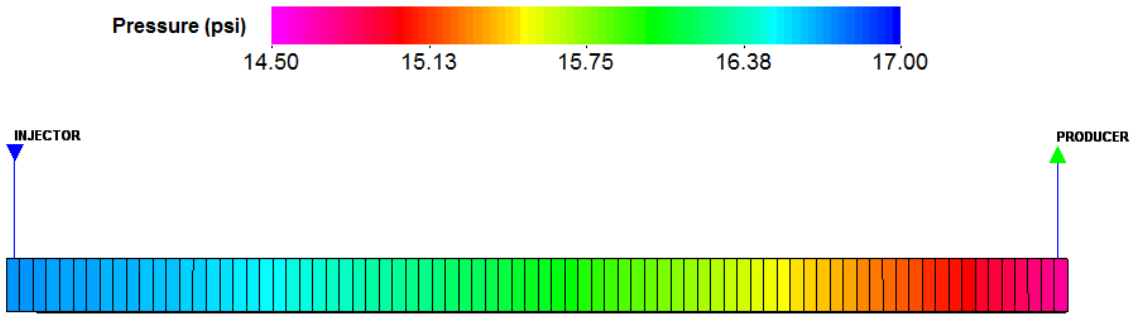

Figure 4-34: The simulation model for homogeneous sandpack experiment.

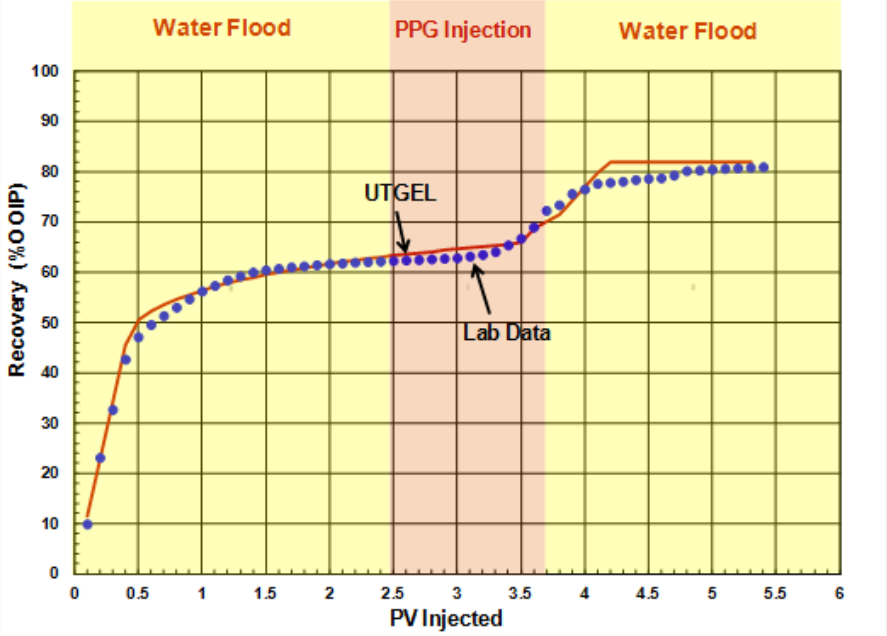

Figure 4-35: Comparison of measured (blue circles) and simulated (red curve) oil recoveries.

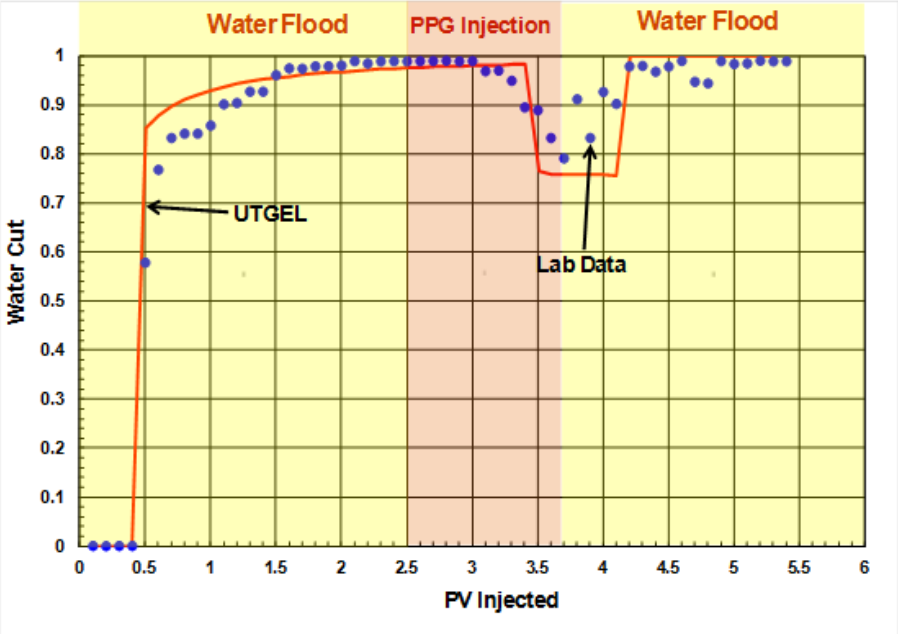

Figure 4-36: Comparison of measured (blue circles) and simulated (red curve) water cuts.

4.4.3 Simulation of Heterogeneous Sandpack Experiment (Without Crossflow)

A Cartesian 2-D model (two layers) was used to simulate the water and PPG injection into the heterogeneous sandpack experiment without crossflow to model and history match the oil recovery and water cut measurements (Figure 4-37). The mineral oil from Fisher Scientific was used. After saturating and preparing both sandpacks, it was flooded with 2.86 PVs of brine at the flow rate of 1 ml/min and then flooded with 0.2 PVs of PPG at the rate of 1 ml/min. Finally, 2.18 PVs of post-water was injected again at the same rate of 1 ml/min. A summary of rock and fluid properties with is given in Table 4-7. Oil recovery was nearly 56% OOIP.

Resistance factor and residual resistance factor parameters were assigned in the input file based on measured data. To model heterogeneous sandpack experiment, the following equations as a function of salinity and flow rate for resistance factor (RF) and residual resistance factor (RRF) are used.

$$RF = 60(C_{SEP})^{-0.52}(\dot{\gamma}_{eq})^{-0.30}, \tag{4.30}$$

$$RRF = 83(C_{SEP})^{-0.54}(\dot{\gamma}_{eq})^{-1.21}. \tag{4.31}$$

Different values of residual oil saturation and relative permeability parameters are used for high and low permeability sandpacks. A comparison of measured and simulated oil recovery is shown in Figure 4-38. Water cut is compared in Figure 4-39. The favorable comparison of the simulated and the experimental results indicates that the gel transport model implemented in the simulator can accurately model gel injection behavior.

Table 4-7: Fluid and petrophysical properties for heterogeneous sandpack experiment without crossflow.

Diameter and Length	2.6 cm, 20 cm
Porosity for each region	0.272 (High perm), 0.375 (Low perm)
Permeability for each region	6778 md (High perm), 1005 md (Low perm)
Initial oil Saturation	0.74 (High perm), 0.82 (Low perm)
Irreducible Water Saturation	0.26 (High perm), 0.18 (Low perm)
Residual Oil Saturation for each region	0.09 md (High perm), 0.32 md (Low perm)
Oil Relative Permeability Endpoint for each region	0.85 md (High perm), 0.68 md (Low perm)
Oil Relative Permeability Exponent for each region	1.6 md (High perm), 2.4 md (Low perm)
Ratio of k_v/k_h	0
Temperature	22.5 ^{0}C
Salinity	1 wt% KCl (0.134 meq/ml)
Mineral Oil Viscosity	195 cp
Duration of Experiment	360 min
Microgel flood:	Pore volumes injected:
1 wt% KCl flood	2.86 PV
2000 ppm PPG in 1 wt% KCl	0.2 PV
1 wt % KCl post flush	2.18 PV

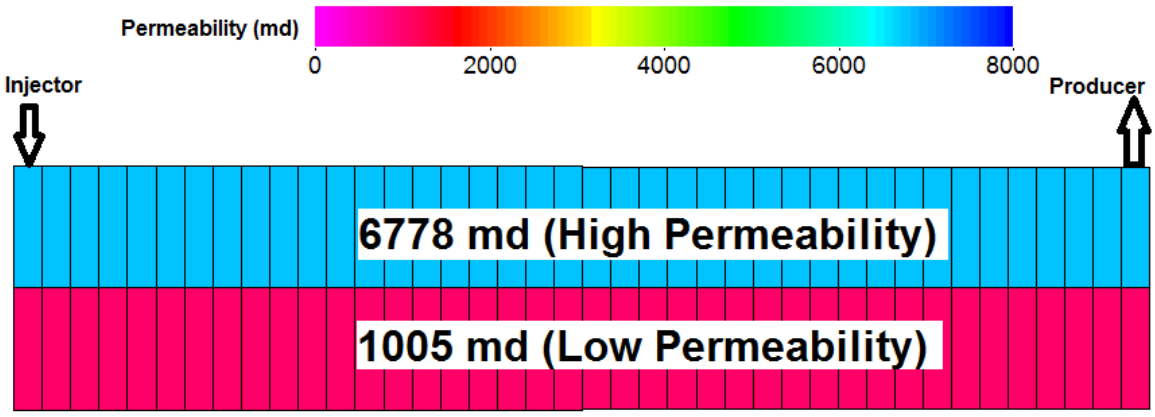

Figure 4-37: The simulation model for heterogeneous sandpack experiment (without crossflow).

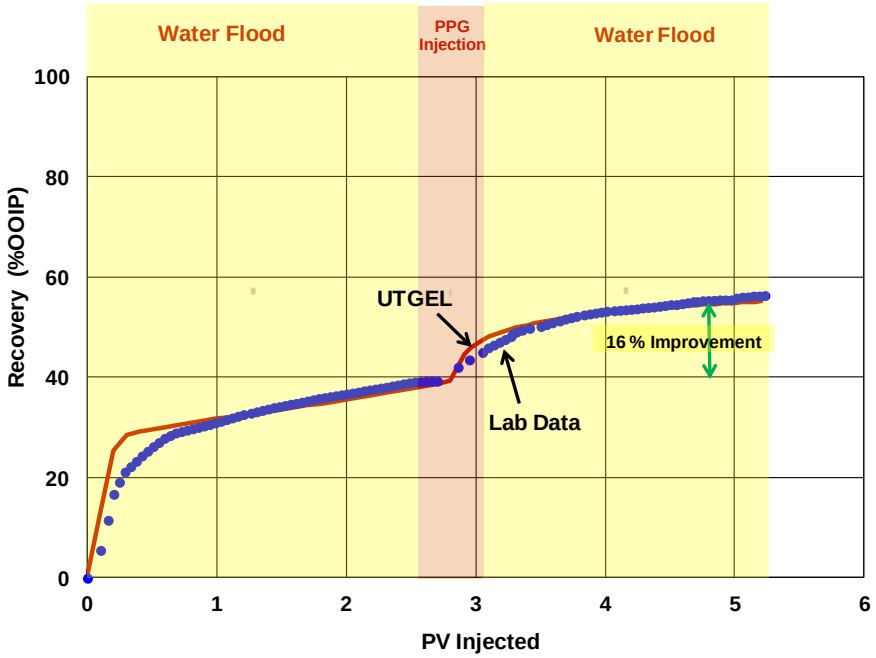

Figure 4-38: Comparison of measured (blue circles) and simulated (red curve) oil recoveries.

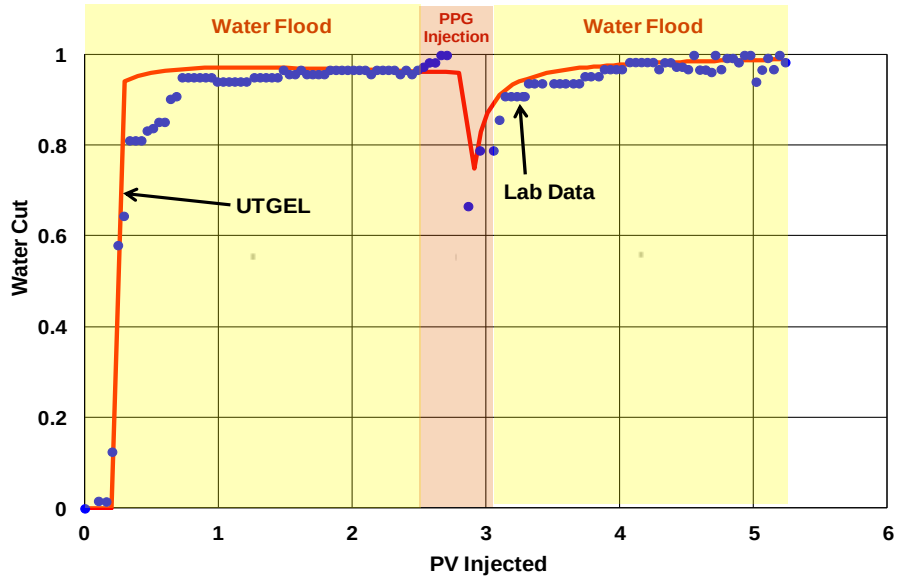

Figure 4-39: Comparison of measured (blue circles) and simulated (red curve) water cuts.

4.4.4 Simulation of Heterogeneous Sandpack Experiment (With Crossflow)

A Cartesian 2-D model (three layers) was used to history match the water and PPG injection into the heterogeneous sandpack experiment with crossflow (Figure 4-40). After preparing and saturating the sandpack with oil to reach irreducible water saturation, it was flooded with 3.19 PVs of brine at the flow rate of 2 ml/min and then flooded with 0.59 PVs of PPG at the rate of 2 ml/min. Finally, 3.23 PVs of post-water was injected again at the same rate of 2 ml/min. The mineral oil from Fisher Scientific was used for this experiment. A summary of rock and fluid properties is shown in Table 4-8. Oil recovery was nearly 71% OOIP.

Different values of residual oil saturation and relative permeability parameters are used for both high and low permeability sandpacks. A comparison of measured and simulated oil recovery is shown in Figure 4-41. Water cut is compared in Figure 4-42. PPG can selectively penetrate into the higher permeability sand while minimizes its penetration into the lower permeability sand or unswept zone. To model heterogeneous sandpack experiment, the following equations as a function of salinity and flow rate for resistance factor (RF) and residual resistance factor (RRF) are used.

$$RF = 47(C_{SEP})^{-0.52}(\dot{\gamma}_{eq})^{-0.32}, \tag{4.32}$$

$$RRF = 73(C_{SEP})^{-0.51}(\dot{\gamma}_{eq})^{-1.27}. \tag{4.33}$$

Table 4-8: Fluid and petrophysical properties for heterogeneous sandpack experiment with crossflow.

Outside Diameter, Inside Diameter and Length	5.08 cm, 2.54 cm, 30 cm
Porosity for each region	0.272 (High perm), 0.375 (Low perm)
Permeability for each region	6778 md (High perm), 1005 md (Low perm)
Initial oil Saturation	0.72
Irreducible Water Saturation	0.28
Residual Oil Saturation for each region	0.09 md (High perm), 0.32 md (Low perm)
Oil Relative Permeability Endpoint for each region	0.85 md (High perm), 0.68 md (Low perm)
Oil Relative Permeability Exponent for each region	1.6 md (High perm), 2.4 md (Low perm)
Ratio of k_v/k_h	0.1
Temperature	22.5 ^{0}C
Salinity	1 wt% KCl (0.134 meq/ml)
Mineral Oil Viscosity	37 cp
Duration of Experiment	867 min
Microgel flood:	Pore volumes injected:
1 wt% KCl flood	3.19 PV
2000 ppm PPG in 1 wt% KCl	0.59 PV
1 wt % KCl post flush	3.23 PV

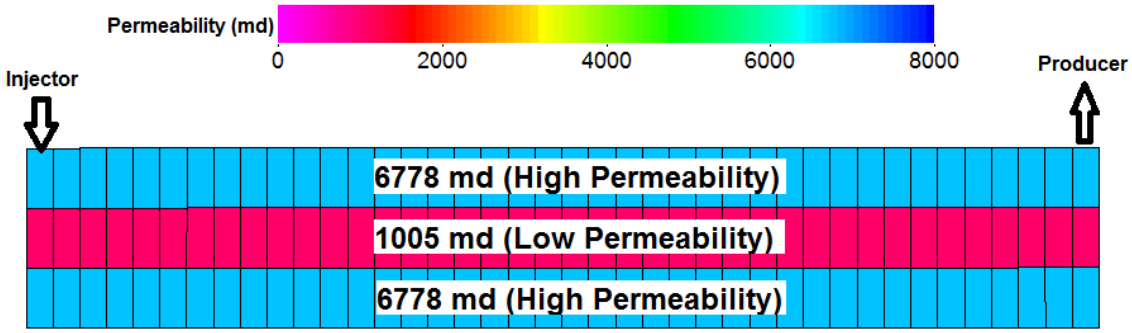

Figure 4-40: The simulation model for heterogeneous sandpack experiment (with crossflow).

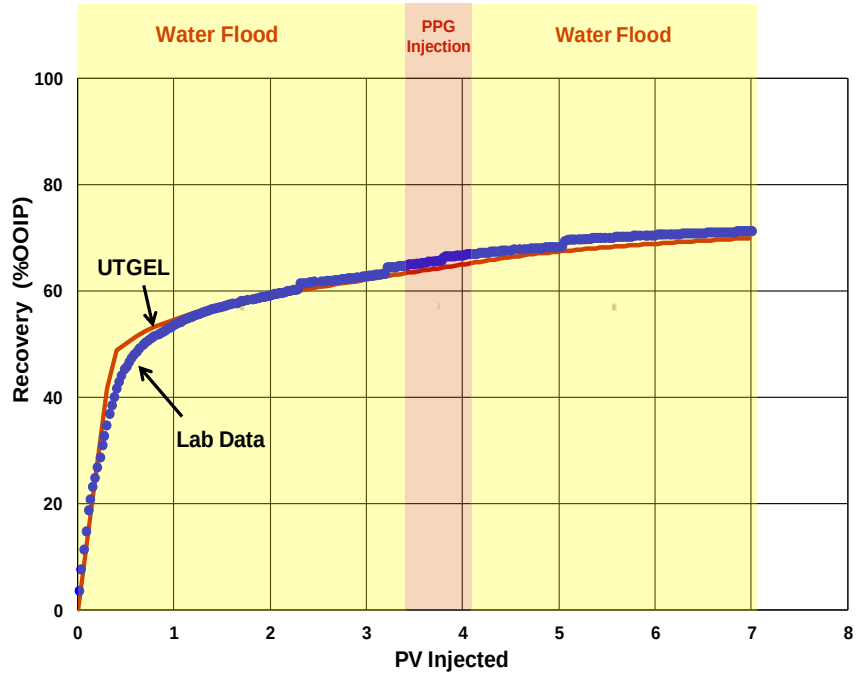

Figure 4-41: Comparison of measured (blue circles) and simulated (red curve) oil recoveries.

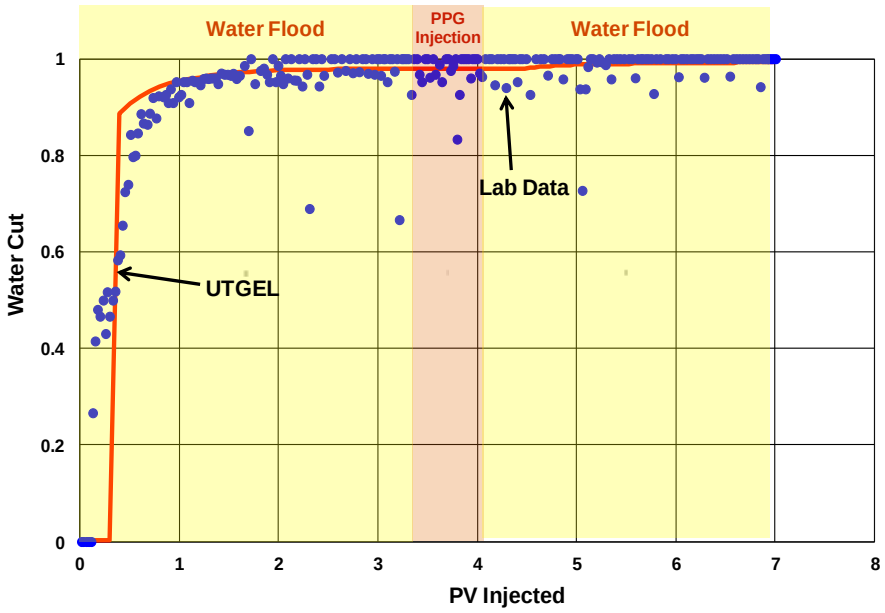

Figure 4-42: Comparison of measured (blue circles) and simulated (red curve) water cuts.

4.4.5 Simulation of Berea Sandstone Coreflood Experiment

1-D numerical model was set up (Figure 4-43) to simulate the water and microgel injection into the Berea sandstone core to history match the measured oil recovery and water cut measurements during both waterflood and microgel injection. A comparison of measured and simulated oil recovery is shown in Figure 4-44 and water cut is compared in Figure 4-45. The comparison shows that simulated oil recovery and water cut were in good agreement with the lab data. The residual oil saturation was reduced by increasing PPG concentration in gridblocks during microgel injection. However, based on experimental results, oil relative permeability endpoint remained constant at 0.654 during whole experiment which shows the minimum effect of microgel on oil relative permeability; the main goal is to reduce water relative permeability. A summary of rock and fluid properties is shown in Table 4-9.

Residual oil saturation measured during gel injection was reduced below that of waterflood. The phenomena have been reported for viscoelastic polymer solutions injected into consolidated cores (Huh and Pope, 2008; Delshad et al., 2008; Li et al., 2014). Many researchers have attributed the effect to increased pressure gradient, pulling effect of elastic polymers, among others. More experimental and theoretical research is required to understand the mechanism causing the reduction in residual oil saturation observed in our PPG experiment. However, in order to history match the oil recovery behavior, we propose a preliminary linear correlation to describe residual oil saturation reduction by increasing gel concentration as

$$w(i) = \frac{C_{PPG,i} - C_{PPG,0}}{C_{PPG,inj} - C_{PPG,0}}, \tag{4.34}$$

$$S_{res,i} = w(i)(S^0_{res,PPG} - S^0_{res,primary}) + S^0_{res,primary}, \quad (4.35)$$

where $C_{PPG,i}$, $S_{res,i}$ are the gel concentration and residual oil saturation in each gridblock, $C_{PPG,0}$, $C_{PPG,inj}$ are the initial and injected gel concentrations, $S^0_{res,primary}$, $S^0_{res,PPG}$ are the residual oil saturation during initial waterflood and end of gel injection. For this experiment, the initial gel concentration in the core, $C_{PPG,0}$, was zero and the injected gel concentration, $C_{PPG,inj}$ was 1000 ppm.

Table 4-9: Fluid and core properties used in microgel experiment.

Width, Height, and Length	2.54 cm, 2.54 cm, 50.8 cm
Porosity, Permeability	0.23, 558.34 md
Initial oil Saturation	0.66
Irreducible Water Saturation	0.34
Pore Volume	185.1 cm^3
Temperature	22.5 ^{0}C
Salinity	1 wt% KCl (0.134 meq/ml)
Mineral Oil Viscosity	37 cp
Residual Oil Saturation	0.374 (Water Inj.), 0.289 (Gel Inj.), 0.223 (Post flush)
Duration of Experiment	376 min
Gel flood:	Pore volumes injected:
1 wt% KCl flood	0.97 PVs
1000 ppm Microgel	0.91 PVs
1 wt % KCl post flush	1.17 PVs

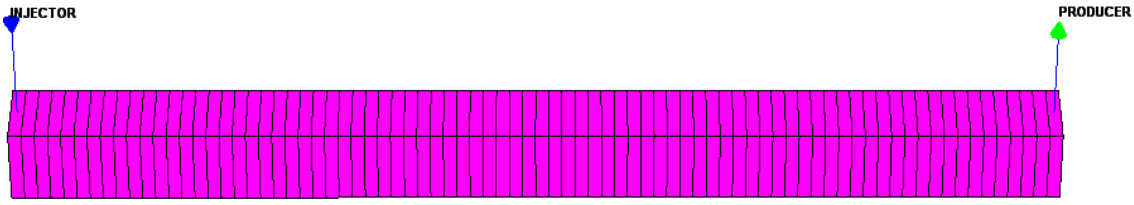

Figure 4-43: The simulation model used for history matching Berea sandstone microgel experiment.

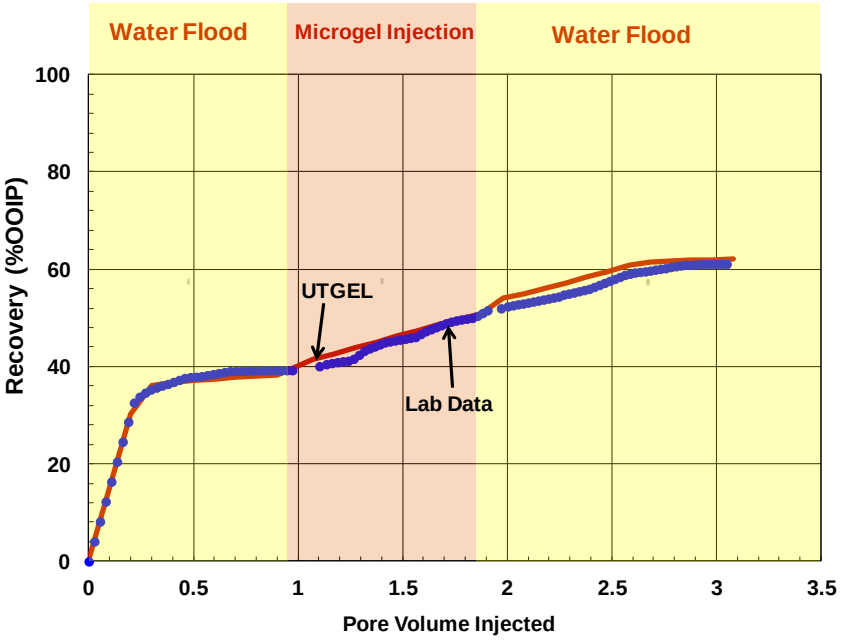

Figure 4-44: Comparison of measured (blue circles) and simulated (red curve) oil recoveries for Berea coreflood.

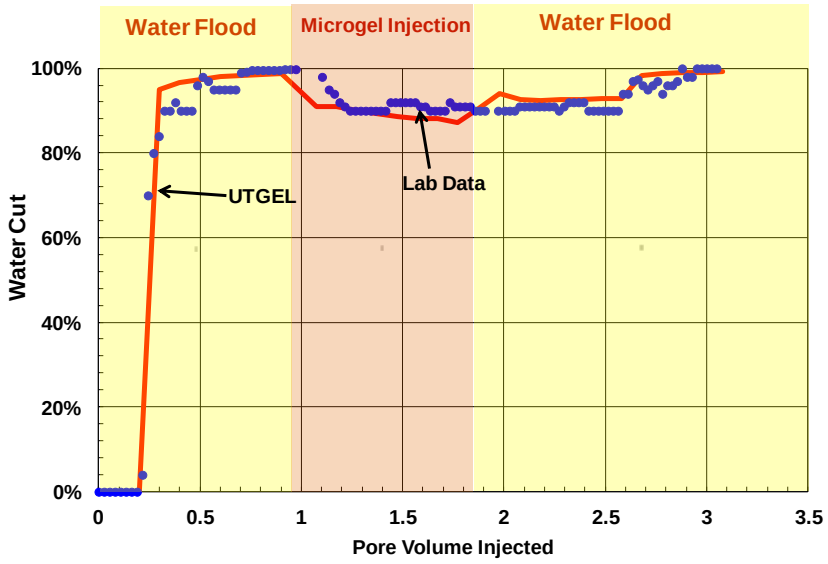

Figure 4-45: Comparison of measured (blue circles) and simulated (red curve) water cuts for Berea coreflood.

4.5 SYNTHETIC SIMULATIONS

4.5.1 Base Case

A Cartesian model was set up to simulate the PPG injection with constant rate injection and production at constant pressure. The base case has a high permeability layer of 1500 md located in the middle and upper and lower layers have a permeability of 50 md (Figure 4-46). Table 4-10 gives the input data including model properties and PPG injection design. Waterflood was compared with PPG flood and the results indicated considerable improvement in oil recovery (around 7% OOIP incremental) and reduction in water cut as shown in Figure 4-47 and Figure 4-48. Oil saturation maps at the end of simulation (2.5 PVs) are shown in Figure 4-49 and Figure 4-50. It is clear from the figures that the layer with higher permeability is more favorable for injected PPG and injected water will divert into upper and lower layers. Several simulations were performed to study the impact of injection design and reservoir properties.

4.5.2 PPG Treatment Size

The typical treatment size is around 5% of the channel volume (CV). However, this can vary from 5% to 15% depending on PPG dilution, vertical to horizontal permeability ratio, and dispersion, among other factors. Figure 4-51 and Figure 4-52 show the incremental oil recovery and water cut sensitivity to gel treatment size. The results demonstrate that higher treatment size is favorable. However, it should be noted that increasing PPG slug above 15% will not have considerable improvement in oil recovery and it will increase cost.

4.5.3 PPG Concentration

The PPG treatment concentration for base case was chosen to be 1000 ppm. However, concentrations of 10,000 and 15,000 ppm were used to investigate the PPG concentration effect on oil recovery. Figure 4-53 and Figure 4-54 show the incremental oil recovery and water cut sensitivity to gel concentration. The results demonstrate that higher PPG concentration is favorable. However, it should be noted that increasing PPG concentration above 15000 ppm will not improve oil recovery.

4.5.4 Permeability Contrast

Permeability contrast between high permeability zone and the rest of the reservoir is one of the key factors affecting the success of conformance treatment. As shown in Figure 4-55, higher contrast in permeability is desirable for better efficiency because thief zone takes more of the injected PPG to divert the flow to the lower permeability zones.

4.5.5 Crossflow

The vertical to horizontal permeability ratio (k_v/k_h) is another factor that can impact the performance of PPG treatment. The lower the k_v/k_h ratio, more PPG will be placed in high permeability with more effective permeability reduction. However, for the large k_v/k_h ratio, PPG can cross flow into low permeability zones, which is undesirable. Figure 4-56 shows the impact of k_v/k_h ratio on incremental oil recovery.

Table 4-10: Base case data used for PPG study and sensitivity simulations.

Model	3-Dimensional Cartesian
No. of Grids	15×15×3
Δx , Δy , Δz	1.5, 1.5, 1.5 m
Porosity and permeability	0.449, (50, 1500, 50) md
Initial Water saturation	30 %
K_v/K_h	0.1
Injection Rate (constant rate)	2.8 m^3/day
Production Pressure (constant pressure)	101.35 Kpa
PPG Concentration	1000 ppm
Waterflood:	**PVs injected:**
1 wt% KCl flood	2.5 PVs
PPG flood:	**PVs injected:**
1 wt% KCl flood	1 PV
1000 ppm PPG in 1 wt% KCl	0.5 PV
1 wt % KCl post flush	1 PV

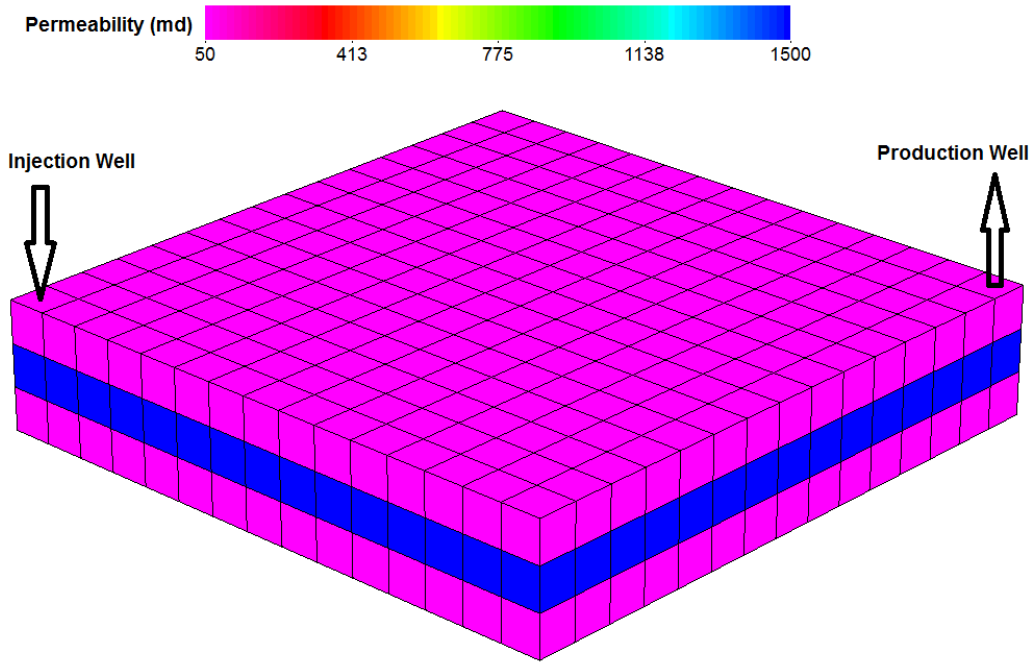

Figure 4-46: Simulation model and permeability representation.

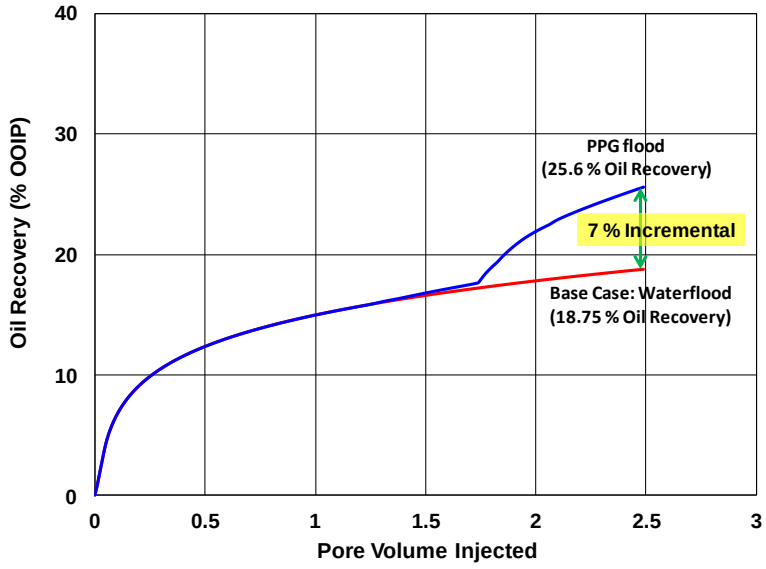

Figure 4-47: Comparison of oil recovery between waterflood and PPG flood for the base case.

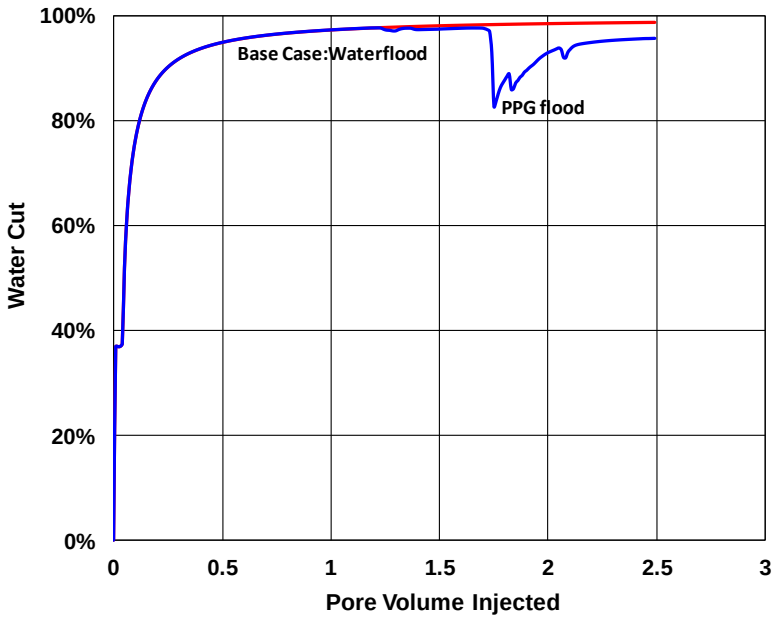

Figure 4-48: Comparison of water cut between waterflood and PPG flood for the base case.

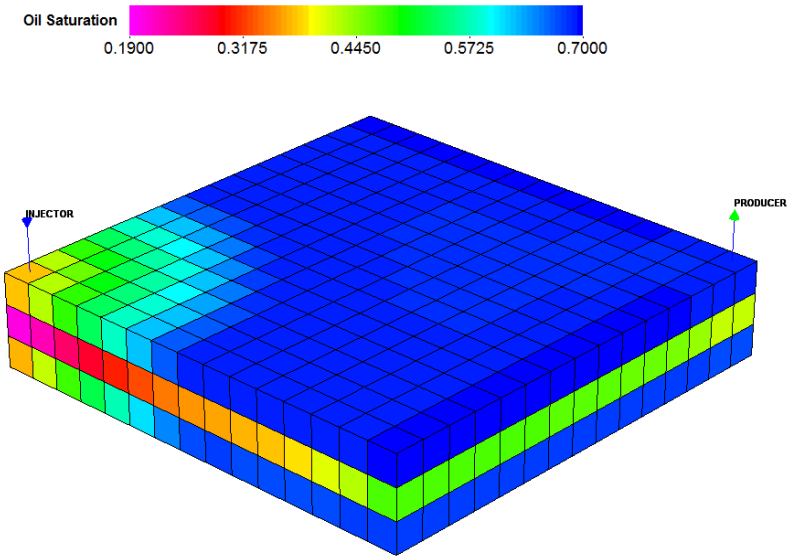

Figure 4-49: Oil saturation after 2.5 PVs for waterflood in the base case simulation.

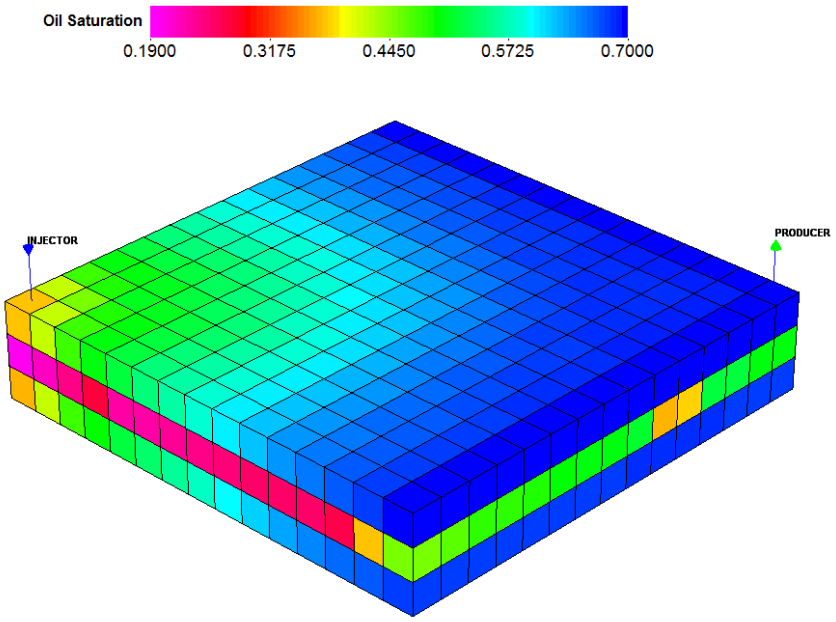

Figure 4-50: Oil saturation after 2.5 PVs for PPG flood in the base case simulation.

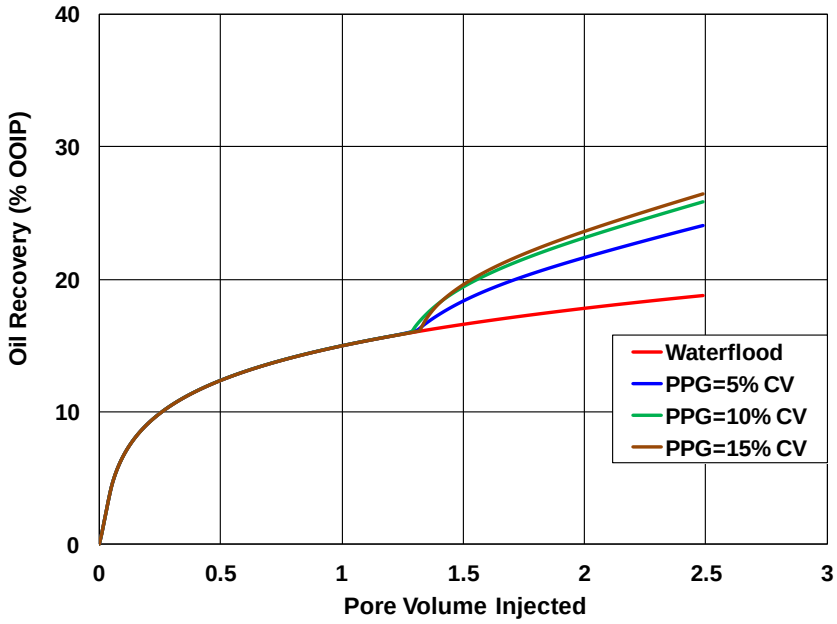

Figure 4-51: Comparison of oil recovery for different treatment sizes.

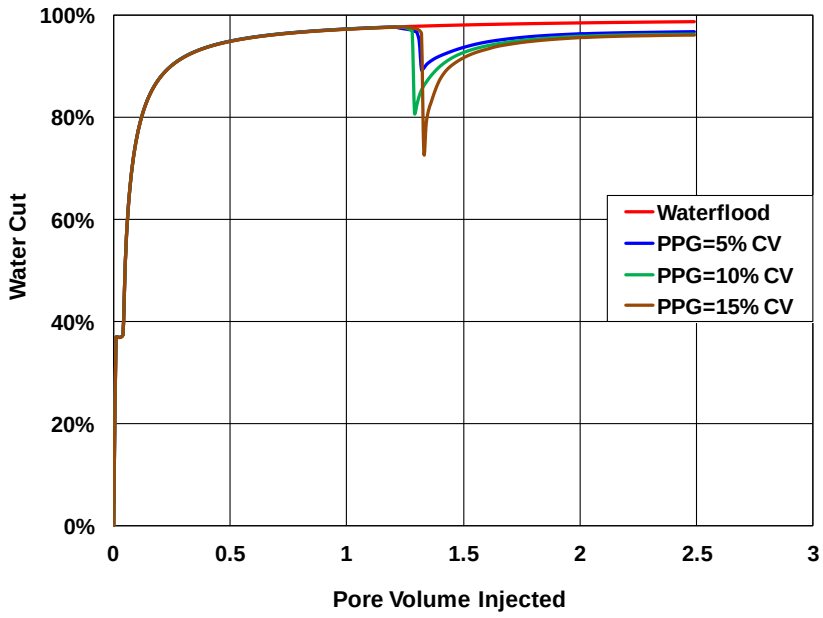

Figure 4-52: Comparison of water cut for different treatment sizes.

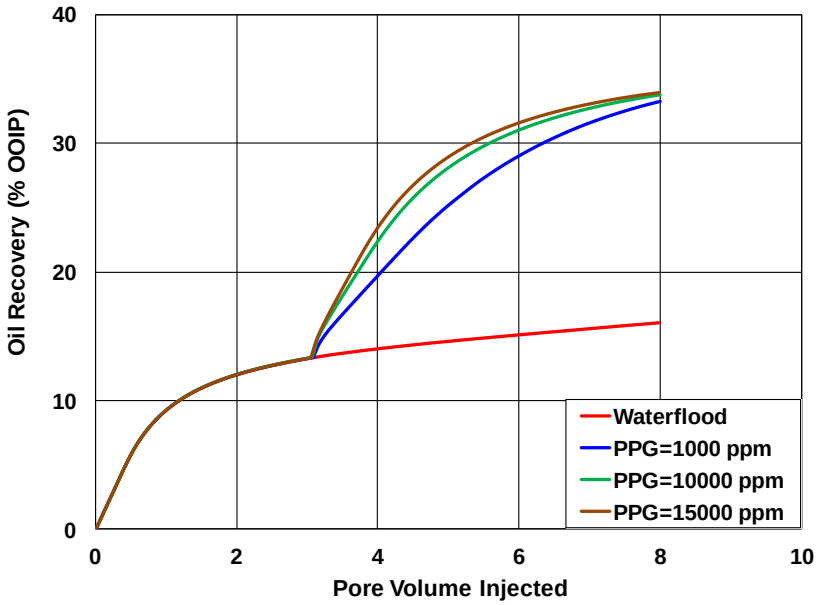

Figure 4-53: Comparison of oil recovery for different PPG concentrations.

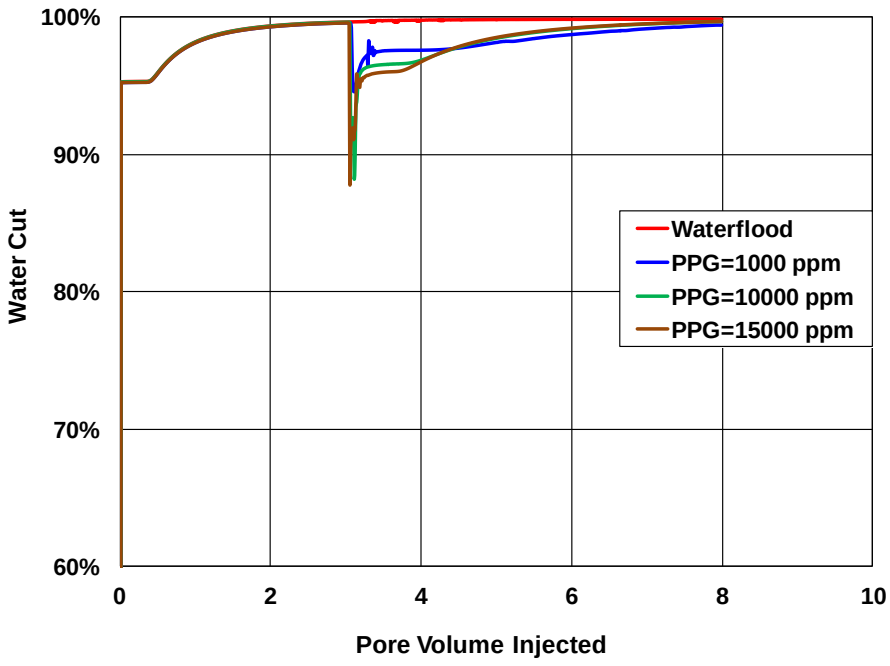

Figure 4-54: Comparison of water cut for different PPG concentrations.

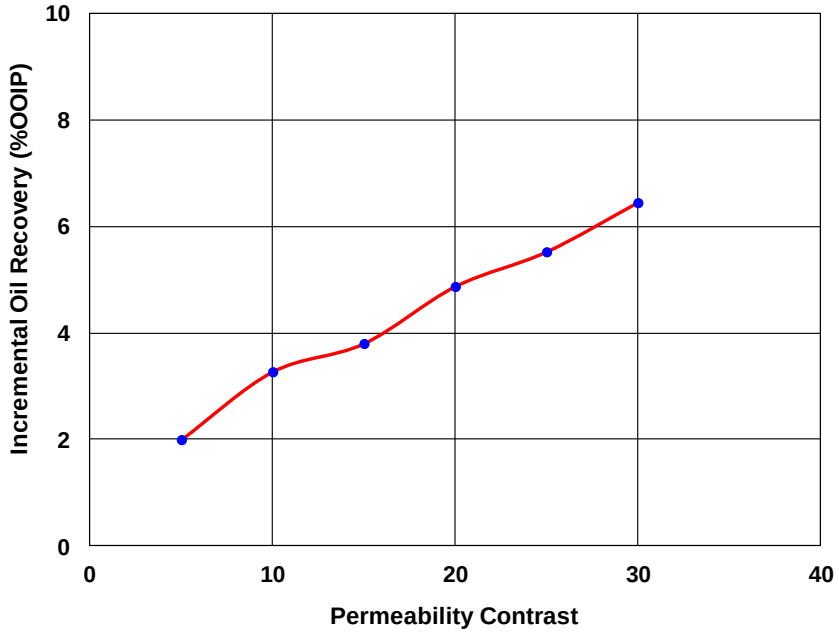

Figure 4-55: Impact of permeability contrast (thief zone and the rest of the reservoir) on incremental oil recovery.

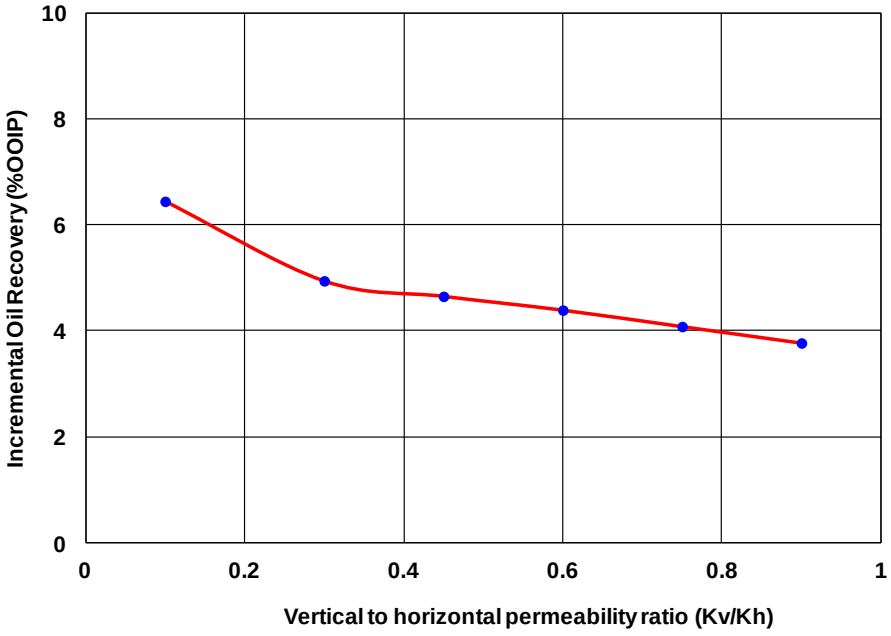

Figure 4-56: Impact of k_v/k_h ratio on incremental oil recovery.

4.6 FIELD-SCALE SIMULATIONS

4.6.1 Karamay Field PPG Conformance Control

The Karamay oil field is an onshore sandstone reservoir in northern China (Delshad et al., 1998). We used the geomodel and well conditions of Karamay as a candidate reservoir for PPG treatment. A pilot area of 42.67×42.67 m2 containing 13 wells was used. The top of the pay zone is at the depth of 289.56 m with a thickness of 10 m. Crude oil and water viscosities at the reservoir temperature of 60 °C are 17.2 and 0.9 cp, respectively. The pay zone has three geological layers and stochastic permeability maps were generated for each layer by use of the matrix-decomposition method and conditioned to the well data (Figure 4-57). The pay zones are isolated from each other by non-communicating shale layers. A Cartesian model with 19×19×3 gridblocks in X, Y, and Z directions is used for this field study. Table 4-11 gives the reservoir and fluid properties. Figure 4-58 shows initial oil saturation distribution. The PPG input parameters were chosen based on measured experimental data. The simulation includes 100 days of waterflood followed by PPG flood for 300 days and followed by post water injection for 600 days.

The comparison of oil recovery and water cut with and without PPG treatment are shown in Figure 4-59 and Figure 4-60. Oil recovery increases by about 14% with significant reduction in water cut using PPG. The success of PPG can be related to heterogeneity of reservoir in which the middle layer has the highest permeability compared to the other two and this made it possible for PPG to block the high permeability gridblocks and water diverts into low permeability zones. The oil saturation distribution after 400 days of waterflood and PPG flood in Figure 4-61 and Figure 4-62

clearly shows that PPG improved sweep efficiency considerably and most of the reservoir oil was produced. However, salinity, temperature, particle sizes, and reservoir heterogeneity control how far PPG propagates into the formation from the injection well. The PPG concentration and also resistance factor at the end of PPG flood (400 days) are shown in Figure 4-63 and Figure 4-64.

Table 4-11: Karamay field and fluid properties for PPG field scale conformance control study.

Model	3-Dimensional Cartesian
No. of grids	19×19×3
Δx, Δy, Δz	10, 10, (3-6-3) m
Reservoir Porosity	0.3
Initial Reservoir Pressure	12238 Kpa
Oil and Water Relative Permeability Endpoint	0.95, 0.20
Temperature	60 ^{0}C
Crude Oil Viscosity	40 cp
Simulation Time	1000 days
PPG Design:	**Time injected:**
Waterflood	100 Days
PPG flood with Concentration of 1000 ppm	300 Days
Post Water Injection	600 Days

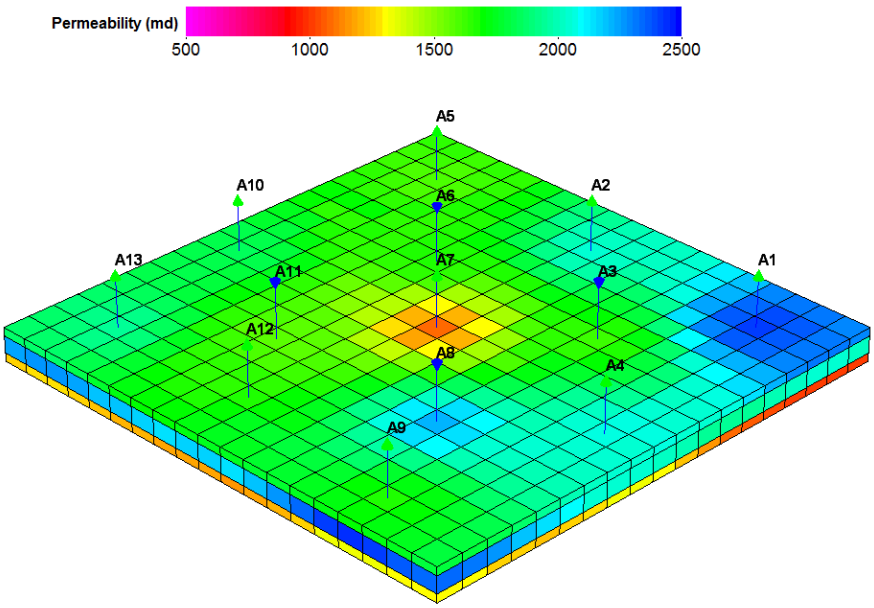

Figure 4-57: Permeability distribution in Karamay field.

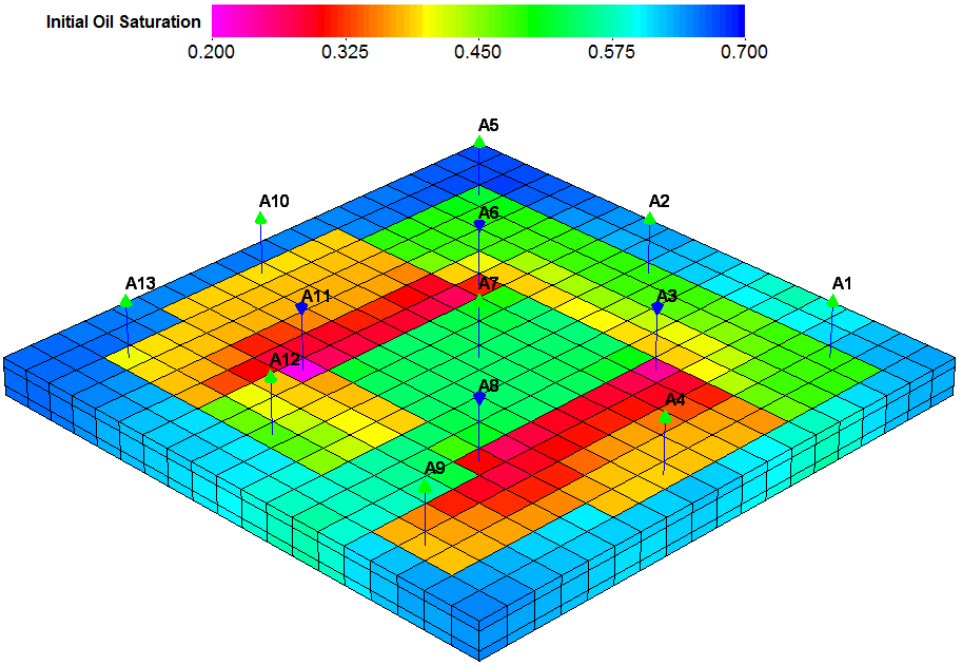

Figure 4-58: Initial oil saturation distribution in Karamay field.

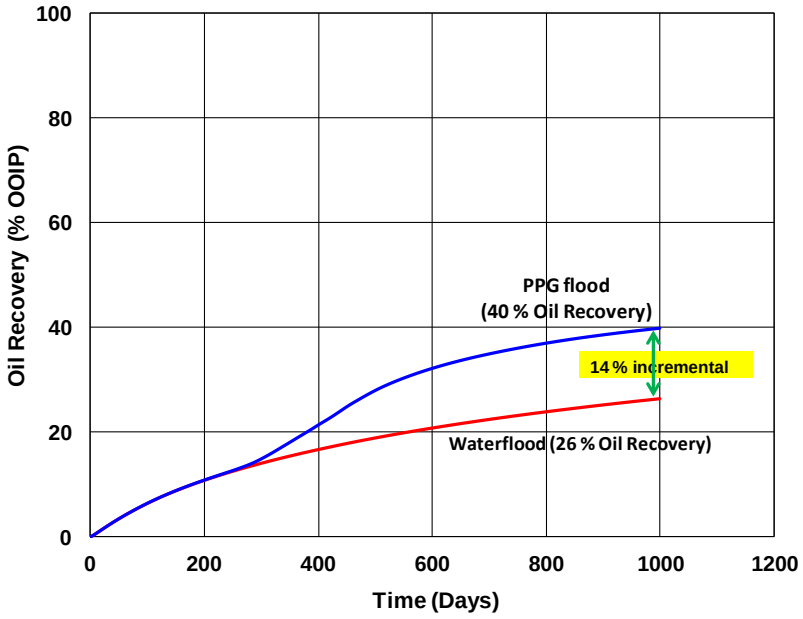

Figure 4-59: Comparison of waterflood and PPG flood oil recoveries in Karamay oil field.

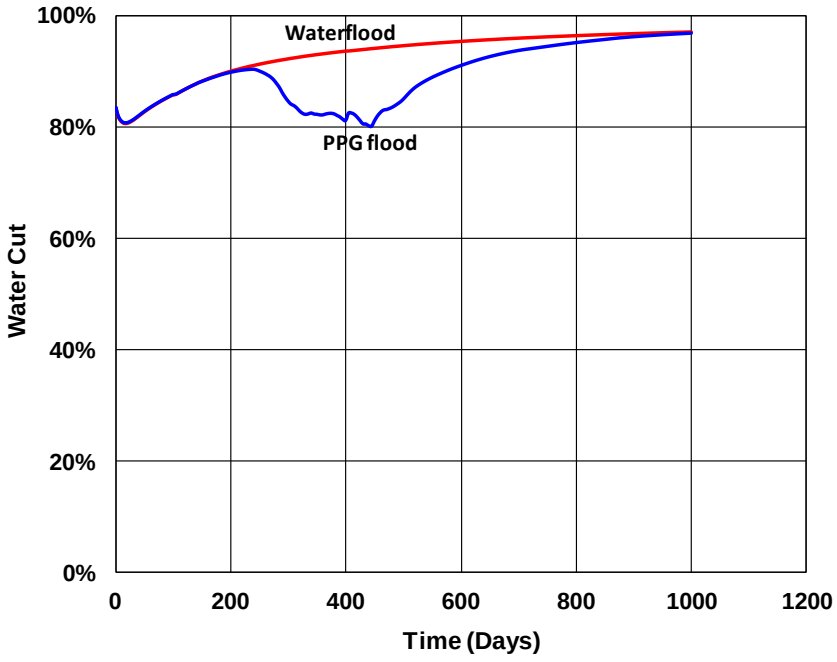

Figure 4-60: Comparison of waterflood and PPG flood water cuts in Karamay oil field.

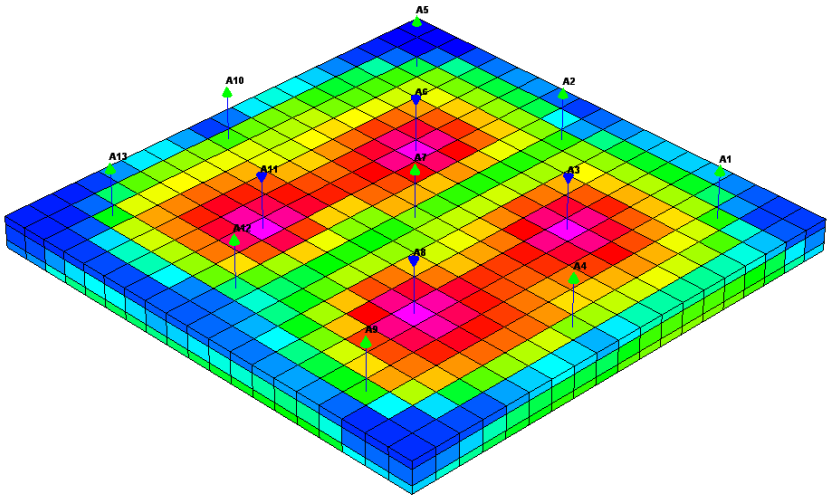

Figure 4-61: Oil saturation after 400 days for waterflood.

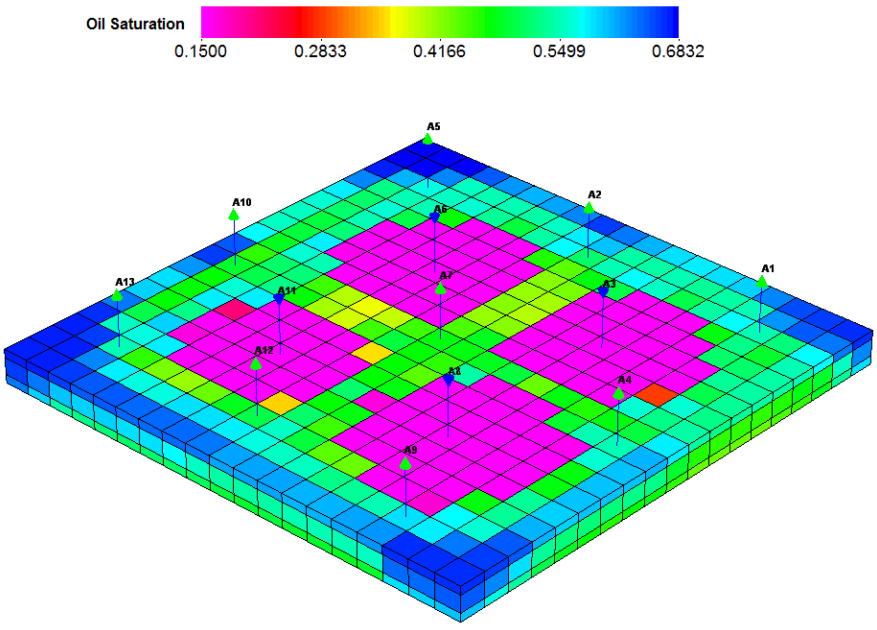

Figure 4-62: Oil saturation after 400 days for PPG flood.

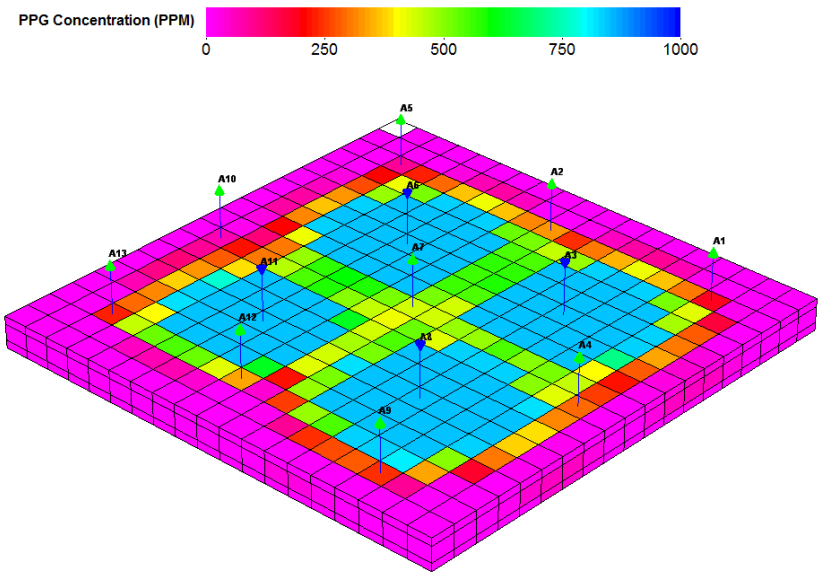

Figure 4-63: PPG concentration after 400 days for PPG flood.

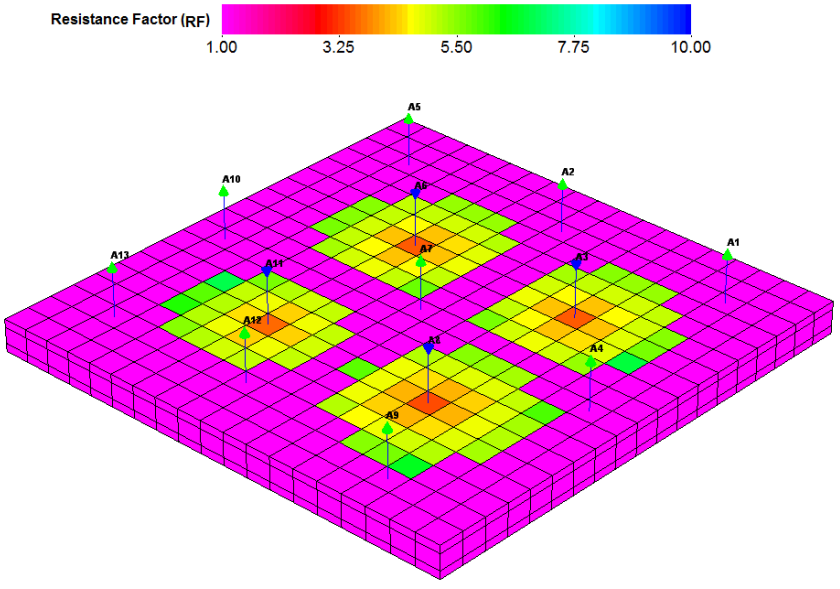

Figure 4-64: Resistance factor after 400 days for PPG flood.

4.6.2 Heterogeneous Permeability Large Scale Model

A Cartesian model was set up where PPG injection is simulated. The injection was at constant rate and production was at constant pressure. Table 4-12 gives the data used. The base case has a high average permeability of 3000 md with Dykstra-Parsons coefficient of 0.88, correlation length of 0.1 in x-axis, correlation length ratio Lx/Ly of 1, and correlation length ratio Lx/Lz of 1000. The generated heterogeneous permeability distribution is shown in Figure 4-65. The model consists of one inverted 5-spot pattern (4 produces, 1 injector) and PPG concentration for injection was 2000 ppm. The base case model (PPG flood) was compared with waterflood and the results indicated that PPG injection has considerable improvement compared to waterflood.

A comparison of simulated oil recovery for PPG flood vs. waterflood is shown in Figure 4-66. Oil recovery increases by about 15% with significant decrease in water cut using PPG. The oil saturation at the end of waterflood and PPG flood in areal direction are shown in Figure 4-67 and Figure 4-68. Also, the oil saturation at the end of waterflood and PPG flood in vertical direction are shown in Figure 4-69 and Figure 4-70. It is clear from the figures that the areas with higher permeability is more favorable for PPG injection and gives better sweep efficiency. Therefore it can be concluded that both areal and vertical sweep efficiency are improved using PPG compared to waterflood.

Figure 4-71 and Figure 4-72 show the incremental oil recovery and oil production rate sensitivity to gel concentration. This sensitivity analysis was performed to optimize the incremental oil recovery from PPG treatment by increasing PPG concentration. Three PPG concentrations of 500, 2000, and 15000 ppm were chosen for sensitivity simulations and the duration of PPG injection was 200 days. The results demonstrate that higher PPG concentration is favorable. However, it should be noted that increasing PPG

concentration above 2000 ppm will not have any impact in oil recovery. The detail of the input data for this simulation is in Appendix A.

Table 4-12: Simulation input parameters for large scale heterogeneous case.

Model	3-Dimensional Cartesian
No. of grids	40×40×3
Δx, Δy, Δz	10, 10, 10 ft
Reservoir Porosity	0.35
Initial Water Saturation	0.15
K_v/K_h	0.1
Crude Oil Viscosity	25 cp
Injection Rate	2500 ft^3/day
Production Bottomhole Pressure	500 psi
Simulation Time	800 days
Waterflood:	**Time injected:**
1 wt% KCl Flood	800 Days
PPG Design:	**Time injected:**
Waterflood	300 Days
PPG flood with Concentration of 2000 ppm	200 Days
Post Water Injection	300 Days

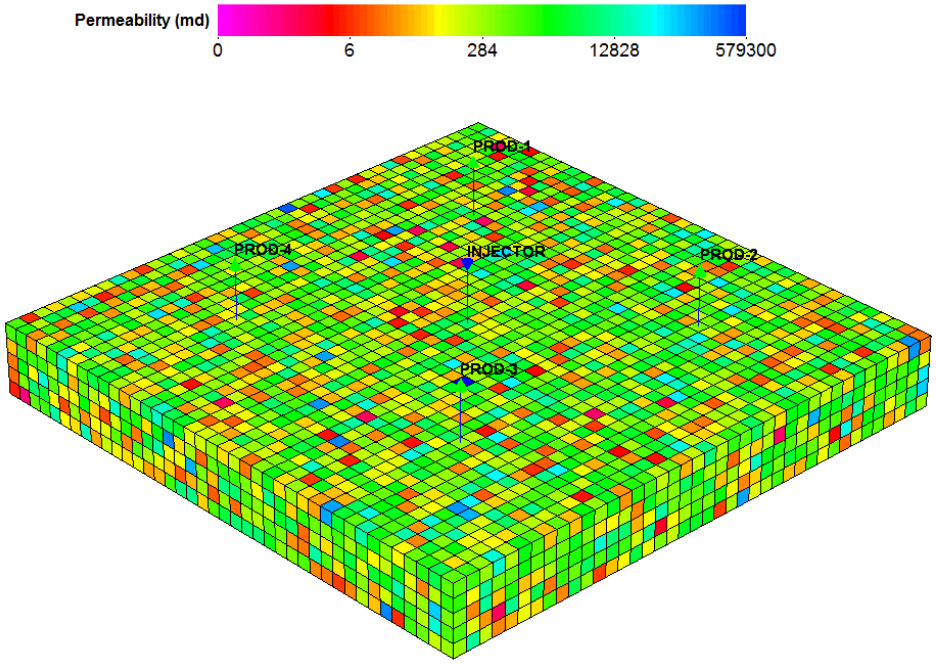

Figure 4-65: The base case heterogeneous permeability distribution representation.

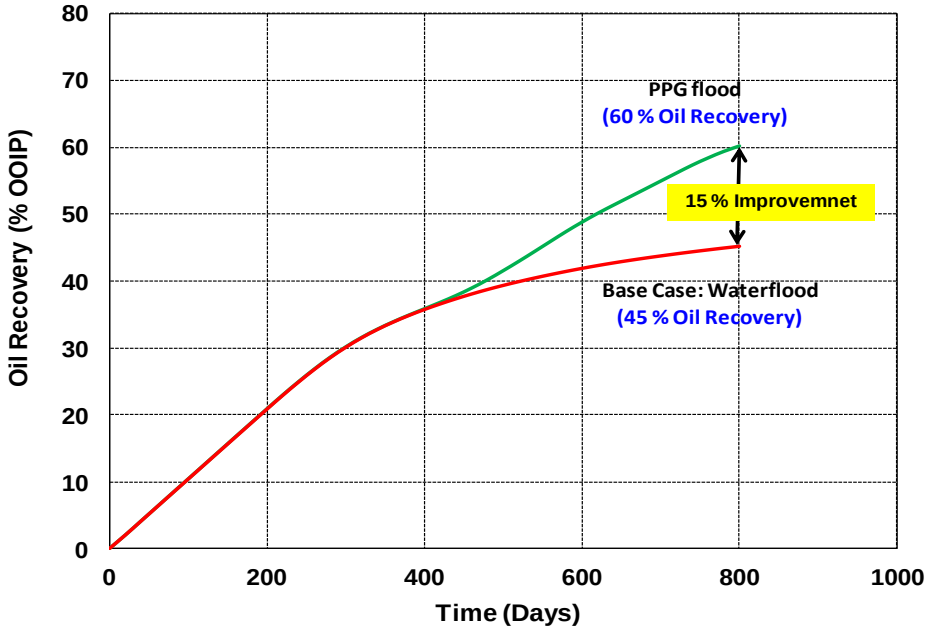

Figure 4-66: Comparison of simulated oil recovery for PPG vs. waterflood.

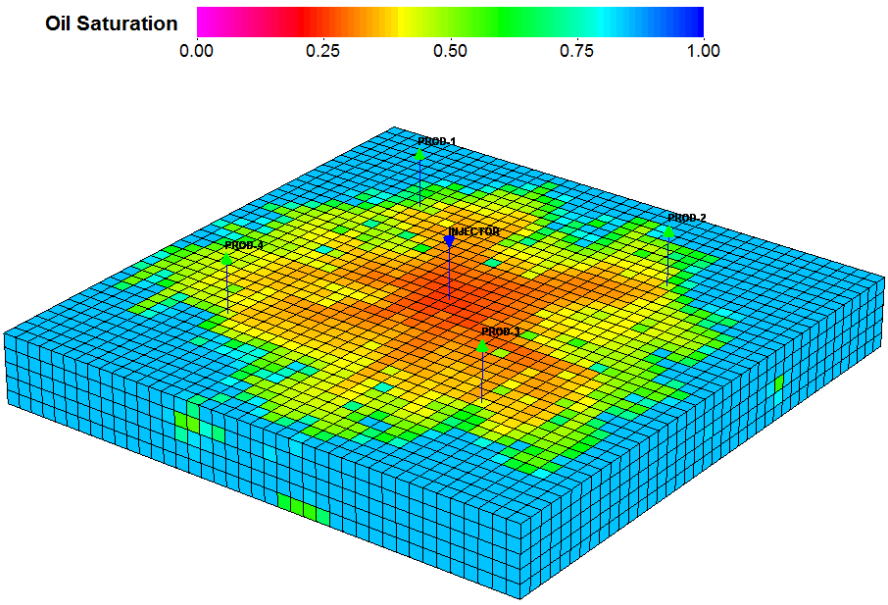

Figure 4-67: Oil saturation distribution at the end of waterflood scenario in areal direction.

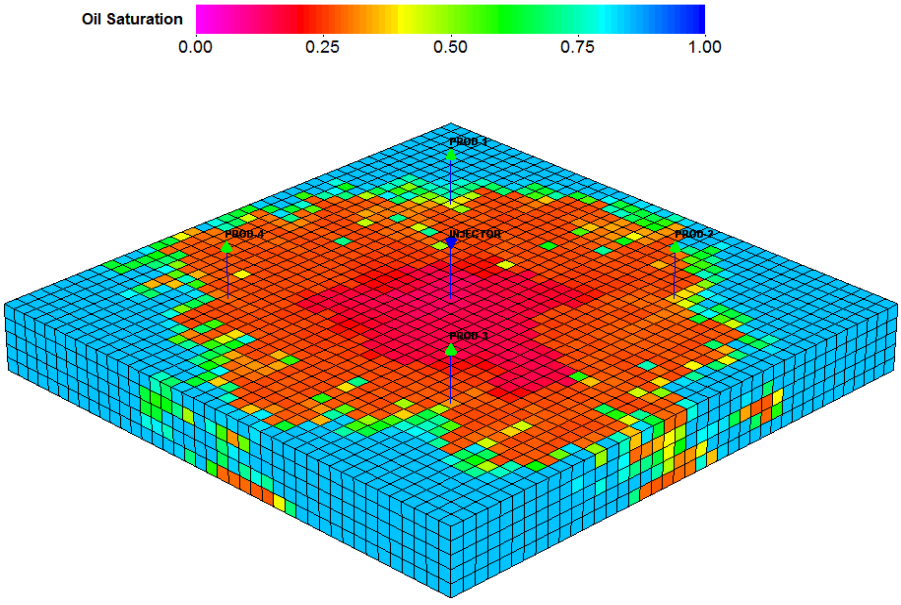

Figure 4-68: Oil saturation distribution at the end of PPG flood scenario in areal direction.

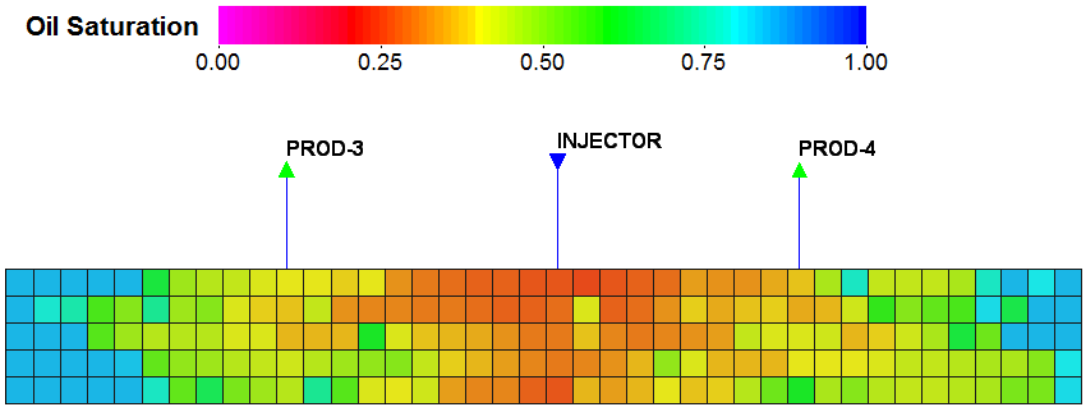

Figure 4-69: Oil saturation distribution at the end of waterflood scenario in vertical direction.

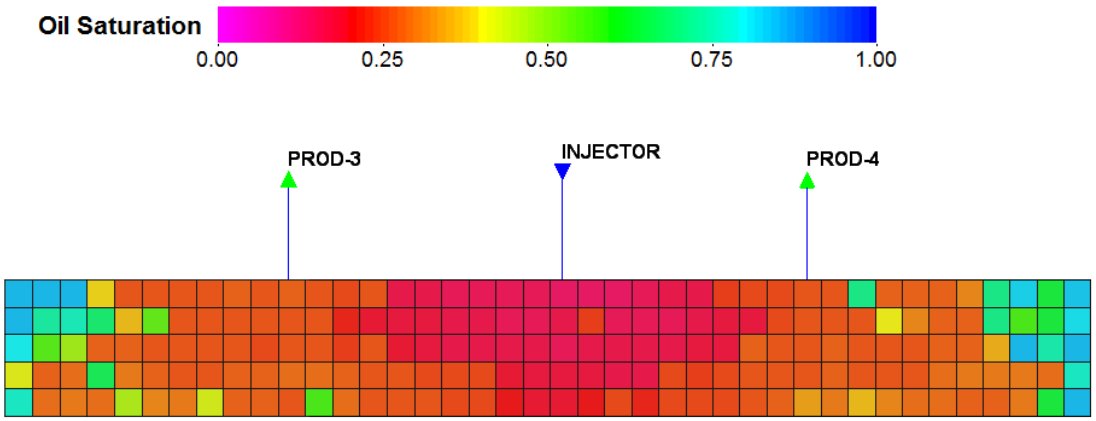

Figure 4-70: Oil saturation distribution at the end of PPG flood scenario in vertical direction.

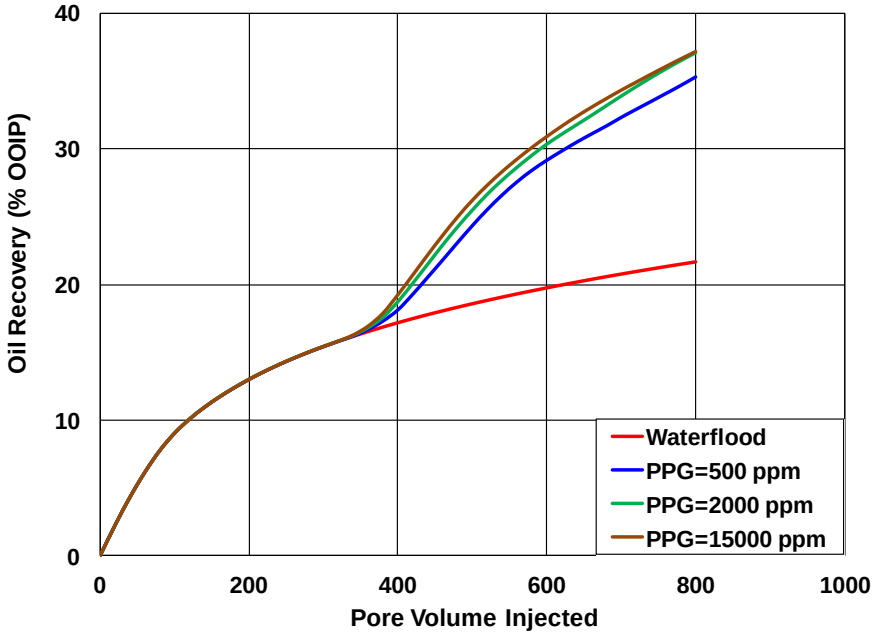

Figure 4-71: Comparison of oil recovery for different PPG concentrations.

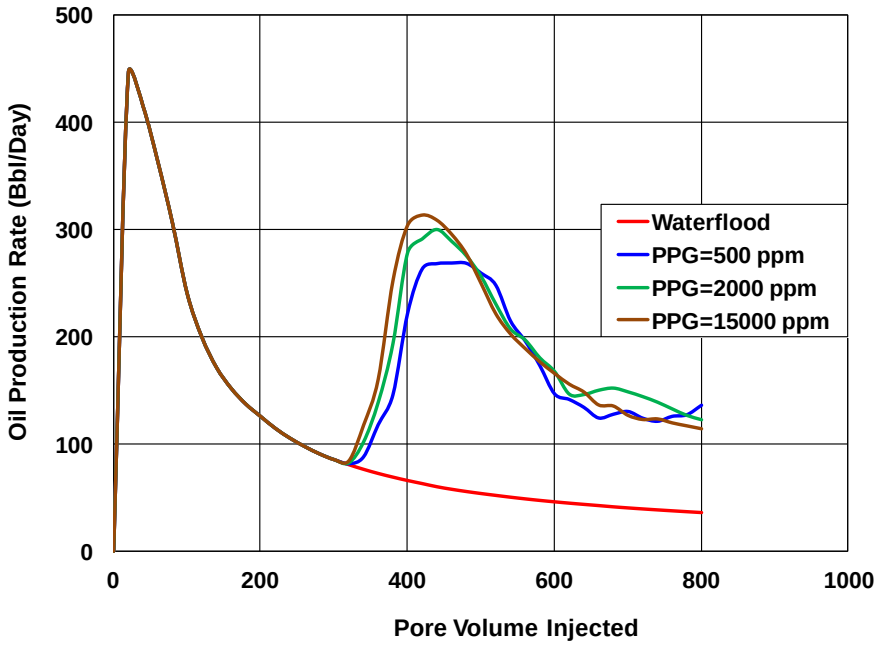

Figure 4-72: Comparison of oil production rate for different PPG concentrations.

4.6.3 PPG vs. Bulk Gel Conformance Control for a Heterogeneous Onshore Field

We used the geomodel and well conditions of a candidate onshore field to compare PPG versus Bulk Gel treatments. A pilot area of 983×1075 m^2 containing 10 injection wells and 7 production wells, all of which are vertical wells with perforation over the entire pay zone, was selected for this study. The average reservoir porosity is around 0.25 but it varies between 0.1 and 0.3, as shown in Figure 4-73. The reservoir permeability is very heterogeneous and varies from 0.1 to 17,000 md (in both vertical and areal direction) as shown in Figure 4-74. The top of the pay zone is at the depth of 1916 ft with a thickness of 37 ft. Crude oil and water viscosities at the reservoir temperature of 72.5 °F are 3.4 and 0.37 cp, respectively. A Cartesian model with 43×47×19 gridblocks in X, Y, and Z directions is used for this field study. Table 4-13 gives the reservoir and fluid properties. The PPG and Bulk Gel input parameters for comparison were chosen based on measured experimental data. Different simulations were performed to investigate the performance of two types of gels, namely; Bulk Gel, and PPG. The production scenarios are summarized as following:

- Base case waterflood: comprised of 7.3 PV of water injection.
- Bulk in-situ gel treatment: comprised of 5.0 PV of pre-treatment water injection, followed by 0.3 PV of bulk gel treatment, and 2.0 PV of post water injection.
- PPG treatment: comprised of 5.0 PV of pre-treatment water injection, followed by 0.3 PV of PPG injection, and 2.0 PV of post water injection.

The comparison of oil recovery and water cut for different production scenarios are shown in Figure 4-75 and Figure 4-76. The oil recovery increases by about 9% for Bulk Gel Flood compared to waterflood. However, PPG flood shows around 21% improvement in oil recovery compared to waterflood. This illustrates that injection of PPG as microgel can be more efficient than generation of in-situ bulk gel in the reservoir by injecting polymer and crosslinker since polymerflood has some disadvantages, such as shear degradation, higher adsorption, and high pressure drop requirement for injection. The detail of the input data for this simulation is in Appendix A.

Table 4-13: UTGEL simulation input parameters.

Model	3-Dimensional Cartesian
No. of grids	43×47×19
Δx, Δy, Δz	75, 75, 2 ft
Initial Water Saturation	0.2
Crude Oil Viscosity	3.4 cp
Injection Rate	Variable for each well
Production Bottomhole Pressure	300 psi
Total Pore Volume Injected	7.3 PV
Waterflood:	**Pore Volume Injected:**
1 wt% KCl Flood	7.3 PV
PPG Design:	**Pore Volume Injected:**
Waterflood	5 PV
PPG flood with Concentration of 2500 ppm	0.3 PV
Post Water Injection	2 PV
Bulk Gel Design:	**Pore Volume Injected:**
Waterflood	5 PV
0.5 %wt Polymer and Crosslinker	0.3 PV
Post Water Injection	2 PV

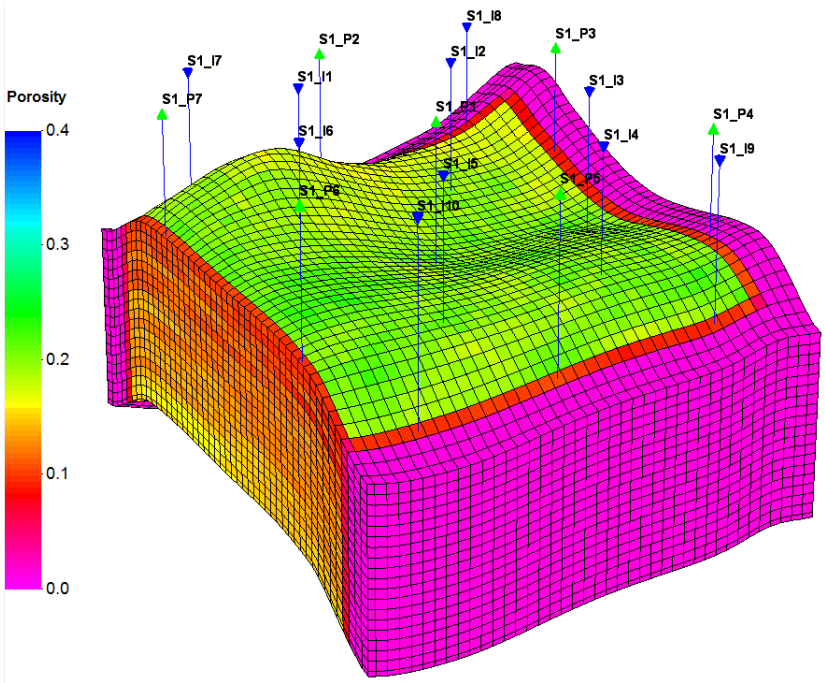

Figure 4-73: Porosity distribution of the heterogeneous onshore field.

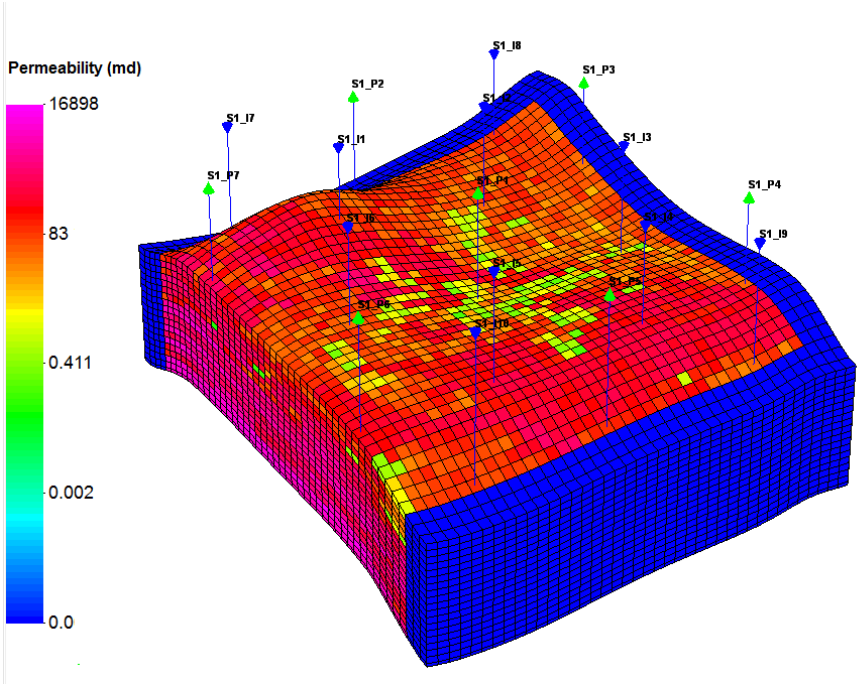

Figure 4-74: Permeability distribution of the heterogeneous onshore field.

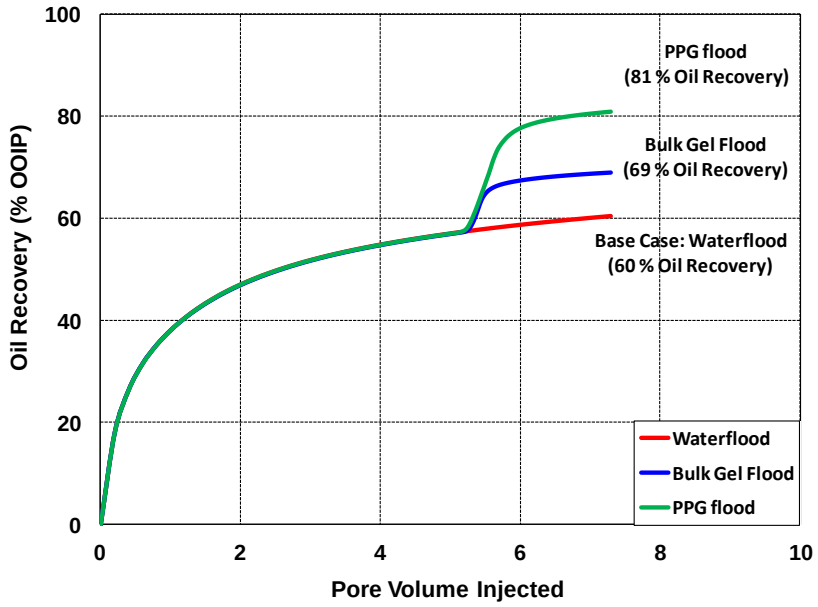

Figure 4-75: Comparison of waterflood, Bulk Gel flood, and PPG flood oil recoveries.

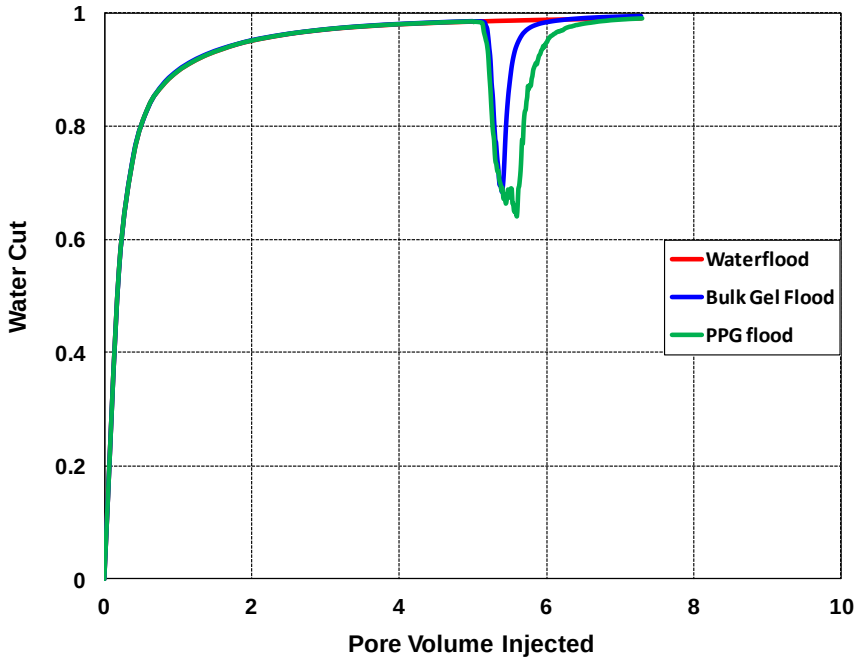

Figure 4-76: Comparison of waterflood, Bulk Gel flood, and PPG flood water cuts.

4.7 SUMMARY AND CONCLUSIONS

- PPG experiments in both fracture and sandpack models were performed successfully to investigate the effect of PPG on improving conformance and reducing water cut.
- PPG injection pressure increased with the increase in flow rate and salinity but decreased with the increase of fracture width.
- Berea coreflood experiment was conducted to understand the transport of PPG microgels and their impact on flow conformance and reducing water production.
- Coreflood results indicated that residual oil saturation after PPG flood is lower than the waterflood residual oil saturation. A simple model is proposed but more mechanistic understanding is underway supported by additional laboratory and theoretical studies.
- Empirical correlations are developed for resistance factor (RF) and residual resistance factor (RRF) using different size conduits and for a wide range of flow rate and brine salinity and hardness.
- We have developed models for gel rheology, adsorption, swelling ratio, resistance factor, and residual resistance factor.
- The gel transport models were implemented in a reservoir simulator and validated against laboratory experiments.
- The numerical studies indicated that main PPG design variables are treatment size, PPG concentration, permeability contrast, and the ratio of vertical to horizontal permeability.
- The normal and rule-of-thumb estimate for slug size is between 5-15% of the Channel Volume (CV). However, the sensitivity simulations showed that

increasing slug volume above 10 % CV will not have considerable impact on final oil recovery. The sensitivity simulations also illustrated that higher concentration is favorable for PPG treatment. However, 10,000 ppm can be considered as the criteria where increasing concentration above that will not increase the final oil recovery. For reservoir properties, higher permeability contrast between layers and lower vertical to horizontal permeability ratio (k_v/k_h) are favorable design parameters for PPG treatment. Higher k_v/k_h will cause the crossflow of PPG from high permeability layer into low permeability layer which brings adverse effect on blocking high permeability channels.

- UTGEL can model the performance of PPG in improving oil recovery in the parallel sandpack systems (with crossflow and without crossflow) which represented a degree of heterogeneity in the experiment design. Resistance factor and gel retention model parameters were used as history matching parameters.
- To history match heterogeneous parallel sandpack experiments (with crossflow and without crossflow), different relative permeability, capillary pressure, and residual saturations are used for high and low permeability zones.
- PPG can preferentially penetrate into the higher permeable layer while minimizing its penetration into the lower permeable layer.
- Pilot scale simulations of Karamay oil field showed that PPG is capable of generating high resistance factor in the high permeability thief zone and increased the incremental recovery by 14% over waterflood.

Chapter 5: Thermally Active Polymers (TAP) for Conformance Control

5.1 INTRODUCTION

In 1996, an industry consortium (BP, Nalco, and ChevronTexaco) conducted a joint research and introduced the new product named Thermally Active Polymer (TAP). TAP expands due to temperature and time and can be used as in-depth conformance control. The main characteristic of TAP is to activate at a specific depth triggered by temperature and block the high permeability layers and divert the injected water into low permeability unswept oil zones (Figure 5-1). TAP can be injected with cold surface water and will activate and expand when temperature exceeds a critical value and blocks high permeability thief zones. The given temperature range will control the depth in the reservoir where adsorption and permeability reduction will happen. However, the main issue in field trial of TAP injection is uncertainty about the amount of incremental oil as the result of the treatment.

Garmeh *et al.* (2012) illustrated that stable and reversible crosslinkers hold the TAP polymers in their initial state due to internal linkage. The hydrolysis can break the reversible linkages leading to expansion in particle sizes. The resistance in high permeability zones will be created by adsorption and retention of TAP on the pore throats. The adsorption and permeability reduction can be controlled by treatment size, TAP concentration and permeability contrast between layers due to reservoir heterogeneity. The idea about activation of TAP returns to model proposed by the vendor which says TAP starts off like small popcorn kernels and move forward with cool

injection water in high permeability and porosity layers. By moving forward, the particles encounter hot water and rocks. Once it reaches certain temperature, the TAP particles pop as shown Figure 5-2 and this irreversible expansion blocks the high permeability layers. The popping level of TAP particles can be controlled by the chemical formulation of TAP and temperature.

The original idea of popping comes from Frampton *et al.* (2004) that activation time of the particles can be determined using slim tube tests and salinity of water impacts the size of popped particles. Slim tube is mainly designed for evaluating propagation of TAP and measuring its popping conditions. However, there is still room for more research to understand the mechanism of TAP activation whether popping happens or it is due to gradual swelling similar to preformed particle gels. Figure 5-3 and Figure 5-4 show the viscosity profile for two TAP polymers at the temperature of 85 ^{0}C and pH of 7. Static bottle tests were used to evaluate the TAP viscosity and activation time. The figures illustrate that the viscosity of TAP grade 9398A is almost double the viscosity of grade 9378A. The viscosity of TAP depends on several factors including TAP concentration, brine composition, and pH.

In this chapter, the mathematical model and equations for activation and propagation of TAP in UTGEL simulator will be presented. Then, different simulations on synthetic cases will be explained to investigate the effect of key controlling factors on the performance of TAP for blocking high permeability thief zones.

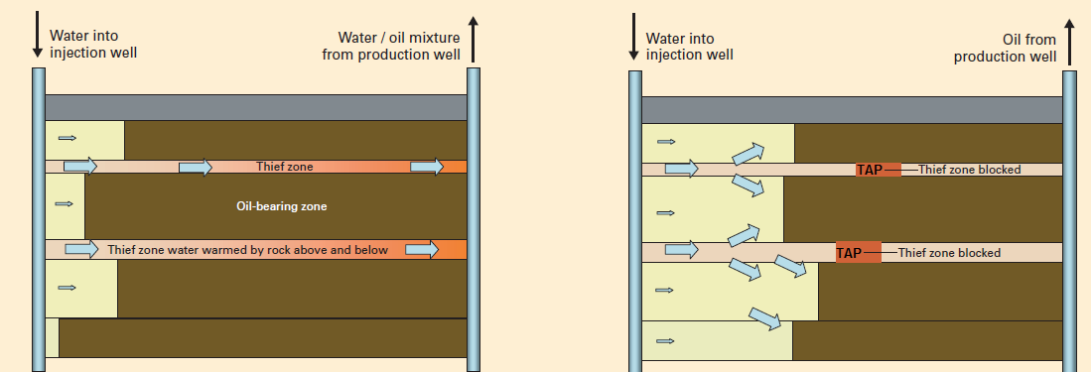

Figure 5-1**:** TAP adsorbs and retains on the surface of the rock in thief zones and diverts the water into low permeability areas.

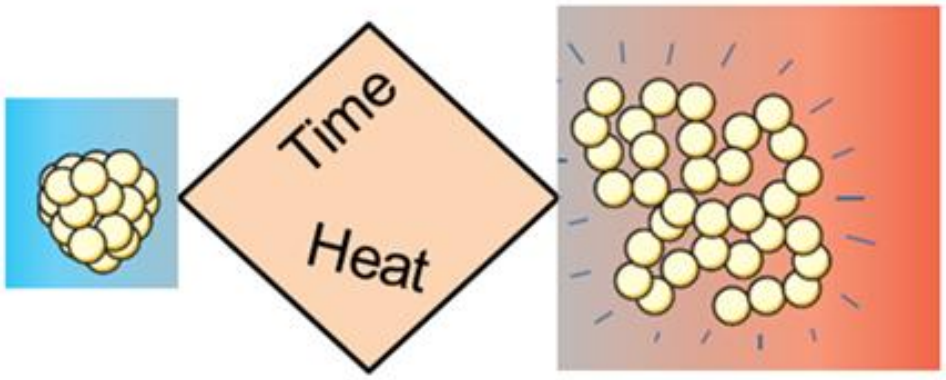

Figure 5-2: Mechanism of TAP activation: TAP will be activated by heat over time and swells several times its original size.

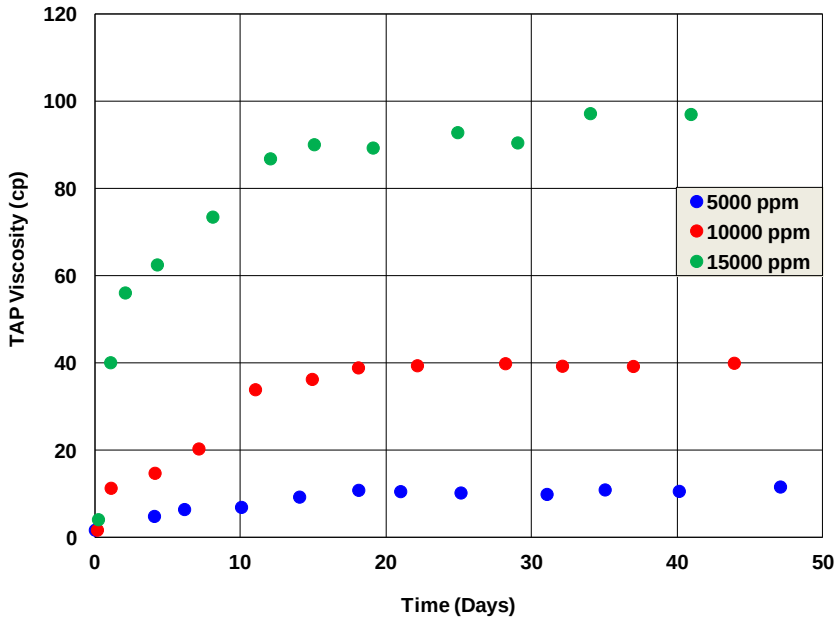

Figure 5-3: The viscosity of 9378A grade TAP for different concentrations at 85 ^{0}C and pH=7 (Salehi *et al.*, 2012).

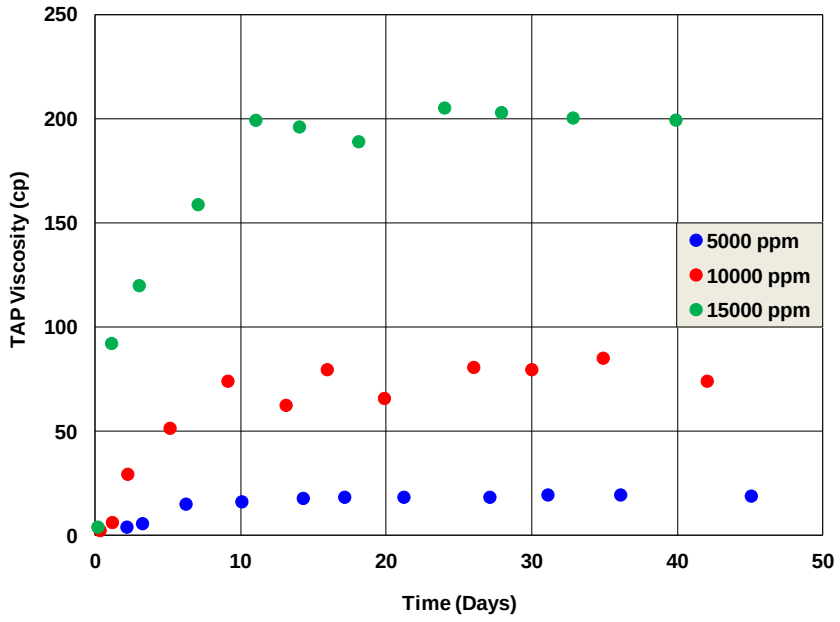

Figure 5-4: The viscosity of 9398A grade TAP for different concentrations at 85 ^{0}C and pH=7 (Salehi *et al.*, 2012).

5.2 MODEL DESCRIPTION

To model thermally active polymers, it is necessary to combine chemical and thermal modules of the compositional simulators. The required information for modeling TAP are rock and fluids heat conductivities, injection and reservoir temperature, TAP viscosity and adsorption measured data from laboratory, and rock heat capacity. The temperature profile of the reservoir will be used to determine the specific TAP treatment and help to specify the optimum location of TAP activation in high permeability thief zone. A brief description of thermally active polymer viscosity, adsorption, and permeability reduction in UTGEL and CMG-STARS will be presented in this section. There are two approaches for modeling TAP conformance:

***Single component approach*:** TAP is injected as a single component in the injector which has low viscosity and low adsorption. The adsorption and viscosity of TAP will increase by heat as a function of time away from the injector and consequently, permeability reduction will happen in thief zones. The rate of increase in viscosity and adsorption depends on the type of TAP. The laboratory viscosity bottle tests can be used to determine the activation region of the TAP based on transit time of the thief zone and popping time of the grade selected.

***Chemical reaction approach*:** TAP is the product of chemical reaction between polymer and cross-linker. Therefore, there will be three water soluble components (polymer, cross-linker, TAP). The gelation reaction which is explained below is a nondecay reaction where total mass will be conserved. The reaction parameters can be determined by tuning laboratory viscosity data and TAP activation can be controlled by time and gridblock temperature.

5.2.1 TAP Model in UTGEL

5.2.1.1 Gelation Reaction:

The reaction between polymer and cross-linker to form TAP Gel (BWG) is modeled by adding reaction term in concentration equations of corresponding components (polymer, crosslinker, and BWG). The reaction rates for polymer, crosslinker, and gel are as following:

$$r_p = -r_{TAP_0} C_{P_0} C_P C_{CL} Exp(B_k(\frac{1}{T} - \frac{1}{T_{ref}})), \tag{5.1}$$

$$r_{CL} = -r_{TAP_0} C_{CL_0} C_P C_{CL} Exp(B_k(\frac{1}{T} - \frac{1}{T_{ref}})), \tag{5.2}$$

$$r_{TAP} = -(r_P + r_{CL}), \tag{5.3}$$

where r_P, r_{CL} and r_{TAP} are the reaction rates of polymer, crosslinker, and TAP, r_{TAP_0} is the reaction rate coefficient, B_k is the temperature coefficient, C_{P_0} and C_{CL_0} are the polymer and crosslinker reaction rate multiplier, respectively; T_{ref} is the reference temperature, and C_P and C_{CL} are the polymer (wt%) and crosslinker (ppm) concentrations, respectively. The reactions take place when the temperature and concentrations of polymer and crosslinker are greater than threshold values.

5.2.1.2 TAP Viscosity

The viscosity of an aqueous solution containing thermally active polymer gel is modeled using the Flory-Huggins equation with additional terms for TAP as following:

$$\mu_{TAP} = \mu_w \left[1 + \left(A_{p1} C_P + A_{p2} C_P{}^2 + A_{p3} C_P{}^3 \right) C_{SEP}^{S_P} E_P + (A_{G1} C_G + A_{G2} C_G{}^2 + A_{G3} (C_G - C_{TG})^3) E_G \right] \quad (5.4)$$

where C_P (wt %) and C_G (ppm) are polymer and gel concentrations in aqueous phase, C_{TG} is the threshold gel concentration, μ_w is the water viscosity, C_{SEP} is effective salinity, S_p is a parameter for the effect of salinity, E_P, E_G are temperature dependent viscosity parameters for polymer and gel, and A_{p1}, A_{p2}, A_{p3}, A_{G1}, A_{G2}, A_{G3} are input parameters.

5.2.1.3 TAP Adsorption

Langmuir isotherm is used to correlate adsorbed concentration with the aqueous-phase concentrations as following:

$$\hat{C}_{TAP} = \frac{a_G C_{TAP}}{1 + b_G C_{TAP}}, \quad (5.5)$$

$$a_G = \left[a_{G,ref} + a_{Gs} (C_S - C_{s,ref}) + a_{GT} (T - T_{ref}) \right] (\bar{k})^{-S_k}, \quad (5.6)$$

where C_{TAP} is the TAP concentration in the aqueous phase (ppm), a_G is the parameter dependent on temperature, and b_G is constant input parameter for adsorption.

5.2.1.4 Permeability Reduction

Adsorption, retention, and filtration can cause the resistance to flow or reduction of the permeability during TAP flow. The following shows the dependency of resistance factor on adsorbed TAP:

$$RF_{TAP} = 1.0 + (RF_{TAP,Max} - 1) \frac{\hat{C}_{TAP}}{\hat{C}_{\mathrm{TAP},Max}}, \quad (5.7)$$

where $\hat{C}_{TAP}$ is adsorbed TAP concentration, $\hat{C}_{\mathrm{TAP},Max}$ is the maximum adsorption capacity, and $RF_{TAP,Max}$ is maximum permeability reduction (input parameter). When both polymer and TAP flow through the rock, the combined resistance factors should be considered for permeability reduction as

$$RF_{Total} = 1.0 + (RF_{P,Max} - 1)\frac{\hat{C}_P}{\hat{C}_{\mathrm{P},Max}} + (RF_{TAP,Max} - 1)\frac{\hat{C}_{TAP}}{\hat{C}_{\mathrm{TAP},Max}}, \tag{5.8}$$

where the first term is the permeability reduction due to polymer and the second term is the permeability reduction due to TAP.

5.2.2 TAP Model in CMG-STARS

The rate of propagation of many additives (surfactants, caustic, and polymers) is strongly affected by their interaction with the rock. These interactions can be chemical (e.g. ion exchange) or mechanical (e.g. blockage, straining capture) or a combination. The capture levels can depend on fluid concentrations, temperature and rock type (CMG-STARS, 2012). The adsorption isotherm can be modeled either in a tabular format or Langmuir isotherm as follows:

$$Ads_i = (\frac{A}{B})(\frac{BZ_i}{1+BZ_i}), \tag{5.9}$$

where Ads_i is the component i adsorption based on Langmuir equation, (A/B) is the slope of Langmuir curve and it quantifies the adsorption sensitivity, and Z_i is the concentration of component i. The adsorption level should decrease as the temperature increases. A typical isothermal Langmuir adsorption curve is shown in Figure 5-5 with

both reversible threshold and irreversible residual adsorption. The adsorption increases as the concentration increases. The reversible threshold illustrates that if the concentration remains lower than point A, then adsorption will be irreversible. However, if the concentration falls between points A and B, then desorption occurs along a straight line from the maximum point reached on the adsorption curve to point C (Garmeh *et al.*, 2012).

The permeability reduction factor for TAP can be related to the pore-scale level of adsorption. Therefore, it can be concluded that the permeability reduction at the pore-scale level will be a combination of adsorption, retention, and filtration.

$$RF = 1.0 + (RF_{Max} - 1.0)\frac{Ads_i}{Ads_{Max}}, \tag{5.10}$$

where Ads_i is adsorbed gel concentration (moles/unit pore volume), Ads_{Max} is the maximum adsorption, and RF_{Max} is an input maximum permeability reduction.

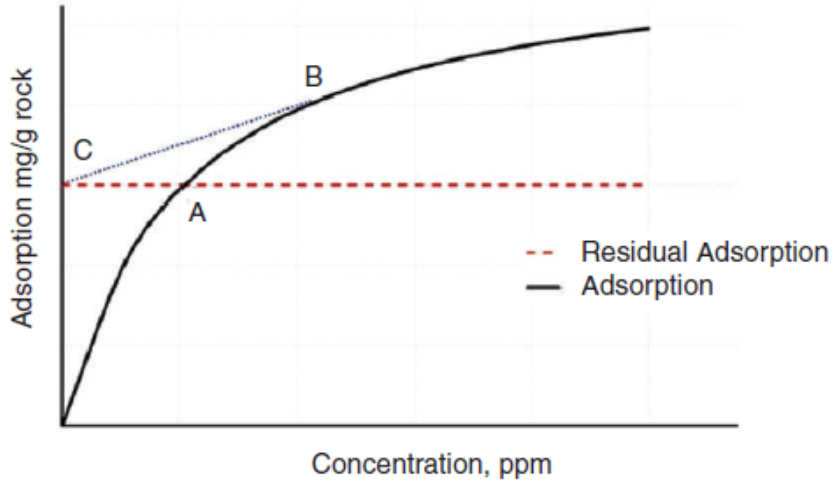

Figure 5-5: Reversible adsorption and irreversible adsorption based on Langmuir adsorption (Garmeh *et al.*, 2012).

5.3 RESULTS AND DISCUSSION

5.3.1 TAP conceptual model using UTGEL

A Cartesian 3D model was set up to simulate the TAP injection for conformance improvement. The injection was at constant rate and production was at constant pressure. The heterogeneous case has a high permeability layer of 1500 md located in the middle and upper and lower layers with a permeability of 50 md with the Dykstra-Parsons coefficient of 0.75 for all layers (Figure 5-6). It should be noted that the activation temperature of TAP in this case was between 130 ^{0}F and 150 ^{0}F. Therefore, two conditions of TAP concentration and the temperature at which TAP is activated are required to observe water diversion from high permeability to lower permeability layers by swelled TAP. Figure 5-7 shows the temperature profile in the reservoir. The typical TAP slug size in field cases is around 5 % of the channel volume as considered in this simulation (20 days TAP injection). However, in different injection designs such as offshore applications, this treatment size can vary from 2% to 10% of the channel volume.

Table 5-1 gives the model data and the injection design. TAP was compared with waterflood and the results indicated that a considerable improvement in oil recovery (around 9% OOIP incremental) and reduction in water cut is achieved using TAP as shown in Figure 5-8 and Figure 5-9. As it is illustrated in Figure 5-10, the average reservoir pressure increases during TAP injection but stable pressure during gel flood can be achieved. Figure 5-11 shows considerable increase in oil flow rate for TAP compared to waterflood. There was considerable improvement in oil recovery using this process in which temperature and residence time are two key design parameters.

Generally, the treatment strategy is to place TAP half way between injector and producer. However, based on the characteristics of TAP grade, it can be placed in different locations of the thief zone. The placement of treatment in thief zone depends on several factors including thief zone permeability, heterogeneity, mobility ratio, reservoir and thief zone temperature, well distance among other factors. The placement of TAP for this heterogeneous case is shown in Figure 5-12 which is almost half way between injector and producer. The permeability reduction map is shown in Figure 5-13 which clearly demonstrates the permeability reduction happens as TAP activated far from the injector. The detail of the input data for this simulation is in Appendix A.

Table 5-1: Properties of model used for TAP conformance control study.

Model	3-Dimensional Cartesian
No. of Grids	15×15×3
Porosity and permeability	0.449, (50, 1500, 50) md
Water saturation	25 %
Ratio of K_v/K_h	0.1
Initial Reservoir Temperature	180 ^{0}F
Injection Fluid Temperature	60 ^{0}F
TAP Activation Temperature Range	130-150 ^{0}F
Injection Rate (constant rate)	250 ft^3/day
Production Pressure (constant pressure)	16.44 psi
TAP Concentration	2000 ppm
Simulation Time	1000 days
Waterflood:	Time injected:
1 wt% KCl flood	1000 Days
TAP flood:	Time injected:
1 wt% KCl flood	450 Days
2000 ppm TAP in 1wt% KCl	20 Days
1 wt% KCl post flush	530 Days

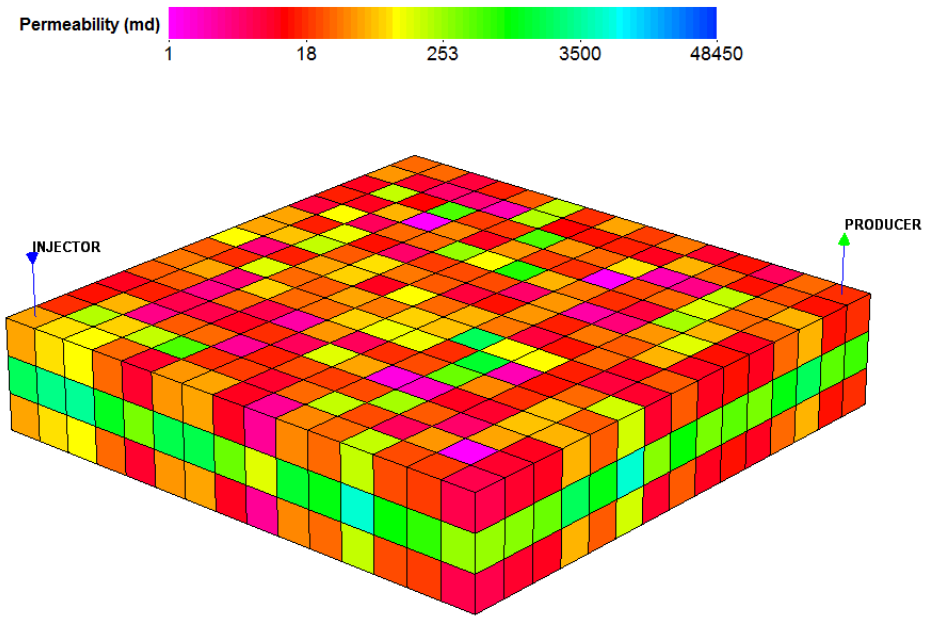

Figure 5-6: The heterogeneous case permeability distribution.

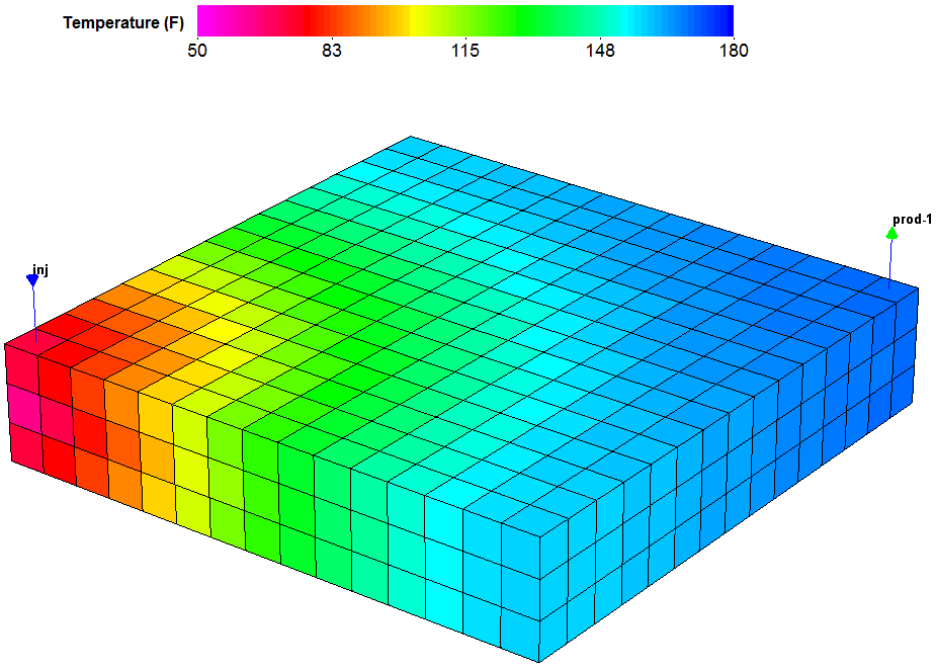

Figure 5-7: Temperature profile during TAP injection.

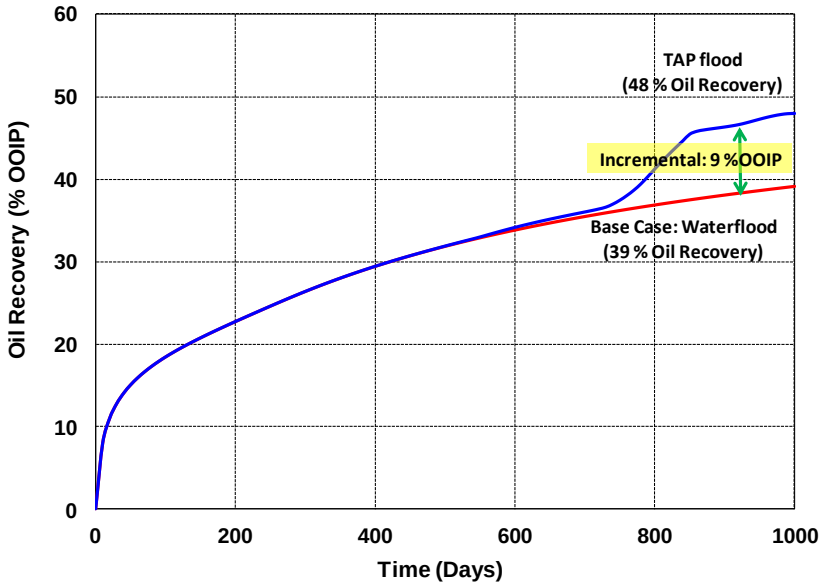

Figure 5-8: Comparison of oil recovery between waterflood and TAP flood for the heterogeneous case using UTGEL.

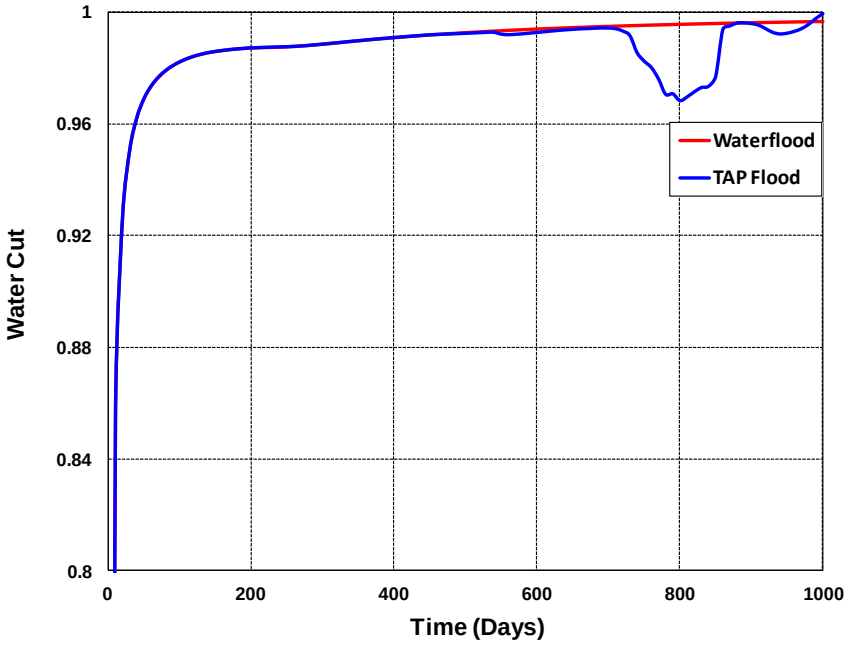

Figure 5-9: Comparison of water cut between waterflood and TAP flood using UTGEL.

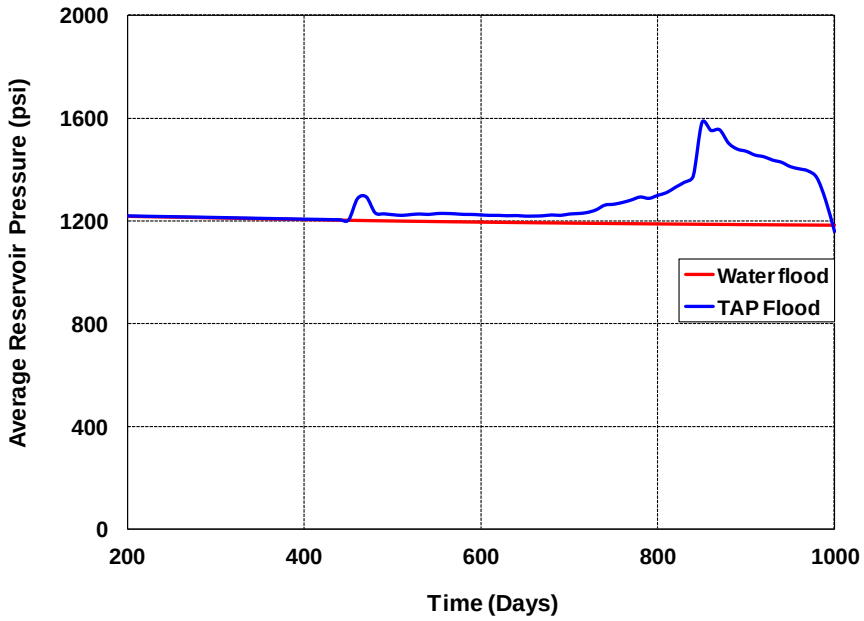

Figure 5-10: Comparison of average reservoir pressure between waterflood and TAP flood using UTGEL.

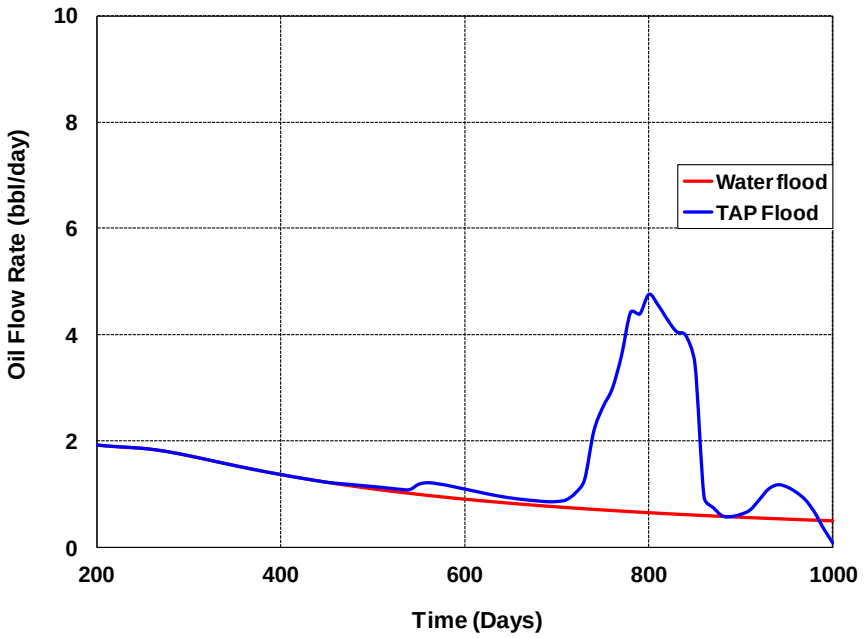

Figure 5-11: Comparison of oil flow rate between waterflood and TAP flood using UTGEL.

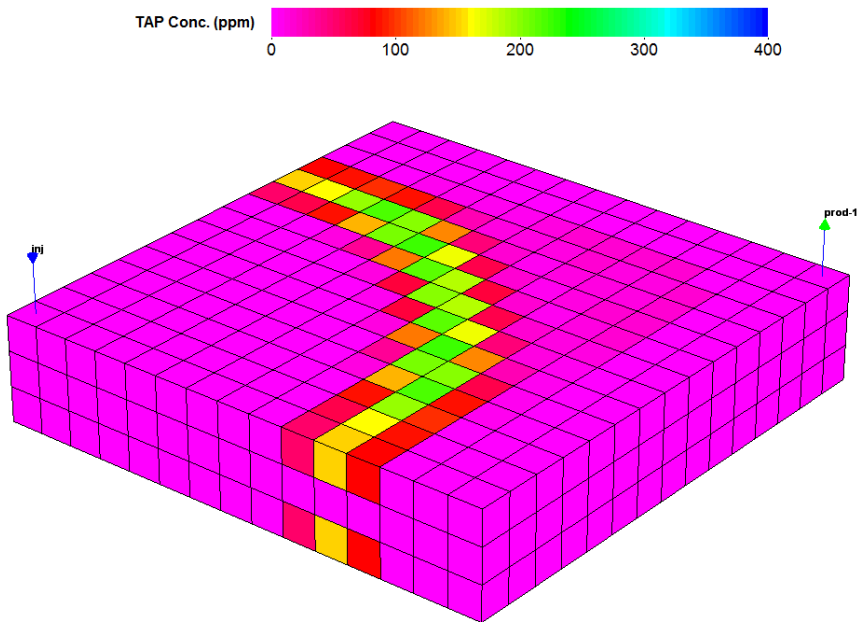

Figure 5-12: TAP concentration in the activation temperature range using UTGEL.

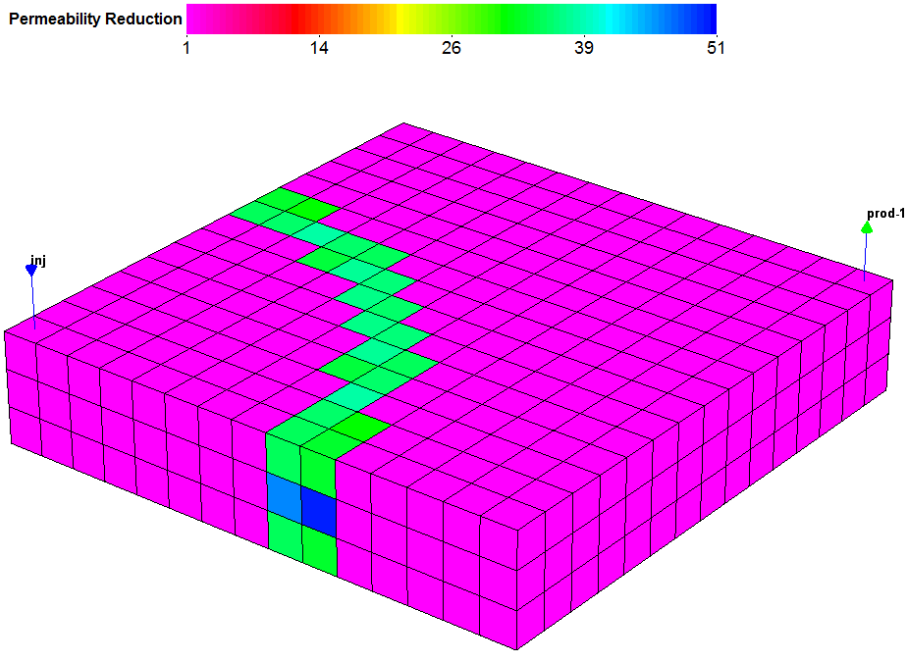

Figure 5-13: Permeability reduction factor in the activation temperature range using UTGEL.

5.3.2 Comparison of UTGEL and CMG-STARS for modeling TAP

A Cartesian model was set up where TAP flood is simulated. The injection was at constant rate and production was at constant pressure. Table 5-2 gives the properties used for this comparison. The base case has a high average permeability layer of 1500 md located in the middle and upper and lower layers with a permeability of 50 md (Figure 5-14). The Kv/Kh ratio of 0.2 is assumed for crossflow between layers. Waterflood was performed for 450 days followed by 20 days of TAP injection followed by 530 days of post water injection. It should be noted that the temperature trigger range for activation of TAP in this case was between 130-160 ^{0}F and TAP is injected at the concentration of 1500 ppm.

The comparison of simulated oil recovery between UTGEL and CMG-STARS shows that two simulators can model TAP in very close agreement. Input adsorption and resistance factor are the same in both simulators. The comparison of waterflood oil recovery between UTGEL and CMG-STARS shows that there is good agreement between the simulators with 39% OOIP waterflood recovery as shown in Figure 5-15. The comparison of TAP simulations shows that there was almost 17% improvement in oil recovery compared to waterflood (Figure 5-16).

The adsorption and permeability reduction of TAP will happen mostly in high permeability layer leading to the improvement in oil recovery. The success of TAP depends on how ineffective the waterflood performance in mature oil reservoirs is. Generally low efficiency waterflooding especially high water cut wells gives better performance of conformance control processes.

Table 5-2: Simulation model parameters for TAP flood comparison between UTGEL and CMG-STARS.

Model	3-Dimensional Cartesian
No. of Grids	15×15×3
Porosity and Permeability	0.45, (50, 1500, 50) md
Water Saturation	35 %
Ratio of K_v/K_h	0.2
Initial Reservoir Temperature	180 ^{0}F
Injection Fluid Temperature	60 ^{0}F
TAP Activation Temperature Range	130-160 ^{0}F
Injection Rate (constant rate)	500 ft^3/day
Production Pressure (constant pressure)	16.44 psi
TAP Concentration	1500 ppm
Simulation Time	1000 days
Waterflood:	Time injected:
1 wt% KCl flood	1000 Days
TAP flood:	Time injected:
1 wt% KCl flood	450 Days
2000 ppm TAP in 1 wt% KCl	20 Days
1 wt % KCl post flush	530 Days

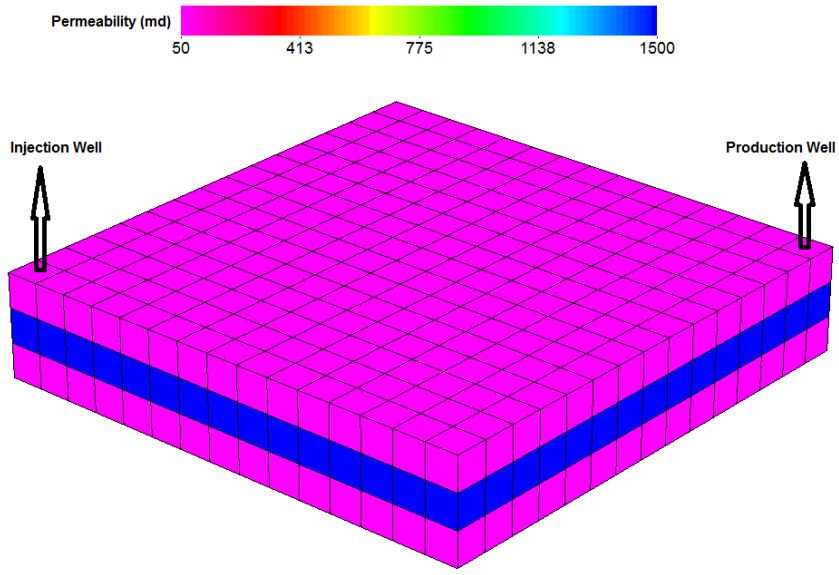

Figure 5-14: The base case permeability distribution.

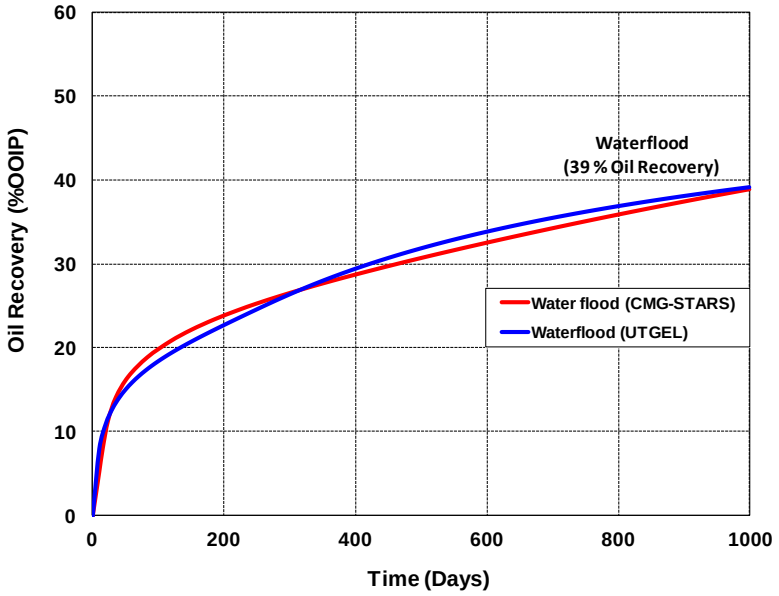

Figure 5-15: Comparison of simulated oil recovery for waterflood between UTGEL and CMG-STARS.

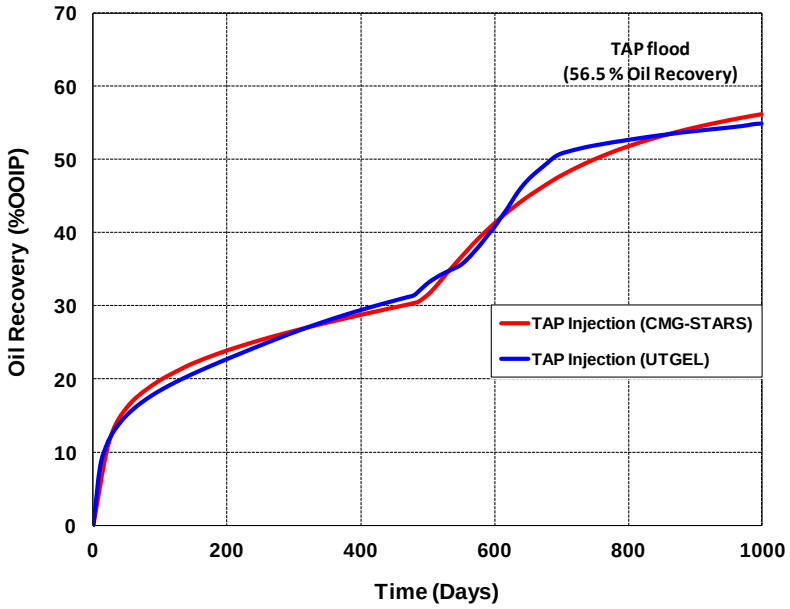

Figure 5-16: Comparison of simulated oil recovery for TAP flood between UTGEL and CMG-STARS.

Chapter 6: Upscaling Methodology for Chemical EOR Processes Using Imbibition and Coreflood Data

6.1 INTRODUCTION

Water flooding is effective for fractured reservoirs if the matrix rock is water-wet, but most of fractured carbonate reservoirs (around 80%) are mixed-wet to oil-wet (Treiber *et al.*, 1972; Roehl and Choquette, 1985; Borchardt and Yen, 1989). The recovery factor in these reservoirs depends on matrix permeability, rock wettability, fracture intensity, and fluid properties (Adibhatla *et al.*, 2005). Alkaline chemicals, such as sodium carbonate, especially in fractured carbonate reservoirs, can diffuse into matrix blocks and may alter wettability from oil-wet to water-wet. In addition, surfactants can alter wettability and reduce interfacial tension (IFT) to increase macroscopic Bond number and, consequently, push water into the matrix.

The oil recovery from fractured carbonate reservoirs is influenced by combined viscous, gravity, and capillary forces, but can be dominated either by spontaneous imbibition or buoyancy, or for some mixed-wet rocks, both buoyancy and spontaneous imbibition can be dominant mechanisms. A three-dimensional multiphase multicomponent chemical compositional simulator, UTCHEM, will be used for modeling chemical EOR processes and aiding to develop a dimensionless scaling group in this study.

During the capillary imbibition process in a highly fractured water-wet rock, where there is small pressure gradient across the matrix blocks, water will flow into the matrix rock and oil will be produced via fractures due to capillary pressure by counter-

current imbibition. Therefore, positive capillary pressures for water-wet rocks indicate higher water pressure in fractures (than pressure in matrix) which pushes water into matrix blocks by force and displaces oil toward fractures (Babadagli, 2003). However, it should be noted that if there are communication between matrix blocks (i.e. not surrounded by fractures in all directions) or the injection rate is high, the process of co-current imbibition can also happen. The rate of imbibition will be a function of matrix block size and permeability. Unfortunately, for oil-wet fractured carbonate rocks the water imbibition recovery without the presence of surfactant is very low because the initial capillary pressure is negative.

Imbibition experiments using surfactants that produce low IFT have been done by several investigators (Hirasaki and Zhang, 2004; Seethepalli *et al.*, 2004a, 2004b; Abidhatla and Mohanty, 2006). Hirasaki and Zhang (2004) suggested that the dominant oil recovery mechanism in low IFT imbibition is buoyancy and wettability alteration. With some anionic surfactants, the IFT can be reduced to ultra-low values where the capillary pressure is reduced to nearly zero. When the capillary pressure is nearly zero, other forces must be present to account for the rapid imbibition observed in many experiments. Simulation results by Abbasi-Asl *et al.* (2010) showed that transverse pressure gradients between the fractures and the matrix can push the surfactant further into the matrix in the dynamic imbibition process. Korrani *et al.* (2013, 2014a, 2014b) mechanistically modeled wettability alteration due to low salinity waterflooding through coupling a geochemical package, IPhreeqc, with compositional reservoir simulators, UTCHEM and UTCOMP. They modeled wettability alteration dynamically using the total ionic strength. Rezaveisi *et al.* (2012) investigated the effect of gravity and oil viscosity on imbibition using experimental data under different wettability conditions.

Imbibition experiments showed that increasing surfactant concentration increased the recovery rate slightly at early times but did not have a considerable effect on final oil recovery. Lu *et al*. (2012b, 2014) performed static and dynamic imbibition experiments using new surfactant formulations and investigated the effect of surfactant on IFT reduction and oil recovery. Capillary imbibition is an efficient process for small size blocks and its effectiveness is reduced by increasing matrix block size. If capillary forces are small due to IFT reduction by surfactant, gravity forces will be significant and a combination of wettability alteration and gravity will dominate during the imbibition process.

Laboratory experiments including coreflood and imbibition tests provide an understanding of oil recovery mechanisms and the effectiveness of different chemical formulations. With the improved understanding of the relationship between the surfactant structure and the performance, surfactant formulations are developed that give promising results even under high temperature and high salinity reservoir conditions (Solairaj *et al*., 2012; Adkins *et al*., 2012; Lu *et al*., 2012a). However, the same recovery or recovery rate at lab scale cannot be expected at larger field scales. The main aim of this chapter is to use laboratory data at different scales to propose a scale-up methodology for predicting chemical EOR processes at reservoir scales. Without these scale-up studies and understanding of involved mechanisms for oil recovery during a chemical flood, it is difficult to design cost-effective, successful chemical processes for fractured carbonate reservoirs.

6.2 UTCHEM SIMULATOR

Extensive research at The University of Texas at Austin results in development of a three dimensional multiphase multicomponent chemical compositional reservoir simulator, UTCHEM, which is capable of simulating different chemical EOR processes (Satoh, 1984; Saad, 1989; Bhuyan, 1989; Delshad *et al*., 1996; Aldejain, 1989 and Liu *et al.*, 1994; Lashgari, 2014b; Korrani *et al.*, 2015). The simulator accounts for surfactant phase behavior, chemical reaction, petrophysical properties, and reservoir heterogeneity. The simulator can generate up to four phases (gas, aqueous, oleic and microemulsion) and uses advanced concepts in high-order numerical accuracy and dispersion control. Microemulsion (ME) is a combination of water, oil, surfactant and co-surfactant which at certain conditions of temperature, pressure and salinity can form a single separate phase which is thermodynamically stable. The simulator can model wettability alteration, capillary pressures, three-phase relative permeabilities (water/gas/organic phases or water/organic/microemulsion phases), dispersion, diffusion, adsorption, chemical reactions, non-equilibrium mass transfer between phases and other related phenomena. Some of the features are listed below (Technical Manual, 2011).

UTCHEM features:

- 3-dimensional finite difference with temperature equation
- IMPES-type formulation
- Third-order finite difference with a flux limiter
- Four phase (water, oil, microemulsion, gas)
- Vertical, horizontal, and deviated wells
- Water/surfactant/oil phase behavior
- Clay/surfactant cation exchange

- Polymer with non-Newtonian rheology (shear thinning/thickening)
- Geochemical reactions

UTCHEM oil reservoir applications:

- Waterflooding
- Single well, partitioning interwell, and single well wettability tracer tests
- Polymer flooding
- Profile control using bulk gel
- Surfactant flooding
- Wettability alteration
- High pH alkaline flooding
- Microbial EOR
- Surfactant/foam and ASP/foam EOR
- Formation damage

6.2.1 Mass Conservation Equations

The main assumptions which are imposed on developing flow equations are as following:

1. The rock and fluids are slightly compressible.
2. Darcy's law applies.
3. Mixing is ideal.
4. Fickian dispersion is used.
5. There exists local thermodynamic equilibrium except for tracers and dissolution of organic components.
6. The boundary conditions of no flow and no dispersive flux across the impermeable boundaries will be used for flow equations.

The mass conservation equation for component κ in terms of overall volume of component κ per unit pore volume is defined as

$$\frac{\partial}{\partial t}\left(\phi \tilde{C}_\kappa \rho_\kappa\right) + \vec{\nabla}\bullet\left[\sum_{\ell=1}^{n_p} \rho_\kappa \left(C_{\kappa\ell}\vec{u}_\ell - \vec{\tilde{D}}_{\kappa\ell}\right)\right] = R_\kappa, \tag{6.1}$$

where

ϕ = porosity, (L^3/L^3)

$\tilde{C}_\kappa$ = overall volumetric concentration of component *k*, (L^3/L^3)

ρ_κ = density of pure component *k* , (m/L^3)

$C_{\kappa\ell}$ = concentration of component *k* in phase ℓ , (L^3/L^3)

$\vec{u}_\ell$ = volumetric flux of phase ℓ , (L/t)

$\vec{\tilde{D}}_{\kappa\ell}$ = dispersive flux of component *k* in phase ℓ , (L^2/t)

R_κ = total source/sink flow for component *k*, (m/L^3t)

The overall volume of component κ per unit pore volume will be computed as follows:

$$\tilde{C}_\kappa = \left(1 - \sum_{k=1}^{n_{cv}} \hat{C}_\kappa\right)\sum_{\ell=1}^{n_p} S_\ell C_{\kappa\ell} + \hat{C}_\kappa, \text{ for } \kappa = 1,\ldots, n_c \tag{6.2}$$

where

$\tilde{C}_\kappa$ = overall volumetric concentration of component κ , (L^3/L^3)

n_{cv} = total number of volume-occupying components

$\hat{C}_\kappa$ = adsorbed concentration of species κ , (L^3/L^3)

n_p = number of phases

S_ℓ = saturation of phase ℓ, (L^3/L^3)

6.2.2 The Pressure Equation

The pressure equation will be formed by summing up the mass balances over all volume-occupying components, and substituting Darcy's law in each of phase flux terms, using the definition of capillary pressure. By knowing that $\sum_{\kappa=1}^{n_{cv}} C_{\kappa\ell} = 1$ (sum of concentrations of all the components in each phase equals to l), the pressure equation in terms of the reference phase pressure (phase 1) will be:

$$\phi C_t \frac{\partial P_1}{\partial t} + \vec{\nabla} \bullet \vec{\vec{K}} \bullet \lambda_{rTc} \vec{\nabla} P_1 = -\vec{\nabla} \bullet \sum_{\ell=1}^{n_p} \vec{\vec{K}} \bullet \lambda_{r\ell c} \vec{\nabla} D + \vec{\nabla} \bullet \sum_{\ell=1}^{n_p} \vec{\vec{K}} \bullet \lambda_{r\ell c} \vec{\nabla} P_{c\ell 1} + \sum_{\kappa=1}^{n_{cv}} Q_\kappa, \tag{6.3}$$

where

C_t = total system compressibility, (Lt^2/m)

$\vec{\vec{K}}$ = permeability tensor, (L^2)

P_1 = pressure of phase 1, (Lt^2/m)

Q_κ = source/sink flow for component κ per bulk volume. (L^3/L^3t)

$P_{c\ell 1}$ = capillary pressure between the given phase ℓ and phase 1, (Lt^2/m)

D = depth, (L)

$\lambda_{r\ell c}$ = relative mobility, (m/Lt)

λ_{rTc} = total relative mobility, (m/Lt)

The relative mobilities ($\lambda_{r\ell c}$ and λ_{rTc}) and total compressibility (C_t)are calculated based on the following equations:

$$\lambda_{r\ell c} = \frac{k_{r\ell}}{\mu_\ell} \sum_{\kappa=1}^{n_{cv}} \rho_\kappa C_{\kappa\ell}, \tag{6.4}$$

$$\lambda_{rTc} = \sum_{\ell=1}^{n_p} \lambda_{r\ell c}, \tag{6.5}$$

$$C_t = C_r + \sum_{\kappa=1}^{n_{cv}} C_\kappa^o \tilde{C}_\kappa, \tag{6.6}$$

where

C_r = rock compressibility

C_κ^o = component compressibility

6.2.3 Relative Permeability-Capillary Pressure Models

Surfactants can alter wettability and reduce IFT to increase capillary number; consequently, residual oil will be mobilized due to reduced capillary forces. The simulator has the capability to model wettability alteration for both static imbibition cell and dynamic corefloods. Relative permeability and capillary pressure for each extreme wetting condition in every gridblock will be calculated in every time step based on the Corey model as following:

$$k_{r\ell} = k_{r\ell}^o S_{n\ell}^{n_\ell}, \tag{6.7}$$

where ℓ refers to water, oil, or microemulsion phase, $k_{r\ell}^o$ is the endpoint relative permeability, n_ℓ is the exponent, and $S_{n\ell}$ is the normalized saturation as computed by

$$S_{n\ell} = \frac{S_\ell - S_{\ell r}}{1 - \sum_{\ell=1}^{n_p} S_{\ell r}}, \qquad \ell = \text{water, oil or microemulsion phase} \tag{6.8}$$

where S_ℓ is the saturation , n_p is the number of phases, and $S_{\ell r}$ is the residual saturation.

The altered relative permeability and capillary pressure will be calculated by interpolating between two initial and final wetting conditions using a factor ω which can either be a constant value or be dependent on surfactant adsorption as shown below (Delshad *et al*., 2006).

$$k_{r\ell}^{altered} = \omega_1 k_{r\ell}^{final} + \left(1-\omega_1\right) k_{r\ell}^{initial}, \tag{6.9}$$

$$P_c^{altered} = \omega_2 P_c^{final} + \left(1-\omega_2\right) P_c^{initial}, \tag{6.10}$$

where ω_1 and ω_2 are the interpolation scaling factors for relative permeability and capillary pressure, respectively, *final* and *initial* refer to the two extreme wetting states, $k_{r\ell}$ is phase ℓ relative permeability, and P_c is the capillary pressure between pair of phases.

The scaling factors ω_1 and ω_2 in Eqs. (6.9) and (6.10) are either constant or dependent on adsorbed surfactant concentration as following:

$$\omega_1 = \omega_2 = \frac{\hat{C}_{surf}}{C_{surf} + \hat{C}_{surf}}, \tag{6.11}$$

where C_{surf} and $\hat{C}_{surf}$ are the total and the adsorbed surfactant concentrations calculated in every gridblock and every time step.

Surfactant effect on IFT and subsequently on residual saturations is incorporated by a dimensionless group, *trapping number*, which is a combination of capillary number and bond number as expressed below to model the effect of capillary, gravity and viscous forces at the pore-scale in three dimensions (Delshad, 1994):

$$N_{T\ell} = \frac{\left| -\vec{\vec{K}} \bullet \vec{\nabla} \Phi_{\ell'} - \vec{\vec{K}} \bullet \left[g\left(\rho_{\ell'} - \rho_{\ell}\right) \vec{\nabla} h \right] \right|}{\sigma_{\ell\ell'}}, \tag{6.12}$$

where $N_{T\ell}$ is dimensionless trapping number, $\vec{\vec{K}}$ is permeability tensor, ρ_l is phase density, h is vertical depth, and σ is interfacial tension. The imbibition process is first initiated by considering surfactant diffusion into a gridblock; IFT is then reduced with the increase in trapping number Eq. (6.12). The residual oil saturation reduces as trapping number increases, with subsequent changes in endpoint relative permeability, endpoint capillary pressure, and exponents of relative permeability curves.

The effect of mobilization on residual phase saturations is modeled as follows (Delshad, 1994):

$$S_{\ell r} = S_{\ell r}^{high} + \frac{S_{\ell r}^{low} - S_{\ell r}^{high}}{1 + T_{\ell} N_{T\ell}}, \tag{6.13}$$

where $S_{\ell r}^{high}$ and $S_{\ell r}^{high}$ are residual saturations for phase-ℓ at high and low trapping numbers, respectively, T_{ℓ} is the trapping parameter for phase ℓ assigned as input and $N_{T\ell}$ is trapping number of phase ℓ. The effect of mobilization on endpoint relative permeabilities is modeled as follows:

$$k_{r\ell}^{o} = k_{r\ell}^{o^{high}} + \frac{S_{\ell' r}^{low} - S_{\ell' r}}{S_{\ell' r}^{low} - S_{\ell' r}^{high}} \left(k_{r\ell}^{o^{high}} - k_{r\ell}^{o^{low}} \right), \tag{6.14}$$

where $k_{r\ell}^{o^{high}}$ and $k_{r\ell}^{o^{low}}$ are phase ℓ endpoint relative permeability at high and low trapping numbers, respectively, $S_{\ell' r}$ corresponds to residual saturation of the conjugate phase ℓ, and $S_{\ell' r}^{low}$ and $S_{\ell' r}^{high}$ are residual saturations at low and high trapping numbers, respectively.

The effect of IFT on capillary pressure is modeled as shown below:

$$P_c = C_{pc} \frac{\sigma_{om}}{\sigma_{ow}} \left(1 - S_{\ell}\right)^{E_{pc}}, \tag{6.15}$$

where C_{pc} and E_{pc} are endpoint and exponent for capillary pressure, respectively, and IFT for oil/microemulsion and oil/water phases are represented by σ_{om} and σ_{ow}, respectively. The parameter C_{pc} takes into account the effect of porosity and permeability using the Leverett J-function.

6.3 SCALE UP METHODOLOGY

Several dimensionless scaling groups exist for modeling imbibition experiments. Essentially, dimensionless time defined as scaling equation includes the characteristic length, viscosity ratio, core geometry, and IFT to predict oil recovery at larger scales under either gravity dominated or capillary dominated mechanisms. These dimensionless groups are applicable only to processes in which IFT remains constant or wettability remains unchanged. Zhang *et al*. (1995) used laboratory results to estimate oil recovery from fractured matrix blocks for field scales that have matrix sizes, boundary conditions, and heterogeneities much different from core scales. He used a shape factor proposed by Kazemi *et al*. (1992) to compensate for the effect of size and boundary conditions of the system for mass transfer between matrix and fracture. This shape factor was modified later by Zhang *et al*. (1995) based on the data provided by Hamon and Vidal (1986). For cylindrical cores there are four boundary conditions: 1) all faces open to imbibition (AFO), 2) two ends open to imbibition (TEO), 3) one end open to imbibition (OEO), 4) two ends closed to imbibition (TEC). A dimensionless group was proposed considering core size, boundary conditions, and fluid viscosities. Other imbibition test data were used to verify the correctness of this generalized dimensionless group.

Al-Lawati and Saleh (1996) achieved the best results for scaling imbibition tests by combining the dimensionless gravity and capillary groups. However, the correlation lacks satisfactory results compared to measured recoveries. For large spatial scales, IFT reduction may cause an increase or decrease in oil recovery, depending on the degree of capillarity and buoyancy.

Mattax and Kyte (1962) introduced their classic scaling group correlating field production rate and matrix block size as follows:

$$t_{\mathrm{D}}=\sqrt{\frac{k}{\phi}}\frac{\sigma}{\mu_{\mathrm{w}}}\frac{1}{\mathrm{L}^{2}}\mathrm{t}, \tag{6.16}$$

where t_D is the dimensionless time, k is permeability, ϕ is porosity, σ is interfacial tension between oil and water, μ_w is the water viscosity, L is the length of the core, and t is the total duration of imbibition experiment. The limitations with this scaling group were the lack of gravity effects, core shape, boundary conditions, and relative permeability functions.

Parsons and Chaney (1966) proposed the following dimensionless scaling group:

$$t_{\mathrm{D2}}=\frac{k}{\phi}\left[\frac{\Delta\rho\mathrm{g}}{\mu\mathrm{L}}\right]\mathrm{t}, \tag{6.17}$$

where $\Delta\rho$ is the density difference between a pair of fluids.

Hagoort (1980) performed one-dimensional gravity drainage oil recovery experiments from oil wet rocks and developed the following dimensionless time for recovery factor:

$$\mathrm{t}_{\mathrm{Dg}}=\frac{\mathrm{k}\mathrm{k}_{\mathrm{ro}}^{0}\Delta\rho\mathrm{g}}{(\mathrm{S}_{\mathrm{oi}}\text{-}\mathrm{S}_{\mathrm{or}})\phi\mu_{\mathrm{o}}\mathrm{L}}t, \tag{6.18}$$

$$E_R=\frac{(S_{oi}-\overline{S_o})}{(S_{oi}-S_{or})}, \tag{6.19}$$

where the recovery factor, E_R, is

$$E_R = \begin{cases} t_{Dg} & \text{for} \quad t_{Dg} < t_{BT} \\ 1 - \dfrac{1 - \dfrac{1}{n}}{(nt_{Dg})^{\frac{1}{n-1}}} & \text{for} \quad t_{Dg} > t_{BT} \end{cases}, \tag{6.20}$$

where $t_{BT} = \dfrac{1}{n}$, k_{ro}^0 is the oil relative permeability endpoint, $\Delta\rho$ is the density difference between oil and water, S_{oi} is initial oil saturation, S_{or} is residual oil saturation, μ_o is oil viscosity, and $\overline{S_o}$ is average oil saturation in the core. The parameter n is the Corey exponent in Haggort's (1980) equation.

Ma *et al*. (1997) improved the above correlation by including a characteristic length for counter-current flow instead of core length. Their work resulted in two different groups using either oil and water viscosities; but finally they introduced the new scaling group as follows:

$$t_D = \sqrt{\frac{k}{\phi}} \frac{\sigma}{\sqrt{\mu_o \mu_w}} \frac{1}{L_C^2} t, \tag{6.21}$$

where t_D is the dimensionless time and L_C is the core characteristic length. The characteristic length is defined based on core geometry by Kazemi *et al*. (1992) as:

$$L_C = \sqrt{\frac{V_b}{\sum \frac{A_i}{d_i}}}, \tag{6.22}$$

where V_b is the core bulk volume, A_i are surface areas exposed to spontaneous imbibition, and d_i are distances to no-flow boundaries.

For the cylindrical core sample, L_c will be defined as follows:

$$L_c = \frac{Ld}{2\sqrt{d^2+2L^2}}, \tag{6.23}$$

where d is the core diameter.

Li and Horne (2002) derived a more general scaling group for spontaneous imbibition by incorporating both gravity and capillary forces in addition to other parameters such as mobility and rock properties. They tested the model using the published data of Schechter *et al*. (1994). The following equation gives the final definition for dimensionless time, t_d :

$$t_d = c^2 \frac{M_e^* P_c (S_{wf} - S_{wi})}{\phi L_c^2} t, \tag{6.24}$$

where c is the ratio of the gravity to capillary forces (*i.e.*, Bond number), M_e^* is the effective mobility, P_c is capillary pressure, S_{wf} is the water saturation at the displacement front, S_{wi} is the initial water saturation, ϕ is porosity, L_c is the characteristic length which is give in Eq. (6.22), and t is the imbibition time.

6.4 MODELING STATIC IMBIBITION EXPERIMENTS

Investigating the mechanism of oil recovery by using new surfactant formulations or alkali is the primary steps for evaluating their performance at field scales. Static imbibition experiments are designed to evaluate the extent of wettability alteration or IFT reduction due to surfactant or alkali. The main objectives of imbibition experiments are summarized as:

- Assess effectiveness of chemical formulation to imbibe and produce oil
- Infer initial and final wetting states
- Infer initial and final capillary pressure and relative permeability curves
- Obtain magnitude of oil recovery and time response due to wettability alteration vs. IFT reduction
- Provide an understanding of oil recovery mechanisms and how to scale up

6.4.1 Experimental Procedure

A vuggy fractured carbonate rock was used in this study (Figure 6-1) and the set up of imbibition cell test is shown in Figure 6-1. The diameter of the large core was 4 inches and the height was 6 inches with a measured porosity and permeability of 14% and 50.6 md. Prior to the imbibition test, contact angle measurements were performed on core slabs and calcite plates. The results indicated that the rock is oil-wet. The original reservoir core was flooded with surrogate crude oil without pre-cleaning and then aged in the crude oil for one week at reservoir temperature of 100 ^{0}C to make it oil-wet similar to the in-situ wettability condition as shown in Figure 6-2. The dead crude oil has a viscosity of 15 cp at 100 ^{0}C and the surrogate oil is the 70 % dead oil mixed with 30 % cyclohexane which has a viscosity of 2.5~3 cp at 100 ^{0}C similar to live oil. It is obvious

from the figure that the core was very vuggy. The anionic surfactant used for the imbibition experiment was Enordet A092, which is a branched C16 alkoxyl sulfonate with 9 ethoxylate (EO) groups. The optimum solubilization ratio is around 28 with an optimal salinity of 43,000 ppm (Figure 6-3). The solubilization ratio is used to calculate IFT as proposed by Huh (1979):

$$\sigma_{\ell 3} = \frac{0.3}{R_{\ell 3}^{\ 2}}, \qquad \ell = 1(\textit{water phase}), 2(\textit{oil phase}) \tag{6.25}$$

where $\sigma_{\ell 3}$ is the IFT between either water-microemulsion or oil-microemulsion phases, and $R_{\ell 3}$ is the solubilization ratio.

After aging the core with crude oil, it was immersed in the imbibition cell filled with the surfactant solution at the optimum salinity. Surfactant diffuses into the core; IFT is reduced and wettability will be altered from oil wet to water wet. Wettability alteration and IFT reduction are the key mechanisms to push oil out of the matrix core by buoyancy where oil accumulates at the top of the cell. Oil comes out of the core from the top and no oil was drained from the sides. This is indicative of gravity as the main driving mechanism for oil recovery but capillarity can also be an additional driving force. Based on the measured IFT after imbibition tests, it was concluded that the surfactant used in imbibition experiment reduces the IFT to a value of 0.05 mN/m with negligible capillary force. Table 6-1 shows the summary of core, crude oil, and surfactant properties for imbibition experiments performed by Mohanty (2010) at reservoir temperature. The first five samples were core plugs and the last one (16A1-1) was large whole core sample which is explained comprehensively in this section. The imbibition recovery data for different core sizes are shown in Figure 6-4.

Table 6-1: The core properties of imbibition experiments performed by Mohanty (2010).

Core ID	N17	N18	AKL-207	SD-17	22A1-1	16A1-1
Diameter (cm)	3.80	3.80	3.80	3.80	3.80	10.16
Length (cm)	4.389	4.455	4.487	7.47	8.075	15.04
Porosity (%)	18.9	16.3	8.3	17.53	9.13	14
Permeability (md)	74.7	66.6	3.02	185	8.95	50.6
Crude oil viscosity, cp	3.5	3.5	2.5	3.5	3.5	3.5
Initial oil saturation	0.835	0.835	0.807	0.646	0.541	0.85
Residual oil saturation	0.45	0.45	0.45	0.32	0.38	0.45
Irreducible water saturation	0.165	0.165	0.193	0.354	0.459	0.15
Temperature (^{0}C)	100	100	100	100	100	100
Surf. conc. (wt%)	0.25	0.25	0.25	0.25	0.25	0.25
Imbibition duration (days)	14	14	14	42	31	57
Total oil recovery (%OOIP)	24	31	28	51.65	28.85	48
Final IFT (mN/m)	8	~3	0.005	0.5	0.5	0.05
Salinity (ppm)	38,000	38,000	38,000	38,000	38,000	38,000
Contact angle (Degree)	80	40	120	120	120	40

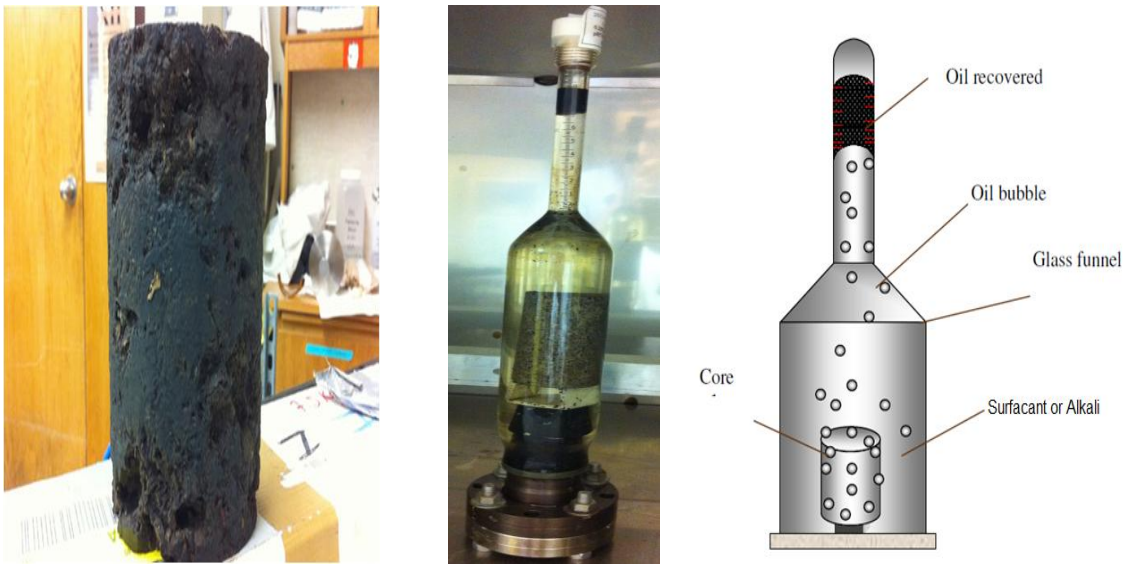

Figure 6-1: The image of vuggy carbonate core and static imbibition experimental set up (Mohanty, 2010).

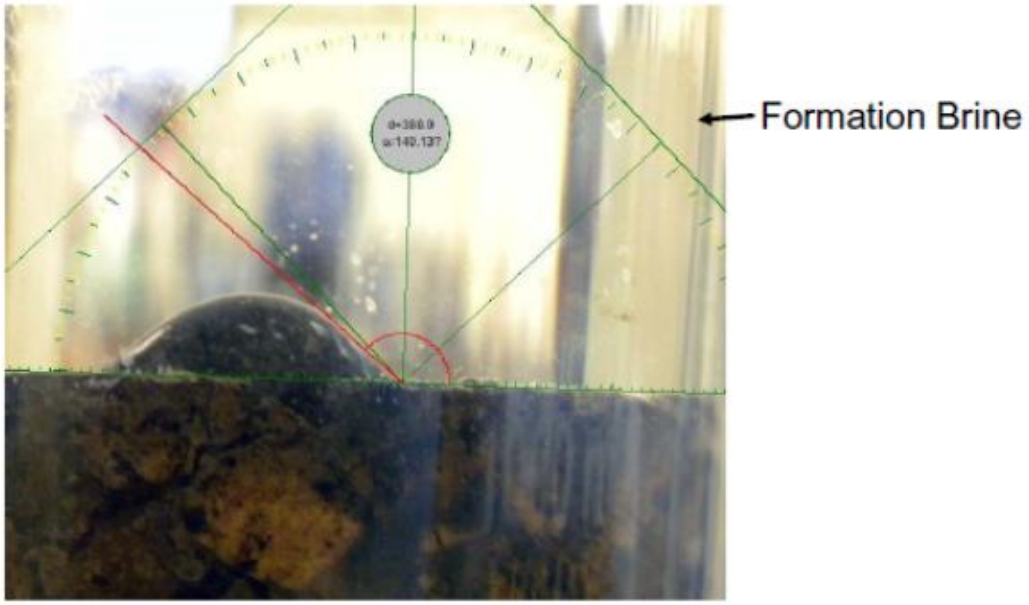

Figure 6-2: Oil-wet core after aging with the crude oil for one week at reservoir temperature of 100 ^{0}C (Mohanty, 2010).

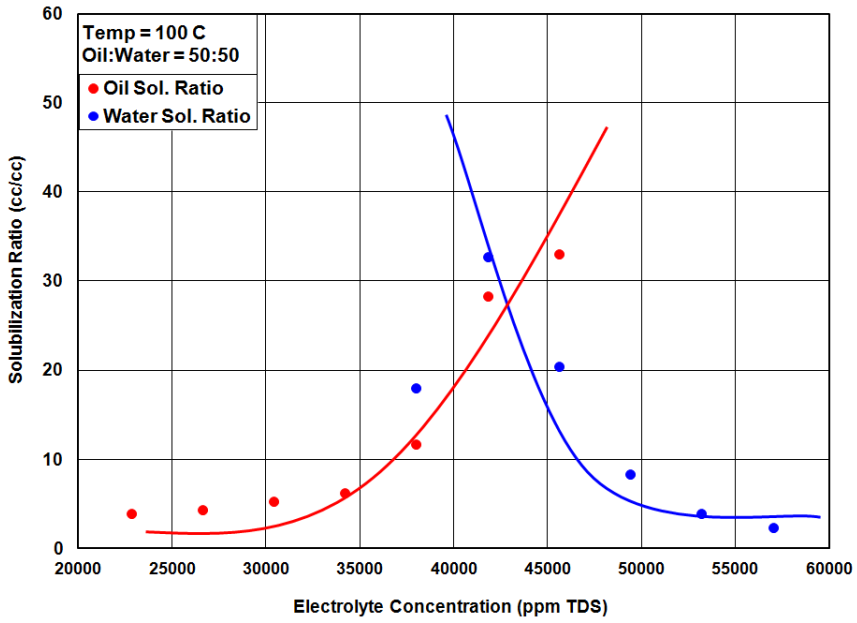

Figure 6-3: Phase behavior for Enordet surfactant and oil at 100 ^{0}C (Oil = 30 % cyclohexane and 70 % crude oil).

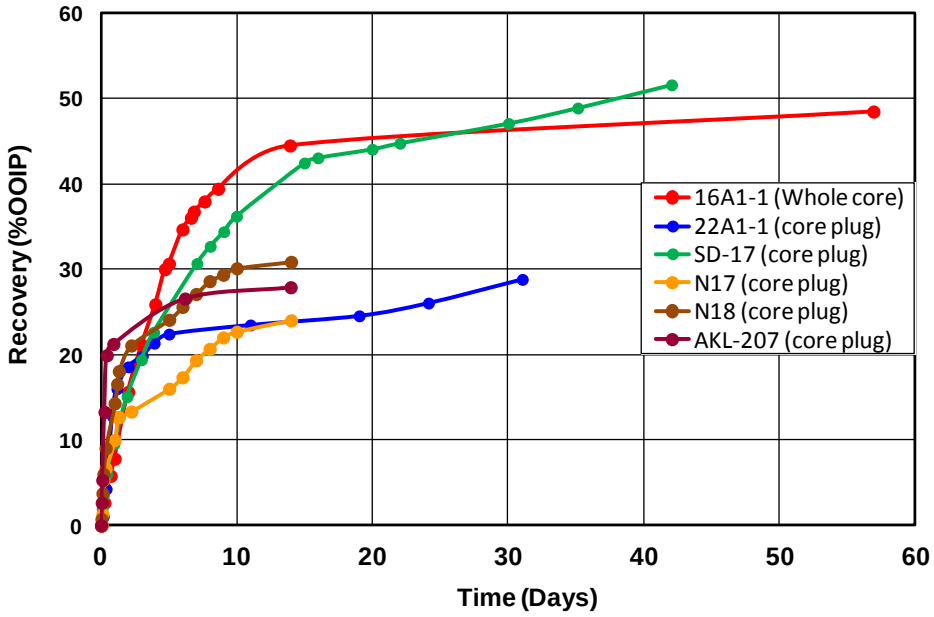

Figure 6-4: Imbibition tests oil recoveries for different core sizes at reservoir temperature (Mohanty, 2010).

6.4.2 Imbibition Test Modeling and the Effect of Matrix Block Size on Oil Recovery

6.4.2.1 Imbibition Test Simulation

Most of the experimental studies on imbibition cell tests were performed using core samples of 1.5 to 4 inches in diameter and 2 to 6 inches in height. The core plug sample (1.5 inch in diameter) was modeled using a Cartesian homogeneous structure with 7×7×7 gridblocks. The middle of the model with 5×5×5 gridblocks is assigned to the core with its properties of permeability and porosity and is saturated with reservoir crude oil. The remaining gridblocks (non-rock) mimic the container filled with the surfactant solution assigning porosity of 1.0, permeability of 1,000 D, and capillary pressure of zero. Then for modeling a larger whole core sample (4 inch in diameter), the size of

gridblocks was kept the same as the smaller core but the number of gridblocks increased to 19×19×19 (Figure 6-5) to investigate upscaling of the process. The blue region is the rock (reservoir porosity and permeability) and has zero initial surfactant concentration, while the red region is filled with 0.25 wt% surfactant concentration. As the surfactant enters the rock gridblocks by molecular diffusion, it gives more favorable relative permeabilities and capillary pressures from oil-wet to water-wet due to wettability alteration effect of surfactant. The gravity and oil buoyancy will then take effect and oil will accumulate at the top of the imbibition cell since the capillary forces become negligible and oil will be released from the pores. The simulations are based on both IFT reduction and wettability alteration using the constant ω factor option (Eqs. (6.9) and (6.10)). The detail of the input data for this simulation is in Appendix A.

The whole core imbibition experiment described previously was mainly gravity-dominated with negligible capillary pressure. There was no oil production when the oil saturated core was placed in the cell filled with brine; this confirms the oil-wet nature of the rock. The entire core and imbibition container model set up has 19×19×19 gridblocks. The middle part of the model with 17×17×17 gridblocks represents the core rock. Therefore, 19×19×2 (top of the core) + 4×18×17 (sides of the core) = 1946 gridblocks remaining will define the container filled with surfactant solution. The properties of rock, oil, and surfactant solution used for imbibition test experiment are given in Table 6-2.

6.4.2.2 Impact of Matrix Block Height

A sensitivity analysis with respect to the number of gridblocks in vertical direction was conducted and considerable change in oil production rate was observed with negligible effect on final oil recovery. Gravity was the main dominant mechanism

for oil recovery in imbibitions tests as explained before and for this reason, increasing the height of the matrix leads to a reduction in oil production rate as shown in Figure 6-6. It should be noted that for different block sizes in vertical direction, almost the same final oil recovery will be achieved but the oil production rate will be higher for larger column height or shorter block size in vertical direction. Gravity segregation will be effective when IFT is adequately low and wettability is altered in the core where both of these conditions are met as explained previously. The oil saturation distributions for different number of grids in vertical direction are shown in Figure 6-7.

Table 6-2: Properties of the large core sample, oil, and surfactant used in the imbibition cell test.

Variable	Unit	Value	Variable	Unit	Value
Core ID	--------	L1 (large core)	Reservoir temperature	°C	100
No. of grids	--------	19×19×19	Oil rel. perm. endpoint	--------	0.7
Core diameter and length	Cm	10.16, 15.04	Surfactant Conc.	wt %	0.25
Porosity	%	14	IFT before surfactant treatment	mN/m	30
Permeability	cm^2	50.6×10^{-11}	IFT after surfactant treatment	mN/m	0.05
Crude oil viscosity	cp	3.5	Contact angle before surfactant treatment	Degrees	150
Initial oil saturation	fraction	0.85	Contact angle after surfactant treatment	Degrees	40
Residual oil saturation	fraction	0.45	Total oil recovery	% OOIP	48

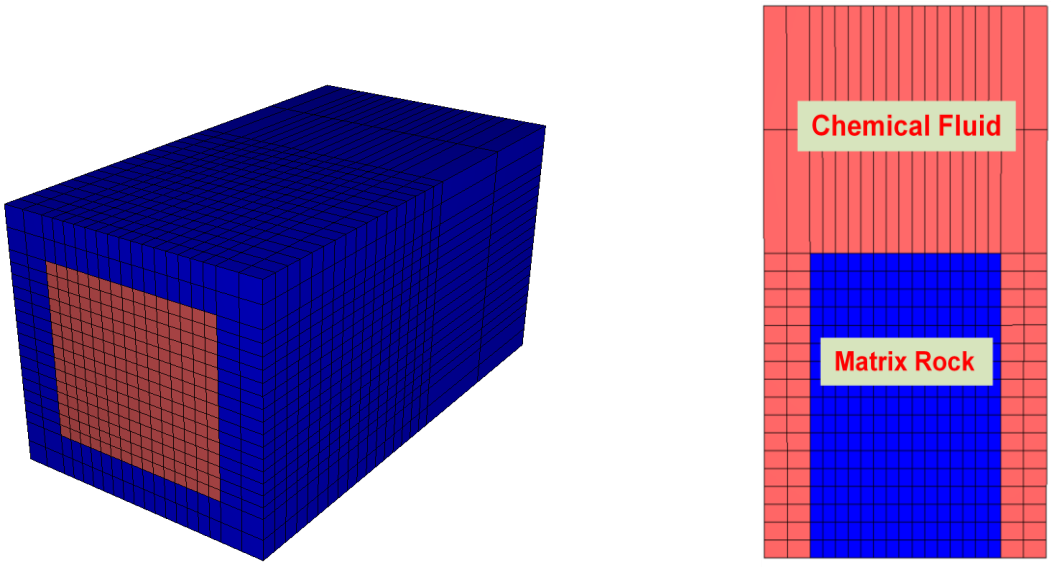

Figure 6-5: 3-D simulation model used to history match whole core in static imbibition test.

6.4.2.3 Impact of Matrix Block Size in the Areal Direction

A sensitivity analysis with respect to the number of gridblocks in the areal direction was conducted and no considerable change in oil recovery was found. The same effective molecular diffusion coefficient for surfactant is used in all the simulation cases. However for the large size in areal direction, it takes much longer time for surfactant to diffuse into the rock and change wettability or reduce IFT. This can be the main reason for slightly lower oil production rate in the larger case. This shows that the main mechanism for recovery was gravity from the top side of the core, where counter-current capillary imbibition in the horizontal direction is negligible as shown in Figure 6-8. Gravity dominant imbibition is co-current and oil production happens only from the top of the core due to density difference between surfactant solution and oil. Due to gravity, water enters into the core mainly from the bottom of the core and oil is produced from the top with higher oil saturation. The oil saturation distributions for different number of

grids in areal direction are shown in Figure 6-9. It is clear that for larger matrix core in areal direction, there is no considerable recovery increase from the top of the cell.

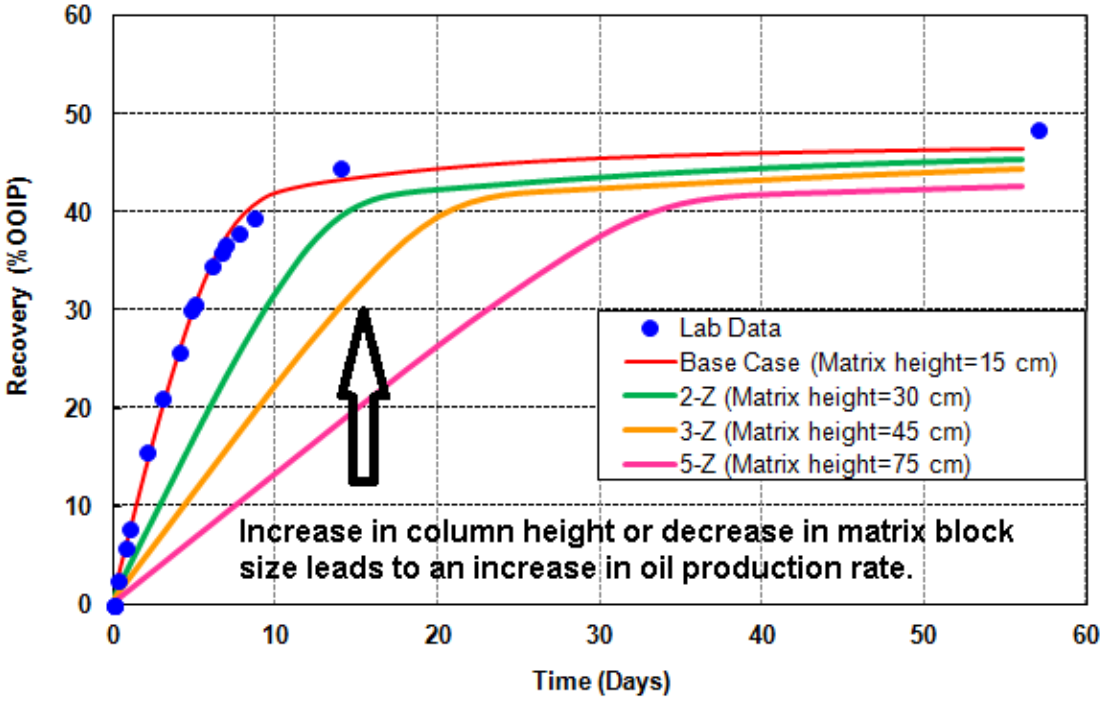

Figure 6-6: Surfactant imbibition cell test: Effect of the matrix block height on oil recovery.

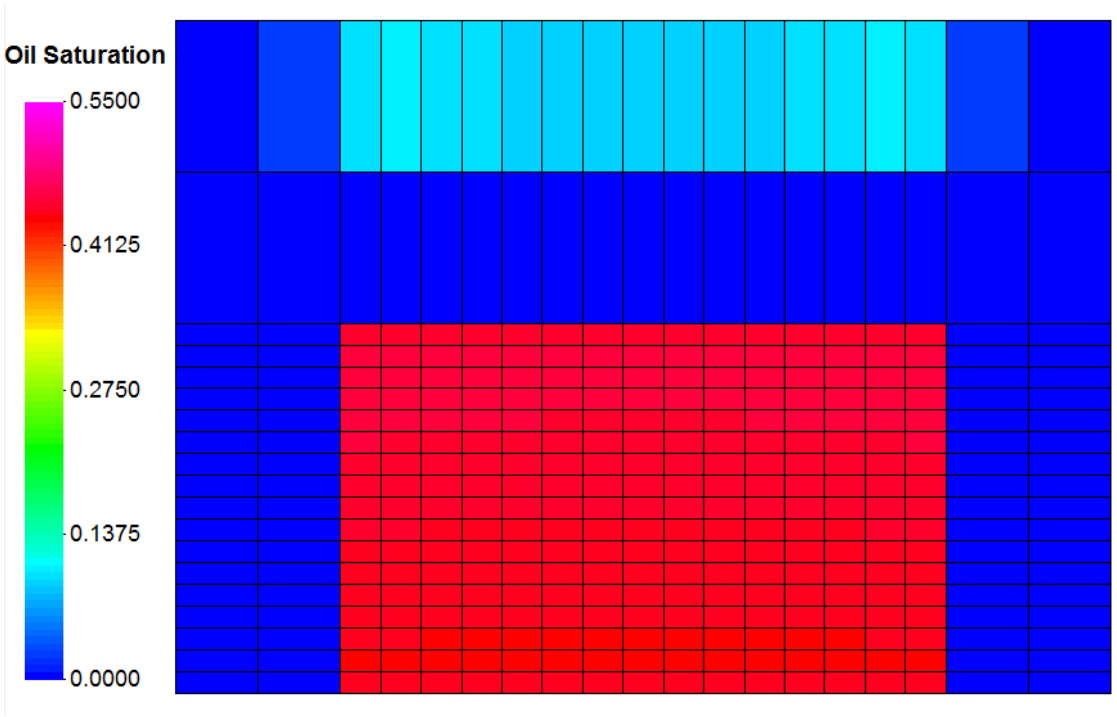
Oil Saturation
0.5500
0.4125
0.2750
0.1375
0.0000

(a)

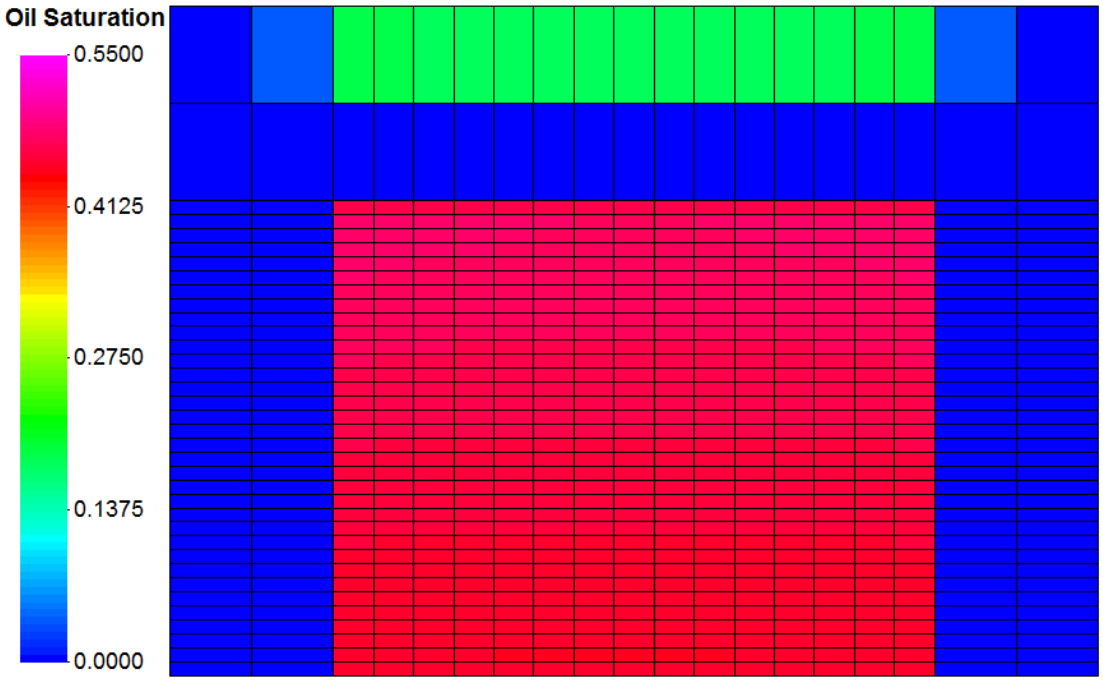
Oil Saturation
0.5500
0.4125
0.2750
0.1375
0.0000

(b)

Figure 6-7.

Figure 6-7, continued.

(c)

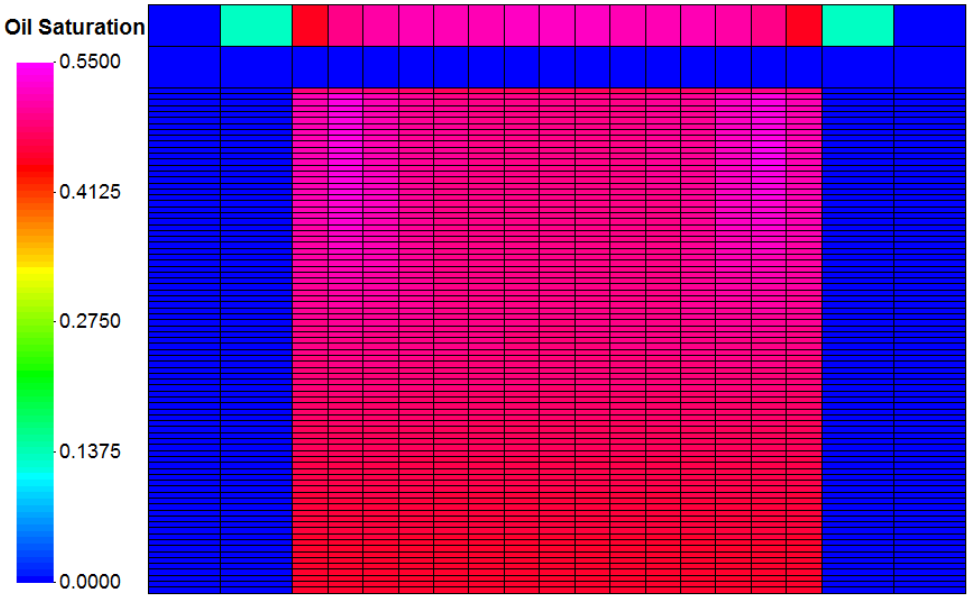

(d)

Figure 6-7: Profiles of oil saturation at 31 days with different grids in vertical direction: Base Case:19×19×19, (b) 19×19×36, (c) 19×19×53, (d) 19×19×87.

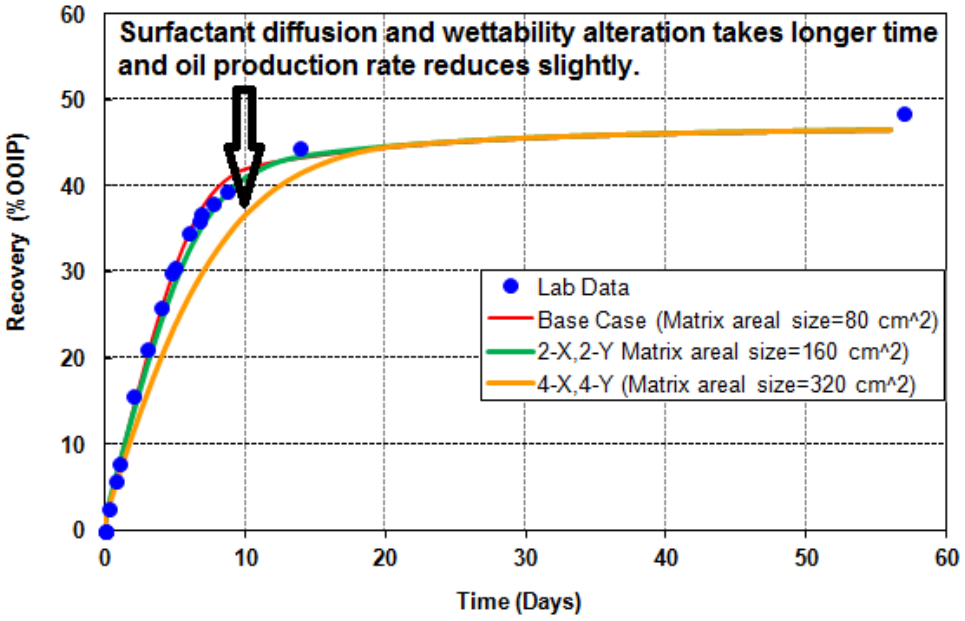

Figure 6-8: Oil recovery of imbibition cell test: Effect of the matrix block areal size on oil recovery.

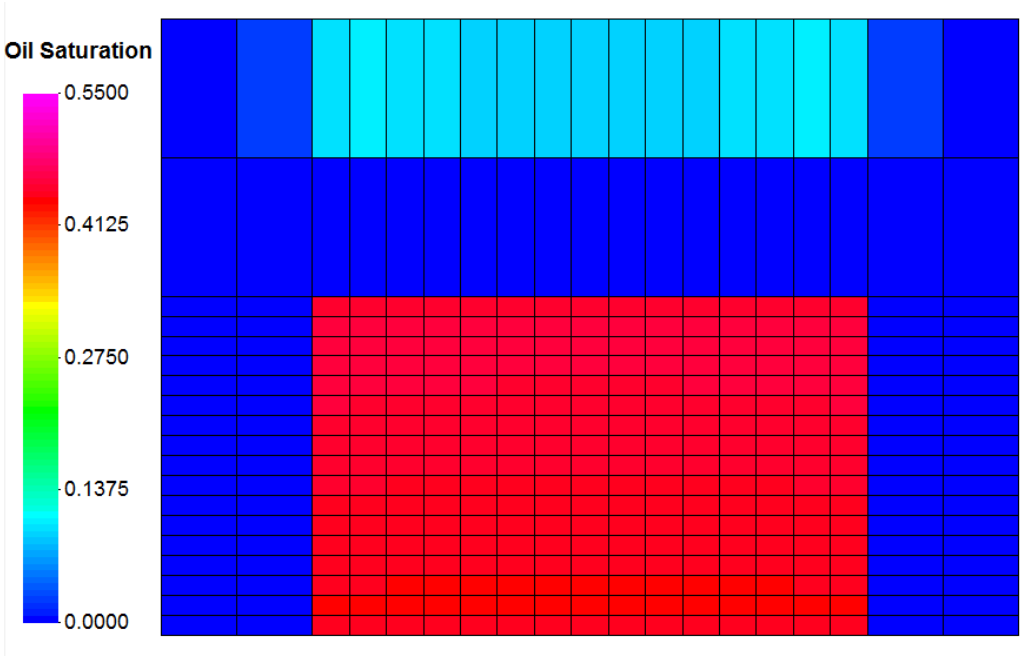

(a)

Figure 6-9.

Figure 6-9, continued.

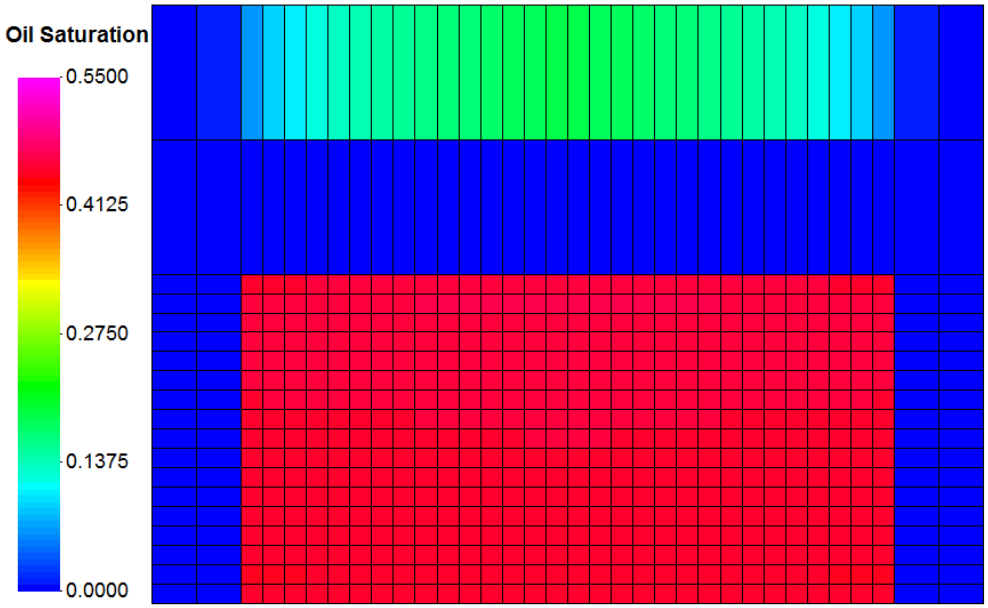

(b)

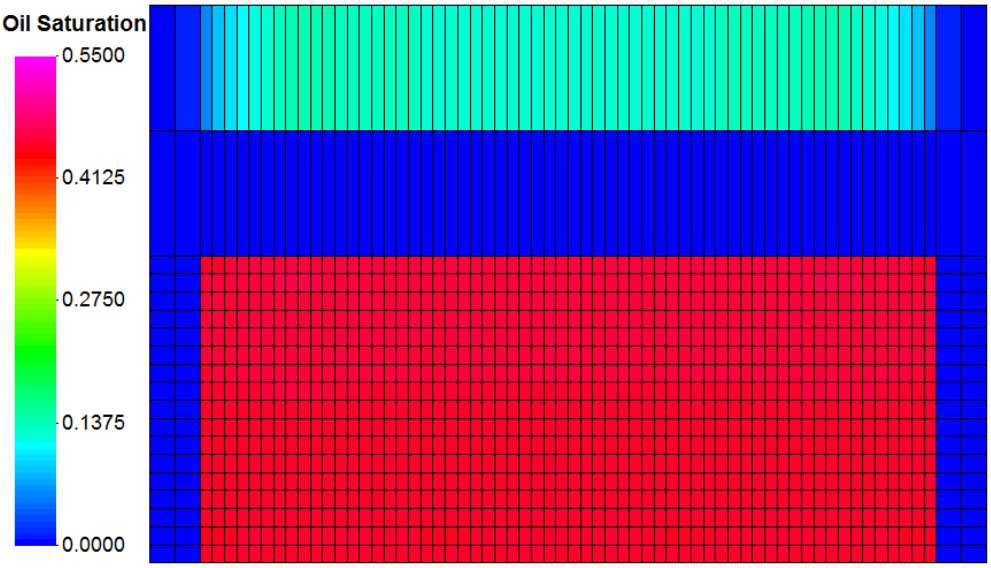

(c)

Figure 6-9: Profiles of oil saturation at 31 days with different grids in areal direction: Base Case:19×19×19, (b) 34×34×19, (c) 64×64×19.

6.4.3 Different Recovery Mechanisms (IFT Reduction vs. Wettability Alteration)

An imbibition cell test had been conducted for a small core with the diameter of 3.81 cm and length of 4.445 cm from the same vuggy fractured carbonate formation. The data were then used for a scale-up exercise where small core results were used to predict the performance of the large core. Contact angle measurements indicated that the rock is oil-wet. The imbibition cell test was performed at reservoir temperature of 100 ^{0}C. Table 6-3 gives rock and fluid properties and imbibition test conditions. The surfactant used for the small core imbibition test was branched C16, 17 alcohol alkoxyl sulfonate (9EO) with 0.5% EDTA as alkali to enhance wettability alteration. Relative permeability and capillary pressure parameters based on simulated recovery curve are shown in Table 6-4. The constant input value of scaling factor $\omega = 0.5$ is selected to evaluate the effect of wettability alteration using two relative permeability curves of oil-wet and water-wet conditions. This value gave very favorable history match of experimental results. It is clear from Eqs. (6.9) and (6.10) that any other values close to 1 or 0 will make either water-wet or oil-wet dominant in the final oil recovery and simulation results. Whereas, experimental data illustrated that the final wettability conditions of the rock was mixed-wet rather than either oil-wet or water-wet which confirms the use of 0.5 for the scaling factor.

Two approaches were used to history match the experiment. The first simulation was based on the hypothesis that both IFT reduction and wettability alteration occur in the core. The second simulation was based on the hypothesis that surfactant changes the core wettability from oil-wet to water-wet with no significant effect in reducing IFT (Goudarzi *et al.*, 2012). In both cases, surfactant can initially enter into the rock only by molecular diffusion with an effective diffusion coefficient of 3.72×10^{-6} m^2/d (4.0×10^{-5}

ft^2/d). A comparison of these two simulations for core S1 is shown in Figure 6-10. The simulation of wettability alteration gives similar recovery to the case of both IFT reduction and wettability alteration. As it is clear from Table 6-3, the oil/water IFT was reduced from 30 to only 3 mN/m when surfactant is used, indicating that ultralow IFT was not achieved. However, the reduction in contact angle to 40 degrees demonstrates and confirms that wettability alteration was the main mechanism for oil recovery. Calculated relative permeability curves for a trapping number of 3.0×10-5 are shown in Figure 6-11.

Table 6-3: Properties of the small core sample, oil, and surfactant used in the imbibition cell test.

Core ID	S1 (small core)
Diameter and length	3.81 cm, 4.455 cm
Porosity, permeability	0.163, 66.6×10^{-11} cm^2
Initial oil saturation	0.835
Irreducible water saturation	0.165
Surf. concentration	0.25 wt%
Oil recovery in surfactant	31 %OOIP
IFT before surfactant treatment	30 mN/m
IFT after surfactant treatment	~3 mN/m
Contact angle before surfactant treatment	150 Degrees
Contact angle after surfactant treatment	40 Degrees
Temperature	100 ^{0}C
Crude oil viscosity	3.5 cp
Residual oil saturation	0.45
Duration of imbibition experiment	14 Days

Table 6-4: Capillary pressure-relative permeability parameters used in the simulation of core S1.

Core S1	Mixed-Wet (preferentially oil-wet)		Water-Wet	
	Oil	Water	Oil	Water
Residual saturation	0.45	0.165	0.45	0.165
Relative permeability endpoint	0.3	0.81	0.56	0.39
Relative permeability exponent	6	1.9	4.5	2.5
Capillary pressure endpoint	5, -5		8.95	
Capillary pressure exponent	2		2.5	
Scaling Factor, ω_1	0.5			

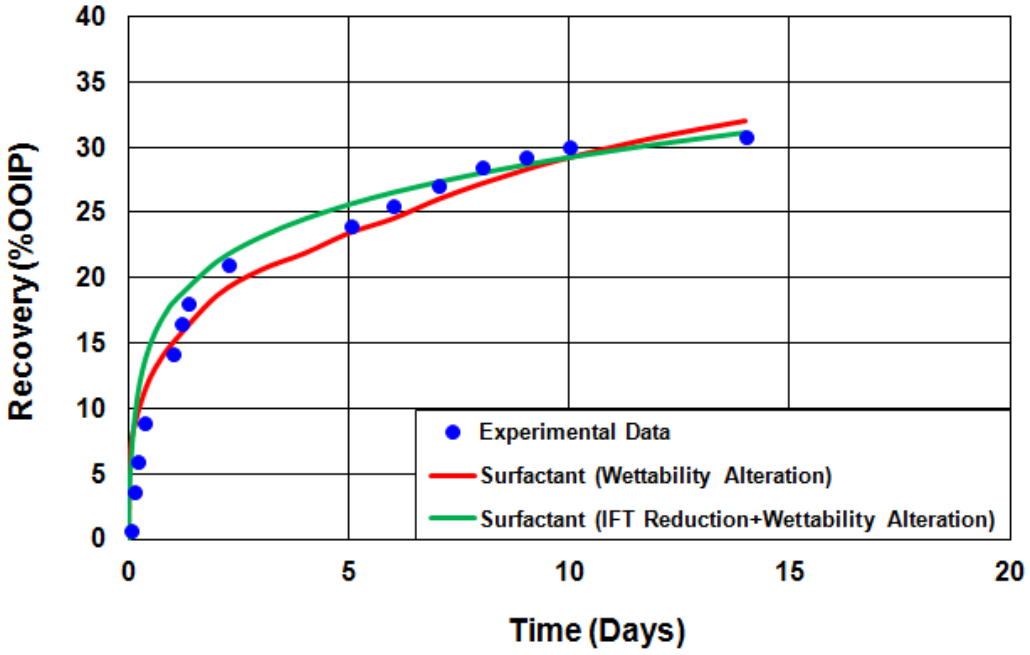

Figure 6-10: Simulated recovery curves using different surfactant model options for core S1.

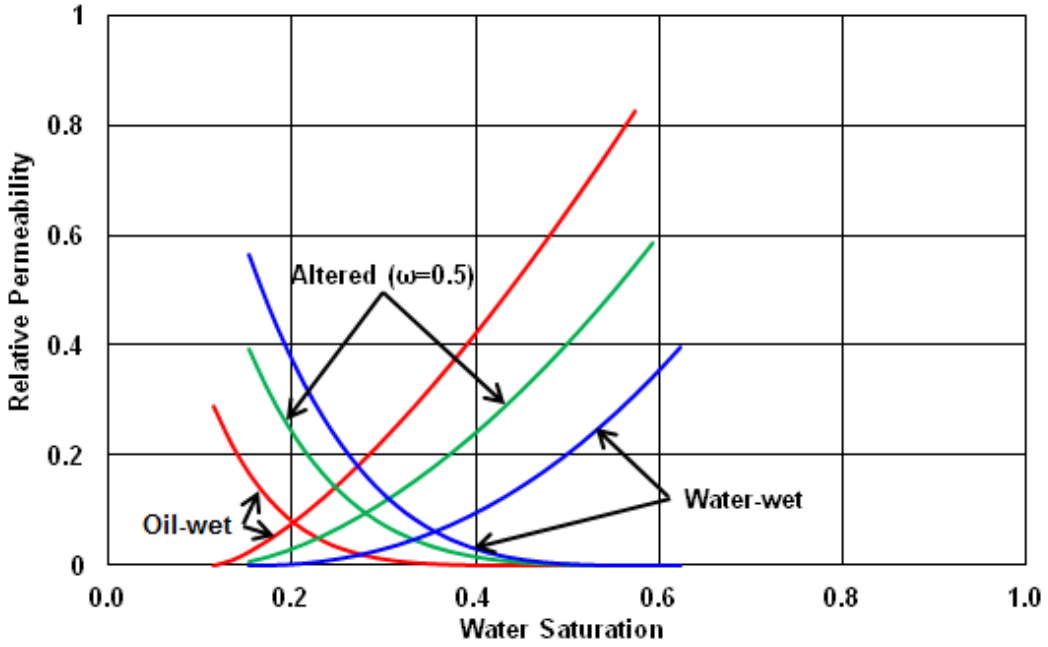

Figure 6-11: Relative permeability curves at different wetting states for NT=3.0×10^{-5}.

6.4.4 Inverse Bond Number

The macroscopic inverse bond number is an indication of the relative importance of capillary forces to gravity forces in the imbibition experiment. This ratio is given by

$$N_B^{-1} = C\frac{\sigma\sqrt{\frac{\phi}{k}}}{\Delta\rho g H}, \tag{6.26}$$

where C is a constant (equal to 0.4 for capillary tube model), H is the height, ϕ, and k are the porosity and permeability.

Schechter *et al*. (1994) found that for a large inverse bond number, $N_B^{-1} > 5$, the flow will be capillary dominated and for a small numbers, $N_B^{-1} < 1$, the flow will be gravity dominated. For $1 < N_B^{-1} < 5$ both capillary and gravity forces are dominant.

Therefore, based on experimental data and using Eq. (6.26), the dominant mechanism of flow can be determined. Table 6-5 gives the inverse Bond number for small and large cores. The simulation results for large core illustrate that oil comes out of the core from the top and no oil was drained from the sides which indicate gravity-dominant mechanism with negligible capillary-dominancy. On the other hand, the small values of inverse Bond number clearly show that gravity is more dominant than capillarity for the large core. However, capillary drive mechanism was more dominant in the recovery from small core as the inverse bond number is higher than 5. Therefore, the recovery mechanism determined by calculating inverse Bond number is consistent with simulation results, another confirmation that Hagoort scaling group is appropriate for this experiment.

Table 6-5: Inverse bond numbers for large and small cores.

Variable	**Unit**	**Value**	**Variable**	**Unit**	**Value**
Core ID	--------	L1 (Large core)	Core ID	--------	S1 (Small core)
IFT	mN/m	5×10^{-2}	IFT	mN/m	3
Porosity	fraction	0.14	Porosity	fraction	0.163
Permeability	cm^2	50.6×10^{-11}	Permeability	cm^2	66.6×10^{-11}
Height	cm	15.04	Height	cm	4.45
Density difference	gr/cm^3	0.2	Density difference	gr/cm^3	0.2
N_B^{-1}	--------	0.1128 < 1	N_B^{-1}	--------	21.5 > 5
Flow Mechanism	**Gravity Dominated**		Flow Mechanism	**Capillary Dominated**	

Delshad *et al*. (2009) investigated upscaling using the following dimensionless group and Hirasaki and Zhang (2004) published experiments in which the mechanism was gravity-dominated:

$$t_D = \frac{t}{t_g} = \frac{\Delta\rho g k}{L\mu_o} t. \tag{6.27}$$

The main goal of our study is to investigate two points:

- **a.** Check the correctness of the dimensionless group (Eq. (6.18)) for large core experiment.
- **b.** Use Eq. (6.18) but include the effect of IFT for both large and small cores which had been conducted under the same reservoir temperature using same surfactant formulation.

6.4.5 Validation of Gravity-Based Dimensionless Time

Firstly, the experiment was modeled and then simulations were performed using the same model parameters but with different core sizes. Simulated oil recoveries for different core sizes were scaled in the vertical direction (core diameter was held constant) using Eq. (6.18) for t_{Dg}. The results are satisfactory as presented in Figure 6-12.

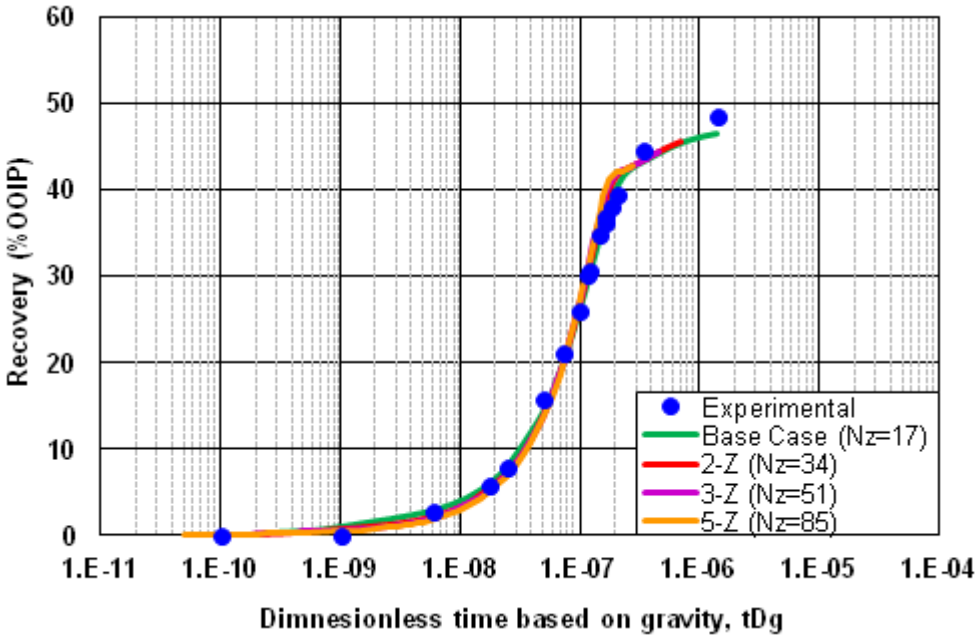

Figure 6-12: Scaling of oil recovery vs. dimensionless time for gravity-dominant flow (effect of matrix block height).

6.4.6 Predicting Recovery Data for Large Core Using Modified Dimensionless Time

In this section, scale up calculations are shown in which the lab results of small core are used to predict the oil recovery for large core and compare the results with the lab recoveries. Gravity-based dimensionless number proposed by Hagoort was used for scaling up the recovery curves. The main reason for choosing Hagoort model was its capability for modeling gravity-dominated imbibition processes (Hagoort, 1980; Adibhatla *et al.*, 2005; Adibhatla and Mohanty, 2006). The Hagoort model includes viscosity, more importantly oil relative permeability but lacks the IFT reduction. We modified Hagoort's model by including IFT factor where it showed a good agreement with oil recovery measured for larger scales.

Table 6-6 shows the properties used to predict oil recovery for large core imbibition test based on the small core results. Similar to Eq. (6.19) for oil recovery, IFT factor was used to incorporate the effect of IFT reduction on oil recovery:

$$IFT\ factor = \frac{\sigma_{initial} - \overline{\sigma}}{\sigma_{initial} - \sigma_{final}}, \tag{6.28}$$

where $\sigma_{initial}$ and σ_{final} are the oil-microemulsion IFT at the start and end of the imbibition test corresponding to S_{oi} and S_{or}. $\overline{\sigma}$ is the average IFT used as a matching parameter to predict recovery. Therefore, the equations to predict oil recovery including effects of gravity, capillarity, scaled by interfacial tension are obtained by inserting the above equation into E qs. (6.18) and (6.19) as given below (Goudarzi *et al.*, 2015):

$$t_{Dg} = \frac{kk_{ro}^{0}\Delta\rho g}{(S_{oi}\text{-}S_{or})\phi\mu_{o}L}\left(\frac{\sigma_{initial} - \overline{\sigma}}{\sigma_{initial} - \sigma_{final}}\right)t, \tag{6.29}$$

$$E_R = \frac{(S_{oi} - \overline{S_o})}{(S_{oi} - S_{or})}\left(\frac{\sigma_{initial} - \overline{\sigma}}{\sigma_{initial} - \sigma_{final}}\right). \tag{6.30}$$

The measured IFT for the small core was 3 mN/m (initial conditions) and it was 0.05 mN/m for the large core (final conditions) as given in Table 6-6. The modified Hagoort equation proposed here does not take into account the effect of wettability but can be applied to any IFT range from high to ultralow values. The predicted recovery curve comparison with measured data achieved for the large core is shown in Figure 6-13. The comparison shows a good agreement between predicted results and experimental data using the scaling groups of recovery factor and imbibition time. It is clear from the figure that there was almost 16 % improvement in prediction with

modified Hagoort compared to the original model. The proposed modified equation for predicting oil recovery is based on initial, final, and an average IFT, $\bar{\sigma}$. Initial and final IFTs are measured but IFT changes in each gridblock during imbibition process and it is not possible to measure IFT at each time step in the lab. Therefore using $\bar{\sigma}$ for the whole process is the main reason for deviation in the middle.

Table 6-6: Parameters used for scale-up of small core S1 to large core L1.

Variable	Unit	Value	Value
Core ID	……..	S1	L1
Absolute permeability	cm^2	66.6×10^{-11}	50.6×10^{-11}
End-point oil relative permeability	fraction	0.45	0.7
Oil viscosity	gr/cm-s	0.035	0.035
Oil density	gr/cm^3	0.8	0.8
Water density	gr/cm^3	1	1
Density difference	gr/cm^3	0.2	0.2
Length	cm	4.445	15.04
Porosity	fraction	0.163	0.14
Initial oil saturation	fraction	0.835	0.85
Residual oil saturation	fraction	0.45	0.45
IFT for the small core (initial conditions)	mN/m	3	
IFT for the large core (final conditions)	mN/m	0.05	

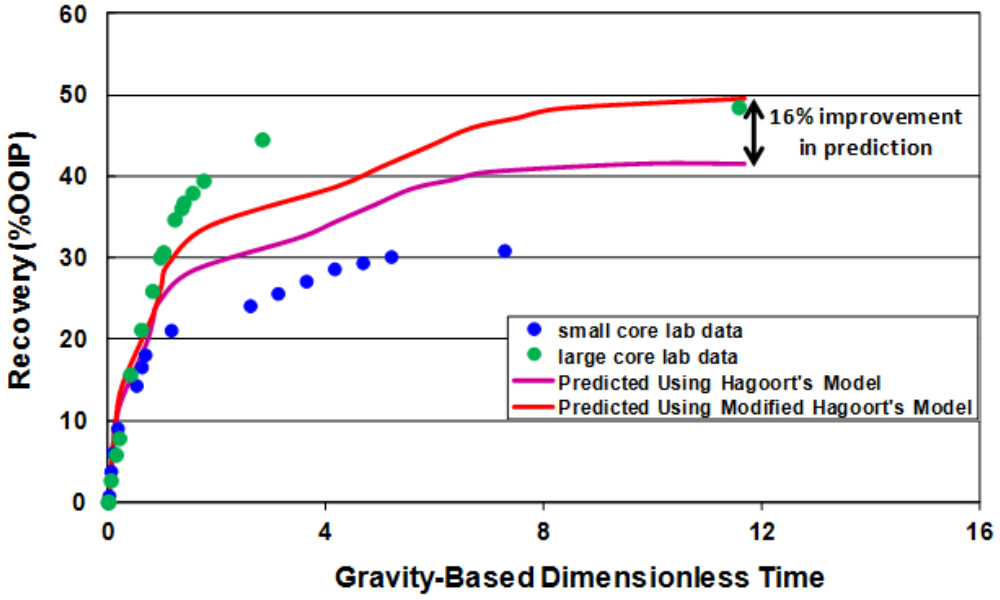

Figure 6-13: Comparison of predicted and lab recovery data for the large core.

6.5 MODELING DYNAMIC EXPERIMENTS (COREFLOOD TESTS)

Coreflood experiments are designed to evaluate the effectiveness of new surfactant formulations or alkali in vuggy/fractured carbonate rocks. The mains objectives of coreflood experiments are summarized as following:

- Assess effectiveness of chemical formulation to propagate in fracture/matrix/vug and produce oil
- Measure chemical retention
- Measure initial and final endpoint relative permeabilities
- Assess impact of pressure gradient
- Use larger cores
- Measurements at reservoir temperature/pressure
- Different drive mechanisms i.e. pressure gradient or gravity stable
- Help in Scale up

In the following sections, mechanistic modeling of coreflood experiment for a whole core sample will be investigated using two different approaches of heterogeneous permeability distribution and explicit fracture modeling. Table 6-7 shows the summary of three coreflood experiments performed by Pope (2010) for heterogeneous carbonate cores at reservoir temperature. The first two samples were core plugs and the last one (AKL-08) was a whole core sample described in the next section. The coreflood recovery data for different core sizes are shown in Figure 6-14. Table 6-8 shows the brine compositions used in the experiments.

Table 6-7: The core properties of coreflood experiments performed by Pope (2010).

Core ID	AKL-01	AKL-S03	AKL-08
Diameter (cm)	3.78	4.83	10.20
Length (cm)	29.79	26.7	27.40
Porosity (%)	16	10	9.7
Permeability (md)	211	1000	6
Crude oil viscosity, cp	2.5	3.0	2.1
Initial oil saturation	0.73	0.76	0.495
Residual oil saturation	0.122	0.05	0.14
Irreducible water saturation	0.27	0.24	0.505
Temperature (^{0}C)	100	100	100
Surfactant concentration (wt%)	1	1	1
Coreflood duration (PV_{inj})	3.55	1.76	1.71
Total oil recovery (%OOIP)	68.73	54.78	61
Salinity (ppm)	117,000	117,000	117,000

Table 6-8: Brine compositions used in all coreflood experiments.

Composition	Formation brine (ppm)	Synthetic seawater (SASW) (ppm)
Na^+	41,473	12,188
Ca^{2+}	3,880	480
Mg^{2+}	145	1,342
Cl^-	70,971	21,133
SO_4^{2-}	500	3,250
TDS	116,969	38,393

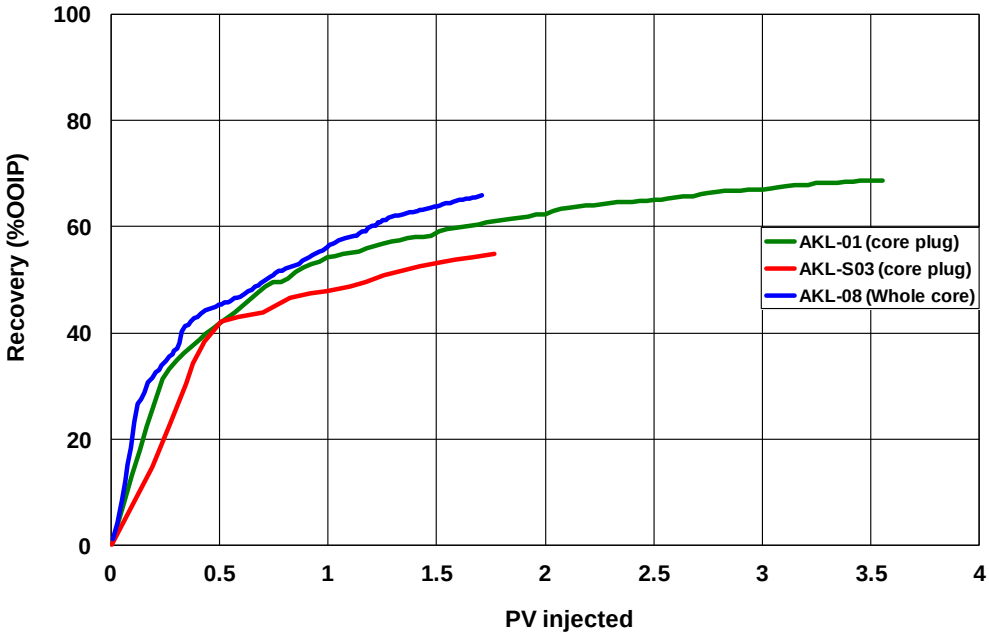

Figure 6-14: Coreflood tests recovery data for different core sizes at reservoir temperature (Pope, 2010).

6.5.1 Experimental Procedure

A reservoir core of about 27.4 cm (10.8 inches) in length and 10.2 cm (4.0 inches) in diameter was used for coreflood experiment and simulation study (AKL-08). The brine permeability was measured to be about 6 md before the core was fractured, which is close to the average matrix permeability. The composite core permeability was about 1970 md after it was fractured. The core is aged with oil and oil flooded to displace brine and measure the oil permeability and residual water saturation followed by a waterflood with formation brine (Table 6-8). The residual oil saturation and water relative permeability were measured. The chemical flood experiment was designed vertically to inject from bottom and produce from top to achieve gravity stable conditions at reservoir temperature of 100 ^{0}C.

A CT scan of the second core was conducted before and after the core was fractured. The images in Figure 6-15 show that the reservoir core is extremely heterogeneous and vuggy before fractures were made (Lu et al., 2012b). Some vugs are connected and some are isolated. The size of the vugs also varied over a wide range. The images in Figure 6-16 show the core after it was fractured corresponding to the same cross-sections shown in Figure 6-15.

After the waterflood, surfactant solution was injected to displace the oil. The surfactant formulation was a mixture of 0.5 wt% C28-25PO-25EO-carboxylate and 0.5 wt% C15-18-IOS surfactants. A 0.25 PV surfactant slug was injected followed by a brine drive. The initial (formation) brine had a salinity of 116,969 ppm TDS with hardness of 4,025 ppm. The salinity of the surfactant slug was 57,000 ppm TDS with a divalent cation concentration of 2300 ppm. The novel Guerbet alkoxy carboxylate and IOS surfactant mixture can tolerate such high temperature, high salinity, and high hardness, and still produce ultra-low IFT with aqueous stability within the range of salinity. After injection of the surfactant slug, about 1.46 PV brine was injected with a salinity of 10,000 ppm TDS. The chemical flood was stopped after about 1.71 PV of injection at an oil cut of about 5%.

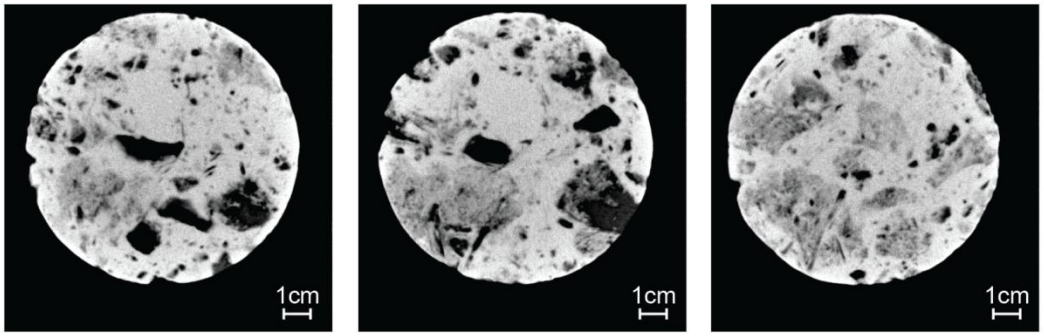

Figure 6-15: CT images of the core before it was fractured (Lu *et al.*, 2012b).

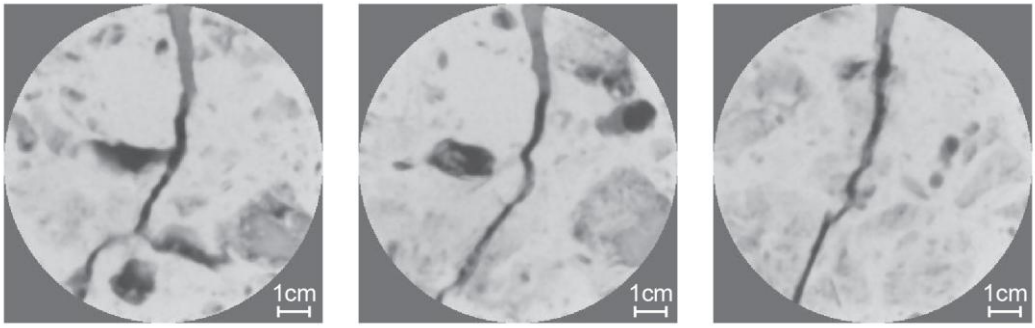

Figure 6-16: CT images of the core after it was fractured (Lu *et al.*, 2012b).

6.5.2 Modeling Coreflood Experiment Using Heterogeneous Permeability Distribution Approach

Two different approaches are adopted to model coreflood experiments in highly vuggy and fractured cores: a) Heterogeneous permeability distribution, b) Explicit fracture. If the fractures are not interconnected and streamlines pass through both vugs and fractures, then random permeability distribution approach is more representative. However, if the fractures are all connected and flow happens mainly through the fracture channels, then using explicit fracture modeling is more appropriate. Because of the contribution of both vugs and fractures in the mentioned coreflood experiment, a random

heterogeneous permeability distribution was used. A Cartesian 5×5×10 grid was used as shown in Figure 6-17. The average brine permeability was 1.9×10^{-12} m^2 (1970 md). A Dykstra-Parsons coefficient of 0.9 was required to match the experimental results. This very high value is consistent with the observed degree of variations in triple porosity/permeability core. The detail of the input data for this coreflood simulation is in Appendix A.

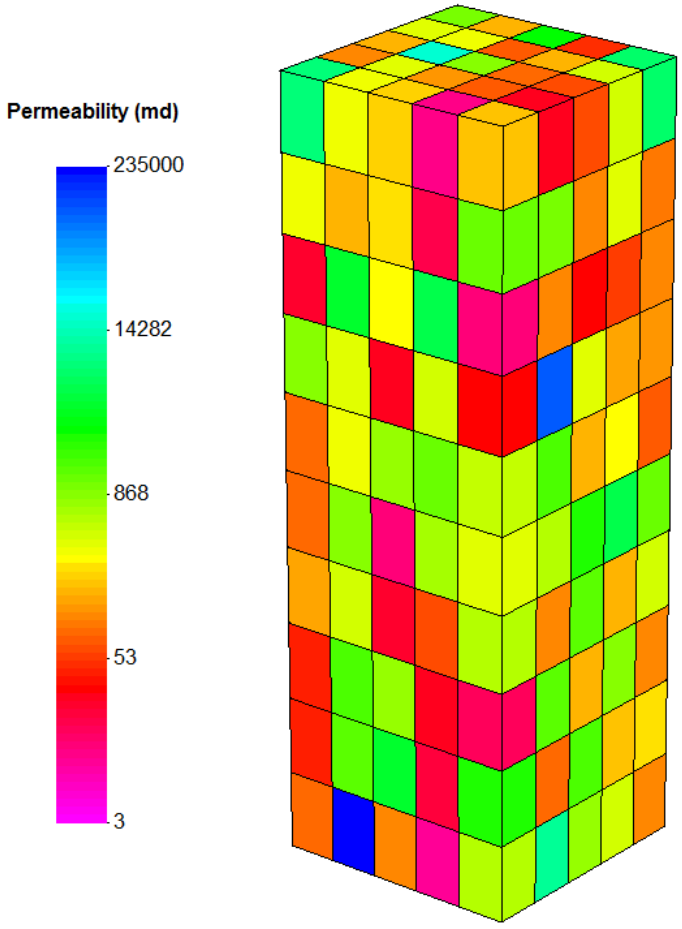

Figure 6-17: Permeability distribution (md) used for modeling the fractured coreflood.

UTCHEM was used to model the surfactant phase behavior, static imbibition, and coreflood experiments. The phase behavior model is based on Hand's rule (Hand, 1939) and uses the ternary diagram for representing different microemulsion phases. The tie lines which join the composition of the equilibrium phases are given as

$$\frac{C_{3\ell}}{C_{2\ell}} = E\left(\frac{C_{3\ell}}{C_{1\ell}}\right)^F, \qquad for \quad \ell = 1, 2, or\, 3 \tag{6.31}$$

where E and F are empirical parameters and ℓ refers to aqueous, oleic or microemulsion phase. For matching measured phase behavior data, parameters E and F were changed. The current formulation in UTCHEM is a symmetrical binodal curve with the value of -1 for F and the value of E in Type I is 0.0028 and 0.00539 in Type II.

The final history match of phase behavior is shown in Figure 6-18. The lab data clearly shows that this formulation equilibrates fast and shows a high optimum solubilization ratio of about 16 at the optimum salinity of about 57,000 ppm. The solubilization ratio of 16 corresponds to an ultra-low IFT of about 1.2×10^{-3} mN/m using the Huh equation (Huh, 1979).

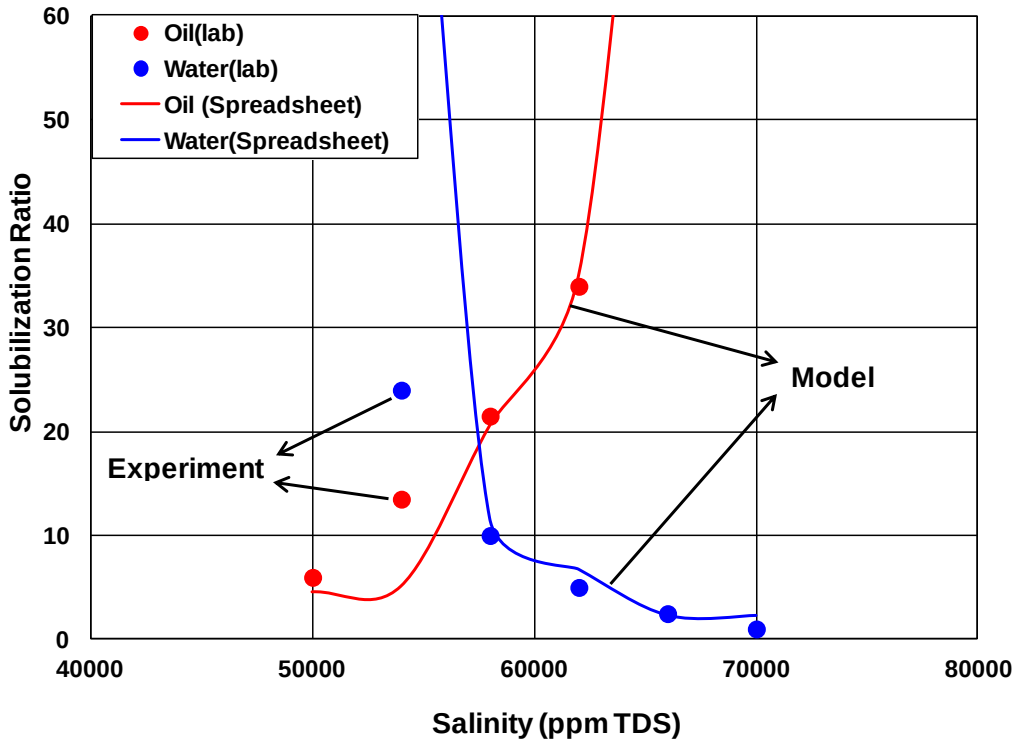

Figure 6-18: Comparison of measured and modeled solubilization ratios at 100 °C.

Figure 6-19 and Figure 6-20 show a good match between the experimental coreflood data and the simulation for total oil recovery, oil saturation, oil cut, and salinity. The relative permeability parameters were adjusted to match the oil recovery. Capillary pressure was neglected in these simulations. The relative permeability parameters are shown in Table 6-9. The oil relative permeability endpoint increased from 0.5 to 0.85 and water relative permeability endpoint decreased from 0.4 to 0.1, as shown in Figure 6-21. The oil relative permeability endpoint increases during wettability alteration from mixed-wet to water-wet. However, for the water phase, the endpoint decreases during the transition from mixed-wet to water-wet.

Figure 6-22 shows the sensitivity of oil recovery to IFT reduction and wettability alteration mechanisms. Simulations with only one of these mechanisms gives lower oil recovery compared to including both. Therefore, it can be realized that both IFT reduction and wettability alteration mechanisms aided in oil recovery. The plot shows that the rate of oil recovery at early times for wettability alteration alone is lower than that due to IFT reduction alone.

The simulated oil saturation at the end of the flood and IFT at the end of surfactant injection are shown in Figure 6-23 and Figure 6-24. Figure 6-23 is before surfactant breakthrough; the subsequent water injection pushes the surfactant slug through the core. These maps indicate that lower oil saturation correlates with lower IFT. The simulation was based on both IFT reduction and wettability alteration. The comparison of oil saturation distribution and the permeability distribution in Figure 6-17 illustrates that oil was mobilized even in low permeability grid blocks.

In field situations, it is desirable to inject the surfactant solution in a horizontal well at the bottom of the fractured reservoir and produce the oil through another horizontal well placed at the top of the reservoir. The horizontal wells will connect to and flood the vertical fractures with the surfactant solution. The transfer of surfactant solution from the fractures to the matrix and the reverse transfer of oil from the matrix to the fracture would be controlled by gravity, interfacial tension and wettability alteration. The rate of transfer can be measured from vertical static and dynamic experiments and then scaled up for the field using the simulator.

Table 6-9: Relative permeability parameters used in the simulation of coreflood.

Core Data	Oil-Wet		Water-Wet	
	Oil	Water	Oil	Water
Residual saturation	0.18	0.50	0.05	0.50
Endpoint relative permeability	0.50	0.40	0.85	0.10
Relative permeability exponent	2.0	2.0	1.5	3.0
Scaling Factor, ω_1	0.5			

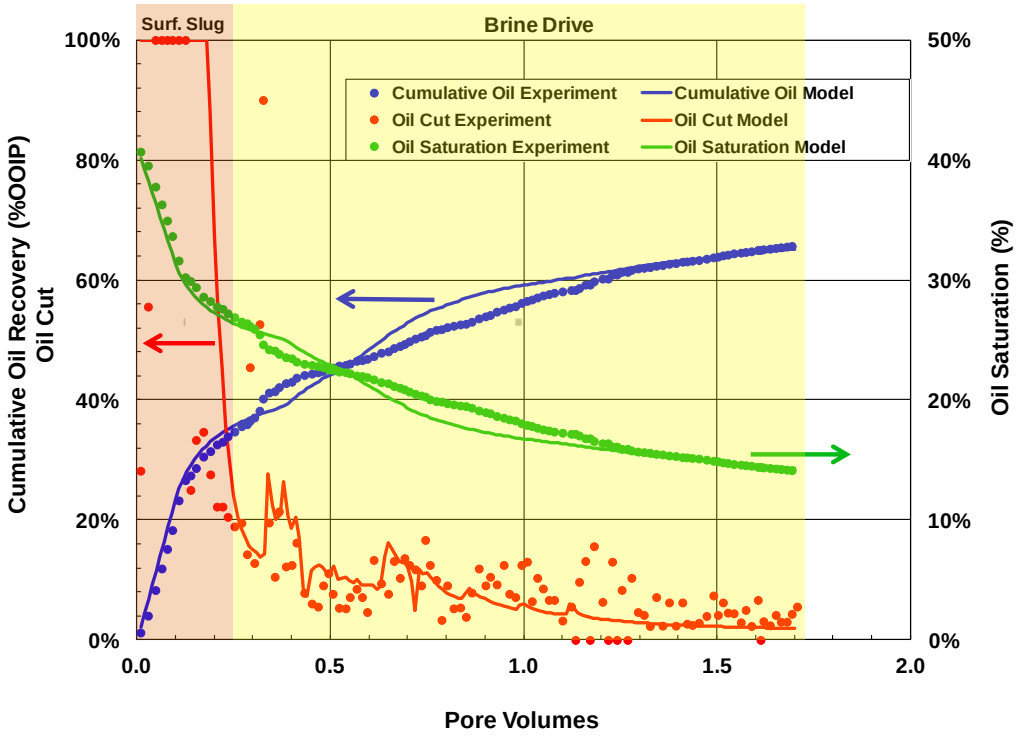

Figure 6-19: Comparison of simulated and measured fractured coreflood results.

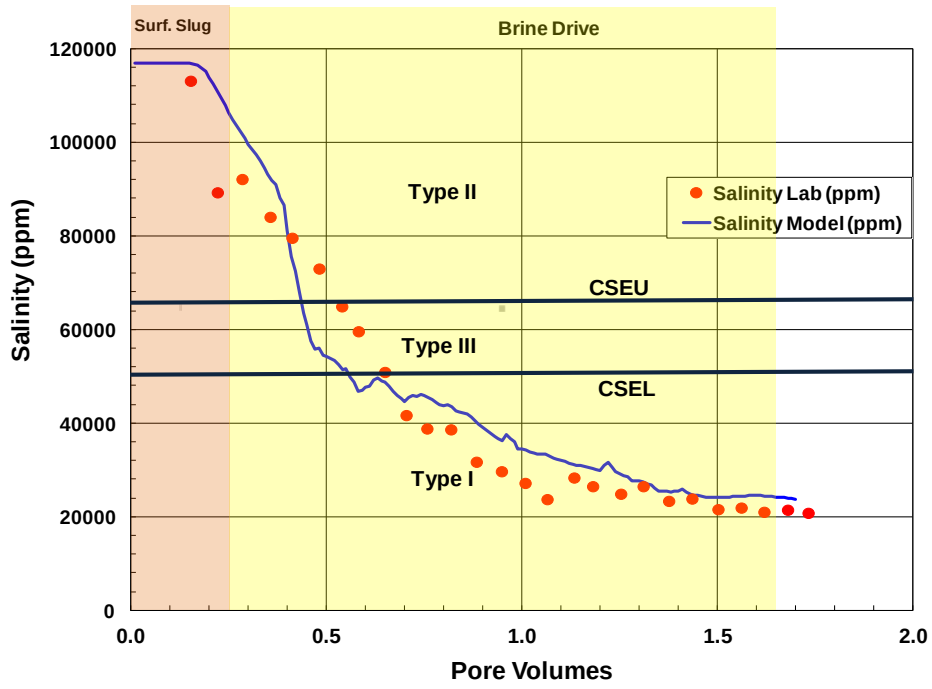

Figure 6-20: Comparison of simulated and measured effluent salinity.

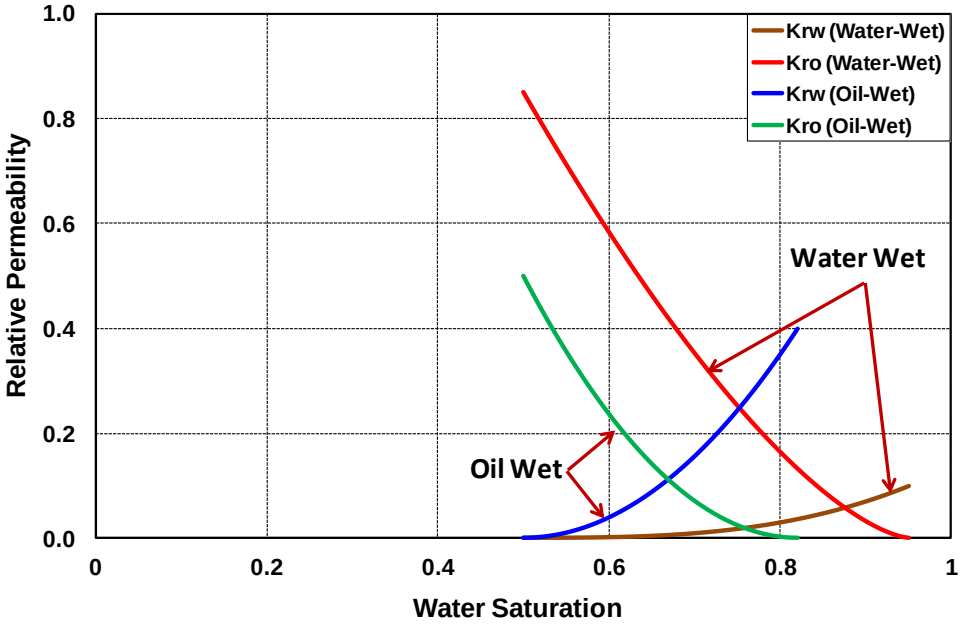

Figure 6-21: Relative permeability curves at different wetting states.

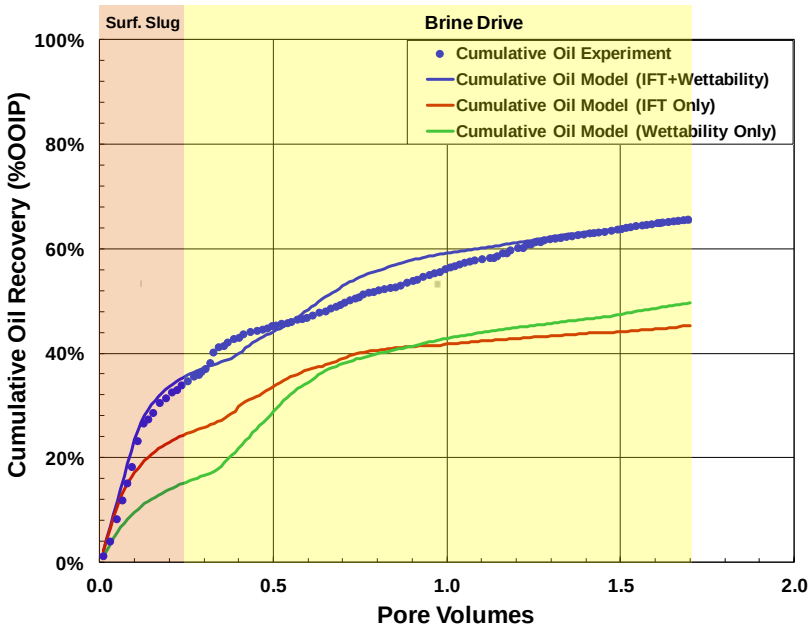

Figure 6-22: Sensitivity simulations to IFT reduction and wettability alteration mechanisms.

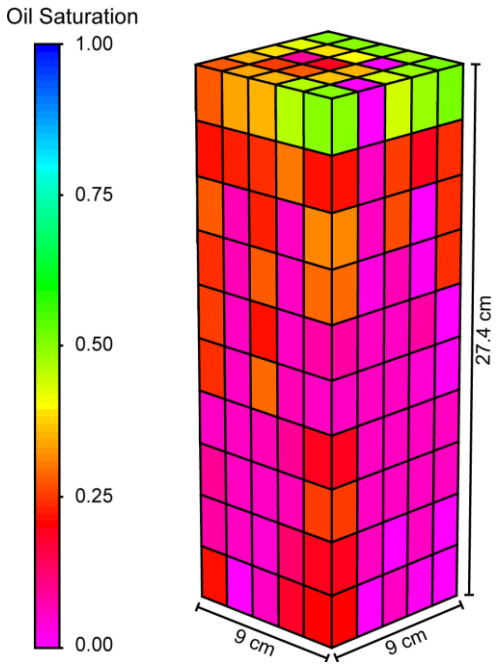

Figure 6-23: Simulated oil saturation profile at the end of surfactant flood (PV_{inj}=1.71).

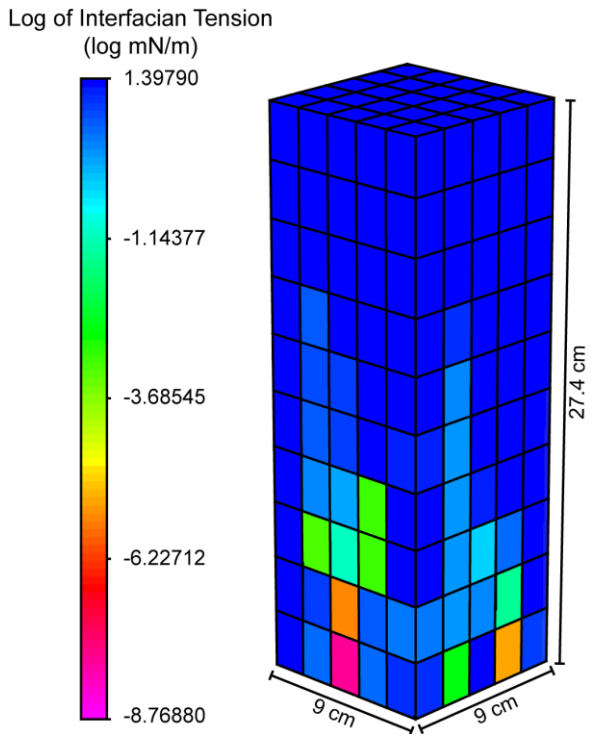

Figure 6-24: Representation of IFT reduction at the end of surfactant flood (PV_{inj}=1.71).

6.5.3 Modeling Coreflood Test Using Explicit Fracture Approach

A Cartesian grid with different fracture densities is used for modeling heterogeneous fractured rock as shown in Figure 6-25 through Figure 6-27. Different combinations of fractures parallel and perpendicular to flow direction are used in explicit fracture models. The fracture thickness was 1/10 of the gridblock size. The average brine permeability was 1.9×10^{-12} m^2 (1970 md) after fractures are generated. The end caps were modeled as fractures and injection-production wells are placed in the center of fracture plates.

The fracture porosity was calculated using the Eq. (6.32). The matrix permeability was 6 md and the fracture permeability was 5000 md. The fracture permeability was

calculated using simulation of single phase flow in the core.

$$\phi_{Core} * Bulk\,Volume_{Core} = \phi_{Fracture} * Bulk\,Volume_{Fracture} + \phi_{Matrix} * Bulk\,Volume_{Matrix}. \quad (6.32)$$

Figure 6-28 and Figure 6-29 show a good match between the measured oil recovery and the simulation using low fracture density model (4 fractures parallel to flow direction, 9 fractures perpendicular to flow direction) and high fracture density model (8 fractures parallel to flow direction, 20 fractures perpendicular to flow direction). The relative permeability parameters were adjusted to match the oil recovery as shown in Figure 6-30 and Figure 6-31. For the 9 fractures perpendicular, the oil relative permeability endpoint increased from 0.18 to 0.69. However, for the 20 fractures perpendicular, the oil relative permeability endpoint increased from 0.5 to 0.8.

Simulation study using different discrete fracture models showed that by increasing the fracture density, the same oil recovery can be achieved with a smaller degree of wettability alteration. Coreflood simulation results with a limited number of explicit fractures indicate that a substantial wettability alteration from mixed-wet to water-wet is required in order to increase oil recovery. However, with a large number of explicit fractures, oil can be recovered with only slight modification in the matrix rock wettability. Thus the interplay between heterogeneity and wettability becomes evident.

These findings are significant as they illustrate that the extent of required wettability alteration in fractured reservoirs will depend on the nature and density of the fracture network. Extensive simulation work and laboratory results demonstrate the validity and ranges of applicability of scale up procedures, and also indicate the importance of viscous and capillary forces in field-scales. The results of this work give insight into the design and optimization of field projects.

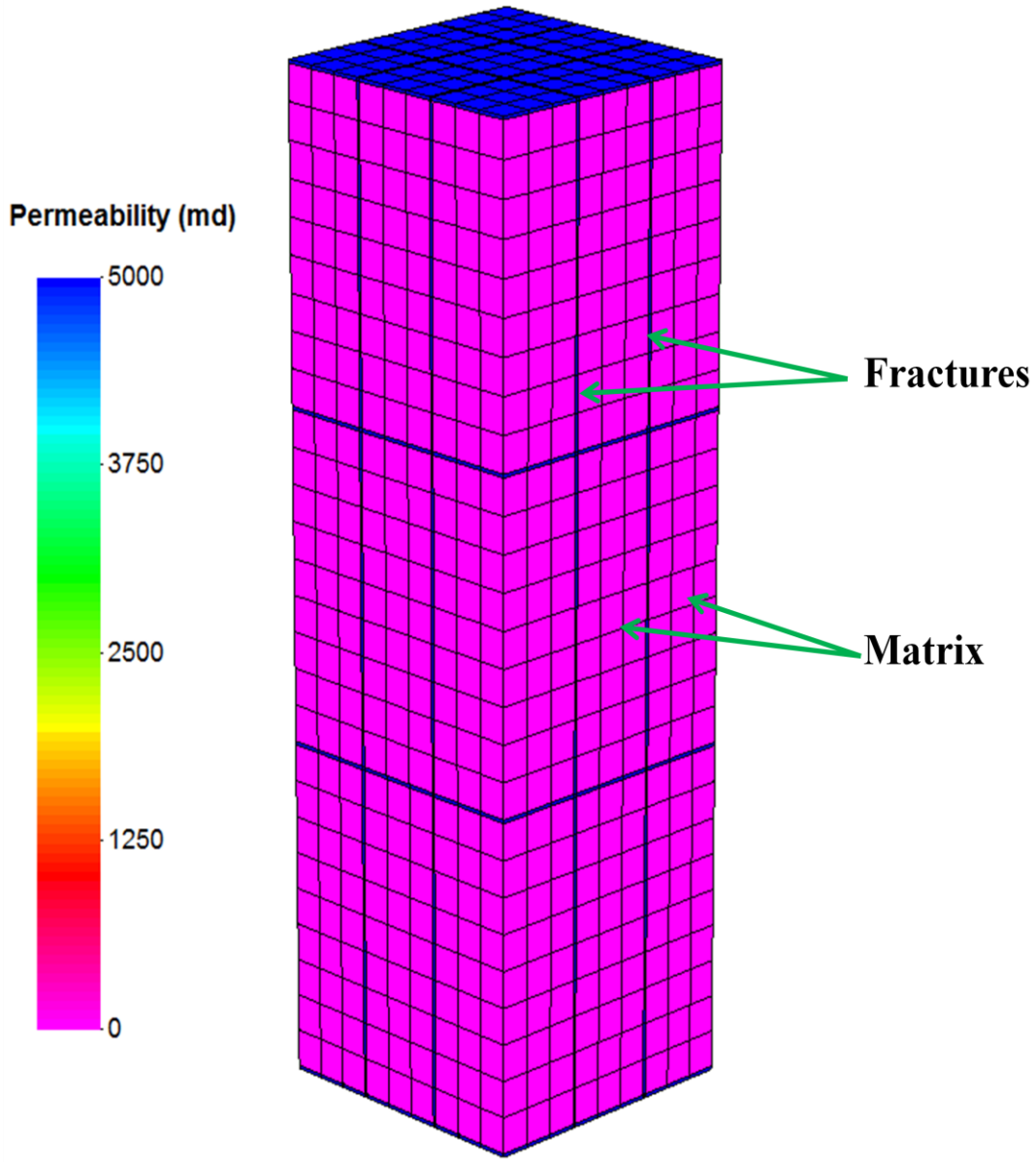

Figure 6-25: Permeability distribution using explicit fracture model (4 fractures parallel to flow direction, 2 fractures perpendicular to flow Direction).

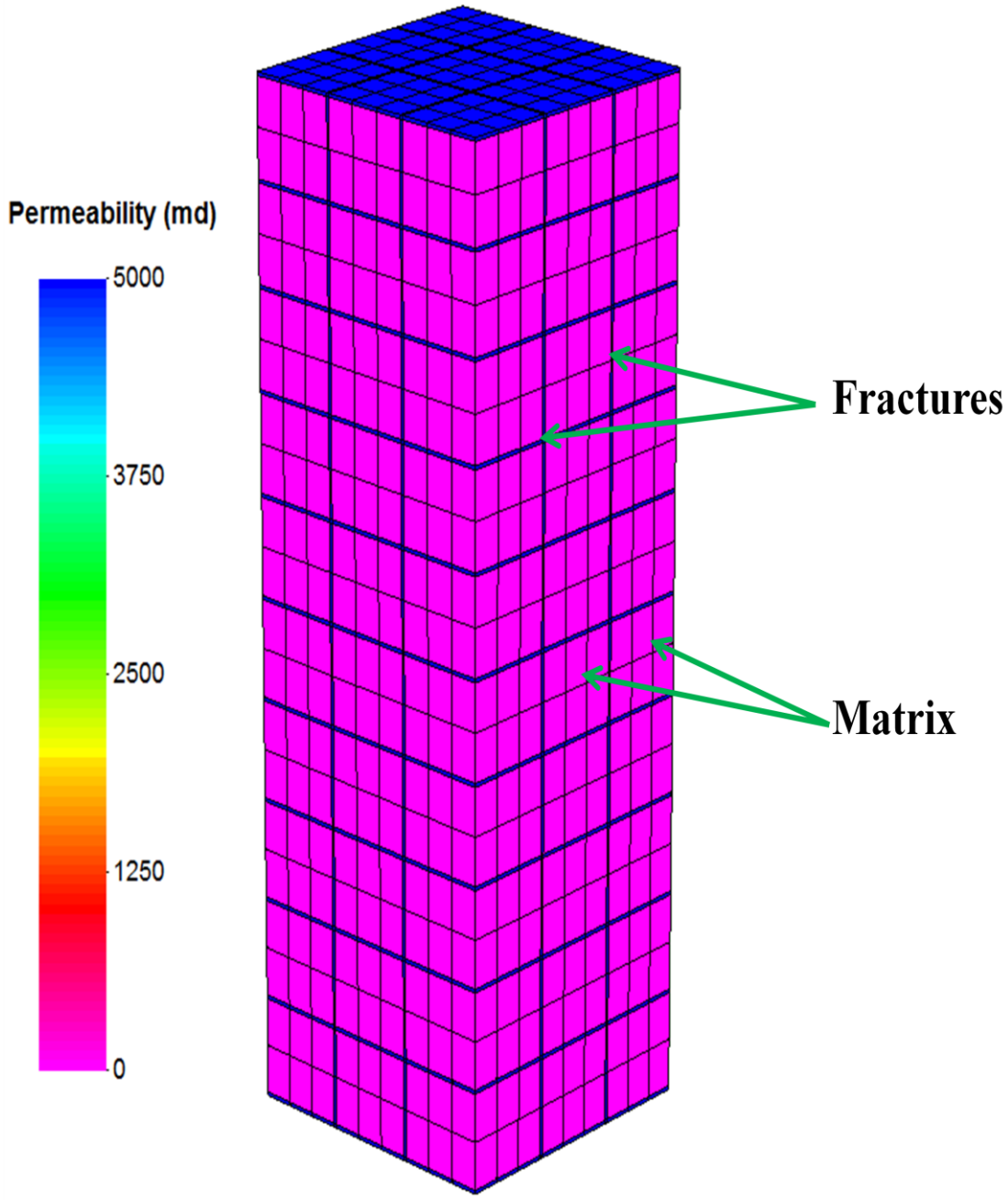

Figure 6-26: Permeability distribution using explicit fracture model (4 fractures parallel to flow direction, 9 fractures perpendicular to flow Direction).

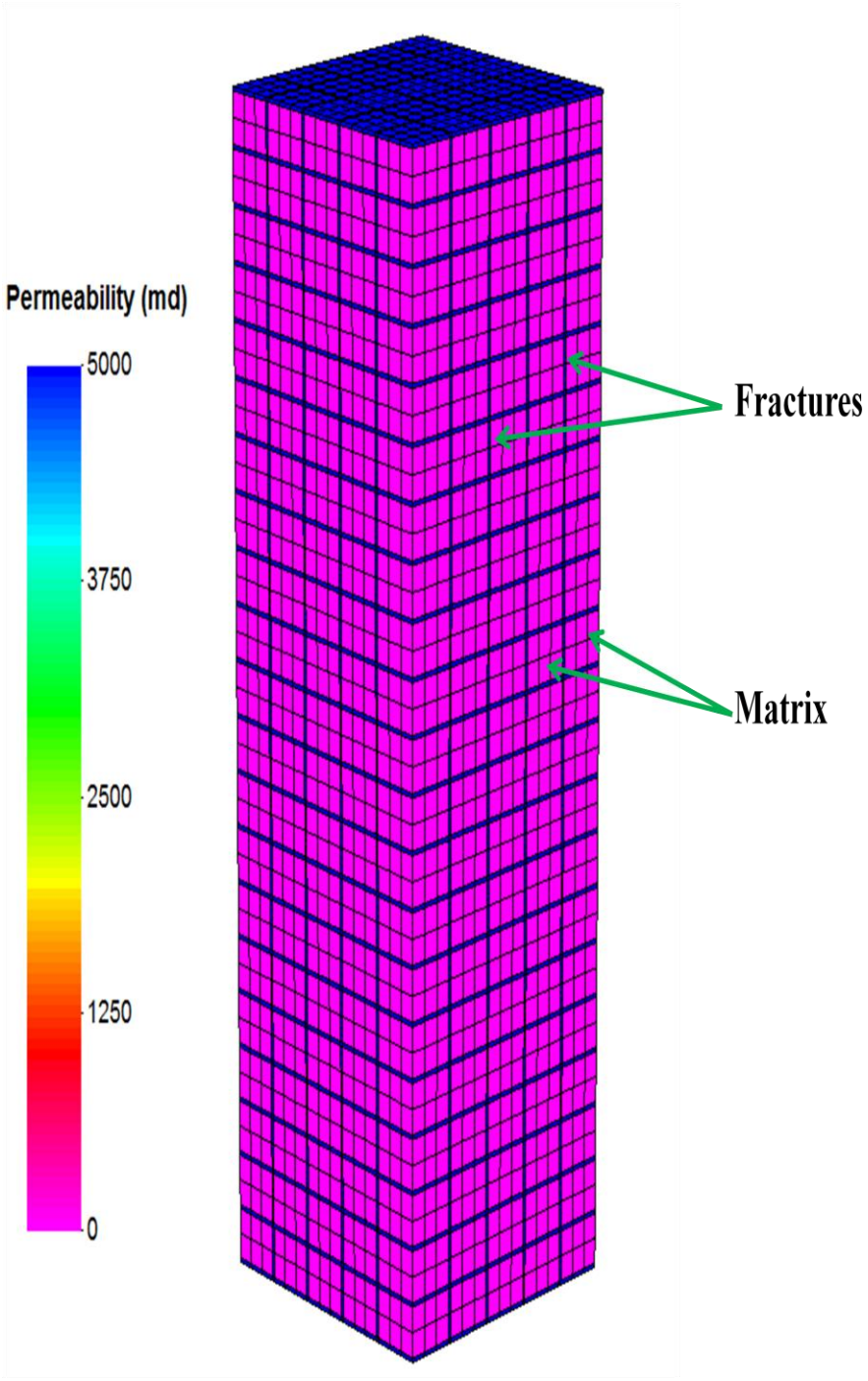

Figure 6-27: Permeability distribution using explicit fracture model (8 fractures parallel to flow direction, 20 fractures perpendicular to flow direction).

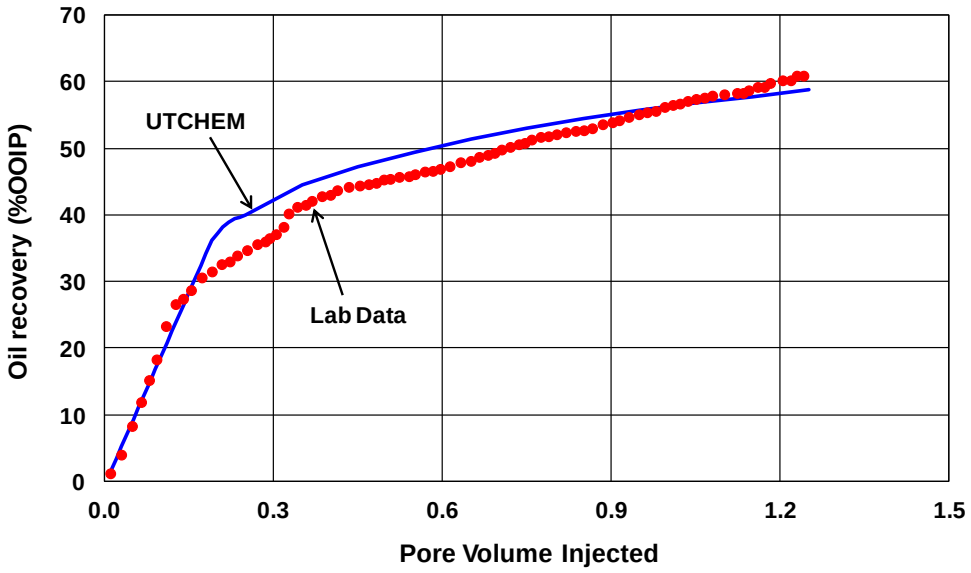

Figure 6-28: Comparison of simulated and measured fractured coreflood oil recovery (4 fractures parallel to flow direction, 9 fractures perpendicular to flow Direction).

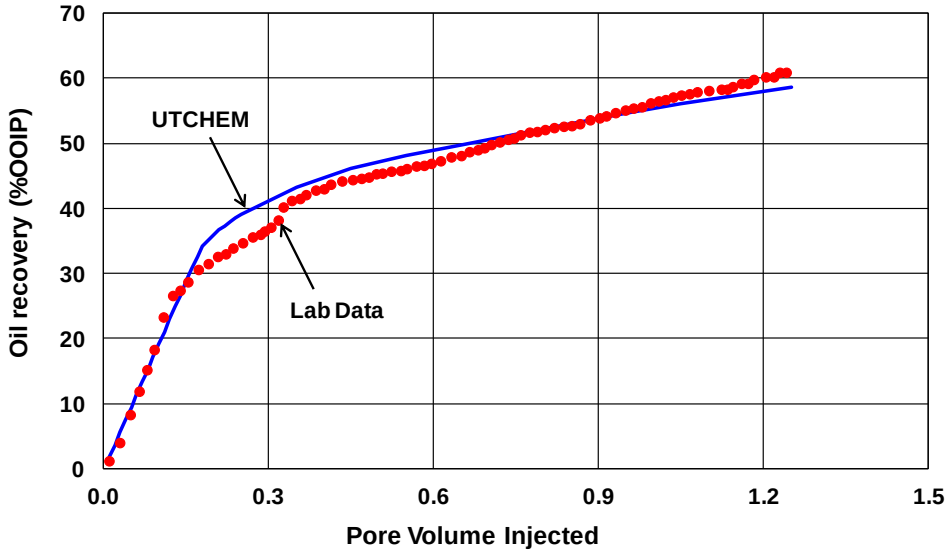

Figure 6-29: Comparison of simulated and measured fractured coreflood oil recovery (8 fractures parallel to flow direction, 20 fractures perpendicular to flow direction).

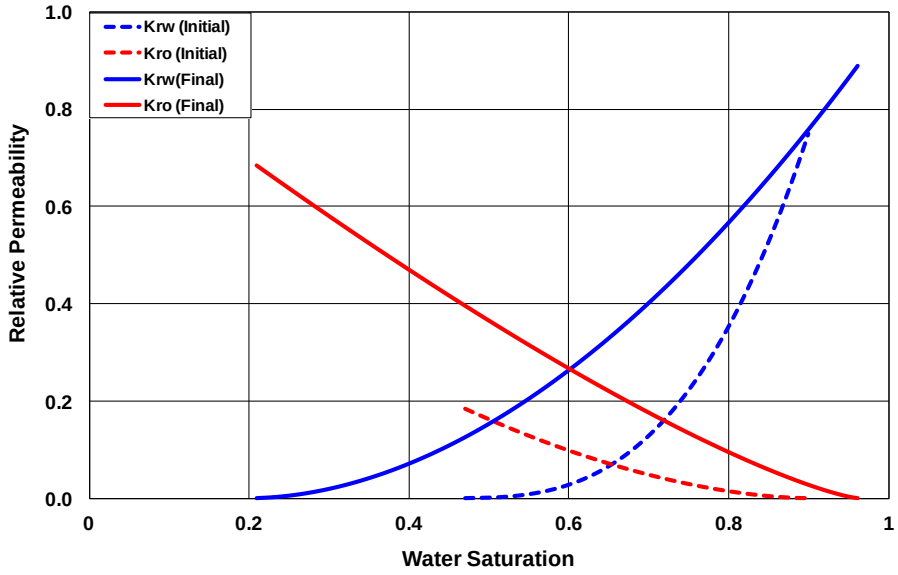

Figure 6-30: Relative permeability curves at initial and final conditions (4 fractures parallel to flow direction, 9 fractures perpendicular to flow direction).

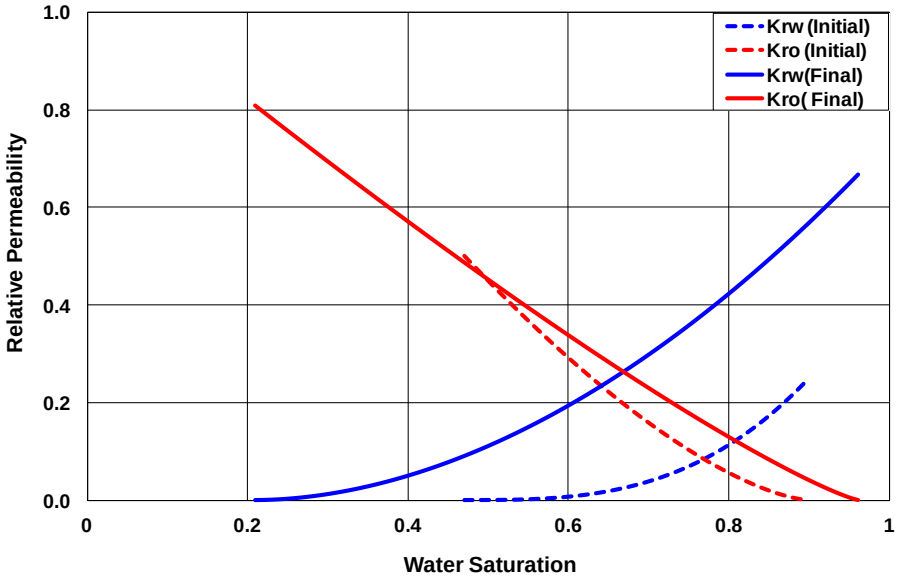

Figure 6-31: Relative permeability curves at initial and final conditions (8 fractures parallel to flow direction, 20 fractures perpendicular to flow direction).

6.6 SUMMARY AND CONCLUSIONS

- Anionic surfactant, Enordet A092, with EDTA as an alkali can alter wettability from oil wet to strongly water-wet conditions. However, higher concentration of divalent cations (i.e. Mg^{2+} and Ca^{2+}) prohibits the degree of wettability alteration.
- Imbibition cell tests were conducted at reservoir temperature using crude oil in different core sizes to study the impact of matrix block size on oil recovery. These data guided us to develop new dimensionless scaling groups for the time of imbibition and recovery factor.
- The experimental results showed that in addition to high permeability, less degree of rock heterogeneity is another factor favorable for wettability alteration and imbibition recovery.
- A published gravity-based dimensionless time was successfully modified and validated against experiments conducted with increasing the height of the core.
- The scale-up results show that increasing the thickness of the core in the vertical direction leads to a reduction in oil production rate and increase in imbibition time linearly.
- Oil recovery for the large core at reservoir temperature was predicted from new dimensionless numbers and the results were in good agreement with measured oil recovery.
- Two different approaches of random permeability distribution and explicit fracture modeling are used to model fractured coreflood experiment.
- The history match of coreflood experiment by explicit fractures illustrated that by increasing the fracture density, the same oil recovery can be achieved with a smaller degree of wettability alteration.

- Coreflood simulation results with a limited number of explicit fractures indicate that a substantial wettability alteration from mixed-wet to water-wet is required in order to increase oil recovery. However, with a large number of explicit fractures, oil can be recovered with only slight modification in the matrix rock wettability. Thus the interplay between heterogeneity and wettability becomes evident.

Chapter 7: Benchmark Study of Different Reservoir Simulators for Chemical EOR Processes

7.1 INTRODUCTION

Recovery from oil reservoirs under natural depletion is referred to as primary production. However, after pressure decline due to production, it is required to increase reservoir pressure by injecting water or gas as a secondary recovery. Moreover, it is recognized that water flooding cannot mobilize viscous oils or oil droplet trapped in smaller pores due to capillary force. There can be further oil recovery after secondary by lowering oil viscosity with thermal methods or decreasing interfacial tension (IFT) between water and oil by adding chemicals such as surfactant or alkali to the injection water. These methods are referred to as Enhanced Oil Recovery processes (Lake, 1989; Green and Willhite, 1998).

Chemical EOR methods have been studied extensively in the lab and field tested for several decades. Because of great advances in recent years, many of the original issues and limitations hindering the application of chemical EOR no longer exist.

Different commercial reservoir simulators can be used for modeling the chemical EOR processes. In this chapter, the performance of VIP and REVEAL for chemical processes will be discussed briefly but the main focus will be on CMG-STARS, ECLIPSE, and UTCHEM due to their worldwide applications. The laboratory coreflood experiments are modeled and compared. Pandey *et al.* (2008) used CMG-STARS extensively to model coreflood experiments for better understanding of flow mechanisms during chemical flood and also generate parameters which will be used subsequently in

field scale simulations. Morel *et al.* (2008) used ECLIPSE polymer module to perform feasibility study of polymer injection in the Dalia field and their studies demonstrated useful results about injectivity and additional oil recovery.

Reveal (Petroleum Experts, 2012) is a full field reservoir simulator from Petroleum Experts with capability for modeling surfactant phase behavior and also mobility control which includes both polymer and gel options. The surfactant module is similar to that in UTCHEM and can define different phase behaviors (Type I, Type II, and Type III) as a function of salinities. Reveal has the capability of modeling polymer and has several polymer-gel kinetics based on shear thinning behavior near wellbore. Reveal has options for permeability reduction, inaccessible pore volume, gelation of polymer and a cross-linker, and degradation. It also includes a foam model for increasing gas phase viscosity especially in heavy oil reservoirs.

VIP (Landmark, 2012), Landmark's reservoir simulation suite, besides its capability for thermal simulation of hot water and steam injection, has capability for polymer flooding in black oil model. In this chapter, we compare chemical models of UTCHEM (version 2011), CMG–STARS (version 2010), and ECLIPSE (version 2009) for polymer, surfactant/polymer, and alkaline/surfactant/polymer floods.

7.2 DIFFERENT CHEMICAL EOR SIMULATORS

There are very few reservoir simulators that have capability of modeling surfactant/polymer floods. Examples include commercial simulators of such as UTCHEM, CMG-STARS, STARS-ME, ECLIPSE, and REVEAL. A brief description of the capability of some of these simulators is presented here.

7.2.1 UTCHEM

UTCHEM is a three dimensional multiphase multicomponent chemical compositional simulator which is capable of simulating different chemical EOR processes (Delshad, 1994). The simulator can account for complex phase behavior and chemical reactions. The simulator can address up to four phases (gas, aqueous, oleic and microemulsion) and uses advanced concepts in high-order numerical accuracy and dispersion control. Microemulsion (ME) is a combination of water, oil, surfactant and co-surfactant which at certain conditions of temperature, pressure and salinity can form a single separate phase which is thermodynamically stable. UTCHEM has the modeling capabilities for wettability alteration, capillary pressures, up to four-phase relative permeabilities as a function of trapping number, full tensor dispersion, molecular diffusion, adsorption, chemical reactions arising during high pH alkaline flooding, non-equilibrium mass transfer between phases and other related phenomena.

7.2.2 ECLIPSE

Schlumberger-ECLIPSE simulator consists of two different modules: ECLIPSE100 is black oil model and ECLIPSE300 is compositional equation of state. ECLIPSE100 is a fully-implicit, three phase, three dimensional, general purpose black oil simulator which can model different chemical EOR processes, including polymer and surfactant flooding. However, ECLIPSE300 runs in fully implicit, IMPES, and adaptive implicit (AIM) modes.

ECLIPSE100 models the effect of varying salt concentrations on polymer viscosity. The viscosity of a fully mixed polymer solution in ECLIPSE100 is defined as a function of the polymer concentration. However, the effect of temperature on polymer

viscosity is ignored. Different features for polymer flooding, including viscosity, permeability reduction, adsorption, and rheology will be compared against UTCHEM in this chapter. There is no separate ME phase and the surfactant model is based on Type I. However, the effect of surfactant viscosity is modeled by modifying water viscosity based on measured ME viscosity (ECLIPSE technical manual, 2009).

7.2.3 CMG-STARS

CMG-STARS is the advanced processes reservoir simulator which includes options such as polymer flooding, surfactant flooding, steam flood, in-situ combustion, etc.

CMG-STARS can be run in fully implicit and adaptive implicit modes. Different features for polymer flooding and surfactant flooding are explained later. The features for polymer flooding include viscosity, permeability reduction, adsorption, and rheology which will be compared against UTCHEM. The surfactant model is based on Type I (water and oil) and there is no microemuslion phase. Interfacial tension reduction can be defined in tabular format as a function of surfactant concentration (CMG-STARS technical manual, 2010).

7.2.4 STARS-ME (CMG)

STARS-ME is a new version of STARS where microemulsion is defined as a separate phase similar to UTCHEM. In fact, gas phase is replaced by ME phase and three phases of water, oil, and ME exist. Phase behavior and relative permeability models are similar to UTCHEM. The phase behavior is defined as the salinity limits for Type III and the height of the binodal curves at three salinity values. The surfactant partitions either

into water phase (under-optimum) or oil phase (over-optimum) or into the middle phase which is optimum conditions. The solubilization ratio leads to reduction in interfacial tension modeled using Huh's correlation (Chun Huh, 1979) similar to UTCHEM.

Phase relative permeabilities are functions of the calculated residual saturations, endpoints, and relative permeability curvature based on Corey function. Each phase relative permeability is calculated using an interpolated relative permeability curvature and endpoint (STARS-ME technical manual, 2011).

The limitations are the lack of gas phase and the effect of buoyancy in the capillary number. STARS-ME is only limited to a total of 9 components with specific names for each component. This module is still under development and therefore we do not include in our benchmark study.

7.3 MODEL DESCRIPTION

7.3.1 Polymer Flood

Polymer flooding is used for improving mobility ratio for better sweep of the remaining bypassed mobile oil after primary and secondary recoveries. The purpose of adding polymer to the injected water is to increase water viscosity and decrease water effective permeability. This will reduce the mobility ratio and better mobilize the original oil with a more uniform displacement front. It is obvious that different parameters such as polymer concentration, viscosity, adsorption on rock minerals, permeability reduction, inaccessible pore volume, etc. are key parameters for controlling an efficient polymer flood.

7.3.1.1 Viscosity vs. Polymer Concentration

UTCHEM models polymer viscosity as a function of polymer concentration, salinity, and divalent cations (hardness) as shown below:

$$\mu_p^0 = \mu_w \left(1+\left(A_{p1} C_{4\ell} + A_{p2} C_{4\ell}^2 + A_{p3} C_{4\ell}^3\right) C_{SEP}^{S_p}\right), \tag{7.1}$$

where $C_{4\ell}$ is the polymer concentration in phase ℓ, μ_w is the water viscosity, C_{SEP} is effective salinity ($\left(\mathrm{C_{SEP}} = \frac{\mathrm{C_5} + \beta_\mathrm{p} \mathrm{C_6}}{\mathrm{C_1}}\right)$), S_p is a parameter for the effect of salinity, and A_{p1}, A_{p2}, A_{p3} are input parameters.

For CMG-STARS, the non-linear mixing rule is applied for calculating polymer viscosity as follows:

$$\ln \mu_p = f(x_a) \ln \mu_a + \frac{1 - f(x_a)}{1 - x_a} \sum_{i \neq a} x_i \ln \mu_i, \tag{7.2}$$

where x_a is the components mole fraction, $f(x_a)$ is the mixing function which depends on x_a and μ_a is component viscosity. The effect of salinity and hardness on polymer viscosity is not modeled.

The polymer viscosity in ECLIPSE (ECLIPSE Technical Manual, 2009) is modeled using an effective polymer viscosity $\mu_{p,eff}$ based on Todd-Longstaff model. The model includes both the effect of dispersion and fingering,

$$\mu_{p,eff} = \mu_m (C_p)^{\omega} . \mu_p^{1-\omega}, \tag{7.3}$$

where $\mu_m(C_p)$ is polymer solution viscosity as an increasing function of polymer concentration (C_p), μ_p is the polymer viscosity at maximum polymer concentration (i.e. injected polymer viscosity) as an input parameter and ω is the Todd-Longstaff mixing input parameter. The model, however, lacks the effect of salinity and hardness on polymer viscosity.

7.3.1.2 Polymer Adsorption

UTCHEM uses Langmuir isotherm for polymer adsorption and includes polymer concentration and salinity as shown below:

$$\hat{C}_4 = \frac{a_4(C_{41})}{1+b_4 C_{41}}, \tag{7.4}$$

$$\mathrm{a_4} = \left(\mathrm{a_{41}} + \mathrm{a_{42}} \mathrm{C_{SEP}}\right)\left(\frac{\mathrm{k_{ref}}}{\mathrm{k}}\right)^{0.5}, \tag{7.5}$$

where C_{41} is the polymer concentration in the aqueous phase 1 and the parameters a_{41}, a_{42}, and b_4 are model input. The reference permeability ($\mathrm{k_{ref}}$) is the permeability which is used for specifying input adsorption parameters.

CMG-STARS uses Langmuir isotherm to calculate polymer adsorption as a non-linear function of salinity and mole fraction of polymer in the aqueous phase,

$$ad = \frac{(tad1 + tad2 * xnacl) * ca}{(1 + tad3 * ca)}, \tag{7.6}$$

where $xnacl$ is the salinity, ca is the mole fraction of polymer in aqueous phase, and $tad1$, $tad2$, $tad3$ are input parameters.

Polymer adsorption in ECLIPSE is calculated using modified Langmuir function as

$$C_{ads} = \frac{aC^m}{1+bC}, \tag{7.7}$$

$$a = (a_1 + a_2 C_{SE})(\frac{K_{ref}}{K})^n, \tag{7.8}$$

where C is the polymer concentration, m is the exponent for concentration dependence, C_{SE} is the salinity, K is gridblock permeability, K_{ref} is the reference permeability, n is the exponent for permeability dependence, and a_1, a_2, b are the adsorption coefficients.

7.3.1.3 Polymer Permeability Reduction

Polymer can reduce the water effective permeability where degree of permeability reduction depends on polymer type, molecular weight, shear effects, and rock properties. The model in UTCHEM is as follows:

$$R_k = 1 + \frac{(R_{k\max} - 1) b_{rk} C_{4\ell}}{1 + b_{rk} C_{4\ell}}, \tag{7.9}$$

$$R_{k,\max} = \min\left\{\left[1 - \frac{c_{rk}\left(A_{p1} C_{SEP}^{Sp}\right)^{1/3}}{\left(\frac{\sqrt{k_x k_y}}{\phi}\right)^{1/2}}\right]^{-4}, rkcut\right\}, \tag{7.10}$$

where $C_{4\ell}$ is polymer concentration, $R_{k\max}$ is the maximum permeability reduction, $rkcut$, b_{rk}, and c_{rk} are input parameters.

For STARS, permeability reduction is related to adsorption or mechanical entrapment which can cause blockage or reduction in permeability as shown below:

$$AKW(I) = \frac{AK(I)\, k_{rw}}{RKW(I)}, \tag{7.11}$$

$$RKW = 1 + \frac{(RRFT - 1)AD(C,T)}{ADMAXT}, \tag{7.12}$$

where AK is permeability, $RRFT$ is the residual resistance factor, $AD(C,T)$ is the adsorption isotherm, and $ADMAXT$ is the maximum adsorption capacity of the rock.

ECLIPSE uses similar equation as

$$R_k = 1.0 + (RRF - 1)\frac{C_p^{\alpha}}{C_p^{\alpha \max}}, \tag{7.13}$$

where RRF, C_p^{α}, and $C_p^{\alpha \max}$ are the residual resistance, polymer adsorption, and maximum adsorption capacity of the rock for polymer in phase α.

7.3.1.4 Polymer Rheology

The viscosity of polymer decreases by increasing shear rate, especially near the injection wellbore. At low shear rates, μ_p is independent of shear rate; however, at higher shear rates the viscosity is reduced and finally a second plateau value close to the water viscosity will be achieved (Lake, 1989). The relationship between polymer viscosity and shear rate in UTCHEM is modeled using Meter's equation (Meter and Bird, 1964) as follows:

$$\mu_p = \mu_w + \frac{\mu_p^0 - \mu_w}{1 + \left(\frac{\dot{\gamma}_{eq}}{\dot{\gamma}_{1/2}} \right)^{P_\alpha - 1}}, \tag{7.14}$$

where μ_p^0 is the polymer viscosity at low shear rate, $\dot{\gamma}_{1/2}$ is the shear rate at which the polymer viscosity is equal to average of μ_p^0 and μ_w, and $\dot{\gamma}_{eq}$ is the equivalent shear rate. Other option available in UTCHEM is unified viscosity model for shear thinning and shear thickening using Carreau's model (Delshad *et al.*, 2008). There is a correction for near wellbore where the fluid velocity is high (Li and Delshad, 2014).

For STARS, shear effect will be included in the tabular format which relates polymer viscosity to fluid velocity. The fluid velocity will be calculated based on Blake–Kozeny equation (Sorbie, 1991) as follows:

$$\dot{\gamma}_{eq} = \frac{\dot{\gamma}_c |u_\ell|}{\sqrt{\bar{k} k_{r\ell} \phi S_\ell}}, \tag{7.15}$$

where $\dot{\gamma}_c$ is the shear rate coefficient which includes non-ideal effect such as slip .

For ECLIPSE, there is a table to input the shear thinning or thickening polymer viscosity as a function of water velocity where,

$$V_w = b_w . \frac{F_w}{\phi A}, \tag{7.16}$$

$$\mu_{sh} = \mu_{w,eff} \left[\frac{1 + (P-1)M}{P} \right], \tag{7.17}$$

where b_w is the water formation volume factor, F_w is water flow rate, A is the flow area between a pair of wells, $\mu_{w,eff}$ is the water viscosity, μ_{sh} is polymer shear viscosity, P,

and M are viscosity thinning or thickening multipliers provided as input. Table 7-1 illustrates the important features of polymer module in each simulator.

Table 7-1: Comparison of polymer model options (Goudarzi *et al.*, 2013).

Polymer Module	UTCHEM	CMG-STARS	ECLIPSE
Viscosity vs. Polymer Conc.	√	√	√
Viscosity vs. Shear Rate	√	√	√
Adsorption	√	√	√
Permeability Reduction	√	√	√
Inaccessible Pore Volume	√	√	√
Effect of Salinity on Viscosity and Adsorption	√	Not Included	Not Included
Effect of Hardness on Viscosity, Adsorption, and Permeability Reduction	√	Not Included	Not Included

7.3.2 Surfactant Flood

Oil droplets can be trapped because of microscopic capillary forces during water injection. This trapping can be shown as a competition between viscous forces to mobilize oil and capillary forces that cause trapping of oil (Lake, 1989). Surfactant injection to lower the water/oil interfacial tension was first performed by Uren and Fahmy (1927). IFT can be reduced from 30 dynes/cm in a typical waterflood to around 10^{-2} dynes/cm, which causes a significant reduction in residual oil saturation (Green and Willhite, 1998).

Surfactant/polymer slug injection should be followed by polymer flooding. The main objective is to use low-cost, high performance surfactants with more innovative ways (Levitt, 2006; Adkins *et al.*, 2012). With the comprehensive understanding of the relationship between the surfactant structure and its performance, surfactant formulations are developed that give invaluable results even under high temperature and high salinity

reservoirs (Solairaj *et al*., 2012; Adkins *et al*., 2012; Lu *et al*., 2012a). Lu *et al*. (2012b) performed dynamic corefloods using new surfactant formulations at reservoir temperature and investigated the effect of surfactant formulation on IFT reduction and oil recovery. Lashgari *et al.* (2014a, 2014b, 2015) presented a steam-surfactant-foam model by having four-phase flow (steam/ oil/water/microemulsion) in equilibrium to reveal the efficiency of hybrid thermal-chemical method in improvement of recovery from heavy oil reservoirs.

Here we compare the surfactant models available in UTCHEM, STARS, and ECLIPSE. Microemulsion viscosity, interfacial tension, and surfactant phase behavior are three key properties that should be considered in any surfactant flood design.

7.3.2.1 Microemulsion Viscosity

Microemulsion (ME) is a thermodynamically stable mixture of water, oil, surfactant/co-surfactant where at certain conditions of temperature, pressure, and salinity can form a separate phase. Viscosity of the ME phase is one of the key factors in the successful design of surfactant flood (Delshad, 1994). Viscous ME can cause plugging, lower injectivity, high retention, and low recovery. Microemulsion viscosity is a function of the composition. UTCHEM can model ME viscosity as a function of water, oil and surfactant concentrations in the ME phase as shown below:

$$\mu_{ME} = C_{13}\,\mu_w\, e^{[\alpha_1(C_{23}+C_{33})]} + C_{23}\,\mu_o\, e^{[\alpha_2(C_{13}+C_{33})]} + C_{33}\,\alpha_3\, e^{[\alpha_4 C_{13}+\alpha_5 C_{33}]}, \qquad (7.18)$$

where C_{13}, C_{23}, C_{33} are the water, oil and surfactant concentrations in ME phase, and α_1, α_2, α_3, α_4, α_5 are input parameters. When polymer is added to the surfactant solution,

water viscosity (μ_w) is replaced with the polymer solution viscosity μ_p^0. Figure 7-1 shows the viscosity of ME phase as a function of oil concentration in microemulsion phase. Taghavifar (2014) proposed a theoretical framework to describe the mechanisms of microemulsion rheology, specifically with the addition of branched co-surfactants, co-solvents, and higher temperature.

There is no option for ME phase or its viscosity in either STARS or ECLIPSE. It is assumed that surfactant solution has viscosity the same as that of the water.

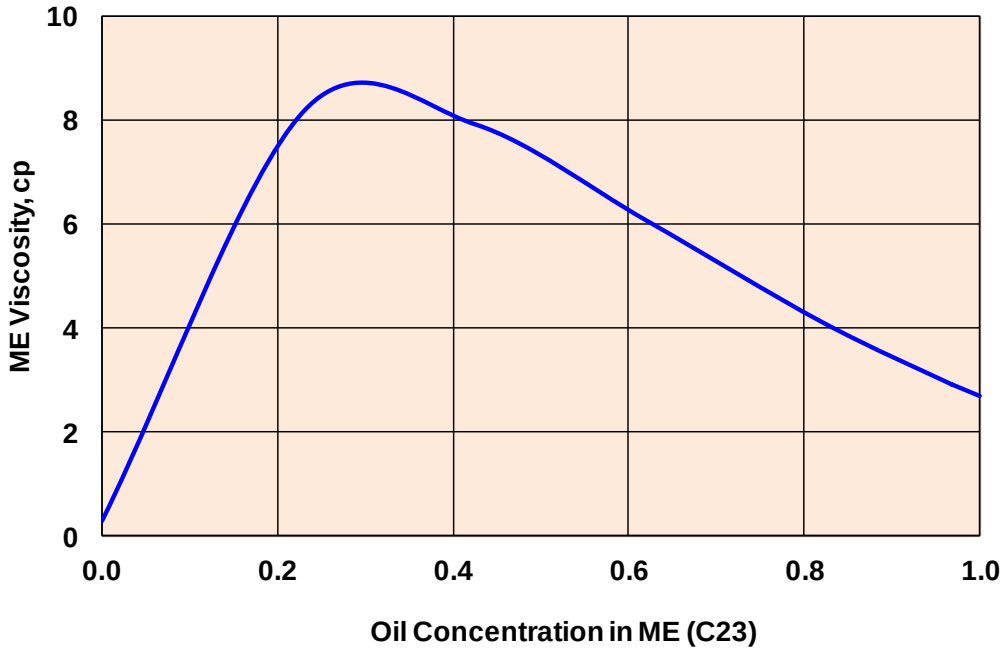

Figure 7-1: ME viscosity as a function of oil concentration in microemulsion phase (Pope, 2011).

7.3.2.2 Interfacial Tension

Interfacial tension (IFT) and its reduction will be controlled by surfactant type, surfactant concentration, injected and formation salinity, as well as hardness, reservoir temperature, and crude oil composition (Green and Willhite, 1998). There exists a strong correlation between the phase behavior of a microemulsion system and IFT (Lake, 1989; Healy and Reed, 1974).

Both Healy and Reed (1974) and Chun Huh (1979) correlations are available in UTCHEM. Huh's correlation correlates IFT with oil solubilization ratio (R_{23}) as

$$\sigma_{23} = \frac{C}{R_{23}^2}, \tag{7.19}$$

$$R_{23} = \frac{C_{23}}{C_{33}}. \tag{7.20}$$

The implementation in UTCHEM includes a correction to ensure the IFT approaches oil/water in the absence of surfactant as follows:

$$\sigma_{l3} = \sigma_{ow} e^{-aR_{l3}} + \frac{CF_{\ell}}{R_{l3}^2}(1 - e^{-aR_{l3}^3}), \tag{7.21}$$

where σ_{ow} is the water/oil IFT, F_{ℓ} is the correction factor, and a is equal to about 10. Figure 7-2 shows oil-ME interfacial tension as a function of oil concentration in microemulsion phase (C_{23}).

A table of IFT as a function of surfactant concentration is provided in both STARS and ECLIPSE. Linear and logarithmic interpolation can be used to calculate IFT at any other concentration and surfactant concentration in the table should increase monotonically down the column.

For ECLIPSE and STARS, the effect of IFT on relative permeability will be modeled by assuming two sets of relative permeability curves at high IFT (low capillary number) and low IFT (high capillary number) and interpolating between these two relative permeability curves. For UTCHEM, the effect of IFT on relative permeability is explained comprehensively in Chapter 6.

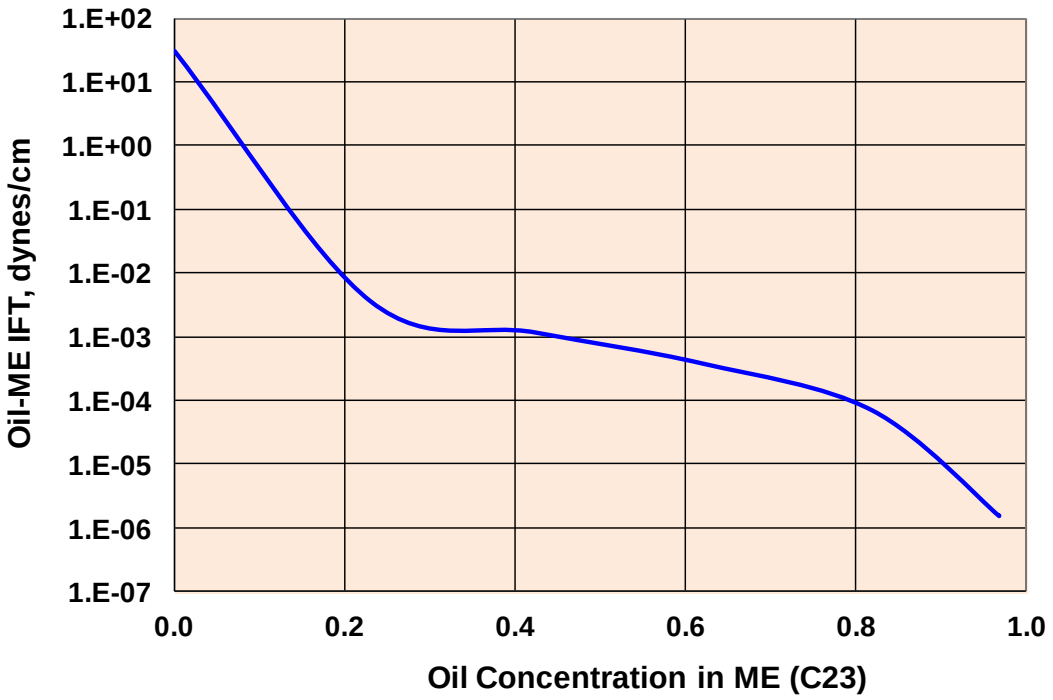

Figure 7-2: Oil-ME interfacial tension as a function of oil concentration in microemulsion phase (Pope, 2011).

7.3.2.3 Microemulsion Phase Behavior

The phase behavior of surfactant at reservoir conditions is very complicated due to many factors influencing its performance. Healy and Reed (1974) showed that the phase behavior strongly depends on brine salinity and there are essentially three different microemulsion types of Type I, Type II, and Type III. The phase behavior model in UTCHEM is based on Hand's rule (Hand, 1939) and uses the ternary diagram for representing different microemulsion phases and tie lines which are distributive curves.

The tie lines which join the composition of the equilibrium phases are given as

$$\frac{C_{3\ell}}{C_{2\ell}} = E\left(\frac{C_{3\ell}}{C_{1\ell}}\right)^F, \qquad for \quad \ell = 1,2,or\,3 \tag{7.22}$$

where E and F are empirical parameters and ℓ refers to aqueous, oleic or microemulsion phase.

At low salinity, there is an excess oil phase which is essentially pure oil and a microemulsion phase which contains water plus electrolytes, surfactant, and some solubilized oil. The tie lines (distribution curves) at low salinity have negative slope. This type of phase environment is called Winsor Type I. For high salinity, an excess water phase and a microemulsion phase containing most of the surfactant and oil, and some solubilized water exist. This type of phase environment is called Winsor Type II. An overall composition at intermediate salinity separates into three phases. These phases are excess oil and water phases and a microemulsion phase whose composition is represented by an invariant point. This phase environment is called Winsor Type III. Figure 7-3 and Figure 7-4 illustrate the experimental set up and different phase behavior types as salinity increases. The effective salinities at which the three equilibrium phases form or disappear

are called lower and upper limits of effective salinity (C_{SEL} and C_{SEU}). Figure 7-5 shows three phase behavior environments as a function of salinity.

There is no ME phase modeled in STARS and ECLIPSE and the effect of salt on phase behavior is not modeled. However, there are two options to specify surfactant partitioning between phases in STARS. The first is irreversible which means surfactant cannot dissolve back into the water and the second is reversible which indicates surfactant can dissolve back into water defined as K values for each component. In summary, Table 7-2 illustrates the key features in each simulator.

Table 7-2: Comparison of surfactant model options (Goudarzi *et al.*, 2013).

Surfactant Module	**UTCHEM**	**CMG-STARS**	**ECLIPSE**
ME Viscosity	√	Not Included	Not Included
Interfacial Tension	√	Tabular Format	Tabular Format
Phase Behavior	√	Not Included	Not Included
Surfactant Adsorption	√	√	√
Ion Exchange Effect	√	√	√
Effective Salinity Window	√	Not Included	Not Included

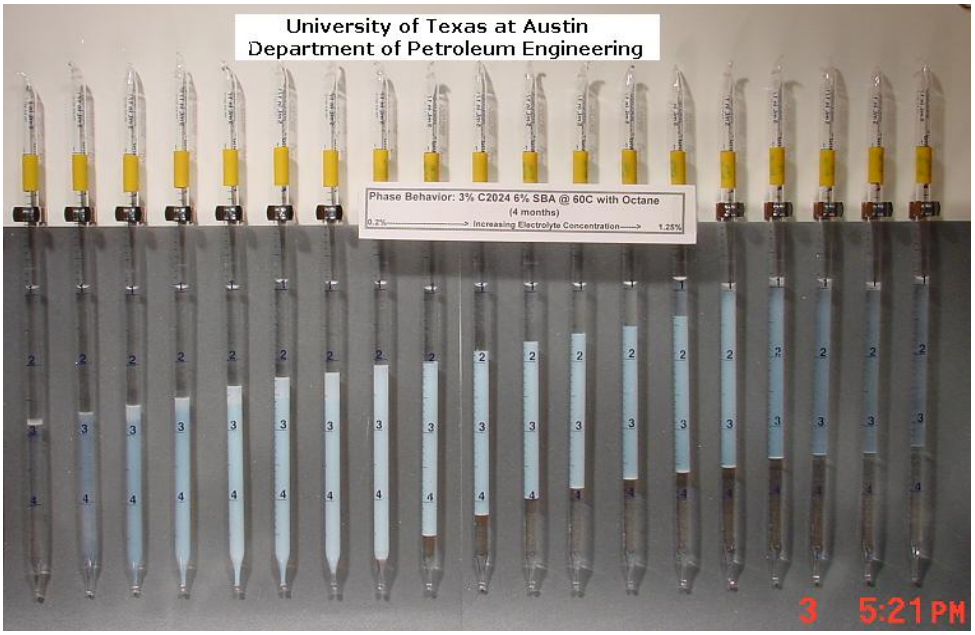

Figure 7-3: Phase behavior samples for surfactant and Octane mixtures (Pope, 2011).

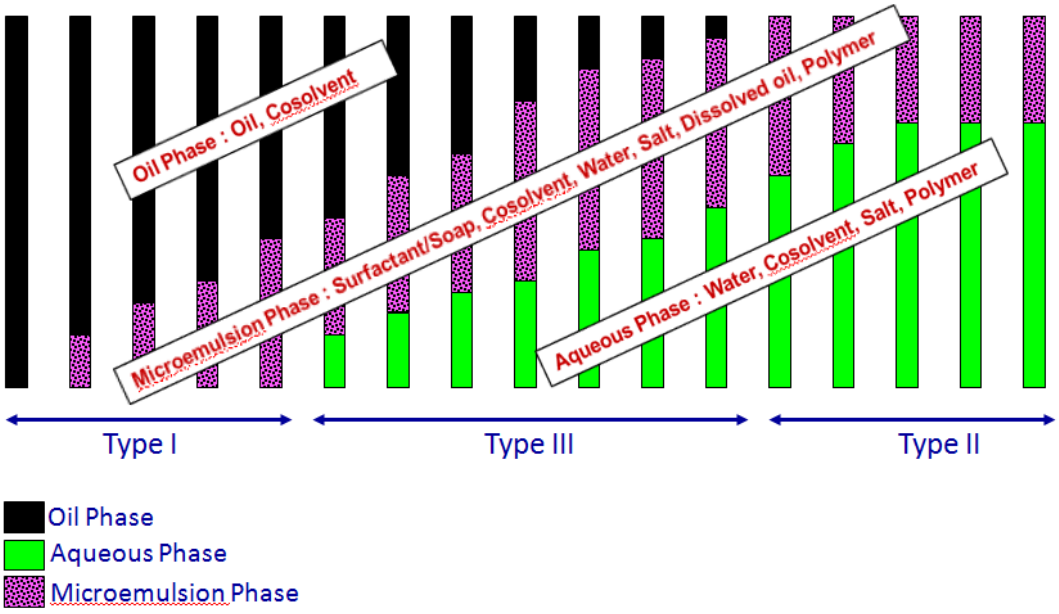

Figure 7-4: Phase behavior illustration of three Windsor Types I, II, III: Salinity increases from left to right.

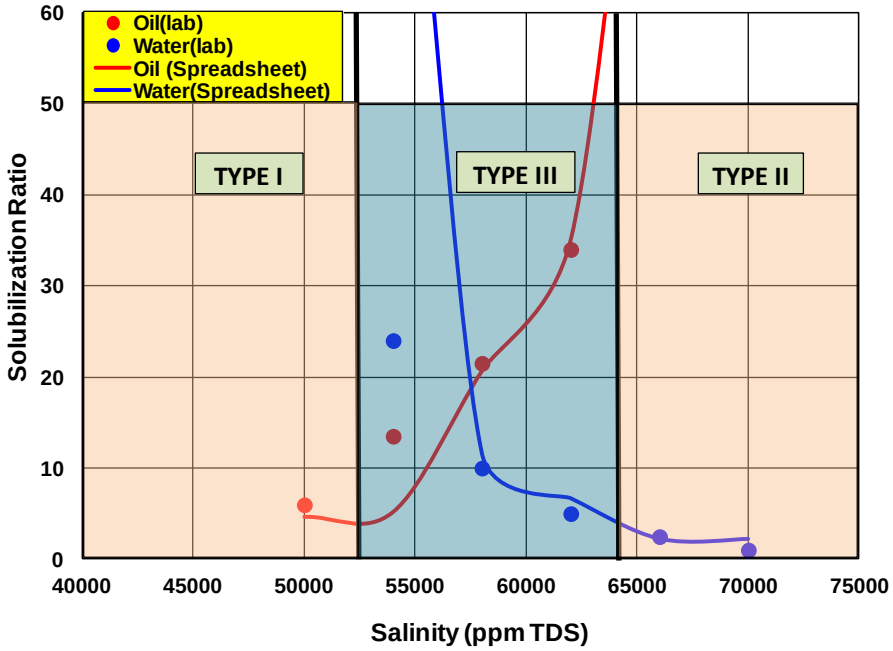

Figure 7-5: Phase behavior (solubilization curves) for surfactant and oil at reservoir temperature.

7.3.3 Alkaline Flood

Alkaline-surfactant-polymer (ASP) flooding is just another version of the surfactant-polymer (SP) flooding process. It uses the surfactants or, sometimes, called petroleum soap generated in-situ from interactions between the alkaline chemicals injected and the in-place acidic components in the crude oil along with the injected surfactants to lower the interfacial tension between the chemical slug and the crude oil to increasing the capillary number and, therefore, lowering the residual oil saturation. The recovery mechanisms of the ASP process are similar to the SP process but interactions of the alkaline chemicals with the reservoir solids and crude oils are much more complex and may cause severe production problems such as the severe emulsions and scales.

However, if we can take the advantage of the in-situ generated surfactants, the economic benefits in chemical costs could be substantial.

Both UTCHEM and STARS model geochemical reactions and consider the effect of in-situ generated soap. Binodal curves for surfactant and soap phase behavior are defined using hand's rule. STARS supports IFT data in a tabular format as explained before but IFT can be modeled using Chun Huh or Healy and Reed model in STARS-ME and tabular format is no longer supported in STARS-ME. It should be noted that polymer model in STARS-ME is the same as that in STARS. Relative permeability curves at high and low capillary number are given as input parameters. The relative permeability is then interpolated as a function of capillary number. Four types of reactions (aqueous phase reactions, dissolution/precipitation reactions, ion exchange with clay, and acid dissociation reactions) are defined and assumed to be in equilibrium. In summary, Table 7-3 illustrates the key features in each simulator.

7.3.3.1 Soap Generation

Surfactant produced from the reaction between the acidic components of crude oil and the injected alkali is the principle mechanism of oil recovery in alkaline flooding. The acid components of the oil are a combination of carboxylic acid, carboxyphenols, porphyrins, or asphaltene fractions. The acid components of the oil are measured as total acid number (TAN). The total acid number is defined as the milligram of potassium hydroxide (KOH) needed to neutralize one gram of crude oil. Fan and Buckley (2006) developed a laboratory procedure to measure the acid number to better reflect the reactivity of the crude oils. The soap generation is generally modeled by partitioning of

acid in the water and subsequent dissociation in aqueous phase to provide soluble anionic surfactant (A^-) which is referred to as soap (UTCHEM technical manual, 2011).

$$HA_o \rightleftarrows HA_W$$

,

$$K_D = \frac{[HA_W]}{[HA_o]} \tag{7.23}$$

where HA_W is the concentration of acid in water and K_D is the partition coefficient of acid between oil and water.

$$HA_W \xrightleftharpoons{K_a} H^+ + A^-, \tag{7.24}$$

where K_a is the reaction constant following the equilibrium relationship as

$$K_a = \frac{[H^+][A^-]}{[HA_W]}. \tag{7.25}$$

Alkali uses OH^- to generate soap by the following reaction:

$$HA_W + OH^- \xrightleftharpoons{K_a} H_2O + A^-. \tag{7.26}$$

7.3.3.2 Simplified ASP Model in UTCHEM

The simplified model captures the key mechanisms of the process but in a way that requires minimum input for the model. The simplified alkaline model will add very little overhead to the computation time when added to the existing surfactant/polymer

model. The following features in simplified ASP model will make large scale ASP simulations reasonable:

- Generation of soap based on acid number and water oil ratio
- Effect of soap on optimum salinity and solubilization ratio at optimum salinity
- Alkali consumption using Langmuir isotherm
- Reduction of synthetic surfactant adsorption as a function of pH

Soap generation is based on an input total acid number (TAN) in the unit of (mg KOH)/(g oil). We assume that acid is either fully or partially converted to soap using an acid conversion factor (K_S) only when there is co-presence of oil and alkali. The generated soap concentration in mole/(L water) is computed using the following equation:

$$C_{soap} = \frac{(TAN)\, K_S\, S_2\, \rho_2}{S_1 (MW_{KOH})}\,, \tag{7.27}$$

where S_2, ρ_2, S_1, and MW_{KOH} are oil saturation, oil density, water saturation, and molecular weight of potassium hydroxide which is 56.1 g/mole. The effect of soap on optimum salinity and solubilization ratio is modeled exactly the same as that for full ASP model.

Table 7-3: Comparison of ASP model options (Goudarzi *et al.*, 2013).

ASP Module	UTCHEM	CMG-STARS	ECLIPSE
Aqueous Reactions	√	Not Included	Not Included
Soap Generation Reaction	√	Not Included	Not Included
Surfactant/Soap Effect on IFT	√	√	√
Alkali Retention	√	√	√
Surfactant Adsorption	√	√	√
Surfactant Adsorption vs. Alkali Concentration	*SF*	√	√

7.4 RESULTS AND DISCUSSION

7.4.1 Polymer Flood Using UTCHEM and CMG-STARS

A Cartesian model was set up where single phase polymer flood is simulated. The injection was at constant rate and production was at constant pressure and different parameters of concentration, adsorption, shear rate, etc. were evaluated. Table 7-4 gives the properties used for this comparison. The comparison of polymer viscosity model between UTCHEM and CMG-STARS is shown in Figure 7-6. This part can be divided into two main case studies:

a. Investigate polymer viscosity model and its impact on injection pressure and average pressure while the polymer adsorption and also viscosity dependency on shear rates are not included. A comparison of injection and average pressure is shown in Figure 7-7. Overall the results are close considering very different models for viscosity as a function of concentration. Figure 7-8 compares water viscosity distributions after 180 days. The comparison illustrates that polymer viscosity front move similarly in both UTCHEM and STARS.

b. Same comparison as part (a) but polymer adsorption and shear effect are included. A comparison of injection and average pressure in Figure 7-9 shows more differences compared to the case (a). Adsorption and shear rate models in UTCHEM use a function whereas CMG-STARS uses tables. The water viscosity profiles after 180 days are shown in Figure 7-10.

Table 7-4: Properties of model used for comparison polymer model between UTCHEM and CMG-STARS.

Model	3-Dimensional Cartesian
No. of Grids	15×15×5
Porosity and permeability	0.19, 100 md
Water saturation	100 %
Injection Rate (constant rate)	561.5 ft^3/day
Production Pressure (constant pressure)	1800 psi
Polymer Concentration	0.25 wt%
Simulation Time	1000 days

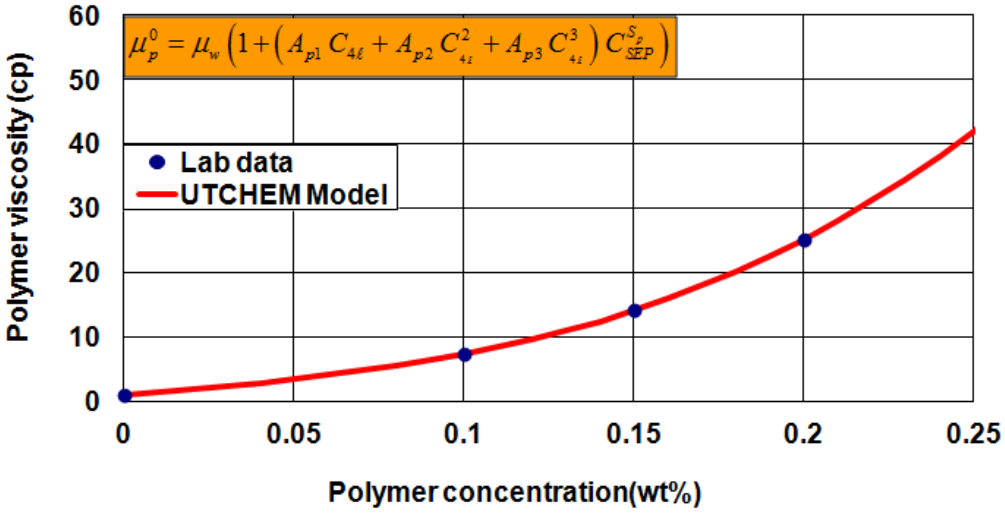

(UTCHEM)

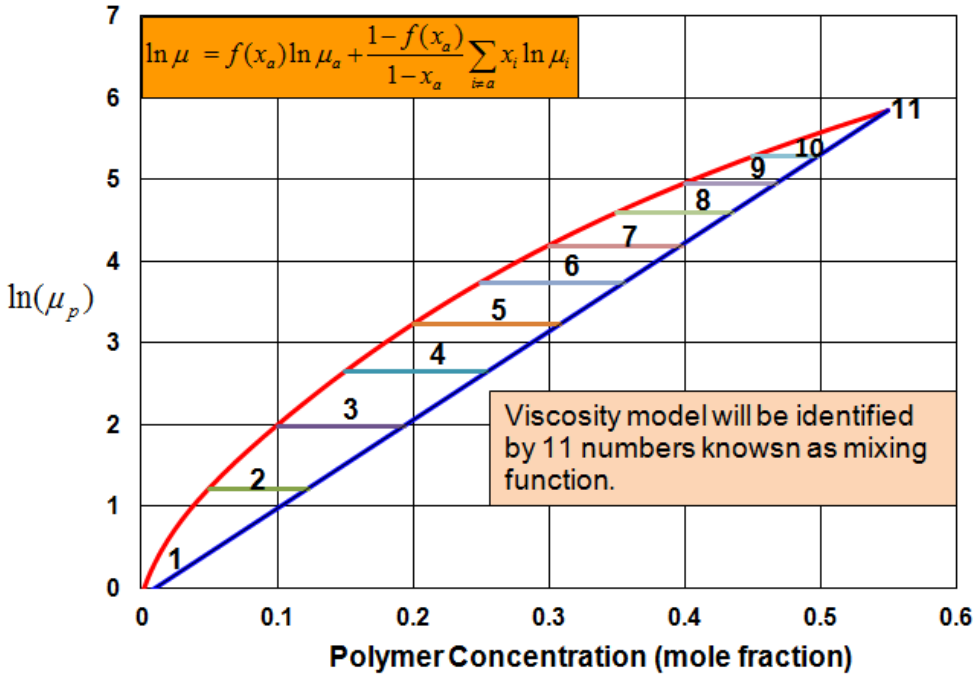

(CMG-STARS)

Figure 7-6: Comparison of polymer viscosity model between UTCHEM and CMG-STARS.

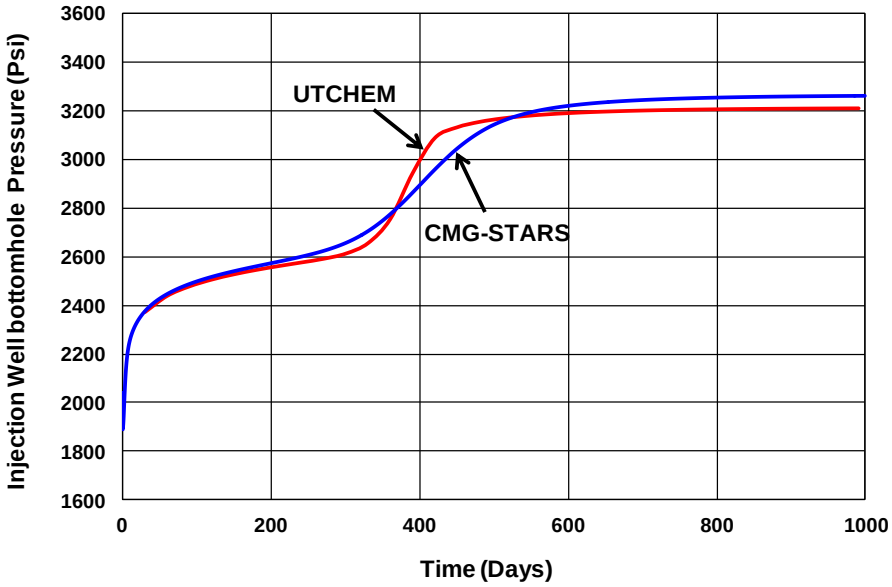

(a)

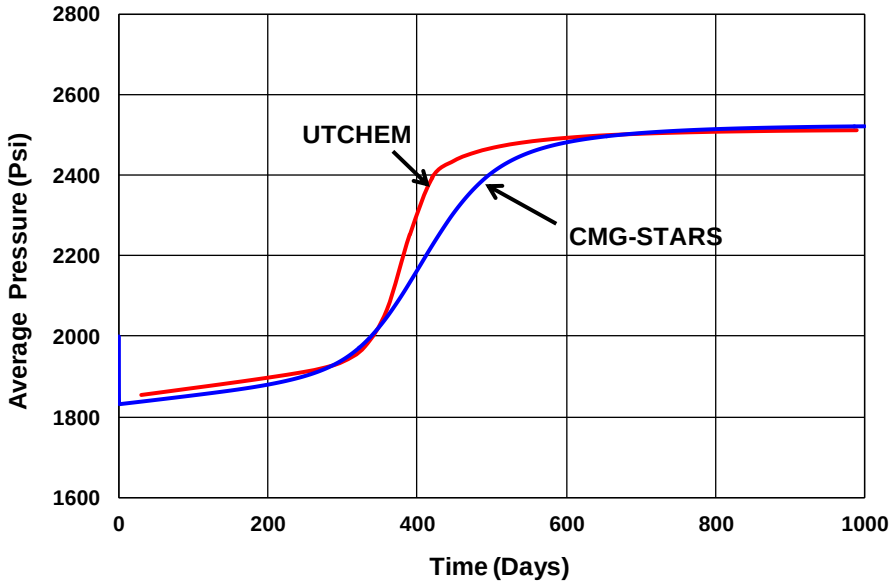

(b)

Figure 7-7: Comparison of (a) injection pressure and (b) average pressure between UTCHEM and CMG-STARS for polymer model (Base case-No polymer adsorption and shear effect).

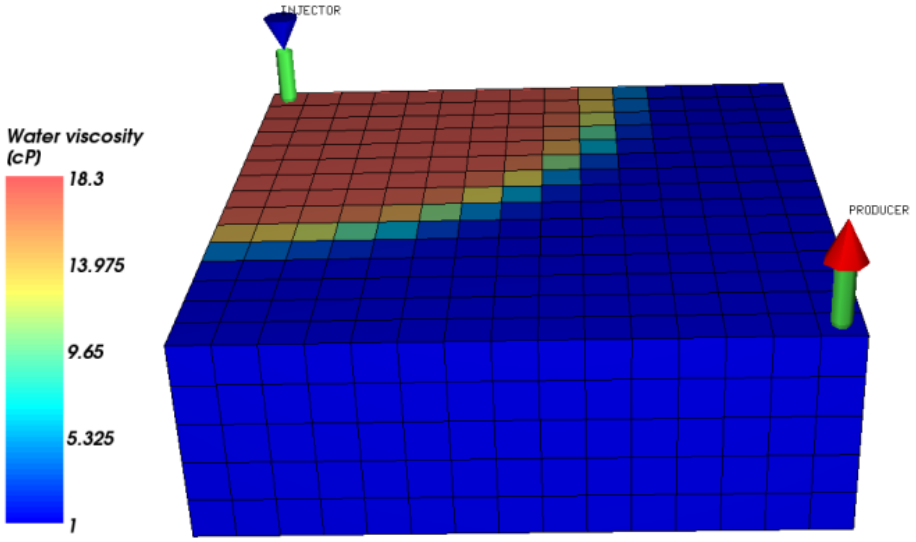

(UTCHEM)

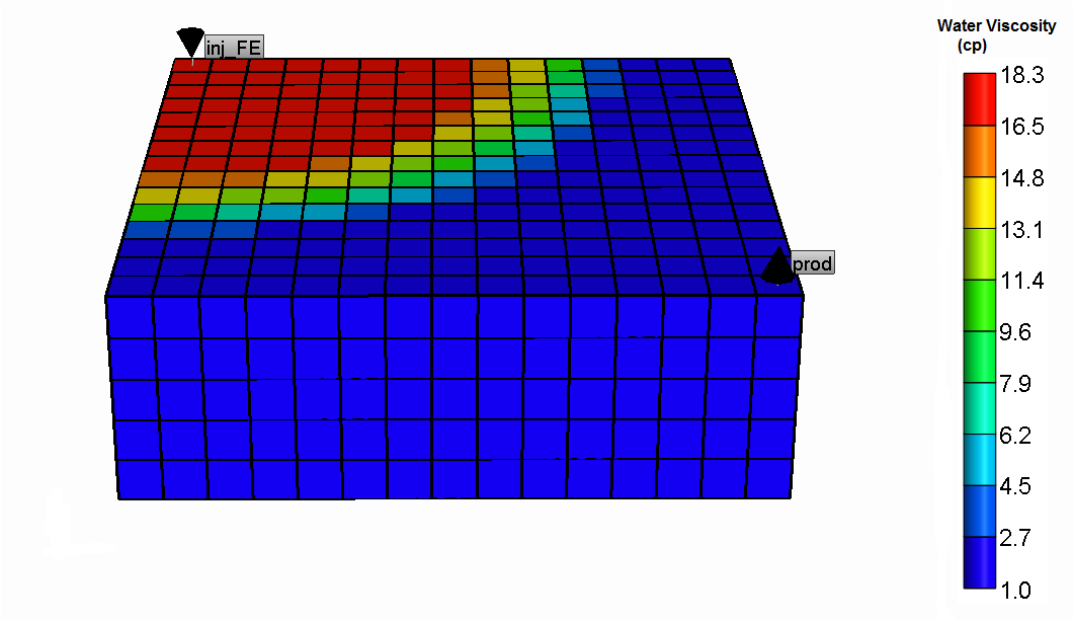

(CMG-STARS)

Figure 7-8: Comparison of water viscosity profile between UTCHEM and CMG-STARS for polymer model (Base case-No polymer adsorption and shear effect).

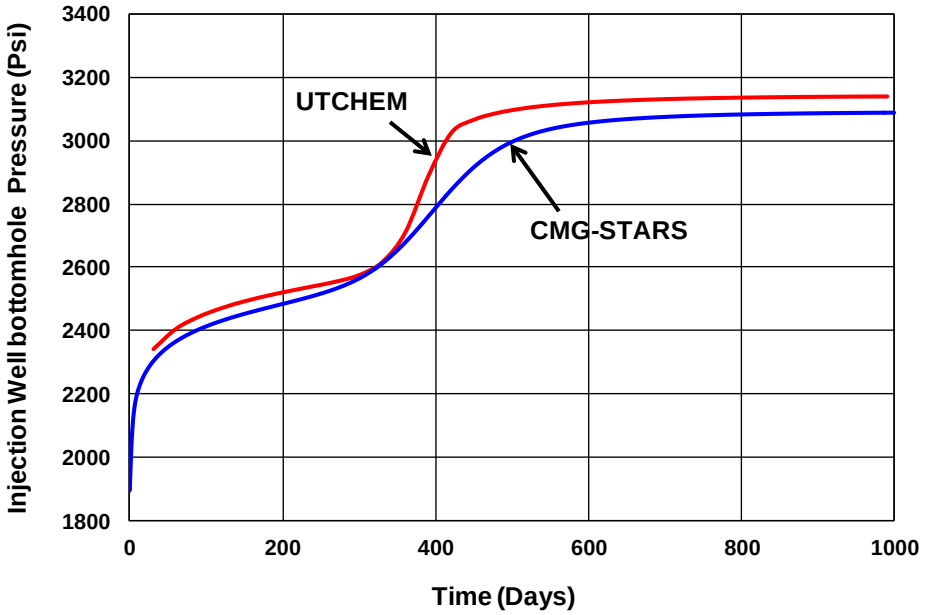

(a)

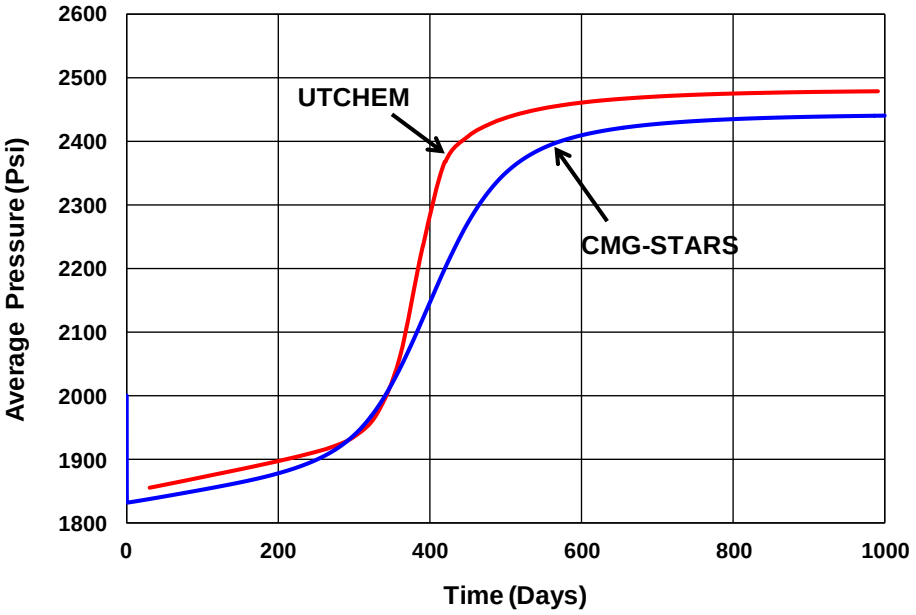

(b)

Figure 7-9: Comparison of (a) injection pressure and (b) average pressure between UTCHEM and CMG-STARS for polymer model (Polymer adsorption and shear effect are included).

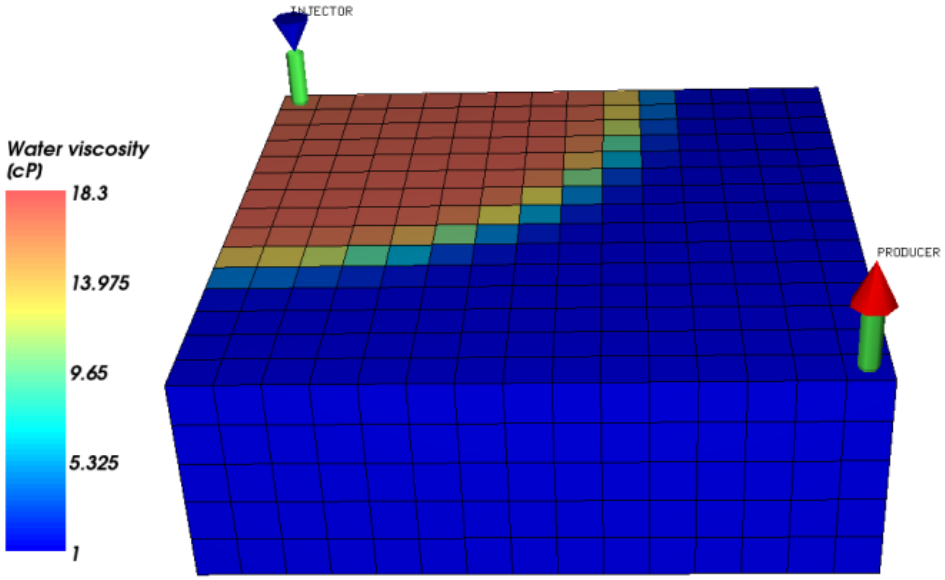

(UTCHEM)

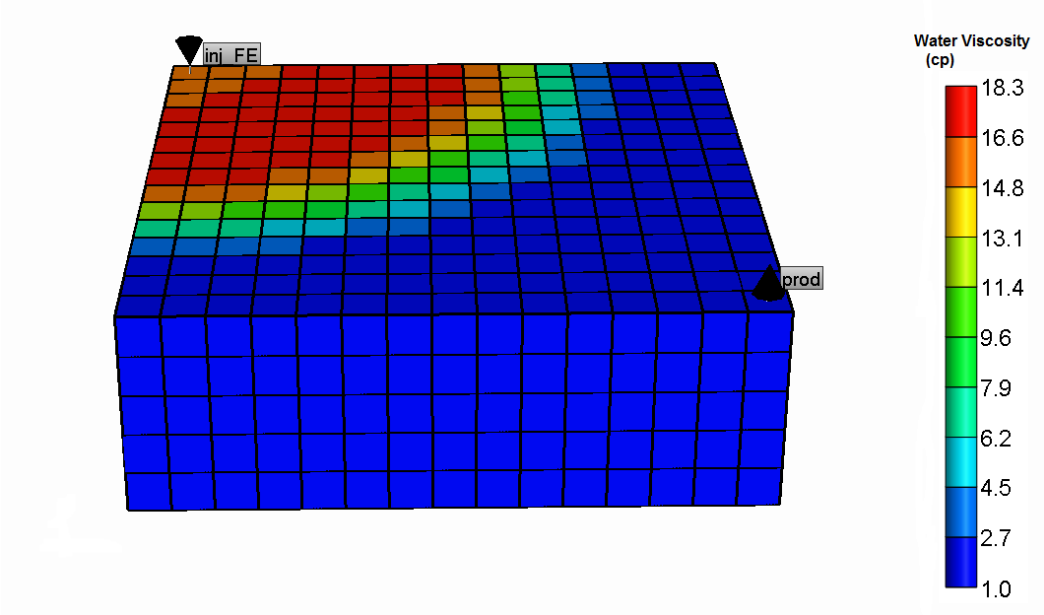

(CMG-STARS)

Figure 7-10: Comparison of water viscosity between UTCHEM and CMG-STARS for polymer model (Polymer adsorption and shear effect are included).

7.4.2 ASP Coreflood Simulations Using UTCHEM and CMG-STARS

7.4.2.1 Experimental Procedure

Mohanty (2012) performed a laboratory coreflood using outcrop Berea core with ASP formulation at ultralow IFT conditions. The dead oil was used for the active oil with pH of around 8.5-9.5 when sodium carbonate was added and soap was generated in-situ. First, the core was saturated with formation brine and then flooded with reservoir dead oil and the core was left in the oven at reservoir temperature of 59 ^{0}C overnight. Then the vertical core was flooded with 3 PVs of synthetic formation brine (SFB) from the bottom of the core at the velocity of 1 ft/d and then flooded with 2 PVs of SFB at the rate of 10 ft/d to reach residual oil saturation before the chemical flood starts. A water preflush was followed by ASP chemical slug, then polymer drive, and finally by post water injection. Oil recovery was nearly 80%. A summary of rock properties and coreflood procedures is shown in Table 7-5.

7.4.2.2 Simulation Results

The objective of this section was to history match ASP coreflood using UTCHEM and CMG-STARS simulators, which provides the key parameters for field scale simulations. Surfactant phase behavior showed a solubilization ratio of around 22 at optimal salinity of 11,000 ppm. Based on Huh's correlation and using optimum solubilization ratio, a very low IFT of 0.00062 dynes/cm was calculated. STARS has no capability for alkali reactions but the effect of alkali on IFT is modeled and surfactant adsorption is provided in the form of input tables. A comparison of oil recoveries and oil saturations between lab data, UTCHEM, and STARS simulators are shown in Figure 7-11 and Figure 7-12. The comparison demonstrates that both UTCHEM and STARS can

model the ASP experiment in good agreement with laboratory data. Pressure drop between lab data and simulators is compared in Figure 7-13. The profile of produced polymer and surfactant concentrations is shown in Figure 7-14 which shows the peak of surfactant concentration after ASP slug which is around 6 PV injected. The experimental results demonstrated that in-situ generated soap (Figure 7-15) leads to ultralow IFT between oil and microemulsion phase as shown in Figure 7-16.

Table 7-5: Fluid and coreflood conditions.

Type	Berea Core
Diameter and Length	3.78 cm, 27.153 cm
Porosity, Permeability	0.18, 300 md
Initial oil Saturation	0.412
Irreducible Water Saturation	0.21
Surf. Concentration	0.5 wt%
Oil Recovery	80% OOIP
IFT	0.00062 mN/m
Temperature	59 ^{0}C
Crude Oil Viscosity	14 cp
Residual Oil Saturation	0.41
Duration of Experiment	0.72 days
Chemical flood:	**Pore volume injected:**
Preflush 0.5% Na_2CO_3, 1.1% NaCl in SFB	0.4 PV
ASP Slug 0.5% surf., 0.25% polymer, 0.5% Na_2CO_3, 1.1% NaCl in SFB	0.3 PV
Polymer Drive 0.25% polymer, 0.5% NaCl in SFB	1 PV
Post Water Injection	2 PV

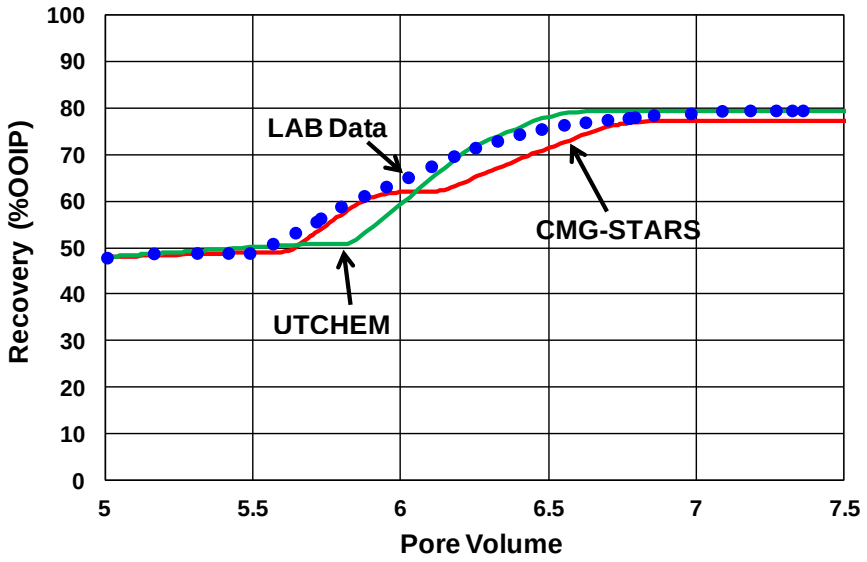

Figure 7-11: Comparison of measured and simulated oil recovery between lab data with UTCHEM and CMG-STARS simulators.

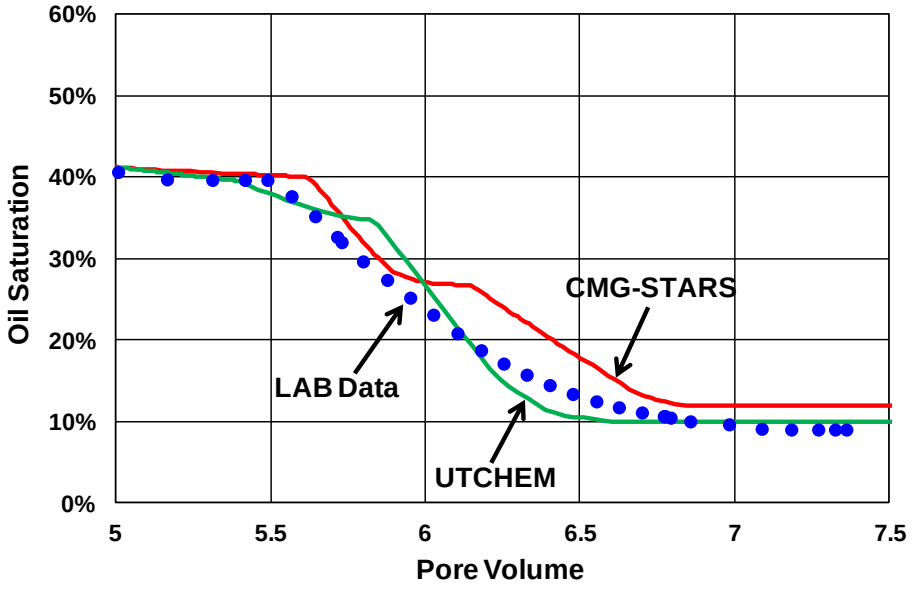

Figure 7-12: Comparison of measured and simulated oil saturation between lab data with UTCHEM and CMG-STARS simulators.

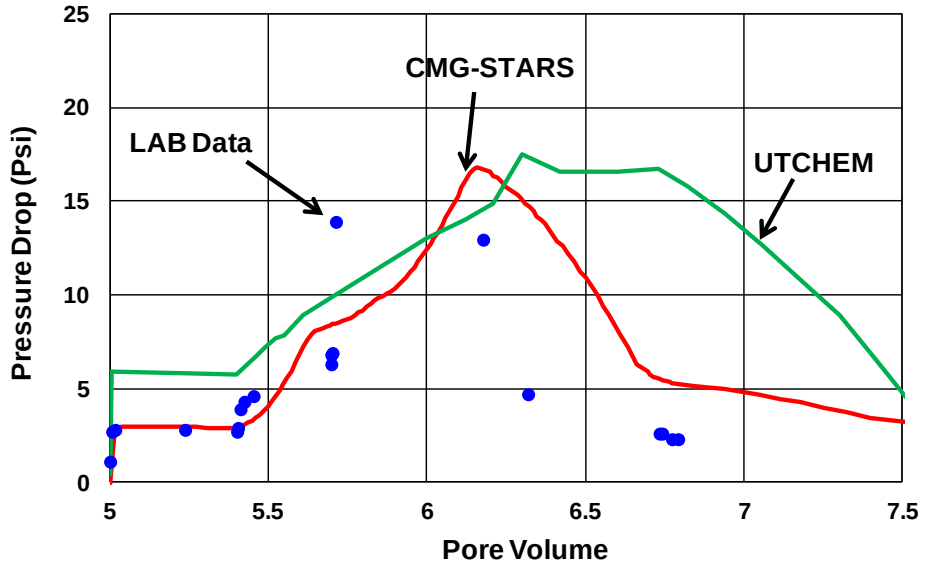

Figure 7-13: Comparison of simulated and measured pressure drop between lab data with UTCHEM and CMG-STARS simulators.

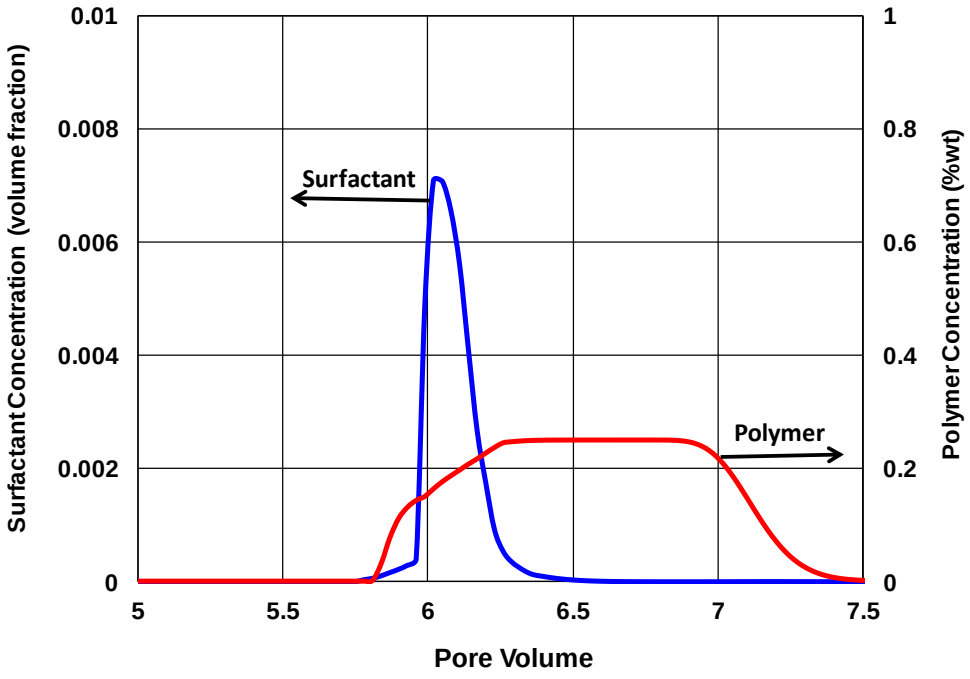

Figure 7-14: Surfactant and polymer concentration at the outlet during chemical flood.

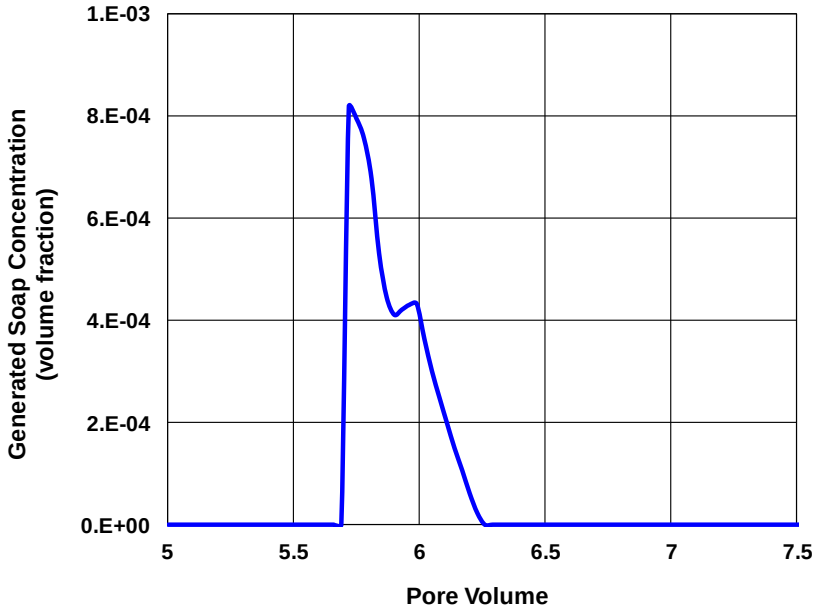

Figure 7-15: Generate soap concentration during ASP injection.

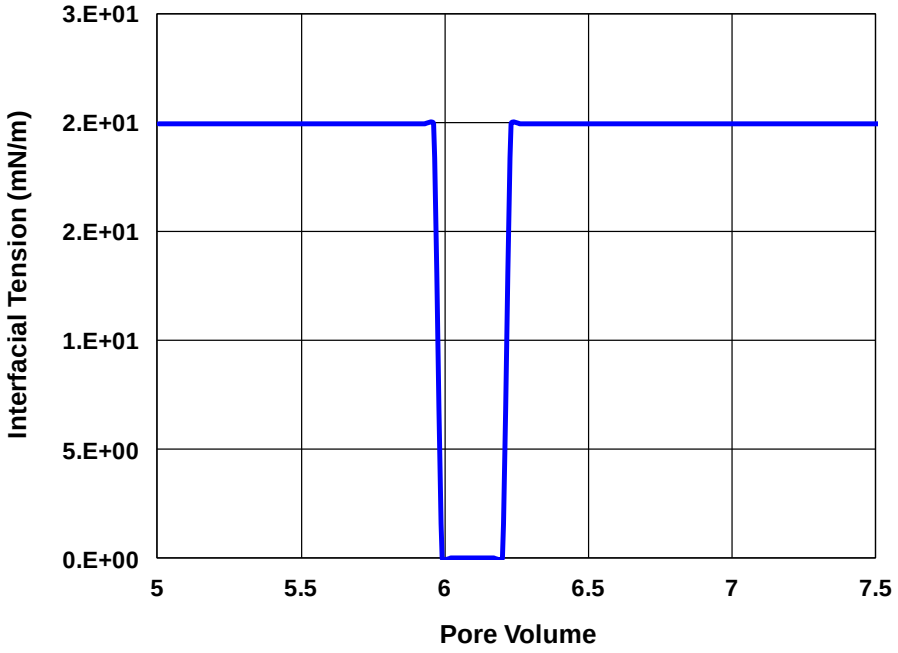

Figure 7-16: IFT profile and its reduction due to injected surfactant and in-situ generated soap inside the core.

7.4.3 Polymer Flood Simulation Using UTCHEM and ECLIPSE

A Cartesian model was set up where single phase polymer flood is simulated. The injection was at constant rate and production was at constant pressure and different parameters of concentration, adsorption, shear rate, etc. were evaluated. Table 7-6 gives the properties used for the comparison of polymer flood between UTCHEM and ECLIPSE. The polymer models were defined for both ECLIPSE and UTCHEM as close as possible by providing polymer property input tables in ECLIPSE calibrated against UTCHEM correlations.

UTCHEM and ECLIPSE are compared for polymer flood based on total oil production, production rate, oil saturation, and polymer concentration. Total simulation time was 1000 days and polymer concentration of 0.15 wt% was chosen. The comparison of total oil production and oil production rate shows that there is good agreement between UTCHEM and ECLIPSE for polymer flood as Figure 7-17 and Figure 7-18 illustrate. Saturation profiles after 1000 days are very close (Figure 7-19). However, it should be noted that ECLIPSE polymer viscosity model lacks the effect of salinity and hardness on viscosity.

There are differences between UTCHEM and ECLIPSE. Firstly, it should be noted that polymer concentration in UTCHEM varies from 0 to 0.15 wt%, equivalent to 0 to 50 lb/stb in ECLIPSE. Secondly, the difference in polymer concentration profiles (Figure 7-20) is because ECLIPSE shows the polymer concentration movement exactly as maximum injected concentration and does not consider the residual oil remained behind polymer front which has effect on polymer concentration, whereas, UTCHEM shows this reduction in polymer concentration which arises from oil and water concentrations left behind polymer flood. The profiles of water and oil concentrations

after 1000 days from UTCHEM simulation are shown in Figure 7-21. The oil concentration map shows that all the remaining mobile oil is produced in most of the gridblocks down to residual oil saturation as a result of effective sweep by polymer flood.

Table 7-6: Polymer flood simulation data between UTCHEM and ECLIPSE.

Model	2-Dimensional Cartesian
No. of grids	10×10×1
Δx , Δy , Δz	75, 75, 30 ft
Porosity, Permeability	0.2, 50 md
Initial Water Saturation	25 %
Initial Reservoir Pressure	4000 psi
Oil Relative Permeability Endpoint	0.8
Water Relative Permeability Endpoint	0.25
Temperature	25 ^{0}C
Crude Oil Viscosity	2 cp
Residual Oil Saturation	0.3
Injection Rate (constant rate)	1123 ft^3/day
Production Pressure (constant pressure)	3999 psi
Polymer Concentration	0.15 wt%
Simulation Time	1000 days

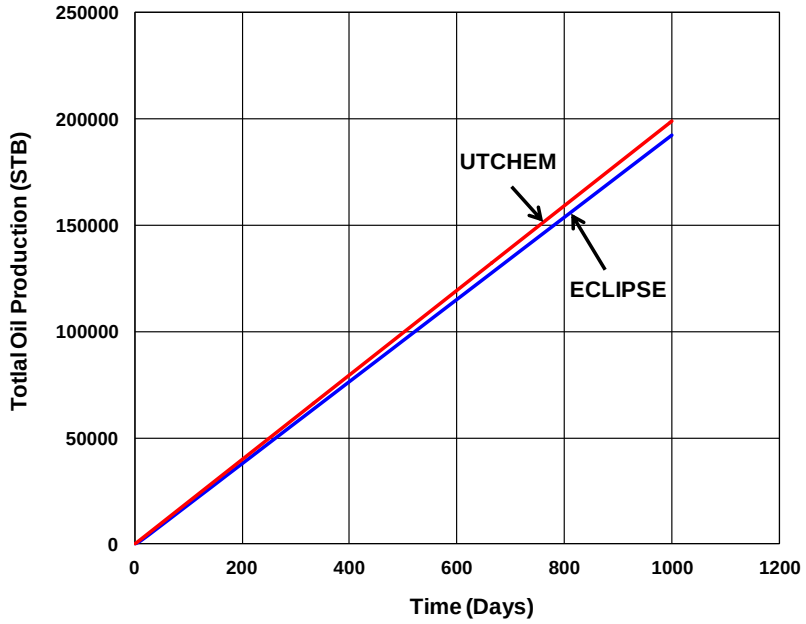

Figure 7-17: Comparison of total oil production between UTCHEM and ECLIPSE for polymer flood.

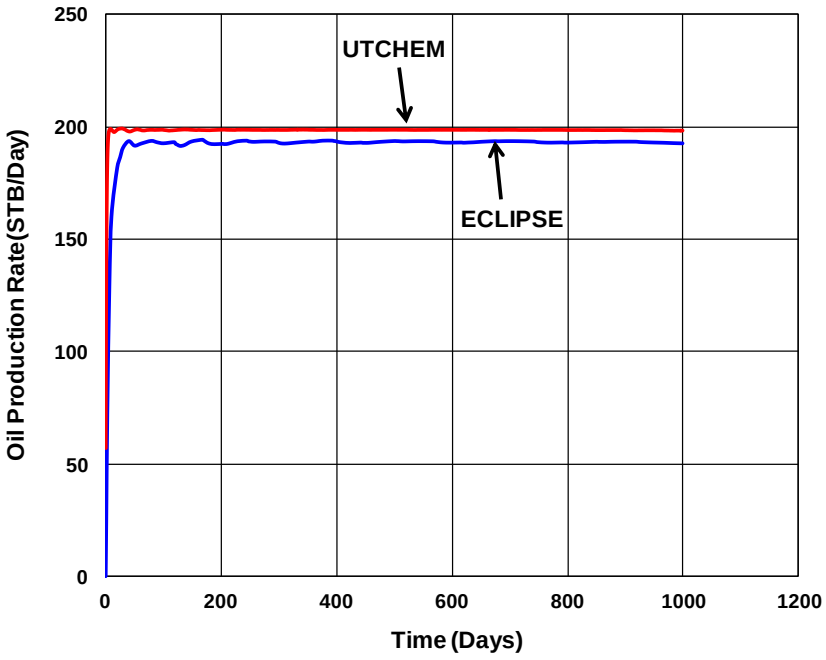

Figure 7-18: Comparison of oil production rate between UTCHEM and ECLIPSE for polymer flood.

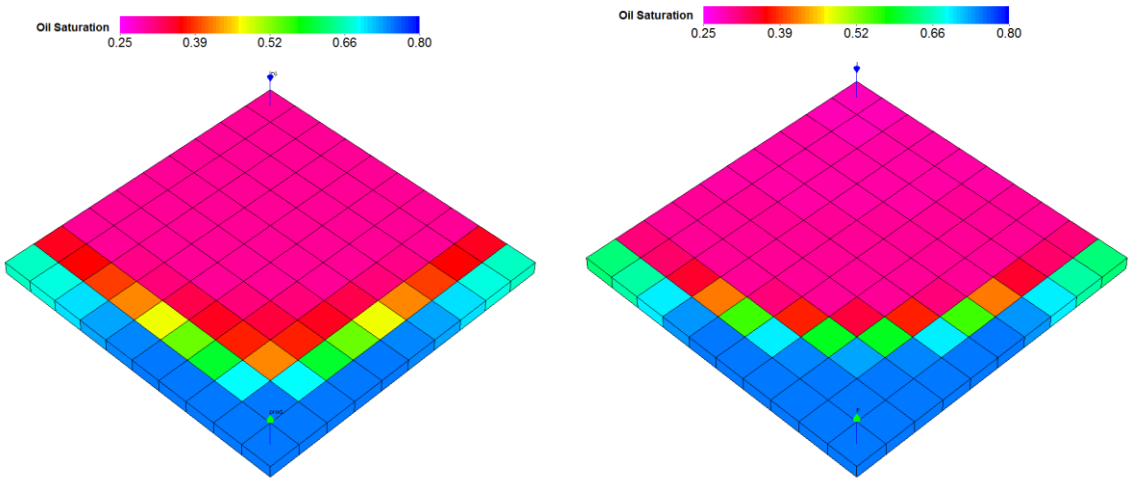

(UTCHEM) (ECLIPSE)

Figure 7-19: Oil saturation profiles after 1000 days in UTCHEM and ECLIPSE for polymer flood.

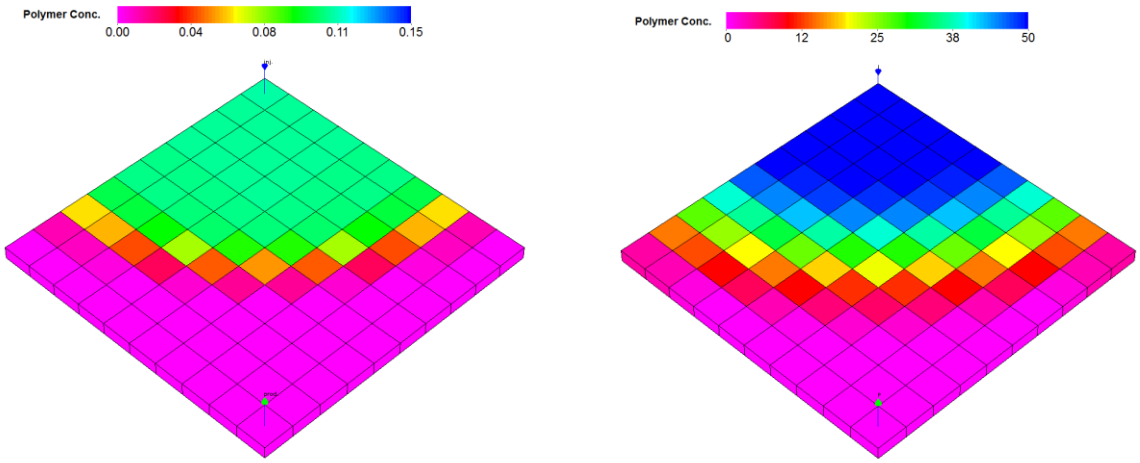

(UTCHEM) (ECLIPSE)

Figure 7-20: Polymer concentration profiles after 1000 days in UTCHEM and ECLIPSE for polymer flood.

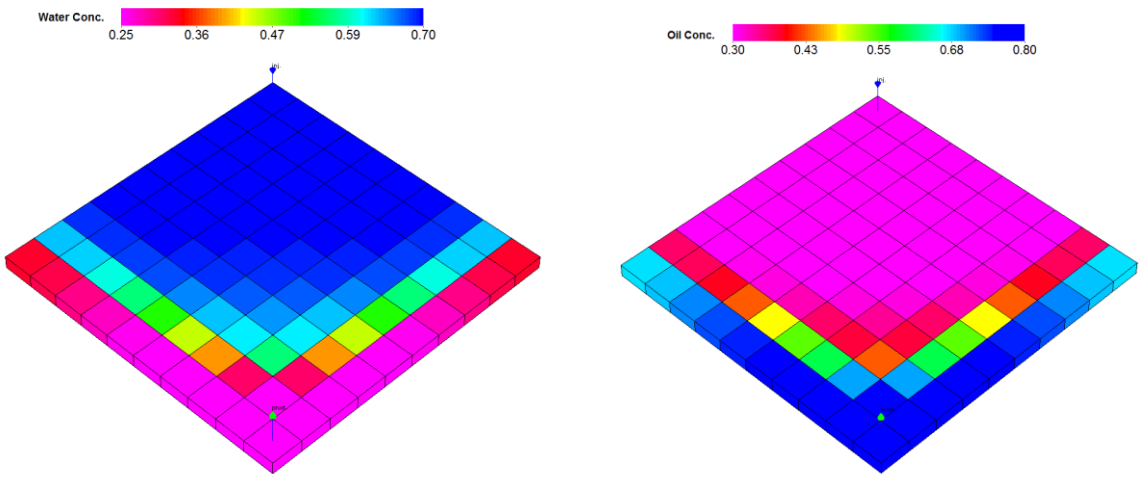

(Water concentration) (Oil concentration)

Figure 7-21: Water and oil concentration profiles after 1000 days in UTCHEM for polymer flood.

7.4.4 Field Scale Surfactant Flood Simulation Using UTCHEM and ECLIPSE

A sector model with 95×192×5 gridblocks in X, Y, and Z directions is used for this field scale simulation. Table 7-7 gives the reservoir and fluid properties. Average reservoir properties for each layer are given in Table 7-8. The distribution of porosity and permeability for the sector model is shown in Figure 7-22. Figure 7-23 shows the distribution of initial oil saturation and initial pressure. The reservoir temperature is about 220 ^{0}F and the initial reservoir pressure is 4000 psi at a reference depth of 6150 ft. The reservoir is described as layered with two units separated by a hard streak barrier that limits the vertical flow between the units. Initially the reservoir was under primary depletion using the central well.

The surfactant models were defined for both ECLIPSE and UTCHEM with an attempt to make the input as close as possible. The simulation was based on waterflood for 3980 days followed by surfactant flood for almost 5000 days. The optimum surfactant concentration of 0.017 vol. fraction was chosen for injection. The crude oil viscosity was around 2 cp implying generated microemulsion viscosity will be low and co-solvent injection to control viscosity is not necessary. The comparison of cumulative oil production shows that there is a good agreement between UTCHEM and ECLIPSE as Figure 7-24 illustrates. Also, the comparison of surfactant injected between UTCHEM and ECLIPSE is shown in Figure 7-25 which demonstrates close agreement between UTCHEM and ECLIPSE during surfactant injection.

Table 7-7: Reservoir and fluid properties for surfactant flood using UTCHEM and ECLIPSE.

Model	3-Dimensional Cartesian
No. of grids	95×192×5
Δx , Δy	40, 50 ft
Initial Reservoir Pressure	4000 psi
Oil Relative Permeability Endpoint	1.0
Water Relative Permeability Endpoint	0.23
Temperature	105 ^{0}C
Crude Oil Viscosity	2 cp
Water Viscosity	0.8 cp
Surfactant Concentration (vol. fraction)	0.017
Simulation Time	8705 days

Table 7-8: Average petrophysical properties per layer.

Layer	K_x, md	K_y, md	K_z, md	ϕ	Δz , ft	S_{wi}
1	3.264	9.806	1.634	0.17393	1.61	0.172
2	4.453	13.358	2.226	0.1694	1.61	0.162
3	1.489	4.466	0.744	0.25714	1.8	0.393
4	1.188	3.564	0.594	0.17344	1.8	0.381
5	0.712	2.136	0.356	0.1187	1.8	0.424

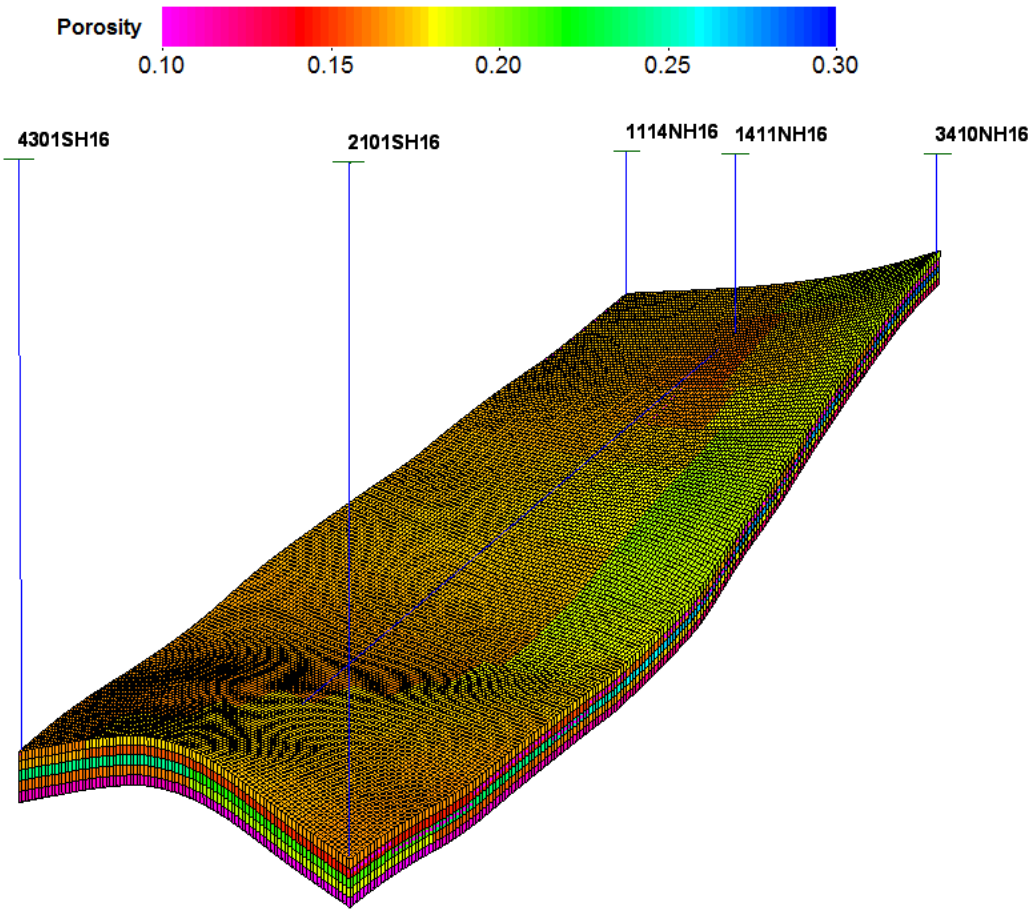
Porosity
0.10
0.15
0.20
0.25
0.30
4301SH16
2101SH16
1114NH16
1411NH16
3410NH16

(a)

Figure 7-22.

Figure 7-22, continued.

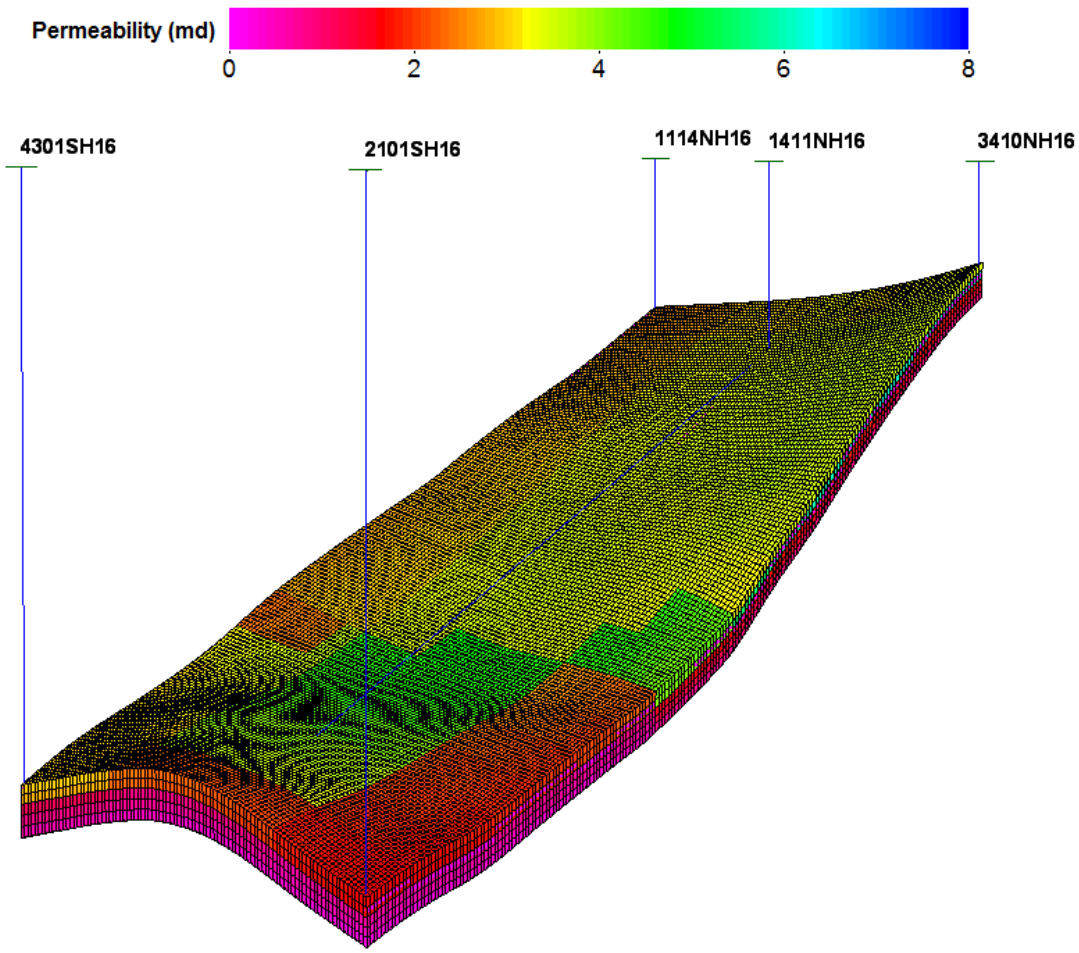

(b)

Figure 7-22: The distribution of (a) porosity and (b) permeability in the sector model.

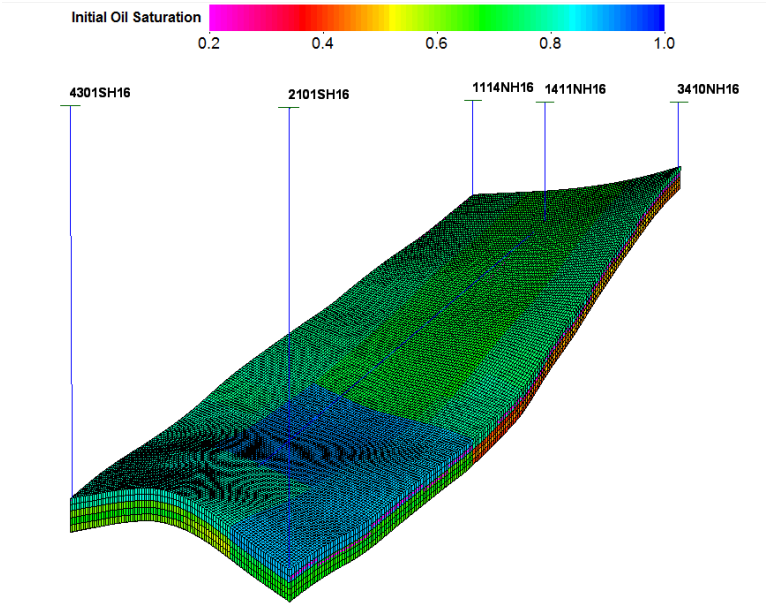

(a)

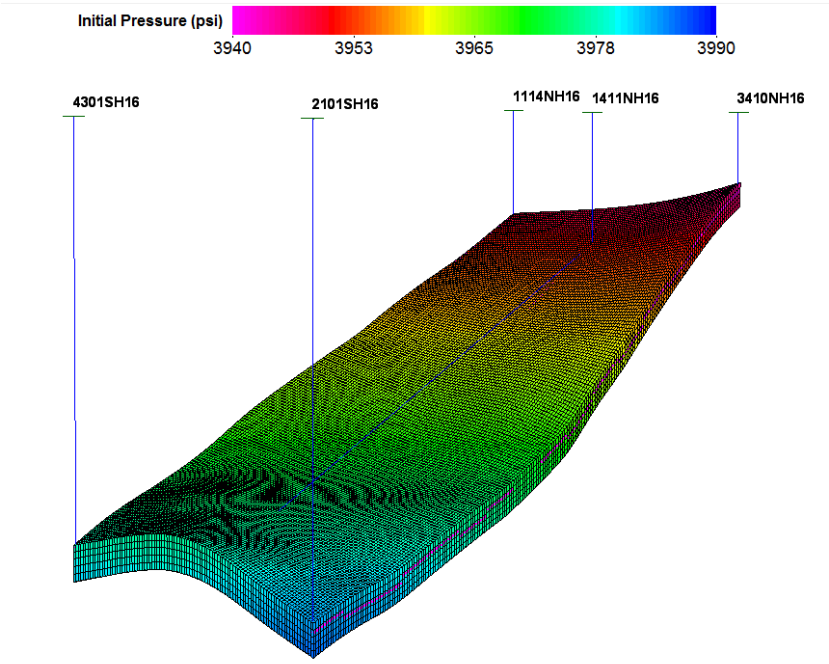

(b)

Figure 7-23: The distribution of (a) initial oil saturation and (b) initial pressure in the sector model.

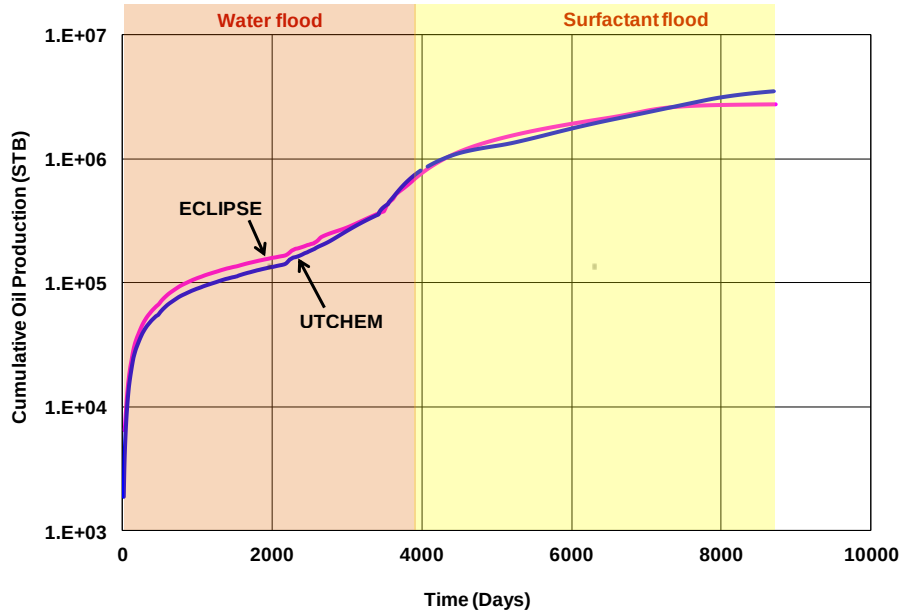

Figure 7-24: Comparison of oil production between UTCHEM and ECLIPSE for surfactant flood.

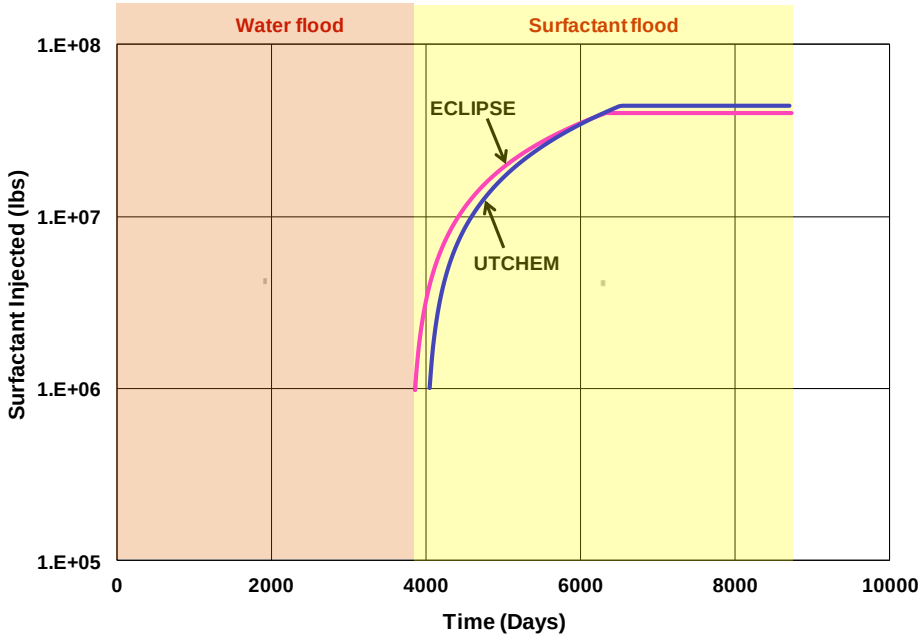

Figure 7-25: Comparison of surfactant injected between UTCHEM and ECLIPSE for surfactant flood.

7.5 SUMMARY AND CONCLUSIONS

- Careful selection of tables in the commercial simulators against UTCHEM correlations leads to a reasonable agreement for different chemical EOR applications.
- Laboratory coreflood results were history matched using both UTCHEM and CMG-STARS with very good agreement.
- Polymer models were compared between UTCHEM and CMG-STARS and also between UTCHEM and ECLIPSE. The results showed differences because of different viscosity models in each simulator.
- The effect of salinity and hardness in polymer model is not considered in either CMG-STARS or ECLIPSE.
- UTCHEM results show a reduction in polymer viscosity as expected when adsorption and subsequent reduction in polymer concentration are modeled. However, CMG-STARS and ECLIPSE give no considerable effect on polymer viscosity compared to the case with no adsorption.
- The surfactant flood for a large field-scale case was modeled using both UTCHEM and ECLIPSE and fairly close results were achieved. Tables for ECLIPSE were generated based on UTCHEM correlations. Water viscosity was replaced with microemulsion viscosity in order to achieve a good comparison.

Chapter 8: Summary, Conclusions and Recommendations for Future Research

In this chapter, we summarize the tasks performed and present the conclusions of this dissertation with several recommendations for future extension.

8.1 SUMMARY AND CONCLUSIONS

Conformance control research:

- PPG experiments were performed both in fracture and sandpack models to investigate the effect of PPG on improving conformance and reducing water cut. The experimental results demonstrated that PPG injection pressure increased with the increase in flow rate and salinity but decreased with the increase of fracture width.
- Several Berea sandstone coreflood experiments were conducted to understand the transport of PPG microgels and their impact on flow conformance and reducing water production. Coreflood results showed that residual oil saturation after PPG flood is lower than the primary waterflood residual oil saturation. A simple model is proposed to simulate the experiment but more mechanistic understanding is required as future work supported by additional laboratory and theoretical studies.
- We developed empirical correlations for resistance factor (RF) and residual resistance factor (RRF) using different size conduits and for a wide range of flow rate, brine salinity, and hardness and the developed correlations are implemented in UTGEL simulator. Also, we have developed models for gel rheology, gel

adsorption, swelling ratio, and gel viscosity.

- The gel transport models were implemented in a reservoir simulator and validated against different types of laboratory experiments.
- UTGEL can model the heterogeneous coreflood experiments including parallel sandpack systems of high and low permeability packs (with cossflow and without crossflow) which represented the degree of heterogeneity. Resistance factor and gel retention model parameters were used as history matching parameters.
- To model heterogeneous parallel sand-pack coreflood experiments (with cossflow and without crossflow), different relative permeability, capillary pressure, and residual saturations are assigned for high and low permeability zones. PPG can penetrate into the high permeability sand-pack and minimize its penetration into the lower permeability sand-pack.
- The numerical studies indicated that main PPG design variables are treatment size, PPG concentration, permeability contrast between layers, degree of reservoir heterogeneity, high water cut, early water breakthrough, mobility ratio, and the ratio of vertical to horizontal permeability.
- The normal and rule-of-thumb estimates for slug size vary from 5% to 15% of the Channel Volume (CV). Our sensitivity simulation results showed that increasing slug volume above 10% CV will not have considerable impact on final oil recovery. Also, the sensitivity simulations illustrated that higher concentration is favorable for PPG treatment. However, increasing concentration beyond 10000 PPM will not increase final oil recovery. For reservoir properties, higher permeability contrast between layers and lower vertical to horizontal permeability ratio (k_v/k_h) are favorable design parameters for PPG treatment. Higher k_v/k_h

will lead to the crossflow of PPG from high permeability layer into low permeability layer which brings adverse effect on blocking high permeability channels.

- Pilot scale simulations of oil field cases showed that PPG has the capability to generate high resistance factor in the high permeability thief zone and increase the oil recovery by around 10-15% and decrease water cut by about 5-10 % over waterflood.

Wettability alteration and scale-up research:

- We modeled wettability alteration process using surfactant and alkaline in fractured carbonate rocks.
- Enordet A092 as anionic surfactant, with EDTA as an alkali, can change wettability from oil wet to strongly water-wet conditions. However, higher concentration of divalent cations (i.e. Mg^{2+} and Ca^{2+}) reduces the degree of wettability alteration.
- The imbibition cell tests were performed at reservoir temperature using reservoir crude oil for different core sizes to study the impact of matrix block size on oil recovery. We developed a new dimensionless scaling group for the imbibition time and recovery factor using the lab data including the IFT effect.
- The experimental results revealed that in addition to high permeability, less heterogeneity is another favorable factor for wettability alteration and rate of imbibition. We modified a published gravity-based dimensionless time and validated against experiments conducted with various size cores.

- The scale-up results illustrated that increasing the height of the core results in a reduction in oil production rate and increase in imbibition time linearly. Oil recovery for the large core at reservoir temperature was estimated using new developed dimensionless numbers and the results were in good agreement with measured oil recovery.
- We modeled dynamic fractured core using two different methods of a) random permeability distribution, b) explicit fracture modeling. If the flow happens through both vugs and fractures, then random permeability distribution method is more representative. However; if the flow happens mainly through the fractures, then using explicit fracture modeling is more accurate.
- The simulation of heterogeneous coreflood experiment by explicit fracture model showed that by increasing fracture density, the same oil recovery can be achieved with a smaller degree of wettability alteration. Coreflood simulation results with a limited number of explicit fractures indicate that a substantial wettability alteration from mixed-wet to water-wet is required in order to increase oil recovery. However, with a greater number of explicit fractures, oil can be recovered with slight modification in the matrix rock wettability. Thus the interaction between heterogeneity and wettability is important.

Benchmark reservoir simulators for chemical features:

- Calibration of polymer and surfactant input tables in the commercial simulators against UTCHEM correlations leads to a reasonable agreement for different

chemical EOR simulations. Laboratory coreflood results were history matched using UTCHEM and CMG-STARS with very good agreement.

- Polymer models were compared between UTCHEM and CMG-STARS and also between UTCHEM and ECLIPSE. The results showed some differences because of different viscosity models. The effect of salinity and hardness in polymer model is not considered in either CMG-STARS or ECLIPSE.
- UTCHEM simulations illustrated that a reduction in polymer viscosity occurs as expected when adsorption and subsequent reduction in polymer concentration is modeled. However, CMG-STARS and ECLIPSE showed no considerable effect on polymer viscosity compared to the case without adsorption.
- A constant salinity Type I surfactant flood for a large field case was modeled using both UTCHEM and ECLIPSE and fairly close agreement were achieved. Tables for ECLIPSE were generated based on UTCHEM correlations. To model microemulsion viscosity in tabular format in ECLIPSE, we replaced water viscosity with microemulsion viscosity and the table values were obtained using viscosity correlation in UTCHEM.

8.2 RECOMMENDATIONS FOR FUTURE RESEARCH

In the following, the recommendations for future study in this area are presented:

- The PPG model in UTGEL simulator used in this dissertation was isothermal. However, several laboratory observations clearly illustrate the pronounced effect of elevated temperatures on the PPG swelling and resistance factor. Hence, it would be more realistic if the new models for PPG swelling with temperature effect is developed and implemented in the simulator rather than only dependent on salinity.
- The developed models for resistance factor and residual resistance factor consider the shear and salinity effect but it lacks the hardness effect. Therefore, it would be required to perform experiments with various divalent cations concentrations and modify the model to include hardness effect as well.
- The PPG rheology in UTGEL is modeled using Meter equation. However, more laboratory data are required to tune the INPUT parameters. Also, decrease in residual oil saturation using nano-sized PPG (nanogel) has not been entirely clear whether and how the IFT can be decreased due to nanogel which leads to reduction in residual oil saturation. More laboratory experiments including IFT measurement are required to better understand the mechanism. A simple linear model for residual oil saturation dependency on PPG concentration is implemented in the UTGEL simulator but definitely there is still room for modification on the model.
- In field applications of PPG for conformance control, injectivity is of great concern because injection rates influence the project economics considerably.

Therefore, it is essentially required to develop and implement a model to improve PPG injectivity calculations in reservoir simulations. The model should consider the effect of PPG rheology and grid size.

- The PPG model in UTGEL only considers the flow of PPG through porous media and assumes that there is no retained PPG in the wellbore. In other words, the flow of PPG inside the wellbore is not modeled. However, several field cases illustrate that there is always injectivity issue during PPG injection which can be an indication of PPG retention inside the wellbore. Hence, it would be more realistic if the flow of PPG in the wellbore is modeled as well and implemented in the simulator.
- In Chapter 6, we used the imbibition test results for a small and a large core to validate the predictability of the newly developed dimensionless number. However, we did not validate our developed scaling group for various sizes of coreflood experiments. Hence, it would be of more interest if the new developed dimensionless number is validated using coreflood experiments with different rock sizes.
- The new developed dimensionless number included IFT reduction factor but it lacks the wettability alteration effect. Hence, it would be of great interest if wettability effect is included and the coreflood experiments with different wettability conditions are used to validate the new scaling group with IFT reduction and wettability alteration effects.

Appendix A: Bulk Gels, Microgels, Static Imbibition Tests, and Fractured Coreflood Sample Input Files

A.1 Bulk Gel Field Case

The following is the input data file for bulk gel field scale simulation in UTGEL simulator. We used this case in Chapter 4 for modeling bulk gel in-situ generation in a heterogeneous field. In order to run this case for conformance control, KGOPT flag in input file should be set KGOPT = 1, 2 or 3 along with required input data for gel permeability reduction, adsorption, etc.

```
CC*************************************************************************************
********
CC                                                                                    *
CC     BRIEF DESCRIPTION OF DATA SET: UTGEL                                           *
CC                                                                                    *
CC*************************************************************************************
********
CC  XYZ AREA 7 spot
*
CC  Injection Details and other properties from DW's Input for coreflood C
*
CC
*
CC  LENGTH (FT) : 2100              PROCESS: Bulk Gel FLOOD CASE (0.3 PV CDG)
*
CC  THICKNESS (FT) : 37             INJ. RATE (FT3/DAY) :
*
CC  WIDTH (FT) : 2400               COORDINATES : CARTESIAN
*
CC  POROSITY : variable             PROD. RATE (FT3/DAY):
*
CC  GRID BLOCKS : 43x47x19          1BBL=5.615 cubic feet
*
CC  DATE : 06/15/2013               A1 Sand - original grid size
*
CC
*
CC*************************************************************************************
********
CC                                                                                    *
CC*************************************************************************************
********
```

```
CC                                                                                      *
CC    RESERVOIR DESCRIPTION                                                             *
CC                                                                                      *
CC*****************************************************************************************
********
CC
CC
*----RUNNO
Onshore Field
CC
CC
*----HEADER
S-1119_finer grids
Modified from CDG Flood case of Abdulmaki Mazen Ramzi, 2012
BUlkgel Flood Case (0.3 PV bulkgel)
CC
CC SIMULATION FLAGS
*---- IMODE IMES IDISPC IREACT ICOORD ITREAC ITC IENG
      1     2    3      0      1      0      0   0
CC
CC NUMBER OF GRID BLOCKS AND FLAG SPECIFIES CONSTANT OR VARIABLE GRID SIZE
*----NX   NY  NZ  IDXYZ  IUNIT
     43    47  19  2       0
CC Grid Properties Given By Chevron
CC CONSTANT GRID BLOCK SIZE IN X, Y, AND Z  (in ft)
*----DX
     43*75
CC Grid Properties Given By Chevron
CC  CONSTANT GRID BLOCK SIZE IN X, Y, AND Z  (in ft)
*----DY
     47*75
CC
CC Grid Properties Given By Chevron
*----DZ  (this is mean from NET from ecl2gocad) total thickness is about 68 ft
     19*2
CC
CC TOTAL NO. OF COMPONENTS, NO. OF TRACERS, NO. OF GEL COMPONENTS
*----N   NTW   NG
     14  0     6
CC
CC  All species must be present even for standard waterflood.
*---- species name
water
oil
surf. (no)
polymer
anion
calcium
alchol (no)
gas (no)
TRACER
ng1 (no)
ng2 (no)
Cr3+
Gel
H+
CC
CC FLAG INDICATING IF THE COMPONENT IS INCLUDED IN CALCULATIONS OR NOT
*----ICF(KC) FOR KC=1,N
      1  1  0  1  1  0  0  0  1   0  0  1  1  1
CC
CC*********************************************************************
CC                                                                     *
CC    OUTPUT OPTIONS                                                    *
```

```
CC                                                                      *
CC**********************************************************************
CC
CC ICUMTM=0==>TIME PRINTING;istop=1==>PV SPEC
CC FLAGS FOR PV OR DAYS
*----ICUMTM  ISTOP
     1       1
CC
CC FLAG INDICATING IF THE PROFILE OF KCTH COMPONENT SHOULD BE WRITTEN
*----IPRFLG(KC),KC=1,N
      1  1  0  1  1  0  0  0  1   0  0  1  1  1
CC
CC FLAG FOR PRES,SAT.,TOTAL CONC.,TRACER CONC.,CAP.,GEL, ALKALINE PROFILES
*----IPPRES IPSAT IPCTOT IPGEL IPTEMP
     1      1     1      0     0
CC  ICKL is phase conc.  (K is component and L is phase)
CC FLAG FOR WRITING SEVERAL PROPERTIES TO UNIT 6 (PROFIL)
*----ICKL IVIS IPER ICNM ICSE
     1    1    1    1    1
CC
CC FLAG FOR WRITING SEVERAL PROPERTIES TO UNIT 6 (PROFIL)
*----IADS  IVEL IRKF IPHSE
     1     0    1    1
CC
CC**********************************************************************
CC                                                                      *
CC    RESERVOIR PROPERTIES                                              *
CC                                                                      *
CC**********************************************************************
CC
CC
CC MAX. SIMULATION TIME
*---- TMAX
      7.3
CC
CC ROCK COMPRESSIBILITY (1/PSI), STAND. PRESSURE(PSIA)
*----COMPR      PSTAND
     0.000008   14.7
CC  Porosity Values For Each Grid Input Given Through Include Files
CC  FLAGS INDICATING CONSTANT OR VARIABLE POROSITY, X,Y,AND Z PERMEABILITY
*----IPOR1 IPERMX IPERMY IPERMZ  IMOD  ITRANZ  INTG
     4     4      4      4       0     0       0
CC Depth To The Top Layer Input Given Through Include Files
CC FLAG FOR CONSTANT OR VARIABLE DEPTH, PRESSURE, WATER SATURATION
*----IDEPTH  IPRESS  ISWI
     4       1       0
CC
CC  4/10/2009 - Chevron
*----PINIT    HINIT
     550.     1965.77185
CC  4/10/2009 - Chevron
CC WATER SATURATION
*----SWI
     0.2
CC formation water  (3000 ppm NaCl)
CC CONSTANT CHLORIDE AND CALCIUM CONCENTRATIONS (MEQ/ML)
*----C50       C60
     0.0513    0.0
CC
CC**********************************************************************
CC                                                                      *
CC PHYSICAL PROPERTY DATA                                               *
CC                                                                      *
CC**********************************************************************
```

```
CC
CC DW
CC OIL CONC. AT PLAIT POINT FOR TYPE II(+) AND TYPE II(-), CMC (do not change)
*---- EPSME
      0.0001
CC SLOPE AND INTERCEPT OF BINODAL CURVE AT ZERO, OPT., AND 2XOPT SALINITY
CC  DW'S INPUT FILE FOR CORE FLOOD C (SPE 113965)
*----HBNS70 HBNC70 HBNS71 HBNC71 HBNS72 HBNC72
     0.0    0.055  0      0.035  0.     0.055
CC SLOPE AND INTERCEPT OF BINODAL CURVE AT ZERO, OPT., AND 2XOPT SALINITY
CC FOR ALCOHOL 2
*----HBNS80 HBNC80 HBNS81 HBNC81 HBNS82 HBNC82
     0.     0.     0.     0.     0.     0.
CC DW'S INPUT FILE FOR CORE FLOOD C (SPE 113965)
CC LOWER AND UPPER EFFECTIVE SALINITY FOR ALCOHOL 1(7) AND ALCOHOL 2 (8)
*----CSEL7     CSEU7     CSEL8  CSEU8
     0.5       0.85      0.     0.
CC DW'S INPUT FILE FOR CORE FLOOD C (SPE 113965)
CC THE CSE SLOPE PARAMETER FOR CALCIUM AND ALCOHOL 1 AND ALCOHOL 2
*----BETA6  BETA7  BETA8
     0.0     0     0.0
CC DW'S INPUT FILE FOR CORE FLOOD C (SPE 113965)
CC FLAG FOR ALCOHOL PART. MODEL AND PARTITION COEFFICIENTS
*----IALC  OPSK7O  OPSK7S  OPSK8O  OPSK8S
     0     0.0      0      0.      0.
CC
CC NO. OF ITERATIONS, AND TOLERANCE
*----NALMAX   EPSALC
     20       .0001
CC DW'S INPUT FILE FOR CORE FLOOD C (SPE 113965)
CC ALCOHOL 1 PARTITIONING PARAMETERS IF IALC=1  (leave as is)
*----AKWC7   AKWS7  AKM7  AK7     PT7
     4.671    1.79   48   35.31  0.222
CC
CC ALCOHOL 2 PARTITIONING PARAMETERS IF IALC=1
*----AKWC8   AKWS8  AKM8  AK8     PT8
     0.      0.     0.    0.      0.
CC
CC  0 = Healy and Reed and 1 is Chun-Huh
*--- ift
     1
CC
CC INTERFACIAL TENSION PARAMETERS
*----CHUH  AHUH
     0.3   10.
CC
CC LOG10 OF OIL/WATER INTERFACIAL TENSION
*----XIFTW
     1.48
CC
CC CAPILLARY DESATURATION PARAMETERS FOR PHASE 1, 2, AND 3
*----ITRAP   T11        T22        T33
     2      2000.      75000.     365.
CC  UTCHEM9P9: new input data
CC relative perm. flag (0:imbibition corey,1:first drainage corey
*----iperm     IRTYPE
     0          0
CC RESIDUAL SATURATION FOR EACH PHASE INPUT GIVEN THROUGH INCLUDE FILES
CC FLAG FOR CONSTANT OR VARIABLE REL. PERM. PARAMETERS
*----ISRW  IPRW  IEW
     4      0    0
CC  CHEVRON - 04/10/2009
CC CONSTANT ENDPOINT REL. PERM. OF PHASES 1,2,AND 3 AT LOW CAPILLARY NO.
*----P1RW  P2RWZ P3RW
```

```
     .30  0.7  0.30
CC CHEVRON - 04/10/2009
CC CONSTANT REL. PERM. EXPONENT OF PHASES 1,2,AND 3 AT LOW CAPILLARY NO.
*----E1W   E2W  E3W
     2     2    2
CC
CC  RES. SATURATION OF PHASES 1,2,AND 3 AT HIGH CAPILLARY NO.
*----S1RC(=SWIR)  S2RC(=SORCHEM)  S3RC(SMER=SWIR)
     0.0001    0.0001   0.0001
CC
CC ENDPOINT REL. PERM. OF PHASES 1,2,AND 3 AT HIGH CAPILLARY NO.
*----P1RC P2RC P3RC
     1.    1.    1.
CC
CC REL. PERM. EXPONENT OF PHASES 1,2,AND 3 AT HIGH CAPILLARY NO.
*----E13CW  E23C E31C
     1    1    1
CC SPE 113965
CC WATER AND OIL VISCOSITY at reference temperature, RESERVOIR TEMPERATURE (leave zero)
*----VIS1   VIS2  TEMPV
     0.37    3.4     0.
CC DW'S INPUT FILE FOR CORE FLOOD C (SPE 113965)
CC MICROEMULSION VISCOSITY PARAMETERS
*----ALPHA1 ALPHA2  ALPHA3  ALPHA4  ALPHA5
       .1     2.5     0.1       0.1     0.1
CC DW'S INPUT FILE FOR CORE FLOOD C (SPE 113965)
CC PARAMETERS TO CALCULATE POLYMER VISCOSITY AT ZERO SHEAR RATE
*----AP1      AP2     AP3
    45        625     1000
CC  DW'S INPUT FILE FOR CORE FLOOD C (SPE 113965)
CC PARAMETER TO COMPUTE CSEP,MIN. CSEP, AND SLOPE OF LOG VIS. VS. LOG CSEP
*----BETAP CSE1  SSLOPE
     1.    .01   -0.377
CC  DW'S INPUT FILE FOR CORE FLOOD C (SPE 113965)
CC PARAMETER FOR SHEAR RATE DEPENDENCE OF POLYMER VISCOSITY (50% shear ~ 10 cP)
*----GAMMAC  GAMHF  POWN   IPMOD  ISHEAR   RWEFF  GAMHF2  IWREATH
      4       30    1.8     0        1       0.4   0.0    1
CC
CC WREATH CORRELATION PARAMETERS
*----WREATHM  WREATHB  WREATHN  WREATHT
     4.7      0.18     0.48     1.0
CC
CC FLAG FOR POLYMER (4) PARTITIONING, PERM. REDUCTION PARAMETERS
*----IPOLYM EPHI3 EPHI4   BRK    CRK     rkcut
     1      1.    1       100   0.045      10
CC
CC SPECIFIC WEIGHT FOR COMPONENTS 1,2,3,7,AND 8 , AND GRAVITY FLAG
*----DEN1  DEN2  DEN3 DEN7 DEN8 IDEN
     .433  .377  .433 .346  0.  2
CC
CC  FLAG FOR CHOICE OF UNITS ( 0:BOTTOMHOLE CONDITION , 1: STOCK TANK)
*-----ISTB
      1
CC
CC  FVF FOR PHASE 1,2,3
*-----(FVF(L),L=1,NPHAS)
      1    1.083    1
CC
CC COMPRESSIBILITY FOR VOL. OCCUPYING COMPONENTS 1,2,3,7,AND 8
*----COMPC(1)  COMPC(2)  COMPC(3)  COMPC(7)  COMPC(8)
     0.000003   0.00001        0.        0.        0.
CC
CC CONSTANT OR VARIABLE PC PARAM., WATER-WET OR OIL-WET PC CURVE FLAG
*----ICPC   IEPC  IOW
```

```
     0       0     0
CC
CC CAPILLARY PRESSURE PARAMETERS, CPC
*----CPC
     0.
CC
CC CAPILLARY PRESSURE PARAMETERS, EPC
*---- EPC
      2.
CC
CC MOLECULAR DIFFUSIVITY OF KCTH COMPONENT IN PHASE 1 (D(KC),KC=1,N)
*----D(1) D(2) D(3) D(4) D(5) D(6) D(7) D(8) D(9) D(10) D(1
     0.   0.   0.   0.    0.  0.  8*0.
CC
CC MOLECULAR DIFFUSIVITY OF KCTH COMPONENT IN PHASE 2 (D(KC),KC=1,N)
*----D(1) D(2) D(3) D(4) D(5) D(6) D(7) D(8) D(9)  D(10)  D(11)
     0.   0.   0.   0.   0.   0.  8*0.
CC
CC MOLECULAR DIFFUSIVITY OF KCTH COMPONENT IN PHASE 3 (D(KC),KC=1,N)
*----D(1) D(2) D(3) D(4) D(5) D(6) D(7) D(8) D(9) D(10)  D(11)
     0.   0.   0.   0.   0.   0.   8*0.
CC  Mojdeh
CC LONGITUDINAL AND TRANSVERSE DISPERSIVITY (ft) OF PHASE 1
*----ALPHAL(1)     ALPHAT(1)
     4             0.4
CC Mojdeh
CC LONGITUDINAL AND TRANSVERSE DISPERSIVITY OF PHASE 2
*----ALPHAL(2)     ALPHAT(2)
     4             0.4
CC Mojdeh
CC LONGITUDINAL AND TRANSVERSE DISPERSIVITY OF PHASE 3
*----ALPHAL(3)     ALPHAT(3)
     4            0.4
CC   Polymer (7 microg/g), surf. (0.3 mg/g)
CC SURFACTANT AND POLYMER ADSORPTION PARAMETERS
*----AD31  AD32  B3D    AD41   AD42  B4D      iadk   iads1   fads refk(mD)
     0.125     0.0  1000.  1   0.    100.       0       0     0   0.
CC
CC PARAMETERS FOR CATION EXCHANGE OF CLAY AND SURFACTANT MW (needed for cation exch)
*----QV      XKC   XKS  EQW
     0.0     0.0   0.0  429.
CC
CC PARAMETERS FOR GELATION KINETICS (THIS LINE ONLY IF IREACT = 1)
*---- KGOPT
      2
CC
CC
*---  AK1         AK2         SCR      X4       X13     X14     X16       WM4
      0.01     903.6E+9      0.25     2.6       0.     0.6     1.0      6.E+6
CC
CC PARAMETERS FOR GEL VISCOSITY (THIS LINE ONLY IF IREACT = 1)
*----  AG1      AG2      CRG     AGK       BGK
     0.0075    2.7E-5     5.     0.035    0.01
CC
CC PARAMETERS FOR GEL RETENTION, NA-H & NA-CR EXCHANGE, INIT. H+ CONC.
*---- A15D      B15D     ICREX    A14D     B14D     CRNAK     HNAK     C160
      1950       100.     1       0         0        1.57E+7   2.      .1258E-7
CC
CC*************************************************************************
CC                                                                        *
CC  WELL DATA                                                             *
CC                                                                        *
CC*************************************************************************
CC
```

```
CC
CC TOTAL NUMBER OF WELLS, WELL RADIUS FLAG, FLAG FOR TIME OR COURANT NO.
*----NWELL   IRO   ITIME  NWELR
      17      2      1     17
CC 4/10/2009
CC WELL ID,LOCATIONS,AND FLAG FOR SPECIFYING WELL TYPE, WELL RADIUS, SKIN
*----IDW  IW   JW   IFLAG    RW     SWELL  IDIR  IFIRST   ILAST    IPRF
     1   16     13     1     0.4     0      3     1        19       0
CC
CC WELL NAME
*---- WELNAM
S1_I1
CC Maximum allowable rate of 2500b/d= 44916.8 cubic feet per day
CC MAX. AND MIN. ALLOWABLE BOTTOMHOLE PRESSURE AND RATE
*----ICHEK   PWFMIN   PWFMAX  QTMIN   QTMAX
     0       300.0    1300.0  0.0     84219
CC
CC WELL ID,LOCATIONS,AND FLAG FOR SPECIFYING WELL TYPE, WELL RADIUS, SKIN
*----IDW  IW   JW   IFLAG    RW     SWELL  IDIR  IFIRST   ILAST    IPRF
      2   30   13  1        0.4    0      3      1       19        0
CC
CC WELL NAME
*---- WELNAM
S1_I2
CC
CC MAX. AND MIN. ALLOWABLE BOTTOMHOLE PRESSURE AND RATE
*----ICHEK   PWFMIN   PWFMAX  QTMIN   QTMAX
     0       300.0    1300.0  0.0     84219
CC
CC WELL ID,LOCATIONS,AND FLAG FOR SPECIFYING WELL TYPE, WELL RADIUS, SKIN
*----IDW  IW   JW   IFLAG    RW     SWELL  IDIR  IFIRST   ILAST    IPRF
     3   36   25  1       0.4    0      3      1       19        0
CC
CC WELL NAME
*---- WELNAM
S1_I3
CC
CC MAX. AND MIN. ALLOWABLE BOTTOMHOLE PRESSURE AND RATE
*----ICHEK   PWFMIN   PWFMAX  QTMIN   QTMAX
     0       300.0    1300.0  0.0     84219
CC
CC WELL ID,LOCATIONS,AND FLAG FOR SPECIFYING WELL TYPE, WELL RADIUS, SKIN
*----IDW  IW   JW   IFLAG    RW     SWELL  IDIR  IFIRST   ILAST    IPRF
     4   30   37    1      0.4    0      3      1       19        0
CC
CC WELL NAME
*---- WELNAM
S1_I4
CC
CC MAX. AND MIN. ALLOWABLE BOTTOMHOLE PRESSURE AND RATE
*----ICHEK   PWFMIN   PWFMAX  QTMIN   QTMAX
     0       300.0    1300.0  0.0     84219
CC
CC WELL ID,LOCATIONS,AND FLAG FOR SPECIFYING WELL TYPE, WELL RADIUS, SKIN
*----IDW  IW   JW   IFLAG    RW     SWELL  IDIR  IFIRST   ILAST    IPRF
     5   16    37     1     0.4    0      3      1      19        0
CC
CC WELL NAME
*---- WELNAM
S1_I5
CC
CC MAX. AND MIN. ALLOWABLE BOTTOMHOLE PRESSURE AND RATE
*----ICHEK   PWFMIN   PWFMAX  QTMIN   QTMAX
     0       300.0    1300.0  0.0     84219
```

```
CC
CC WELL ID,LOCATIONS,AND FLAG FOR SPECIFYING WELL TYPE, WELL RADIUS, SKIN
*----IDW  IW   JW   IFLAG    RW     SWELL  IDIR  IFIRST   ILAST    IPRF
     6   10   25    1     0.4     0      3      1       19         0
CC
CC WELL NAME
*---- WELNAM
S1_I6
CC
CC MAX. AND MIN. ALLOWABLE BOTTOMHOLE PRESSURE AND RATE
*----ICHEK   PWFMIN   PWFMAX  QTMIN   QTMAX
     0       300.0    1300.0  0.0     84219
CC
CC WELL ID,LOCATIONS,AND FLAG FOR SPECIFYING WELL TYPE, WELL RADIUS, SKIN
*----IDW  IW   JW   IFLAG    RW     SWELL  IDIR  IFIRST   ILAST    IPRF
      7   10     5     1     0.4     0      3      1       19         0
CC
CC WELL NAME
*---- WELNAM
S1_I7
CC
CC MAX. AND MIN. ALLOWABLE BOTTOMHOLE PRESSURE AND RATE
*----ICHEK   PWFMIN   PWFMAX  QTMIN   QTMAX
     0       300.0    1300.0  0.0     84219
CC
CC WELL ID,LOCATIONS,AND FLAG FOR SPECIFYING WELL TYPE, WELL RADIUS, SKIN
*----IDW  IW   JW   IFLAG    RW     SWELL  IDIR  IFIRST   ILAST    IPRF
     8   36    5     1     0.4       0      3      1       19      0
CC
CC WELL NAME
*---- WELNAM
S1_I8
CC
CC MAX. AND MIN. ALLOWABLE BOTTOMHOLE PRESSURE AND RATE
*----ICHEK   PWFMIN   PWFMAX  QTMIN   QTMAX
     0       300.0    1300.0  0.0     84219
CC
CC WELL ID,LOCATIONS,AND FLAG FOR SPECIFYING WELL TYPE, WELL RADIUS, SKIN
*----IDW  IW   JW   IFLAG    RW     SWELL  IDIR  IFIRST   ILAST    IPRF
     9   36  44     1     0.4     0      3      1       19            0
CC
CC WELL NAME
*---- WELNAM
S1_I9
CC
CC MAX. AND MIN. ALLOWABLE BOTTOMHOLE PRESSURE AND RATE
*----ICHEK   PWFMIN   PWFMAX  QTMIN   QTMAX
     0       300.0    1300.0  0.0     84219
CC
CC WELL ID,LOCATIONS,AND FLAG FOR SPECIFYING WELL TYPE, WELL RADIUS, SKIN
*----IDW  IW   JW   IFLAG    RW     SWELL  IDIR  IFIRST   ILAST    IPRF
     10   10    44     1     0.4     0      3      1       19     0
CC
CC WELL NAME
*---- WELNAM
S1_I10
CC
CC MAX. AND MIN. ALLOWABLE BOTTOMHOLE PRESSURE AND RATE
*----ICHEK   PWFMIN   PWFMAX  QTMIN   QTMAX
     0       300.0    1300.0  0.0     84219
CC
CC WELL ID,LOCATIONS,AND FLAG FOR SPECIFYING WELL TYPE, WELL RADIUS, SKIN
*----IDW  IW   JW   IFLAG    RW     SWELL  IDIR  IFIRST   ILAST    IPRF
     11  22   25    2      0.4    0      3      1      19     0
```

```
CC
CC WELL NAME
*---- WELNAM
S1_P1
CC   DW, max 10000 bbls/d
CC MAX. AND MIN. ALLOWABLE BOTTOMHOLE PRESSURE AND RATE
*----ICHEK   PWFMIN   PWFMAX  QTMIN   QTMAX
     0       300.0      1300.   0.0     -56146.0
CC
CC WELL ID,LOCATIONS,AND FLAG FOR SPECIFYING WELL TYPE, WELL RADIUS, SKIN
*----IDW  IW   JW   IFLAG    RW     SWELL  IDIR  IFIRST   ILAST    IPRF
     12  22   5     2       0.4    0      3      1       19      0
CC
CC WELL NAME
*---- WELNAM
S1_P2
CC
CC MAX. AND MIN. ALLOWABLE BOTTOMHOLE PRESSURE AND RATE
*----ICHEK   PWFMIN   PWFMAX  QTMIN   QTMAX
     0       300.0      1400.   0.0    -28073
CC
CC WELL ID,LOCATIONS,AND FLAG FOR SPECIFYING WELL TYPE, WELL RADIUS, SKIN
*----IDW  IW   JW   IFLAG    RW     SWELL  IDIR  IFIRST   ILAST    IPRF
     13  40   13     2       0.4    0      3      1       19     0
CC
CC WELL NAME
*---- WELNAM
S1_P3
CC
CC MAX. AND MIN. ALLOWABLE BOTTOMHOLE PRESSURE AND RATE
*----ICHEK   PWFMIN   PWFMAX  QTMIN   QTMAX
     0       300.0      1400.   0.0     -28073
CC
CC WELL ID,LOCATIONS,AND FLAG FOR SPECIFYING WELL TYPE, WELL RADIUS, SKIN
*----IDW  IW   JW   IFLAG    RW     SWELL  IDIR  IFIRST   ILAST    IPRF
     14  40   37    2      0.4    0      3      1       19      0
CC
CC WELL NAME
*---- WELNAM
S1_P4
CC
CC MAX. AND MIN. ALLOWABLE BOTTOMHOLE PRESSURE AND RATE
*----ICHEK   PWFMIN   PWFMAX  QTMIN   QTMAX
     0       300.0      1400.   0.0     -28073
CC
CC WELL ID,LOCATIONS,AND FLAG FOR SPECIFYING WELL TYPE, WELL RADIUS, SKIN
*----IDW  IW   JW   IFLAG    RW     SWELL  IDIR  IFIRST   ILAST    IPRF
     15  22   44    2      0.4    0      3      1       19        0
CC
CC WELL NAME
*---- WELNAM
S1_P5
CC
CC MAX. AND MIN. ALLOWABLE BOTTOMHOLE PRESSURE AND RATE
*----ICHEK   PWFMIN   PWFMAX  QTMIN   QTMAX
     0       300.0      1400.   0.0    -28073
CC
CC WELL ID,LOCATIONS,AND FLAG FOR SPECIFYING WELL TYPE, WELL RADIUS, SKIN
*----IDW  IW   JW   IFLAG    RW     SWELL  IDIR  IFIRST   ILAST    IPRF
     16  4    37    2       0.4    0      3      1       19      0
CC
CC WELL NAME
*---- WELNAM
S1_P6
```

```
CC
CC MAX. AND MIN. ALLOWABLE BOTTOMHOLE PRESSURE AND RATE
*----ICHEK   PWFMIN   PWFMAX  QTMIN   QTMAX
     0       300.0      1400.   0.0     -28073
CC
CC WELL ID,LOCATIONS,AND FLAG FOR SPECIFYING WELL TYPE, WELL RADIUS, SKIN
*----IDW  IW   JW   IFLAG    RW     SWELL  IDIR  IFIRST   ILAST    IPRF
     17   4   13     2       0.4    0      3      1      19         0
CC
CC WELL NAME
*---- WELNAM
S1_P7
CC
CC MAX. AND MIN. ALLOWABLE BOTTOMHOLE PRESSURE AND RATE
*----ICHEK   PWFMIN   PWFMAX  QTMIN   QTMAX
     0       300.0      1400.   0.0     -28073
CC
CC
*----ID   QI    C
     1  44916.8     1.    0.   0.    0.    0.05130  0.     2*0   4*0  2*0
     1    0.        0.    0.   0.    0.    0.       0.     6*0   2*0
     1    0.        0.    0.   0.    0.    0.       0.     6*0   2*0
CC
CC
*----ID   QI    C
     2   44916.8   1.    0.   0.    0.    0.05130   0.     2*0   4*0  2*0
     2    0.        0.    0.   0.    0.    0.        0.     6*0   2*0
     2    0.        0.    0.   0.    0.    0.        0.     6*0   2*0
CC
CC
*----ID   QI    C
     3  44916.8     1.    0.   0.    0.    0.05130 0.     2*0   4*0 2*0
     3    0.        0.    0.   0.    0.    0.      0.     6*0   2*0
     3    0.        0.    0.   0.    0.    0.      0.     6*0   2*0
CC
CC id,INJ. RATE AND INJ. COMP. FOR RATE CONS. WELLS FOR EACH PHASE(L=1,3)
*----id  QI(M,L)  C(M,KC,L) (need to keep 2nd and 3rd lines for oil and ME)
     4  44916.8     1.    0.   0.    0.    0.05130 0.     2*0   4*0  2*0
     4    0.        0.    0.   0.    0.    0.      0.     6*0   2*0
     4    0.        0.    0.   0.    0.    0.      0.     6*0   2*0
CC
CC
*----id  QI(M,L)  C(M,KC,L) (need to keep 2nd and 3rd lines for oil and ME)
     5  44916.8     1.    0.   0.    0.    0.05130 0.     2*0   4*0  2*0
     5    0.        0.    0.   0.    0.    0.      0.     6*0   2*0
     5    0.        0.    0.   0.    0.    0.      0.     6*0   2*0
CC
CC id,INJ. RATE AND INJ. COMP. FOR RATE CONS. WELLS FOR EACH PHASE(L=1,3)
*----id  QI(M,L)  C(M,KC,L) (need to keep 2nd and 3rd lines for oil and ME)
     6  44916.8     1.    0.   0.    0.    0.05130 0.     2*0  4*0 2*0
     6    0.        0.    0.   0.    0.    0.      0.     6*0   2*0
     6    0.        0.    0.   0.    0.    0.      0.     6*0   2*0
CC
CC id,INJ. RATE AND INJ. COMP. FOR RATE CONS. WELLS FOR EACH PHASE(L=1,3)
*----id  QI(M,L)  C(M,KC,L) (need to keep 2nd and 3rd lines for oil and ME)
     7  22458.4     1.    0.   0.    0.    0.05130 0.     2*0  4*0 2*0
     7    0.        0.    0.   0.    0.    0.      0.     6*0   2*0
     7    0.        0.    0.   0.    0.    0.      0.     6*0   2*0
CC
CC
*----id  QI(M,L)  C(M,KC,L) (need to keep 2nd and 3rd lines for oil and ME)
     8  22458.4     1.    0.   0.    0.    0.05130 0.     2*0  4*0 2*0
     8    0.        0.    0.   0.    0.    0.      0.     6*0   2*0
     8    0.        0.    0.   0.    0.    0.      0.     6*0   2*0
```

```
CC
CC id,INJ. RATE AND INJ. COMP. FOR RATE CONS. WELLS FOR EACH PHASE(L=1,3)
*----id  QI(M,L)  C(M,KC,L) (need to keep 2nd and 3rd lines for oil and ME)
     9  22458.4     1.    0.   0.    0.    0.05130 0.     2*0  4*0  2*0
     9    0.        0.    0.   0.    0.    0.      0.     6*0   2*0
     9    0.        0.    0.   0.    0.    0.      0.     6*0   2*0
CC
CC id,INJ. RATE AND INJ. COMP. FOR RATE CONS. WELLS FOR EACH PHASE(L=1,3)
*----id  QI(M,L)  C(M,KC,L) (need to keep 2nd and 3rd lines for oil and ME)
     10  22458.4     1.    0.   0.    0.    0.05130 0.     2*0  4*0  2*0
     10    0.        0.    0.   0.    0.    0.      0.     6*0   2*0
     10    0.        0.    0.   0.    0.    0.      0.     6*0   2*0
CC
CC   Pressure constrained producer
*----WELL ID   PWF
     11         300.0
CC
CC   Pressure constrained producer
*----WELL ID   PWF
     12         300.0
CC
CC   Pressure constrained producer
*----WELL ID   PWF
     13         300.0
CC
CC   Pressure constrained producer
*----WELL ID   PWF
     14         300.0
CC
CC   Pressure constrained producer
*----WELL ID   PWF
     15         300.0
CC
CC   Pressure constrained producer
*----WELL ID   PWF
     16         300.0
CC
CC   Pressure constrained producer
*----WELL ID   PWF
     17         300.0
CC
CC CUM. INJ. TIME , AND INTERVALS (PV OR DAY) FOR WRITING TO OUTPUT FILES (3.7.8)
*----TINJ      CUMPR1  CUMHI2  WRHPV(HIST) WRPRF(PLOT) RSTC
    5         4.9     4.9     0.2          0.5        4.9
CC
CC FOR IMES=2 ,THE INI. TIME STEP,CONC. TOLERANCE,MAX.,MIN. time steps
*----DT             DCLIM     CNMAX   CNMIN
     0.00001        0.001     0.2     0.01
CC
CC IRO, ITIME, NEW FLAGS FOR ALL THE WELLS
*---- IRO ITSTEP IFLAG
       2   1     10*1  7*2
CC
CC NUMBER OF WELLS CHANGES IN LOCATION OR SKIN OR PWF
*----NWEL1
     0
CC
CC NUMBER OF WELLS WITH RATE CHANGES, ID - SP FLOOD INTO 10 INJECTORS
*----NWEL2   ID
     10       1 2 3 4 5 6 7 8 9 10
CC
CC id,INJ. RATE AND INJ. COMP. FOR RATE CONS. WELLS FOR EACH PHASE(L=1,3)
*----id  QI(M,L)  C(M,KC,L) (need to keep 2nd and 3rd lines for oil and ME)
     1  14036.5     1.    0.   0.    0.5    0.7116  0  0  6*0  0.2E-4
```

```
     1    0.        0.    0.   0.    0.    0.      0.         6*0   2*0
     1    0.        0.    0.   0.    0.    0.      0.         6*0   2*0
CC
CC id,INJ. RATE AND INJ. COMP. FOR RATE CONS. WELLS FOR EACH PHASE(L=1,3)
*----id  QI(M,L)  C(M,KC,L) (need to keep 2nd and 3rd lines for oil and ME)
     2  14036.5     1.    0.   0.    0.5    0.7116  0  0  6*0  0.2E-4
     2    0.        0.    0.   0.    0.    0.      0.         6*0   2*0
     2    0.        0.    0.   0.    0.    0.      0.         6*0   2*0
CC
CC
*----id  QI(M,L)  C(M,KC,L) (need to keep 2nd and 3rd lines for oil and ME)
     3 14036.5     1.    0.   0.    0.5    0.7116  0  0  6*0  0.2E-4
     3    0.        0.    0.   0.    0.    0.      0.         6*0   2*0
     3    0.        0.    0.   0.    0.    0.      0.         6*0   2*0
CC
CC
*----id  QI(M,L)  C(M,KC,L) (need to keep 2nd and 3rd lines for oil and ME)
     4  14036.5     1.    0.   0.    0.5    0.7116  0  0  6*0  0.2E-4
     4    0.        0.     0.   0.    0.    0.      0.         6*0   2*0
     4    0.        0.     0.   0.    0.    0.      0.         6*0   2*0
CC
CC id,INJ. RATE AND INJ. COMP. FOR RATE CONS. WELLS FOR EACH PHASE(L=1,3)
*----id  QI(M,L)  C(M,KC,L) (need to keep 2nd and 3rd lines for oil and ME)
     5  14036.5     1.    0.   0.    0.5    0.7116  0  0  6*0  0.2E-4
     5    0.        0.    0.   0.    0.    0.      0.         6*0  2*0
     5    0.        0.    0.   0.    0.    0.      0.         6*0  2*0
CC
CC id,INJ. RATE AND INJ. COMP. FOR RATE CONS. WELLS FOR EACH PHASE(L=1,3)
*----id  QI(M,L)  C(M,KC,L) (need to keep 2nd and 3rd lines for oil and ME)
     6  14036.5     1.    0.   0.    0.5    0.7116  0  0  6*0  0.2E-4
     6    0.        0.    0.   0.    0.    0.      0.         6*0  2*0
     6    0.        0.    0.   0.    0.    0.      0.         6*0  2*0
CC
CC id,INJ. RATE AND INJ. COMP. FOR RATE CONS. WELLS FOR EACH PHASE(L=1,3)
*----id  QI(M,L)  C(M,KC,L) (need to keep 2nd and 3rd lines for oil and ME)
     7  7018.25     1.    0.   0.    0.5    0.7116  0  0  6*0  0.2E-4
     7    0.        0.    0.   0.    0.    0.      0.         6*0  2*0
     7    0.        0.    0.   0.    0.    0.      0.         6*0  2*0
CC
CC id,INJ. RATE AND INJ. COMP. FOR RATE CONS. WELLS FOR EACH PHASE(L=1,3)
*----id  QI(M,L)  C(M,KC,L) (need to keep 2nd and 3rd lines for oil and ME)
     8   7018.25     1.    0.   0.    0.5    0.7116  0  0  6*0  0.2E-4
     8    0.        0.    0.   0.    0.    0.      0.         6*0  2*0
     8    0.        0.    0.   0.    0.    0.      0.         6*0  2*0
CC
CC id,INJ. RATE AND INJ. COMP. FOR RATE CONS. WELLS FOR EACH PHASE(L=1,3)
*----id  QI(M,L)  C(M,KC,L) (need to keep 2nd and 3rd lines for oil and ME)
     9   7018.25     1.    0.   0.    0.5    0.7116  0  0  6*0  0.2E-4
     9    0.        0.    0.   0.    0.    0.      0.         6*0  2*0
     9    0.        0.    0.   0.    0.    0.      0.         6*0  2*0
CC
CC id,INJ. RATE AND INJ. COMP. FOR RATE CONS. WELLS FOR EACH PHASE(L=1,3)
*----id  QI(M,L)  C(M,KC,L) (need to keep 2nd and 3rd lines for oil and ME)
     10  7018.25     1.    0.   0.    0.5    0.7116  0  0  6*0  0.2E-4
     10    0.        0.    0.   0.    0.    0.      0.         6*0  2*0
     10    0.        0.    0.   0.    0.    0.      0.         6*0  2*0
CC
CC CUM. INJ. TIME , AND INTERVALS (PV OR DAY) FOR WRITING TO OUTPUT FILES (3.7.8)
*----TINJ    CUMPR1  CUMHI2 WRHPV(HIST) WRPRF(PLOT) RSTC
     5.3     0.01    0.1   0.01        0.1        0.05
CC CDG Inj.
CC FOR IMES=2 ,THE INI. TIME STEP,CONC. TOLERANCE,MAX.,MIN. time steps
*----DT             DCLIM     CNMAX   CNMIN
     0.00001       0.005     0.05   0.001
```

```
CC
CC IRO, ITIME, NEW FLAGS FOR ALL THE WELLS
*---- IRO ITIME IFLAG
       2   1     10*1  7*2
CC
CC NUMBER OF WELLS changes IN LOCATION OR SKIN OR PWF
*----NWEL1
      0
CC
CC NUMBER OF WELLS WITH RATE changes, id
*----NWEL2   Id
     10      1 2 3 4 5 6 7 8 9 10
CC
CC id,INJ. RATE AND INJ. COMP. FOR RATE CONS. WELLS FOR EACH PHASE(L=1,3)
*----id  QI(M,L)  C(M,KC,L) (need to keep 2nd and 3rd lines for oil and ME)
     1  14036.5     1.    0.   0.    0.0  0.0513   0.     0  7*0
     1    0.        0.    0.   0.    0.    0.      0.       6*0   2*0
     1    0.        0.    0.   0.    0.    0.      0.       6*0   2*0
CC
CC id,INJ. RATE AND INJ. COMP. FOR RATE CONS. WELLS FOR EACH PHASE(L=1,3)
*----id  QI(M,L)  C(M,KC,L) (need to keep 2nd and 3rd lines for oil and ME)
     2  14036.5     1.    0.   0.    0.0  0.0513   0.       0   7*0
     2    0.        0.    0.   0.    0.    0.      0.        6*0   2*0
     2    0.        0.    0.   0.    0.    0.      0.        6*0   2*0
CC
CC id,INJ. RATE AND INJ. COMP. FOR RATE CONS. WELLS FOR EACH PHASE(L=1,3)
*----id  QI(M,L)  C(M,KC,L) (need to keep 2nd and 3rd lines for oil and ME)
     3  14036.5     1.    0.   0.    0.0  0.0513   0.       0    7*0
     3    0.        0.    0.   0.    0.    0.      0.        6*0   2*0
     3    0.        0.    0.   0.    0.    0.      0.        6*0   2*0
CC
CC id,INJ. RATE AND INJ. COMP. FOR RATE CONS. WELLS FOR EACH PHASE(L=1,3)
*----id  QI(M,L)  C(M,KC,L) (need to keep 2nd and 3rd lines for oil and ME)
     4  14036.5     1.    0.   0.    0.0  0.0513   0.       0   7*0
     4    0.        0.    0.   0.    0.    0.      0.        6*0   2*0
     4    0.        0.    0.   0.    0.    0.      0.        6*0   2*0
CC
CC id,INJ. RATE AND INJ. COMP. FOR RATE CONS. WELLS FOR EACH PHASE(L=1,3)
*----id  QI(M,L)  C(M,KC,L) (need to keep 2nd and 3rd lines for oil and ME)
     5  14036.5    1.    0.   0.    0.0  0.0513   0.      0    7*0
     5    0.        0.    0.   0.    0.    0.      0.        6*0  2*0
     5    0.        0.    0.   0.    0.    0.      0.        6*0  2*0
CC
CC id,INJ. RATE AND INJ. COMP. FOR RATE CONS. WELLS FOR EACH PHASE(L=1,3)
*----id  QI(M,L)  C(M,KC,L) (need to keep 2nd and 3rd lines for oil and ME)
     6  14036.5     1.    0.   0.    0.0  0.0513   0.      0   7*0
     6    0.        0.    0.   0.    0.    0.      0.        6*0  2*0
     6    0.        0.    0.   0.    0.    0.      0.        6*0  2*0
CC
CC id,INJ. RATE AND INJ. COMP. FOR RATE CONS. WELLS FOR EACH PHASE(L=1,3)
*----id  QI(M,L)  C(M,KC,L) (need to keep 2nd and 3rd lines for oil and ME)
     7    7018.25        1.    0.   0.    0.0  0.0513   0.       0      7*0
     7    0.             0.    0.   0.    0.    0.      0.       6*0    2*0
     7    0.             0.    0.   0.    0.    0.      0.       6*0    2*0
CC
CC id,INJ. RATE AND INJ. COMP. FOR RATE CONS. WELLS FOR EACH PHASE(L=1,3)
*----id  QI(M,L)  C(M,KC,L) (need to keep 2nd and 3rd lines for oil and ME)
     8    7018.25        1.    0.   0.    0.0  0.0513   0.       0      7*0
     8    0.             0.    0.   0.    0.    0.      0.       6*0    2*0
     8    0.             0.    0.   0.    0.    0.      0.       6*0    2*0
CC
CC id,INJ. RATE AND INJ. COMP. FOR RATE CONS. WELLS FOR EACH PHASE(L=1,3)
*----id  QI(M,L)  C(M,KC,L) (need to keep 2nd and 3rd lines for oil and ME)
     9    7018.25        1.    0.   0.    0.0  0.0513   0.       0      7*0
```

```
     9    0.             0.    0.   0.    0.    0.      0.        6*0    2*0
     9    0.             0.    0.   0.    0.    0.      0.        6*0    2*0
CC
CC id,INJ. RATE AND INJ. COMP. FOR RATE CONS. WELLS FOR EACH PHASE(L=1,3)
*----id  QI(M,L)  C(M,KC,L) (need to keep 2nd and 3rd lines for oil and ME)
     10    7018.25        1.    0.   0.    0.0  0.0513   0.        0    7*0
     10    0.             0.    0.   0.    0.    0.      0.        6*0  2*0
     10    0.             0.    0.   0.    0.    0.      0.        6*0  2*0
CC post flush formation water injection
CC CUM. INJ. TIME , AND INTERVALS (PV OR DAY) FOR WRITING TO OUTPUT FILES (3.7.8)
*----TINJ      CUMPR1  CUMHI2 WRHPV(HIST) WRPRF(PLOT) RSTC
     7.3       0.5    0.5   0.01        0.3        0.3
CC
CC FOR IMES=2 ,THE INI. TIME STEP,CONC. TOLERANCE,MAX.,MIN. time steps
*----DT             DCLIM     CNMAX   CNMIN
     0.01     0.001     0.05   0.001
```

A.2 Preformed Particle Gel (PPG) Heterogeneous Case

The following is the input data file for PPG heterogeneous case simulation in UTGEL simulator. We used this case in Chapter 4 for modeling PPG injection to improve sweep efficiency. In order to run this case for conformance control, KGOPT flag in input file should be set KGOPT = 4 along with required input data for gel permeability reduction, adsorption, etc.

```
CC*************************************************************************
CC                                                                       *
CC    BRIEF DESCRIPTION OF DATA SET: UTGEL                               *
CC                                                                       *
CC*************************************************************************
CC                                                                       *
CC                                                                       *
CC                                                                       *
CC  LENGTH (FT) :    15         PROCESS :  PPG Flood                     *
CC  THICKNESS (FT) : 75          INJ. RATE (FT3/Day) : 1000              *
CC  WIDTH (FT) :     75         COORDINATES : CARTESIAN                  *
CC  POROSITY :       0.449                                               *
CC  GRID BLOCKS :    15x15x3                                             *
CC  DATE :           5/12/2014                                           *
CC                                                                       *
CC*************************************************************************
CC
CC*************************************************************************
CC                                                                       *
CC    RESERVOIR DESCRIPTION                                              *
CC                                                                       *
CC*************************************************************************
CC
CC
*----RUNNO
PPG Flood
CC
CC
*----HEADER
CC
CC
CC
CC
CC SIMULATION FLAGS
*---- IMODE IMES IDISPC IREACT  ICOORD ITREAC ITC  IENG  IFRAC
        1    2    3       1      1     0      0    0        0
CC
CC NUMBER OF GRID BLOCKS AND FLAG SPECIFIES CONSTANT OR VARIABLE GRID SIZE
*----NX     NY   NZ   IDXYZ  IUNIT
     15    15     3     0       0
CC
CC  VARIABLE GRID BLOCK SIZE IN X
*----DX           DY          DZ
```

```
     5             5          5
CC
CC TOTAL NO. OF COMPONENTS, NO. OF TRACERS, NO. OF GEL COMPONENTS
*----N   NTW  NG
     14   0   6
CC
CC
*---- SPNAME(I),I=1,N
WATER
OIL
none
Polymer
SALT
none
none
none
none
none
none
none
none
ppg
CC
CC FLAG INDICATING IF THE COMPONENT IS INCLUDED IN CALCULATIONS OR NOT
*----ICF(KC) FOR KC=1,N
   1  1  0  1  1 0  0 0 0 0 0 0 0 1
CC
CC*********************************************************************
CC                                                                    *
CC    OUTPUT OPTIONS                                                  *
CC                                                                    *
CC*********************************************************************
CC
CC
CC  FLAG FOR PV OR DAYS FOR OUTPUT AND STOP THE RUN
*----ICUMTM  ISTOP
       1     1
CC
CC FLAG INDICATING IF THE PROFILE OF KCTH COMPONENT SHOULD BE WRITTEN
*----IPRFLG(KC),KC=1,N
     1  1  0  1  0  0 0 0 0 0 0 0 0  1
CC
CC FLAG FOR PRES,SAT.,TOTAL CONC.,TRACER CONC.,CAP.,GEL, ALKALINE PROFILES
*----IPPRES IPSAT IPCTOT IPGEL  ITEMP
      1      1      1      1    0
CC
CC FLAG FOR WRITING SEVERAL PROPERTIES
*----ICKL IVIS IPER ICNM  ICSE
      0     1    0    0    0
CC
CC FLAG FOR WRITING SEVERAL PROPERTIES TO PROF
*----IADS  IVEL IRKF IPHSE
      0     0    1    0
CC
CC*********************************************************************
CC                                                                    *
CC    RESERVOIR PROPERTIES                                            *
CC                                                                    *
CC*********************************************************************
CC
CC
CC MAX. SIMULATION TIME (days)
*---- TMAX
       8
```

```
CC
CC ROCK COMPRESSIBILITY (1/PSI), STAND. PRESSURE(PSIA)
*----COMPR   PSTAND
      0.      1000.
CC
CC FLAGS INDICATING CONSTANT OR VARIABLE POROSITY, X,Y,AND Z PERMEABILITY
*----IPOR1 IPERMX IPERMY IPERMZ  IMOD  ITRNZ  INTG
       0      2     3      3      0     0      0
CC
CC VARIABLE POROSITY
*----PORC1
    0.449
CC
CC VARIABLE X-PERMEABILITY (MILIDARCY)
*----PERMX(1)
   49.64         16.90         12.86         10.42         24.70         30.72         24.83
87.69        46.57        48.10
   7.216        14.17        9.598        40.19        29.45
   80.87         161.0         53.35         15.22         23.79         45.04         16.51
4.752        62.27        14.75
   88.83        10.24         149.2        8.468        27.00
   86.91         69.28         4.031         6.676         4.078         4.325         121.7
14.42        159.5        100.5
   6.093        54.22        11.33        5.019        7.897
   29.30         145.0         24.13         6.707         28.84         67.72         27.13
46.47        24.67        12.59
   29.20        1.366        417.5        4.257        14.89
   9.176         445.6         29.55         10.29         7.042         28.49         25.29
69.15        81.28        5.466
   28.62        35.19        19.37        2.602        23.35
   43.83         15.54         3.498         16.49         2.995         27.50         46.67
9.712        30.01        19.18
   223.7        10.03        19.29        168.2        142.5
   43.87         18.89         14.78         5.925         41.38         69.22         30.13
93.57        23.80        20.75
   86.36        40.30        443.7        11.00        16.83
   10.40         8.309         20.72         114.1         5.967         106.0         68.38
27.09        7.612        22.65
   640.7        19.62        42.50        12.37        45.58
   3.695         26.11         19.85         49.33         16.18         102.2         59.25
52.65        12.30        4.979
   53.72        17.52        28.44        13.92        18.30
   34.36         141.9         20.15         1.864         20.51         16.53         1615.
31.24        38.83        40.64
   33.26        1.320        79.02        9.689        29.92
   26.96         21.39         192.8         2.459         325.8         1056.         92.94
7.551        13.71        3.163
   15.85        22.21        2.782        56.37        8.845
   153.7         5.535         24.75         9.826         37.09         2.538         86.96
12.88        32.42        4.696
   8.087        26.88        4.099        29.06        12.11
   22.84         39.10         4.885         8.536         16.21         12.92         15.41
29.53        25.24        41.16
   188.1        111.7        142.0        12.59        5.551
   19.40         1.492         44.38         57.28         63.36         26.15         7.403
9.518        56.07        119.8
   52.96        28.36        30.71        20.26        28.01
   6.980         8.380         10.45         53.09         25.92         137.9         8.817
25.39        10.14        12.50
   9.974        28.09        53.73        12.42        15.78
   1489.         506.9         385.9         312.6         741.1         921.7         745.0
2631.        1397.        1443.
   216.5        425.1        287.9        1206.        883.5
   2426.         4830.         1601.         456.7         713.8         1351.         495.4
```

142.6 1868. 442.6
2665. 307.1 4476. 254.0 809.9
2607. 2078. 120.9 200.3 122.3 129.8 3651.
432.5 4784. 3016.
182.8 1627. 339.8 150.6 236.9
879.0 4351. 724.0 201.2 865.2 2032. 813.8
1394. 740.1 377.7
876.1 40.99 0.1253E+05 127.7 446.8
275.3 0.1337E+05 886.6 308.6 211.3 854.6 758.8
2074. 2438. 164.0
858.7 1056. 581.2 78.06 700.6
1315. 466.2 105.0 494.6 89.86 825.0 1400.
291.4 900.4 575.4
6711. 301.0 578.6 5046. 4276.
1316. 566.7 443.5 177.8 1241. 2077. 903.8
2807. 714.0 622.6
2591. 1209. 0.1331E+05 330.0 504.9
311.9 249.3 621.5 3423. 179.0 3179. 2052.
812.6 228.3 679.4
0.1922E+05 588.7 1275. 371.2 1367.
110.8 783.4 595.4 1480. 485.3 3067. 1777.
1580. 368.9 149.4
1611. 525.7 853.3 417.6 548.9
1031. 4257. 604.6 55.91 615.2 495.9 0.4845E+05
937.1 1165. 1219.
997.7 39.61 2371. 290.7 897.6
808.9 641.8 5784. 73.77 9773. 0.3167E+05 2788.
226.5 411.2 94.90
475.5 666.2 83.46 1691. 265.4
4611. 166.0 742.5 294.8 1113. 76.15 2609.
386.4 972.7 140.9
242.6 806.5 123.0 871.8 363.3
685.3 1173. 146.6 256.1 486.2 387.7 462.4
886.0 757.3 1235.
5644. 3350. 4261. 377.6 166.5
582.1 44.76 1332. 1718. 1901. 784.4 222.1
285.6 1682. 3593.
1589. 850.8 921.4 607.7 840.3
209.4 251.4 313.6 1593. 777.6 4138. 264.5
761.7 304.3 374.9
299.2 842.7 1612. 372.6 473.3
49.64 16.90 12.86 10.42 24.70 30.72 24.83
87.69 46.57 48.10
7.216 14.17 9.598 40.19 29.45
80.87 161.0 53.35 15.22 23.79 45.04 16.51
4.752 62.27 14.75
88.83 10.24 149.2 8.468 27.00
86.91 69.28 4.031 6.676 4.078 4.325 121.7
14.42 159.5 100.5
6.093 54.22 11.33 5.019 7.897
29.30 145.0 24.13 6.707 28.84 67.72 27.13
46.47 24.67 12.59
29.20 1.366 417.5 4.257 14.89
9.176 445.6 29.55 10.29 7.042 28.49 25.29
69.15 81.28 5.466
28.62 35.19 19.37 2.602 23.35
43.83 15.54 3.498 16.49 2.995 27.50 46.67
9.712 30.01 19.18
223.7 10.03 19.29 168.2 142.5
43.87 18.89 14.78 5.925 41.38 69.22 30.13
93.57 23.80 20.75
86.36 40.30 443.7 11.00 16.83
10.40 8.309 20.72 114.1 5.967 106.0 68.38
27.09 7.612 22.65

```
   640.7       19.62       42.50       12.37       45.58
   3.695         26.11         19.85         49.33         16.18         102.2         59.25
52.65       12.30       4.979
   53.72       17.52       28.44       13.92       18.30
   34.36         141.9         20.15         1.864         20.51         16.53         1615.
31.24       38.83       40.64
   33.26       1.320       79.02       9.689       29.92
   26.96         21.39         192.8         2.459         325.8         1056.         92.94
7.551       13.71       3.163
   15.85       22.21       2.782       56.37       8.845
   153.7         5.535         24.75         9.826         37.09         2.538         86.96
12.88       32.42       4.696
   8.087       26.88       4.099       29.06       12.11
   22.84         39.10         4.885         8.536         16.21         12.92         15.41
29.53       25.24       41.16
   188.1       111.7       142.0       12.59       5.551
   19.40         1.492         44.38         57.28         63.36         26.15         7.403
9.518       56.07       119.8
   52.96       28.36       30.71       20.26       28.01
   6.980         8.380         10.45         53.09         25.92         137.9         8.817
25.39       10.14       12.50
   9.974       28.09       53.73       12.42       15.78
CC
CC VARIABLE Y-PERMEABILITY (MILIDARCY) FOR LAYER K = 1,NZ
*----PERMY(1)
     1
CC
CC VARIABLE Z-PERMEABILITY
*----PERMZC (MILIDARCY)
     0.1
CC
CC FLAG FOR CONSTANT OR VARIABLE DEPTH, PRESSURE, WATER SATURATION
*----IDEPTH  IPRESS  ISWI
      0        0       0
CC
CC VARIABLE DEPTH (FT)
*----D111
    0.0
CC
CC CONSTANT PRESSURE (PSIA)
*----PRESS1
     14.7
CC
CC CONSTANT INITIAL WATER SATURATION
*----SWI
     0.6
CC
CC CONSTANT CHLORIDE AND CALCIUM CONCENTRATIONS (MEQ/ML)
*----C50       C60
    0.134      0.0
CC
CC*********************************************************************
CC                                                                     *
CC    PHYSICAL PROPERTY DATA                                           *
CC                                                                     *
CC*********************************************************************
CC
CC
CC CMC
*----  EPSME
      .0001
CC SLOPE AND INTERCEPT OF BINODAL CURVE AT ZERO, OPT., AND 2XOPT SALINITY
CC FOR ALCOHOL 1
*----HBNS70 HBNC70 HBNS71 HBNC71 HBNS72 HBNC72
```

```
     0.     .030    0.   .030     0.0   .030
CC SLOPE AND INTERCEPT OF BINODAL CURVE AT ZERO, OPT., AND 2XOPT SALINITY
CC FOR ALCOHOL 2
*----HBNS80 HBNC80 HBNS81 HBNC81 HBNS82 HBNC82
     0.     0.     0.     0.     0.     0.
CC
CC LOWER AND UPPER EFFECTIVE SALINITY FOR ALCOHOL 1 AND ALCOHOL 2
*----CSEL7  CSEU7  CSEL8  CSEU8
     .65   .9   0.     0.
CC
CC THE CSE SLOPE PARAMETER FOR CALCIUM AND ALCOHOL 1 AND ALCOHOL 2
*----BETA6  BETA7  BETA8
     0.0    0.    0.
CC
CC FLAG FOR ALCOHOL PART. MODEL AND PARTITION COEFFICIENTS
*----IALC  OPSK7O  OPSK7S  OPSK8O  OPSK8S
     0     0.      0.      0.      0.
CC
CC NO. OF ITERATIONS, AND TOLERANCE
*----NALMAX   EPSALC
     20       .0001
CC
CC ALCOHOL 1 PARTITIONING PARAMETERS IF IALC=1
*----AKWC7   AKWS7  AKM7  AK7     PT7
     4.671   1.79   48.   35.31   .222
CC
CC ALCOHOL 2 PARTITIONING PARAMETERS IF IALC=1
*----AKWC8   AKWS8  AKM8  AK8     PT8
     0.      0.     0.    0.      0.
CC
CC
*--- IFT MODEL FLAG
      0
CC
CC INTERFACIAL TENSION PARAMETERS
*----G11  G12     G13   G21   G22    G23
     13.  -14.8   .007  13.2   -14.5  .010
CC
CC LOG10 OF OIL/WATER INTERFACIAL TENSION
*----XIFTW
     1.477
CC
CC CAPILLARY DESATURATION PARAMETERS FOR PHASE 1, 2, AND 3
*----ITRAP   T11        T22        T33
     0       1865.      28665.46      364.2
CC
CC REL. PERM. AND PC CURVES
*---- IPERM    IRTYPE
        0       0
CC
CC FLAG FOR CONSTANT OR VARIABLE REL. PERM. PARAMETERS
*----ISRW  IPRW  IEW
     0      0    0
CC
CC CONSTANT RES. SATURATION OF PHASES 1,2,AND 3 AT LOW CAPILLARY NO.
*----S1RWC  S2RWC  S3RWC
     .147    .25    .147
CC
CC CONSTANT ENDPOINT REL. PERM. OF PHASES 1,2,AND 3 AT LOW CAPILLARY NO.
*----P1RW      P2RW       P3RW
     .13771   0.7148      .13771
CC
CC CONSTANT REL. PERM. EXPONENT OF PHASES 1,2,AND 3 AT LOW CAPILLARY NO.
*----E1W         E2W     E3W
```

```
     4.1817   2.40475   4.1817
CC
CC WATER AND OIL VISCOSITY , RESERVOIR TEMPERATURE
*----VIS1   VIS2  TEMPV
      1      95     0.0
CC
CC VISCOSITY PARAMETERS
*----ALPHA1 ALPHA2  ALPHA3  ALPHA4  ALPHA5
     0.0     0.0      0.0   0.000865    4.153
CC
CC PARAMETERS TO CALCULATE POLYMER VISCOSITY AT ZERO SHEAR RATE
*----AP1      AP2     AP3
     1.5      50     2200
CC
CC PARAMETER TO COMPUTE CSEP,MIN. CSEP, AND SLOPE OF LOG VIS. VS. LOG CSEP
*----BETAP CSE1  SLOPE
     1     .01   .0
CC
CC PARAMETER FOR SHEAR RATE DEPENDENCE OF POLYMER VISCOSITY
*----GAMMAC       GAMHF      POWN    IPMOD   ishear  rweff   GAMHF2  iwreath
       4         19051.7      1.6     0       0       0.25    0        0
CC
CC FLAG FOR POLYMER PARTITIONING, PERM. REDUCTION PARAMETERS
*----IPOLYM EPHI3 EPHI4     BRK      CRK    RKCUT
     1      1.    1         100.     0.13    10
CC
CC SPECIFIC WEIGHT FOR COMPONENTS 1,2,3,7,AND 8 , AND GRAVITY FLAG
*----DEN1    DEN2     DEN3     DEN7     DEN8  IDEN
     62.899  49.857  62.399   49.824      0     2
CC
CC  FLAG FOR CHOICE OF UNITS ( 0:BOTTOMHOLE CONDITION , 1: STOCK TANK)
*-----ISTB
      0
CC
CC COMPRESSIBILITY FOR VOL. OCCUPYING COMPONENTS 1,2,3,7,AND 8
*----COMPC(1)      COMPC(2)     COMPC(3)  COMPC(7)  COMPC(8)
     0.00264E-03  0.005E-3         0         0         0
CC
CC CONSTANT OR VARIABLE PC PARAM., WATER-WET OR OIL-WET PC CURVE FLAG
*----ICPC   IEPC  IOW
     0       0   0
CC
CC CAPILLARY PRESSURE PARAMETERS, CPC
*----CPC
   0.
CC
CC CAPILLARY PRESSURE PARAMETERS, EPC
*---- EPC
      0.
CC
CC MOLECULAR DIFFUSIVITY OF KCTH COMPONENT IN PHASE 1 (D(KC),KC=1,N)
*----D(1) D(2) D(3) D(4) D(5) D(6)
     0.   0.   0.   0.   0.   0.  0.0  0.0  0.0  0.0  0.0  0.0  0.0 0.0
CC
CC MOLECULAR DIFFUSIVITY OF KCTH COMPONENT IN PHASE 2 (D(KC),KC=1,N)
*----D(1) D(2) D(3) D(4) D(5) D(6)
     0.   0.   0.   0.   0.   0.  0.0  0.0  0.0  0.0  0.0  0.0 0.0 0.0
CC
CC MOLECULAR DIFFUSIVITY OF KCTH COMPONENT IN PHASE 3 (D(KC),KC=1,N)
*----D(1) D(2) D(3) D(4) D(5) D(6)
     0.   0.   0.   0.   0.   0.  0.0  0.0  0.0  0.0  0.0  0.0 0.0  0.0
CC
CC LONGITUDINAL AND TRANSVERSE DISPERSIVITY OF PHASE 1
*----ALPHAL(1)     ALPHAT(1)
```

```
     0.0            0.0
CC
CC LONGITUDINAL AND TRANSVERSE DISPERSIVITY OF PHASE 2
*----ALPHAL(2)     ALPHAT(2)
     0.0            0.0
CC
CC LONGITUDINAL AND TRANSVERSE DISPERSIVITY OF PHASE 3
*----ALPHAL(3)     ALPHAT(3)
    0.0            0.0
C
CC SURFACTANT AND POLYMER ADSORPTION PARAMETERS
*----AD31     AD32  B3D    AD41   AD42  B4D  IADK, IADS1, FADS refk
     0.        .0  1000.  0.672   0.0  1      0      0      0   0
CC
CC PARAMETERS FOR CATION EXCHANGE OF CLAY AND SURFACTANT
*----QV     XKC   XKS  EQW
      0     0.    0.   804
cc
cc
*---  KGOPT
      4
CC
CC
* -- IRKPPG         RKCUTPPG             DPPG          APPGS         PPGNS         DCRICWS
TOLPPGIN     IRF

      2             100000000           0.0001268       28.68        -0.296          0.045
50          1
CC
CC
* --  APPGFR         PPGNFR        APPGRFR        PPGNRFR      CSEP
       450.340       -0.664        250.340       -0.464      0.561
cc
cc
*---  ADPPGA         ADPPGB        RESRKFAC     TOLPPGRK
       0.0            0.0            8.5          100
CC
CC
* ---- APPG1       APPG2     GAMCPG     GAMHFPG     POWNPG    ISROPPG    PPGKinetics
        0.1         0.4        0.0        0.0        0.0          0            0
CC
CC*********************************************************************
CC                                                                     *
CC    WELL DATA                                                        *
CC                                                                     *
CC*********************************************************************
CC
CC
CC TOTAL NUMBER OF WELLS, WELL RADIUS FLAG, FLAG FOR TIME OR COURANT NO.
*----NWELL   IRO   ITIME  NWREL
      2      2      1      2
CC
CC WELL ID,LOCATIONS,AND FLAG FOR SPECIFYING WELL TYPE, WELL RADIUS, SKIN
*----IDW   IW    JW    IFLAG    RW     SWELL  IDIR   IFIRST  ILAST  IPRF
      1    1     1      1       .5     0.      3      1        3    0
CC
CC WELL NAME
*---- WELNAM
INJECTOR
CC
CC ICHEK MAX. AND MIN. ALLOWABLE BOTTOMHOLE PRESSURE AND RATE
*----ICHEK   PWFMIN   PWFMAX    QTMIN    QTMAX
      0      0.0       5801.6    0.0     5615.
CC
```

```
CC WELL ID, LOCATION, AND FLAG FOR SPECIFYING WELL TYPE, WELL RADIUS, SKIN
*----IDW  IW   JW   IFLAG    RW     SWELL  IDIR  IFIRST   ILAST    IPRF
     2    15   15   2       .5       0.     3     1         3       0
CC
CC WELL NAME
*---- WELNAM
PRODUCER
CC
CC MAX. AND MIN. ALLOWABLE BOTTOMHOLE PRESSURE AND RATE
*----ICHEK  PWFMIN   PWFMAX  QTMIN   QTMAX
      0     0.0      5000.   0.0     50000.
CC
CC ID,INJ. RATE AND INJ. COMP. FOR RATE CONS. WELLS FOR EACH PHASE (L=1,3)
*----ID  QI(M,L)  C(M,KC,L)
     1    1000     1.   0.  0.     0.   0.134    0.    0.    0.    0.   0.   0.   0.   0.
0.
     1     0.      0.   0.  0.     0.   0.       0.    0.    0.    0.   0.   0.   0.   0.
0.
     1     0.      0.   0.  0.     0.   0.       0.    0.    0.    0.   0.   0.   0.   0.
0.
CC
CC ID, BOTTOM HOLE PRESSURE FOR PRESSURE CONSTRAINT WELL (IFLAG=2 OR 3)
*----ID   PWF
     2    14.7
CC
CC CUM. INJ. TIME , AND INTERVALS (PV OR DAY) FOR WRITING TO OUTPUT FILES
*----TINJ    CUMPR1   CUMHI1     WRHPV   WRPRF      RSTC
     3         1       1          0.01     1         10
CC
CC FOR IMES=2 ,THE INI. TIME STEP,CONC. TOLERANCE,MAX.,MIN. COURANT NO.
*----DT      DCLIM      CNMAX   CNMIN
     0.01    0.01       0.1     0.01
CC-----------------------------------------------------Gel flood---------------------------
CC IRO, ITIME, NEW FLAGS FOR ALL THE WELLS
*---- IRO ITIME IFLAG
       2   1     1  2
CC
CC NUMBER OF WELLS CHANGES IN LOCATION OR SKIN OR PWF
*----NWEL1
      0
CC
CC NUMBER OF WELLS WITH RATE CHANGES, ID
*----NWEL1   ID
     1        1
CC
CC ID,INJ. RATE AND INJ. COMP. FOR RATE CONS. WELLS FOR EACH PHASE (L=1,3)
*----ID  QI(M,L)  C(M,KC,L)
     1   1000       1.0    0.   0.     0.    0.134    0.    0.   0.   0.    0.   0.   0.
0.  2000.
     1    0.        0.     0.   0.     0.    0.       0.    0.   0.   0.    0.   0.   0.
0.  0.
     1    0.        0.     0.   0.     0.    0.       0.    0    0.   0.    0.   0.   0.
0.  0.
CC
CC CUM. INJ. TIME , AND INTERVALS (PV) FOR WRITING TO OUTPUT FILES
*----TINJ   CUMPR1  CUMHI1(PROFIL) WRHPV(HIST) WRPRF(PLOT) RSTC
      5       1       1              0.01        1         10
CC
CC FOR IMES=2 ,THE INI. TIME STEP,CONC. TOLERANCE,MAX.,MIN. COURANT NO.
*----DT        DCLIM       dtMAX      dtMIN
     0.01      0.01        0.1        0.01
CC34567890---------2---------3---------4---------5---------6---------7---------8
CC IRO, ITIME, NEW FLAGS FOR ALL THE WELLS ( WATER INJ.)
*---- IRO ITIME IFLAG
```

```
       2   1     1  2
CC
CC NUMBER OF WELLS CHANGES IN LOCATION OR SKIN OR PWF
*----NWEL1
     0
CC
CC NUMBER OF WELLS WITH RATE CHANGES, ID
*----NWEL1   ID
     1        1
CC
CC ID,INJ. RATE AND INJ. COMP. FOR RATE CONS. WELLS FOR EACH PHASE (L=1,3)
*----ID  QI(M,L)  C(M,KC,L)
     1   1000        1.0    0.   0.      0.   0.134       0.      0.     0.     0.       0.
0.    0.   0.    0.
     1    0.         0.     0.   0.      0.   0.          0.      0.     0.     0.       0.
0.    0.   0.    0.
     1    0.         0.     0.   0.      0.   0.          0.      0.     0.     0.       0.
0.    0.   0.    0.
CC
CC CUM. INJ. TIME , AND INTERVALS (PV) FOR WRITING TO OUTPUT FILES
*----TINJ   CUMPR1  CUMHI1(PROFIL)  WRHPV(HIST) WRPRF(PLOT) RSTC
       8      1       1               0.01        1         10
CC
CC FOR IMES=2 ,THE INI. TIME STEP,CONC. TOLERANCE,MAX.,MIN. COURANT NO.
*----DT        DCLIM     CNMAX   CNMIN


     0.01      0.01       0.1     0.01
```

A.3 Thermally Active Polymers (TAP) Heterogeneous Case

The following is the input data file for TAP heterogeneous case simulation in UTGEL simulator. We used this case in Chapter 5 for modeling TAP injection to block thief zones and improve sweep efficiency. In order to run this case for conformance control, KGOPT flag in input file should be set KGOPT = 6 along with required input data for gel permeability reduction, adsorption, etc.

```
CC*************************************************************************
CC                                                                       *
CC              BRIEF DESCRIPTION OF DATA SET                            *
CC                                                                       *
CC*************************************************************************
CC                                                                       *
CC                                                                       *
CC                                                                       *
CC  LENGTH (FT) :      75           PROCESS :  TAP Flood                 *
CC  THICKNESS (FT) :   75           INJ. Rate (Ft3/Day) :  842           *
CC  WIDTH (FT) :       15         COORDINATES : CARTESIAN                 *
CC  POROSITY :        0.449                                              *
CC  GRID BLOCKS :   15x15x3                                              *
CC  DATE :   10/12/2014                                                  *
CC                                                                       *
CC*************************************************************************
CC
CC*************************************************************************
CC                                                                       *
CC    RESERVOIR DESCRIPTION                                              *
CC                                                                       *
CC*************************************************************************
CC
CC
*----RUNNO
TAP Test Case
CC
CC
*----HEADER
CC
CC
CC
CC
CC SIMULATION FLAGS
*---- IMODE IMES IDISPC IREACT  ICOORD ITREAC ITC  IENG
        1    2     3       0      1     0      0    1    0
CC
CC NUMBER OF GRID BLOCKS AND FLAG SPECIFIES CONSTANT OR VARIABLE GRID SIZE
*----NX     NY    NZ  IDXYZ  IUNIT
     15     15    3     0      0
CC
CC  CONSTANT GRID BLOCK SIZE IN X, Y, Z direction
```

```
*----    DX           DY          DZ
         5           5           5
CC
CC TOTAL NO. OF COMPONENTS, NO. OF TRACERS, NO. OF GEL COMPONENTS
*----N   NTW  NG
     15   0   7
CC
CC
*---- SPNAME(I),I=1,N
WATER
OIL
none
POLYMER
SALT
none
none
none
none
none
none
none
none
BW
CL
CC
CC FLAG INDICATING IF THE COMPONENT IS INCLUDED IN CALCULATIONS OR NOT
*----ICF(KC) FOR KC=1,N
   1  1  0  1  1 1  0 0 0 0 0 0 0 1 0
CC
CC*************************************************************************
CC                                                                       *
CC    OUTPUT OPTIONS                                                     *
CC                                                                       *
CC*************************************************************************
CC
CC
CC  FLAG FOR PV OR DAYS FOR OUTPUT AND STOP THE RUN
*----ICUMTM  ISTOP
       0      0
CC
CC FLAG INDICATING IF THE PROFILE OF KCTH COMPONENT SHOULD BE WRITTEN
*----IPRFLG(KC),KC=1,N
     1  1  0  1 1  0  0 0 0 0 0 0 1  1 1
CC
CC FLAG FOR PRES,SAT.,TOTAL CONC.,TRACER CONC.,CAP.,GEL, ALKALINE PROFILES
*----IPPRES IPSAT IPCTOT IPGEL  ITEMP
      1      1      1      1    1
CC
CC FLAG FOR WRITING SEVERAL PROPERTIES
*----ICKL IVIS IPER ICNM  ICSE
      0     1    0    0    0
CC
CC FLAG FOR WRITING SEVERAL PROPERTIES TO PROF
*----IADS  IVEL IRKF IPHSE
      1     0    1    0
CC
CC*************************************************************************
CC                                                                       *
CC    RESERVOIR PROPERTIES                                               *
CC                                                                       *
CC*************************************************************************
CC
CC
CC MAX. SIMULATION TIME (PVs)
```

```
*---- TMAX
      100
CC
CC ROCK COMPRESSIBILITY (1/PSI), STAND. PRESSURE(PSIA)
*----COMPR    PSTAND
    0     0
CC
CC FLAGS INDICATING CONSTANT OR VARIABLE POROSITY, X,Y,AND Z PERMEABILITY
*----IPOR1 IPERMX IPERMY IPERMZ  IMOD  ITRNZ  INTG
       0      2     3      3      0     0      0
CC
CC VARIABLE POROSITY
*----PORC1
     0.449
CC
CC VARIABLE X-PERMEABILITY (MILIDARCY)
*----PERMX(1)
   49.64       16.90       12.86       10.42       24.70       30.72       24.83
87.69       46.57       48.10
   7.216       14.17       9.598       40.19       29.45
   80.87       161.0       53.35       15.22       23.79       45.04       16.51
4.752       62.27       14.75
   88.83       10.24       149.2       8.468       27.00
   86.91       69.28       4.031       6.676       4.078       4.325       121.7
14.42       159.5       100.5
   6.093       54.22       11.33       5.019       7.897
   29.30       145.0       24.13       6.707       28.84       67.72       27.13
46.47       24.67       12.59
   29.20       1.366       417.5       4.257       14.89
   9.176       445.6       29.55       10.29       7.042       28.49       25.29
69.15       81.28       5.466
   28.62       35.19       19.37       2.602       23.35
   43.83       15.54       3.498       16.49       2.995       27.50       46.67
9.712       30.01       19.18
   223.7       10.03       19.29       168.2       142.5
   43.87       18.89       14.78       5.925       41.38       69.22       30.13
93.57       23.80       20.75
   86.36       40.30       443.7       11.00       16.83
   10.40       8.309       20.72       114.1       5.967       106.0       68.38
27.09       7.612       22.65
   640.7       19.62       42.50       12.37       45.58
   3.695       26.11       19.85       49.33       16.18       102.2       59.25
52.65       12.30       4.979
   53.72       17.52       28.44       13.92       18.30
   34.36       141.9       20.15       1.864       20.51       16.53       1615.
31.24       38.83       40.64
   33.26       1.320       79.02       9.689       29.92
   26.96       21.39       192.8       2.459       325.8       1056.       92.94
7.551       13.71       3.163
   15.85       22.21       2.782       56.37       8.845
   153.7       5.535       24.75       9.826       37.09       2.538       86.96
12.88       32.42       4.696
   8.087       26.88       4.099       29.06       12.11
   22.84       39.10       4.885       8.536       16.21       12.92       15.41
29.53       25.24       41.16
   188.1       111.7       142.0       12.59       5.551
   19.40       1.492       44.38       57.28       63.36       26.15       7.403
9.518       56.07       119.8
   52.96       28.36       30.71       20.26       28.01
   6.980       8.380       10.45       53.09       25.92       137.9       8.817
25.39       10.14       12.50
   9.974       28.09       53.73       12.42       15.78
   1489.       506.9       385.9       312.6       741.1       921.7       745.0
2631.       1397.       1443.
```

```
   216.5       425.1       287.9       1206.       883.5
   2426.       4830.       1601.       456.7       713.8       1351.       495.4
142.6       1868.       442.6
   2665.       307.1       4476.       254.0       809.9
   2607.       2078.       120.9       200.3       122.3       129.8       3651.
432.5       4784.       3016.
   182.8       1627.       339.8       150.6       236.9
   879.0       4351.       724.0       201.2       865.2       2032.       813.8
1394.       740.1       377.7
   876.1       40.99     0.1253E+05    127.7       446.8
   275.3     0.1337E+05    886.6       308.6       211.3       854.6       758.8
2074.       2438.       164.0
   858.7       1056.       581.2       78.06       700.6
   1315.       466.2       105.0       494.6       89.86       825.0       1400.
291.4       900.4       575.4
   6711.       301.0       578.6       5046.       4276.
   1316.       566.7       443.5       177.8       1241.       2077.       903.8
2807.       714.0       622.6
   2591.       1209.     0.1331E+05    330.0       504.9
   311.9       249.3       621.5       3423.       179.0       3179.       2052.
812.6       228.3       679.4
  0.1922E+05   588.7       1275.       371.2       1367.
   110.8       783.4       595.4       1480.       485.3       3067.       1777.
1580.       368.9       149.4
   1611.       525.7       853.3       417.6       548.9
   1031.       4257.       604.6       55.91       615.2       495.9     0.4845E+05
937.1       1165.       1219.
   997.7       39.61       2371.       290.7       897.6
   808.9       641.8       5784.       73.77       9773.     0.3167E+05    2788.
226.5       411.2       94.90
   475.5       666.2       83.46       1691.       265.4
   4611.       166.0       742.5       294.8       1113.       76.15       2609.
386.4       972.7       140.9
   242.6       806.5       123.0       871.8       363.3
   685.3       1173.       146.6       256.1       486.2       387.7       462.4
886.0       757.3       1235.
   5644.       3350.       4261.       377.6       166.5
   582.1       44.76       1332.       1718.       1901.       784.4       222.1
285.6       1682.       3593.
   1589.       850.8       921.4       607.7       840.3
   209.4       251.4       313.6       1593.       777.6       4138.       264.5
761.7       304.3       374.9
   299.2       842.7       1612.       372.6       473.3
   49.64       16.90       12.86       10.42       24.70       30.72       24.83
87.69       46.57       48.10
   7.216       14.17       9.598       40.19       29.45
   80.87       161.0       53.35       15.22       23.79       45.04       16.51
4.752       62.27       14.75
   88.83       10.24       149.2       8.468       27.00
   86.91       69.28       4.031       6.676       4.078       4.325       121.7
14.42       159.5       100.5
   6.093       54.22       11.33       5.019       7.897
   29.30       145.0       24.13       6.707       28.84       67.72       27.13
46.47       24.67       12.59
   29.20       1.366       417.5       4.257       14.89
   9.176       445.6       29.55       10.29       7.042       28.49       25.29
69.15       81.28       5.466
   28.62       35.19       19.37       2.602       23.35
   43.83       15.54       3.498       16.49       2.995       27.50       46.67
9.712       30.01       19.18
   223.7       10.03       19.29       168.2       142.5
   43.87       18.89       14.78       5.925       41.38       69.22       30.13
93.57       23.80       20.75
   86.36       40.30       443.7       11.00       16.83
```

```
   10.40       8.309       20.72       114.1       5.967       106.0       68.38
27.09       7.612       22.65
   640.7       19.62       42.50       12.37       45.58
   3.695       26.11       19.85       49.33       16.18       102.2       59.25
52.65       12.30       4.979
   53.72       17.52       28.44       13.92       18.30
   34.36       141.9       20.15       1.864       20.51       16.53       1615.
31.24       38.83       40.64
   33.26       1.320       79.02       9.689       29.92
   26.96       21.39       192.8       2.459       325.8       1056.       92.94
7.551       13.71       3.163
   15.85       22.21       2.782       56.37       8.845
   153.7       5.535       24.75       9.826       37.09       2.538       86.96
12.88       32.42       4.696
   8.087       26.88       4.099       29.06       12.11
   22.84       39.10       4.885       8.536       16.21       12.92       15.41
29.53       25.24       41.16
   188.1       111.7       142.0       12.59       5.551
   19.40       1.492       44.38       57.28       63.36       26.15       7.403
9.518       56.07       119.8
   52.96       28.36       30.71       20.26       28.01
   6.980       8.380       10.45       53.09       25.92       137.9       8.817
25.39       10.14       12.50
   9.974       28.09       53.73       12.42       15.78
CC
CC VARIABLE Y-PERMEABILITY (MILIDARCY) FOR LAYER K = 1,NZ
*----PERMY(1)
     1.0
CC
CC VARIABLE Z-PERMEABILITY
*----PERMZC (MILIDARCY)
     0.1
CC
CC FLAG FOR CONSTANT OR VARIABLE DEPTH, PRESSURE, WATER SATURATION
*----IDEPTH  IPRESS  ISWI
      0        0       0
CC
CC VARIABLE DEPTH (FT)
*----D111
      0.0
CC
CC CONSTANT PRESSURE (PSIA)
*----PRESS1
     2000
CC
CC CONSTANT INITIAL WATER SATURATION
*----SWI
     0.25
CC
CC CONSTANT CHLORIDE AND CALCIUM CONCENTRATIONS (MEQ/ML)
*----C50         C60
     0.134       0.0
CC
CC*********************************************************************
CC                                                                     *
CC    PHYSICAL PROPERTY DATA                                           *
CC                                                                     *
CC*********************************************************************
CC
CC
CC CMC
*----  EPSME
      .0001
CC SLOPE AND INTERCEPT OF BINODAL CURVE AT ZERO, OPT., AND 2XOPT SALINITY
```

```
CC FOR ALCOHOL 1
*----HBNS70 HBNC70 HBNS71 HBNC71 HBNS72 HBNC72
     0.     .030    0.   .030     0.0   .030
CC
CC Slope of Height of Binodal Curve vs Temperature
*---- hbnt0     hbnt1     hbnt2     cset
        0          0          0         0
CC SLOPE AND INTERCEPT OF BINODAL CURVE AT ZERO, OPT., AND 2XOPT SALINITY
CC FOR ALCOHOL 2
*----HBNS80 HBNC80 HBNS81 HBNC81 HBNS82 HBNC82
     0.     0.     0.     0.     0.     0.
CC
CC LOWER AND UPPER EFFECTIVE SALINITY FOR ALCOHOL 1 AND ALCOHOL 2
*----CSEL7  CSEU7  CSEL8  CSEU8
     .65   .9   0.     0.
CC
CC THE CSE SLOPE PARAMETER FOR CALCIUM AND ALCOHOL 1 AND ALCOHOL 2
*----BETA6  BETA7  BETA8
     0.0    0.    0.
CC
CC FLAG FOR ALCOHOL PART. MODEL AND PARTITION COEFFICIENTS
*----IALC  OPSK7O  OPSK7S  OPSK8O  OPSK8S
     0     0.      0.      0.      0.
CC
CC NO. OF ITERATIONS, AND TOLERANCE
*----NALMAX   EPSALC
     20       .0001
CC
CC ALCOHOL 1 PARTITIONING PARAMETERS IF IALC=1
*----AKWC7   AKWS7  AKM7  AK7     PT7
     4.671   1.79   48.   35.31   .222
CC
CC ALCOHOL 2 PARTITIONING PARAMETERS IF IALC=1
*----AKWC8   AKWS8  AKM8  AK8     PT8
     0.      0.     0.    0.      0.
CC
CC
*--- IFT MODEL FLAG
      0
CC
CC INTERFACIAL TENSION PARAMETERS
*----G11  G12     G13   G21   G22    G23
     13.  -14.8   .007  13.2   -14.5  .010
CC
CC LOG10 OF OIL/WATER INTERFACIAL TENSION
*----XIFTW
     1.477
CC
CC CAPILLARY DESATURATION PARAMETERS FOR PHASE 1, 2, AND 3
*----ITRAP   T11        T22        T33
     0        0.         0.        0.
CC
CC REL. PERM. AND PC CURVES
*---- IPERM    IRTYPE
        0       0
CC
CC FLAG FOR CONSTANT OR VARIABLE REL. PERM. PARAMETERS
*----ISRW  IPRW  IEW
     0      0    0
CC
CC CONSTANT RES. SATURATION OF PHASES 1,2,AND 3 AT LOW CAPILLARY NO.
*----S1RWC       S2RWC       S3RWC
     0.05         0.22        0.05
CC
```

```
CC CONSTANT ENDPOINT REL. PERM. OF PHASES 1,2,AND 3 AT LOW CAPILLARY NO.
*----P1RW       P2RW       P3RW
      0.3       0.9        0.3
CC
CC CONSTANT REL. PERM. EXPONENT OF PHASES 1,2,AND 3 AT LOW CAPILLARY NO.
*----E1W         E2W       E3W
     1.4         3.6       1.4
CC
CC WATER AND OIL VISCOSITY , RESERVOIR TEMPERATURE
*----VIS1    VIS2        TSTAND
     0.9     10.0        60.0
cc
cc oil viscosity parameters
*--- bv1   bv2
      0     0
CC
CC VISCOSITY PARAMETERS
*----ALPHA1 ALPHA2  ALPHA3  ALPHA4  ALPHA5
     0.0     0.0      0.0   0.000865    4.153
CC
CC PARAMETERS TO CALCULATE POLYMER VISCOSITY AT ZERO SHEAR RATE
*----AP1     AP2     AP3
      45.    833.0   428.
CC
CC PARAMETER TO COMPUTE CSEP,MIN. CSEP, AND SLOPE OF LOG VIS. VS. LOG CSEP
*----BETAP CSE1  SLOPE
     1     .01   .0
CC
CC PARAMETER FOR SHEAR RATE DEPENDENCE OF POLYMER VISCOSITY
*----GAMMAC      GAMHF     POWN    IPMOD   ishear  rweff   GAMHF2  iwreath
       4         19051.7   1.6     0       0       0.25    0        0
CC
CC FLAG FOR POLYMER PARTITIONING, PERM. REDUCTION PARAMETERS
*----IPOLYM EPHI3 EPHI4 BRK    CRK    RKCUT
     1      1.    1      0.    0.0     10
CC
CC SPECIFIC WEIGHT FOR COMPONENTS 1,2,3,7,AND 8 , AND GRAVITY FLAG
*----DEN1    DEN2      DEN3      DEN7     DEN8  IDEN
    0.433    0.347     0.433       0       0     2
CC
CC  FLAG FOR CHOICE OF UNITS ( 0:BOTTOMHOLE CONDITION , 1: STOCK TANK)
*-----ISTB
      0
CC
CC COMPRESSIBILITY FOR VOL. OCCUPYING COMPONENTS 1,2,3,7,AND 8
*----COMPC(1)   COMPC(2)     COMPC(3)  COMPC(7)  COMPC(8)
        0          0             0         0         0
CC
CC CONSTANT OR VARIABLE PC PARAM., WATER-WET OR OIL-WET PC CURVE FLAG
*----ICPC   IEPC  IOW
     0       0   0
CC
CC CAPILLARY PRESSURE PARAMETERS, CPC
*----CPC
     0.
CC
CC CAPILLARY PRESSURE PARAMETERS, EPC
*---- EPC
      2.
CC
CC MOLECULAR DIFFUSIVITY OF KCTH COMPONENT IN PHASE 1 (D(KC),KC=1,N)
*----D(1) D(2) D(3) D(4) D(5) D(6)
  0    0.   0.   0.   0.   0.   0.  0.0  0.0  0.0  0.0  0.0  0.0  0.0 0.0
CC
```

```
CC MOLECULAR DIFFUSIVITY OF KCTH COMPONENT IN PHASE 2 (D(KC),KC=1,N)
*----D(1) D(2) D(3) D(4) D(5) D(6)
  0   0.   0.   0.   0.   0.   0.  0.0  0.0  0.0  0.0  0.0  0.0 0.0 0.0
CC
CC MOLECULAR DIFFUSIVITY OF KCTH COMPONENT IN PHASE 3 (D(KC),KC=1,N)
*----D(1) D(2) D(3) D(4) D(5) D(6)
  0   0.   0.   0.   0.   0.   0.  0.0  0.0  0.0  0.0  0.0  0.0 0.0  0.0
CC
CC LONGITUDINAL AND TRANSVERSE DISPERSIVITY OF PHASE 1
*----ALPHAL(1)     ALPHAT(1)
     0            0
CC
CC LONGITUDINAL AND TRANSVERSE DISPERSIVITY OF PHASE 2
*----ALPHAL(2)     ALPHAT(2)
     0            0
CC
CC LONGITUDINAL AND TRANSVERSE DISPERSIVITY OF PHASE 3
*----ALPHAL(3)     ALPHAT(3)
     0            0
C
CC SURFACTANT AND POLYMER ADSORPTION PARAMETERS
*----AD31     AD32  B3D    AD41    AD42  B4D  IADK, IADS1, FADS refk
     0.        .0   1000.   0.0     0.0    1     0      0      0   0
CC
CC PARAMETERS FOR CATION EXCHANGE OF CLAY AND SURFACTANT
*----QV     XKC   XKS  EQW
      0     0.    0.   804
cc
cc
*---  KGOPT
      6
CC
CC
*---- IRKFOLD
      2
CC
CC
*----CRKPOL CRKBWG CLIMBWG
      2     6.8    200
CC
CC
*---- AG1        AG2     AG3
      .005    .00260     0
CC
CC
*---- ALPHBWP  ALPHBWG
      0         0
CC
CC
*---- ADBWGLIM
      2.3
CC
CC
*---- ADBWG0 ADBWGS ADBWGT ADBWGK ADBWG
       2.66     0     6     -0.01   10.
CC
CC
*---- TEMTRBWG   TEMTRMBWG    CCRLRBWG     CPOLRBWG    CBWGRBWG
       130           160         0.0          0.0         0.0
CC
CC
*---- BWB0    BWKC0
        0       0
CC
```

```
CC
*---- BWRKCP0,BWRKCC0
      1e-3      1e-3
cc
cc
*--- initial res. temp (F)
     180.
cc
cc silica - rock heat cap. - 35 btu/ft3-F,
*--- dens     crtc     cvspr       cvsp(1)  cvsp(2)   cvsp(3)
      165      24     0.1454        1        0.50      0.0
cc
cc
*--- ihlos
      0
CC
CC*********************************************************************
CC                                                                     *
CC    WELL DATA                                                        *
CC                                                                     *
CC*********************************************************************
CC
CC
CC TOTAL NUMBER OF WELLS, WELL RADIUS FLAG, FLAG FOR TIME OR COURANT NO.
*----NWELL   IRO   ITIME  NWREL
        2     1       1        2
CC
CC WELL ID,LOCATIONS,AND FLAG FOR SPECIFYING WELL TYPE, WELL RADIUS, SKIN
*---- IDW    IW    JW    IFLAG    RW       SWELL   IDIR   IFIRST   ILAST   IPRF
       1     1     1       1     0.003       0       3      1       3      0
CC
CC WELL NAME
*----  WELNAM
inj
CC
CC ICHEK , MAX. AND MIN. ALLOWABLE BOTTOMHOLE PRESSURE AND RATE
*---- ICHEK     PWFMIN     PWFMAX    QTMIN    QTMAX
        0          0         30000      0        9000
CC
CC WELL ID,LOCATIONS,AND FLAG FOR SPECIFYING WELL TYPE, WELL RADIUS, SKIN
*---- IDW    IW    JW    IFLAG    RW     SWELL   IDIR   IFIRST   ILAST   IPRF
       2     15     15       2   0.003     0       3      1       3      0
CC
CC WELL NAME
*----  WELNAM
prod-1
CC
CC ICHEK , MAX. AND MIN. ALLOWABLE BOTTOMHOLE PRESSURE AND RATE
*---- ICHEK     PWFMIN     PWFMAX    QTMIN    QTMAX
        0          0         30000      0        50000
CC
CC  ID,INJ. RATE AND INJ. COMP. FOR RATE CONS. WELLS FOR EACH PHASE (L=1,3)
*----  ID     QI(M,L)     C(M,KC,L)
       1     842.25       1   0  0  0    0.134    0    0   0  0  0 0    0    0.    0    0
       1      0           0   0  0  0    0        0    0   0  0  0 0    0    0.    0    0
       1      0           0   0  0  0    0        0    0   0  0  0 0    0    0.    0    0
cc
cc
*--- id  tinj
     1    60
CC
CC ID, BOTTOM HOLE PRESSURE FOR PRESSURE CONSTRAINT WELL (IFLAG=2 OR 3)
*----  ID    PWF
       2      1000
```

```
CC
CC CUM. INJ. TIME , AND INTERVALS (PV OR DAY) FOR WRITING TO OUTPUT FILES
*---- TINJ     CUMPR1     CUMHI1     WRHPV     WRPRF      RSTC
       450      10.        10.        10.         10.       100000
CC
CC THE INI. TIME STEP,CONC. TOLERANCE,MAX.,MIN. time steps
*----  DT       DELC       DTMAX      DTMIN
       0.01    0.1        0.4      0.04
CC---------2---------3---------4---------5---------6---------7---------8-----------------
---------
CC IRO, ITIME, NEW FLAGS FOR ALL THE WELLS ( WATER INJ.)
*---- IRO ITIME IFLAG
       2   1     1  2
C
CC NUMBER OF WELLS CHANGES IN LOCATION OR SKIN OR PWF
*----NWEL1
     0
CC
CC NUMBER OF WELLS WITH RATE CHANGES, ID
*----NWEL1   ID
     1        1
CC
CC  ID,INJ. RATE AND INJ. COMP. FOR RATE CONS. WELLS FOR EACH PHASE (L=1,3)
*----  ID     QI(M,L)     C(M,KC,L)
       1    842.25       1   0  0  0    0.134    0         0   0  0  0   0    0  0.
2000          0
       1      0          0   0  0  0    0        0         0   0  0  0   0    0  0.    0
0
       1      0          0   0  0  0    0        0         0   0  0  0   0    0  0.    0
0
cc
cc
*--- id  tinj
     1   60
CC
CC CUM. INJ. TIME , AND INTERVALS (PV OR DAY) FOR WRITING TO OUTPUT FILES
*---- TINJ     CUMPR1     CUMHI1     WRHPV      WRPRF      RSTC
      670        10         10         10         10       100000
CC
CC THE INI. TIME STEP,CONC. TOLERANCE,MAX.,MIN. time steps
*----  DT        DELC       DTMAX     DTMIN
       0.01     0.1        0.4      0.004
CC---------2---------3---------4---------5---------6---------7---------8-----------------
-------------
CC IRO, ITIME, NEW FLAGS FOR ALL THE WELLS ( WATER INJ.)
*---- IRO ITIME IFLAG
       2   1     1  2
C
CC NUMBER OF WELLS CHANGES IN LOCATION OR SKIN OR PWF
*----NWEL1
     0
CC
CC NUMBER OF WELLS WITH RATE CHANGES, ID
*----NWEL1   ID
     1        1
CC
CC  ID,INJ. RATE AND INJ. COMP. FOR RATE CONS. WELLS FOR EACH PHASE (L=1,3)
*----  ID     QI(M,L)     C(M,KC,L)
       1     842.25       1   0  0  0    0.134    0         0   0  0  0 0    0  0.    0
0
       1      0          0   0  0  0    0        0         0   0  0  0 0    0  0.    0
0
       1      0          0   0  0  0    0        0         0   0  0  0 0    0  0.    0
0
```

```
cc
cc
*--- id  tinj
     1   60
CC
CC CUM. INJ. TIME , AND INTERVALS (PV OR DAY) FOR WRITING TO OUTPUT FILES
*---- TINJ     CUMPR1     CUMHI1     WRHPV     WRPRF      RSTC
      1000       10.        10         10        10       100000
CC
CC THE INI. TIME STEP,CONC. TOLERANCE,MAX.,MIN. time steps
*----  DT        DELC        DTMAX       DTMIN
       0.01     0.1        0.4      0.04
```

A.4 Static Imbibition Test Case

The following is the input data file for static imbibition test in UTCHEM simulator. We used this case in Chapter 6 for modeling imbibition experiments to investigate wettability alteration and IFT reduction using surfactant solution. In order to run this case for wettability alteration, IWALT flag in input file should be set IWALT=1 along with relative permeability and capillary pressure data before and after wettability alteration.

```
CC*********************************************************************
CC                                                                     *
CC     BRIEF DESCRIPTION OF DATA SET: UTCHEM (VERSION 9.95)            *
CC                                                                     *
CC*********************************************************************
CC                                                                     *
CC  Surfactant Imbibition (CORE), 5x5x5                                *
CC                                                                     *
CC  LENGTH (FT): 0.111                                                 *
CC  THICKNESS (FT) : 0.146                                             *
CC  WIDTH (FT) : 0.111                    POROSITY :    0.163          *
CC  NJ. RATE (FT3/DAY) : NA                                            *
CC  GRID BLOCKS : 7x7x7               COORDINATE : CARTESIAN           *
CC  DATE : 06/23/2012                                                  *
CC                                                                    *
CC*********************************************************************
CC
CC*********************************************************************
CC                                                                     *
CC    RESERVOIR DESCRIPTION                                            *
CC                                                                     *
CC*********************************************************************
CC
CC Run number
*---- RUNNO
CC
CC0
CC Title and run description
*----
Surfactant Imbibition in a 5x5x5 core inside a 7x7x7 model
Cartesian Coord with Square Core with same XArea and Pore Volume
0.05 % Surf in solution outside core WITH WETTABILITY ALTERATION
CC
CC SIMULATION FLAGS
*---- IMODE IMES IDISPC ICWM ICAP IREACT IBIO ICOORD ITREAC ITC  IGAS  IENG
       1    3     3     0    0     0     0     1      0     0    0     0  0       0
CC
CC no. of gridblocks,flag specifies constant or variable grid size,unit
*---- NX    NY    NZ  IDXYZ  IUNIT
      7     7    7     2      0
```

```
CC
CC GRID SIZE OF BLOCK IN X DIRECTION
*---- DX(I), FOR I=1 TO NX
          0.04      0.0222    0.0222    0.0222    0.0222    0.0222    0.04
CC
CC GRID SIZE OF BLOCK IN Y DIRECTION
*---- DY(I), FOR I=1 TO NY
          0.04      0.0222    0.0222    0.0222    0.0222    0.0222    0.04
CC
CC GRID SIZE OF BLOCK IN Z DIRECTION
*----DZ(I), FOR I=1 TO NZ
        0.1     0.1     0.0292    0.0292    0.0292    0.0292    0.0292
CC
CC total no. of components,no. of tracers,no. of gel components
*----n    no    ntw    nta    ngc    ng    noth
     6    0      0      0      0     0      0
CC
CC Name of the components
*----spname(i) for i=1 to n
Water
Oil
Surf.
Polymer
Chloride
Calcium
CC
CC flag indicating if the component is included in calculations or not
*----icf(kc) for kc=1,n
      1  1  1  0  1  1
CC
CC*********************************************************************
CC                                                                     *
CC    OUTPUT OPTIONS                                                   *
CC                                                                     *
CC*********************************************************************
CC
CC
CC FLAG TO WRITE TO UNIT 3,FLAG FOR PV OR DAYS TO PRINT OR TO STOP THE RUN
*---- ICUMTM  ISTOP  IOUTGMS
        0       0       2
CC
CC FLAG INDICATING IF THE PROFILE OF KCTH COMPONENT SHOULD BE WRITTEN
*---- IPRFLG(KC),KC=1,N
        1  1  1  0  1  1
CC
CC FLAG FOR PRES.,SAT.,TOTAL CONC.,TRACER CONC.,CAP.,GEL, ALKALINE PROFILES
*---- IPPRES IPSAT IPCTOT IPBIO IPCAP IPGEL IPALK IPTEMP IPOBS
        1      1      1      0     0     0     0     0      0
CC
CC FLAG FOR WRITING SEVERAL PROPERTIES TO UNIT 4 (Prof)
*---- ICKL IVIS IPER ICNM ICSE IHYSTP IFOAMP INONEQ
       1    0    1    1    1    1    0    0
CC
CC FLAG  for variables to PROF output file
*---- IADS IVEL IRKF IPHSE
       0    0    0    0
CC
CC*********************************************************************
CC                                                                     *
CC    RESERVOIR PROPERTIES                                             *
CC                                                                     *
CC*********************************************************************
CC
CC
```

```
CC MAX. SIMULATION TIME ( DAYS)
*---- TMAX
      14
CC
CC ROCK COMPRESSIBILITY (1/PSI), STAND. PRESSURE(PSIA)
*---- COMPR                PSTAND
        0                   0
CC
CC FLAGS INDICATING CONSTANT OR VARIABLE POROSITY, X,Y,AND Z PERMEABILITY
*---- IPOR1  IPERMX IPERMY IPERMZ IMOD
        2      2      3      3     0   0   0
CC
CC VARIABLE POROSITY OVER RESERVOIR
*---- POR(I),FOR I=1 TO NX*NY*NZ
          1         1         1         1         1         1         1
          1         1         1         1         1         1         1
          1         1         1         1         1         1         1
          1         1         1         1         1         1         1
          1         1         1         1         1         1         1
          1         1         1         1         1         1         1
          1         1         1         1         1         1         1
          1         1         1         1         1         1         1
          1         1         1         1         1         1         1
          1         1         1         1         1         1         1
          1         1         1         1         1         1         1
          1         1         1         1         1         1         1
          1         1         1         1         1         1         1
          1         1         1         1         1         1         1
          1         1         1         1         1         1         1
          1       0.163     0.163     0.163     0.163     0.163       1
          1       0.163     0.163     0.163     0.163     0.163       1
          1       0.163     0.163     0.163     0.163     0.163       1
          1       0.163     0.163     0.163     0.163     0.163       1
          1       0.163     0.163     0.163     0.163     0.163       1
          1         1         1         1         1         1         1
          1         1         1         1         1         1         1
          1       0.163     0.163     0.163     0.163     0.163       1
          1       0.163     0.163     0.163     0.163     0.163       1
          1       0.163     0.163     0.163     0.163     0.163       1
          1       0.163     0.163     0.163     0.163     0.163       1
          1       0.163     0.163     0.163     0.163     0.163       1
          1         1         1         1         1         1         1
          1         1         1         1         1         1         1
          1       0.163     0.163     0.163     0.163     0.163       1
          1       0.163     0.163     0.163     0.163     0.163       1
          1       0.163     0.163     0.163     0.163     0.163       1
          1       0.163     0.163     0.163     0.163     0.163       1
          1       0.163     0.163     0.163     0.163     0.163       1
          1         1         1         1         1         1         1
          1         1         1         1         1         1         1
          1       0.163     0.163     0.163     0.163     0.163       1
          1       0.163     0.163     0.163     0.163     0.163       1
          1       0.163     0.163     0.163     0.163     0.163       1
          1       0.163     0.163     0.163     0.163     0.163       1
          1       0.163     0.163     0.163     0.163     0.163       1
          1         1         1         1         1         1         1
CC
```

```
CC VARIABLE PERMEABILITY OVER RESERVOIR
*---- PERMX(I),FOR I=1 TO NX*NY*NZ
       100000     100000       100000     100000     100000     100000       100000
       100000     100000       100000     100000     100000     100000       100000
       100000     100000       100000     100000     100000     100000       100000
       100000     100000       100000     100000     100000     100000       100000
       100000     100000       100000     100000     100000     100000       100000
       100000     100000       100000     100000     100000     100000       100000
       100000     100000       100000     100000     100000     100000       100000
       100000     100000       100000     100000     100000     100000       100000
       100000     100000       100000     100000     100000     100000       100000
       100000     100000       100000     100000     100000     100000       100000
       100000     100000       100000     100000     100000     100000       100000
       100000     100000       100000     100000     100000     100000       100000
       100000     100000       100000     100000     100000     100000       100000
       100000     66.6         66.6         66.6     66.6           66.6
100000
       100000     66.6         66.6         66.6     66.6           66.6
100000
       100000     66.6         66.6         66.6     66.6           66.6
100000
       100000     66.6         66.6         66.6     66.6           66.6
100000
       100000     66.6         66.6         66.6     66.6           66.6
100000
       100000     100000       100000     100000     100000     100000       100000
       100000     100000       100000     100000     100000     100000       100000
       100000     66.6         66.6         66.6     66.6           66.6
100000
       100000     66.6         66.6         66.6     66.6           66.6
100000
       100000     66.6         66.6         66.6     66.6           66.6
100000
       100000     66.6         66.6         66.6     66.6           66.6
100000
       100000     66.6         66.6         66.6     66.6           66.6
100000
       100000     100000       100000     100000     100000     100000       100000
       100000     100000       100000     100000     100000     100000       100000
       100000     66.6         66.6         66.6     66.6           66.6
100000
       100000     66.6         66.6         66.6     66.6           66.6
100000
       100000     66.6         66.6         66.6     66.6           66.6
100000
       100000     66.6         66.6         66.6     66.6           66.6
100000
       100000     66.6         66.6         66.6     66.6           66.6
100000
       100000     100000       100000     100000     100000     100000       100000
```

```
       100000      100000        100000      100000     100000     100000       100000
       100000      66.6          66.6          66.6     66.6           66.6
100000
       100000      66.6          66.6          66.6     66.6           66.6
100000
       100000      66.6          66.6          66.6     66.6           66.6
100000
       100000      66.6          66.6          66.6     66.6           66.6
100000
       100000      66.6          66.6          66.6     66.6           66.6
100000
       100000      100000        100000      100000     100000     100000       100000
CC
CC Y DIRECTION PERMEABILITY IS DEPENDENT ON X DIRECTION PERMEABILITY
*---- CONSTANT PERMEABILITY MULTIPLIER FOR Y DIRECTION PERMEABILITY
        1
CC
CC Z DIRECTION PERMEABILITY IS DEPENDENT ON X DIRECTION PERMEABILITY
*---- CONSTANT PERMEABILITY MULTIPLIER FOR Z DIRECTION PERMEABILITY
        0.95
CC
CC FLAG FOR CONSTANT OR VARIABLE DEPTH, PRESSURE, WATER SATURATION,INITIAL AQUEOUS PHASE
cOMPOSITIONS
*----IDEPTH  IPRESS  ISWI  ICWI
       0       1      2      2
CC
CC CONSTANT DEPTH (FT)
*---- D111
       0.5
CC
CC INITIAL PRESSURE FOR A POINT AT A SPECIFIED DEPTH IS SPECIFIED
*---- PINIT  HINIT
      14.7    0
CC
CC INITIAL WATER SATURATION FOR EACH GRIDBLOCk IS SPECIFIED
*---- S(I),I=1 TO NX*NY*NZ
          1         1         1         1         1         1         1
          1         1         1         1         1         1         1
          1         1         1         1         1         1         1
          1         1         1         1         1         1         1
          1         1         1         1         1         1         1
          1         1         1         1         1         1         1
          1         1         1         1         1         1         1
          1         1         1         1         1         1         1
          1         1         1         1         1         1         1
          1         1         1         1         1         1         1
          1         1         1         1         1         1         1
          1         1         1         1         1         1         1
          1         1         1         1         1         1         1
          1         1         1         1         1         1         1
          1         0.165      0.165      0.165      0.165      0.165      1
          1         0.165      0.165      0.165      0.165      0.165      1
          1         0.165      0.165      0.165      0.165      0.165      1
          1         0.165      0.165      0.165      0.165      0.165      1
          1         0.165      0.165      0.165      0.165      0.165      1
          1         1         1         1         1         1         1
          1         1         1         1         1         1         1
          1         0.165      0.165      0.165      0.165      0.165      1
          1         0.165      0.165      0.165      0.165      0.165      1
          1         0.165      0.165      0.165      0.165      0.165      1
          1         0.165      0.165      0.165      0.165      0.165      1
          1         0.165      0.165      0.165      0.165      0.165      1
          1         1         1         1         1         1         1
```

```
          1         1         1         1         1         1         1
          1         0.165      0.165      0.165      0.165      0.165      1
          1         0.165      0.165      0.165      0.165      0.165      1
          1         0.165      0.165      0.165      0.165      0.165      1
          1         0.165      0.165      0.165      0.165      0.165      1
          1         0.165      0.165      0.165      0.165      0.165      1
          1         1         1         1         1         1         1
          1         1         1         1         1         1         1
          1         0.165      0.165      0.165      0.165      0.165      1
          1         0.165      0.165      0.165      0.165      0.165      1
          1         0.165      0.165      0.165      0.165      0.165      1
          1         0.165      0.165      0.165      0.165      0.165      1
          1         0.165      0.165      0.165      0.165      0.165      1
          1         1         1         1         1         1         1
          1         1         1         1         1         1         1
          1         0.165      0.165      0.165      0.165      0.165      1
          1         0.165      0.165      0.165      0.165      0.165      1
          1         0.165      0.165      0.165      0.165      0.165      1
          1         0.165      0.165      0.165      0.165      0.165      1
          1         0.165      0.165      0.165      0.165      0.165      1
          1         1         1         1         1         1         1
CC
CC INITIAL CONCENTRATION IN THE AQUEOUS PHASE AT Ith GRIDBLOCK
*---- cwi(I,KW) for i=1, NXxNYxNZ, for kw=1,n(8+no)
        0.9995  0.9995  0.9995  0.9995  0.9995  0.9995  0.9995
        0.9995  0.9995  0.9995  0.9995  0.9995  0.9995  0.9995
        0.9995  0.9995  0.9995  0.9995  0.9995  0.9995  0.9995
        0.9995  0.9995  0.9995  0.9995  0.9995  0.9995  0.9995
        0.9995  0.9995  0.9995  0.9995  0.9995  0.9995  0.9995
        0.9995  0.9995  0.9995  0.9995  0.9995  0.9995  0.9995
        0.9995  0.9995  0.9995  0.9995  0.9995  0.9995  0.9995
        0.9995  0.9995  0.9995  0.9995  0.9995  0.9995  0.9995
        0.9995  0.9995  0.9995  0.9995  0.9995  0.9995  0.9995
        0.9995  0.9995  0.9995  0.9995  0.9995  0.9995  0.9995
        0.9995  0.9995  0.9995  0.9995  0.9995  0.9995  0.9995
        0.9995  0.9995  0.9995  0.9995  0.9995  0.9995  0.9995
        0.9995  0.9995  0.9995  0.9995  0.9995  0.9995  0.9995
        0.9995  1       1       1       1       1       0.9995
        0.9995  1       1       1       1       1       0.9995
        0.9995  1       1       1       1       1       0.9995
        0.9995  1       1       1       1       1       0.9995
        0.9995  1       1       1       1       1       0.9995
        0.9995  0.9995  0.9995  0.9995  0.9995  0.9995  0.9995
        0.9995  0.9995  0.9995  0.9995  0.9995  0.9995  0.9995
        0.9995  1       1       1       1       1       0.9995
        0.9995  1       1       1       1       1       0.9995
        0.9995  1       1       1       1       1       0.9995
        0.9995  1       1       1       1       1       0.9995
        0.9995  1       1       1       1       1       0.9995
        0.9995  0.9995  0.9995  0.9995  0.9995  0.9995  0.9995
        0.9995  0.9995  0.9995  0.9995  0.9995  0.9995  0.9995
        0.9995  1       1       1       1       1       0.9995
        0.9995  1       1       1       1       1       0.9995
        0.9995  1       1       1       1       1       0.9995
        0.9995  1       1       1       1       1       0.9995
        0.9995  1       1       1       1       1       0.9995
        0.9995  0.9995  0.9995  0.9995  0.9995  0.9995  0.9995
        0.9995  0.9995  0.9995  0.9995  0.9995  0.9995  0.9995
        0.9995  1       1       1       1       1       0.9995
        0.9995  1       1       1       1       1       0.9995
        0.9995  1       1       1       1       1       0.9995
        0.9995  1       1       1       1       1       0.9995
```

```
        0.9995  1       1       1       1       1       0.9995
        0.9995  0.9995  0.9995  0.9995  0.9995  0.9995  0.9995
        0.9995  0.9995  0.9995  0.9995  0.9995  0.9995  0.9995
        0.9995  1       1       1       1       1       0.9995
        0.9995  1       1       1       1       1       0.9995
        0.9995  1       1       1       1       1       0.9995
        0.9995  1       1       1       1       1       0.9995
        0.9995  1       1       1       1       1       0.9995
        0.9995  0.9995  0.9995  0.9995  0.9995  0.9995  0.9995
CC
CC INITIAL CONCENTRATION IN THE AQUEOUS PHASE AT Ith GRIDBLOCK
*---- cwi(I,KW) for i=1, NXxNYxNZ, for kw=1,n(8+no)
        0       0       0       0       0       0       0
        0       0       0       0       0       0       0
        0       0       0       0       0       0       0
```

```
        0.0005  0.0005  0.0005  0.0005  0.0005  0.0005  0.0005
        0.0005  0.0005  0.0005  0.0005  0.0005  0.0005  0.0005
        0.0005  0.0005  0.0005  0.0005  0.0005  0.0005  0.0005
        0.0005  0.0005  0.0005  0.0005  0.0005  0.0005  0.0005
        0.0005  0.0005  0.0005  0.0005  0.0005  0.0005  0.0005
        0.0005  0.0005  0.0005  0.0005  0.0005  0.0005  0.0005
        0.0005  0.0005  0.0005  0.0005  0.0005  0.0005  0.0005
        0.0005  0.0005  0.0005  0.0005  0.0005  0.0005  0.0005
        0.0005  0.0005  0.0005  0.0005  0.0005  0.0005  0.0005
        0.0005  0.0005  0.0005  0.0005  0.0005  0.0005  0.0005
        0.0005  0.0005  0.0005  0.0005  0.0005  0.0005  0.0005
        0.0005  0.0005  0.0005  0.0005  0.0005  0.0005  0.0005
        0.0005  0.0005  0.0005  0.0005  0.0005  0.0005  0.0005
        0.0005  0.0005  0.0005  0.0005  0.0005  0.0005  0.0005
        0.0005  0       0       0       0       0       0.0005
        0.0005  0       0       0       0       0       0.0005
        0.0005  0       0       0       0       0       0.0005
        0.0005  0       0       0       0       0       0.0005
        0.0005  0       0       0       0       0       0.0005
        0.0005  0.0005  0.0005  0.0005  0.0005  0.0005  0.0005
        0.0005  0.0005  0.0005  0.0005  0.0005  0.0005  0.0005
        0.0005  0       0       0       0       0       0.0005
        0.0005  0       0       0       0       0       0.0005
        0.0005  0       0       0       0       0       0.0005
        0.0005  0       0       0       0       0       0.0005
        0.0005  0       0       0       0       0       0.0005
        0.0005  0.0005  0.0005  0.0005  0.0005  0.0005  0.0005
        0.0005  0.0005  0.0005  0.0005  0.0005  0.0005  0.0005
        0.0005  0       0       0       0       0       0.0005
        0.0005  0       0       0       0       0       0.0005
        0.0005  0       0       0       0       0       0.0005
        0.0005  0       0       0       0       0       0.0005
        0.0005  0       0       0       0       0       0.0005
        0.0005  0.0005  0.0005  0.0005  0.0005  0.0005  0.0005
        0.0005  0.0005  0.0005  0.0005  0.0005  0.0005  0.0005
        0.0005  0       0       0       0       0       0.0005
        0.0005  0       0       0       0       0       0.0005
        0.0005  0       0       0       0       0       0.0005
        0.0005  0       0       0       0       0       0.0005
        0.0005  0       0       0       0       0       0.0005
        0.0005  0.0005  0.0005  0.0005  0.0005  0.0005  0.0005
CC
CC INITIAL CONCENTRATION IN THE AQUEOUS PHASE AT Ith GRIDBLOCK
*---- cwi(I,KW) for i=1, NXxNYxNZ, for kw=1,n(8+no)
        0.48    0.48    0.48    0.48    0.48    0.48    0.48
        0.48    0.48    0.48    0.48    0.48    0.48    0.48
        0.48    0.48    0.48    0.48    0.48    0.48    0.48
        0.48    0.48    0.48    0.48    0.48    0.48    0.48
        0.48    0.48    0.48    0.48    0.48    0.48    0.48
        0.48    0.48    0.48    0.48    0.48    0.48    0.48
        0.48    0.48    0.48    0.48    0.48    0.48    0.48
        0.48    0.48    0.48    0.48    0.48    0.48    0.48
        0.48    0.48    0.48    0.48    0.48    0.48    0.48
        0.48    0.48    0.48    0.48    0.48    0.48    0.48
        0.48    0.48    0.48    0.48    0.48    0.48    0.48
        0.48    0.48    0.48    0.48    0.48    0.48    0.48
```

```
        0.48    0.48    0.48    0.48    0.48    0.48    0.48
        0.48    0.48    0.48    0.48    0.48    0.48    0.48
        0.48    0.48    0.48    0.48    0.48    0.48    0.48
        0.48    0.65    0.65    0.65    0.65    0.65    0.48
        0.48    0.65    0.65    0.65    0.65    0.65    0.48
        0.48    0.65    0.65    0.65    0.65    0.65    0.48
        0.48    0.65    0.65    0.65    0.65    0.65    0.48
        0.48    0.65    0.65    0.65    0.65    0.65    0.48
        0.48    0.48    0.48    0.48    0.48    0.48    0.48
        0.48    0.48    0.48    0.48    0.48    0.48    0.48
        0.48    0.65    0.65    0.65    0.65    0.65    0.48
        0.48    0.65    0.65    0.65    0.65    0.65    0.48
        0.48    0.65    0.65    0.65    0.65    0.65    0.48
        0.48    0.65    0.65    0.65    0.65    0.65    0.48
        0.48    0.65    0.65    0.65    0.65    0.65    0.48
        0.48    0.48    0.48    0.48    0.48    0.48    0.48
        0.48    0.48    0.48    0.48    0.48    0.48    0.48
        0.48    0.65    0.65    0.65    0.65    0.65    0.48
        0.48    0.65    0.65    0.65    0.65    0.65    0.48
        0.48    0.65    0.65    0.65    0.65    0.65    0.48
        0.48    0.65    0.65    0.65    0.65    0.65    0.48
        0.48    0.65    0.65    0.65    0.65    0.65    0.48
        0.48    0.48    0.48    0.48    0.48    0.48    0.48
        0.48    0.48    0.48    0.48    0.48    0.48    0.48
        0.48    0.65    0.65    0.65    0.65    0.65    0.48
        0.48    0.65    0.65    0.65    0.65    0.65    0.48
        0.48    0.65    0.65    0.65    0.65    0.65    0.48
        0.48    0.65    0.65    0.65    0.65    0.65    0.48
        0.48    0.48    0.48    0.48    0.48    0.48    0.48
        0.48    0.48    0.48    0.48    0.48    0.48    0.48
        0.48    0.65    0.65    0.65    0.65    0.65    0.48
        0.48    0.65    0.65    0.65    0.65    0.65    0.48
        0.48    0.65    0.65    0.65    0.65    0.65    0.48
        0.48    0.65    0.65    0.65    0.65    0.65    0.48
        0.48    0.48    0.48    0.48    0.48    0.48    0.48
CC
CC INITIAL CONCENTRATION IN THE AQUEOUS PHASE AT Ith GRIDBLOCK
*---- cwi(I,KW) for i=1, NXxNYxNZ, for kw=1,n(8+no)
        0       0       0       0       0       0       0
        0       0       0       0       0       0       0
        0       0       0       0       0       0       0
        0       0       0       0       0       0       0
        0       0       0       0       0       0       0
        0       0       0       0       0       0       0
        0       0       0       0       0       0       0
        0       0       0       0       0       0       0
        0       0       0       0       0       0       0
        0       0       0       0       0       0       0
        0       0       0       0       0       0       0
        0       0       0       0       0       0       0
        0       0       0       0       0       0       0
        0       0       0       0       0       0       0
        0       0       0       0       0       0       0
        0       0       0       0       0       0       0
        0       0       0       0       0       0       0
        0       0       0       0       0       0       0
        0       0       0       0       0       0       0
        0       0       0       0       0       0       0
        0       0       0       0       0       0       0
        0       0       0       0       0       0       0
        0       0       0       0       0       0       0
        0       0       0       0       0       0       0
        0       0       0       0       0       0       0
        0       0       0       0       0       0       0
        0       0       0       0       0       0       0
        0       0       0       0       0       0       0
```

```
        0       0       0       0       0       0       0
        0       0       0       0       0       0       0
        0       0       0       0       0       0       0
        0       0       0       0       0       0       0
        0       0       0       0       0       0       0
        0       0       0       0       0       0       0
        0       0       0       0       0       0       0
        0       0       0       0       0       0       0
        0       0       0       0       0       0       0
        0       0       0       0       0       0       0
        0       0       0       0       0       0       0
        0       0       0       0       0       0       0
        0       0       0       0       0       0       0
        0       0       0       0       0       0       0
        0       0       0       0       0       0       0
        0       0       0       0       0       0       0
        0       0       0       0       0       0       0
        0       0       0       0       0       0       0
        0       0       0       0       0       0       0
        0       0       0       0       0       0       0
        0       0       0       0       0       0       0
        0       0       0       0       0       0       0
CC
CC**********************************************************************
CC                                                                     *
CC    PHYSICAL PROPERTY DATA                                           *
CC                                                                     *
CC**********************************************************************
CC
CC
CC OIL CONC. AT PLAIT POINT FOR TYPE II(+)AND TYPE II(-), CMC
*---- c2plc  c2prc   epsme   ihand
        0      1     0.00005    0
CC
CC flag indicating type of phase behavior parameters
*---- ifghbn
        0
CC SLOPE AND INTERCEPT OF BINODAL CURVE AT ZERO, OPT., AND 2XOPT SALINITY
CC FOR ALCOHOL 1
*---- hbns70   hbnc70   hbns71   hbnc71   hbns72   hbnc72
        0    0.0044        0       0.0073      0     0.1
CC SLOPE AND INTERCEPT OF BINODAL CURVE AT ZERO, OPT., AND 2XOPT SALINITY
CC FOR ALCOHOL 2
*---- hbns80  hbnc80  hbns81  hbnc81  hbns82  hbnc82
        0       0       0       0       0       0
CC
CC LOWER AND UPPER EFFECTIVE SALINITY FOR ALCOHOL 1 AND ALCOHOL 2
*---- csel7   cseu7   csel8   cseu8
       0.85     0.95     0       0
CC
CC THE CSE SLOPE PARAMETER FOR CALCIUM AND ALCOHOL 1 AND ALCOHOL 2
*---- beta6    beta7    beta8
        0        0       0
CC
CC FLAG FOR ALCOHOL PART. MODEL AND PARTITION COEFFICIENTS
*---- ialc   opsk7o   opsk7s   opsk8o   opsk8s
        0      0        0        0        0
CC
CC NO. OF ITERATIONS, AND TOLERANCE
*---- nalmax     epsalc
        20       0.0001
```

```
CC
CC ALCOHOL 1 PARTITIONING PARAMETERS IF IALC=1
*---- akwc7     akws7    akm7     ak7      pt7
       4.671    1.79      48     35.31    0.222
CC
CC ALCOHOL 2 PARTITIONING PARAMETERS IF IALC=1
*---- akwc8     akws8    akm8    ak8     pt8
        0         0        0      0       0
CC
CC ift model flag
*----  ift
        1
CC
CC INTERFACIAL TENSION PARAMETERS
*---- chuh     ahuh
      0.2       9
CC
CC LOG5 OF OIL/WATER INTERFACIAL TENSION
*---- xiftw
       1.3
CC
CC ORGANIC MASS TRANSFER FLAG
*---- imass icor
        0       0
cc
cc
*----IWALT  iwalf
      1     0
CC
CC
*----fw1  pcw1
    0.5   0.5
CC
CC CAPILLARY DESATURATION PARAMETERS FOR PHASE 1, 2, AND 3
*---- itrap      t11      t22      t33
        2       15000    1862     5000
CC
CC Altered CAPILLARY DESATURATION PARAMETERS FOR PHASE 1, 2, AND 3 after wettability
alteration
*---- t11      t22      t33
      2500       6500  5000
CC
CC  FLAG FOR RELATIVE PERMEABILITY AND CAPILLARY PRESSURE MODEL
*---- iperm
        0   0   0
CC
CC FLAG FOR CONSTANT OR VARIABLE REL. PERM. PARAMETERS
*---- isrw    iprw    iew
        2      2       2
CC
CC Residual saturation of aqueous phase displaced by oil or gas at low capillary number
for I gridblock
*---- s1rw(i),FOR I=1 TO NX*NY*NZ
          0.0001         0.0001         0.0001         0.0001         0.0001
0.0001         0.0001
          0.0001         0.0001         0.0001         0.0001         0.0001
0.0001         0.0001
          0.0001         0.0001         0.0001         0.0001         0.0001
0.0001         0.0001
          0.0001         0.0001         0.0001         0.0001         0.0001
0.0001         0.0001
          0.0001         0.0001         0.0001         0.0001         0.0001
0.0001         0.0001
```

```
          0.0001         0.0001         0.0001         0.0001         0.0001
0.0001         0.0001
          0.0001         0.0001         0.0001         0.0001         0.0001
0.0001         0.0001
          0.0001         0.0001         0.0001         0.0001         0.0001
0.0001         0.0001
          0.0001         0.0001         0.0001         0.0001         0.0001
0.0001         0.0001
          0.0001         0.0001         0.0001         0.0001         0.0001
0.0001         0.0001
          0.0001         0.0001         0.0001         0.0001         0.0001
0.0001         0.0001
          0.0001         0.0001         0.0001         0.0001         0.0001
0.0001         0.0001
          0.0001         0.0001         0.0001         0.0001         0.0001
0.0001         0.0001
          0.0001         0.0001         0.0001         0.0001         0.0001
0.0001         0.0001
          0.0001         0.165      0.165      0.165      0.165      0.165      0.0001
          0.0001         0.165      0.165      0.165      0.165      0.165      0.0001
          0.0001         0.165      0.165      0.165      0.165      0.165      0.0001
          0.0001         0.165      0.165      0.165      0.165      0.165      0.0001
          0.0001         0.165      0.165      0.165      0.165      0.165      0.0001
          0.0001         0.0001         0.0001         0.0001         0.0001
0.0001         0.0001
          0.0001         0.0001         0.0001         0.0001         0.0001
0.0001         0.0001
          0.0001         0.165      0.165      0.165      0.165      0.165      0.0001
          0.0001         0.165      0.165      0.165      0.165      0.165      0.0001
          0.0001         0.165      0.165      0.165      0.165      0.165      0.0001
          0.0001         0.165      0.165      0.165      0.165      0.165      0.0001
          0.0001         0.165      0.165      0.165      0.165      0.165      0.0001
          0.0001         0.0001         0.0001         0.0001         0.0001
0.0001         0.0001
          0.0001         0.0001         0.0001         0.0001         0.0001
0.0001         0.0001
          0.0001         0.165      0.165      0.165      0.165      0.165      0.0001
          0.0001         0.165      0.165      0.165      0.165      0.165      0.0001
          0.0001         0.165      0.165      0.165      0.165      0.165      0.0001
          0.0001         0.165      0.165      0.165      0.165      0.165      0.0001
          0.0001         0.165      0.165      0.165      0.165      0.165      0.0001
          0.0001         0.0001         0.0001         0.0001         0.0001
0.0001         0.0001
          0.0001         0.0001         0.0001         0.0001         0.0001
0.0001         0.0001
          0.0001         0.165      0.165      0.165      0.165      0.165      0.0001
          0.0001         0.165      0.165      0.165      0.165      0.165      0.0001
          0.0001         0.165      0.165      0.165      0.165      0.165      0.0001
          0.0001         0.165      0.165      0.165      0.165      0.165      0.0001
          0.0001         0.165      0.165      0.165      0.165      0.165      0.0001
          0.0001         0.0001         0.0001         0.0001         0.0001
0.0001         0.0001
CC
```

```
CC Residual saturation of oleic phase displaced by water at low capillary number for I
gridblock
*---- s2rw(i),FOR I=1 TO NX*NY*NZ
       0.0001  0.0001  0.0001  0.0001  0.0001  0.0001  0.0001
       0.0001  0.0001  0.0001  0.0001  0.0001  0.0001  0.0001
       0.0001  0.0001  0.0001  0.0001  0.0001  0.0001  0.0001
       0.0001  0.0001  0.0001  0.0001  0.0001  0.0001  0.0001
       0.0001  0.0001  0.0001  0.0001  0.0001  0.0001  0.0001
       0.0001  0.0001  0.0001  0.0001  0.0001  0.0001  0.0001
       0.0001  0.0001  0.0001  0.0001  0.0001  0.0001  0.0001
       0.0001  0.0001  0.0001  0.0001  0.0001  0.0001  0.0001
       0.0001  0.0001  0.0001  0.0001  0.0001  0.0001  0.0001
       0.0001  0.0001  0.0001  0.0001  0.0001  0.0001  0.0001
       0.0001  0.0001  0.0001  0.0001  0.0001  0.0001  0.0001
       0.0001  0.0001  0.0001  0.0001  0.0001  0.0001  0.0001
       0.0001  0.45    0.45    0.45    0.45    0.45    0.0001
       0.0001  0.45    0.45    0.45    0.45    0.45    0.0001
       0.0001  0.45    0.45    0.45    0.45    0.45    0.0001
       0.0001  0.45    0.45    0.45    0.45    0.45    0.0001
       0.0001  0.45    0.45    0.45    0.45    0.45    0.0001
       0.0001  0.0001  0.0001  0.0001  0.0001  0.0001  0.0001
       0.0001  0.0001  0.0001  0.0001  0.0001  0.0001  0.0001
       0.0001  0.45    0.45    0.45    0.45    0.45    0.0001
       0.0001  0.45    0.45    0.45    0.45    0.45    0.0001
       0.0001  0.45    0.45    0.45    0.45    0.45    0.0001
       0.0001  0.45    0.45    0.45    0.45    0.45    0.0001
       0.0001  0.45    0.45    0.45    0.45    0.45    0.0001
       0.0001  0.0001  0.0001  0.0001  0.0001  0.0001  0.0001
       0.0001  0.0001  0.0001  0.0001  0.0001  0.0001  0.0001
       0.0001  0.45    0.45    0.45    0.45    0.45    0.0001
       0.0001  0.45    0.45    0.45    0.45    0.45    0.0001
       0.0001  0.45    0.45    0.45    0.45    0.45    0.0001
       0.0001  0.45    0.45    0.45    0.45    0.45    0.0001
       0.0001  0.45    0.45    0.45    0.45    0.45    0.0001
       0.0001  0.0001  0.0001  0.0001  0.0001  0.0001  0.0001
       0.0001  0.0001  0.0001  0.0001  0.0001  0.0001  0.0001
       0.0001  0.45    0.45    0.45    0.45    0.45    0.0001
       0.0001  0.45    0.45    0.45    0.45    0.45    0.0001
       0.0001  0.45    0.45    0.45    0.45    0.45    0.0001
       0.0001  0.45    0.45    0.45    0.45    0.45    0.0001
       0.0001  0.45    0.45    0.45    0.45    0.45    0.0001
       0.0001  0.0001  0.0001  0.0001  0.0001  0.0001  0.0001
CC
CC Residual saturation of microemulsion phase displaced by water or oil at low capillary
number for I gridblock
*---- s3rw(i),FOR I=1 TO NX*NY*NZ
         0.0001         0.0001         0.0001         0.0001         0.0001
0.0001         0.0001
         0.0001         0.0001         0.0001         0.0001         0.0001
0.0001         0.0001
         0.0001         0.0001         0.0001         0.0001         0.0001
0.0001         0.0001
         0.0001         0.0001         0.0001         0.0001         0.0001
0.0001         0.0001
```

```
          0.0001          0.0001          0.0001          0.0001          0.0001
0.0001          0.0001
          0.0001          0.0001          0.0001          0.0001          0.0001
0.0001          0.0001
          0.0001          0.0001          0.0001          0.0001          0.0001
0.0001          0.0001
          0.0001          0.0001          0.0001          0.0001          0.0001
0.0001          0.0001
          0.0001          0.0001          0.0001          0.0001          0.0001
0.0001          0.0001
          0.0001          0.0001          0.0001          0.0001          0.0001
0.0001          0.0001
          0.0001          0.0001          0.0001          0.0001          0.0001
0.0001          0.0001
          0.0001          0.0001          0.0001          0.0001          0.0001
0.0001          0.0001
          0.0001          0.0001          0.0001          0.0001          0.0001
0.0001          0.0001
          0.0001          0.165       0.165       0.165       0.165       0.165       0.0001
          0.0001          0.165       0.165       0.165       0.165       0.165       0.0001
          0.0001          0.165       0.165       0.165       0.165       0.165       0.0001
          0.0001          0.165       0.165       0.165       0.165       0.165       0.0001
          0.0001          0.165       0.165       0.165       0.165       0.165       0.0001
          0.0001          0.0001          0.0001          0.0001          0.0001
0.0001          0.0001
          0.0001          0.0001          0.0001          0.0001          0.0001
0.0001          0.0001
          0.0001          0.165       0.165       0.165       0.165       0.165       0.0001
          0.0001          0.165       0.165       0.165       0.165       0.165       0.0001
          0.0001          0.165       0.165       0.165       0.165       0.165       0.0001
          0.0001          0.165       0.165       0.165       0.165       0.165       0.0001
          0.0001          0.165       0.165       0.165       0.165       0.165       0.0001
          0.0001          0.0001          0.0001          0.0001          0.0001
0.0001          0.0001
          0.0001          0.0001          0.0001          0.0001          0.0001
0.0001          0.0001
          0.0001          0.165       0.165       0.165       0.165       0.165       0.0001
          0.0001          0.165       0.165       0.165       0.165       0.165       0.0001
          0.0001          0.165       0.165       0.165       0.165       0.165       0.0001
          0.0001          0.165       0.165       0.165       0.165       0.165       0.0001
          0.0001          0.165       0.165       0.165       0.165       0.165       0.0001
          0.0001          0.0001          0.0001          0.0001          0.0001
0.0001          0.0001
          0.0001          0.0001          0.0001          0.0001          0.0001
0.0001          0.0001
          0.0001          0.165       0.165       0.165       0.165       0.165       0.0001
          0.0001          0.165       0.165       0.165       0.165       0.165       0.0001
          0.0001          0.165       0.165       0.165       0.165       0.165       0.0001
          0.0001          0.165       0.165       0.165       0.165       0.165       0.0001
          0.0001          0.165       0.165       0.165       0.165       0.165       0.0001
```

```
          0.0001         0.0001         0.0001         0.0001         0.0001
0.0001         0.0001
CC
CC Altered Residual saturation of aqueous phase displaced by oil or gas at low capillary
number for I gridblock
*---- s1rw(i),FOR I=1 TO NX*NY*NZ
          0.0001         0.0001         0.0001         0.0001         0.0001
0.0001         0.0001
          0.0001         0.0001         0.0001         0.0001         0.0001
0.0001         0.0001
          0.0001         0.0001         0.0001         0.0001         0.0001
0.0001         0.0001
          0.0001         0.0001         0.0001         0.0001         0.0001
0.0001         0.0001
          0.0001         0.0001         0.0001         0.0001         0.0001
0.0001         0.0001
          0.0001         0.0001         0.0001         0.0001         0.0001
0.0001         0.0001
          0.0001         0.0001         0.0001         0.0001         0.0001
0.0001         0.0001
          0.0001         0.0001         0.0001         0.0001         0.0001
0.0001         0.0001
          0.0001         0.0001         0.0001         0.0001         0.0001
0.0001         0.0001
          0.0001         0.0001         0.0001         0.0001         0.0001
0.0001         0.0001
          0.0001         0.0001         0.0001         0.0001         0.0001
0.0001         0.0001
          0.0001         0.0001         0.0001         0.0001         0.0001
0.0001         0.0001
          0.0001         0.0001         0.0001         0.0001         0.0001
0.0001         0.0001
          0.0001         0.165      0.165      0.165      0.165      0.165      0.0001
          0.0001         0.165      0.165      0.165      0.165      0.165      0.0001
          0.0001         0.165      0.165      0.165      0.165      0.165      0.0001
          0.0001         0.165      0.165      0.165      0.165      0.165      0.0001
          0.0001         0.165      0.165      0.165      0.165      0.165      0.0001
          0.0001         0.0001         0.0001         0.0001         0.0001
0.0001         0.0001
          0.0001         0.0001         0.0001         0.0001         0.0001
0.0001         0.0001
          0.0001         0.165      0.165      0.165      0.165      0.165      0.0001
          0.0001         0.165      0.165      0.165      0.165      0.165      0.0001
          0.0001         0.165      0.165      0.165      0.165      0.165      0.0001
          0.0001         0.165      0.165      0.165      0.165      0.165      0.0001
          0.0001         0.165      0.165      0.165      0.165      0.165      0.0001
          0.0001         0.0001         0.0001         0.0001         0.0001
0.0001         0.0001
          0.0001         0.0001         0.0001         0.0001         0.0001
0.0001         0.0001
          0.0001         0.165      0.165      0.165      0.165      0.165      0.0001
```

```
          0.0001         0.165      0.165      0.165      0.165      0.165      0.0001
          0.0001         0.165      0.165      0.165      0.165      0.165      0.0001
          0.0001         0.165      0.165      0.165      0.165      0.165      0.0001
          0.0001         0.165      0.165      0.165      0.165      0.165      0.0001
          0.0001         0.0001         0.0001         0.0001         0.0001
0.0001         0.0001
          0.0001         0.0001         0.0001         0.0001         0.0001
0.0001         0.0001
          0.0001         0.165      0.165      0.165      0.165      0.165      0.0001
          0.0001         0.165      0.165      0.165      0.165      0.165      0.0001
          0.0001         0.165      0.165      0.165      0.165      0.165      0.0001
          0.0001         0.165      0.165      0.165      0.165      0.165      0.0001
          0.0001         0.165      0.165      0.165      0.165      0.165      0.0001
          0.0001         0.0001         0.0001         0.0001         0.0001
0.0001         0.0001
CC
CC Residual saturation of oleic phase displaced by water at low capillary number for I
gridblock
*---- s2rw(i),FOR I=1 TO NX*NY*NZ
        0.0001  0.0001  0.0001  0.0001  0.0001  0.0001  0.0001
        0.0001  0.0001  0.0001  0.0001  0.0001  0.0001  0.0001
        0.0001  0.0001  0.0001  0.0001  0.0001  0.0001  0.0001
        0.0001  0.0001  0.0001  0.0001  0.0001  0.0001  0.0001
        0.0001  0.0001  0.0001  0.0001  0.0001  0.0001  0.0001
        0.0001  0.0001  0.0001  0.0001  0.0001  0.0001  0.0001
        0.0001  0.0001  0.0001  0.0001  0.0001  0.0001  0.0001
        0.0001  0.0001  0.0001  0.0001  0.0001  0.0001  0.0001
        0.0001  0.0001  0.0001  0.0001  0.0001  0.0001  0.0001
        0.0001  0.0001  0.0001  0.0001  0.0001  0.0001  0.0001
        0.0001  0.0001  0.0001  0.0001  0.0001  0.0001  0.0001
        0.0001  0.0001  0.0001  0.0001  0.0001  0.0001  0.0001
        0.0001  0.0001  0.0001  0.0001  0.0001  0.0001  0.0001
        0.0001  0.45    0.45    0.45    0.45    0.45    0.0001
        0.0001  0.45    0.45    0.45    0.45    0.45    0.0001
        0.0001  0.45    0.45    0.45    0.45    0.45    0.0001
        0.0001  0.45    0.45    0.45    0.45    0.45    0.0001
        0.0001  0.45    0.45    0.45    0.45    0.45    0.0001
        0.0001  0.0001  0.0001  0.0001  0.0001  0.0001  0.0001
        0.0001  0.0001  0.0001  0.0001  0.0001  0.0001  0.0001
        0.0001  0.45    0.45    0.45    0.45    0.45    0.0001
        0.0001  0.45    0.45    0.45    0.45    0.45    0.0001
        0.0001  0.45    0.45    0.45    0.45    0.45    0.0001
        0.0001  0.45    0.45    0.45    0.45    0.45    0.0001
        0.0001  0.45    0.45    0.45    0.45    0.45    0.0001
        0.0001  0.0001  0.0001  0.0001  0.0001  0.0001  0.0001
        0.0001  0.0001  0.0001  0.0001  0.0001  0.0001  0.0001
        0.0001  0.45    0.45    0.45    0.45    0.45    0.0001
        0.0001  0.45    0.45    0.45    0.45    0.45    0.0001
        0.0001  0.45    0.45    0.45    0.45    0.45    0.0001
        0.0001  0.45    0.45    0.45    0.45    0.45    0.0001
        0.0001  0.45    0.45    0.45    0.45    0.45    0.0001
        0.0001  0.0001  0.0001  0.0001  0.0001  0.0001  0.0001
        0.0001  0.0001  0.0001  0.0001  0.0001  0.0001  0.0001
        0.0001  0.45    0.45    0.45    0.45    0.45    0.0001
        0.0001  0.45    0.45    0.45    0.45    0.45    0.0001
        0.0001  0.45    0.45    0.45    0.45    0.45    0.0001
        0.0001  0.45    0.45    0.45    0.45    0.45    0.0001
        0.0001  0.45    0.45    0.45    0.45    0.45    0.0001
        0.0001  0.0001  0.0001  0.0001  0.0001  0.0001  0.0001
        0.0001  0.0001  0.0001  0.0001  0.0001  0.0001  0.0001
        0.0001  0.45    0.45    0.45    0.45    0.45    0.0001
        0.0001  0.45    0.45    0.45    0.45    0.45    0.0001
```

```
        0.0001  0.45    0.45    0.45    0.45    0.45    0.0001
        0.0001  0.45    0.45    0.45    0.45    0.45    0.0001
        0.0001  0.45    0.45    0.45    0.45    0.45    0.0001
        0.0001  0.0001  0.0001  0.0001  0.0001  0.0001  0.0001
CC
CC Residual saturation of microemulsion phase displaced by water or oil at low capillary
number for I gridblock
*---- s3rw(i),FOR I=1 TO NX*NY*NZ
          0.0001          0.0001          0.0001          0.0001          0.0001
0.0001          0.0001
          0.0001          0.0001          0.0001          0.0001          0.0001
0.0001          0.0001
          0.0001          0.0001          0.0001          0.0001          0.0001
0.0001          0.0001
          0.0001          0.0001          0.0001          0.0001          0.0001
0.0001          0.0001
          0.0001          0.0001          0.0001          0.0001          0.0001
0.0001          0.0001
          0.0001          0.0001          0.0001          0.0001          0.0001
0.0001          0.0001
          0.0001          0.0001          0.0001          0.0001          0.0001
0.0001          0.0001
          0.0001          0.0001          0.0001          0.0001          0.0001
0.0001          0.0001
          0.0001          0.0001          0.0001          0.0001          0.0001
0.0001          0.0001
          0.0001          0.0001          0.0001          0.0001          0.0001
0.0001          0.0001
          0.0001          0.0001          0.0001          0.0001          0.0001
0.0001          0.0001
          0.0001          0.0001          0.0001          0.0001          0.0001
0.0001          0.0001
          0.0001          0.0001          0.0001          0.0001          0.0001
0.0001          0.0001
          0.0001          0.0001          0.0001          0.0001          0.0001
0.0001          0.0001
          0.0001          0.165       0.165       0.165       0.165       0.165       0.0001
          0.0001          0.165       0.165       0.165       0.165       0.165       0.0001
          0.0001          0.165       0.165       0.165       0.165       0.165       0.0001
          0.0001          0.165       0.165       0.165       0.165       0.165       0.0001
          0.0001          0.165       0.165       0.165       0.165       0.165       0.0001
          0.0001          0.0001          0.0001          0.0001          0.0001
0.0001          0.0001
          0.0001          0.0001          0.0001          0.0001          0.0001
0.0001          0.0001
          0.0001          0.165       0.165       0.165       0.165       0.165       0.0001
          0.0001          0.165       0.165       0.165       0.165       0.165       0.0001
          0.0001          0.165       0.165       0.165       0.165       0.165       0.0001
          0.0001          0.165       0.165       0.165       0.165       0.165       0.0001
          0.0001          0.165       0.165       0.165       0.165       0.165       0.0001
          0.0001          0.0001          0.0001          0.0001          0.0001
0.0001          0.0001
          0.0001          0.0001          0.0001          0.0001          0.0001
0.0001          0.0001
          0.0001          0.165       0.165       0.165       0.165       0.165       0.0001
          0.0001          0.165       0.165       0.165       0.165       0.165       0.0001
          0.0001          0.165       0.165       0.165       0.165       0.165       0.0001
          0.0001          0.165       0.165       0.165       0.165       0.165       0.0001
          0.0001          0.165       0.165       0.165       0.165       0.165       0.0001
          0.0001          0.0001          0.0001          0.0001          0.0001
0.0001          0.0001
```

```
          0.0001         0.0001         0.0001         0.0001         0.0001
0.0001         0.0001
          0.0001         0.165      0.165      0.165      0.165      0.165      0.0001
          0.0001         0.165      0.165      0.165      0.165      0.165      0.0001
          0.0001         0.165      0.165      0.165      0.165      0.165      0.0001
          0.0001         0.165      0.165      0.165      0.165      0.165      0.0001
          0.0001         0.165      0.165      0.165      0.165      0.165      0.0001
          0.0001         0.0001         0.0001         0.0001         0.0001
0.0001         0.0001
          0.0001         0.0001         0.0001         0.0001         0.0001
0.0001         0.0001
          0.0001         0.165      0.165      0.165      0.165      0.165      0.0001
          0.0001         0.165      0.165      0.165      0.165      0.165      0.0001
          0.0001         0.165      0.165      0.165      0.165      0.165      0.0001
          0.0001         0.165      0.165      0.165      0.165      0.165      0.0001
          0.0001         0.165      0.165      0.165      0.165      0.165      0.0001
          0.0001         0.0001         0.0001         0.0001         0.0001
0.0001         0.0001
CC
CC Endpoint relative permeability of water at low capillary number for I gridblock
*---- p1rw(i) ,FOR I=1 TO NX*NY*NZ
          1         1         1         1         1         1         1
          1         1         1         1         1         1         1
          1         1         1         1         1         1         1
          1         1         1         1         1         1         1
          1         1         1         1         1         1         1
          1         1         1         1         1         1         1
          1         1         1         1         1         1         1
          1         1         1         1         1         1         1
          1         1         1         1         1         1         1
          1         1         1         1         1         1         1
          1         1         1         1         1         1         1
          1         1         1         1         1         1         1
          1         1         1         1         1         1         1
          1         1         1         1         1         1         1
          1         0.7       0.7       0.7       0.7       0.7       1
          1         0.7       0.7       0.7       0.7       0.7       1
          1         0.7       0.7       0.7       0.7       0.7       1
          1         0.7       0.7       0.7       0.7       0.7       1
          1         0.7       0.7       0.7       0.7       0.7       1
          1         1         1         1         1         1         1
          1         1         1         1         1         1         1
          1         0.7       0.7       0.7       0.7       0.7       1
          1         0.7       0.7       0.7       0.7       0.7       1
          1         0.7       0.7       0.7       0.7       0.7       1
          1         0.7       0.7       0.7       0.7       0.7       1
          1         0.7       0.7       0.7       0.7       0.7       1
          1         1         1         1         1         1         1
          1         1         1         1         1         1         1
          1         0.7       0.7       0.7       0.7       0.7       1
          1         0.7       0.7       0.7       0.7       0.7       1
          1         0.7       0.7       0.7       0.7       0.7       1
          1         0.7       0.7       0.7       0.7       0.7       1
          1         0.7       0.7       0.7       0.7       0.7       1
          1         1         1         1         1         1         1
          1         1         1         1         1         1         1
          1         0.7       0.7       0.7       0.7       0.7       1
          1         0.7       0.7       0.7       0.7       0.7       1
          1         0.7       0.7       0.7       0.7       0.7       1
          1         0.7       0.7       0.7       0.7       0.7       1
          1         0.7       0.7       0.7       0.7       0.7       1
          1         1         1         1         1         1         1
          1         1         1         1         1         1         1
```

```
          1         0.7       0.7       0.7       0.7       0.7       1
          1         0.7       0.7       0.7       0.7       0.7       1
          1         0.7       0.7       0.7       0.7       0.7       1
          1         0.7       0.7       0.7       0.7       0.7       1
          1         0.7       0.7       0.7       0.7       0.7       1
          1         1         1         1         1         1         1
CC
CC Endpoint relative permeability of oil at low capillary number for I gridblock
*---- p2rw(i) ,FOR I=1 TO NX*NY*NZ
          1         1         1         1         1         1         1
          1         1         1         1         1         1         1
          1         1         1         1         1         1         1
          1         1         1         1         1         1         1
          1         1         1         1         1         1         1
          1         1         1         1         1         1         1
          1         1         1         1         1         1         1
          1         1         1         1         1         1         1
          1         1         1         1         1         1         1
          1         1         1         1         1         1         1
          1         1         1         1         1         1         1
          1         1         1         1         1         1         1
          1         1         1         1         1         1         1
          1         1         1         1         1         1         1
          1         0.23      0.23      0.23      0.23      0.23      1
          1         0.23      0.23      0.23      0.23      0.23      1
          1         0.23      0.23      0.23      0.23      0.23      1
          1         0.23      0.23      0.23      0.23      0.23      1
          1         0.23      0.23      0.23      0.23      0.23      1
          1         1         1         1         1         1         1
          1         1         1         1         1         1         1
          1         0.23      0.23      0.23      0.23      0.23      1
          1         0.23      0.23      0.23      0.23      0.23      1
          1         0.23      0.23      0.23      0.23      0.23      1
          1         0.23      0.23      0.23      0.23      0.23      1
          1         0.23      0.23      0.23      0.23      0.23      1
          1         1         1         1         1         1         1
          1         1         1         1         1         1         1
          1         0.23      0.23      0.23      0.23      0.23      1
          1         0.23      0.23      0.23      0.23      0.23      1
          1         0.23      0.23      0.23      0.23      0.23      1
          1         0.23      0.23      0.23      0.23      0.23      1
          1         0.23      0.23      0.23      0.23      0.23      1
          1         1         1         1         1         1         1
          1         1         1         1         1         1         1
          1         0.23      0.23      0.23      0.23      0.23      1
          1         0.23      0.23      0.23      0.23      0.23      1
          1         0.23      0.23      0.23      0.23      0.23      1
          1         0.23      0.23      0.23      0.23      0.23      1
          1         0.23      0.23      0.23      0.23      0.23      1
          1         1         1         1         1         1         1
CC
CC Endpoint relative permeability of microemulsion at low capillary number for I
gridblock
*---- p3rw(i) ,FOR I=1 TO NX*NY*NZ
          1         1         1         1         1         1         1
          1         1         1         1         1         1         1
```

```
          1         1         1         1         1         1         1
          1         1         1         1         1         1         1
          1         1         1         1         1         1         1
          1         1         1         1         1         1         1
          1         1         1         1         1         1         1
          1         1         1         1         1         1         1
          1         1         1         1         1         1         1
          1         1         1         1         1         1         1
          1         1         1         1         1         1         1
          1         1         1         1         1         1         1
          1         1         1         1         1         1         1
          1         1         1         1         1         1         1
          1         0.7       0.7       0.7       0.7       0.7       1
          1         0.7       0.7       0.7       0.7       0.7       1
          1         0.7       0.7       0.7       0.7       0.7       1
          1         0.7       0.7       0.7       0.7       0.7       1
          1         0.7       0.7       0.7       0.7       0.7       1
          1         1         1         1         1         1         1
          1         1         1         1         1         1         1
          1         0.7       0.7       0.7       0.7       0.7       1
          1         0.7       0.7       0.7       0.7       0.7       1
          1         0.7       0.7       0.7       0.7       0.7       1
          1         0.7       0.7       0.7       0.7       0.7       1
          1         0.7       0.7       0.7       0.7       0.7       1
          1         1         1         1         1         1         1
          1         1         1         1         1         1         1
          1         0.7       0.7       0.7       0.7       0.7       1
          1         0.7       0.7       0.7       0.7       0.7       1
          1         0.7       0.7       0.7       0.7       0.7       1
          1         0.7       0.7       0.7       0.7       0.7       1
          1         0.7       0.7       0.7       0.7       0.7       1
          1         1         1         1         1         1         1
          1         1         1         1         1         1         1
          1         0.7       0.7       0.7       0.7       0.7       1
          1         0.7       0.7       0.7       0.7       0.7       1
          1         0.7       0.7       0.7       0.7       0.7       1
          1         0.7       0.7       0.7       0.7       0.7       1
          1         0.7       0.7       0.7       0.7       0.7       1
          1         1         1         1         1         1         1
CC
CC Altered Endpoint relative permeability of water at low capillary number for I
gridblock
*---- p1rw(i) ,FOR I=1 TO NX*NY*NZ
          1         1         1         1         1         1         1
          1         1         1         1         1         1         1
          1         1         1         1         1         1         1
          1         1         1         1         1         1         1
          1         1         1         1         1         1         1
          1         1         1         1         1         1         1
          1         1         1         1         1         1         1
          1         1         1         1         1         1         1
          1         1         1         1         1         1         1
          1         1         1         1         1         1         1
          1         1         1         1         1         1         1
          1         1         1         1         1         1         1
          1         1         1         1         1         1         1
```

```
          1         1         1         1         1         1         1
          1         1         1         1         1         1         1
          1       0.3       0.3       0.3       0.3       0.3       1
          1       0.3       0.3       0.3       0.3       0.3       1
          1       0.3       0.3       0.3       0.3       0.3       1
          1       0.3       0.3       0.3       0.3       0.3       1
          1       0.3       0.3       0.3       0.3       0.3       1
          1         1         1         1         1         1         1
          1         1         1         1         1         1         1
          1       0.3       0.3       0.3       0.3       0.3       1
          1       0.3       0.3       0.3       0.3       0.3       1
          1       0.3       0.3       0.3       0.3       0.3       1
          1       0.3       0.3       0.3       0.3       0.3       1
          1       0.3       0.3       0.3       0.3       0.3       1
          1         1         1         1         1         1         1
          1         1         1         1         1         1         1
          1       0.3       0.3       0.3       0.3       0.3       1
          1       0.3       0.3       0.3       0.3       0.3       1
          1       0.3       0.3       0.3       0.3       0.3       1
          1       0.3       0.3       0.3       0.3       0.3       1
          1       0.3       0.3       0.3       0.3       0.3       1
          1         1         1         1         1         1         1
          1         1         1         1         1         1         1
          1       0.3       0.3       0.3       0.3       0.3       1
          1       0.3       0.3       0.3       0.3       0.3       1
          1       0.3       0.3       0.3       0.3       0.3       1
          1       0.3       0.3       0.3       0.3       0.3       1
          1       0.3       0.3       0.3       0.3       0.3       1
          1         1         1         1         1         1         1
CC
CC Altered Endpoint relative permeability of oil at low capillary number for I gridblock
*---- p2rw(i) ,FOR I=1 TO NX*NY*NZ
          1         1         1         1         1         1         1
          1         1         1         1         1         1         1
          1         1         1         1         1         1         1
          1         1         1         1         1         1         1
          1         1         1         1         1         1         1
          1         1         1         1         1         1         1
          1         1         1         1         1         1         1
          1         1         1         1         1         1         1
          1         1         1         1         1         1         1
          1         1         1         1         1         1         1
          1         1         1         1         1         1         1
          1         1         1         1         1         1         1
          1         1         1         1         1         1         1
          1         1         1         1         1         1         1
          1         1         1         1         1         1         1
          1       0.5       0.5       0.5       0.5       0.5       1
          1       0.5       0.5       0.5       0.5       0.5       1
          1       0.5       0.5       0.5       0.5       0.5       1
          1       0.5       0.5       0.5       0.5       0.5       1
          1       0.5       0.5       0.5       0.5       0.5       1
          1         1         1         1         1         1         1
          1         1         1         1         1         1         1
          1       0.5       0.5       0.5       0.5       0.5       1
          1       0.5       0.5       0.5       0.5       0.5       1
          1       0.5       0.5       0.5       0.5       0.5       1
```

```
          1         0.5       0.5       0.5       0.5       0.5       1
          1         0.5       0.5       0.5       0.5       0.5       1
          1         1         1         1         1         1         1
          1         1         1         1         1         1         1
          1         0.5       0.5       0.5       0.5       0.5       1
          1         0.5       0.5       0.5       0.5       0.5       1
          1         0.5       0.5       0.5       0.5       0.5       1
          1         0.5       0.5       0.5       0.5       0.5       1
          1         0.5       0.5       0.5       0.5       0.5       1
          1         1         1         1         1         1         1
          1         1         1         1         1         1         1
          1         0.5       0.5       0.5       0.5       0.5       1
          1         0.5       0.5       0.5       0.5       0.5       1
          1         0.5       0.5       0.5       0.5       0.5       1
          1         0.5       0.5       0.5       0.5       0.5       1
          1         0.5       0.5       0.5       0.5       0.5       1
          1         1         1         1         1         1         1
          1         1         1         1         1         1         1
          1         0.5       0.5       0.5       0.5       0.5       1
          1         0.5       0.5       0.5       0.5       0.5       1
          1         0.5       0.5       0.5       0.5       0.5       1
          1         0.5       0.5       0.5       0.5       0.5       1
          1         0.5       0.5       0.5       0.5       0.5       1
          1         1         1         1         1         1         1
CC
CC Altered Endpoint relative permeability of microemulsion at low capillary number for I
gridblock
*---- p3rw(i) ,FOR I=1 TO NX*NY*NZ
          1         1         1         1         1         1         1
          1         1         1         1         1         1         1
          1         1         1         1         1         1         1
          1         1         1         1         1         1         1
          1         1         1         1         1         1         1
          1         1         1         1         1         1         1
          1         1         1         1         1         1         1
          1         1         1         1         1         1         1
          1         1         1         1         1         1         1
          1         1         1         1         1         1         1
          1         1         1         1         1         1         1
          1         1         1         1         1         1         1
          1         1         1         1         1         1         1
          1         1         1         1         1         1         1
          1         1         1         1         1         1         1
          1         0.3       0.3       0.3       0.3       0.3       1
          1         0.3       0.3       0.3       0.3       0.3       1
          1         0.3       0.3       0.3       0.3       0.3       1
          1         0.3       0.3       0.3       0.3       0.3       1
          1         0.3       0.3       0.3       0.3       0.3       1
          1         1         1         1         1         1         1
          1         1         1         1         1         1         1
          1         0.3       0.3       0.3       0.3       0.3       1
          1         0.3       0.3       0.3       0.3       0.3       1
          1         0.3       0.3       0.3       0.3       0.3       1
          1         0.3       0.3       0.3       0.3       0.3       1
          1         0.3       0.3       0.3       0.3       0.3       1
          1         1         1         1         1         1         1
          1         1         1         1         1         1         1
          1         0.3       0.3       0.3       0.3       0.3       1
          1         0.3       0.3       0.3       0.3       0.3       1
          1         0.3       0.3       0.3       0.3       0.3       1
          1         0.3       0.3       0.3       0.3       0.3       1
          1         0.3       0.3       0.3       0.3       0.3       1
          1         1         1         1         1         1         1
          1         1         1         1         1         1         1
```

```
          1         0.3       0.3       0.3       0.3       0.3       1
          1         0.3       0.3       0.3       0.3       0.3       1
          1         0.3       0.3       0.3       0.3       0.3       1
          1         0.3       0.3       0.3       0.3       0.3       1
          1         0.3       0.3       0.3       0.3       0.3       1
          1         1         1         1         1         1         1
          1         1         1         1         1         1         1
          1         0.3       0.3       0.3       0.3       0.3       1
          1         0.3       0.3       0.3       0.3       0.3       1
          1         0.3       0.3       0.3       0.3       0.3       1
          1         0.3       0.3       0.3       0.3       0.3       1
          1         0.3       0.3       0.3       0.3       0.3       1
          1         1         1         1         1         1         1
CC
CC Relative permeability  exponent of aqueous phase at low capillary number for I
gridblock
*---- e1w(i) ,FOR I=1 TO NX*NY*NZ
          1         1         1         1         1         1         1
          1         1         1         1         1         1         1
          1         1         1         1         1         1         1
```

```
          1         1.9      1.9      1.9      1.9      1.9      1
          1         1         1         1         1         1         1
CC
CC Relative permeability  exponent of oleic phase at low capillary number for I gridblock
*---- e2w(i) ,FOR I=1 TO NX*NY*NZ
          1         1         1         1         1         1         1
          1         1         1         1         1         1         1
          1         1         1         1         1         1         1
          1         1         1         1         1         1         1
          1         1         1         1         1         1         1
          1         1         1         1         1         1         1
          1         1         1         1         1         1         1
          1         1         1         1         1         1         1
          1         1         1         1         1         1         1
          1         1         1         1         1         1         1
          1         1         1         1         1         1         1
          1         1         1         1         1         1         1
          1         1         1         1         1         1         1
          1         1         1         1         1         1         1
          1         6      6      6      6      6      1
          1         6      6      6      6      6      1
          1         6      6      6      6      6      1
          1         6      6      6      6      6      1
          1         6      6      6      6      6      1
          1         1         1         1         1         1         1
          1         1         1         1         1         1         1
          1         6      6      6      6      6      1
          1         6      6      6      6      6      1
          1         6      6      6      6      6      1
          1         6      6      6      6      6      1
          1         6      6      6      6      6      1
          1         1         1         1         1         1         1
          1         1         1         1         1         1         1
          1         6      6      6      6      6      1
          1         6      6      6      6      6      1
          1         6      6      6      6      6      1
          1         6      6      6      6      6      1
          1         6      6      6      6      6      1
          1         1         1         1         1         1         1
          1         1         1         1         1         1         1
          1         6      6      6      6      6      1
          1         6      6      6      6      6      1
          1         6      6      6      6      6      1
          1         6      6      6      6      6      1
          1         6      6      6      6      6      1
          1         1         1         1         1         1         1
          1         1         1         1         1         1         1
          1         6      6      6      6      6      1
          1         6      6      6      6      6      1
          1         6      6      6      6      6      1
          1         6      6      6      6      6      1
          1         6      6      6      6      6      1
          1         1         1         1         1         1         1
CC
CC Relative permeability  exponent of microemulsion phase at low capillary number for I
gridblock
*---- e3w(i) ,FOR I=1 TO NX*NY*NZ
          1         1         1         1         1         1         1
          1         1         1         1         1         1         1
          1         1         1         1         1         1         1
          1         1         1         1         1         1         1
          1         1         1         1         1         1         1
          1         1         1         1         1         1         1
```

```
          1         1         1         1         1         1         1
          1         1         1         1         1         1         1
          1         1         1         1         1         1         1
          1         1         1         1         1         1         1
          1         1         1         1         1         1         1
          1         1         1         1         1         1         1
          1         1         1         1         1         1         1
          1         1         1         1         1         1         1
          1         1         1         1         1         1         1
          1       1.9       1.9       1.9       1.9       1.9         1
          1       1.9       1.9       1.9       1.9       1.9         1
          1       1.9       1.9       1.9       1.9       1.9         1
          1       1.9       1.9       1.9       1.9       1.9         1
          1       1.9       1.9       1.9       1.9       1.9         1
          1         1         1         1         1         1         1
          1         1         1         1         1         1         1
          1       1.9       1.9       1.9       1.9       1.9         1
          1       1.9       1.9       1.9       1.9       1.9         1
          1       1.9       1.9       1.9       1.9       1.9         1
          1       1.9       1.9       1.9       1.9       1.9         1
          1       1.9       1.9       1.9       1.9       1.9         1
          1         1         1         1         1         1         1
          1         1         1         1         1         1         1
          1       1.9       1.9       1.9       1.9       1.9         1
          1       1.9       1.9       1.9       1.9       1.9         1
          1       1.9       1.9       1.9       1.9       1.9         1
          1       1.9       1.9       1.9       1.9       1.9         1
          1       1.9       1.9       1.9       1.9       1.9         1
          1         1         1         1         1         1         1
          1         1         1         1         1         1         1
          1       1.9       1.9       1.9       1.9       1.9         1
          1       1.9       1.9       1.9       1.9       1.9         1
          1       1.9       1.9       1.9       1.9       1.9         1
          1       1.9       1.9       1.9       1.9       1.9         1
          1       1.9       1.9       1.9       1.9       1.9         1
          1         1         1         1         1         1         1
CC
CC Altered Relative permeability  exponent of aqueous phase at low capillary number for I
gridblock
*---- e1w(i) ,FOR I=1 TO NX*NY*NZ
          1         1         1         1         1         1         1
          1         1         1         1         1         1         1
          1         1         1         1         1         1         1
          1         1         1         1         1         1         1
          1         1         1         1         1         1         1
          1         1         1         1         1         1         1
          1         1         1         1         1         1         1
          1         1         1         1         1         1         1
          1         1         1         1         1         1         1
          1         1         1         1         1         1         1
          1         1         1         1         1         1         1
          1         1         1         1         1         1         1
          1         1         1         1         1         1         1
          1         1         1         1         1         1         1
          1         1         1         1         1         1         1
          1         1         1         1         1         1         1
          1       2.5       2.5       2.5       2.5       2.5         1
          1       2.5       2.5       2.5       2.5       2.5         1
```

```
          1         2.5       2.5       2.5       2.5       2.5       1
          1         2.5       2.5       2.5       2.5       2.5       1
          1         2.5       2.5       2.5       2.5       2.5       1
          1         1          1         1          1         1         1
          1         1          1         1          1         1         1
          1         2.5       2.5       2.5       2.5       2.5       1
          1         2.5       2.5       2.5       2.5       2.5       1
          1         2.5       2.5       2.5       2.5       2.5       1
          1         2.5       2.5       2.5       2.5       2.5       1
          1         2.5       2.5       2.5       2.5       2.5       1
          1         1          1         1          1         1         1
          1         1          1         1          1         1         1
          1         2.5       2.5       2.5       2.5       2.5       1
          1         2.5       2.5       2.5       2.5       2.5       1
          1         2.5       2.5       2.5       2.5       2.5       1
          1         2.5       2.5       2.5       2.5       2.5       1
          1         2.5       2.5       2.5       2.5       2.5       1
          1         1          1         1          1         1         1
          1         1          1         1          1         1         1
          1         2.5       2.5       2.5       2.5       2.5       1
          1         2.5       2.5       2.5       2.5       2.5       1
          1         2.5       2.5       2.5       2.5       2.5       1
          1         2.5       2.5       2.5       2.5       2.5       1
          1         2.5       2.5       2.5       2.5       2.5       1
          1         1          1         1          1         1         1
          1         1          1         1          1         1         1
          1         2.5       2.5       2.5       2.5       2.5       1
          1         2.5       2.5       2.5       2.5       2.5       1
          1         2.5       2.5       2.5       2.5       2.5       1
          1         2.5       2.5       2.5       2.5       2.5       1
          1         2.5       2.5       2.5       2.5       2.5       1
          1         1          1         1          1         1         1
CC
CC Altered Relative permeability  exponent of oleic phase at low capillary number for I
gridblock
*---- e2w(i) ,FOR I=1 TO NX*NY*NZ
          1         1         1         1         1         1
          1         1         1         1         1         1
          1         1         1         1         1         1
          1         1         1         1         1         1
          1         1         1         1         1         1
          1         1         1         1         1         1
          1         1         1         1         1         1
          1         1         1         1         1         1
          1         1         1         1         1         1
          1         1         1         1         1         1
          1         1         1         1         1         1
          1         1         1         1         1         1
          1         1         1         1         1         1
          1         1         1         1         1         1
          1         1         1         1         1         1
          1         7.5       7.5       7.5       7.5       7.5       1
          1         7.5       7.5       7.5       7.5       7.5       1
          1         7.5       7.5       7.5       7.5       7.5       1
          1         7.5       7.5       7.5       7.5       7.5       1
          1         7.5       7.5       7.5       7.5       7.5       1
          1         1          1         1          1         1         1
          1         1          1         1          1         1         1
          1         7.5       7.5       7.5       7.5       7.5       1
          1         7.5       7.5       7.5       7.5       7.5       1
          1         7.5       7.5       7.5       7.5       7.5       1
          1         7.5       7.5       7.5       7.5       7.5       1
          1         7.5       7.5       7.5       7.5       7.5       1
          1         1          1         1          1         1         1
```

```
          1         1         1         1         1         1         1
          1         7.5       7.5       7.5       7.5       7.5       1
          1         7.5       7.5       7.5       7.5       7.5       1
          1         7.5       7.5       7.5       7.5       7.5       1
          1         7.5       7.5       7.5       7.5       7.5       1
          1         7.5       7.5       7.5       7.5       7.5       1
          1         1         1         1         1         1         1
          1         1         1         1         1         1         1
          1         7.5       7.5       7.5       7.5       7.5       1
          1         7.5       7.5       7.5       7.5       7.5       1
          1         7.5       7.5       7.5       7.5       7.5       1
          1         7.5       7.5       7.5       7.5       7.5       1
          1         7.5       7.5       7.5       7.5       7.5       1
          1         1         1         1         1         1         1
          1         1         1         1         1         1         1
          1         7.5       7.5       7.5       7.5       7.5       1
          1         7.5       7.5       7.5       7.5       7.5       1
          1         7.5       7.5       7.5       7.5       7.5       1
          1         7.5       7.5       7.5       7.5       7.5       1
          1         7.5       7.5       7.5       7.5       7.5       1
          1         1         1         1         1         1         1
CC
CC Altered Relative permeability  exponent of microemulsion phase at low capillary number
for I gridblock
*---- e3w(i) ,FOR I=1 TO NX*NY*NZ
          1         1         1         1         1         1         1
          1         1         1         1         1         1         1
          1         1         1         1         1         1         1
          1         1         1         1         1         1         1
          1         1         1         1         1         1         1
          1         1         1         1         1         1         1
          1         1         1         1         1         1         1
          1         1         1         1         1         1         1
          1         1         1         1         1         1         1
          1         1         1         1         1         1         1
          1         1         1         1         1         1         1
          1         1         1         1         1         1         1
          1         1         1         1         1         1         1
          1         1         1         1         1         1         1
          1         2.5       2.5       2.5       2.5       2.5       1
          1         2.5       2.5       2.5       2.5       2.5       1
          1         2.5       2.5       2.5       2.5       2.5       1
          1         2.5       2.5       2.5       2.5       2.5       1
          1         2.5       2.5       2.5       2.5       2.5       1
          1         1         1         1         1         1         1
          1         1         1         1         1         1         1
          1         2.5       2.5       2.5       2.5       2.5       1
          1         2.5       2.5       2.5       2.5       2.5       1
          1         2.5       2.5       2.5       2.5       2.5       1
          1         2.5       2.5       2.5       2.5       2.5       1
          1         2.5       2.5       2.5       2.5       2.5       1
          1         1         1         1         1         1         1
          1         1         1         1         1         1         1
          1         2.5       2.5       2.5       2.5       2.5       1
          1         2.5       2.5       2.5       2.5       2.5       1
          1         2.5       2.5       2.5       2.5       2.5       1
```

```
          1         2.5      2.5      2.5      2.5      2.5      1
          1         2.5      2.5      2.5      2.5      2.5      1
          1         1         1         1         1         1         1
          1         1         1         1         1         1         1
          1         2.5      2.5      2.5      2.5      2.5      1
          1         2.5      2.5      2.5      2.5      2.5      1
          1         2.5      2.5      2.5      2.5      2.5      1
          1         2.5      2.5      2.5      2.5      2.5      1
          1         2.5      2.5      2.5      2.5      2.5      1
          1         1         1         1         1         1         1
CC
CC  RES. SATURATION OF PHASES 1,2,AND 3 AT HIGH CAPILLARY NO.
*----S1RC  S2RC  S3RC
     .0    .0    .0
CC
CC ENDPOINT REL. PERM. OF PHASES 1,2,AND 3 AT HIGH CAPILLARY NO.
*----P1RC  P2RC  P3RC
     1.    1.    1.
CC
CC REL. PERM. EXPONENT OF PHASES 1,2,AND 3 AT HIGH CAPILLARY NO.
*----E13C  E23C  E31C
     1.     1.    1.
CC
CC WATER AND OIL VISCOSITY , RESERVOIR TEMPERATURE
*---- VIS1    VIS2   TSTAND
       1       3.5       0
CC
CC COMPOSITIONAL PHASE VISCOSITY PARAMETERS
*----   ALPHAV1   ALPHAV2   ALPHAV3   ALPHAV4  ALPHAV5
         2         2         0         0.9       0.7
CC
CC PARAMETERS TO CALCULATE POLYMER VISCOSITY AT ZERO SHEAR RATE
*---- AP1      AP2      AP3
       13      64     75
CC
CC PARAMETER TO COMPUTE CSEP,MIN. CSEP, AND SLOPE OF LOG VIS. VS. LOG CSEP
*---- BETAP    CSE1     SSLOPE
       1      0.01     -0.2398
CC
CC PARAMETER FOR SHEAR RATE DEPENDENCE OF POLYMER VISCOSITY
*---- GAMMAC   GAMHF   POWN    ipmod  ishear   rweff
       130       400    2.3     0      0      0.25
CC
CC CC FLAG FOR POLYMER PARTITIONING, PERM. REDUCTION PARAMETERS
*---- IPOLYM    EPHI3    EPHI4    BRK     CRK
        1         1       1       100    0.12   5
CC
CC SPECIFIC WEIGHT FOR COMPONENTS 1,2,3,7,8 ,Coeffient of oil and GRAVITY FLAG
*---- DEN1     DEN2    DEN23     DEN3    DEN7    DEN8    IDEN
      0.433     0.382     0.382     0.433     0.346    0        2
CC
CC FLAG FOR CHOICE OF UNITS ( 0:BOTTOMHOLE CONDITION , 1: STOCK TANK)
*----- ISTB
        0
CC
CC COMPRESSIBILITY FOR VOL. OCCUPYING COMPONENTS 1,2,3,7,AND 8
*---- COMPC(1)  COMPC(2)  COMPC(3)  COMPC(7)  COMPC(8)
         0         0         0         0         0
CC
CC CONSTANT OR VARIABLE PC PARAM., WATER-WET OR OIL-WET PC CURVE FLAG
*---- ICPC    IEPC   IOW
       2       2      2
CC
CC  CAPILLARY PRESSURE ENDPOINT FOR GRIDBLOCK
```

```
*---- CPC(I),I=1 TO NX*NY*NZ
          0         0         0         0         0         0         0
          0         0         0         0         0         0         0
          0         0         0         0         0         0         0
          0         0         0         0         0         0         0
          0         0         0         0         0         0         0
          0         0         0         0         0         0         0
          0         0         0         0         0         0         0
          0         0         0         0         0         0         0
          0         0         0         0         0         0         0
          0         0         0         0         0         0         0
          0         0         0         0         0         0         0
          0         0         0         0         0         0         0
          0         0         0         0         0         0         0
          0         0         0         0         0         0         0
          0         5    5    5    5    5    0
          0         5    5    5    5    5    0
          0         5    5    5    5    5    0
          0         5    5    5    5    5    0
          0         5    5    5    5    5    0
          0         0         0         0         0         0         0
          0         0         0         0         0         0         0
          0         5    5    5    5    5    0
          0         5    5    5    5    5    0
          0         5    5    5    5    5    0
          0         5    5    5    5    5    0
          0         5    5    5    5    5    0
          0         0         0         0         0         0         0
          0         0         0         0         0         0         0
          0         5    5    5    5    5    0
          0         5    5    5    5    5    0
          0         5    5    5    5    5    0
          0         5    5    5    5    5    0
          0         5    5    5    5    5    0
          0         0         0         0         0         0         0
          0         0         0         0         0         0         0
          0         5    5    5    5    5    0
          0         5    5    5    5    5    0
          0         5    5    5    5    5    0
          0         5    5    5    5    5    0
          0         5    5    5    5    5    0
          0         0         0         0         0         0         0
          0         0         0         0         0         0         0
          0         5    5    5    5    5    0
          0         5    5    5    5    5    0
          0         5    5    5    5    5    0
          0         5    5    5    5    5    0
          0         5    5    5    5    5    0
          0         0         0         0         0         0         0
c
c
*------------
          343*2
c
c
*--------
          0         0         0         0         0         0         0
          0         0         0         0         0         0         0
          0         0         0         0         0         0         0
          0         0         0         0         0         0         0
          0         0         0         0         0         0         0
          0         0         0         0         0         0         0
          0         0         0         0         0         0         0
```

```
          0         0         0         0         0         0         0
          0         0         0         0         0         0         0
          0         0         0         0         0         0         0
          0         0         0         0         0         0         0
          0         0         0         0         0         0         0
          0         0         0         0         0         0         0
          0         0         0         0         0         0         0
          0         0         0         0         0         0         0
          0        -5    -5    -5    -5    -5     0
          0        -5    -5    -5    -5    -5     0
          0        -5    -5    -5    -5    -5     0
          0        -5    -5    -5    -5    -5     0
          0        -5    -5    -5    -5    -5     0
          0         0         0         0         0         0         0
          0         0         0         0         0         0         0
          0        -5    -5    -5    -5    -5     0
          0        -5    -5    -5    -5    -5     0
          0        -5    -5    -5    -5    -5     0
          0        -5    -5    -5    -5    -5     0
          0        -5    -5    -5    -5    -5     0
          0         0         0         0         0         0         0
          0         0         0         0         0         0         0
          0        -5    -5    -5    -5    -5     0
          0        -5    -5    -5    -5    -5     0
          0        -5    -5    -5    -5    -5     0
          0        -5    -5    -5    -5    -5     0
          0        -5    -5    -5    -5    -5     0
          0         0         0         0         0         0         0
          0         0         0         0         0         0         0
          0        -5    -5    -5    -5    -5     0
          0        -5    -5    -5    -5    -5     0
          0        -5    -5    -5    -5    -5     0
          0        -5    -5    -5    -5    -5     0
          0        -5    -5    -5    -5    -5     0
          0         0         0         0         0         0         0
c
c
*--------
        343*2
c
c
*---  S STAR
       343*0.35
CC
CC CONSTANT OR VARIABLE PC PARAM., WATER-WET OR OIL-WET PC CURVE FLAG
*---- ICPC    IEPC   IOW
       2       0      0
CC
CC  CAPILLARY PRESSURE ENDPOINT FOR GRIDBLOCK
*---- CPC0
       0       0       0       0       0       0       0       0       0       0
       0       0       0       0       0       0       0       0       0       0
       0       0       0       0       0       0       0       0       0       0
       0       0       0       0       0       0       0       0       0       0
       0       0       0       0       0       0       0       0       0       0
       0       0       0       0       0       0       0       0       0       0
       0       0       0       0       0       0       0       0       0       0
```

```
        0       0       0       0       0       0       0       0       0       0
        0       0       0       0       0       0       0       0       0       0
        0       0       0       0       0       0       0       0       0       0
        0       0       0       0       0       0       8.95    8.95    8.95    8.95
        8.95    0       0       8.95    8.95    8.95    8.95    8.95    0       0
        8.95    8.95    8.95    8.95    8.95    0       0       8.95    8.95    8.95
        8.95    8.95    0       0       8.95    8.95    8.95    8.95    8.95    0
        0       0       0       0       0       0       0       0       0       0
        0       0       0       0       0       8.95    8.95    8.95    8.95    8.95
        0       0       8.95    8.95    8.95    8.95    8.95    0       0       8.95
        8.95    8.95    8.95    8.95    0       0       8.95    8.95    8.95    8.95
        8.95    0       0       8.95    8.95    8.95    8.95    8.95    0       0
        0       0       0       0       0       0       0       0       0       0
        0       0       0       0       0       8.95    8.95    8.95    8.95    0
        0       8.95    8.95    8.95    8.95    8.95    0       0       8.95    8.95
        8.95    8.95    8.95    0       0       8.95    8.95    8.95    8.95    8.95
        0       0       8.95    8.95    8.95    8.95    8.95    0       0       0
        0       0       0       0       0       0       0       0       0       0
        0       0       0       8.95    8.95    8.95    8.95    8.95    0       0
        8.95    8.95    8.95    8.95    8.95    0       0       8.95    8.95    8.95
        8.95    8.95    0       0       8.95    8.95    8.95    8.95    8.95    0
        0       8.95    8.95    8.95    8.95    8.95    0       0       0       0
        0       0       0       0       0       0       0       0       0       0
        0       0       8.95    8.95    8.95    8.95    8.95    0       0       8.95
        8.95    8.95    8.95    8.95    0       0       8.95    8.95    8.95    8.95
        8.95    0       0       8.95    8.95    8.95    8.95    8.95    0       0
        8.95    8.95    8.95    8.95    8.95    0       0       0       0       0
        0       0       0
CC
CC CAPILLARY PRESSURE PARAMETER, EPC0
*---- EPC0
       2.5
CC
CC MOLECULAR DIFFUSION COEF. KCTH COMPONENT IN PHASE 1
*---- D(KC,1),KC=1,N
         0        0        0.0065   0        0        0
CC
CC MOLECULAR DIFFUSION COEF. KCTH COMPONENT IN PHASE 2
*---- D(KC,2),KC=1,N
         0        0        0        0        0        0
CC
CC MOLECULAR DIFFUSION COEF. KCTH COMPONENT IN PHASE 3
*---- D(KC,3),KC=1,N
         0        0        0.0065        0        0        0
CC
CC LONGITUDINAL AND TRANSVERSE DISPERSIVITY OF PHASE 1
*---- ALPHAL(1)     ALPHAT(1)
         0           0
CC
CC LONGITUDINAL AND TRANSVERSE DISPERSIVITY OF PHASE 2
*---- ALPHAL(2)     ALPHAT(2)
         0           0
CC
CC LONGITUDINAL AND TRANSVERSE DISPERSIVITY OF PHASE 3
*---- ALPHAL(3)     ALPHAT(3)
         0           0
CC
CC flag to specify organic adsorption calculation
*---- iadso
        0
CC
CC SURFACTANT AND POLYMER ADSORPTION PARAMETERS
*---- AD31    AD32   B3D    AD41   AD42   B4D   IADK  IADS1   FADS   REFK
      0      0    1000    0     0     100     0     0      0      50
```

```
CC
CC PARAMETERS FOR CATION EXCHANGE OF CLAY AND SURFACTANT
*---- QV      XKC     XKS     EQW
      0    0     0      804
CC
CC*********************************************************************
CC                                                                     *
CC    WELL DATA                                                        *
CC                                                                     *
CC*********************************************************************
CC
CC
CC FLAG FOR SPECIFIED BOUNDARY AND ZONE IS MODELED
*---- IBOUND     IZONE
       0      0
CC
CC TOTAL NUMBER OF WELLS, WELL RADIUS FLAG, FLAG FOR TIME OR COURANT NO.
*---- NWELL   IRO    ITIME    NWREL
       1      2       0        1
CC
CC WELL ID,LOCATIONS,AND FLAG FOR SPECIFYING WELL TYPE, WELL RADIUS, SKIN
*---- IDW    IW    JW    IFLAG    RW     SWELL   IDIR   IFIRST   ILAST   IPRF
       1     1     1       1      0.001       0       3      1      1      0
CC
CC WELL NAME
*----  WELNAM
Fake
CC
CC ICHEK , MAX. AND MIN. ALLOWABLE BOTTOMHOLE PRESSURE AND RATE
*---- ICHEK     PWFMIN     PWFMAX    QTMIN    QTMAX
       0          0         10      0        10
CC
CC  ID,INJ. RATE AND INJ. COMP. FOR RATE CONS. WELLS FOR EACH PHASE (L=1,3)
*----  ID     QI(M,L)     C(M,KC,L)
       1      0      1      0      0      0      0      0
       1      0      0      0      0      0      0      0
       1      0      0      0      0      0      0      0
CC
CC CUM. INJ. TIME , AND INTERVALS (PV OR DAY) FOR WRITING TO OUTPUT FILES
*---- TINJ     CUMPR1     CUMHI1     WRHPV     WRPRF      RSTC
       0.1      0.01        0.01        0.01      0.01       0.01
CC
CC THE INI. TIME STEP,CONC. TOLERANCE,MAX.,MIN. time steps
*----  DT     DELC(I)              DTMAX            DTMIN
       1E-09          0.0005      0.0005      0.000008      0.001      0.001      0.001
0.001      0.0000001
CC
CC
*----IBMOD
       0
CC
CC
*----IRO ITIME IFLAG
       2       0       1
CC
CC NUMBER OF WELLS changes IN LOCATION OR SKIN OR PWF
*----NWEL1
      0
CC
CC NUMBER OF WELLS WITH RATE changes, id
*----NWEL1
     0
CC
CC CUM. INJ. TIME , AND INTERVALS (PV OR DAY) FOR WRITING TO OUTPUT FILES
```

```
*---- TINJ     CUMPR1     CUMHI1     WRHPV     WRPRF      RSTC
       1      0.1        0.1        0.1      0.1       0.1
CC
CC THE INI. TIME STEP,CONC. TOLERANCE,MAX.,MIN. time steps
*----  DT     DELC(I)              DTMAX            DTMIN
       1E-09          0.0005      0.0005      0.000008      0.001      0.001      0.001
0.001      0.0000001
CC
CC
*----IBMOD
       0
CC
CC
*----IRO ITIME IFLAG
       2       0       1
CC
CC NUMBER OF WELLS changes IN LOCATION OR SKIN OR PWF
*----NWEL1
      0
CC
CC NUMBER OF WELLS WITH RATE changes, id
*----NWEL1
     0
CC
CC CUM. INJ. TIME , AND INTERVALS (PV OR DAY) FOR WRITING TO OUTPUT FILES
*---- TINJ     CUMPR1     CUMHI1     WRHPV     WRPRF      RSTC
       10       1        1        1      1       1
CC
CC THE INI. TIME STEP,CONC. TOLERANCE,MAX.,MIN. time steps
*----  DT     DELC(I)              DTMAX            DTMIN
       1E-09          0.0005      0.0005      0.000008      0.001      0.001      0.001
0.001     0.0000001
CC
CC
*----IBMOD
       0
CC
CC
*----IRO ITIME IFLAG
       2       0       1
CC
CC NUMBER OF WELLS changes IN LOCATION OR SKIN OR PWF
*----NWEL1
      0
CC
CC NUMBER OF WELLS WITH RATE changes, id
*----NWEL1
     0
CC
CC CUM. INJ. TIME , AND INTERVALS (PV OR DAY) FOR WRITING TO OUTPUT FILES
*---- TINJ     CUMPR1     CUMHI1     WRHPV     WRPRF      RSTC
       150      2        2        2      2       2
CC
CC THE INI. TIME STEP,CONC. TOLERANCE,MAX.,MIN. time steps
*----  DT     DELC(I)              DTMAX            DTMIN
       1E-09          0.0005      0.0005      0.000008      0.001      0.001      0.001
0.001      0.0000001
```

A.5 Heterogeneous Fractured Coreflood Case

The following is the input data file for heterogeneous vuggy fractured coreflood in UTCHEM simulator. We used this case in Chapter 6 for modeling coreflood experiment to investigate wettability alteration and IFT reduction dynamically using surfactant solution. In order to run this case for wettability alteration, IWALT flag in input file should be set IWALT=1 along with relative permeability and capillary pressure data before and after wettability alteration.

```
CC**********************************************************************
CC                                                                     *
CC     BRIEF DESCRIPTION OF DATA SET : UTCHEM (VERSION 9.95 )          *
CC                                                                     *
CC**********************************************************************
CC                                                                     *
CC  Surfactant Hetregenous Coreflood test                              *
CC                                                                     *
CC  LENGTH (FT):  0.899                                                *
CC  THICKNESS (FT) : 0.295                                             *
CC  WIDTH (FT) :    0.295            POROSITY : 0.097                  *
CC  NJ. RATE (FT3/DAY) : 0.00168                                       *
CC  GRID BLOCKS : 5x5x10               COORDINATE : CARTESIAN          *
CC  DATE : 6/8/2012                                                    *
CC                                                                    *
CC**********************************************************************
CC
CC**********************************************************************
CC                                                                     *
CC    RESERVOIR DESCRIPTION                                            *
CC                                                                     *
CC**********************************************************************
CC
CC Run number
*---- RUNNO
CC
CC
CC Title and run description
*---- title(i)
PEMEX-Surfactant AKL-523 core flood core
Cartesian Coord with Square Core with same XArea and Pore Volume
1 % Surf in solution
CC
CC SIMULATION FLAGS
*---- IMODE IMES IDISPC ICWM ICAP IREACT IBIO ICOORD ITREAC ITC  IGAS  IENG
        1    1     3     0    0     0     0     1      0     0    0     0
CC
```

```
CC no. of gridblocks,flag specifies constant or variable grid size,unit
*---- NX    NY    NZ  IDXYZ  IUNIT
      5     5     10    2      0
CC
CC GRID SIZE OF BLOCK IN X DIRECTION
*---- DX(I), FOR I=1 TO NX
          5*0.059
CC
CC GRID SIZE OF BLOCK IN Y DIRECTION
*---- DY(I), FOR I=1 TO NY
          5*0.059
CC
CC GRID SIZE OF BLOCK IN Z DIRECTION
*----DZ(I), FOR I=1 TO NZ
          10*0.0899
CC
CC total no. of components,no. of tracers,no. of gel components
*----n    no    ntw    nta    ngc    ng    noth
     6    0      0      0      0     0      0
CC
CC Name of the components
*----spname(i) for i=1 to n
Water
Oil
Surf.
Polymer
Chloride
Calcium
CC
CC flag indicating if the component is included in calculations or not
*----icf(kc) for kc=1,n
      1   1   1   0   1   1
CC
CC*********************************************************************
CC                                                                     *
CC    OUTPUT OPTIONS                                                   *
CC                                                                     *
CC*********************************************************************
CC
CC
CC FLAG TO WRITE TO UNIT 3,FLAG FOR PV OR DAYS TO PRINT OR TO STOP THE RUN
*---- ICUMTM  ISTOP  IOUTGMS
        1       1       0
CC
CC FLAG INDICATING IF THE PROFILE OF KCTH COMPONENT SHOULD BE WRITTEN
*---- IPRFLG(KC),KC=1,N
        1   1  1   0   1   1
CC
CC FLAG FOR PRES.,SAT.,TOTAL CONC.,TRACER CONC.,CAP.,GEL, ALKALINE PROFILES
*---- IPPRES IPSAT IPCTOT IPBIO IPCAP IPGEL IPALK IPTEMP IPOBS
        1      1      1      0     0     0     0     0      0
CC
CC FLAG FOR WRITING SEVERAL PROPERTIES TO UNIT 4 (Prof)
*---- ICKL IVIS IPER ICNM ICSE IHYSTP IFOAMP INONEQ
       1    1   1    1    1    0    0    0
CC
CC FLAG  for variables to PROF output file
*---- IADS IVEL IRKF IPHSE
       1    1    0    1
CC
CC*********************************************************************
CC                                                                     *
CC    RESERVOIR PROPERTIES                                             *
CC                                                                     *
```

```
CC*********************************************************************
CC
CC
CC MAX. SIMULATION TIME ( DAYS)
*---- TMAX
       1.71
CC
CC ROCK COMPRESSIBILITY (1/PSI), STAND. PRESSURE(PSIA)
*---- COMPR               PSTAND
        1e-7                  1000
CC
CC FLAGS INDICATING CONSTANT OR VARIABLE POROSITY, X,Y,AND Z PERMEABILITY
*---- IPOR1  IPERMX IPERMY IPERMZ IMOD
        0      2      3      3     0   0   0
CC  Reported average
CC VARIABLE POROSITY OVER RESERVOIR
*---- POR(I),FOR I=1 TO NX*NY*NZ
      0.097
CC  Stoichastioc average of 1970, vdp=0.9
CC VARIABLE PERMEABILITY OVER RESERVOIR
*---- PERMX(I),FOR I=1 TO NX*NY*NZ
    972.6       171.3       2613.       46.59       6654.
   371.8        323.9       74.41       161.0       427.3
   156.0      0.1886E+05    879.6       78.33       64.21
   115.9        383.6       128.0       73.03       26.80
   8252.        326.6       217.4       10.38       198.5
   2099.        34.15       2353.       2433.       90.55
   5773.        305.3       2641.       55.75       372.6
   212.3        614.6       1390.       700.5       105.4
   1090.        1643.       497.2       5509.       1034.
   324.9        171.7       246.1       19.11       1075.
   2351.        3611.       154.0       35.69       109.0
   286.4        18.95       374.5       7940.       53.70
   58.18        166.7       6118.       225.4       30.82
   18.61        3214.       335.2       94.80       104.6
   25.20        3996.       282.5       5099.       11.18
   423.9        963.2       48.50       421.7       131.2
   221.4        413.5       1067.       1077.       145.9
   353.5        1429.       323.2       188.5       394.8
   312.2        3037.       1179.     0.2788E+05  0.1056E+06
   815.5        375.4       25.96       456.5       31.14
   68.03        5.519       63.88       408.6       74.13
   44.21        44.83       468.8       77.59       296.5
   5091.        349.4       2116.       3.206       159.8
   429.7        172.0       79.67       220.9       1430.
   83.53        336.2       709.9       1102.       528.1
   799.6        8.542       2385.     0.1043E+05    1188.
   178.1        11.66       50.04       134.9       5127.
   258.2        456.8       440.2       273.9       2262.
   14.89      0.1202E+06    925.7       219.3       570.4
   83.11        882.8       12.70       697.4       357.2
   800.7        75.78       24.13       2328.       418.4
   6211.        730.3       116.1       80.85       176.9
   30.67        834.7       305.4       370.1       1321.
   144.2        8.981       143.8     0.3069E+05    101.8
   151.1        442.9       23.68       59.95       545.2
   82.84        60.71       138.6     0.5475E+05    112.0
   1645.        34.54       429.2       1118.       850.3
   667.9        20.80       50.68       3490.       171.5
   245.5        116.7       2958.       761.5       1295.
   41.21        1612.       724.2       26.30       16.19
   16.23        1219.       876.9       1102.       237.0
   5268.        166.2       72.08       3.385       201.8
   3.887        1587.       107.9       402.7       1593.
```

```
   229.5       354.2       112.0       404.5       83.39
   41.52       1286.       3897.       20.28       2183.
   544.9       1081.       1640.       517.5       109.6
  0.3090E+05   241.6       338.2       565.7       438.1
   58.97       405.5       660.7       396.6       718.8
   235.0       4868.       30.08       2024.      0.1077E+05
   81.45      0.2350E+06   110.7       9.339       555.2
CC
CC Y DIRECTION PERMEABILITY IS DEPENDENT ON X DIRECTION PERMEABILITY
*---- CONSTANT PERMEABILITY MULTIPLIER FOR Y DIRECTION PERMEABILITY
        1
CC
CC Z DIRECTION PERMEABILITY IS DEPENDENT ON X DIRECTION PERMEABILITY
*---- CONSTANT PERMEABILITY MULTIPLIER FOR Z DIRECTION PERMEABILITY
        1
CC
CC FLAG FOR CONSTANT OR VARIABLE DEPTH, PRESSURE, WATER SATURATION,INITIAL AQUEOUS PHASE
cOMPOSITIONS
*----IDEPTH  IPRESS  ISWI  ICWI
       0       1      0     -1
CC
CC CONSTANT DEPTH (FT)
*---- D111
        0
CC
CC INITIAL PRESSURE FOR A POINT AT A SPECIFIED DEPTH IS SPECIFIED
*---- PINIT  HINIT
      14.7    0
CC
CC INITIAL WATER SATURATION FOR EACH GRIDBLOCk IS SPECIFIED
*---- S(I),I=1 TO NX*NY*NZ
     0.588
CC
CC     C50    C60 Formation brine of 116969 ppm
*---- cwi(I,KW) for i=1, NXxNYxNZ, for kw=1,n(8+no)
       1.999   0.0
CC
CC*********************************************************************
CC                                                                    *
CC    PHYSICAL PROPERTY DATA                                          *
CC                                                                    *
CC*********************************************************************
CC
CC
CC OIL CONC. AT PLAIT POINT FOR TYPE II(+)AND TYPE II(-), CMC
*---- c2plc  c2prc   epsme   ihand
        0      1     0.0001    0
CC
CC flag indicating type of phase behavior parameters
*---- ifghbn
        0
CC SLOPE AND INTERCEPT OF BINODAL CURVE AT ZERO, OPT., AND 2XOPT SALINITY
CC FOR ALCOHOL 1
*---- hbns70   hbnc70   hbns71   hbnc71   hbns72   hbnc72
        0      0.035       0       0.029     0       0.035
CC SLOPE AND INTERCEPT OF BINODAL CURVE AT ZERO, OPT., AND 2XOPT SALINITY
CC FOR ALCOHOL 2
*---- hbns80  hbnc80  hbns81  hbnc81  hbns82  hbnc82
        0       0       0       0       0       0
CC
CC LOWER AND UPPER EFFECTIVE SALINITY FOR ALCOHOL 1 AND ALCOHOL 2
*---- csel7   cseu7   csel8   cseu8
       0.86     1.06     0       0
CC
```

```
CC THE CSE SLOPE PARAMETER FOR CALCIUM AND ALCOHOL 1 AND ALCOHOL 2
*---- beta6    beta7    beta8
        0        0       0
CC
CC FLAG FOR ALCOHOL PART. MODEL AND PARTITION COEFFICIENTS
*---- ialc   opsk7o   opsk7s   opsk8o   opsk8s
        0      0        0        0        0
CC
CC NO. OF ITERATIONS, AND TOLERANCE
*---- nalmax     epsalc
        20       0.0001
CC
CC ALCOHOL 1 PARTITIONING PARAMETERS IF IALC=1
*---- akwc7     akws7    akm7     ak7      pt7
       4.671    1.79      48     35.31    0.222
CC
CC ALCOHOL 2 PARTITIONING PARAMETERS IF IALC=1
*---- akwc8     akws8    akm8    ak8     pt8
        0         0        0      0       0
CC
CC ift model flag
*----  ift
        1
CC
CC INTERFACIAL TENSION PARAMETERS
*---- chuh     ahuh
      0.3      9
CC
CC LOG10 OF OIL/WATER INTERFACIAL TENSION
*---- xiftw
       1.3979
CC
CC ORGANIC MASS TRANSFER FLAG
*---- imass icor
        0       0
cc
cc
*----IWALT  iwalf
      1     0
c
c
*---
       0.5     0.5
CC
CC CAPILLARY DESATURATION PARAMETERS FOR PHASE 1, 2, AND 3
*---- itrap      t11      t22      t33
       2        59074    6500    5000
c
c
*
                6500     59074    5000
CC
CC  FLAG FOR RELATIVE PERMEABILITY AND CAPILLARY PRESSURE MODEL
*---- iperm
        0   0   0
CC
CC FLAG FOR CONSTANT OR VARIABLE REL. PERM. PARAMETERS
*---- isrw    iprw    iew
        0       0       0
CC
CC Residual saturation of aqueous phase displaced by oil or gas at low capillary number
for I gridblock
*---- s 1,2,3rw(i),FOR I=1 TO NX*NY*NZ
       0.5    0.18  0.5
```

```
c
c    Alt s
**
       0.5  0.05  0.5
CC   kro measure in lab
CC Endpoint relative permeability of water at low capillary number for I gridblock
*---- p1, 2 3 rw(i) ,FOR I=1 TO NX*NY*NZ
        0.40  0.50    0.40
c
c    Alt pr
*
      0.10     0.85   0.10
CC
CC Relative permeability  exponent of aqueous phase at low capillary number for I
gridblock
*---- e1, 2, 3 w(i) ,FOR I=1 TO NX*NY*NZ
          2   2.0   2
CC
CC    Alt   ei
*
         3   1.5   3
CC  high cap press
CC  RES. SATURATION OF PHASES 1,2,AND 3 AT HIGH CAPILLARY NO.
*----S1RC  S2RC  S3RC
     0.    0.    .0
CC
CC ENDPOINT REL. PERM. OF PHASES 1,2,AND 3 AT HIGH CAPILLARY NO.
*----P1RC  P2RC  P3RC
     1.    1.    1.
CC
CC REL. PERM. EXPONENT OF PHASES 1,2,AND 3 AT HIGH CAPILLARY NO.
*----E13C  E23C  E31C
     1.     1.    1.
CC  Diluted akal oil at 100 C
CC WATER AND OIL VISCOSITY , RESERVOIR TEMPERATURE
*---- VIS1    VIS2   TSTAND
       0.33     2.1      0
CC
CC COMPOSITIONAL PHASE VISCOSITY PARAMETERS
*----   ALPHAV1   ALPHAV2   ALPHAV3   ALPHAV4  ALPHAV5
          1        2.5        .1        0.1       0.1
CC
CC PARAMETERS TO CALCULATE POLYMER VISCOSITY AT ZERO SHEAR RATE
*---- AP1      AP2      AP3
      60       100     200
CC
CC PARAMETER TO COMPUTE CSEP,MIN. CSEP, AND SLOPE OF LOG VIS. VS. LOG CSEP
*---- BETAP    CSE1     SSLOPE
       1      0.01     -0.2
CC
CC PARAMETER FOR SHEAR RATE DEPENDENCE OF POLYMER VISCOSITY
*---- GAMMAC  GAMHF  POWN       IPMOD   ISHEAR  RWEFF   GAMH2
        4     20.    1.8        0      0        0.5   0
CC
CC CC FLAG FOR POLYMER PARTITIONING, PERM. REDUCTION PARAMETERS
*---- IPOLYM    EPHI3    EPHI4    BRK     CRK    rcut
        1         1       0.7       100     0      10
CC  Den water = 1.05g/cc     Den Oil =  0.83g/cc
CC SPECIFIC WEIGHT FOR COMPONENTS 1,2,3,7,8 ,Coeffient of oil and GRAVITY FLAG
*---- DEN1       DEN2    DEN23     DEN3      DEN7    DEN8    IDEN
      0.455      0.359     0.359   0.455     0.346    0        2
CC
CC FLAG FOR CHOICE OF UNITS ( 0:BOTTOMHOLE CONDITION , 1: STOCK TANK)
*----- ISTB
```

```
        0
CC
CC COMPRESSIBILITY FOR VOL. OCCUPYING COMPONENTS 1,2,3,7,AND 8
*---- COMPC(1)  COMPC(2)  COMPC(3)  COMPC(7)  COMPC(8)
         0         0         0         0         0
CC
CC CONSTANT OR VARIABLE PC PARAM., WATER-WET OR OIL-WET PC CURVE FLAG
*---- ICPC    IEPC   IOW
       0       0      1
CC
CC  CAPILLARY PRESSURE ENDPOINT FOR GRIDBLOCK
*---- CPC(I),I=1 TO NX*NY*NZ
           -0.01
CC
CC
*---
         3
CC
CC    Alt
*---- ICPC    IEPC   IOW
       0       0      0
CC
CC
*   cpc
   0.0
CC
CC
*    epc
    3
CC
CC MOLECULAR DIFFUSION COEF. KCTH COMPONENT IN PHASE 1
*---- D(KC,1),KC=1,N
         0         0         0.0000          0         0         0
CC
CC MOLECULAR DIFFUSION COEF. KCTH COMPONENT IN PHASE 2
*---- D(KC,2),KC=1,N
         0         0         0.0000      0         0         0
CC
CC MOLECULAR DIFFUSION COEF. KCTH COMPONENT IN PHASE 3
*---- D(KC,3),KC=1,N
         0         0         0.0000         0         0         0
CC
CC LONGITUDINAL AND TRANSVERSE DISPERSIVITY OF PHASE 1
*---- ALPHAL(1)     ALPHAT(1)
         0.01           0
CC
CC LONGITUDINAL AND TRANSVERSE DISPERSIVITY OF PHASE 2
*---- ALPHAL(2)     ALPHAT(2)
         0.01           0
CC
CC LONGITUDINAL AND TRANSVERSE DISPERSIVITY OF PHASE 3
*---- ALPHAL(3)     ALPHAT(3)
         0.01           0
CC
CC flag to specify organic adsorption calculation
*---- iadso
        0
CC
CC SURFACTANT AND POLYMER ADSORPTION PARAMETERS
*---- AD31    AD32    B3D     AD41   AD42   B4D   IADK  IADS1   FADS   REFK
      5.5     0.5    1000     1      0     100     0     0      0      50
CC
CC PARAMETERS FOR CATION EXCHANGE OF CLAY AND SURFACTANT
*---- QV      XKC     XKS     EQW
```

```
      0    0     0      804
CC
CC*********************************************************************
CC                                                                     *
CC    WELL DATA                                                        *
CC                                                                     *
CC*********************************************************************
CC
CC
CC FLAG FOR SPECIFIED BOUNDARY AND ZONE IS MODELED
*---- IBOUND     IZONE
        0        0
CC
CC TOTAL NUMBER OF WELLS, WELL RADIUS FLAG, FLAG FOR TIME OR COURANT NO.
*---- NWELL   IRO    ITIME    NWREL
        2      2       0       2
CC Deviated Injector 1
CC WELL ID,LOCATIONS,AND FLAG FOR SPECIFYING WELL TYPE, WELL RADIUS, SKIN
*----IDW   IW     JW    IFLAG    RW     SWELL  IDIR   IFIRST  ILAST   IPRF
      1     3    3      1      0.01    3      3    10       10   0
CC
CC WELL NAME
*----  WELNAM
Injector
CC
CC ICHEK , MAX. AND MIN. ALLOWABLE BOTTOMHOLE PRESSURE AND RATE
*---- ICHEK     PWFMIN     PWFMAX    QTMIN    QTMAX
        0          0         10      0        10
CC Deviated producer 2
CC WELL ID,LOCATIONS,AND FLAG FOR SPECIFYING WELL TYPE, WELL RADIUS, SKIN
*----IDW   IW     JW    IFLAG    RW     SWELL  IDIR   IFIRST  ILAST   IPRF
      2     3      3      2      0.01    3      3      1       1       0
CC
CC WELL NAME
*----  WELNAM
Producer
CC
CC ICHEK , MAX. AND MIN. ALLOWABLE BOTTOMHOLE PRESSURE AND RATE
*---- ICHEK     PWFMIN     PWFMAX    QTMIN    QTMAX
        0          0         10      0        10
CC  0.033 ml/min, at 57000 ppm
CC  ID,INJ. RATE AND INJ. COMP. FOR RATE CONS. WELLS FOR EACH PHASE (L=1,3)
*----  ID     QI(M,L)     C(M,KC,L)
       1      0.00168    0.99   0      0.01   0      0.974      0
       1      0          0      0      0      0      0          0
       1      0          0      0      0      0      0          0
CC
CC  ID,INJ. RATE AND INJ. COMP. FOR RATE CONS. WELLS FOR EACH PHASE (L=1,3)
*----  ID     QI(M,L)     C(M,KC,L)
       2     14.7
CC
CC CUM. INJ. TIME , AND INTERVALS (PV OR DAY) FOR WRITING TO OUTPUT FILES
*---- TINJ     CUMPR1     CUMHI1     WRHPV     WRPRF      RSTC
      0.25      0.02        0.01        0.01      0.01       0.1
CC
CC THE INI. TIME STEP,CONC. TOLERANCE,MAX.,MIN. time steps
*---- DT DELC DTMAX DTMIN
       1E-4  0.003   0.2     0.01
cc
cc
*--- ibmod
     0
cc
cc
```

```
*---  iro  itime  iflag
      2     0     1        2
cc
cc
*--- nwel1
     0
cc
cc
*--- nwel2
     2    1    2
CC      Sea water 10000 ppm , 0.033 ml/min
CC ID,INJ. RATE AND INJ. COMP. FOR RATE CONS. WELLS FOR EACH PHASE (L=1,3)
*----ID  QI(M,L)  C(M,KC,L)
       1      0.00168   1      0      0      0      0.171      0
       1      0          0      0      0      0      0          0
       1      0          0      0      0      0      0          0
CC
CC ID, BOTTOM HOLE PRESSURE FOR PRESSURE CONSTRAINT WELL (IFLAG=2 OR 3)
*----  ID     QI(M,L)     C(M,KC,L)
       2     14.7
CC
CC CUM. INJ. TIME , AND INTERVALS (PV OR DAY) FOR WRITING TO OUTPUT FILES
*---- TINJ     CUMPR1     CUMHI1     WRHPV     WRPRF      RSTC
      1.71      0.01          0.01      0.01       0.01        1
CC
CC FOR IMES=2 ,THE INI. TIME STEP,CONC. TOLERANCE,MAX.,MIN. courant numbers
*----  DT DCLIM cnMAX cnMIN 0.0005 0.0005 0.000008 0.001 0.001 0.001 0.001 0.0000001
        1E-4   0.003   0.2     0.01
```

References

Abbasi-Asl, Y., Pope, G. A., and Delshad, M., 2010. "Mechanistic Modeling of Chemical Transport in Naturally Fractured Oil Reservoirs," SPE 129661 presented at SPE IOR Symposium, Tulsa, OK, April 24-28.

Abdulbaki, M., 2012. "Simulation Study of Polymer Microgel Conformance Treatments," Master's Thesis, The University of Texas at Austin.

Abdulbaki, M., Huh, C., Sepehrnoori, K., Delshad, M., and Varavei, A., 2014. "A critical review on use of polymer microgels for conformance control purposes," *Journal of Petroleum Science and Engineering*, 122: 741-753.

Abouie, A., 2015. "Development and Application of a Compositonal Wellbore Simulator for Modeling Flow Assurance Issues and Optimization of Field Production," Master's Thesis, The University of Texas at Austin.

Adibhatla, B., Sun, X., and Mohanty, K. K., 2005. "Numerical Studies of Oil Production from Initially Oil-Wet Fracture Blocks by Surfactant Brine Imbibition," Paper SPE 97687, presented at the International Improved Oil Recovery Conference, Kuala Lumpur, Malaysia, December 5-6.

Adibhatla, B., and Mohanty, K. K., 2006. "Oil Recovery from Fractured Carbonates by Surfactant-Aided Gravity Drainage: Laboratory Experiments and Mechanistic Simulations," SPE 99773 presented at SPE IOR Symposium, Tulsa, OK, April 22-26.

Adkins, S., Arachchilage, G. P., Solairaj, S., Lu, J., Weerasooriya, U., and Pope, G. A., 2012. "Development of Thermally and Chemically Stable Large-Hydrophobe Alkoxy Carboxylate Surfactants," SPE 154256 presented at SPE IOR Symposium, Tulsa, OK, April 14-18.

Al-Anazi, H. A., and Sharma, M. M., 2002a. "Evaluation of a pH-Sensitive Polymer for Gravel-Packing Operations," *SPE Drilling and Completion Technology Journal*, 17: 28-36.

Al-Anazi, H. A., and Sharma, M. M., 2002b. "Use of a pH Sensitive Polymer for Conformance Control," Paper SPE 73782, presented at the International Symposium and Exhibition on Formation Damage Control, Lafayette, Louisiana, February 20-21.

Aldejain, A., 1989. "Implementation of a Dual Porosity Model in a Chemical Flooding Simulator," Ph.D. Dissertation, The University of Texas at Austin, Austin, Texas.

Al-Lawati, S. and Saleh, S., 1996. "Oil Recovery in Fractured Oil Reservoirs by Low IFT Imbibition Process," Paper SPE 36688, presented at the SPE Annual Technical Conference and Exhibition, Denver, Colorado, October 6-9.

Almohsin, A., Bai, B., Imqam, A., Wei, M., Kang, W., Delshad, M., and Sepehrnoori, K., 2014. "Transport of Nanogel through Porous Media and Its Resistance to Water Flow" Paper SPE 169078, presented at the SPE Symposium on Improved Oil Recovery, Tulsa, Oklahoma, April 12-16.

Al-Muntasheri, G. A., Nasr-El-Din, H. A., Al-Noaimi, K. R., and Zitha, P. L. J., 2009. "A Study of Polyacrylamide-Based Gels Crosslinked With Polyethyleneimine," *SPE Journal*, 14: 245-251.

Al-Muntasheri, G. A., Nasr-El-Din, H. A., Al-Noaimi, K. R., and Zitha, P. L. J., 2007. "A Study of Polyacrylamide-Based Gels Crosslinked With Polyethyleneimine," Paper SPE 105925, presented at the SPE International Symposium on Oilfield Chemistry, Houston, Texas, February 28- March 2.

Anderson, W. G., 1986. "Wettability Literature Survey-Part 2: Wettability Measurements," *Journal of Petroleum Technology*, 38: 1246-1262.

Anderson, G. A., 2006. "Simulation of Chemical Flood Enhanced Oil Recovery Processes Including the Effects of Reservoir Wettability," Master's Thesis, The University of Texas at Austin.

Austad, T., and Milter, J., 1997. "Spontaneous Imbibition of Water Into Low Permeable Chalk at Different Wettabilities Using Surfactants," Paper SPE 37236, presented at the International Symposium on Oilfield Chemistry, Houston, Texas, February 18-21.

Babadagli, T., 2003. "Analysis of Oil Recovery by Spontaneous Imbibition of Surfactant Solution," Paper SPE 84866, presented at the International Improved Oil Recovery Conference, Kuala Lumpur, Malaysia, October 20-21.

Babu, D. K., and Odeh, A. S., 1988. "Productivity of a Horizontal Well Appendices A and B," Paper SPE 18334, presented at the SPE Annual Technical Conference and Exhibition, Houston, Texas, October 2-5.

Bai, B., Li., Y., and Liu, X., 1999. "New development of water Shutoff and profile control in oilfields in china," *Journal of Oil Drilling and Production Technology*, 20: 3.

Bai, B., Li, L., Liu, Y., Wang, Z., Liu, H., 2004a. "Preformed particle gel for conformance control: factors affecting its properties and applications," Paper SPE 89389, presented at the SPE/DOE 14th Symposium on Improved Oil Recovery, Tulsa, Oklahoma, April 17-21.

Bai, B., Li, L., Liu, Y., Coste, J., Li, L., 2004b. "Preformed particle gel for conformance control: transport mechanism through porous media," Paper SPE 89468, presented at the SPE/DOE 14th Symposium on Improved Oil Recovery, Tulsa, Oklahoma, April 17-21.

Bai, B., Li, L., Liu, Y., Liu, H., Wang, Z., and You, C., 2007a. "Conformance control by preformed particle gel: factors affecting its properties and applications," *SPE Reservoir Evaluation and Engineering Journal*, 10: 415-421.

Bai, B., Liu, Y., Coste, J. P., and Li, L., 2007b. "Preformed particle gel for conformance control: transport mechanism through porous media," *SPE Reservoir Evaluation and Engineering Journal*, 10: 176-184.

Bai, B., Huang, F., Liu, Y., Seright, R.S., and Wang, Y., 2008. "Case study on preformed particle gel for in-depth fluid diversion," Paper SPE 113997, presented at the SPE/DOE Improved Oil Recovery Symposium, Tulsa, Oklahoma, April 19-23.

Bai, B., 2010. "Preformed particle gel (PPG) for conformance control," RPSEA contract No: 07123-02, Midland, Texas, February 3.

Bai, B., Wei, M., and Liu, Y., 2013. "Field and Lab Experience with a Successful Preformed Particle Gel Conformance Control Technology," Paper SPE 164511, presented at the SPE Production and Operations Symposium, Oklahoma City, Oklahoma, March 23-26.

Bai, B., 2013, 2014. Private communication.

Barreau, P., Bertin, H., Lasseux, D., Glenat, P., and Zaitoun, A., 1997. "Water Control in Producing Wells: Influence of an Adsorbed-Polymer Layer on Relative Permeabilities and Capillary Pressure," *SPE Reservoir Engineering Journal*, 12: 234-239.

Bennett, K. E., Fitzjohn, J. L., Harmon, R. A., and Yates, P. C., 1988. "Colloidal silica-based fluid diversions," U.S. Patent No. 4,732,213.

Bhuyan, D., 1989. "Development of an Alkaline/Surfactant/Polymer Compositional Reservoir Simulator," Ph.D. Dissertation, The University of Texas at Austin, Austin, Texas, December.

Bird, R. B., Stewart, W. E., and Lightfoot, E. N., 1976. Transport Phenomena, John Wiley & Sons, 42-46, 62-63, New York.

Bird, R. B., Armstrong, R. C., and Hassager, O., 1977. Dynamics of Polymeric Liquids, Vol. 1: Fluid Mechanics, John Wiley & Sons.

Bird, R. B., Dai, G. C., and Yarusso, B. J., 1983. "The Rheology and Flow of Viscoplastic Materials," *Reviews in Chemical Engineering*.

Bohdanecky, M., and Kovar, J., 1982. Viscosity of Polymer Solutions. Polymer Science Library, Vol 2, Elsevier.

Borchardt, J. K., and Yen, T. F., 1989. "Enhanced Recovery and Production Stimulation," ACS Symposium Series, American Chemical Society, Washington, D.C.

Brannon-Peppas, L., and Peppas, N. A., 1988. "Structural Analysis of Charged Polymeric Networks," *Polymer Bulletin Journal*, 20: 285-289.

Buckley, J. S., Liu, Y., and Monsterleet, S., 1998. "Mechanisms of Wettability Alteration by Crude Oils" *SPE Journal*, 3: 54-61.

Buckley, J. S., and Morrow, N. R., 1990. "Characterization of Crude Oil Wetting Behavior by Adhesion Tests," Paper SPE 20263, presented at the SPE/DOE Symposium on Improved Oil Recovery, Tulsa, Oklahoma, April 22-25.

Budtova, T. V., Budtov, V. P., Navard, P., and Frenkel, S. Y., 1994. "Rheological Properties of Highly Swollen Hydrogel Suspensions," *Journal of Applied Polymer Science*, 52: 721-726.

Castelijns, H., 2007. "Two-Phase Reactive Transport of an Oil-Soluble Chemical: an NMR Study," Ph.D. Dissertation, Delft University of Technology, Delft.

Cavalcante Filho, J. S. A., Shakiba, M., Moinfar, M., and Sepehrnoori, K., 2015. "Implementation of a Preprocessor for Embedded Discrete Fracture Modeling in an IMPEC Compositional Reservoir Simulator," Paper SPE 173289, Presented at the SPE Reservoir Simulation Symposium, Houston, Texas, February 23-25.

Chang, K. T., Frampton, H., and Morgan, J. C., 2002. "Composition and Method for Recovering Hydrocarbon Fluids from a Subterranean Reservoir" US Patent No. 6,454,003.

Chang, H. L., Sui, X., Xiao, L., Liu, H., Guo, Z., Yao, Y., Xiao, Y., Chen, G., Song, K., and Mack, J. C., 2004. "Successful Field Pilot of In-Depth Colloidal Dispersion Gel (CDG) Technology in Daqing Oil Field," Paper SPE 89460, presented at the SPE/DOE Fourteenth Symposium on Improved Oil Recovery, Tulsa, Oklahoma, April 17-21.

Chang, H. L., Zhang, Z. Q., Wang, Q. M., Xu, Z. S., Guo, Z. D., Sun, H. Q., Cao, X. L., and Qiao, Q., 2006. "Advances in Polymer Flooding and Alkaline/Surfactant/Polymer Processes as Developed and Applied in the People's Republic of China," *Journal of Petroleum Technology*, 58: 84-89.

Chauveteau, G., and Sorbie, K., 1991. Mobility control by polymers: Basic Concepts in Enhanced Oil Recovery Processes. Elsevier Science Publishers, Amsterdam, The Netherlands, Vol. 33, Chapter 2.

Chauveteau, G., Omari, A., Tabary, R., Renard, M., Veerapen, J., and Rose, J., 2001. "New Size-Controlled Microgels for Oil Production," Paper SPE 64988, presented at the SPE International Symposium on Oilfield Chemistry, Houston, Texas, February 13-16.

Chauveteau, G., Tabary, R., Le Bon, C., Renard, M., Feng, Y., and Omari, A., 2003. "In-Depth Permeability Control by Adsorption of Soft Size-Controlled Microgels," Paper SPE 82228, presented at the SPE European Formation Damage Conference, The Hague, Netherlands, May 13-14.

Chauveteau, G., Tabary, R., Blin, N., Renard, M., Rousseau, D., and Faber, R., 2004. "Disproportionate Permeability Reduction by Soft Preformed Microgels," Paper SPE 89390, presented at the SPE/DOE 14th Improved Oil Recovery Symposium, Tulsa, Oklahoma, April 17-21.

Chen, P., and Mohanty, K. K., 2012. "Surfactant-Mediated Spontaneous Imbibition in Carbonate Rocks at Harsh Reservoir Conditions," Paper SPE 153960, presented at the SPE Improved Oil Recovery Symposium, Tulsa, Oklahoma, April 14-18.

Cheung, S., Ng, R., Frampton, H., Chang, K. T., and Morgan, J., 2007. "A swelling polymer for in-depth profile modification: update on field applications," presented at the SPE Applied Technology Workshop of "Chemical Methods for Reducing Water Production", San Antonio, Texas, March 4-6.

Choi, S. K., Ermel, Y. M., Bryant, S. L., Huh, C., and Shrma, M. M., 2006. "Transport of a pH-Sensitive Polymer in Porous Media for Novel Mobility Control Applications," Paper SPE 99656, presented at the SPE/DOE Improved Oil Recovery Symposium, Tulsa, Oklahoma, 22-26 April.

Choi, S. K., Shrma, M. M., Bryant, S. L., and Huh, C., 2010. "pH-Sensitive Polymers for Novel Conformance-Control and Polymer-Flood Applications," *SPE Reservoir Evaluation and Engineering Journal*, 13: 926-939.

CMG-STARS Technical Manual, 2010.

Coste, J. P., Liu, Y., Bai, B., Li, Y., Shen, P., Wang, Z., and Zhu, G., 2000. "In-Depth Fluid Diversion by Pre-Gelled Particles: Laboratory Study and Pilot Testing," Paper SPE 59362, presented at the SPE/DOE Improved Oil Recovery Symposium, Tulsa, Oklahoma, April 3-5.

Cozic, C., Rousseau, D., and Tabary, R., 2009. "Novel insights into microgel systems for water control," *SPE Production & Operations Journal*, 24: 590–601.

Craig, F. F., 1971. "The Reservoir Engineering Aspects of Waterflooding," Monograph Series, SPE, 24: 590–601.

Cui, X., Li, Z., Cao, X., Song, X., and Zhang, X., 2011, "A Novel PPG Enhanced Surfactant-Polymer System for EOR," Paper SPE 143506, presented at the SPE Enhanced Oil Recovery Conference, Kuala Lumpur, Malaysia, July 19-21.

Darabi, H., Sepehrnoori, K., and Kalaei, M. H., 2012. "Modeling of Wettability Alteration Due to Asphaltene Deposition in Oil Reservoirs," Paper SPE 159554, presented at the SPE Annual Technical Conference and Exhibition, San Antonio, Texas, October 8-10.

Delshad, M., UTCHEM Technical Manual, 1994.

Delshad, M., Pope, G. A., and Sepehrnoori, K., 1996. "A compositional simulator for modeling surfactant enhanced aquifer remediation, 1 Formulation," *Journal of Contaminant Hydrology*, 23: 303-327.

Delshad, M., Han, W., Pope, G. A., Sepehrnoori, K., Wu, W., Yang, R., and Zhao, L., 1998. "Alkaline/Surfactant/Polymer Flood Predictions for the Karamay Oil Field," Paper SPE 39610, presented at the SPE/DOE Improved Oil Recovery Symposium, Tulsa, Oklahoma, April 19-22.

Delshad, M., Najafabadi, N. F., Anderson, G. A., Pope, G. A., and Sepehrnoori, K., 2006. "Modeling Wettability Alteration in Naturally Fractured Reservoirs," Paper SPE 100081, presented at the SPE/DOE Symposium on Improved Oil Recovery, Tulsa, Oklahoma, April 22-26.

Delshad, M., Kim, D. H., Oluwaseun, A. M., Huh, C., and Pope, G. A., 2008. "Mechanistic Interpretation and Utilization of Viscoelastic Behavior of Polymer Solutions for Improved Polymer-Flood Efficiency," Paper SPE 113620, presented at the SPE/DOE Symposium on Improved Oil Recovery, Tulsa, Oklahoma, April 20-23.

Delshad, M., Najafabadi, N. F., and Sepehrnoori, K., 2009. "Scale Up Methodology for Wettability Modification in Fractured Carbonates," Paper SPE 118915, presented at the SPE Improved Oil Recovery Symposium, Tulsa, Oklahoma, February 2-4.

Diaz, D., Somaruga, C., Norman, C., and Romero, J., 2008. "Colloidal Dispersion Gels Improve Oil Recovery in a Heterogeneous Argentina Waterflood," Paper SPE 113320, presented at the SPE/DOE Improved Oil Recovery Symposium, Tulsa, Oklahoma, 19-23 April.

ECLIPSE Technical Manual, 2009.

Edmondson, T. A., 1965. "Effect of Temperature on Waterflooding," *Journal of Canadian Petroleum Technology*, 4: 236-242.

Elsharafi, M. O., and Bai, B., 2012. "Effect of Weak Particle Gel on Unswept Oil Zones/Areas during Conformance Control Treatments," *Journal of the Industrial and Engineering Chemistry Research*, 51: 11547-11554.

Faber, M. J., Joosten, G. J. P., Hashmi, K. A., and Gruenenfelder, M., 1998. "Water shut-off field experience with a relative permeability modification system in the Marmul field (Oman)," Paper SPE 39633, presented at the SPE/DOE Improved Oil Recovery Symposium, Tulsa, Oklahoma, April 19-22.

Fan, T., and Buckley, J. S., 2006. "Acid Number Measurements Revisited," SPE 99884 presented at SPE/DOE Symposium on Improved Oil Recovery, Tulsa, OK, April 22-26.

Farhadinia, M. A., Chen, P., Delshad, M., Mohanty, K. K., and Rodriguez, F. G., 2011. "A Systematic Study of Oil Recovery Mechanisms from a Fractured and Vuggy Carbonate Reservoir," Paper SPE 147317, presented at the SPE Annual Technical Conference and Exhibition, Colorado, Denver, October 30-November 2.

Feng, Y., Tabary, R., Renard, M., LeBon, C., Omari, A., Chauveteau, G., 2003. "Characteristics of microgels designed for water shutoff and profile control," Paper SPE 80203, presented at SPE International Symposium on Oilfield Chemistry, Houston, Texas, February 5-7.

Fielding, R. C. Jr., Gibbons, D. H., and Legrand, F. P., 1994. "In-Depth Drive Fluid Diversion Using an Evolution of Colloidal Dispersion Gels and New Bulk Gels: An Operational Case History of North Rainbow Ranch Unit," Paper SPE 27773, presented at SPE/DOE Ninth Symposium on Improved Oil Recovery, Tulsa, Oklahoma, April 17-20.

Fischer, H., and Morrow, N. R., 2005. "Spontaneous Imbibition with Matched Liquid Viscosities," Paper SPE 96812, presented at the Annual Technical Conference and Exhibition, Dallas, Texas, October 9-12.

Frampton, H., Morgan, J. C., Cheung, S. K., Munson, L., Chang, K. T., and Williams, D., 2004. "Development of a Novel Waterflood Conformance Control System" Paper SPE 89391, presented at the SPE/DOE Fourteenth Symposium on Improved Oil Recovery, Tulsa, Oklahoma, April 17-21.

Galli, G., Morra, D., Ghaddab, F., Tesconi, M., Manrique, E., and Freeman, G., 2012. "Thermally Activated Particle Treatment to Improve Sweep Efficiency: Pilot Test Results and Field Scale Application Design in El Borma Field (Tunisia)" Paper SPE 154042, presented at the Eighteenth SPE Improved Oil Recovery Symposium, Tulsa, Oklahoma, April 14-18.

Ganguly, S., Willhite, G. P., Green, D. W., and McCool, C. S., 2003. "Effect of Flow Rate on Disproportionate Permeability Reduction," Paper SPE 80205, presented at the International Symposium on Oilfield Chemistry, Houston, Texas, February 5-7.

Gardner, D. C., 1983. "Rheological Characterization of Crosslinked and Delayed Crosslinked Fracturing Fluids Using a Closed-Loop Pipe Viscometer," Paper SPE 12028, presented at the Annual Technical Conference and Exhibition, San Francisco, California, October 5-8.

Garmeh, R., Izadi, M., Salehi, M., Romero, J. L., Thomas, C. P., and Manrique, E. J., 2012. "Thermally Active Polymer to Improve Sweep Efficiency of Water Floods: Simulation and Pilot Design Approaches," *SPE Reservoir Evaluation and Engineering Journal*, 15: 86-97.

Ghaddab, F., Kaddour, K., Tesconi, M., Brancolini, A., Carniani, C. and Galli, G., 2010. "El Borma - Bright Water: A Tertiary Method for Enhanced Oil Recovery for a Mature Field," Paper SPE 136140, presented at the Production and Operations Conference and Exhibition, Tunis, Tunisia, June 8-10.

Gilliland, H. E., and Conley, F. R., 1976. "Pilot Flood Mobilizes Residual Oil," *Oil &Gas Journal*, 43-48.

Goudarzi, A., Delshad, M., Mohanty, K. K., and Sepehrnoori, K., 2015. "Surfactant oil recovery in fractured carbonates: Experiments and modeling of different matrix dimensions," *Journal of Petroleum Science and Engineering*, 125: 136-145.

Goudarzi, A., Delshad, M., Mohanty, K. K., and Sepehrnoori, K., 2012. "Impact of Matrix Block Size on Oil Recovery Response Using Surfactants in Fractured Carbonates," Paper SPE 160219, presented at the SPE Annual Technical Conference and Exhibition, San Antonio, Texas, October 8-10.

Goudarzi, A., Delshad, M., and Sepehrnoori, K., 2013. "A Critical Assessment of Several Reservoir Simulators for Modeling Chemical Enhanced Oil Recovery Processes," Paper SPE 163578, Presented at the SPE Reservoir Simulation Symposium, The Woodlands, Texas, February 18-20.

Goudarzi, A., Zhang, H., Varavei, A., Hu, Y., Delshad, M., Bai, B., and Sepehrnoori, K., 2013, "Water Management in Mature Oil Fields using Preformed Particle Gels," Paper SPE 165356, presented at the SPE Western Regional & AAPG Pacific Section Meeting, Monterey, California, April, 19-25.

Goudarzi, A., Almohsin, A., Varavei, A., Delshad, M., Bai, B., and Sepehmoori, K., 2014. "New Experiments and Models for Conformance Control Microgels," Paper SPE 169159, presented at the SPE Symposium on Improved Oil Recovery, Tulsa, Oklahoma, April 12-16.

Goudarzi, A., Zhang, H., Varavei, A., Taksaudom, P., Hu, Y., Delshad, M., Bai, B., and Sepehmoori, K., 2015. "A laboratory and simulation study of preformed particle gels for water Conformance Control," *Fuel Journal*, 140: 502-513.

Grattoni, C. A., Al-Sharji, H. H., Yang, C., Muggeridge, A. H., and Zimmerman, R. W., 2001. "Rheology and Permeability of Crosslinked Polyacrylamide Gel," *Journal of Colloidal and Interface Science*, 240: 601-607.

Graue, A., Viksund, B. G., and Baldwin, B. A., 1998. "Reproducible Wettability Alteration of Low-Permeable Outcrop Chalk," Paper SPE 39622, presented at the SPE/DOE Symposium on Improved Oil Recovery, Tulsa, Oklahoma, April 19-22.

Graue, A., and Bogne, T., 1999. "Wettability Effects on Oil Recovery Mechanisms in Fractured Reservoirs," Paper SPE 56672, presented at the SPE Annual Technical Conference and Exhibition, Houston, Texas, October 3-6.

Graue, A., Aspenes, E., Bogno, T., Moe, R. W., and Ramsdal, J., 2002. "Alteration of wettability and wettability heterogeneity," *Journal of Petroleum Science and Engineering*, 33: 3-17.

Green, D. W., Willhite, G. P., 1998. Enhanced Oil Recovery, AIME Memorial Fund, Society of Petroleum Engineers.

Gupta, R., and Mohanty, K. K., 2007. "Temperature Effects on Surfactant-Aided Imbibition into Fractured Carbonates," Paper SPE 110204, presented at the SPE Annual Technical Conference and Exhibition, Anaheim, California, November 11-14.

Gupta, R., and Mohanty, K. K., 2008. "Wettability Alteration of Fractured Carbonate Reservoirs," Paper SPE 113407, presented at the SPE/DOE Improved Oil Recovery Symposium, Tulsa, Oklahoma, April 19-23.

Gupta, R., Mohan, K., and Mohanty, K. K., 2009. "Surfactant Screening for Wettability Alteration in Oil-Wet Fractured Carbonates," Paper SPE 124822, presented at the SPE Annual Technical Conference and Exhibition, New Orleans, Lousiana, October 4-7.

Hagoort, J., 1980. "Oil Recovery by Gravity Drainage," *SPE Journal*, 20,139-150.

Hamon, G. and Vidal, J., 1986. "Scaling-Up the Capillary Imbibition Process from Laboratory Experiments on Homogeneous and Heterogeneous Samples," Paper SPE 15852, presented at the SPE European Petroleum Conference, London, United Kingdom, October 20-22.

Hand, D. B., 1939. "Dineric Distribution: I. The Distribution of a Consolute Liquid Between Two Immiscible Liquids," *Journal of Physics and Chem*, 34: 1961-2000.

Healy, R. N., and Reed, R. L., 1974. "Physicochemical Aspects of Microemulsion Flooding," *SPE Journal*, 14: 491-501.

Hendraningrat, L., Li, S., and Torsaeter, O., 2013. "A Coreflood Investigation of Nanofluid Enhanced Oil Recovery in Low-Medium Permeability Berea Sandstone," Paper SPE 164106, presented at the SPE International Symposium on Oilfield Chemistry, The Woodlands, Texas, April 8-10.

Hirasaki, G. J., 1982. "Interpretation of the Change in Optimal Salinity with Overall Surfactant Concentration," *SPE Journal*, 22: 971-982.

Hirasaki, G. J., 1991. "Wettability Fundamentals and surface forces", *SPE Journal*, 6: 217-226.

Hirasaki, G. J. and Zhang, L. D., 2004. "Surface Chemistry of Oil Recovery from Fractured, Oil-Wet, Carbonate Formations," Paper SPE 80988, presented at the International Symposium on Oilfield Chemistry, Houston, Texas, February 5-8.

Hirasaki, G. J., Miller, C. A., and Puerto, M., 2008. "Recent Advances in Surfactant EOR," Paper IPTC 115386, presented at the International Petroleum Technology Conference, Kuala Lumpur, Malaysia, December 3-5.

Huh, C., 1979. "Interfacial Tension and Solubilizing Ability of a Microemulsion Phase that Coexists with Oil and Brine," *Journal of Colloidal and Interface Science*, 71: 408-428.

Huh, C., Choi, S. K., and Sharma, M. M., 2005. "A rheological model for pH-sensitive ionic polymer solutions for optimal mobility-control applications," Paper SPE 96914, presented at the SPE Annual Technical Conference and Exhibition, Dallas, Texas, October 9-12.

Huh, C., and Pope, G. A., 2008. "Residual Oil Saturation from Polymer Floods: Laboratory Measurements and Theoretical Interpretation", Paper SPE 113417, presented at the SPE/DOE Symposium on Improved Oil Recovery, Tulsa, Oklahoma, April 20-23.

Hunt, J. A., 1987. "An experimental study of the kinetics of the crosslinking reaction between chromium(III) and polyacrylamide," Ph.D. dissertation, University of Kansas, Lawrence.

Husband, M., Ohms, D., Frampton, H., Carhart, S., Carlson, B., Morgan, J. C., and Chang, K. T., 2010. "Results of a Three-Well Waterflood Sweep Improvement Trial in the Prudhoe Bay Field Using a Thermally Activated Particle System," Paper SPE 129967, presented at the Improved Oil Recovery Symposium, Tulsa, Oklahoma, April 24-28.

Iler, R. K., 1979. The chemistry of silica: solubility, polymerization, colloid and surface properties, and biochemistry, John Wiley & Sons, New York.

Imqam, A., Bai, B., Al-Ramadan, M., Wei, M., Delshad, M., and Sepehrnoori, K., 2014. "Preformed particle gel extrusion through open conduits during conformance control treatments," SPE 169107 presented at SPE Improved Oil Recovery Symposium, Tulsa, Oklahoma, April 12-16.

Imqam, A., and Bai, B., 2015a. "Optimizing the strength and size of preformed particle gels for better conformance control treatment," *Fuel Journal*, 148: 178–185.

Imqam, A., 2015b. "Particle Gel Propagation and Blocking Behavior Through High Permeability Streaks and Fractures," Ph.D. dissertation, Missouri University of Science and Technology, Rolla, Missouri.

Izgec, O., and Shook, G. M., 2012. "Design Considerations of Waterflood Conformance Control with Temperature-Triggered Low Viscosity Sub-Micron Polymer," Paper SPE 153898, presented at the Western Regional Meeting, Bakersfield, California, March 19-23.

Jadhunandan, P. P., and Morrow, N. R., 1995. "Effect of Wettability on Waterflood Recovery for Crude Oil/Brine/Rock Systems," *SPE Reservoir Engineering Journal*, 10: 40-46.

Jain, R., McCool, C. S., Green, D. W., Willhite, G. P., and Michnick, M. J., 2005. "Reaction Kinetics of the Uptake of Chromium (III) Acetate by Polyacrylamide," *SPE Journal* 10: 247-255.

Johnson, C. E., 1976. "Status of Caustic and Emulsion Methods," *Journal of Petroleum Technology*, 28: 85-92.

Jurinak, J. J., Summers, L. E., and Bennett, K. E., 1989. "Oilfield application of colloidal silica gel," Paper SPE 18505, presented at the SPE International Symposium on Oilfield Chemistry, Houston, Texas, February 8-10.

Kalaei, M. H., Green, D. W., and Willhite, G. P., 2012. "A New Dynamic Wettability Alteration Model for Oil-Wet Cores During Surfactant Solution Imbibition," Paper SPE 153329, presented at the SPE Improved Oil Recovery Symposium, Tulsa, Oklahoma, April 14-18.

Kamath, J., Meyer, R. F., and Nakagawa, F. M., 2001. "Understanding Waterflood Residual Oil Saturation of Four Carbonate Rock Types," Paper SPE 71505, presented at the SPE Annual Technical Conference and Exhibition, New Orleans, Louisiana, September 30-October 3.

Kazemi, H., Gilman, J. R., and Elsharkawy, A. M., 1992. "Analytical and Numerical Solution of Oil Recovery from Fractured Reservoirs with Empirical Transfer Functions," *SPE Reservoir Engineering Journal*, 7: 219-227.

Kong, X., and Ohadi, M., 2010. "Applications of Micro and Nano Technologies in the Oil and Gas Industry- An Overview of the Recent Progress," Paper SPE 138241, presented at the Abu Dhabi International Petroleum Exhibition and Conference, Abu Dhabi, UAE, November 1-4.

Korrani, A. K. N., Sepehrnoori, K., Delshad, M., 2013. "A Novel Mechanistic Approach for Modeling Low Salinity Water Injection," Paper SPE 166523, Presented at the SPE Annual Technical Conference and Exhibition, New Orleans, Louisiana, September 30-October 2.

Korrani, A. K. N., Jerauld, G. R. and Sepehrnoori, K., 2014a. "Coupled Geochemical-Based Modeling of Low Salinity Waterflooding," Paper SPE 169115, presented at the SPE Improved Oil Recovery Symposium, Tulsa, Oklahoma, April 12-16.

Korrani, A. K. N., 2014b. "Mechanistic Modeling of Low Salinity Water Injection," Ph.D. Dissertation, The University of Texas at Austin, Austin, Texas, December.

Korrani, A. K. N., Sepehrnoori, K., and Delshad, M., 2015. "Coupling IPhreeqc with UTCHEM to model reactive flow and transport," *Journal of Computer and Geosciences*, 82: 152-169.

Kristensen, R., Lund, T., Titov, V. I., and Akimov, N. I., 1993. "Laboratory evaluation and field tests of a silicate gel system aimed to be under North Sea conditions," paper presented at the seventh European IOR Symposium, Moscow, Russia, October 26-29.

Kurian, P., and Chang, K. N., 2011. "Composition and Method for Recovering Hydrocarbon Fluids from a Subterranean Reservoir," U.S. Patent No. 7,902,127B2.

Lake, L. W., 1989. Enhanced Oil Recovery, Prentice Hall Inc., Englewood Cliffs.

Landmark, 2012. http://www.halliburton.com/ps/default.aspx?pageid=888&navid=226&prodid.

Lashgari, H. R., Lotfollahi, M., Delshad, M., Sepehrnoori, K., DeRouffignac, E., 2014a. "Steam-Surfactant-Foam Modeling in Heavy Oil Reservoirs," Paper SPE 170178, Presented at the Heavy Oil Conference, Calgary, Alberta, Canada, June 10-12.

Lashgari, H. R., 2014b. "Development of a Four-Phase Thermal-Chemical Reservoir Simulator for Heavy Oil," Ph.D. Dissertation, The University of Texas at Austin, Austin, Texas, December.

Lashgari, H. R., Rabaa, W. E., Chan, H., Vaidya, R., 2014c. "Estimation of Hydraulic Fracture Contribution in Medium to High Permeability Reservoirs" Paper SPE 169554, presented at the SPE Western North American and Rocky Mountain Joint Regional Meeting, Denver, Colorado, April 16-18.

Lashgari, H. R., Sepehrnoori, K., Delshad, M., DeRouffignac, E., 2015. "Development of a Four-Phase Chemical-Gas Model in an IMPEC Reservoir Simulator," Paper SPE 173250, Presented at the SPE Reservoir Simulation Symposium, Houston, Texas, February 23-25.

Levitt, D. B., Jackson, A. C., Heinson, C., Britton, L. N., Malik, T., Dwarakanath, V., and Pope, G. A., 2006, "Identification and Evaluation of High-Performance EOR Surfactants," Paper SPE 100089, presented at the SPE/DOE Symposium on Improved Oil Recovery, Tulsa, Oklahoma, April 22-26.

Li, L., and Bai, B., 2001. "Evaluation methods of performed particle gel", A report to PetroChina, December.

Li, Z., and Delshad, M., 2014. "Development of an Analytical Injectivity Model for Non-Newtonian Polymer Solutions," *SPE Journal*, 19: 381-389.

Li, Z., Delshad, M., Lotfollahi, M., Koh, H., Luo, H., Chang, H. L., Zhang, J., Dempsey, P., Lucas-Clements, C., and Brennan, B., 2014. "Polymer Flooding of a Heavy Oil Reservoir with an Active Aquifer," Paper SPE 169149, presented at the SPE Symposium on Improved Oil Recovery, Tulsa, Oklahoma, April 12-16.

Li, K., and Horne, R. N., 2002. "A General Scaling Method for Spontaneous Imbibition," Paper SPE 77544, presented at the SPE Annual Technical Conference and Exhibition, San Antonio, Texas, September 29-October 2.

Li, L., and Lee, S. H., 2008. "Efficient field-scale simulation of black oil in a naturally fractured reservoir through discrete fracture networks and homogenized media," *SPE Reservoir Evaluation & Engineering Journal*, 11: 750-758.

Liang, J. T., Sun, H., and Seright, R. S., 1995. "Why Do Gels Reduce Water Permeability More Than Oil Permeability?," *SPE Reservoir Engineering Journal*, 10: 282-286.

Liang, J., and Seright, R. S., 2000. "Wall-Effect/Gel-Droplet Model of Disproportionate Permeability Reduction," Paper SPE 59344, presented at the SPE/DOE Improved Oil Recovery Symposium, Tulsa, Oklahoma, April 3-5.

Lin, E., 1981. "A study of micellar/polymer flooding using a compositional simulator," Ph.D. Dissertation, The University of Texas at Austin.

Liu, J., Delshad, M., Pope, G. A., and Sepehrnoori, K., 1994. "Application of Higher Order Flux-Limited Methods in Compositional Simulations," *Journal of Transport in Porous Media*, 16: 1-29.

Liu, S., Zhang, D. L., Yan, W., Puerto, M., Hirasaki, G. J., and Miller, C. A., 2008. "Favorable Attributes of Alkaline-Surfactant-Polymer Flooding," *SPE Journal*, 13: 5-16.

Lockhart, T. P., and Albonico, P., 1994. "New Chemistry for the placement of Chromium (III)/Polymer Gels in High-Temperature Reservoirs," *SPE Production & Facilities Journal*, 9: 273-279.

Lu, J., Britton, C., Solairaj, S., Liyanage, P. J., Kim, D. H., Adkins, S., Arachchilage, G. P., Weerasooriya, U., and Pope, G. A., 2012a. "Novel Large-Hydrophobe Alkoxy Carboxylate Surfactants for Enhanced Oil Recovery," Paper SPE 154256, presented at SPE IOR Symposium, Tulsa, OK, April 14-18.

Lu, J., Goudarzi, A., Chen, P., Kim, D. H., Britton, C., Delshad, M., Mohanty, K. K., Weerasooriya, U., and Pope, G. A., 2012b. "Surfactant Enhanced Oil Recovery from Naturally Fractured Reservoirs," Paper SPE 159979, presented at the SPE Annual Technical Conference and Exhibition, San Antonio, Texas, October 8-10.

Lu, J., Goudarzi, A., Chen, P., Kim, D. H., Delshad, M., Mohanty, K. K., Sepehrnoori, K., Weerasooriya, U., and Pope, G. A., 2014. "Enhanced oil recovery from high-temperature high-salinity naturally fractured carbonate reservoirs by surfactant flood," *Journal of Petroleum Science and Engineering*, 124: 122-131.

Lu, X., and Song, K., 2000. "Performance and Evaluation Methods of Colloidal Dispersion Gels in the Daqing Oil Field," Paper SPE 59466, presented at the SPE Asia Pacific Conference on Integrated Modeling for Asset Management, Yokohama, Japan, April 25-26.

Ma, S., Morrow, N. R., and Zhang, X., 1997. "Generalized Scaling of Spontaneous Imbibition Data for Strongly Water-Wet Systems," *Journal of Petroleum Science and Engineering*, 18: 165-178.

Mack, J. C., and Smith, J. E., 1994. "In-depth Colloidal Dispersion Gels Improve Oil Recovery Efficiency," Paper SPE 27780, presented at the SPE/DOE 9th Symposium on Improved Oil Recovery, Tulsa, Oklahoma, April 17-20.

Maini, B. B., and Batycky, J. P., 1985. "Effect of Temperature on Heavy-Oil/Water Relative Permeabilities in Horizontally and Vertically Drilled Core Plugs," *Journal of Petroleum Technology*, 37: 1500-1510.

Manrique, E. J., Garmeh, R., Izadi, M., Salehi, M., Romero, J., Aye, N., Thomas, C. P., and Shevelev, P, 2012. "In-depth Sweep Efficiency Improvement: Screening Criteria and Engineering Approach for Pattern Evaluation and Potential Field Implementation," Paper SPE 160749, Presented at the SPE Russian Oil & Gas Exploration & Production Technical Conference and Exhibition, Moscow, Russia, October 16-18.

Mattax, C. C., and Kyte, J. R., 1962. "Imbibition Oil Recovery from Fractured Water Drive Reservoirs," *SPE Journal*, 2: 177-184.

McCool, C. S., Li, X., and Wilhite, G. P., 2009. "Flow of a Polyacrylamide/Chromium Acetate System in a Long Conduit," *SPE Journal*, 14: 54-66.

Meister, J., 1985. "Bulk Gel Strength Tester," Paper SPE 13567, presented at the SPE Oilfield and Geothermal Chemistry Symposium, Phoenix, Arizona, March 9-11.

Mercado, M., Acuna, J. C., Caballero, C., Vasquez, J., and Soriano, E., 2009. "Successful Field Application of a High-temperature Conformance Polymer in Mexico," Paper SPE 120966, presented at the SPE International Symposium on Oilfield Chemistry, The Woodlands, Texas, April 20-22.

Meter, D. M., and Bird, R. B., 1964. "Tube Flow of Non-Newtonian Polymer Solutions," *Journal of the American Institute of Chemical Engineers*, 10: 878-881.

Mirzaei, M., DiCarlo, D. A., and Pope, G. A., 2013. "Visualization and Analysis of Surfactant Imbibition into Oil-Wet Fractured Cores," Paper SPE 166129, presented at the SPE Annual Technical Conference and Exhibition, New Orleans, Louisiana, September 30-October 2.

Mohanty, K. K., 2010, 2012. Private communication.

Mohebbinia, S., Sepehrnoori, K., Korrani, A. K. N., and Johns, R. T., 2014. "Simulation of Asphaltene Precipitation during Gas Injection Using PC-SAFT EOS," Paper SPE 170697, presented at the SPE Annual Technical Conference and Exhibition, Amsterdam, The Netherlands, October 27-29.

Moinfar, A., Varavei, A., Sepehrnoori, K., and Johns, R. T., 2012. "Development of a Novel and Computationally-Efficient Discrete-Fracture Model to Study IOR Processes in Naturally Fractured Reservoirs," Paper SPE 154246, presented at the Eighteenth SPE Improved Oil Recovery Symposium, Tulsa, Oklahoma, April 14-18.

Moinfar, A., Varavei, A., Sepehrnoori, K., and Johns, R. T., 2013. "Development of a Coupled Dual Continuum and Discrete Fracture Model for the Simulation of Unconventional Reservoirs," Paper SPE 163647, presented at the SPE Reservoir Simulation Symposium, The Woodlands, Texas, February 18-20.

Mollaei, A., Lake, L. W., and Delshad, M., 2011. "Application and variance based sensitivity analysis of surfactant-polymer flooding using modified chemical flood predictive model," *Journal of Petroleum Science and Engineering*, 79: 25-36.

Morel, D., Vert, M., Jouenne, S., and Nahas, E., 2008. "Polymer Injection in Deep Offshore Field: The Dalia Angola Case," Paper SPE 116672, presented at the SPE Annual Technical Conference and Exhibition, Denver, Colorado, September 21-24.

Morrow, N. R., Lim, H. T., and Ward, J. S., 1986. "Effect of Crude-Oil-Induced Wettability Changes on Oil Recovery," *Formation Evaluation Journal* 1: 89-103.

Muhammed, F. A., 2011. "Experimental study of the interaction between surfactant and preformed particle gels," Master's Thesis, Missouri University of Science and Technology, Rolla, Missouri.

Muhammed, F. A., 2014. "Study and pilot test on a novel EOR method-coupling PPG conformance control and surfactant flooding," Ph.D. dissertation, Missouri University of Science and Technology, Rolla, Missouri.

Muhammed, F. A., Bai, B., and Al Brahim, A., 2014. "A Simple Technique to Determine the Strength of Millimeter-Sized Particle Gel," Paper SPE 169106, presented at the SPE Improved Oil Recovery Symposium, Tulsa, Oklahoma, April 12-16.

Muruaga, E., Flores, M., Norman, C., and Romero, J., 2008. "Combining Bulk Gels and Colloidal Dispersion Gels for Improved Volumetric Sweep Efficiency in a Mature Waterflood," Paper SPE 113334, presented at the SPE/DOE Improved Oil Recovery Symposium, Tulsa, Oklahoma, April 19-23.

Mustoni, J. L., Cabrera, F. A., Manrique, E. J., and Norman, C. A., 2012. "Application of a Thermally Activated Particle System for Improved Sweep Efficiency in a Multilayer, Geologically Complex Waterflood," Paper SPE 153331, presents at the Improved Oil Recovery Symposium, Tulsa, Oklahoma, April 14-18.

Nelson, R. C., and Pope, G. A., 1978. "Phase Relationships in chemical Flooding," *SPE Journal*, 18: 325-338.

Nelson, R. A., 2001. Geological Analysis of Naturally Fractured Reservoirs, Second Edition, Gulf Professional Publishing.

Nolen, J. S., and Berry, D. W., 1972. "Tests of the stability and time-step sensitivity of semi-implicit reservoir simulation techniques," *Society of Petroleum Engineering Journal*, 12: 253-266.

Ogolo, N. A., Olafuyi, O. A., and Onyekonwu, M. O., 2012. "Enhanced Oil Recovery Using Nanoparticles," Paper SPE 160847, presented at the Saudi Arabia Section Technical Symposium and Exhibition, Al-Khobar, Saudi Arabia, April 1-4.

Ogunberu, A. L., and Asghari, K., 2004. "Water Permeability Reduction Under Flow-Induced Polymer Adsorption" Paper SPE 89855, presented at the SPE International Petroleum Conference, Puebla, Mexico, November 7-9.

Ohms, D., McLeod, J., Graff, C. J., Frampton, H., Morgan, J. C., Cheung, S., Yancey, K., and Chang, K. T., 2009. "Incremental Oil Success from Waterflood Sweep Improvement in Alaska," Paper SPE 121761, presented at the International Symposium on Oilfield Chemistry, The Woodlands, Texas, April 20-22.

Onbergenov, U., 2012. "Simulation of Thermally Active and pH-Sensitive Polymers for Conformance Control," Master's Thesis, The University of Texas at Austin.

Pandey, A., Beliveau, D., Corbishley, D. W., and Kumar, M. S., 2008. "Design of an ASP Pilot for the Mangala Field: Laboratory Evaluations and Simulation Studies," Paper SPE 113131, presented at the Indian Oil and Gas Technical Conference and Exhibition , Mumbai, India, March 4-6.

Parsons, R. W., and Chaney, P. R., 1966. "Imbibition Model Studies on Water-Wet Carbonate Rocks," *SPE Journal*, 6: 26-34.

Patil, S., Dandekar, A. Y., Patil, S. L., and Khataniar, S., 2008. "Low Salinity Brine Injection for EOR on Alaska North Slope (ANS)," Paper IPTC 12004, presented at the International Petroleum Technology Conference, Kuala Lumpur, Malaysia, December 3-5.

Peaceman, D. W., 1983. "Interpretation of well-block pressures in numerical reservoir simulation with nonsquare gridblocks and anisotropic permeability," *Society of Petroleum Engineering Journal*, 23: 531-543.

Petroleum Experts, 2012. http://www.petex.com/products/?ssi=8.

Pope, G.A., 2010, 2011. Private communication.

Poston, S. W., Ysrael, S., Hossain, A. K. M. S, and Montgomery, E. F., 1970. "The Effect of Temperature on Irreducible Water Saturation and Relative Permeability of Unconsolidated Sands," *SPE Journal*, 10: 171-180.

Pritchett, J., Frampton, H., Brinkman, J., Cheung, S., Morgan, J., Chang, K. T., Williams, D., and Goodgame, J., 2003. "Field Application of a New In-Depth Waterflood Conformance Improvement Tool," Paper SPE 84897, presented at the International Improved Oil Recovery Conference, Kuala Lumpur, Malaysia, October 20-21.

Putra, E., Fidra, Y., and Schechter, D. S., 1999. "Use of Experimental and Simulation Results for Estimating Critical and Optimum Water Injection Rates in Naturally Fractured Reservoirs," Paper SPE 56431, presented at the SPE Annual Technical Conference and Exhibition, Houston, Texas, October 3-6.

Ranganathan, R., Lewis, R., McCool, C. S., Green, D. W., and Willhite G. P., 1998. "Experimental Study of the Gelation Behavior of a Polyacrylamide/Aluminum Citrate Colloidal-Dispersion Gel System", *SPE Journal*, 3: 337-343.

Rezaveisi, M., Ayatollahi, S., and Rostami, B., 2012. "Experimental investigation of matrix wettability effects on water imbibition in fractured artificial porous media," *Journal of Petroleum Science and Engineering*, 86: 165-171.

Riccardo, Po., 1994. "Water-absorbent polymers: A patent survey," *Journal of Macromolecular Science*, Part C: Polymer Reviews, 34: 607-662.

Roehl, P. O., and Choquette, P. W., 1985. "Carbonate Petroleum Reservoirs," New York, Springer-Verlag.

Rousseau, D., Chauveteau, G., Renard, M., Tabary, R., Zaitoun, A., Mallo, P., Braun, O., and Omari, A., 2005. "Rheology and transport in porous media of new water shutoff/conformance control microgels," Paper SPE 93254, presented at SPE International Symposium on Oilfield Chemistry, Houston, Texas, February 2-4.

Roussennac, B., and Toschi, C., 2010. "Brightwater Trial in Salema Field (Campos Basin, Brazil)," Paper SPE 131299, presented at the SPE EUROPEC/EAGE Annual Conference and Exhibition, Barcelona, Spain, June 14-17.

Russel, W. B., Saville, D. A., and Schowalter, W. R., 1989. Colloidal Dispersions, Cambridge University Press, Cambridge, U.K.

Saad, N., 1989. "Field Scale Studies with a 3-D Chemical Flooding Simulator," Ph.D. Dissertation, The University of Texas at Austin, Austin, Texas.

Salehi, M., Thomas, C. P., Kevwitch, R. M., Manrique, E. J., Garmeh, R., and Izadi, M., 2012. "Performance Evaluation of Thermally-Actiavted Polymers for Conformance Control Applications," Paper SPE 154022, Presented at the Eighteenth SPE Improved Oil Recovery Symposium, Tulsa, Oklahoma, Aril 14-18.

Satoh, T., "Treatment of Phase Behavior and Associated Properties Used in Micellar-Polymer Flood Simulator," Master's Thesis, The University of Texas at Austin, Austin, Texas, 1984.

Schembre, J. M., Tang, G. Q., and Kovscek, A. R., 2006. "Wettability alteration and oil recovery by water imbibition at elevated temperatures," *Journal of Petroleum Science and Engineering*, 52: 131-148.

Schechter, D. S., Zhou, D., and Orr, F. M., Jr., 1994. "Low IFT Drainage and Imbibition," *Journal of Petroleum Science and Engineering*, 11: 283-300.

Schneider, F. N., and Owens, W. W., 1982. "Steady-State Measurements of Relative Permeability for Polymer/Oil Systems," *SPE Journal*, 22: 79-86.

Seethepalli, A., Adibhatla, B., and Mohanty, K. K., 2004a. "Physicochemical Interactions During Surfactant Flooding of Carbonate Reservoirs," *SPE Journal*, 9: 411-418.

Seethepalli, A., Adibhatla, B., and Mohanty, K. K., 2004b. "Wettability Alteration during Surfactant Flooding of Carbonate Reservoirs," Paper SPE 89423, presented at the SPE/DOE Fourteenth Symposium on Improved Oil Recovery, Tulsa, Oklahoma, April 17-21.

Seright, R. S., and Martin, F. D., 1991. "Impact of gelation pH, rock permeability and lithology on the performance of a monomer-based gel," Paper SPE 20999, presented at the SPE International Symposium on Oilfield Chemistry, Anaheim, California, February 20-22.

Seright, R. S., and Liang, J., 1994. "A Survey of Field Applications of Gel Treatments for Water Shutoff," Paper SPE 26991, presented at III Latin American/Caribbean Petroleum Engineering Conference, Buenos Aires, Argentina, April 27-29.

Seright, R. S., 1995. "Gel placement in fractured systems," *SPE Production and Facilities Journal*, 10: 241-248.

Seright, R. S., 1997. "Improved methods for water shutoff," Annual Technical Progress Report, DOE Contract: DOE/PC/91008-4, November.

Seright, R. S., 1999. "Mechanism for gel propagation through fractures," Paper SPE 55628, presented at the SPE Rocky Mountain Regional Meeting, Gillette, Wyoming, May 15-18.

Seright, R. S., 2000. "Gel propagation through fractures," Paper SPE 59316, presented at the SPE/DOE Symposium on Improved Oil Recovery, Tulsa, Oklahoma, April 3-5.

Seright, R. S., 2001. "Gel Propagation Through Fractures," *SPE Production and Facilities Journal*, 16: 225-231.

Seright, R. S., 2003. "Washout of Cr(III)-Acetate-HPAM Gels from Fractures," Paper SPE 80200, presented at the SPE International Symposium on Oilfield Chemistry, Houston, Texas, February 5-7.

Seright, R. S., 2004. "Conformance improvement using gels," Annual Technical Progress Report, DOE Contract: DE-FC26-01BC15316, September.

Seright, R. S., 2006. "Cleanup of Oil Zones After a Gel Treatment," *SPE Production and Facilities Journal*, 21: 237-244.

Seright, R. S., 2009. "Disproportionate Permeability Reduction with Pore-Filling Gels," *SPE Journal*, 14: 5-13.

Shakiba, M., 2014. "Modeling and Simulation of Fluid Flow in Naturally and Hydraulically Fractured Reservoirs Using Embedded Discrete Fracture Model (EDFM)," Master's Thesis, The University of Texas at Austin.

Sheng, J., 2011. Modern Chemical Enhanced Oil Recovery: Theory and Practice. Amsterdam: Elsevier, Print.

Shi, J., Varavei, A., Huh, C., Delshad, M., Sepehrnoori, K., and Li, X., 2011a. "Transport Model Implementation and Simulation of Microgel Processes for Conformance and Mobility Control Purposes," *Journal of Energy and Fuels*" 25: 5063-5075.

Shi, J., Varavei, A., Huh, C., Delshad, M., Sepehrnoori, K., and Li, X., 2011b. "Viscosity Model of Preformed Microgels for Conformance and Mobility Control," *Journal of Energy and Fuels*" 25: 5033-5037.

Smith, J. E., Lui, H., and Guo, Z. D., 2000. "Laboratory Studies of In-Depth Colloidal Dispersion Gel Technology for Daqing Oil Field," Paper SPE 62610, presented at the SPE/AAPG Western Regional Meeting, Long Beach, California, June 19-23.

Smith, J. E., Mack, J. C., and Nicol, A. B., 1996. "The Adon Road - An In-Depth Gel Case History," Paper SPE 35352, presented at the SPE/DOE Tenth Symposium on Improved Oil Recovery, Tulsa, Oklahoma, April 21-24.

Smith, J. E., 1989. "The Transition Pressure: A Quick Method for Quantifying Polyacrylamide Gel Strength," Paper SPE 18739, presented at the SPE International Symposium on Oilfield Chemistry, Houston, Texas, February 8-10.

Solairaj, S., Britton, C., Lu, J., Kim, D. H., Weerasooriya, U., and Pope, G. A., 2012. "New Correlation to Predict the Optimum Surfactant Structure for EOR," SPE 154262 presented at SPE IOR Symposium, Tulsa, OK, April 14-18.

Sorbie, K. S., 1991. Polymer-Improved Oil Recovery, CRC Press Inc., Boca Raton, Florida.

Sorbie, K. S., and Seright, R. S., 1992. "Gel Placement in Heterogeneous Systems With Crossflow," Paper SPE 24192, presented at the SPE/DOE Eighth Symposium on Enhanced Oil Recovery, Tulsa, Oklahoma, April 22-24.

Sparlin, D. D., and Hagen, R. W., 1984. "Controlling water in producing operations," Part III: remedial cementing techniques. *World Oil*, 63-65.

Spildo, K., Skauge, A., Aarra, M. G., and Tweheyo, M. T., 2009. "A New Polymer Application for North Sea Reservoirs," *SPE Reservoir Evaluation & Engineering Journal*, 12: 427-432.

Standnes, D. C., and Austad, T., 2000. "Wettability alteration in chalk: 2. Mechanisms for wettability alteration from oil-wet to water-wet using surfactants," *Journal of Petroleum Science and Engineering*, 28: 123-143.

Standnes, D. C., and Austad, T., 2002. "Wettability alteration in carbonates, Interaction between cationic surfactant and carboxylates as a key factor in wettability alteration from oil-wet to water-wet conditions," *Journal of Colloids and surfaces* 216: 243-259.

STARS-ME Technical Manual, 2011.

Stavland, A., and Nilsson, S., 2001. "Segregated Flow is the Governing Mechanism of Disproportionate Permeability Reduction in Water and Gas Shutoff," Paper SPE 71510, presented at the SPE Annual Technical Conference and Exhibition, New Orleans, Louisiana, September 30-October 3.

Sydansk, R. D., Al-Dhafeeri, A. M., Xiong, Y., and Seright, R. S., 2004. "Polymer gels formulated with a combination of high- and low-molecular-weight polymers provide improved performance for water-shutoff treatments of fractured production wells," *SPE Production & Facilities Journal*, 19: 229-236.

Sydansk, R. D., and Moore, P. E., 1992. "Gel conformance treatments increase oil production in Wyoming," *Oil and Gas Journal*, 40-45.

Sydansk, R. D., 1990. "A Newly Developed Chromium (III) Gel Technology," *SPE Reservoir Engineering Journal*, 5: 346-352.

Sydansk, R. D., and Seright, R. S., 2007. "When and Where Relative Permeability Modification Water-Shutoff Treatments Can be Successfully Applied," *SPE Production & Operations Journal*, 22: 236-247.

Taksaudom, P., 2014. "Simulation Study of Preformed Particle Gel for Conformance Control," Master's Thesis, The University of Texas at Austin.

Tavassoli, S., Pope, G. A., and Sepehrnoori, K., 2015. "Frontal-Stability Analysis of Surfactant Floods," *SPE Journal*, 20: 471-482.

Thrasher, D. R., Denyer, P., Timchuk, A. S., Zemtsov, Y. V., and Akinin, D. V., 2013. "First Application in Russia of Bright Water Chemical for Waterflood Sweep Improvement in the Samotlor Field," paper presented at the seventeenth European IOR Symposium, St. Petersburg, Russia, April 16-18.

Thurston, G. B., Ozon, P. M., and Pope, G. A., 1987. "The viscoelasticity and gelation of some polyacrylamide and xanthan gum solutions," presented at AICHE meeting, March.

Tongwa, P., and Bai, B., 2014. "A more superior preformed particle gel with potential application for conformance control in mature oilfields," *Journal of Petroleum Exploration and Production Technology*, 5: 201-210.

Torsaeter, O., and Abtahi, M., 2003. "Experimental Reservoir Engineering Laboratory Workbook," Norwegian University of Science and Technology.

Towns, M., Angarita, M. L., Thrasher, D., Denyer, P., Nabil, M. M., Bayoumi, R. S. and Kinawy, M. M., 2013. "Enhacing Oil Recovery in Gulf of Suez by Deep Conformance Control using a Thermally Activated Particle System," Paper SPE 164650, presented at the Thirteenth North Africa Technical Conference and Exhibition, Cairo, Egypt, April 15-17.

Treiber, L. E., Archer, D. L., and Owens, W. W., 1972. "A Laboratory Evaluation of the Wettability of Fifty Oil-Producing Reservoirs," *SPE Journal*, 12: 531-540.

Tweheyo, M. T., Holt, T., and Torsaeter, O., 1999. "An experimental study of the relationship between wettability and oil production characteristics," *Journal of Petroleum Science and Engineering*, 24: 179-188.

Uren, L. C., and Fahmy, E. H. 1927. "Factors Influencing the Recovery of Petroleum from Unconsolidated Sands by Waterflooding," Petroleum Development and Technology, AIME 318.

UTCHEM Technical Manual, 2011.

UTGEL Technical Manual, 2014

Vinsome, P. K., and Westerveld, J., 1980. "A simple method for predicting cap and base rock heat losses in thermal reservoir simulators," *Journal of Canadian Petroleum Technology*, 19: 87-90.

Wang, J., 2013. "Theoretical Investigations on Enhanced Oil Recovery by Chemical Flooding in High Water-Cut Reservoirs," Ph.D. Dissertation, China University of Petroleum, Beijing, China.

Wang, J., Liu, H., Wang, Z., Xu, J., and Yuan, D., 2013. "Numerical simulation of preformed particle gel flooding for enhancing oil recovery," *Journal of Petroleum Science and Engineering*, 112: 248-257.

Wang, J., Liu, H., Wang, Z., Hou, P., 2012. "Experimental Investigation on the Filtering Flow Law of Pre-gelled Particle in Porous Media," *Transport Porous Media Journal*, 94: 69-86.

Wang, Y., and Seright, R. S., 2006. "Correlating Gel Rheology with Behavior during Extrusion through Fractures," Paper SPE 99462, presented at the SPE/DOE Symposium on Improved Oil Recovery, Tulsa, Oklahoma, April 22-26.

Wang, W., Gu, Y., and Liu, Y., 2003. "Applications of Weak Gel for In-Depth Profile Modification and Oil Displacement," *Journal of Canadian Petroleum Technology*, 42: 54-61.

Willhite, G. P., Green, D. W., and McCool, C. S. 2001. "Increased Oil Recovery from Mature Oil Fields Using Gelled Polymer Treatments," Annual Report, DOE Contract: DE-AC26-99BC15209, Washington, DC.

Willhite, G. P., Green, D. W., and McCool, C. S. 2003. "Increased Oil Recovery from Mature Oil Fields using Gelled Polymer Treatments," Final Report, DOE Contract: DE-AC26-99BC15209.

Wreath, D., Pope, G. A., and Sepehrnoori, K., 1990. "Dependence of polymer apparent viscosity on the permeable media and flow conditions," *In Situ Journal*, 14: 263-284.

Wu, Yu-Shu., Bai, B., 2008. "Modeling particle gel propagation in porous media," Paper SPE 115678, presented at the SPE Annual Technical Conference and Exhibition, Denver, Colorado, September 21-24.

Yanez, P. A. P., Mustoni, J. L., Relling, M. F., Chang, K. T., Hopkinson, P., and Frampton, H., 2007. "New Attempt in Improving Sweep Efficiency at the Mature Koluel Kaike and Piedra Clavada Waterflooding Projects of the S. Jorge Basin in Argentina," Paper SPE 107923, presented at the Latin American and Caribbean Petroleum Engineering Conference, Buenos Aires, Argentina, April 15-18.

Zaitoun, A., and Kohler, N., 1988. "Two-Phase Flow Through Porous Media: Effect of an Adsorbed Polymer Layer," Paper SPE 18085, presented at the SPE Annual Technical Conference and Exhibition, Houston, Texas, October 2-5.

Zaitoun, A., Kohler, N., and Guerrinl, Y., 1991. "Improved Polyacrylamide Treatments for Water Control in Producing Wells," *Journal of Petroleum Technology*, 43: 862-867.

Zaitoun, A., Bertin, H., and Lasseux, D., 1998. "Two-Phase Flow Property Modifications by Polymer Adsorption," Paper SPE 39631, presented at the SPE/DOE Improved Oil Recovery Symposium, Tulsa, Oklahoma, April 19-22.

Zhang, X., Morrow, N. R., Ma, S., 1995. "Experimental Verification of a Modified Scaling Group for Spontaneous Imbibition," Paper SPE 30762, presented at the SPE Annual Technical Conference and Exhibition, Dallas, Texas, October 22-25.

Zhang, H., Challa, R., Bai, B., Tang, X., and Wang, J., 2010. "Using screening test results to predict the effective viscosity of swollen superabsorbent polymer particles extrusion through an open fracture," *Industrial & Engineering Chemistry Research Journal*, 49: 12284–12293.

Zhang, H., and Bai, B., 2010, "Preformed Particle Gel Transport through Open Fractures and its Effect on Water Flow," Paper SPE 129908, presented at the SPE Improved Oil Recovery Symposium, Tulsa, Oklahoma, April 24-28.

Zitha, P. L. J., 2000. Well Treatment and Water Shutoff by Polymer Gels, Delft University Press, Delft.